Title

Strategy Development in Natural Product Total Synthesis: Part I. Function Driven Synthesis of Xiamycin Sesquiterpenoids Part II. Progress toward the Symmetry-inspired Total Synthesis of Melicolones A & B

Author

Bakanas, Ian

Publication Date

2022

Peer reviewed|Thesis/dissertation

Strategy Development in Natural Product Total Synthesis: Part I. Function Driven Synthesis of Xiamycin Sesquiterpenoids Part II. Progress toward the Symmetry-inspired Total Synthesis of Melicolones A & B

By

Ian J Bakanas

A dissertation submitted in partial satisfaction of the

requirements for the degree of

Doctor of Philosophy

in

Chemistry

in the

Graduate Division

of the

University of California, Berkeley

Committee in charge:

Professor Richmond Sarpong, Chair
Professor Thomas Maimone
Professor Xavier Darzacq

Fall 2022

Abstract

Strategy Development in Natural Product Total Synthesis: Part I. Function Driven Synthesis of Xiamycin Sesquiterpenoids Part II. Progress toward the Symmetry-inspired Total Synthesis of Melicolones A & B

by

Ian J Bakanas

Doctor of Philosophy in Chemistry

University of California, Berkeley

Professor Richmond Sarpong, Chair

Two major motivations can be attributed to natural product total synthesis: a search for function, and the development of strategies for complex molecule synthesis. The work described in this dissertation covers both topics with critical analysis of methodologies and synthesis practices.

Chapter 1 provides a statement on the current field of total synthesis highlighting enduring contributions, motivations, and future directions.

Chapters 2 and 3 focus on two total synthesis projects that arose as part of a collaboration in the Sarpong group with scientists at Corteva Argriscience for the identification and development of natural products as antifeedant molecules—a search for function. Chapter 2 describes the total synthesis and biological evaluation of xiamycin-type indolosesquiterpenoids utilizing a 'benzannulation of carvone strategy'. Chapter 3 discusses progress toward broadening this synthesis strategy to paspaline-type indole diterpenoids.

Chapters 4 and 5 initiate a discussion on strategy and tactics in synthesis. Chapter 4 focuses on symmetry inspired strategies and symmetry tactics, the distinction between the two, and how they can each be greatly simplifying in synthesis. Chapter 5 expands on classifications of C–H oxidation reactions, examines their use in natural product synthesis, and gives insights into their strategic application through case study analysis.

Chapter 6 details progress toward the synthesis of the polyprenylated acylphloroglucinol natural products melicolones A & B utilizing a hidden symmetry strategy. Chapter 7 discusses a broad approach toward several bicyclic natural product cores through the divergent C–C cleavage of a common intermediate—the development of strategies for complex molecule synthesis.

Overall, this work explores studies in indoloterpene function as well as symmetry and C–C cleavage strategies for complex molecule synthesis.

In memory of Dr. Nick O'Connor

Table of Contents

Acknowledgements

Richmond, thank you for believing in me and giving me a place to cook. It's indescribably easier to believe in yourself when someone you respect believes in you. I hope I can accomplish all the things you think I can.

To the Sarpong group, thank you for being my home away from home and my family away from family. Meggie specifically, for all the help and the positivity.

Magnus Pfaffenbach, thank you for being a great mentor and teammate. Working on the xiamycins with you taught me how to think and most importantly, how to plan a day.

Nick O'Connor, we miss you. Your selflessness made sure that we never felt alone.

Solène Miaskewicz, thank you for showing me the value of leading with kindness and joy. Everyone felt better after talking with you.

To Jess Tang and Gian Reber, thank you for your help. I think we were chasing something challenging and wholly worthwhile.

Brian Wang, your creativity inspired, and your optimism was so admirable. Thank you for showing me that anything was possible in the future.

Jack Hayward-Cooke, watching you become a leader has been a joy, stay the course.

Hasan Celik, thanks for keeping the NMR facility lights on. We all appreciate your hard, hard work.

Kerry Jones, a great friend, an honest friend, and a joy to be around. Congratulations on all your success keep going and be great.

Bobby Lusi, I scrolled back through the hundreds (maybe thousands) of messages we sent back and forth during phys org readings. I wouldn't be the chemist I am without arguing with you, coming to bother you with my ideas, and listening to your talks.

Justin Jurczyk, everyone needs a friend to hold dry ice with. Our smoothie runs, basketball chats, and accidentally matching outfits kept my head above. Thank you.

Katie Blackford, thanks for being more fun than the rest of us.

Harry Bergman, VC university is going to be a huge hit.

Ethan Ebinger and Johnathan Kupfer, bright lights in a dark time.

To my parents, brothers, and the boys, thanks for making sure Medford was always my home.

To Kelsey, thanks for being a reminder of where we came from. We're just getting started.

Chapter 1
A Perspective on Total Synthesis in 2022

1.1 A short essay on the state and future of total synthesis

The science of natural product synthesis rests on the same axis of exploration as many of the natural sciences. Discoveries of new species, fundamental particles, biological processes, and cellular structures are all driven by scientists pushing boldly into the unknown and building on each other's discoveries to build a more complete understanding of the natural world. Organic chemistry and the science of total synthesis evolved in the same way. Our longstanding explorations—starting from the Wöhler synthesis of urea[1] in 1828—take the form of building some of the most complex molecules that nature can offer. Given nearly two centuries of progress, the field today would be unrecognizable to Wöhler, as would the structure of benzene, the concept of a nucleus, and indoor plumbing—we have come a long way.

Many accounts,[2] essays,[3] and opinion pieces[4] have been written on the state and future of total synthesis. Syntheses seem to be getting ever shorter, new methodologies open rich strategic avenues, and we routinely see chemists achieving the syntheses of molecules that possess significant bioactivity.[5] Despite these successes and the outstanding challenges that have been laid bare, some argue that we have solved the challenge of making molecules and that total synthesis does not provide the same value to chemistry as it once did.[4] Opinions aside, it is clear from the number and quality of published syntheses that the field is thriving.[6] Still, I wonder if the return on investment of synthesis is as high as it once was. Few total synthesis campaigns afford the target natural product in useful yields, the number of discoveries that fall out of syntheses[2f] may have diminished as methodology development has become a dominant field (though this is difficult to quantify), and the challenges of the field remain daunting. What is the enduring value of total synthesis and how will it develop in the future? In partial answer, Heathcock[3] notes this quote from Woodward during a time of transition in the field of synthesis:

"Of course, [people] make much use of excuses for activities which lead to discovery, and the lure of unknown structures has in the past yielded a huge dividend of unsought fact, which has been of major importance in building organic chemistry as a science. Should a surrogate now be needed, we do not hesitate to advocate the case for synthesis." –R.B Woodward, 1963[7]

It is clarifying in this moment, I think, to ponder what the endgame of synthetic organic chemistry would look like. Put simply: *the ability to make any reasonable organic structure with ease and speed*. Recent concepts in skeletal and molecular editing[8]—reactions which disrupt the

core structure of a molecule at a late-stage (think benzene to pyridine, piperidine to pyrrolidine, etc.)—may challenge this goal. Perhaps better then to define the endgame as: *total, programmable control of structure and reactivity*. If the purpose of synthesis lies in building organic chemistry as a science, then its value should be attributed to how it contributes to bringing us to the endgame of organic chemistry. On the road to total control, we will always need a means of testing new promising methodologies. Time and time again, we see that certain reactions routinely fail in complex settings. Problems that we have 'solved' in simple systems are exposed en route to our targets. In a simple way, use of a method in synthesis validates that methodology's reliability, reproducibility, and scalability as each step relies on the material throughput of all prior steps. Toward predicting the outcome of a reaction, computational tools have become increasingly popular. As a field, we now routinely use computational tools to model reactions,[9] predict selectivities,[10] and parse out parameters that contribute to those outcomes.[11] However, while these considerations provide a sense of the energy surface of a reaction, they do not predict in a practical sense how well a reaction will work. Machine learning and data science approaches are looking to solve this problem but are still emerging.[12] Shenvi and coworkers coined the term "chemofidelity", [13] meaning a reaction's robustness independent of molecular context. This concept is eminently useful for synthesis planning as one could favor the use of reactions with high chemofidelity to increase chances of success. However, there is currently no empirical basis for the chemofidelity of various reaction classes. A systematic review of the synthesis literature might illuminate which reactions have the highest chemofidelity and therefore inform choices made in a synthesis campaign. Machine learning and data science approaches will have their place in the coming age of making molecules, but in the meantime, the best way to determine a reaction outcome is to find a robust procedure from the total synthesis literature and set it up in the laboratory.

Baran has highlighted that total synthesis papers are widely read and rank among the most read papers each year in the Journal of the American Chemical Society (JACS).[6] With an audience comes the potential for impact and education. While the reactions used in medicinal chemistry have remained relatively stagnant[14] with only a few reactions breaking into the toolbox in recent years, natural product synthesis has incorporated a wide variety of transformational methodologies (Figure 1B). Over the course of my chemistry career, the new reaction classes that have interested me most have been transition metal hydrogen atom transfer (TM-HAT)[15], proton coupled electron transfer (PCET),[16] and visible-light palladium catalysis,[17] which all caught my eye because they changed fundamental ways I thought about reactivity. These methodologies allow for access to radical intermediates and/or activation of strong bonds under mild conditions all wrapped in interesting new reaction mechanisms that were elucidated right before my eyes in real time—much like history in the making. It is no coincidence that all three of these reactions will appear in one or more places in the following chapters; the reactions I found most interesting were at the forefront of my mind when tackling problems or designing a synthesis. In the same way, chemists who are struggling with synthesis problems are inspired by the total synthesis literature that they consume.

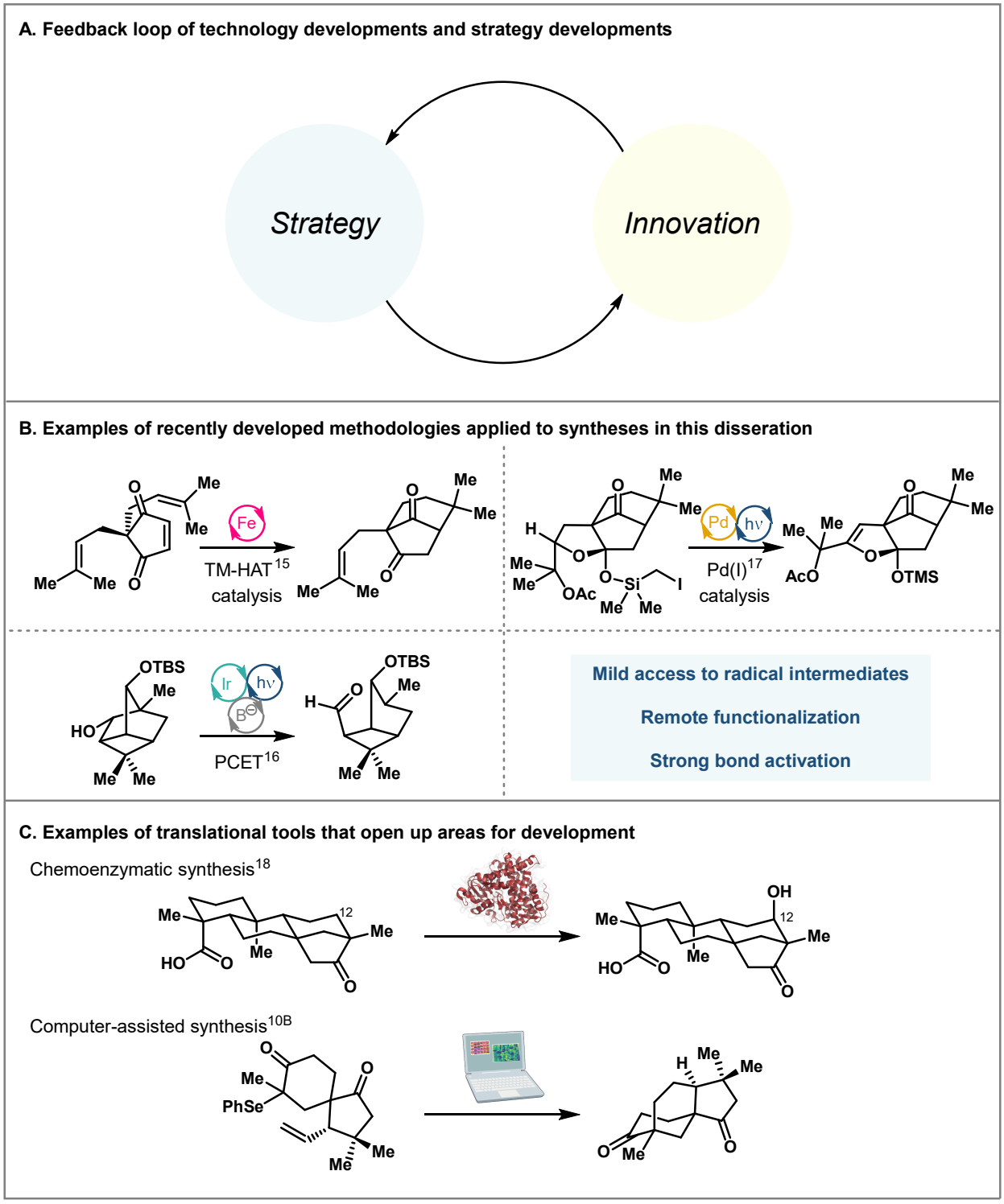

Figure 1.1 A. Dynamic of discovery in synthesis **B.** Select emerging methodologies featured in this dissertation **C.** Select syntheses from Renata and coworkers and Newhouse and coworkers that incorporate non-traditional chemistry tools

Methodologies are also designed and developed to tackle specific problems in synthesis. In this way, the complexity of natural products gives a clear understanding of the roadblocks on the way to control. An excellent illustration of this is in the work of Renata and coworkers (see Chapter 5 for more details) on the application of biocatalysis for selective C–H oxidation in several total syntheses.[18] Biocatalytic C–H oxidation methods hold the promise of evolvable site selectivity which would unlock tremendous possibilities for synthesis planning. Toward this end, they have repeatedly demonstrated their ability to control selectivity in terpene scaffolds and leverage that oxidation in order to achieve highly efficient syntheses. These syntheses would be impossible without the methodology development, but the methodology is given meaning and direction by application. Thus, we can see a clear feedback loop in the science of synthesis (Figure 1A). Methodological innovations unlock new strategies for total synthesis, while at the same time the complex problems unearthed in the process of synthesis inspire new solutions that lead to methodological innovations. It is impossible to know what the fields of C–H functionalization,[19] C–C bond cleavage,[20] and many others would look like in the absence of total synthesis, but, at the very least, they are richer and better explored for it.

With emerging methodologies and technologies, it is inevitable that synthesis will change in the coming years. Our group has successfully implemented and showcased C–H oxidation and C–C cleavage strategies. In particular, chiral pool remodeling[21] and break-it-to-make-it strategies have found great success in recent years. In my opinion, the next dimension of total synthesis will incorporate translational tools, both overtly and routinely. The Renata group, as mentioned above, is ahead of the curve on this, regularly incorporating biocatalysis into their syntheses. The major roadblocks for these concepts are, of course, paucity of resources and expertise. However, those same barriers mean that those areas are rich for exploration. For example, a prevailing attitude in our laboratory was that photoredox reactions are unreliable. However, the use of standardized photoreactors, dozens of Kessil lamps, and acquisition of a library of catalysts have completely changed the chemistry that we can do—the cephanolide synthesis[22] is a great example of this. Computer-assisted synthesis, chemoenzymatic synthesis, further application of electrochemical synthesis,[23] photoredox catalysis,[24] perhaps mechanochemistry,[25] supramolecular catalysis,[26] and so on all hold real promise for exploration in coming years (Figure 1C).

The inherent barriers associated with new methods can even keep us from routine use of other useful catalysts: chiral phosphoric acids, organophotocatalysts, peptide catalysts, modern dinuclear metal complexes, salen complexes, and the like, as their preparation are a time and resource sink. Further commodification of these reagents can help to break down the barriers, and so can collaboration (as our group is still benefiting from several generous donations). Advancements in computer-assisted retrosynthesis planning,[27] automation,[28] and high-throughput experimentation,[29] might reduce the strain on chemists—allowing one's effort to go a little further in terms of results. However, these advances have a way to go before their successful implementation, and even then, there will be concerns about their equitable distribution. Development of infrastructure for production of catalysts and equitable access to

these technologies will be crucial for the advancement of the field. It is very possible that there is a trove of extremely useful chemistry lying in wait that is kept at bay by painful catalyst synthesis. Part of the next era of synthesis will involve breaking down these barriers and studying how each of these tools can move us toward the endgame of organic chemistry.

In my opinion, an enduring legacy of total synthesis will always be its value as a training field. It has long been said[30] that the breadth of chemistry that a chemist is exposed to in making a natural product, the nature of the problem-solving that they engage in, and the repeated failures they experience along the way all contribute to a fantastic education in synthetic organic chemistry. At its core, natural product synthesis requires us to plant the flag—to point boldly at a target and say I will do everything I can to make exactly that molecule. I often compare it to going to the moon. The purpose is not necessarily to collect moonrocks, it is to build the rocket ship—to engineer and discover and create the technology that will take us there. Over the course of the next six chapters of this dissertation, I will discuss my journey to the moon—I never quite got to leave my footprint, but I did learn quite a bit about making engines along the way.

1.2 References

(1) Wöhler, F. Ueber Künstliche Bildung Des Harnstoffs. *Annalen der Physik* **1828**, *88*, 253–256.

(2) (a) Molinski, T. F. All Natural: The Renaissance of Natural Products Chemistry. *Org. Lett.* **2014**, *16*, 3849–3855. (b) Mulzer, J. Trying to Rationalize Total Synthesis. *Nat. Prod. Rep.* **2014**, *31*, 595–603. (c) Terpenoid- and Shikimate-Derived Natural Product Total Synthesis: A Personal Analysis and Commentary on the Importance of the Papers That Appear in This Virtual Issue. *Org. Lett.* **2013**, *15*, 3181–3198. (d) Nicolaou, K. C. Perspectives in Total Synthesis: A Personal Account. Tetrahedron 2003, 59, 6683–6738. (e) Denmark, S. E. The Interplay of Invention, Discovery, Development, and Application in Organic Synthetic Methodology: A Case Study. J. Org. Chem. 2009, 74, 2915–2927. (f) Armaly, A. M.; DePorre, Y. C.; Groso, E. J.; Riehl, P. S.; Schindler, C. S. Discovery of Novel Synthetic Methodologies and Reagents during Natural Product Synthesis in the Post-Palytoxin Era. *Chem. Rev*. **2015**, *115*, 9232–9276.

(3) (ac) Ball, P. Chemistry: Why Synthesize? *Nature* **2015**, *528*, 327–329. (b) Gaich, T.; Baran, P. S. Aiming for the Ideal Synthesis. *J. Org. Chem.* **2010**, *75*, 4657–4673. (c) Heathcock, C. H. As We Head into the 21st Century, Is There Still Value in Total Synthesis of Natural Products as a Research Endeavor? In *Chemical Synthesis: Gnosis to Prognosis*; Chatgilialoglu, C., Snieckus, V., Eds.; NATO ASI Series; Springer Netherlands: Dordrecht, 1996; pp 223–243. (d) Seebach, D. Organic Synthesis—Where now? *Angew. Chem. Int. Ed.* **1990**, *29*, 1320–1367. (e) Whitesides, G. M. Complex Organic Synthesis: Structure, Properties, and/or Function? *Isr. J. Chem.* **2018**, *58*, 142–150. (f) Trauner, D. The Chemist and the Architect. *Angew. Chem. Int. Ed.* **2018**, *57*, 4177–4191. (g) Wender, P. A.; Miller, B. L. Synthesis at the Molecular Frontier. *Nature* **2009**, *460*, 197–201. (h) Nicolaou, K. C.; Vourloumis, D.; Winssinger, N.; Baran, P. S. The Art and Science of Total Synthesis at the Dawn of the Twenty-First Century. *Angew. Chem. Int. Ed.* **2000**, *39*, 44–122.

(4) (a) Keasling, J. D.; Mendoza, A.; Baran, P. S. A Constructive Debate. *Nature* **2012**, *492*, 188–189. (b) Lowe, D. *The End of Synthesis*. https://www.science.org/content/blog-post/end-synthesis (accessed 2022-11-29).

(5) (a) for a recent example Mitcheltree, M. J.; Pisipati, A.; Syroegin, E. A.; Silvestre, K. J.; Klepacki, D.; Mason, J. D.; Terwilliger, D. W.; Testolin, G.; Pote, A. R.; Wu, K. J. Y.; Ladley, R. P.; Chatman, K.; Mankin, A. S.; Polikanov, Y. S.; Myers, A. G. A Synthetic Antibiotic Class Overcoming Bacterial Multidrug Resistance. *Nature* **2021**, *599*, 507–512. (b) Roush, W. R. Total Synthesis of Biologically Active Natural Products. *J. Am. Chem. Soc.* **2008**, *130*, 6654–6656.

(6) Baran, P. S. Natural Product Total Synthesis: As Exciting as Ever and Here To Stay. *J. Am. Chem. Soc.* **2018**, *140*, 4751–4755.

(7) Woodward, R. B.; Cava, M. P.; Ollis, W. D.; Hunger, A.; Daeniker, H. U.; Schenker, K. The Total Synthesis of Strychnine. *Tetrahedron* **1963**, *19*, 247–288.

(8) Jurczyk, J.; Woo, J.; Kim, S. F.; Dherange, B. D.; Sarpong, R.; Levin, M. D. Single-Atom Logic for Heterocycle Editing. *Nat. Synth* **2022**, *1*, 352–364.

(9) (a) Elkin, M.; R. Newhouse, T. Computational Chemistry Strategies in Natural Product Synthesis. *Chem. Soc. Rev.* **2018**, *47*, 7830–7844; (b) Eun, J.; Newhouse, T. R. Computational Decoding. *Nat. Rev. Chem.* **2022**, *6*, 168–169; (c) Schuppe, A. W.; Liu, Y.; Newhouse, T. R. An Invocation for Computational Evaluation of Isomerization Transforms: Cationic Skeletal Reorganizations as a Case Study. *Nat. Prod. Rep.* **2021**, *38*, 510–527. (d) Xu, G.; Elkin, M.; Tantillo, D. J.; Newhouse, T. R.; Maimone, T. J. Traversing Biosynthetic Carbocation Landscapes in the Total Synthesis of Andrastin and Terretonin Meroterpenes. *Angew. Chem. Int. Ed* **2017**, *56*, 12498–12502.

(10) (a) Xu, G.; Elkin, M.; Tantillo, D. J.; Newhouse, T. R.; Maimone, T. J. Traversing Biosynthetic Carbocation Landscapes in the Total Synthesis of Andrastin and Terretonin Meroterpenes. *Angew. Chem. Int. Ed*. *56*, 12498–12502. (b) Zhang, P.; Eun, J.; Elkin, M.; Zhao, Y.; Cantrell, R. L.; Newhouse, T. R. A Neural Network Model Informs Total Synthesis of Clovane Sesquiterpenoids. *ChemRxiv* **2021**, DOI: 10.26434/chemrxiv-2021- 41d5z.

(11) Williams, W. L.; Zeng, L.; Gensch, T.; Sigman, M. S.; Doyle, A. G.; Anslyn, E. V. The Evolution of Data-Driven Modeling in Organic Chemistry. *ACS Cent. Sci.* **2021**, *7*, 1622–1637.

(12) (a) Kearnes, S. M.; Maser, M. R.; Wleklinski, M.; Kast, A.; Doyle, A. G.; Dreher, S. D.; Hawkins, J. M.; Jensen, K. F.; Coley, C. W. The Open Reaction Database. *J. Am. Chem. Soc.* **2021**, *143*, 18820–18826. (b) Żurański, A. M.; Martinez Alvarado, J. I.; Shields, B. J.; Doyle, A. G. Predicting Reaction Yields via Supervised Learning. *Acc. Chem. Res.* **2021**, *54*, 1856–1865.

(13) Green, S. A.; Crossley, S. W. M.; Matos, J. L. M.; Vásquez-Céspedes, S.; Shevick, S. L.; Shenvi, R. A. The High Chemofidelity of Metal-Catalyzed Hydrogen Atom Transfer. *Acc. Chem. Res.* **2018**, *51*, 2628–2640.

(14) Brown, D. G.; Boström, J. Analysis of Past and Present Synthetic Methodologies on Medicinal Chemistry: Where Have All the New Reactions Gone? *J. Med. Chem.* **2016**, *59*, 4443–4458.

(15) (a) Crossley, S. W. M.; Obradors, C.; Martinez, R. M.; Shenvi, R. A. Mn-, Fe-, and Co-Catalyzed Radical Hydrofunctionalizations of Olefins. *Chem. Rev.* **2016**, *116*, 8912–9000. (b) Shevick, S. L.; Wilson, C. V.; Kotesova, S.; Kim, D.; Holland, P. L.; Shenvi, R. A. Catalytic Hydrogen Atom Transfer to Alkenes: A Roadmap for Metal Hydrides and Radicals. *Chem. Sci.* **2020**, *11*, 12401–12422.

(16) (a) Gentry, E. C.; Knowles, R. R. Synthetic Applications of Proton-Coupled Electron Transfer. *Acc. Chem. Res.* **2016**, *49*, 1546–1556. (b) Miller, D. C.; Tarantino, K. T.; Knowles, R. R. Proton-Coupled Electron Transfer in Organic Synthesis: Fundamentals, Applications, and Opportunities. *Top. Curr. Chem.* **2016**, *374*, 30.

(17) Chuentragool, P.; Kurandina, D.; Gevorgyan, V. Catalysis with Palladium Complexes Photoexcited by Visible Light. *Angew. Chem. Int. Ed.* **2019**, *58*, 11586–11598.

(18) Stout, C. N.; Renata, H. Reinvigorating the Chiral Pool: Chemoenzymatic Approaches to Complex Peptides and Terpenoids. *Acc. Chem. Res.* **2021**, *54*, 1143–1156.

(19) Abrams, D. J.; Provencher, P. A.; Sorensen, E. J. Recent Applications of C–H Functionalization in Complex Natural Product Synthesis. *Chem. Soc. Rev.* **2018**, *47*, 8925–8967.

(20) Wang, B.; Perea, M. A.; Sarpong, R. Transition Metal-Mediated C−C Single Bond Cleavage: Making the Cut in Total Synthesis. *Angew. Chem. Int. Ed.* **2020**, *59*, 18898–18919.

(21) Lusi, R. F.; Perea, M. A.; Sarpong, R. C–C Bond Cleavage of α-Pinene Derivatives Prepared from Carvone as a General Strategy for Complex Molecule Synthesis. *Acc. Chem. Res.* **2022**, *55*, 746–758.

(22) Sennari, G.; Gardner, K. E.; Wiesler, S.; Haider, M.; Eggert, A.; Sarpong, R. Unified Total Syntheses of Benzenoid Cephalotane-Type Norditerpenoids: Cephanolides and Ceforalides. *J. Am. Chem. Soc.* **2022**, *144*, 19173–19185.

(23) A) Kingston, C.; Palkowitz, M. D.; Takahira, Y.; Vantourout, J. C.; Peters, B. K.; Kawamata, Y.; Baran, P. S. A Survival Guide for the “Electro-Curious.” *Acc. Chem. Res.* **2020**, *53*, 72–83. (b) Yan, M.; Kawamata, Y.; Baran, P. S. Synthetic Organic Electrochemical Methods Since 2000: On the Verge of a Renaissance. *Chem. Rev.* **2017**, *117*, 13230–13319.

(24) Pitre, S. P.; Overman, L. E. Strategic Use of Visible-Light Photoredox Catalysis in Natural Product Synthesis. *Chem. Rev.* **2022**, *122*, 1717–1751.

(25) Do, J.-L.; Friščić, T. Mechanochemistry: A Force of Synthesis. *ACS Cent. Sci.* **2017**, *3*, 13–19.

(26) Morimoto, M.; Bierschenk, S. M.; Xia, K. T.; Bergman, R. G.; Raymond, K. N.; Toste, F. D. Advances in Supramolecular Host-Mediated Reactivity. *Nat. Catal.* **2020**, *3*, 969–984.

(27) (a) Coley, C. W.; Rogers, L.; Green, W. H.; Jensen, K. F. Computer-Assisted Retrosynthesis Based on Molecular Similarity. *ACS Cent. Sci.* **2017**, *3*, 1237–1245. (b) Hardy, M. A.; Nan, B.; Wiest, O.; Sarpong, R. Strategic Elements in Computer-Assisted Retrosynthesis: A Case Study of the Pupukeanane Natural Products. *Tetrahedron* **2022**, *104*, 132584. (c) Mikulak-Klucznik, B.; Gołębiowska, P.; Bayly, A. A.; Popik, O.; Klucznik, T.; Szymkuć, S.; Gajewska, E. P.; Dittwald, P.; Staszewska-Krajewska, O.; Beker, W.; Badowski, T.; Scheidt, K. A.; Molga, K.; Mlynarski, J.; Mrksich, M.; Grzybowski, B. A. Computational Planning of the Synthesis of Complex Natural Products. *Nature* **2020**, *588*, 83–88. (d) Shen, Y.; Borowski, J. E.; Hardy, M. A.; Sarpong, R.; Doyle, A. G.; Cernak, T. Automation and Computer-Assisted Planning for Chemical Synthesis. *Nat. Rev. Methods Primers* **2021**, *1*, 1–23.

(28) Trobe, M.; Burke, M. D. The Molecular Industrial Revolution: Automated Synthesis of Small Molecules. *Angew. Chem. Int. Ed.* **2018**, *57*, 4192–4214.

(29) For a recent example of successful use of HTE Prieto Kullmer, C. N.; Kautzky, J. A.; Krska, S. W.; Nowak, T.; Dreher, S. D.; MacMillan, D. W. C. Accelerating Reaction Generality and Mechanistic Insight through Additive Mapping. *Science* **2022**, *376*, 532–539.

(30) See discussion in section 3 of ref. 3C

Chapter 2
Total Synthesis of Xiamycin Sesquiterpenoids

2.1 Introduction to xiamycin sesquiterpenoids and synthesis plan

The 'xiamycin-type' secondary metabolites (Figure 2.1) were first isolated from a range of *Streptomyces* species in 2010. These molecules represent the first examples of indolosesquiterpenoids from bacterial sources, and new members continue to be discovered to this day.[1] The emerging biological activity of these indolosesquiterpenoids has sparked interest in employing them as a starting point for the development of pharmaceuticals and agrochemicals. For example, xiamycin A (**2-1**) displays antibiotic and anti-HIV activity,[2a] whereas its C-16 epimer, oridamycin A (**2-2**), exhibits modest activity against the water mold *Saprolegnia parasitica*.[1b] On the basis of this latter bioactivity, we have become especially interested in profiling the agrochemical potential of the xiamycins as fungicides against a broad range of fungal pathogens that significantly impact crop yields. Notably, we sought to identify new chemotypes active against wheat leaf blotch (*Zymoseptoria tritici*) which has been known to cause up to 50% crop yield loss in the European Union (EU).[3a] While there are known fungicides to combat this fungus, newer compounds that possess novel modes of action are critical to addressing the resistance shifts that continue to emerge for many damage-causing fungi.[3b]

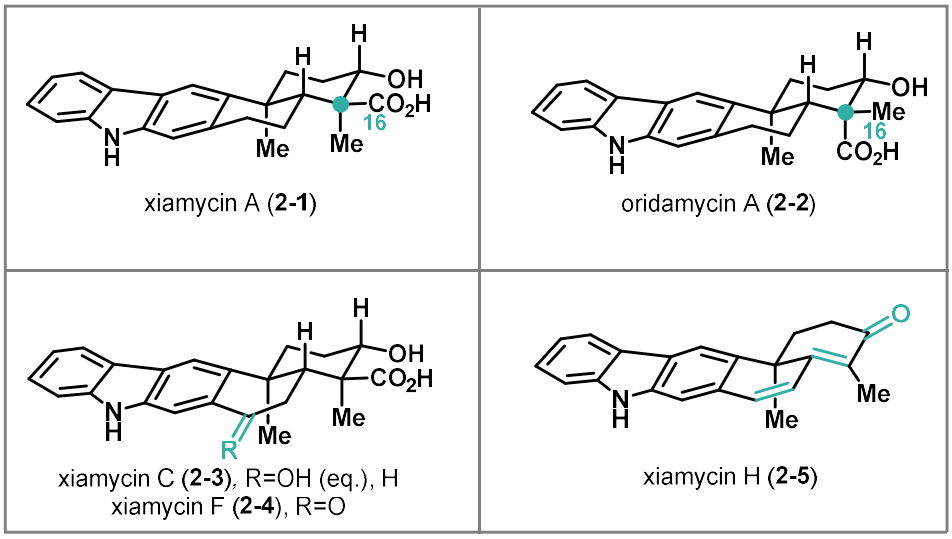

Figure 2.1. Selected members of the xiamycin and oridamycin families

Xiamycin A and oridamycin A have drawn significant attention from synthetic chemists as reflected in the number of total syntheses of these molecules completed over the last five years (Scheme 2.1a).[2] Structurally, they are composed of a challenging pentacyclic framework,

including a carbazole nucleus fused to a *trans*-decalin ring system that bears four contiguous stereocenters.

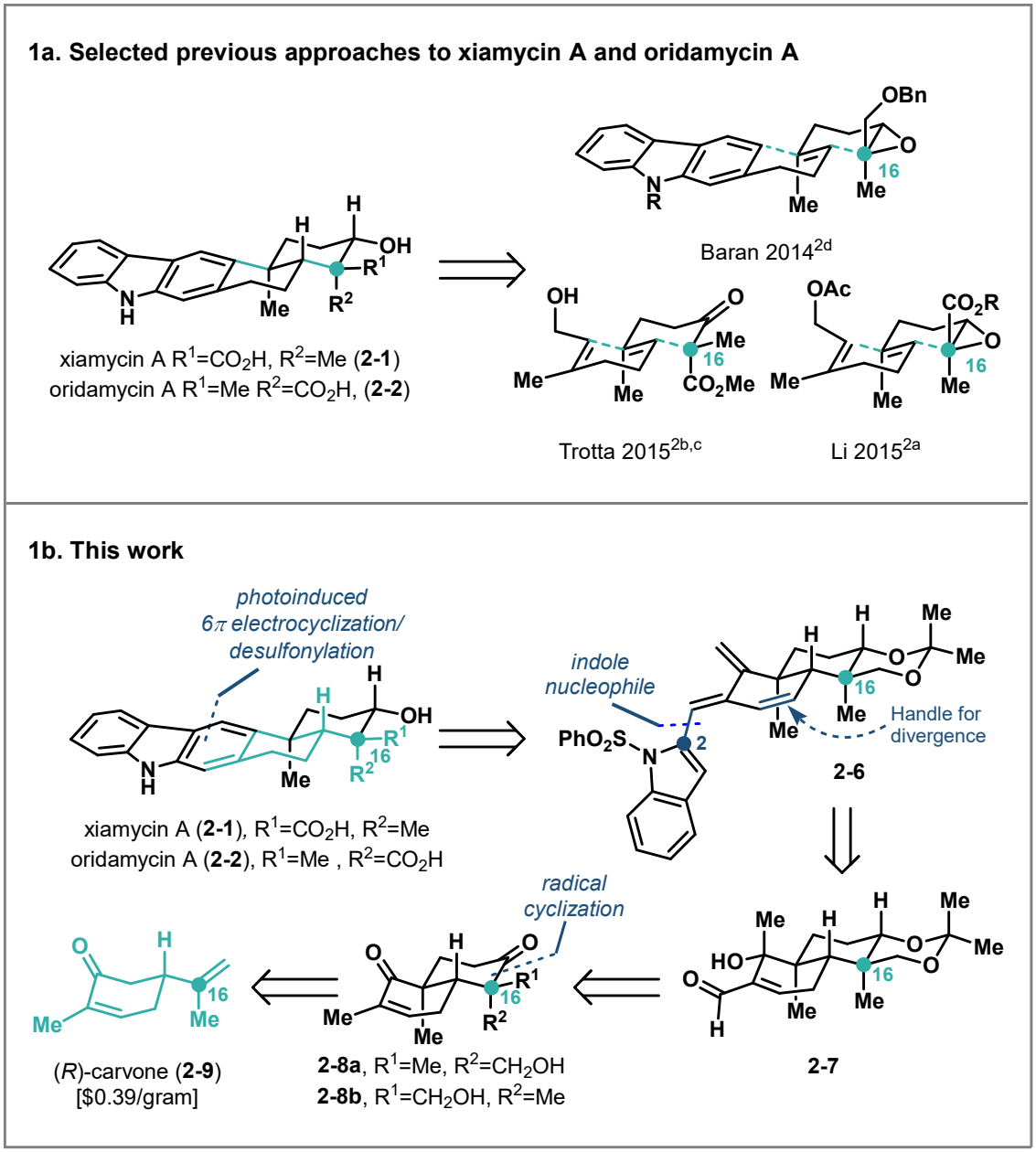

Scheme 2.1 A. Summary of selected previous approaches**. B.** Xiamycin family retrosynthesis from carvone

Two previous syntheses of these natural products by Li and Trotta employ a benzannulation strategy to forge the carbazole moiety. Notably, Baran, Li, and Trotta all utilize polycyclizations to form the *trans*-decalin system.[2] Our group has had a standing interest in divergent[4] syntheses of terpenoid natural products utilizing carvone as a starting material.[5]

Carvone is of particular interest to us because of its ready availability in either enantiomeric form,[6] and its highly modifiable cyclic structure, which allows for rapid elaboration.[7] The syntheses that we report herein are complementary to previous approaches to the xiamycin-type indolosesquiterpenoids. Specifically, we begin from a cyclic 'chiral pool' compound (carvone), which obviates the need for a polycyclization to build the framework of these molecules, thus presenting a unique opportunity for divergence that has culminated in the synthesis of additional congeners of the xiamycin-type indolo-terpenoids than had been previously achieved. In our initial synthesis considerations, we envisioned an expansion of our reported[5m] 'benzannulation of carvone' strategy whereby the α-methyl group of carvone would be exploited in a C–C bond and concomitant six-membered ring formation. Here, we report the realization of this strategy in the total syntheses of xiamycins A, C, F, H (**2-1, 2-3, 2-4, 2-5**) and oridamycin A (**2-2**). As part of an ongoing program to identify novel natural-product derived small molecules relevant to crop protection, we also describe the first systematic investigation of their anti-fungal activity.

Retrosynthetically (Scheme 2-1b), we envisioned **2-1** and **2-2** arising from a late-stage carbazole-forming benzannulation sequence. However, unlike in some of the previous syntheses of these indolosesquiterpenoids, which employed a thermally induced benzannulation, our synthetic plan was to effect a photoinduced olefin isomerization/6π-electrocyclization sequence of triene **2-6**.[8] Triene **2-6** would in turn emerge from the addition of an indole nucleophile to α,β-unsaturated aldehyde **2-7**. Intermediate **2-7** was traced back to known[9] *trans*-decalin C-16 epimers **2-8a** and **2-8b** from which both configurations of the C-16 stereocenter could be accessed, leading to the synthesis of the xiamycin and oridamycin natural product families. Compounds **2-8a** and **2-8b** are accessible through a known four-step sequence from inexpensive and commercially available (*R*)-carvone (**2-9**).

2.2 Forward synthesis

Our synthesis studies commenced with the construction of the key *trans*-decalin system (Scheme 2). Following the precedent of Omura and Nagamitsu,[9] keto-alcohols **2-8a** and **2-8b** were prepared in four steps from (*R*)-carvone (**2-9**) in multigram quantities. Evans reduction[10] of keto-alcohol **2-8a** using tetramethylammonium triacetoxyborohydride ($Me_4NBH(OAc)_3$) gave the desired equatorial alcohol **2-10** as a single diastereomer, which was unambiguously confirmed by X-ray crystallographic analysis.[11] Following acetonide formation, addition of MeLi to the α,β-unsaturated ketone group yielded the corresponding tertiary alcohol as a single isomer. Subsequent allylic oxidation using SeO_2 formed aldehyde **2-7**, which was coupled with 2-lithiated *N*-(phenylsulfonyl)indole[12] reagent **2-11** to produce an inconsequential mixture of diastereomeric alcohols in almost quantitative yield. The elimination of both hydroxy groups proved challenging. Under several conditions (e.g., using the Burgess reagent, MsCl/DIPEA, or $SOCl_2$/py), only elimination of the secondary hydroxy group was observed. Fortunately, Martin's sulfurane cleanly effected double dehydration at room temperature affording triene **6** in gram quantities.

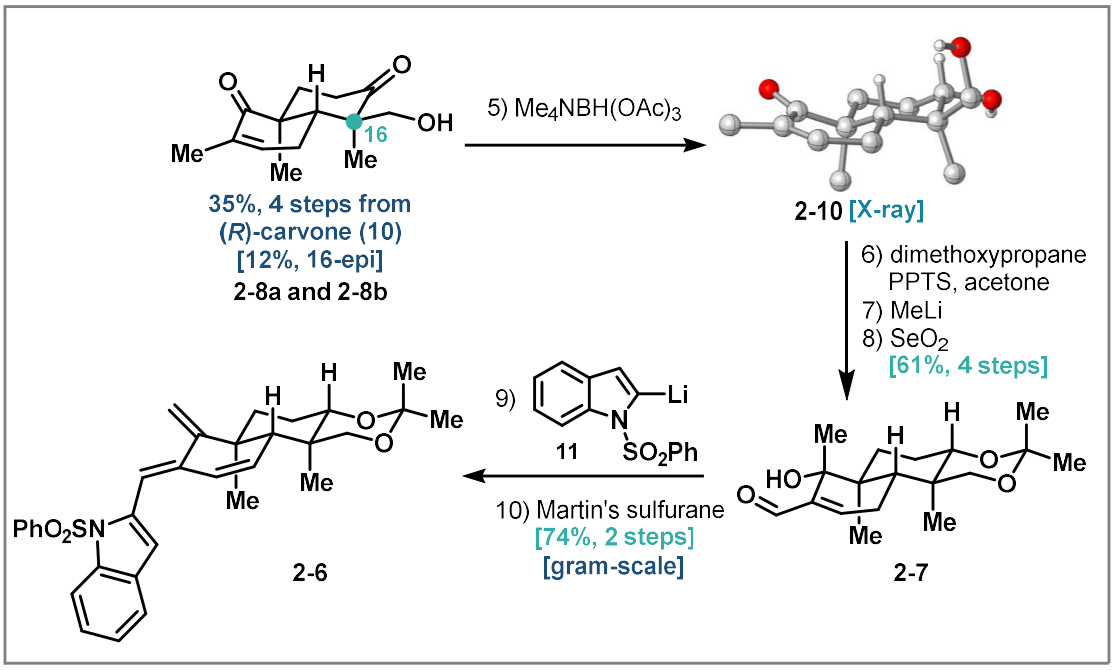

Scheme 2.2. Synthesis of the 6π-electrocyclization precursor **2-6**

Having established an efficient route to precursor **2-6**, we began to explore our proposed benzannulation sequence to forge the 2,3-fused carbazole.[13] Due to the geometric constraint imposed by the trisubstituted (*E*)-double bond in **2-6**, a thermal 6π-electrocyclization/aromatization sequence under aerobic conditions, as demonstrated in the Li and Trotta syntheses of related molecules, was not successful. This prompted us to attempt a photochemical benzannulation[14,15] wherein *E*/*Z* isomerization of the double bond could be effected (Table 2-1). To our surprise, irradiation of **2-6** with UVB light (310 nm) in degassed benzene led to the direct isolation of desulfonylated carbazole **2-12** in 28% yield as the only detectable product (entry 1).[16] After extensive experimentation, we found that irradiation with UVA light (350 nm) in aq. EtOH increased the yield of **2-12** to 44% (entry 2). The solubility of the starting material, as well as the yield, were further increased by adding THF to the reaction medium (entry 3). The use of other polar protic solvents (MeOH, *i*PrOH, HFIP) proved inferior. Polar aprotic solvents such as MeCN led only to isolation of trace amounts of **2-12** (entry 4). The addition of water was found to be beneficial in this case (entry 5) whereas the addition of radical scavengers (1,4-cyclohexadiene, entry 6) to possibly capture a potentially formed sulfonyl radical and prevent polymerization did not improve the yields. Attempts to buffer the resulting sulfinic acid byproduct by the addition of base (Na_2CO_3, entry 7) only led to a decrease in yield. Only scant reports of the photochemical desulfonylation of amines and indoles are known.[17] The existing methods rely on an initial electron transfer from an appropriate donor (e.g., amines, electron-rich aromatics) to the excited state indole moiety. Applying these known conditions, which use DABCO (entry 8) and NEt_3 (entry 9) as amine sources or anisole (entry 10), gave **2-12** in only low (5–33%) yield. While irradiation with blue LED light gave comparable yields to the optimized

conditions (entry 11), longer wavelength visible light did not induce carbazole formation (entry 12).[18]

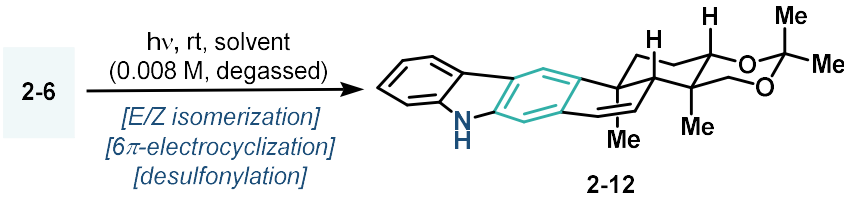

entry	wavelength (nm)[a]	conditions[d]	yield[e]
1	310 / 350	PhH, 1 h	28% / 33%
2	310 / 350	5% aq. EtOH, 1 h	30% / 44%
3	**350**	**10% aq. EtOH/THF, 1 h**	**46%**
4	350	MeCN, 1 h	<5%
5	350	50% aq. MeCN, 0.5 h	23%
6	310	PhH, 1,4-CHD, 0.2 h	30%
7	350	5% aq. EtOH, Na_2CO_3 0.5 h	<5%
8	350	5% aq. MeOH, DABCO, 0.5 h	<5%
9	350	NEt_3, nBu$_3$SnH, MeCN, 0.5 h	<5%
10	350	5% aq. EtOH, anisole, $NaBH_4$, 1.5 h	33%
11	400[b]	5% aq. EtOH, 1.5 h	30%
12	500-800[c]	5% aq. EtOH, 40°C, 1.5 h	no reaction

[a] Luzchem photobox; [b] Kessil blue LED; [c] Sunlite tungsten lamp; [d] Reactions were performed in pyrex glass tubes; 5% aq. EtOH refers to technical grade (95%); [e] Isolated yield.

Table 2.1. Optimization of the key photocyclization/desulfonylation reaction

With access to carbazole **2-12** using our best conditions (entry 3), hydrogenation of the styrenyl double bond and subsequent cleavage of the acetonide yielded diol **2-13** in 60% yield over two steps (Scheme 2-3). Unfortunately, oxidation of the primary hydroxy group to give aldehyde **2-14** (not shown) led to substantial decomposition under standard conditions such as TEMPO/PIDA, presumably due to the free carbazole nitrogen. We therefore opted to install the aldehyde group first. Addition of 2-lithiated *N*-(phenylsulfonyl)indole **2-11** to aldehyde **2-7** gave diol **2-15**, which was subjected to a one-pot double dehydration followed by acetonide cleavage using Martin's sulfurane and 6M HCl, respectively, to give the corresponding triene diol (not shown). Oxidation of the primary alcohol group under TEMPO/PIDA conditions gave a hydroxy-aldehyde which underwent the key photocyclization/desulfonylation to give aldehyde **2-16** in 21% over 3 steps.[19] Finally, Pinnick oxidation[20] followed by hydrogenation with Pd/C reduced the styrenyl double bond to complete the synthesis of xiamycin A (**2-1**) in a total of 14 steps from (*R*)-

carvone (**2-9**). The spectroscopic data obtained for **2-1** were identical to those reported in literature.[4a]

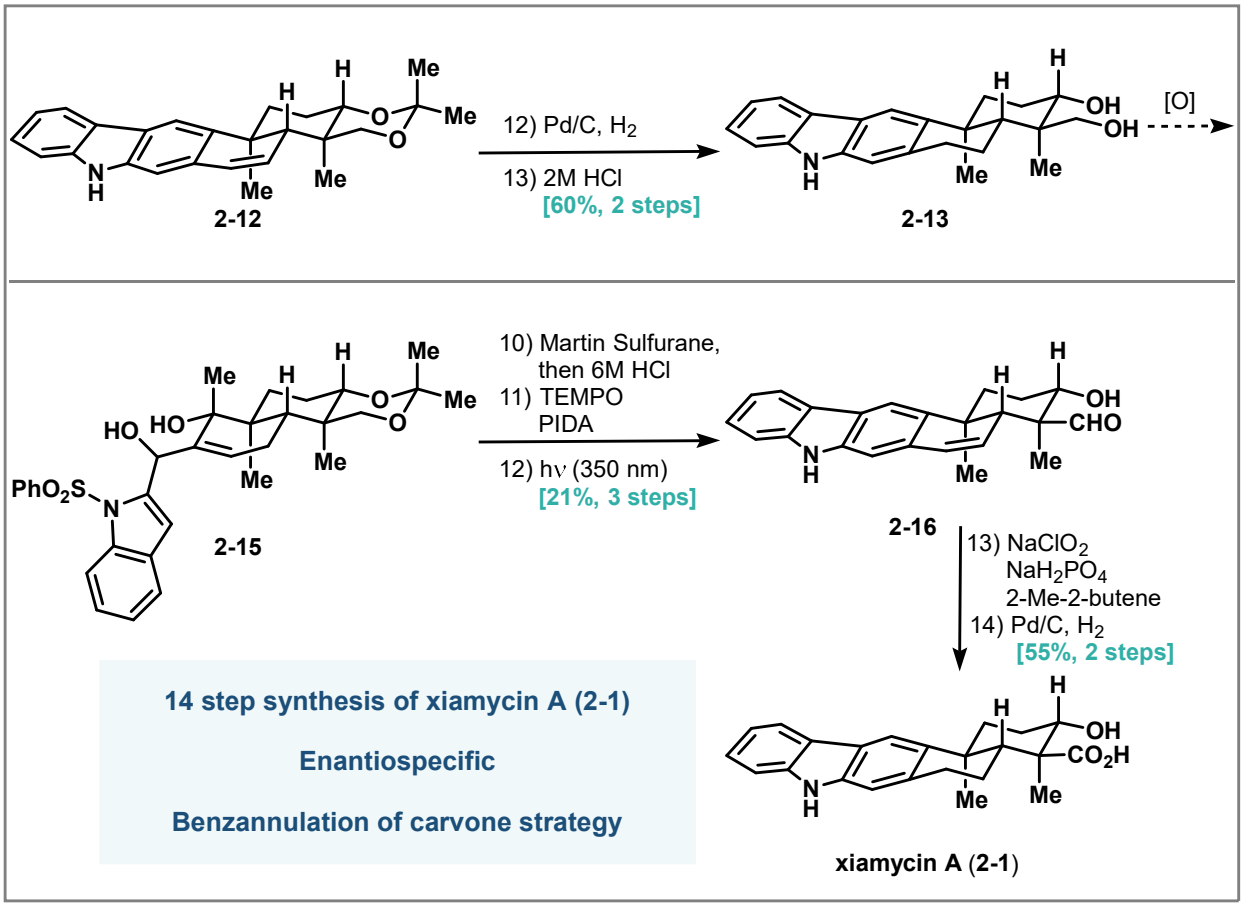

Scheme 2.3. Completion of total synthesis of xiamycin A (**2-1**)

We have also utilized the minor keto-alcohol diastereomer **2-8b** in an analogous sequence to complete a total synthesis of oridamycin A (**2-2**, Scheme 2-4). Thus, subjecting minor diastereomer **2-8b** to Narasaka–Prasad reduction[21] conditions yielded boronate ester **2-17,** which was cleaved by methanolysis on acidic silica to afford desired *syn*-diol **2-18** in 74% yield. The total synthesis of oridamycin A (**2-2**) was successfully completed by following the established route described above (i.e., steps 6–14; see the experimental section for details).

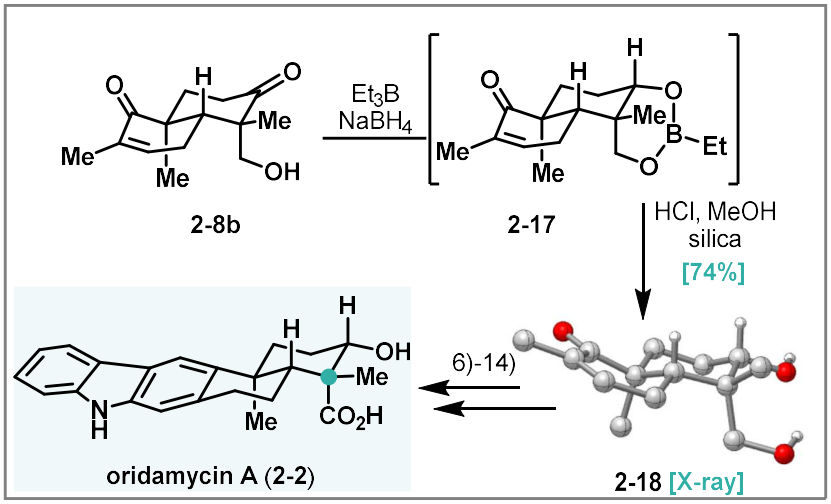

Scheme 2.4. Total synthesis of oridamycin A (**2-2**)

In line with our initial plan, access to **2-16** has provided a common late-stage intermediate that we have applied to the synthesis of several other xiamycin congeners (Scheme 5). Specifically, we envisioned that the styrenyl double bond of **2-16** would serve as a handle for functionalization. Indeed, Mukaiyama hydration of **2-16** followed by Pinnick oxidation gave xiamycin C (**2-3**) and 19-*epi*-xiamycin C as a separable mixture of diastereomers, as well as xiamycin F (**2-4**). This sequence represents the first total syntheses of these natural products as well as the associated C-19 epimer of **2-3**.

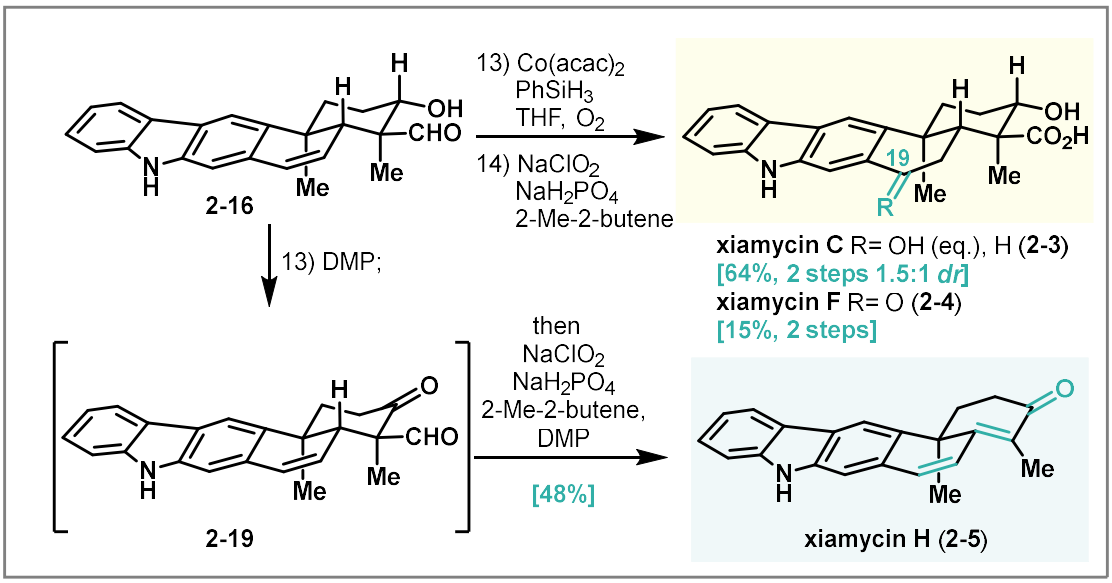

Scheme 2.5. Completion of the syntheses of xiamycin C (**2-4**), F (**2-4**), and H (**2-5**) from common intermediate **2-16**

As a testament to the versatility of our route, we then sought to prepare the only known xiamycin congener that bears an alkene functional group (i.e., xiamycin H; **2-5**). Oxidation of alcohol aldehyde **2-16** with Dess–Martin periodinane first yielded keto-aldehyde **2-19**, which, in one-pot, underwent oxidative decarboxylation under Pinnick oxidation conditions to form xiamycin H (**2-5**) in 48% yield.

2.3 Evaluation of xiamycin family antifeedant activity

Our syntheses of the xiamycins have also provided access to a number of synthetic intermediates which have been screened for bioactivity. Specifically, the *in vitro* fungitoxicity of these small molecules against three agriculturally relevant pathogens: wheat leaf blotch, rice blast (*Pyricularia oryza*) and corn smut (*Ustilago maydis*) was evaluated. At a concentration of 10 ppm, it was found that none of the materials demonstrated significant activity against wheat leaf blotch. Of the natural products tested, only xiamycin H (**2-5**) demonstrated partial (60%) growth inhibition of rice blast. Compound **2-7** demonstrated good activity toward the control of corn smut (100% growth inhibition) over other pathogens, whereas compound **S2-23** (from hydrogenation of **2-12**) demonstrated some selectivity toward the control of rice blast (70% growth inhibition). These initial screening data provide a promising foundation for additional studies to identify even more potent derivatives of this class of natural products.

2.4 Conclusion and outlook

In summary, we have accomplished the divergent, enantiospecific total synthesis of the indolosesquiterpenoids xiamycin A (**2-1**), xiamycin C (**2-3**), xiamycin F (**2-4**), oridamycin A (**2-2**), as well as xiamycin H (**2-5**) in a maximum of ten steps from known compound **2-9**. A key feature in the formation of the characteristic carbazole moiety is a photoinduced 6π-electrocyclization with concomitant desulfonylation, which represents a rare example of this type of transformation. These syntheses proceed in a total of 13–14 steps from carvone and are highly scalable, providing enough material for a preliminary bioactivity screen. Evaluation of the fungicidal activity of these compounds revealed that xiamycin H and some of the synthetic intermediates display notable inhibition of agriculturally relevant pathogens that could set the stage for the identification of new small molecules for crop protection.

The following chapter of this dissertation will discuss the xiamycin (**2-1**) synthesis as it relates to our broader studies on indole diterpenoid and indolosesquiterpenoid natural products. Our plan was to unify these syntheses through a common 'chiral-pool' approach initiated from (*R*)-carvone (**2-9**). Ultimately, our efforts in this regard were unsuccessful but they whole picture will be presented that resulted in this synthesis.

2.5 Experimental

General Considerations

Unless otherwise noted, all reactions were performed in flame or oven-dried glassware fitted with rubber septa under a positive pressure of nitrogen using standard Schlenk techniques. Air- and moisture-sensitive liquids were transferred via syringe or stainless steel cannula through rubber septa. Solids were added under inert gas or were dissolved in appropriate solvents. Low temperature-reactions were carried out in a Dewar vessel filled with a cooling agent: acetone/dry ice (−78 °C), H_2O/ice (0 °C). Reaction temperatures above 23 °C were conducted in an oil bath or in a heated metal block (reactions conducted in vials). The reactions were magnetically stirred and monitored by NMR spectroscopy or analytical thin-layer chromatography (TLC), using glass plates precoated with silica gel (Silicycle Siliaplates, glass backed, extra hard layer, 60 Å, 250 µm thickness, F254 indicator). TLC plates were visualized by exposure to ultraviolet light (254 nm), were stained by submersion in aqueous potassium permanganate solution (KMnO4), p-anisaldehyde, or ceric ammonium molybdate solution (CAM), and were developed by heating with a heat gun. Flash-column chromatography on silica gel was performed as described by Still et al.,1 employing silica gel (Silicycle silica gel, 40–63 µm particle size). Organic solutions were concentrated under reduced pressure on a temperature-controlled rotary evaporator equipped with a dry ice/isopropanol condenser. The yields refer to chromatographically and spectroscopically (^{1}H and ^{13}C NMR) pure material.

Materials

Unless noted below, commercial reagents were purchased from Sigma Aldrich, Acros Organics, ChemImpex, Oakwood Chemical, Combi-blocks, TCI, and/or Alfa Aesar, and used without additional purification. Solvents were purchased from Fisher Scientific, Acros Organics, Alfa Aesar, and Sigma Aldrich. Tetrahydrofuran (THF), diethyl ether (Et_2O), acetonitrile (CH_3CN), benzene, toluene (PhMe), methanol (MeOH), and triethylamine (Et_3N) were sparged with argon and dried by passing through alumina columns using argon in a Glass Contour solvent purification system. Dichloromethane (CH_2Cl_2, DCM) was freshly distilled over calcium hydride under a N_2 atmosphere prior to each use.

NMR spectroscopy

NMR spectral data were obtained using deuterated solvents, obtained from Cambridge Isotope Laboratories, Inc. ^{1}H NMR and ^{13}C NMR data were recorded on Bruker AVB-400, AVQ-400, AV-500, NEO-500, AV-600 or AV-700 spectrometers operating at 400 MHz, 400 MHz, 500 MHz, 500 MHz, 600 MHz, 700 MHz for proton nuclei (100 MHz, 100 MHz, 125 MHz, 125 MHz, 150 MHz, 175 MHz for carbon nuclei), respectively. Proton chemical shifts are expressed in parts per million

(ppm, δ scale) and are referenced to residual protium in the NMR solvent ($CHCl_3$: δ 7.26). Carbon chemical shifts are expressed in parts per million (δ scale, assigned carbon atom) and are referenced to the carbon resonance of the NMR solvent ($CDCl_3$: δ 77.16). ^1H NMR spectroscopic data are reported as follows: Chemical shift in ppm (multiplicity, coupling constants J (Hz), integration) (e.g. "5.21 (t, 3 J = 7.3 Hz, ^1H)"). The multiplicities are abbreviated with s (singlet), br s (broad singlet), d (doublet), t (triplet), q (quartet), p (pentet), se (sextet), h (heptet), m (multiplet) and app (apparent multiplicity). In case of combined multiplicities, the multiplicity with the larger coupling constant is stated first. Except for multiplets, the chemical shift of all signals, as well for centrosymmetric multiplets, is reported as the center of the resonance range. Data for ^{13}C spectroscopy are reported in terms of chemical shift (δ ppm). Additionally to 1D NMR experiments, 2D NMR techniques such as homonuclear correlation spectroscopy (COSY), heteronuclear single quantum coherence (HSQC), heteronuclear multiple bond coherence (HMBC) and nuclear Overhauser enhancement spectroscopy (NOESY) were used to assist structure elucidation. All raw FID files were processed and the spectra analyzed using the program MestReNOVA 11.0 from Mestrelab Research S. L.

Note: The AVB-400, AVQ-400, AV-500, DRX-500 and AV-600 instruments were partially supported by NIH grants SRR023679A, RR02424A-01, S10RR03353-01 and 1S10RR016634-01, and NSF grants CHE-9633007, CHE-8208992, CHE-0130862, and CHE-8703048. The AV-700 instrument was supported by the Berkeley College of Chemistry NMR facility.

Mass spectrometry

Mass spectral data were obtained from the Mass Spectral Facility at the University of California, Berkeley, on a Finnigan/Thermo LTQ-FT instrument (ESI). Data acquisition and processing were performed using the XcaliburTM software.

IR spectroscopy

IR spectroscopic data were recorded on a Bruker ALPHA FT-IR spectrophotometer using a diamond attenuated total reflectance (ATR) accessory. If required, substances were dissolved in dichloromethane prior to direct application on the ATR unit. Data are represented as follows: frequency of absorption (cm^{-1}), and intensity of absorption (s = strong, m = medium, w = weak, br = broad).

X-ray analysis

Single-crystal X-ray diffraction experiments were performed at the UC Berkeley CHEXRAY crystallographic facility. Measurements of all compounds were performed on a Rigaku XtaLAB P200 rotating anode equipped with a Pilatus 200K hybrid pixel array detector. Data were collected using Cu Kα radiation (λ = 1.54184 Å). Crystals were kept at 100(2) K throughout

collection. Data collection was performed with CrysAlisPro. 2 Data processing was done using CrysAlisPro and included either a multi-scan absorption or faceindexed absorption correction applied using the SCALE3 ABSPACK scaling algorithm within CrysAlisPro. All structures were solved with SHELXT.3 Structures were refined with SHELXL.4 All non-hydrogen atoms were refined anisotropically, and hydrogen atoms were either included at the geometrically calculated positions and refined using a riding model or located as Q peaks in the Fourier difference map.

Note: The instruments are supported by an NIH Shared Instrumentation Grant S10-RR027172.

UV-Vis spectroscopy

UV-Vis spectroscopy was performed on a Varian 5000 UV-Vis-NIR spectrometer using quartz cuvettes with a path length of 1 cm. Data were collected using DCM as a solvent with an absorbance window between 230 and 650 nm.

Synthetic procedures and analytical data

Synthesis of diol 2-10

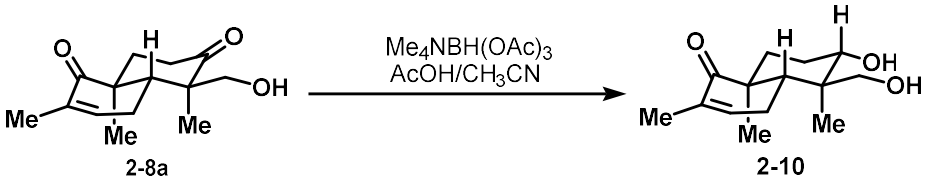

To a solution of $Me_4NHB(OAc)_3$ (10.2 g of >90% pure Acros material, 34.9 mmol, 5.50 equiv) in 22.5 mL of MeCN (0.280 M) was added 22.5 mL of glacial AcOH (0.280 M) under N_2, and the resulting colorless solution was stirred 30 min at room temperature, after which time it was added via cannula to a stirring solution of ketone **2-8a** (1.50 g, 6.35 mmol, 1.00 equiv) dissolved in 22.5 mL MeCN at room temperature. The clear solution was stirred for 3 h at room temperature and then quenched by addition of sat. aq. Rochelle's salt solution. The resulting milky biphasic mixture was diluted with EtOAc and vigorously stirred for 1 h. A solution of sat. aq. $NaHCO_3$ was carefully added while stirring. After the gas evolution ceased, the aq. layer was extracted four times with EtOAc, washed three times with sat. aq. $NaHCO_3$, followed by sat. aq. NaCl solution and dried over $MgSO_4$. This material was used in the next reaction without further purification. An analytical sample was prepared by flash column chromatography (PE:EtOAc = 1:1) to afford diol **2-10** as a white solid. Suitable crystals for X-ray analysis were obtained after crystallization from a Hexane/EtOAc (1:1) solution.

R_f = 0.23 (Hexane:EtOAc = 1:3), UV-active, blue spot (CAM).

^{1}H-NMR (600 MHz, $CDCl_3$): δ = 6.64 (d, *J* = 4.8 Hz, 1H), 3.68–3.58 (m, 2H), 3.39 (d, *J* = 10.6 Hz, 1H), 3.04 (br s, 2H), 2.39–2.29 (m, 1H), 2.18 (d, *J* = 19.1 Hz, 1H), 1.91 (d, *J* = 14.3 Hz, 1H), 1.79 (dd, *J* = 11.5, 4.2 Hz, 1H), 1.75 (d, *J* = 4.0 Hz, 1H), 1.72 (s, 3H), 1.70–1.60 (m, 1H), 1.47 (td, *J* = 14.0, 4.0 Hz, 1H), 1.06 (s, 3H), 0.99 (s, 3H) ppm.

^{13}C–NMR (150 MHz, $CDCl_3$): δ = 205.4, 143.4, 133.2, 75.4, 69.6, 44.4, 42.9, 42.5, 31.4, 26.6, 24.1, 17.9, 16.4, 11.9 ppm.

IR (neat): ν = 3410, 2933, 1657, 1356, 1039, 998, 733, 544 cm^{-1}.

HRMS (ESI, *m/z*): $[M+H]^+$ calcd. for $C_{14}H_{23}O_3$, 239.1640; found 239.1640.

$[\alpha]_D^{22}$ –21.4 (c = 1.00, MeOH); lit.[9a] **$[\alpha]_D^{27}$** -20.3 (c = 1.00, MeOH

Synthesis of acetonide 2-23

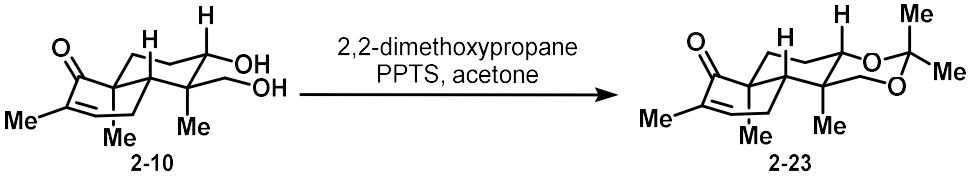

To a solution of crude diol in acetone (80.0 mL, 80.0 mM) was added PPTS (399 mg, 1.58 mmol, 0.250 equiv), followed by 2,2-dimethoxypropane (7.90 mL, 63.5 mmol, 10.0 equiv) at room temperature. After stirring for 14 h, the reaction mixture was quenched by the addition of sat. aq. $NaHCO_3$. The aq. layer was extracted three times with EtOAc, washed with sat. aq. NaCl solution and dried over $MgSO_4$. After removal of the solvent *in vacuo*, this material was used in the next reaction without further purification. An analytical sample was prepared by flash column chromatography (PE:EtOAc = 3:1) to afford acetonide **2-23** as a white solid.

R_f = 0.51 (Hexane:EtOAc = 2:1), UV-active, blue spot (CAM).

^{1}H-NMR (600 MHz, $CDCl_3$): δ = 6.60 (d, *J* = 5.5 Hz, 1H), 3.52–3.47 (m, 3H), 2.34 (ddt, *J* = 18.8, 11.7, 2.3 Hz, 1H), 2.02–1.90 (m, 2H), 1.73 (s, 3H), 1.67–1.55 (m, 4H), 1.41 (s, 6H), 1.19 (s, 3H), 1.07 (s, 3H) ppm.

^{13}C-NMR (150 MHz, $CDCl_3$): δ = 204.7, 142.3, 133.6, 99.3, 76.7, 71.9, 45.0, 44.5, 37.2, 31.9, 29.9, 23.6, 23.5, 19.2, 18.5 16.5, 12.9 ppm.

IR (neat): ν = 2989, 2943, 2864, 1672, 1444, 1392, 1205, 1042, 846 cm^{-1}.

HRMS (ESI, *m*/*z*): $[M+H]^+$ calcd. for $C_{17}H_{27}O_3$, 279.1960; found 279.1954.

M.p. = 79 °C

$[\alpha]_D^{22}$ –39.3 (c = 1.00, MeOH)

Synthesis of tertiary alcohol 2-20

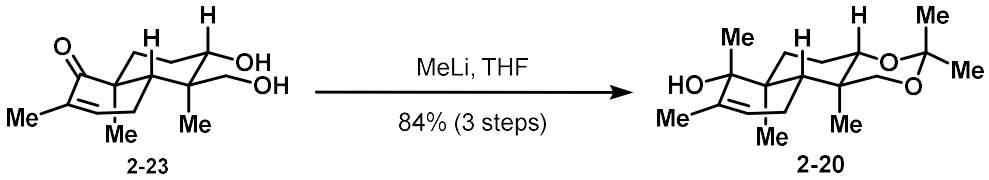

2-23 2-20

MeLi (8.70 mL of a 1.60 M Et_2O solution, 14.0 mmol, 2.20 equiv) was added dropwise to a solution of the crude acetonide **2-23** in THF (63.0 mL, 0.100 M) at –78 °C. After being stirred for 1.5 h at –78 °C, the reaction mixture was quenched by the addition of sat. aq. NH_4Cl. The aq. layer was extracted three times with EtOAc, washed with sat. aq. NaCl solution and dried over $MgSO_4$. After removal of the solvent *in vacuo*, the residue was purified by gradient flash chromatography (Yamazen, eluting with 13-34% EtOAc in hexanes) to afford 1.56 g (84%, over 3 steps) of alcohol **2-20** as a white solid.

R_f = 0.48 (Hexane:EtOAc = 2:1), non UV-active, blue spot (CAM).

^{1}H-NMR (500 MHz, $CDCl_3$): δ = 5.29 (s, 1H), 3.52–3.47 (m, 1H), 3.46 (s, 2H), 2.02–1.90 (m, 1H), 1.70 (s, 3H), 1.69–1.60 (m, 4H), 1.56–1.49 (m, 2H), 1.45 (s, 3H), 1.42 (s, 3H), 1.29 (s, 3H), 1.22 (s, 1H), 1.17 (s, 3H), 1.07 (s, 3H) ppm.

^{13}C-NMR (125 MHz, $CDCl_3$): δ = 138.7, 121.1, 99.2, 77.9, 77.5, 72.7, 40.8, 40.4, 37.1, 30.5, 30.0, 23.8, 23.7, 23.1, 19.4, 18.0, 15.7, 12.4 ppm.

IR (neat): ν = 3499, 2987, 2943, 2897, 1452, 1378, 1284, 1206, 1102, 860 cm^{-1}.

HRMS (EI, *m*/*z*): $[M]^+$ calcd. for $C_{18}H_{30}O_3$, 294.2195; found 294.2192.

M.p. = 182 °C

$[\alpha]_D^{22}$ –27.9 (c = 1.00, MeOH)

Synthesis of aldehyde 2-7

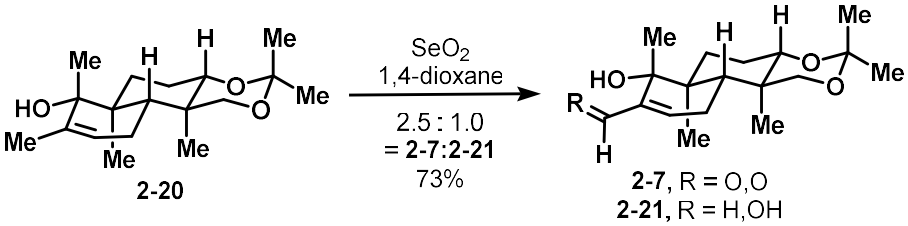

A mixture of alcohol **2-20** (1.69 g, 5.76 mmol, 1.00 equiv) and selenium dioxide (1.60 g, 14.4 mmol, 2.50 equiv) was dissolved in 1,4-dioxane (58.0 mL, 0.100 M) and then placed in an oil bath at 90 °C. After stirring for 2h, the resulting brown mixture was cooled to room temperature and quenched by the addition of distilled water. The aq. phase was extracted three times with EtOAc and the combined organic layers were washed with sat. aq. NaCl solution. The solution was dried over $MgSO_4$ and concentrated *in vacuo*. The crude products were purified by gradient flash chromatography (Yamazen, eluting with 13-34% EtOAc in hexanes) to afford 0.910 g of aldehyde **2-7** as a yellow solid and 0.370 g (73% combined yield, **2-7**:**2-21** = 2.5:1.0) of alcohol **2-21** as a yellow foam.

2-7: R_f = 0.57 (Hexane:EtOAc = 1:1), UV-active, blue spot (CAM).

^{1}H-NMR (500 MHz, $CDCl_3$): δ = 9.35 (s, 1H), 6.67 (br s, 1H), 4.20 (s, 1H), 3.55–3.47 (m, 3H), 2.42–2.32 (m, 1H), 2.15–2.07 (m, 1H), 1.77–1.64 (m, 3H), 1.57–1.50 (m, 2H), 1.46 (s, 3H), 1.43 (s, 6H), 1.21 (s, 3H), 1.05 (s, 3H) ppm.

^{13}C-NMR (125 MHz, $CDCl_3$): δ = 196.3, 151.6, 145.0, 99.3, 77.3, 75.9, 72.5, 40.2, 39.7, 37.0, 30.0, 29.4, 25.4, 25.1, 23.6, 19.3, 15.7, 12.4 ppm.

IR (neat): ν = 3498, 2987, 2942, 1688, 1638, 1378, 1221, 1208, 862 cm^{-1}.

HRMS (ESI, *m*/*z*): $[M–H]^-$ calcd. for $C_{18}H_{27}O_4$, 307.1915; found 307.1915.

$[\alpha]_D^{22}$ –60.1 (c = 1.00, MeOH)

M.p. = 195 °C

2-21:

R_f = 0.19 (Hexane:EtOAc = 1:1), UV-active, blue spot (CAM).

^{1}H-NMR (500 MHz, $CDCl_3$): δ = 5.57 (br s, 1H), 4.37 (d, *J* = 11.6 Hz, 1H), 3.92 (d, *J* = 11.6 Hz, 1H), 3.54–3.41 (m, 3H), 2.23 (br s, 2H), 2.09–1.99 (m, 1H), 1.76 (dt, *J* = 18.4, 4.5 Hz, 1H), 1.70–1.58 (m, 3H), 1.58–1.50 (m, 2H), 1.45 (s, 3H), 1.42 (s, 3H), 1.37 (s, 3H), 1.17 (s, 3H), 1.04 (s, 3H) ppm.

^{13}C-NMR (125 MHz, $CDCl_3$): δ = 141.1, 125.6, 99.2, 78.9, 72.6, 65.2, 40.6, 40.3, 37.1, 30.0, 29.8, 24.9, 23.8, 22.9, 19.3, 15.8, 12.3 ppm.

IR (neat): ν = 3407, 2988, 2943, 2898, 2876, 1378, 1258, 1205, 1100, 1075, 859, 737 cm^{-1}.

HRMS (ESI, *m*/*z*): $[M–H]^-$ calcd. for $C_{18}H_{29}O_4$, 309.2070; found 309.2071.

$[\alpha]_D^{22}$ –8.0 (c = 0.80, MeOH)

Conversion of undesired 2-21 to aldehyde 2-7

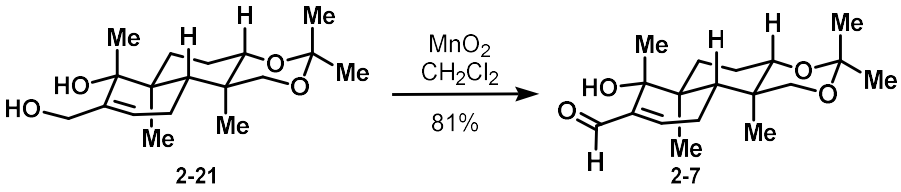

A mixture of alcohol **2-21** (600 mg, 1.95 mmol, 1.00 equiv) and manganese dioxide (2.03 g, 23.3 mmol, 12.0 equiv) in DCM (32.0 mL, 60.0 mM) was stirred for 16 h at room temperature. After filtering through celite (EtOAc eluent), the solution was concentrated *in vacuo* and the crude material was purified by gradient flash chromatography (Yamazen, eluting with 24-45% EtOAc in hexanes) to afford 489 mg (81%) of aldehyde **2-7** as a yellow solid.

Synthesis of adduct 2-15

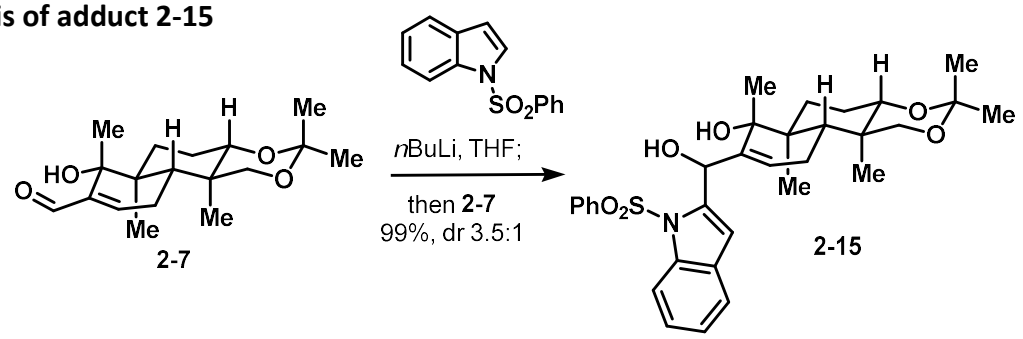

Trace water was removed from 1-(phenylsulfonyl)-1*H*-indole (3.65 g, 14.2 mmol, 3.50 equiv) via azeotropic distillation with benzene. Then, it was dissolved in THF (700 mL) and cooled to –78°C. A solution of *n*BuLi (8.75 ml of a 1.60 M solution in pentane, 14.0 mmol, 3.45 equiv) was added dropwise. The yellow solution was stirred at 0 °C for 1 h. During this time, trace water was removed from aldehyde **2-7** (1.25 g, 4.04 mmol, 1.00 equiv) via azeotropic distillation with benzene. Then it was dissolved in THF (20.0 mL) and added via cannula transfer into the solution containing the 2-lithio-indole over the course of 5 minutes at –78°C. After stirring the resulting solution at –78°C for 1 h, the solution was warmed to 0 °C and stirred additional 1 h before being quenched with sat. aq. NH_4Cl. The aq. layer was extracted three times with EtOAc and the combined organic layers were washed with sat. aq. NaCl, dried over $MgSO_4$, filtered, and concentrated. The residue was purified via gradient flash chromatography (Yamazen, eluting with 46–67% EtOAc in hexanes) to yield a mixture of diastereomers of alcohol **2-15** as a yellow foam (2.27 g, 99% combined yield, dr = 3.5:1) which was used in the next reaction. Analytical samples were prepared via gradient flash chromatography (Yamazen, eluting with 39–59% EtOAc in hexanes).

Major isomer:

R_f = 0.36 (Hexane:EtOAc = 1:1), UV-active, blue spot (CAM).

^{1}H-NMR (500 MHz, $CDCl_3$): δ = 8.11 (d, *J* = 8.5 Hz, 1H), 7.74 (d, *J* = 7.9 Hz, 2H), 7.51–7.47 (m, 2H), 7.40–7.34 (m, 2H), 7.30–7.27 (m, 1H), 7.25–7.20 (m, 1H), 6.91 (s, 1H), 6.16 (s, 1H), 5.05 (br s, 1H), 4.09 (br s, 1H), 3.55–3.49 (m, 1H), 3.48–3.43 (m, 1H), 3.42–3.37 (m, 1H), 2.43 (br s, 1H), 1.94–1.84 (m, 1H), 1.75–1.66 (m, 2H), 1.65–1.62 (m, 2H), 1.61 (s, 3H), 1.59–1.53 (m, 2H), 1.46 (s, 3H), 1.42 (s, 3H), 1.13 (s, 3H), 1.07 (s, 3H) ppm.

^{13}C-NMR (125 MHz, $CDCl_3$): δ = 142.3, 141.9, 138.6, 137.5, 133.8, 129.6, 129.3 (2x), 126.4 (2x), 125.3, 124.7, 124.0, 121.1, 115.0, 112.7, 99.2, 79.8, 77.9, 72.5, 68.1, 40.7, 40.3, 37.0, 30.0, 29.9, 24,7, 23.8, 22.9, 19.4, 15.9, 12.2 ppm.

IR (neat): ν = 3418, 2989, 2944, 1447, 1372, 1173, 1091, 726 cm^{-1}.

HRMS (ESI, *m*/*z*): $[M–H]^-$ calcd. for $C_{32}H_{38}NO_6S$, 564.2425; found 564.2414.

$[\alpha]_D^{22}$ –42.0 (c = 1.00, MeOH)

Minor isomer:

R_f = 0.33 (Hexane:EtOAc = 1:1), UV-active, blue spot (CAM).

^{1}H-NMR (500 MHz, $CDCl_3$): δ = 8.07 (d, *J* = 8.2 Hz, 1H), 7.83 (d, *J* = 8.2 Hz, 2H), 7.55–7.49 (m, 1H), 7.46 (d, *J* = 7.6 Hz, 1H), 7.43–7.39 (m, 2H), 7.34–7.27 (m, 1H), 7.25–7.20 (m, 1H), 6.76 (s, 1H), 6.05 (d, *J* = 3.7 Hz, 1H), 5.85 (br s, 1H), 3.54–3.34 (m, 3H), 3.11 (d, *J*= 4.9 Hz, 1H), 2.19–2.09 (m, 1H), 1.85 (dt, *J* = 18.5, 4.8 Hz, 1H), 1.76 (s, 1H), 1.70–1.76 (m, 1H), 1.66–1.60 (m, 1H), 1.55–1.49 (m, 1H), 1.47 (s, 3H), 1.46 (s, 3H), 1.43 (s, 3H), 1.20 (s, 3H), 1.07 (s, 3H) ppm.

^{13}C-NMR (125 MHz, $CDCl_3$): δ = 144.1, 143.0, 138.3, 137.5, 134.1, 129.4 (2x), 129.0, 126.7 (2x), 125.8, 125.1, 124.1, 121,3, 114.9, 111.4, 99.2, 77.9, 72.6, 66.0, 40.7, 40.6, 37.1, 30.2, 30.0, 24.7, 23.8, 23.1, 19.4, 16.0, 12.5 ppm.

IR (neat): ν = 3422, 2989. 2943, 1448, 1172, 1091, 738, 726, 590 cm^{-1}.

HRMS (ESI, *m*/*z*): $[M–H]^-$ calcd. for $C_{32}H_{38}NO_6S$, 564.2425; found 564.2414.

$[\alpha]_D^{22}$ +58.0 (c = 1.00, MeOH)

Synthesis of diene 2-6

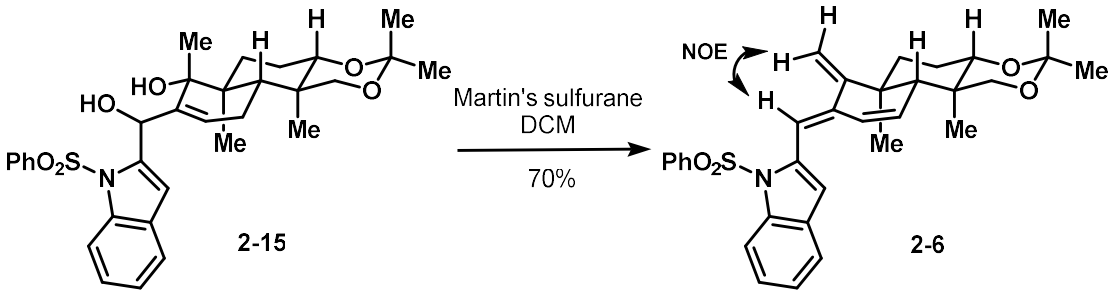

Martin's sulfurane (5.00 g, 7.44 mmol, 2.40 equiv) was added as a solid to a solution of alcohol **2-15** (1.76 g, 3.10 mmol, 1.00 equiv) in DCM (74.4 mL, 40.0 mM) at room temperature. After being stirred for 20 min, the reaction mixture was quenched by the addition of sat. aq. $NaHCO_3$. The aq. layer was extracted three times with DCM, washed with sat. aq. NaCl solution and dried over $MgSO_4$. After removal of the solvent *in vacuo*, the residue was purified by gradient flash chromatography (Yamazen, eluting with 5–26% EtOAc in hexanes) to afford 1.15 g (70%) of compound **2-6** as a yellow solid. The double bond geometry was confirmed by a 2D-NOESY experiment.

R_f = 0.48 (Hexane:EtOAc = 3:1), UV-active, green spot (*p*-anisaldehyde).

^{1}H-NMR (500 MHz, $CDCl_3$): δ = 8.24 (d, *J* = 8.5 Hz, 1H), 7.68 (d, *J* = 8.4 Hz, 2H), 7.50–7.44 (m, 1H), 7.42 (d, *J* = 7.6 Hz, 1H), 7.36–7.24 (m, 2H), 7.24–7.20 (m, 1H), 7.08 (s, 1H), 6.54 (s, 1H), 6.51 (d, *J* = 10.1 Hz, 1H), 5.59 (d, *J* = 10.1 Hz, 1H), 5.29 (s, 1H), 4.84 (s, 1H), 3.61 (d, *J* = 10.4 Hz, 2H), 3.49 (d, *J* = 10.7 Hz, 1H), 2.11 (s, 1H), 1.92–1.80 (m, 3H), 1.73–1.65 (m, 1H), 1.47 (s, 3H), 1.45 (s, 3H), 1.15 (s, 3H), 1.12 (s, 3H) ppm.

^{13}C-NMR (125 MHz, $CDCl_3$): δ = 156.9, 138.6, 138.4, 137.2, 137.0, 133.8, 130.11, 130.0, 129.1 (2x), 126.7 (2x), 125.9, 125.1, 124.2, 120.8, 115.4, 115.3, 113.6, 105.3, 99.5, 71.8, 49.0, 40.5, 36.9, 34.5, 29.9, 24.2, 21.0, 19.4, 12.8 ppm.

IR (neat): ν = 2990, 2940, 2864, 1370, 1174, 1146, 1091, 725 cm^{-1}.

HRMS (ESI, *m*/*z*): $[M+H]^+$ calcd. for $C_{32}H_{36}O_4NS$, 530.2360; found 530.2359.

M.p. = 131 °C

$[\alpha]_D^{22}$ –151.2 (c = 1.00, MeOH)

Synthesis of carbazole 2-12

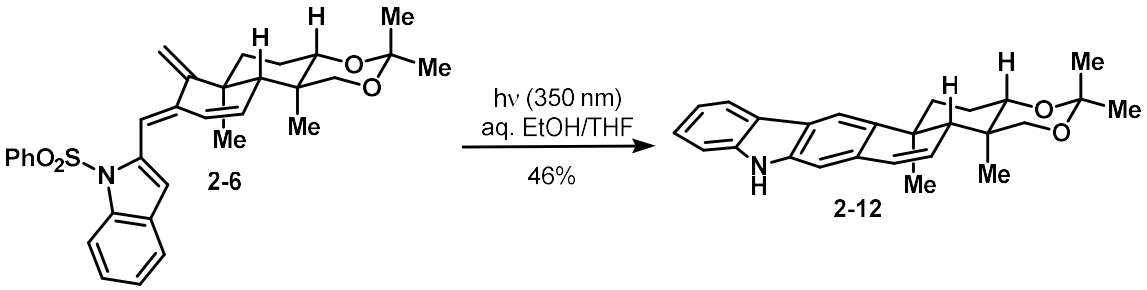

A pyrex glass tube (11 cm tall, 1 cm diameter), equipped with a screw cap, was charged with a solution of acetonide **2-6** (57.0 mg, 0.108 mmol, 1.00 equiv) in 5% aq. ethanol (10.7 mL) and THF (1.20 mL). The vessel was degassed by bubbling a stream of nitrogen through the solution for 45 min. The pale yellow solution was then irradiated for 1 h with UV-A light (350 nm) in a Luzchem photobox at room temperature. After reducing the EtOH *in vacuo*, the residue was dissolved in EtOAc and water. The aq. layer was extracted three times with EtOAc and the combined organic layers were dried over $MgSO_4$, filtered and concentrated *in vacuo*. Gradient flash chromatography (Yamazen, eluting with 5–26% EtOAc in hexanes) provided 19.0 mg (46%) of carbazole **2-12** as a yellow oil.

The stability of the product against irradiation with UV-A (350 nm) light was confirmed by irradiating 5 mg of **2-33** in 5% aq. EtOH (1.60 mL, 8.00 mM) for 2 h at room temperature. After the work-up described above, the material was fully recovered indicating no change by TLC and NMR analysis.

R_f = 0.46 (Hexane:EtOAc = 3:1), UV-active, pink spot (*p*-anisaldehyde)

^{1}H-NMR (700 MHz, C_6D_6): δ = 8.09 (d, *J* = 8.2 Hz, 1H), 7.82 (s, 1H), 7.38 (t, *J* = 7.5 Hz, 1H), 7.25 (t, *J* = 7.5 Hz, 1H), 7.09 (d, *J* = 8.0 Hz, 1H), 6.85 (s, 1H), 6.69 (dd, *J* = 9.3, 2.7 Hz, 1H), 6.63 (br s, 1H), 5.70–5.65 (m, 1H), 3.68 (d, *J* = 10.6 Hz, 1H), 3.46 (dd, *J* = 11.7, 2.9 Hz, 1H), 3.28 (d, *J* = 10.6 Hz, 1H), 2.08 (d, *J* = 12.8 Hz, 1H), 1.93–1.84 (m, 1H), 1.75–1.67 (m, 2H), 1.61 (s, 3H), 1.44 (s, 3H), 1.36 (s, 3H), 1.18 (s, 3H) ppm.

^{13}C-NMR (176 MHz, C_6D_6): δ = 140.7, 140.5, 138.4, 131.8, 130.0, 127.4, 125.8, 124.3, 123.2, 120.3, 119.8, 113.8, 111.0, 109.0, 99.3, 77.2, 71.9, 47.4, 38.3, 36.4, 35.1, 30.4, 24.8, 22.8, 19.5, 13.8 ppm.

IR (neat): ν = 3412, 2937, 2859, 1736, 1449, 1333, 1257, 1194, 811 cm^{-1}.

HRMS (ESI, *m*/*z*): $[M–H]^-$ calcd. for $C_{26}H_{28}O_2N$, 386.2117; found 386.2120.

$[\alpha]_D^{22}$ –105.2 (c = 1.00, MeOH)

Hydrogenation of 2-12 to give carbazole 2-23

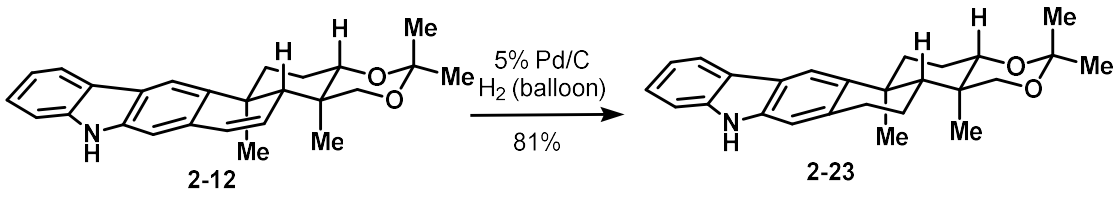

Hydrogen from a balloon was bubbled through a mixture of carbazole **2-12** (19.0 mg, 0.0490 mmol, 1.00 equiv) and 5% Pd/C (11.5 mg, 0.110 mmol, 2.20 equiv) in MeOH (1.60 mL, 30.0 mM) for 1 min. The mixture was then vigorously stirred under an atmosphere of hydrogen (balloon) for 4 h at room temperature. After filtering the mixture through celite (EtOAc/MeOH eluent), the solution was concentrated *in vacuo* and the crude material was purified by gradient flash chromatography (Yamazen, eluting with 5–26% EtOAc in hexanes) to afford 15.0 mg (81%) of carbazole **2-23** as a colorless oil.

R_f = 0.44 (Hexane:EtOAc = 3:1), UV-active, purple spot (*p*-anisaldehyde).

^{1}H-NMR (500 MHz, $CDCl_3$): δ = 8.01 (d, *J* = 7.6 Hz, 1H), 7.93 (s, 1H), 7.84 (br s, 1H), 7.36 (d, *J* = 3.7 Hz, 2H), 7.19 (dt, *J* = 7.7, 3.9 Hz, 1H), 7.08 (s, 1H), 3.70–3.61 (m, 2H), 3.53 (d, *J* = 10.7 Hz, 1H), 3.19–3.11 (m, 1H), 3.09–2.99 (m, 1H), 2.63 (d, *J* = 12.5 Hz, 1H), 1.97–1.79 (m, 4H), 1.76–1.70 (m, 1H), 1.67–1.60 (m, 1H), 1.47 (s, 3H), 1.45 (s, 3H), 1.33 (s, 3H), 1.22 (s, 3H) ppm.

^{13}C-NMR (125 MHz, $CDCl_3$): δ = 141.9, 140.1, 138.2, 133.5, 125.5, 123.7, 122.0, 120.0, 119.3, 115.4, 110.6, 110.0, 99.2, 77.5, 72.7, 46.1, 38.2, 37.9, 37.2, 30.4, 30.0, 26.6, 24.7, 19.4, 18.3, 12.4 ppm.

IR (neat): ν = 2989, 2940, 1465, 1379, 1242, 1108, 853, 728 cm^{-1}.

HRMS (ESI, *m*/*z*): $[M–H]^-$ calcd. for $C_{26}H_{30}NO_2$, 388.2282; found 388.2276.

$[\alpha]_D^{22}$ +47.7 (c = 0.60, MeOH)

Synthesis of free diol 2-13

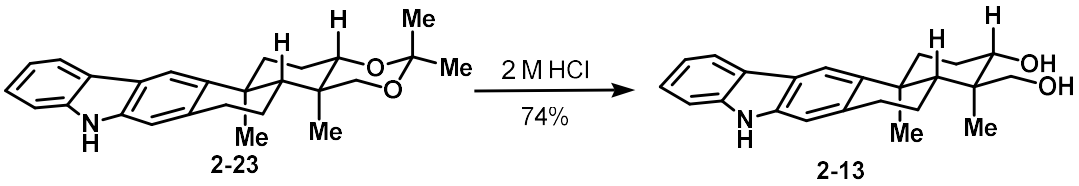

To a solution of carbazole **2-23** (15.0 mg, 0.0380 mmol, 1.00 equiv) in THF (400 µL) was added 2.00 M aq. HCl (400 µL) and the mixture was vigorously stirred for 1 h at room temperature. The solution was quenched by the addition of sat. aq. $NaHCO_3$ at 0 °C. The mixture was warmed to room temperature and additional sat. aq. $NaHCO_3$ was added until the gas evolution ceased. Solid NaCl was added and the aq. layer was extracted five times with EtOAc and dried over $MgSO_4$. After removal of the solvent *in vacuo*, gradient flash chromatography (Yamazen, eluting with 50–70% EtOAc in hexanes) afforded 10.0 mg (74%) of diol **2-13** as a pale-yellow oil.

R_f = 0.25 (Hexane:EtOAc = 1:2), UV-active, blue spot (CAM).

^{1}H-NMR (500 MHz, $CDCl_3$): δ = 8.00 (d, *J* = 7.5 Hz, 1H), 7.94 (s, 1H), 7.84 (br s, 1H), 7.36 (d, *J* = 3.5 Hz, 2H), 7.19 (dt, *J* = 7.6, 3.9 Hz, 1H), 7.07 (s, 1H), 3.84 (d, *J* = 10.6 Hz, 1H), 3.80–3.75 (m, 1H), 3.52 (d, *J* = 10.6 Hz, 1H), 3.17–3.10 (m, 1H), 3.08–3.02 (m, 1H), 2.58–2.53 (m, 1H), 1.93–1.86 (m, 3H), 1.81–1.76 (m, 1H), 1.75–1.69 (m, 1H), 1.55 (d, *J* = 10.2 Hz, 1H), 1.33 (s, 3H), 1.07 (s, 3H) ppm.

^{13}C-NMR (150 MHz, $CDCl_3$): δ = 141.4, 140.0, 138.1, 133.5, 125.4, 123.6, 121.9, 119.9, 119.2, 115.6, 110.4, 109.7, 76.9, 72.3, 44.9, 42.2, 37.7, 37.4, 31.0, 27.8, 25.8, 19.3, 11.2 ppm.

IR (neat): ν = 3413, 2938, 2872, 1466, 1441, 1264, 1066, 1015, 732 cm^{-1}.

HRMS (ESI, *m*/*z*): $[M–H]^-$ calcd. for $C_{23}H_{26}NO_2$, 348.1969; found 348.1963.

$[\alpha]_D^{22}$ +58.4 (c = 0.50, MeOH)

Synthesis of triene 2-24

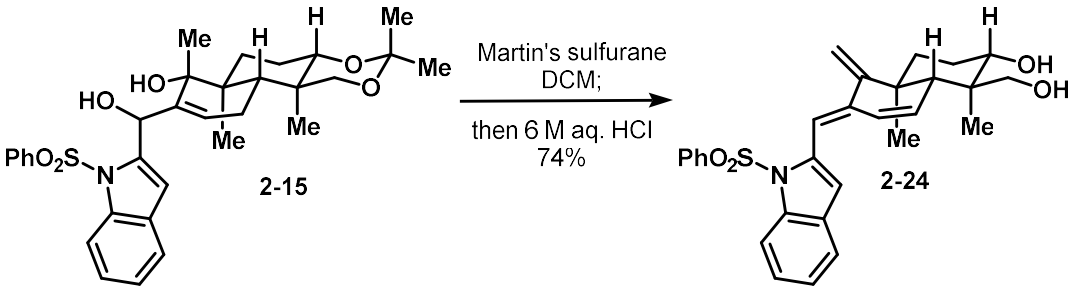

Martin's sulfurane (5.00 g, 7.44 mmol, 2.40 equiv) was added as a solid to a solution of alcohol **2-15** (1.76 g, 3.10 mmol, 1.00 equiv) in DCM (37.2 mL, 80.0 mM) at room temperature. After being stirred for 25 min, an aq. solution of 6 M HCl (37.2 mL) was added at 0 °C. The resulting brown solution was stirred at room temperature for 1.5 h before being quenched by the addition of sat. aq. $NaHCO_3$ at 0 °C. The mixture was warmed to room temperature and additional sat. aq. $NaHCO_3$ was added under stirring until the gas evolution ceased. The mixture was transferred into a sep. funnel and solid NaCl was added. The aq. layer was then extracted four times with EtOAc and dried over $MgSO_4$. After removal of the solvent *in vacuo*, the crude material was purified by gradient flash chromatography (Yamazen, eluting with 50–70% EtOAc in hexanes) affording 1.1 g (74%) of diol **2-24** as a yellow solid in 95% purity.

R_f = 0.22 (Hexane:EtOAc = 1:2), UV-active, blue spot (CAM).

^{1}H-NMR (500 MHz, $CDCl_3$): δ = 8.24 (d, *J* = 8.6 Hz, 1H), 7.68 (d, *J* = 8.1 Hz, 2H), 7.51–7.41 (m, 2H), 7.41–7.33 (m, 3H), 7.08 (s, 1H), 6.55 (s, 1H), 6.52 (d, *J* = 10.4 Hz, 1H), 5.72 (d, *J* = 10.1 Hz, 1H), 5.30 (s, 1H), 4.85 (s, 1H), 3.75 (d, *J* = 10.4 Hz, 2H), 3.47 (d, *J* = 10.6 Hz, 1H), 2.47 (br s, 2H), 2.18 (s, 1H), 1.93–1.74 (m, 4H), 1.11 (s, 3H), 1.00 (s, 3H) ppm.

^{13}C-NMR (125 MHz, $CDCl_3$): δ = 156.7, 138.6, 138.5, 137.2, 137.1, 133.7, 131.1, 130.1, 129.1, 126.7, 125.9, 125.1, 124.2, 120.7, 115.3, 115.1, 113.6, 105.8, 76.7, 71.1, 47.6, 42.0, 40.2, 33.9, 27.5, 20.1, 11.6 ppm.

IR (neat): ν = 3382, 2935, 1447, 1370, 1174, 1090, 725 cm^{-1}.

M.p. = 181 °C

$[\alpha]_D^{22}$ –178.3 (c = 1.00, MeOH)

Synthesis of aldehyde 2-26

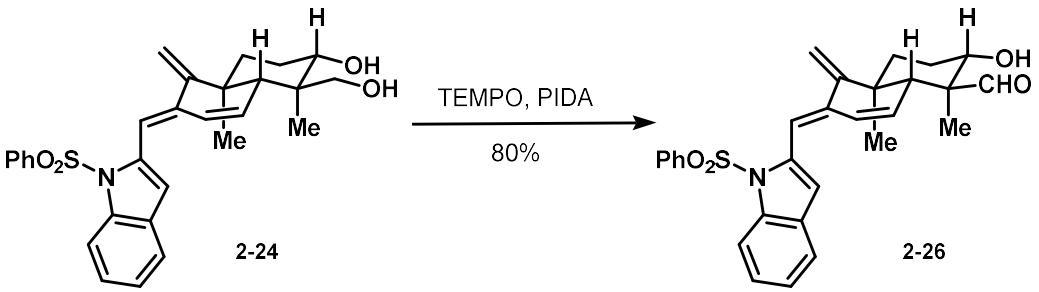

To a solution of diol **2-24** (706 mg, 1.45 mmol, 1.00 equiv) in DCM (11.9 mL) and H_2O (11.9 mL) was added TEMPO (294 mg, 1.88 mmol, 1.30 equiv), followed by PIDA (604 mg, 0.570 mmol, 1.30 equiv) as solids in one portion. The resulting orange-brown mixture was vigorously stirred for 4 h at room temperature before being quenched by the addition of sat. aq. $NaHCO_3$ and sat. aq. NaS_2O_3 (ca. 4:1). The mixture was transferred into a sep. funnel and solid NaCl was added. The aq. layer was then extracted four times with EtOAc, washed with sat. aq. NaCl, dried over $MgSO_4$, and filtered. After removal of the solvent *in vacuo*, this material was used in the next reaction without further purification. Alternatively, the sample was purified by by gradient flash chromatography (Yamazen, eluting with 30–50% EtOAc in hexanes) affording 564 mg (80%) of aldehyde **2-26** as an orange foam.

R_f = 0.21 (Hexane:EtOAc = 2:1), UV-active, blue spot (CAM).

^{1}H-NMR (400 MHz, $CDCl_3$): δ = 9.50 (s, 1H), 8.28 (d, *J* = 8.3 Hz, 1H), 7.70 (d, *J* = 7.8 Hz, 2H), 7.55–7.45 (m, 2H), 7.36 (q, *J* = 7.8 Hz, 3H), 7.29 (d, *J* = 9.3 Hz, 1H), 6.59 (s, 1H), 6.55 (dd, *J* = 10.0, 2.7 Hz, 1H), 5.46–5.36 (m, 2H), 4.93 (s, 1H), 3.96 (d, *J* = 9.6 Hz, 1H), 2.64 (s, 1H), 2.08–2.00 (m, 1H), 1.99–1.83 (m, 3H), 1.76 (br s, 1H), 1.22 (s, 3H), 1.16 (s, 3H) ppm.

^{13}C-NMR (100 MHz, $CDCl_3$): δ = 205.9, 155.9, 138.4, 138.1, 137.3, 136.7, 133.8, 130.1, 129.1 (3x), 126.7 (2x), 126.4, 125.2, 124.2, 120.8, 116.1, 115.3, 113.8, 106.1, 72.0, 54.7, 45.7, 39.1, 33.8, 27.1, 20.0, 9.8 ppm.

IR (neat): ν = 2932, 1722, 1447, 1368, 1173, 1119, 724 cm^{-1}.

HRMS (ESI, *m*/*z*): $[M–H]^-$ calcd. for $C_{29}H_{28}NSO_4$, 486.1745; found 486.1743.

$[\alpha]_D^{22}$ –186.5 (c = 1.00, MeOH)

Synthesis of acid 2-25

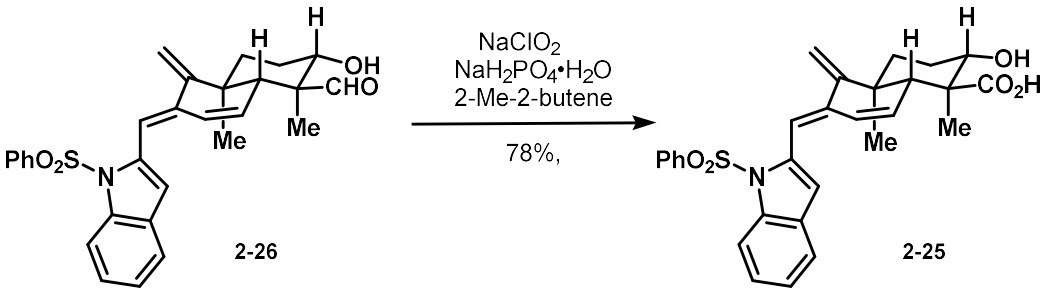

To a solution of the crude aldehyde in acetone (13.9 mL), H_2O (6.90 mL), and 2-Me-2-butene (1.32 mL, 17.3 mmol, 12.0 equiv) was added a mixture of $NaClO_2$ (861mg, 9.50 mmol, 6.00 equiv, ~90% techn.) and $NaH_2PO_4•H_2O$ (1.99 g, 14.4 mmol, 10.0 equiv) at 0 °C. The mixture was warmed to room temperature and stirred for 2 h before being quenched by the addition of sat. aq. NaCl and sat. aq. NH_4Cl (ca. 1:1). The mixture was transferred into a sep. funnel and solid NaCl was added. The aq. layer was then extracted six times with EtOAc and dried over $MgSO_4$. After concentrating the solution *in vacuo*, the crude material was purified by gradient flash chromatography (Yamazen, eluting with 0–10% MeOH in DCM) to afford 569 mg (78%) of acid **2-25** as a yellow oil.

R_f = 0.38 (7% MeOH in DCM), UV-active, blue spot (CAM).

^{1}H-NMR (700 MHz, CD_3OD): δ = 8.19 (d, *J* = 8.4 Hz, 1H), 7.64 (d, *J* = 8.0 Hz, 2H), 7.54 (t, *J* = 7.5 Hz, 1H), 7.47 (d, *J* = 7.5 Hz, 1H), 7.39–7.34 (m, 2H), 7.32 (t, *J* = 7.7 Hz, 1H), 7.23 (t, *J* = 7.7 Hz, 1H), 7.01 (s, 1H), 6.62 (s, 1H), 6.51 (d, *J* = 9.7 Hz, 1H), 5.63 (d, *J* = 9.7 Hz, 1H), 5.29 (s, 1H), 4.90 (s, 1H), 4.12–4.07 (m, 1H), 2.74 (s, 1H), 1.92–1.82 (m, 4H), 1.20 (s, 3H), 1.12 (s, 3H) ppm.

^{13}C-NMR (176 MHz, CD_3OD): δ = 180.2, 158.7, 139.9, 139.4, 138.5, 138.1, 135.1, 133.3, 131.7, 130.2 (2x), 127.6 (2x), 126.4, 126.1, 125.3, 122.0, 116.2, 116.1, 114.8, 105.6, 75.7, 53.6, 50.9, 40.8, 35.2, 28.1, 20.7, 12.4 ppm.

IR (neat): ν = 3357, 2927, 1697, 1447, 1359, 1173, 1088, 970, 748, 685 cm^{-1}.

HRMS (ESI, *m/z*): $[M–H]^-$ calcd. for $C_{29}H_{28}NO_5S$, 502.1694; found 502.1681.

$[\alpha]_D^{22}$ –173.6 (c = 0.50, MeOH)

Synthesis of carbazole aldehyde 2-16

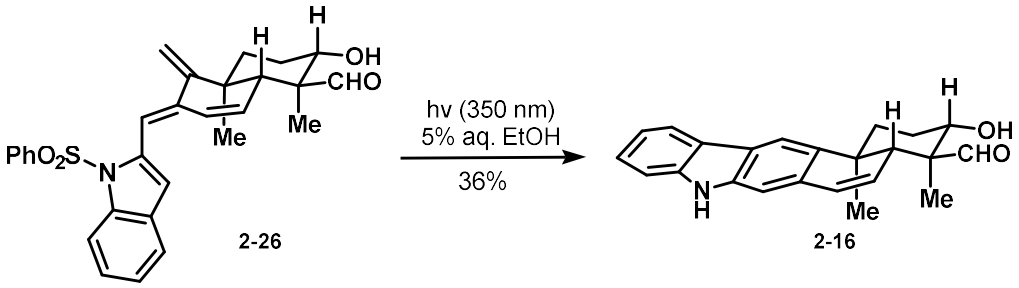

A pyrex glass tube (11 cm tall, 1 cm diameter), equipped with a screw cap, was charged with a solution of aldehyde **2-26** (90.0 mg, 0.184 mmol, 1.00 equiv) in 5% aq. ethanol (9.00 mL, 20.0 mM). The vessel was degassed by bubbling a stream of nitrogen through the solution for 45 min. The mixture was then irradiated for 4 h with UV-A light (350 nm) in a Luzchem photobox at room temperature. After reducing the EtOH *in vacuo*, the residue was dissolved in EtOAc and sat. aq. NaCl. The aq. layer was extracted four times with EtOAc and the combined organic layers were dried over $MgSO_4$, filtered and concentrated *in vacuo* the crude material was purified by gradient flash chromatography (Yamazen, eluting with 13–42% EtOAc in Hexanes) provided 23 mg (36%) of carbazole **2-16** as a white foam.

R_f = 0.25 (Hexane:EtOAc = 2:1), UV-active, blue spot (CAM).

^{1}H-NMR (700 MHz, CD_3OD): δ = 9.48 (s, 1H), 8.03 (d, *J* = 7.5 Hz, 1H), 7.99 (br s, 1H), 7.85 (s, 1H), 7.43–7.36 (m, 2H), 7.22 (t, *J* = 6.4 Hz, 1H), 7.13 (s, 1H), 6.71 (dd, *J* = 9.5, 2.9 Hz, 1H), 5.66 (dd, *J* = 9.5, 2.0 Hz, 1H), 3.98 (dd, *J* = 10.8, 4.2 Hz, 1H), 2.76 (s, 1H), 2.49 (d, *J* = 12.4 Hz, 1H), 2.12–2.07 (m, 1H), 2.07–1.95 (m, 2H), 1.62 (br s, 1H), 1.34 (s, 3H), 1.19 (s, 3H) ppm.

^{13}C-NMR (176 MHz, CD_3OD): δ = 206.3, 140.2, 139.1, 138.1, 131.2, 130.7, 127.1, 125.9, 123.7, 123.0, 120.1, 119.7, 113.8, 110.8, 109.1, 71.8, 54.5, 44.5, 37.2, 34.5, 27.3, 22.0, 10.3 ppm.

IR (neat): ν = 3294, 2937, 2825, 1717, 1242, 1023, 716 cm^{-1}.

HRMS (ESI, *m*/*z*): $[M–H]^-$ calcd. for $C_{23}H_{22}NO_2$, 344.1656; found 344.1653.

$[\alpha]_D^{22}$ –24.2 (c = 0.90, MeOH)

Synthesis of carbazole acid 2-27

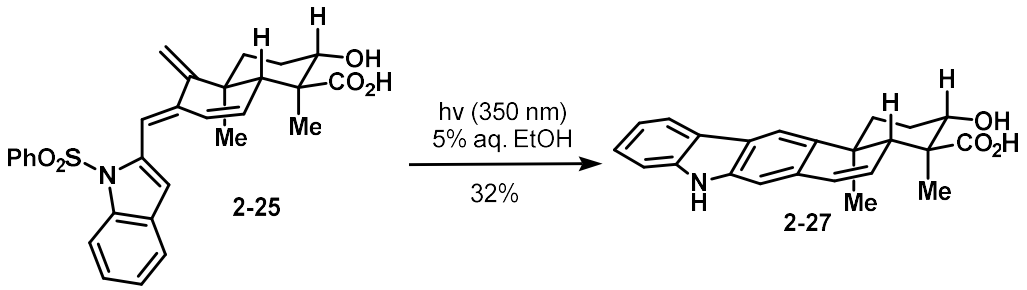

A pyrex glass tube (11 cm tall, 1 cm diameter), equipped with a screw cap, was charged with a solution of acid **2-25** (43mg, 0.085 mmol, 1.0 equiv) in 5% aq. ethanol (9.50 mL). The vessel was degassed by bubbling a stream of nitrogen through the solution for 45 min. The mixture was then irradiated for 1.5 h with UV-A light (350 nm,) in a Luzchem photobox at room temperature. After reducing the EtOH *in vacuo*, the residue was dissolved in EtOAc, water, and sat. aq. NaCl. The aq. layer was extracted six times with EtOAc and the combined organic layers were dried over $MgSO_4$, filtered and concentrated *in vacuo*. The crude material was purified by gradient flash chromatography (Yamazen, eluting with 0–10% MeOH in DCM) to afford 10 mg (32%) of acid **2-27** as a pale yellow solid.

The stability of the product against irradiation with UV-A (350 nm) light was confirmed by irradiating 5.0 mg of **2-27** in 5% aq. EtOH (1.7 mL, 0.0080 M) for 2 h at room temperature. After the work-up described above, the material was fully recovered indicating no change by TLC and NMR analysis.

$\mathbf{R_f}$ = 0.35 (7% MeOH in DCM), UV-active, blue spot (CAM).

^{1}H-NMR (700 MHz, CD_3OD): δ = 8.00 (d, *J* = 8.0 Hz, 1H), 7.85 (s, 1H), 7.39 (d, *J* = 8.0 Hz, 1H), 7.31 (t, *J* = 7.5 Hz, 1H), 7.14–7.10 (m, 2H), 6.70 (dd, *J* = 9.7, 2.7 Hz, 1H), 5.80 (d, *J* = 9.7 Hz, 1H), 4.18 (dd, *J* = 11.7, 4.2 Hz, 1H), 2.83 (br s, 1H), 2.49 (d, *J* = 12.4 Hz, 1H), 2.04–1.98 (m, 3H), 1.35 (s, 3H), 1.15 (s, 3H) ppm.

^{13}C-NMR (176 MHz, CD_3OD): δ = 180.6, 142.0, 140.2, 139.9, 132.3, 131.0, 128.9, 126.2, 124.7, 123.8, 120.7, 119.6, 114.1, 111.6, 109.8, 75.7, 53.5, 49.6, 38.7, 35.9, 28.5, 22.3, 12.9 ppm.

IR (neat): ν = 2926, 1699, 1447, 1371, 1243, 1144, 1075, 734, 588 cm^{-1}.

HRMS (ESI, *m*/*z*): $[M–H]^-$ calcd. for $C_{23}H_{22}NO_3$, 360.1605; found 360.1598.

$[\alpha]_D^{22}$ –6.9 (c = 1.00, MeOH)

Alternative synthesis of carbazole acid 2-27

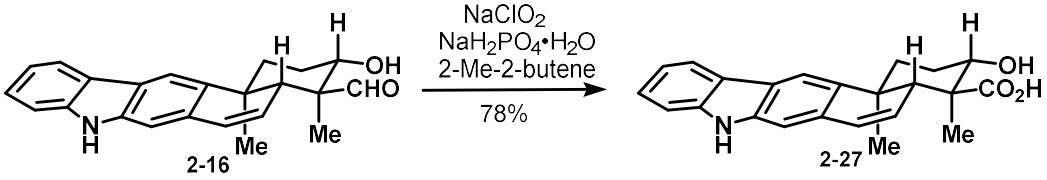

To a solution of the aldehyde **2-16** (90.7 mg, 0.263 mmol, 1.00 equiv) in acetone (3.50 mL), H_2O (1.75 mL), and 2-Me-2-butene (335 µL, 3.16 mmol, 12.0 equiv) was added a mixture of $NaClO_2$ (143 mg, 1.58 mmol, 6.00 equiv, ~90% techn.) and $NaH_2PO_4 \bullet H_2O$ (363 mg, 2.63 mmol, 10.0 equiv) at 0 °C. The mixture was warmed to room temperature and stirred for 2 h before being quenched by the addition of sat. aq. NaCl and sat. aq. NH_4Cl (ca. 1:1). The mixture was transferred into a sep. funnel and solid NaCl was added. The aq. layer was then extracted six times with EtOAc and dried over $MgSO_4$. After concentrating the solution *in vacuo*, the crude material was purified by gradient flash chromatography (Yamazen, eluting with 0-10% MeOH in DCM) to afford 74 mg (78%) of acid **2-27** as a yellow foam.

Synthesis of xiamycin A (2-1)

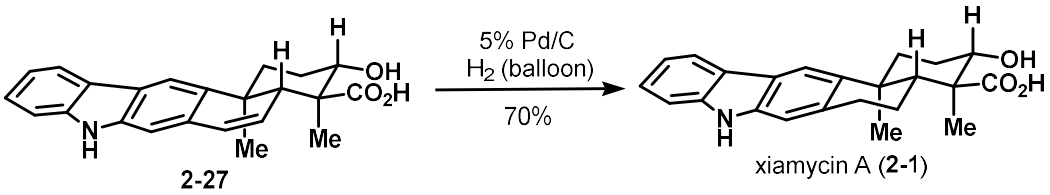

Xiamycin A (2-10): Hydrogen from a balloon was bubbled through a mixture of carbazole **2-27** (10 mg, 0.027 mmol, 1.0 equiv) and 5% Pd/C (9.0 mg, 0.080 mmol, 3.0 equiv) in MeOH (900 µL) for 1 min. The mixture was then vigorously stirred under an atmosphere of hydrogen (balloon) for 3.5 h at room temperature. After filtering the mixture through celite (EtOAc/MeOH eluent), the solution was concentrated *in vacuo* and the crude material was purified by preparative thin layer chromatography (10% MeOH in DCM) to afford 7 mg (70%) of xiamycin A **(2-1)** as a pale yellow solid. The hydrogenation reaction can also be performed using crude carbazole **2-27** to give xiamycin A (**2-1**) in the same overall yield (22%, 2 steps, 1 purification).

$\mathbf{R_f}$ = 0.25 (7% MeOH in DCM), UV-active, blue spot (CAM).

^{1}H-NMR (700 MHz, CD_3OD): δ = 7.97 (d, *J* = 8.0 Hz, 1H), 7.94 (s, 1H), 7.35 (d, *J* = 8.0 Hz, 1H), 7.29 (t, *J* = 7.9 Hz, 1H), 7.09 (t, *J* = 7.5 Hz, 1H), 7.07 (s, 1H), 4.10 (dd, *J* = 10.5, 7.5 Hz, 1H), 3.15–3.08 (m, 1H), 3.08–2.99 (m, 1H), 2.64 (d, *J* = 12.8 Hz, 1H), 2.14 (d, *J* = 11.8 Hz, 1H), 2.08–1.98 (m, 1H), 1.93–1.88 (m, 2H), 1.78–1.72 (m, 1H), 1.58–1.53 (m, 1H), 1.30 (s, 3H), 1.25 (s, 3H) ppm.

^{13}C-NMR (176 MHz, CD_3OD): δ = 181.3, 142.0, 141.8, 140.1, 134.0, 126.0, 124.6, 123.1, 120.6, 119.3, 116.4, 111.4, 110.8, 76.3, 54.9, 47.9, 39.0, 32.1, 28.7, 26.3, 22.6, 11.4 ppm.

IR (neat): ν = 3409, 2932, 1694, 1465, 1242, 1066 cm^{-1}.

HRMS (ESI, *m*/*z*): $[M–H]^-$ calcd. for $C_{23}H_{24}NO_3$, 362.1762; found 362.1754.

$[\alpha]_D^{22}$ +123.5 (c = 0.40, MeOH); lit.[2a] **$[\alpha]_D^{23}$** +137.6 (c = 0.40, MeOH)

Synthesis of xiamycin C and F (2-10):

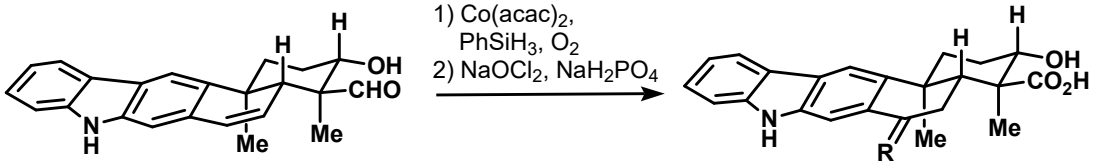

2-16

xiamycin C R= OH (eq.), H (**2-3**)
[64%, 2 steps 1.5:1 *dr*]
xiamycin F R= O (**2-4**)
[15%, 2 steps]

Oxygen from a balloon was bubbled through a mixture of carbazole **2-16** (15 mg, 0.043 mmol, 1.0 equiv), $Co(acac)_2$ (3.3 mg, 0.013 mmol, 0.30 equiv), and $PhSiH_3$ (8.0 ul, 0.067 mmol, 1.5 equiv) in THF (900 µL) for 1 min. The mixture was then stirred under an atmosphere of oxygen (balloon) for 12 h at room temperature. This mixture was then filtered through a silica plug with EtOAc and concentrated *in vacuo*. The crude mixture of diastereomeric alcohols and ketone was then directly subjected Pinnick oxidation conditions as the crude mixture decomposed upon all attempts at characterization and separation. The hydration reaction can also be performed with HFIP as the solvent which led to increased relative yield of the alcohols, and a shorter reaction time of 1 hour.

To a solution of the crude aldehydes in acetone (0.8 mL), H_2O (0.4 mL), and 2-Me-2-butene (115 µL, 1.1 mmol, 25 equiv) was added a mixture of $NaClO_2$ (27 mg, 0.3 mmol, 7.0 equiv, ~90% techn.) and $NaH_2PO_4 \bullet H_2O$ (60 mg, 0.44 mmol, 10 equiv) at 0 °C. The mixture was warmed to room temperature and stirred for 2 h before being quenched by the addition of sat. aq. NaCl and sat. aq. NH_4Cl (ca. 1:1). The mixture was transferred into a sep. funnel and solid NaCl was added. The aq. layer was then extracted six times with EtOAc and dried over $MgSO_4$. After concentrating the solution in vacuo, the crude material was purified by preporatory thin layer chromatography (95:5:1 DCM:MeOH:AcOH) to afford 10.4 mg (64% 1.5:1 *dr*) xiamycin C (**2-**3) as an amorphous yellow solid, and 2.4 mg (16%) xiamycin F (**2-4** as an amorphous yellow solid.

Xiamycin C (2-3):

R_f = 0.18 (10% MeOH in DCM), UV-active, blue spot (CAM).

^{1}H-NMR (600 MHz, CD_3OD) δ8.00 (d, J = 7.7 Hz, 1H),7.94 (s, 1H), 7.58 (s, 1H), 7.37 (d, J = 8.0 Hz, 1H), 7.31 (dd, J = 7.9, 8.0 Hz, 1H), 7.10 (d, J = 7.9, 8.0 Hz 1H), 4.89 (m, 1H), 4.09 (dd, J = 8.0, 6.6 Hz, 1H), 2.63 (ddd, J = 13.2, 3.4, 3.2, Hz, 1H), 2.19 (d, J = 12.6 Hz, 1H) ,2.09 – 1.95 (m, 2H), 1.93 – 1.82 (m, 3H), 1.75 – 1.65 (m, 1H), 1.38 (s, 3H),1.26 (s, 3H).

^{13}C-NMR (151MHz, CD_3OD): δ = 180.4, 142.3, 142.1, 140.1, 137.9, 126.3, 124.5, 124.0, 120.8, 119.3, 116.3, 111.5, 110.1, 76.8, 72.3, 55.1, 46.0, 39.2, 39.0, 33.3, 28.4, 26.9, 12.7.

IR (neat): ν = 3670, 2932, 1684, 1352, 1242, 1066 cm^{-1}.

HRMS (ESI, *m*/*z*): $[M–H]^-$ calcd. for $C_{23}H_{24}NO_4$, 378.1711; found 378.1708.

$[\alpha]_D^{22}$ +120.6 (c = 0.10, MeOH); lit.[1c] **$[\alpha]_D^{20}$** +123.6(c = 0.1, MeOH)

C19epi-Xiamycin C:

R_f = 0.14 (10% MeOH in DCM), UV-active, blue spot (CAM).

^{1}H-NMR (700 MHz, CD_3OD): δ = 7.97 (d, *J* = 8.0 Hz, 1H), 7.94 (s, 1H), 7.35 (d, *J* = 8.0 Hz, 1H), 7.29 (t, *J* = 7.9 Hz, 1H), 7.09 (t, *J* = 7.5 Hz, 1H), 7.07 (s, 1H), 4.10 (dd, *J* = 10.5, 7.5 Hz, 1H), 3.15–3.08 (m, 1H), 3.08–2.99 (m, 1H), 2.64 (d, *J* = 12.8 Hz, 1H), 2.14 (d, *J* = 11.8 Hz, 1H), 2.08–1.98 (m, 1H), 1.93–1.88 (m, 2H), 1.78–1.72 (m, 1H), 1.58–1.53 (m, 1H), 1.30 (s, 3H), 1.25 (s, 3H) ppm.

^{13}C-NMR (176 MHz, CD_3OD): δ = 181.3, 142.0, 141.8, 140.1, 134.0, 126.0, 124.6, 123.1, 120.6, 119.3, 116.4, 111.4, 110.8, 76.3, 54.9, 47.9, 39.0, 32.1, 28.7, 26.3, 22.6, 11.4 ppm.

IR (neat): ν = 3409, 2932, 1694, 1465, 1242, 1066 cm^{-1}.

HRMS (ESI, *m*/*z*): $[M–H]^-$ calcd. for $C_{23}H_{24}NO_4$, 378.1711; found 378.1708.

$[\alpha]_D^{22}$ +117.2 (c = 0.40, MeOH)

Xiamycin F (2-4):

R_f = 0.34 (10% MeOH in DCM), UV-active, blue spot (CAM).

^{1}H-NMR (700 MHz, CD_3OD): δ = 7.97 (d, *J* = 8.0 Hz, 1H), 7.94 (s, 1H), 7.35 (d, *J* = 8.0 Hz, 1H), 7.29 (t, *J* = 7.9 Hz, 1H), 7.09 (t, *J* = 7.5 Hz, 1H), 7.07 (s, 1H), 4.10 (dd, *J* = 10.5, 7.5 Hz, 1H), 3.15–3.08 (m, 1H), 3.08–2.99 (m, 1H), 2.64 (d, *J* = 12.8 Hz, 1H), 2.14 (d, *J* = 11.8 Hz, 1H), 2.08–1.98 (m, 1H), 1.93–1.88 (m, 2H), 1.78–1.72 (m, 1H), 1.58–1.53 (m, 1H), 1.30 (s, 3H), 1.25 (s, 3H) ppm.

^{13}C-NMR (226 MHz, CD_3OD): δ = 201.1, 180.1, 147.7, 144.0, 139.6, 130.1, 129.4, 128.8, 123.8, 122.3, 120.4, 116.2, 112.3, 110.7, 76.0, 54.3, 46.9, 38.8, 38.7, 38.3, 28.4, 24.9, 11.1

IR (neat): ν = 3411, 2945, 1694, 1646, 1470, 1240, 1070 cm^{-1}.

HRMS (ESI, *m*/*z*): $[M–H]^-$ calcd. for $C_{23}H_{22}NO_4$, 376.1554; found 376.1552.

$[\alpha]_D^{22}$ +130.1 (c = 0.40, MeOH)

Synthesis of xiamycin H (2-5)

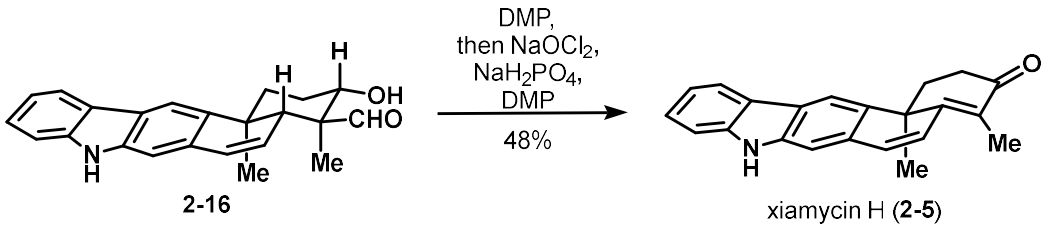

2-16 xiamycin H (**2-5**)

Dess-Martin periodinane (14 mg, 0.032 mmol, 1.1 equiv) (DMP) was added to a solution of carbazole **2-16** (10 mg, 0.029 mmol, 1.0 equiv) in DCM (900 µL). The mixture was then vigorously stirred at room temperature for 30 minutes. To this mixture mixture was added acetone (900 µL), water (450 µL) and 2-Me-2-butene (85 µL, 0.8 mmol, 25 equiv), followed by $NaOCl_2$ (18 mg, 0.3 mmol, 7.0 equiv, ~90% techn.), $NaH_2PO_4 \bullet H_2O$ (40 mg, 0.29 mmol, 10 equiv), and DMP (25 mg, 0.058 mmol, 2 equiv). This yellow heterogenous mixture was stirred vigorously at room temperature for 3 hours. The reaction mixture was diluted with sat. aq. NaCl and extracted 3 times with EtOAc. The combined organic layers were dried over $MgSO_4$, filtered, and concentrated *in vacuo*. The crude material was purified by preparative thin layer chromatography (30% EtOAc in Hexanes) to afford 4.3 mg (48%) of xiamycin H (**2-5**) as a bright yellow amorphous solid.

Comparison of the spectral data for xiamycin H to the natural sample[5] showed strong agreement in the ^{1}H-NMR, but poor resolution made comparison of the ^{13}CNMR difficult (presumably due to its sparing solubility in CD_3OD).

R_f = 0.4 (33% EtOAc in Hexanes), UV-active, visibly yellow spot.

^{1}H-NMR (600 MHz, CD_3OD) δ = 8.16 (s, 1H), 8.06 (d, *J* = 7.9 Hz, 1H), 7.42 (d, *J* = 8.1 Hz, 1H), 7.40 – 7.32 (m, 2H), 7.15 (t, *J* = 7.5 Hz, 1H), 7.05 (d, *J* = 9.8 Hz, 1H), 6.76 (d, *J* = 9.8 Hz, 1H), 3.00 – 2.95 (m, 1H), 2.89 – 2.82 (m, 1H), 2.71 – 2.64 (m, 1H), 2.38 – 2.32, 1.92 (s, 3H), 1.49 (s, 3H).

^{13}C NMR (151 MHz, MeOD) δ = 200.5, 160.2, 156.3, 142.5, 140.1, 137.8, 136.6, 130.1, 129.4, 127.0, 125.0, 124.3, 123.4, 121.1, 120.0, 116.5, 111.8, 40.6, 35.1, 34.9, 31.3, 10.6.

IR (neat): ν = 2932, 1644, 1602, 1558, 1465, 1242, 1066 cm^{-1}.

HRMS (ESI, *m*/*z*): $[M–H]^-$ calcd. for $C_{22}H_{18}NO$, 312.1394; found 312.1392.

$[\alpha]_D^{22}$ +41.5 (c = 0.40, $CHCl_3$)

Synthesis of syn-diol 2-18

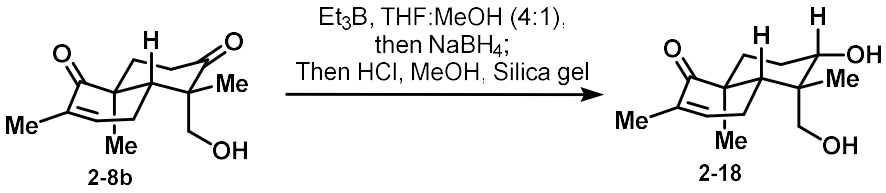

Et_3B (7.81 mL of a 1.00M THF solution, 1.10 equiv) was added to a mixture of THF (56.8 mL) and MeOH (14.2 mL) under a N_2 atmosphere and the resulting colorless solution was stirred for 1 hour at room temperature. The solution was cooled to –78 °C after which 1.70 g of ketone **2-8b** (7.10 mmol, 1.00 equiv) in THF (10.0 mL) was added dropwise and stirred at –78 °C for 30 minutes. $NaBH_4$ (402 mg, 10.6 mmol, 1.50 equiv) was added as a solid and the resulting solution was stirred at –78 °C for 3 hours. The solution was diluted with EtOAc and quenched by the addition of sat. aq. NH_4Cl. The aq. layer was extracted three time with EtOAc and the combined organic layers were washed with sat. aq. NaCl, and dried over $MgSO_4$. After the removal of solvent *in vacuo* the resulting boronate ester was loaded onto a silica gel column that was further acidifed with conc. HCl, and eluted with methanol. After removal of solvent *in vacuo* this material was used in the next reaction without further purification. An analytical sample was prepared by flash column chromatography (PE:EtOAc = 1:1) to afford diol **2-18** as a white solid. Suitable crystals for X-ray analysis were obtained after crystallization from a Hexane/EtOAc (1:1) solution.

$\mathbf{R_f}$ = 0.22 (Hexane:EtOAc = 1:3), UV-active, blue spot (CAM).

^{1}H-NMR (400 MHz, $CDCl_3$) δ = 6.67 (dt, *J* = 6.1, 1.9 Hz, 1H), 4.26 (d, *J* = 11.0 Hz, 1H), 3.72 (s, 2H), 3.48 (d, *J* = 11.0 Hz, 1H), 3.45–3.36 (m, 1H), 2.43–2.30 (m, 1H), 2.19 (ddt, *J* = 19.0, 11.7, 2.5 Hz, 1H), 1.91 (d, *J* = 14.1 Hz, 1H), 1.86–1.76 (m, 2H), 1.70 (dt, *J* = 2.8, 1.4 Hz, 3H), 1.64 (dd, *J* = 11.7, 4.2 Hz, 1H), 1.51–1.40 (m, 1H), 1.21 (s, 3H), 0.95 (s, 3H) ppm.

^{13}C-NMR (126 MHz, $CDCl_3$) δ = 205.2, 143.8, 133.0, 80.0, 64.4, 48.8, 44.4, 42.5, 31.5, 27.3, 23.9, 21.9, 18.1, 16.3 ppm.

IR (neat): ν = 3417, 2944, 1660, 1353, 1032, 991, 739, 547 cm^{-1}.

HRMS (EI, *m*/*z*): $[M]^+$ calcd. for $C_{14}H_{22}O_3$, 238.1569; found 238.1572.

M.p. = 136 °C

$[\alpha]_D^{22}$ –28.2 (c = 1.00, MeOH)

Synthesis of acetonide 2-28

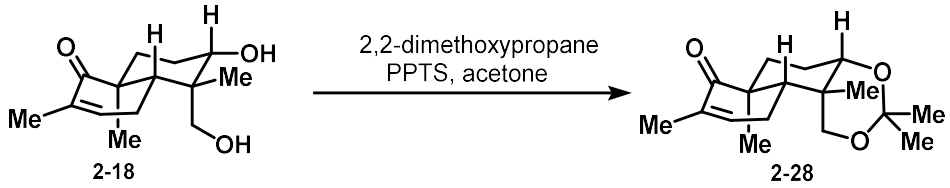

To a solution of crude diol **2-18** in acetone (98.0 mL, 80.0 mM) was added PPTS (490 mg, 1.95 mmol, 0.250 equiv), followed by 2,2-dimethoxypropane (9.80 mL, 78.1 mmol, 10.0 equiv) at room temperature. After stirring for 14 h, the reaction mixture was quenched by the addition of sat. aq. $NaHCO_3$. The aq. layer was extracted three times with EtOAc, washed with sat. aq. NaCl solution and dried over $MgSO_4$. After removal of the solvent *in vacuo*, this material was used in the next reaction without further purification. An analytical sample was prepared by flash column chromatography (PE:EtOAc = 3:1) to afford acetonide **2-28** as a white solid.

R_f = 0.49 (Hexane:EtOAc = 2:1), UV-active, blue spot (CAM).

^{1}H-NMR (700 MHz, $CDCl_3$) δ = 6.64 (d, *J* = 5.9 Hz, 1H), 4.06 (d, *J* = 11.4 Hz, 1H), 3.47 (dd, *J* = 8.4, 3.6 Hz, 1H), 3.28 (d, *J* = 11.5 Hz, 1H), 2.30 (dt, *J* = 18.9, 5.1 Hz, 1H), 2.16 (ddt, *J* = 18.8, 11.8, 2.5 Hz, 1H), 1.96 (dtd, *J* = 13.2, 8.1, 4.6 Hz, 1H), 1.88 (ddd, *J* = 13.5, 7.9, 5.2 Hz, 1H), 1.78 (ddd, *J* = 13.9, 8.4, 4.6 Hz, 1H), 1.74 (d, *J* = 2.7 Hz, 3H), 1.69 (dt, *J* = 12.0, 5.4 Hz, 2H), 1.42 (s, 3H), 1.36 (s, 3H), 1.18 (s, 6H) ppm.

^{13}C-NMR (176 MHz, $CDCl_3$) δ = 204.7, 142.6, 133.4, 99.2, 75.7, 64.2, 45.9, 44.0, 37.7, 27.8, 26.9, 25.2, 25.1, 24.2, 23.3, 19.8, 16.5 ppm.

IR (neat): ν = 2988, 2949, 2876, 1670, 1445, 1432, 1247, 1153, 1077, 864 cm^{-1}.

HRMS (EI, *m/z*): $[M+H]^+$ calcd. for $C_{17}H_{27}O_3$, 279.1960; found 279.1959.

$[\alpha]_D^{22}$ –42.7 (c = 1.00, MeOH)

Synthesis of tertiary alcohol 2-29

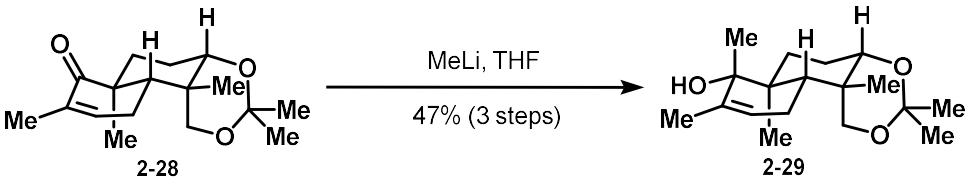

MeLi (10.7 mL of a 1.60 M Et_2O solution, 17.2 mmol, 2.20 equiv) was added dropwise to a solution of the crude acetonide **2-28** in THF (78.0 mL, 0.100 M) at –78 °C. After being stirred for 1.5 h at –78 °C, the reaction mixture was quenched by the addition of sat. aq. NH_4Cl. The aq. layer was extracted three times with EtOAc, washed with sat. aq. NaCl solution and dried over $MgSO_4$. After removal of the solvent *in vacuo*, the residue was purified by gradient flash chromatography (Yamazen, eluting with 13–34% EtOAc in hexanes) to afford 1.09 g (47%, over 3 steps) of alcohol **2-29** as a white solid.

R_f = 0.46 (Hexane:EtOAc = 2:1), non UV-active, blue spot (CAM).

^{1}H-NMR (600 MHz, $CDCL_3$) δ = 5.33 (ddt, *J* = 3.8, 2.5, 1.4 Hz, 1H), 4.08 (d, *J* = 11.4 Hz, 1H), 3.51 (dd, *J* = 7.9, 3.1 Hz, 1H), 3.23 (d, *J* = 11.4 Hz, 1H), 1.98 (dd, *J* = 17.4, 1.6 Hz, 1H), 1.94-1.88 (m, 1H), 1.82-1.73 (m, 1H), 1.72-1.50 (m, 8H), 1.42 (s, 3H), 1.37 (s, 3H), 1.28 (s, 3H), 1.17 (s, 3H), 1.11 (s, 3H) ppm.

^{13}C-NMR (151 MHz, CDCl3) δ 138.68, 121.41, 98.99, 78.09, 76.02, 64.14, 42.44, 39.35, 37.37, 27.37, 26.59, 26.09, 25.19, 25.11, 23.09, 22.88, 17.97, 17.83 ppm.

IR (neat): ν = 3511, 2986, 2961, 2952, 2897, 1454, 1378, 1250, 1098 cm^{-1}.

HRMS (EI, *m/z*): $[M]^+$ calcd. for $C_{18}H_{30}O_3$, 294.2195; found 294.2199.

$[\alpha]_D^{22}$ –33.2 (c = 1.00, MeOH)

Synthesis of aldehyde 2-30

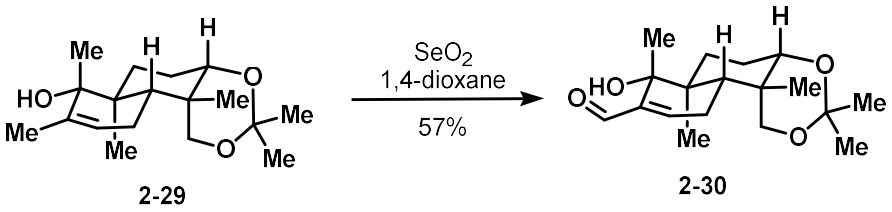

2-29 2-30

A mixture of alcohol **2-29** (1.00 g, 3.40 mmol, 1.00 equiv) and selenium dioxide (940 mg, 8.50 mmol, 2.50 equiv) was dissolved in 1,4-dioxane (34.0 mL, 0.100 M) and then placed in an oil bath at 90 °C. After stirring for 2 h, the resulting brown mixture was cooled to room temperature and quenched by the addition of distilled water. The aq. phase was extracted three times with EtOAc and the combined organic layers were washed with sat. aq. NaCl solution. The solution was dried over $MgSO_4$ and concentrated *in vacuo*. The crude products were purified by gradient flash chromatography (Yamazen, eluting with 13–34% EtOAc in hexanes) to afford 600 mg of aldehyde **2-30** (57%) as an orange solid, in this case no allylic alcohol was isolated.

R_f = 0.54 (Hexane:EtOAc = 1:1), UV-active, blue spot (CAM).

^{1}H-NMR (500 MHz, $CDCl_3$) δ = 9.39 (s, 1H), 6.73 (dd, *J* = 4.7, 2.5 Hz, 1H), 4.14 (d, *J* = 11.3 Hz, 1H), 3.57 (dd, *J* = 7.8, 2.8 Hz, 1H), 3.28 (d, *J* = 11.3 Hz, 1H), 2.45 (dt, *J* = 20.4, 5.0 Hz, 1H), 2.26–2.16 (m, 1H), 1.94 (dd, *J* = 13.7, 5.6 Hz, 1H), 1.86 –1.77 (m, 1H), 1.69 (ddt, *J* = 17.3, 12.1, 7.1 Hz, 3H), 1.45 (d, *J* = 4.9 Hz, 6H), 1.41 (s, 3H), 1.23 (s, 3H), 1.16 (s, 3H) ppm.

^{13}C-NMR (176 MHz, $CDCl_3$) δ 196.24, 151.67, 144.98, 99.27, 76.08, 75.61, 64.00, 41.22, 39.01, 37.32, 26.45, 26.33, 26.08, 25.17, 24.92, 24.87, 18.18 ppm.

IR (neat): ν = 3515, 2988, 2944, 2899, 1739, 1670, 1638, 1457, 1286, 1221, 1208, 1157, 863 cm^{-1}.

HRMS (ESI, *m*/*z*): $[M–H]^-$ calcd. for $C_{18}H_{27}O_4$, 307.1915; found 307.1916.

M.p. = 184°C

$[\alpha]_D^{22}$ –119.1 (c = 1.00, MeOH)

Synthesis of adduct 2-31

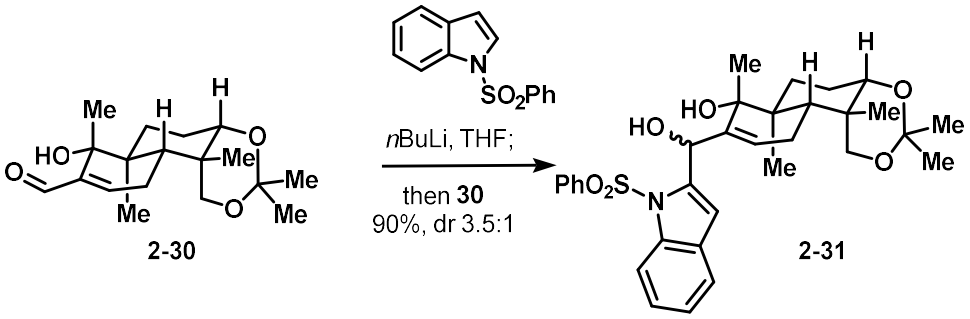

Trace water was removed from 1-(phenylsulfonyl)-1*H*-indole (1.17 g, 4.55 mmol, 3.50 equiv) via azeotropic distillation with benzene. Then, it was dissolved in THF (30.0 mL) and cooled to –78°C. A solution of *n*BuLi (2.80 ml of a 1.60 M solution in pentane, 4.49 mmol, 3.45 equiv) was added dropwise. The yellow solution was stirred at 0 °C for 1 h. During this time, trace water was removed from aldehyde **2-30** (400 mg, 1.30 mmol, 1.00 equiv) via azeotropic distillation with benzene. Then it was dissolved in THF (8.00 mL) and added via cannula transfer into the solution containing the 2-lithio-indole over the course of 5 minutes at –78°C. After stirring the resulting solution at –78°C for 1 h, the solution was warmed to 0 °C and stirred additional 1 h before being quenched with sat. aq. NH_4Cl. The aq. layer was extracted three times with EtOAc and the combined organic layers were washed with sat. aq. NaCl, dried over $MgSO_4$, filtered, and concentrated. The residue was purified via gradient flash chromatography (Yamazen, eluting with 46–67% EtOAc in hexanes) to yield a mixture of diastereomers of alcohol **2-31** as a yellow foam (661 mg, 90% combined yield, *dr* = 3.5:1) which was used in the next reaction. Analytical samples were prepared via gradient flash chromatography (Yamazen, eluting with 39–59% EtOAc in hexanes).

Major isomer:

R_f = 0.35 (Hexane:EtOAc = 1:1), UV-active, blue spot (CAM).

^{1}H-NMR (700 MHz, $CDCl_3$) δ = 8.16 (d, *J* = 8.4 Hz, 1H), 7.80–7.75 (m, 2H), 7.56–7.50 (m, 2H), 7.45–7.39 (m, 2H), 7.34–7.30 (m, 1H), 7.27 (t, *J* = 7.5 Hz, 1H), 6.94 (s, 1H), 6.19 (s, 1H), 5.15 (dd, *J* = 4.8, 2.5 Hz, 1H), 4.07 (d, *J* = 11.5 Hz, 2H), 3.56 (dd, *J* = 7.7, 3.1 Hz, 1H), 3.20 (d, *J* = 11.4 Hz, 1H), 2.33 (s, 1H), 2.02–1.91 (m, 2H), 1.79–1.62 (m, 6H), 1.59 (s, 3H), 1.45 (s, 3H), 1.41 (s, 3H), 1.28 (s, 1H), 1.21 (s, 3H), 1.17 (s, 3H) ppm.

^{13}C-NMR (176 MHz, CDCl3) δ = 142.2, 142.0, 138.6, 137.5, 133.7, 129.5, 129.2, 126.3, 125.6, 124.6, 123.9, 121.0, 114.9, 112.4, 99.2, 79.9, 75.7, 67.9, 64.1, 60.4, 41.8, 39.7, 37.5, 27.1, 26.4, 26.0, 25.3, 25.0, 24.6, 22.8, 18.2, 14.2 ppm.

IR (neat): ν = 3460, 2986, 2933, 1447, 1372, 1173, 1091, 1020, 726, 592 cm^{-1}.

HRMS (ESI, *m/z*): $[M–H]^-$ calcd. for $C_{32}H_{38}NO_6S$, 564.2425; found 564.2422.

$[\alpha]_D^{22}$ –25.4 (c = 1.00, MeOH)

Minor isomer:

R_f = 0.33 (Hexane:EtOAc = 1:1), UV-active, blue spot (CAM).

^{1}H NMR (500 MHz, Chloroform-d) δ 8.08 (d, J = 8.3 Hz, 1H), 7.87 – 7.81 (m, 2H), 7.56 – 7.51 (m, 1H), 7.49 – 7.41 (m, 3H), 7.30 (dd, J = 7.3, 1.4 Hz, 1H), 7.24 (d, J = 7.5 Hz, 1H), 6.78 (s, 1H), 6.05 (d, J = 5.4 Hz, 1H), 5.82 (dd, J = 4.9, 2.4 Hz, 1H), 4.08 (d, J = 11.3 Hz, 1H), 3.54 (dd, J = 7.3, 3.1 Hz, 1H), 3.22 (d, J = 11.2 Hz, 1H), 2.96 (d, J = 5.6 Hz, 1H), 2.14 (dt, J = 18.2, 4.9 Hz, 1H), 1.93 (d, J = 18.0 Hz, 3H), 1.74 (dd, J = 11.7, 5.0 Hz, 2H), 1.68 – 1.59 (m, 2H), 1.44 (d, J = 16.4 Hz, 9H), 1.17 (d, J = 7.4 Hz, 6H) ppm.

^{13}C-NMR (151 MHz, $CDCl_3$): δ = 144.2, 143.5, 138.4, 137.6, 134.1, 129.5, 129.1, 126.7, 126.2, 125.1, 124.1, 121.2, 114.9, 111.3, 99.4, 78.2, 75.5, 66.2, 64.5, 42.1, 39.8, 37.7, 27.0, 26.3, 26.2, 25.3, 25.1, 24.4, 23.2, 18.7 ppm.

IR (neat): ν = 3460, 2986, 2933, 1447, 1372, 1173, 1091, 1020, 726, 592 cm^{-1}.

HRMS (ESI, *m/z*): $[M+Na]^+$ calcd. for $NaC_{32}H_{37}NO_6S$, 588.2390; found 588.2396.

$[\alpha]_D^{22}$ +31.1 (c = 0.4, MeOH)

Synthesis of triene diol 2-32

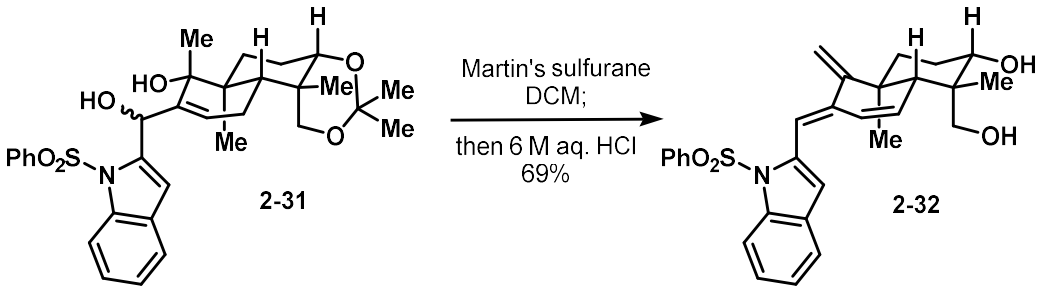

Martin's sulfurane (1.43 g, 2.12 mmol, 2.40 equiv) was added as a solid to a solution of alcohol **2-31** (500 mg, 0.885 mmol, 1.00 equiv) in DCM (8.90 mL, 0.100 M) at room temperature. After being stirred for 25 min, an aq. solution of 6 M HCl (8.90 mL) was added at 0 °C. The resulting brown solution was stirred at room temperature for 1.5 h before being quenched by the addition of sat. aq. $NaHCO_3$ at 0 °C. The mixture was warmed to room temperature and additional sat. aq. $NaHCO_3$ was added unter stirring until the gas evolution ceased. The mixture was transferred into a sep. funnel and solid NaCl was added. The aq. layer was then extracted four times with EtOAc and dried over $MgSO_4$. After removal of the solvent *in vacuo*, the crude material was purified by gradient flash chromatography (Yamazen, eluting with 50–70% EtOAc in hexanes) affording 299 mg (69%) of diol **2-32** as an orange foam.

R_f = 0.21 (Hexane:EtOAc = 1:2), UV-active, blue spot (CAM).

^{1}H-NMR (700 MHz, $CDCl_3$) δ = 8.27 (d, *J* = 8.4 Hz, 1H), 7.70 (dd, *J* = 8.0, 1.3 Hz, 2H), 7.50 (t, *J* = 7.5 Hz, 1H), 7.46 (d, *J* = 7.7 Hz, 1H), 7.37–7.31 (m, 2H), 7.27 (t, *J* = 7.5 Hz, 1H), 7.08 (s, 1H), 6.58 (s, 1H), 6.55 (dd, *J* = 10.1, 3.3 Hz, 1H), 5.90 (dd, *J* = 10.1, 2.1 Hz, 1H), 5.32 (s, 1H), 4.86 (s, 1H), 4.30 (d, *J* = 11.6 Hz, 1H), 3.62 (dd, *J* = 11.5, 4.8 Hz, 1H), 3.41 (d, *J* = 11.6 Hz, 1H), 2.26 (s, 1H), 2.07–2.01 (m, 1H), 1.99 (dq, *J* = 9.1, 4.1 Hz, 1H), 1.88 (dt, *J* = 13.1, 3.5 Hz, 1H), 1.81 (td, *J* = 13.3, 3.8 Hz, 1H), 1.34 (s, 3H), 1.06 (s, 3H) ppm.

^{13}C-NMR (125 MHz, $CDCl_3$): δ = 156.7, 138.6, 138.5, 137.2, 137.1, 133.7, 131.1, 130.1, 129.1, 126.7, 125.9, 125.1, 124.2, 120.7, 115.3, 115.1, 113.6, 105.8, 76.7, 71.1, 47.6, 42.0, 40.2, 33.9, 27.5, 20.1, 11.6 ppm.

IR (neat): ν = 3386, 2960, 2919, 1449, 1371, 1174, 1120, 1090, 725, 570 cm^{-1}.

HRMS (ESI, *m*/*z*): $[M–H]^-$ calcd. for $C_{29}H_{28}NSO_4$, 488.1901; found 488.1897.

$[\alpha]_D^{22}$ –148.0 (c = 1.00, MeOH)

Synthesis of aldehyde 2-33

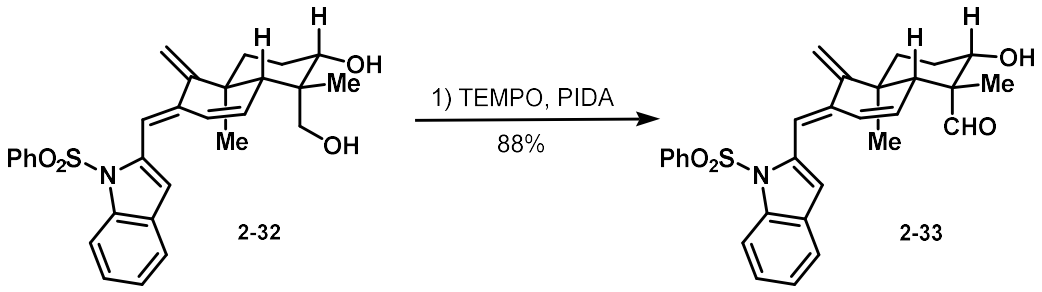

To a solution of diol **2-32** (210 mg, 0.440 mmol, 1.00 equiv) in DCM (3.60 mL) and H_2O (3.60 mL) was added TEMPO (89.0 mg, 0.570 mmol, 1.30 equiv), followed by PIDA (183 mg, 0.570 mmol, 1.30 equiv) as solids in one portion. The resulting orange-brown mixture was vigorously stirred for 4 h at room temperature before being quenched by the addition of sat. aq. $NaHCO_3$ and sat. aq. NaS_2O_3 (ca. 4:1). The mixture was transferred into a sep. funnel and solid NaCl was added. The aq. layer was then extracted four times with EtOAc, washed with sat. aq. NaCl, dried over $MgSO_4$, and filtered. After removal of the solvent *in vacuo*, the crude material was purified by gradient flash chromatography (Yamazen, eluting with 30–50% EtOAc in hexanes) affording aldehyde **2-33** (185 mg, 88%) as a pale orange foam.

R_f = 0.18 (Hexane:EtOAc = 2:1), UV-active, blue spot (CAM)

^{1}H NMR (600 MHz, $CDCl_3$) δ = 9.77 (s, 1H), 8.24 (d, *J* = 8.5 Hz, 1H), 7.67 (d, *J* = 7.9 Hz, 2H), 7.47 (t, *J* = 7.5 Hz, 1H), 7.44 (d, *J* = 7.9 Hz, 1H), 7.32 (dt, *J* = 14.9, 7.8 Hz, 3H), 7.24 (d, *J* = 7.6 Hz, 1H), 7.11 (s, 1H), 6.64-6.58 (m, 1H), 6.57 (s, 1H), 6.08 (d, *J* = 10.2 Hz, 1H), 5.39 (s, 1H), 4.92 (s, 1H), 3.35 (s, 1H), 3.22 (d, *J* = 10.3 Hz, 1H), 2.32 (s, 1H), 2.12 (dt, *J* = 13.9, 4.2 Hz, 1H), 2.05–1.96 (m, 1H), 1.92–1.86 (m, 1H), 1.80 (td, *J* = 13.4, 3.7 Hz, 1H), 1.39 (s, 3H), 1.32–1.21 (m, 1H), 0.98 (s, 3H).

^{13}C-NMR (151 MHz, CDCl3) δ = 207.5, 154.8, 138.4, 137.7, 137.1, 136.5, 133.6, 129.9, 128.9, 128.2, 126.5, 126.1, 125.1, 124.0, 120.6, 116.0, 115.1, 113.5, 106.9, 53.4, 52.2, 39.9, 34.0, 28.6, 19.1, 18.9 ppm.

IR (neat): ν = 3536, 2976, 2932, 2919, 1734, 1448, 1371, 1173, 1119, 1074, 724, 507 cm^{-1}.

HRMS (ESI, *m*/*z*): $[M–H]^-$ calcd. for $C_{29}H_{28}NSO_4$, 486.1745; found 486.1741.

$[\alpha]_D^{22}$ –125.6 (c = 1.00, MeOH)

Synthesis of carbazole 2-34

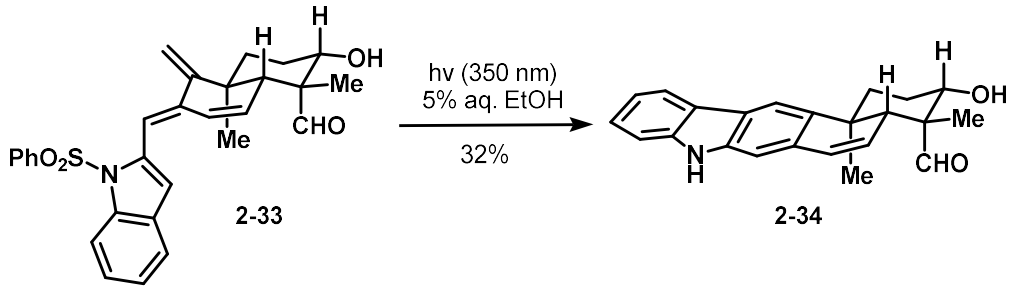

A pyrex glass tube (11 cm tall, 1 cm diameter), equipped with a screw cap, was charged with a solution of aldehyde **2-33** (90.0 mg, 0.184 mmol, 1.00 equiv) in 5% aq. ethanol (9.00 mL, 20.0 mM). The vessel was degassed by bubbling a stream of nitrogen through the solution for 45 min. The mixture was then irradiated for 4 h with UV-A light (350 nm) in a Luzchem photobox at room temperature. After reducing the EtOH *in vacuo*, the residue was dissolved in EtOAc and sat. aq. NaCl. The aq. layer was extracted four times with EtOAc and the combined organic layers were dried over $MgSO_4$, filtered and concentrated *in vacuo* the crude material was purified by gradient flash chromatography (Yamazen, eluting with 13–42% EtOAc in Hexanes) provided 20 mg (36%) of carbazole **2-34** as a white foam.

R_f = 0.20 (Hexane:EtOAc = 2:1), UV-active, blue spot (CAM).

^{1}H-NMR (400 MHz, $CDCl_3$): δ = 9.96 (s, 1H), 8.06–8.02 (m, 2H), 7.88 (s, 1H), 7.39 (m 2H), 7.26 – 7.22 (m, 1H), 7.12 (s, 1H), 6.78 (dd, *J* = 9.7, 3.2 Hz, 1H), 6.28 (dd, *J* = 9.7, 2.7 Hz, 1H), 3.41 (s, 2H), 2.49 (dt, *J* = 12.7, 3.3 Hz, 1H), 2.37 (t, *J* = 3.0 Hz, 1H), 2.19 (dd, *J* = 13.0, 4.0 Hz, 1H), 2.10 – 2.00 (m, 1H), 1.94 (td, *J* = 13.5, 13.1, 3.6 Hz, 1H), 1.43 (s, 3H), 1.02 (s, 3H).

^{13}C-NMR (101 MHz, CD_3OD): δ = 208.0, 140.0, 138.0, 138.0, 130.8, 130.3, 125.7, 125.1, 123.4, 122.9, 120.0, 119.5, 114.1, 110.6, 108.9, 52.0, 51.1, 37.8, 34.7, 28.8, 20.8, 19.0.

IR (neat): ν = 3294, 2937, 2825, 1717, 1242, 1023, 716 cm^{-1}.

HRMS (ESI, *m*/*z*): $[M–H]^-$ calcd. for $C_{23}H_{22}NO_2$, 344.1656; found 344.1654.

$[\alpha]_D^{22}$ –181.1 (c = 1.00, MeOH)

Synthesis of carbazole acid 2-35

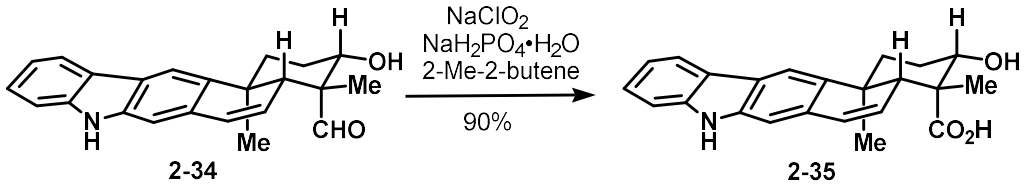

To a solution of the aldehyde **2-34** (20 mg, 0.058 mmol, 1.0 equiv) in acetone (900 µL), H_2O (450 µL), and 2-Me-2-butene (152 µL, 3.16 mmol, 25.0 equiv) was added a mixture of $NaClO_2$ (36.5 mg, 0.406 mmol, 7.00 equiv, ~90% techn.) and $NaH_2PO_4•H_2O$ (80.0 mg, 0.578 mmol, 10.0 equiv) at 0 °C. The mixture was warmed to room temperature and stirred for 2 h before being quenched by the addition of sat. aq. NaCl and sat. aq. NH_4Cl (ca. 1:1). The mixture was transferred into a sep. funnel and solid NaCl was added. The aq. layer was then extracted six times with EtOAc and dried over $MgSO_4$. After concentrating the solution *in vacuo*, the crude material was purified by gradient flash chromatography (Yamazen, eluting with 0-10% MeOH in DCM) to afford 18.8 mg (90%) of acid **2-35** as a yellow foam.

R_f = 0.25 (7% MeOH in DCM), UV-active, blue spot (CAM).

^{1}H-NMR (400 MHz, CD_3OD): δ = δ 8.00 (d, *J* = 7.8 Hz, 1H), 7.80 (s, 1H), 7.40 (d, *J* = 8.1 Hz, 1H), 7.33 (ddd, *J* = 8.1, 7.0, 1.2 Hz, 1H), 7.14 (ddd, *J* = 8.1, 7.0, 1.1 Hz, 1H), 7.09 (s, 1H), 6.60 (d, *J* = 9.9 Hz, 1H), 6.46 (d, *J* = 9.9 Hz, 1H), 3.26 (dd, *J* = 12.1, 4.3 Hz, 1H), 2.38 (dt, *J* = 13.0, 3.6 Hz, 1H), 2.28 – 2.17 (m, 2H), 1.92 (dt, *J* = 12.8, 3.8 Hz, 1H), 1.80 – 1.70 (m, 1H), 1.49 (s, 3H), 1.24–1.28 (m, 1H), 1.04 (s, 3H).

^{13}C NMR (101 MHz, CD_3OD):δ = 180.5, 141.9, 140.0, 139.1, 132.2, 129.8, 128.2, 126.2, 124.7, 123.6, 120.6, 119.6, 114.9, 111.6, 109.4, 78.9, 52.7, 39.3, 36.3, 29.8, 24.1, 21.2.

IR (neat): ν = 3403, 2982, 2970, 1736, 1478, 1372, 1244, 1042 cm^{-1}.

HRMS (ESI, *m/z*): $[M–H]^-$ calcd. for $C_{23}H_{22}NO_3$, 360.1605; found 360.1601.

$[\alpha]_D^{22}$ –123.1 (c = 1.00, MeOH)

Synthesis of oridamycin A (2-2)

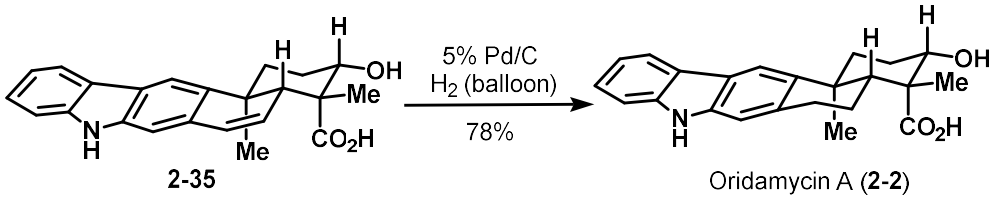

Hydrogen from a balloon was bubbled through a mixture of crude carbazole **2-35** and 5% Pd/C (32.7 mg, 0.308 mmol, 2.00 equiv) in MeOH (0.900 mL) for 1 min. The mixture was then vigorously stirred under an atmosphere of hydrogen (balloon) for 3.5 h at room temperature. After filtering the mixture through celite (EtOAc/MeOH eluent), the solution was concentrated *in vacuo* and the crude material was purified by preparative thin layer chromatography (10% MeOH in DCM) to afford 10.7 mg (20%, 3 steps) of oridamycin A (**2-2**) as a pale yellow solid.
$\mathbf{R_f}$ = 0.25 (7% MeOH in DCM), UV-active, blue spot (CAM).

^{1}H-NMR (700 MHz, CD_3OD) δ = 7.96 (d, *J* = 8.0 Hz, 1H), 7.96 (s, 1H), 7.34 (d, *J* = 8.0 Hz, 1H), 7.28 (t, *J* = 7.6 Hz, 1H), 7.08 (d, *J* = 7.6 Hz, 1H), 7.07 (s, 1H), 3.26 (d, *J* = 11.5 Hz, 1H), 3.10 (dd, *J* = 16.2, 4.6 Hz, 1H), 2.98 (ddd, *J* = 16.2, 4.6 Hz, 1H), 2.60 (dd, *J* = 13.2, 2.0 Hz, 1H), 2.34 (d, *J* = 13.2 Hz, 1H), 2.25 (dd, *J* = 13.9, 6.0 Hz, 1H), 2.20-2.15 (m, 1H), 1.98-1.92 (m, 1H), 1.65–1.60 (m, 1H), 1.54 (m, 1H), 1.51 (s, 3H), 1.29 (s, 3H) ppm.

^{13}C NMR (176 MHz, CD_3OD):δ = 181.0, 142.0, 140.3, 140.1, 134.5, 126.1, 124.6, 123.2, 120.6, 119.3, 117.5, 111.4, 110.7, 79.0, 54.0, 49.9, 39.9, 39.6, 34.0, 30.2, 24.8, 24.5, 22.5.

IR (neat): ν = 3412, 2980, 1695, 1465, 1259, 1089 cm^{-1}.

HRMS (ESI, *m/z*): $[M–H]^-$ calcd. for $C_{23}H_{24}NO_3$, 362.1762; found 362.1756.

M.p. = 183 °C lit.[2c] **M.p.** = 180 °C.

$[\alpha]_D^{22}$ +100.3 (c = 0.4, MeOH) lit[6]: **$[\alpha]_D^{30}$** +93.3 (c = 0.2, MeOH)

Chemical Shifts of ^{1}H-NMR for Natural and Synthetic Xiamycin A (2-1)

Sarpong **(700 MHz, CD_3OD)**	**Natural[1c]** **(500 MHz, CD_3OD)**	**Ang Li[2a]** **(400 MHz, CD_3OD)**
7.97 (d, *J* = 8.0 Hz, 1H)	7.96 (d, *J* = 8.0 Hz, 1H)	7.97 (d, *J* = 8.0 Hz, 1H)
7.94 (s, 1H)	7.91 (s, 1H)	7.93 (s, 1H)
7.35 (d, *J* = 8.0 Hz, 1H)	7.35 (d, *J* = 8.0 Hz, 1H)	7.35 (d, *J* = 8.0 Hz, 1H)
7.29 (t, *J* = 7.9 Hz, 1H)	7.28 (dt, *J* = 7.0, 1.0 Hz, 1H)	7.29 (t, *J* = 7.2 Hz, 1H)
7.09 (t, *J* = 7.5 Hz, 1H)	7.08 (dt, *J* = 7.0, 1.0 Hz, 1H)	7.09 (d, *J* = 7.2 Hz, 1H)
7.07 (s, 1H)	7.07 (s, 1H)	7.06 (s, 1H)
4.10 (dd, *J* = 10.5, 7.5 Hz, 1H)	4.09 (dd, *J* = 10.5, 7.5 Hz, 1H)	4.10 (dd, *J* = 10.4, 7.3 Hz, 1H)
3.15–3.08 (m, 1H) 3.08–2.99 (m, 1H)	3.09 (m, 2H)	3.15–3.01 (m, 1H) 3.11–2.96 (m, 1H)
2.64 (d, *J* = 12.8 Hz, 1H)	2.58 (dt, *J* = 13.1, 1.5 Hz, 1H)	2.62 (dd, *J* = 13.2, 3.0, 1H)
2.14 (d, *J* = 11.8 Hz, 1H)	2.18 (dd, *J* = 12.6, 2.3 Hz, 1H)	2.16 (dd, *J* = 12.4, 1.8 Hz, 1H)
2.08–1.98 (m, 1H)	2.00 (qd, *J* = 12.6, 7.3 Hz, 1H)	2.08–1.95 (m, 1H)
1.93–1.88 (m, 2H)	1.90 (m, 1H) 1.86 (qd, *J* = 13.1, 2.9 Hz, 1H)	1.93–1.89 (m, 1H) 1.89–1.85 (m, 1H)
1.78–1.72 (m, 1H)	1.76 (dt, *J* = 12.3, 6.7 Hz, 1H)	1.78–1.70 (m, 1H)
1.58–1.53 (m, 1H)	1.56 (m, 1H)	1.54 (dd, *J* = 13.0, 7.2 Hz, 1H)

1.30 (s, 3H)	1.28 (s, 3H)	1.29 (s, 3H)
1.25 (s, 3H)	1.23 (s, 3H)	1.24 (s, 3H)

Chemical Shifts of ^{13}C-NMR for Natural and Synthetic Xiamycin A (2-1)

Sarpong (176 MHz, CD_3OD)	**Natural[1c] (151 MHz, CD_3OD)**	**Ang Li[2a] (101 MHz, CD_3OD)**
181.3	181.3	181.2
142.0	142.0	142.0
141.8	141.8	141.8
140.1	140.1	140.1
134.0	134.0	134.0
126.0	126.0	126.0
124.6	124.7	124.7
123.1	123.1	123.1
120.6	120.5	120.6
119.3	119.3	119.3
116.4	116.3	116.3
111.4	111.5	111.4
110.8	110.8	110.8
76.3	76.3	76.3
54.9	54.9	54.9
47.9	47.9	47.9
39.0	39.0	39.0
38.3	38.3	38.3
32.1	32.0	32.0
28.7	28.6	28.6

26.3	26.3	26.3
22.6	22.6	22.6
11.4	11.4	11.4

Chemical Shifts of ^{1}H-NMR for Natural and Synthetic Xiamycin C (2-3)

Sarpong **(600 MHz, CD_3OD)**	**Natural[1d]** **(500 MHz, CD_3OD)**
8.00 (d, *J* = 7.7 Hz, 1H)	8.00 (d, *J* = 8.0 Hz, 1H)
7.94 (s, 1H)	7.94 (s, 1H)
7.58 (s, 1H)	7.58 (s, 1H)
7.37 (d, *J* = 8.0 Hz, 1H)	7.38 (d, *J* = 8.0 Hz, 1H)
7.31 (dd, *J* = 7.9, 8.0 Hz, 1H)	7.31 (dd, *J* = 8.0, 8.0 Hz, 1H)
7.10 (d, *J* = 7.9, 8.0 Hz 1H)	7.10 (dd, *J* = 8.0, 8.0 Hz, 1H)
4.89 (m, 1H)	4.91 (dd, *J* = 10.0, 7.5 Hz, 1H)
4.09 (dd, *J* = 8.0, 6.6 Hz, 1H)	4.08 (dd, *J* = 8.0, 6.5 Hz, 1H)
2.63 (ddd, *J* = 13.2, 3.4, 3.2, Hz, 1H)	2.62 (ddd, *J* = 13.0, 3.5, 3.5 Hz, 1H)
2.19 (d, *J* = 12.6 Hz, 1H)	2.20 (dd, *J* = 12.0, 2.0 Hz, 1H)
2.09 – 1.95 (m, 2H)	1.97 (m, 2H)
1.93 – 1.82 (m, 3H)	1.93 (m, 1H)
	1.89 (m, 2H)
1.75 – 1.65 (m, 1H)	1.70 (m, 1H)
1.38 (s, 3H)	1.38 (s, 3H)
1.26 (s, 3H)	1.26 (s, 3H)

Chemical Shifts of ^{13}C-NMR for Natural and Synthetic Xiamycin C (2-3)

Sarpong **(176 MHz, CD_3OD)**	**Natural[1d]** **(125 MHz, CD_3OD)**
180.4	182.0
142.3	142.4
142.1	141.7
140.1	140.2
137.9	137.6
126.3	126.4
124.5	124.4
124.0	124.1
120.8	120.8
119.3	119.4
116.3	116.3
111.5	111.6
110.1	110.1
76.8	76.3
72.3	72.2
55.1	54.8

46.0	46.1
39.2	39.2
39.0	39.0
33.3	33.2
28.4	28.5
26.9	26.8
12.7	11.9

Chemical Shifts of ^{1}H-NMR for Natural and Synthetic Xiamycin F (2-4)

Sarpong **(700 MHz, CD_3OD)**	**Natural[1E]** **(500 MHz, CD_3OD)**
8.16–8.13 (d, *J* = 7.6 Hz, 1H)	8.16 (d, *J* = 8.0 Hz, 1H)
8.12 (s, 1H)	8.12 (s, 1H)
8.05 (s, 1H)	8.06 (s, 1H)
7.47–7.42 (m, 2H)	7.47 (m, 1H) 7.47 (m, 1H)
7.19 (td, *J* = 6.8, 2.0 Hz, 1H)	7.20 (m, 1H)
4.13–4.06 (m, 1H)	4.13 (m, 1H)
2.91 (t, *J* = 15.9 Hz, 1H)	2.96 (m, 1H)
2.72–2.64 (m, 2H)	2.73 (m, 2H) 2.67 (m, 1H)
2.57 (d, *J* = 11.8 Hz, 1H)	2.43 (d, *J* = 17.5 Hz, 1H)
1.98–1.90 (m, 3H)	1.96 (m, 2H) 1.94 (m, 1H)
1.35 (s, 3H)	1.39 (s, 3H)
1.30 (s, 3H)	1.33 (s, 3H)

Chemical Shifts of ^{13}C-NMR for Natural and Synthetic Xiamycin F (2-4)

Sarpong (176 MHz, CD_3OD)	Natural[1E] (150 MHz, CD_3OD)
201.1	201.3
180.1	180.0
147.7	147.5
144.0	143.9
139.6	139.6
130.1	130.2
129.4	129.5
128.8	128.6
123.8	123.8
122.3	122.2
120.4	120.3
116.2	116.1
112.3	112.2
110.7	110.7
76.0	76.8
54.3	54.3
46.9	46.8

38.8	38.7
38.7	38.2
38.3	38.2
28.4	28.3
24.9	24.8
11.2	11.2

Chemical Shifts of ^{1}H-NMR for Natural and Synthetic Xiamycin H (2-5)

Sarpong **(700 MHz, CD_3OD)**	**Natural[1E]** **(500 MHz, CD_3OD)**
8.16 (s)	8.16 (s)
8.06 (d, *J* = 7.9 Hz, 1H)	8.07 (d, *J* = 8.0 Hz, 1H)
7.42 (d, *J* = 8.1 Hz, 1H)	7.43 (d, *J* = 7.8 Hz, 1H)
7.36 (t, *J* = 7.5 Hz, 1H)	7.36 (ddd, *J* = 8.4, 7.2, 1.2 Hz, 1H)
7.35 (s, 1H)	7.35 (s, 1H)
7.15 (t, *J* = 7.5 Hz, 1H)	7.15 (ddd, *J* = 8.4, 7.2, 1.2 Hz, 1H)
7.05 (d, *J* = 9.8 Hz, 1H)	7.05 (d, *J* = 9.6 Hz, 1H)
6.76 (d, *J* = 9.8 Hz, 1H)	6.76 (d, *J* = 9.6 Hz, 1H)
2.98 (m, 1H)	2.98 (m, 1H)
2.85 (m, 1H)	2.85 (m, 1H)
2.66 (m, 1H)	2.67 (m, 1H)
2.35 (m, 1H)	2.35 (m, 1H)
1.92 (s, 3H)	1.92 (s, 3H)
1.49 (s, 3H)	1.49 (s, 3H)

Chemical Shifts of ^{13}C-NMR for Natural and Synthetic Xiamycin H (2-5)

Sarpong **(176 MHz, CD_3OD)**	**Natural[1E]** **(151 MHz, CD_3OD)**
200.5	200.7
160.2	160.2
156.3	142.6
140.1	139.5
137.8	138.0
136.6	136.7
130.1	130.3
129.4	129.4
127.0	127.2
125.1	125.8
124.3	124.4
123.4	123.6
121.1	121.2
120.2	120.2
116.5	116.7
111.8	112.0
111.8	112.0

40.6	40.7
35.1	35.2
34.9	35.0
31.3	31.4
10.6	10.7

Chemical Shifts of ^{1}H-NMR for Natural and Synthetic Oridamycin A (2-2)

Sarpong **(700 MHz, CD_3OD)**	**Natural[1B]** **(600 MHz, CD_3OD)**	**Ang Li[2A]** **(400 MHz, CD_3OD)**
7.96 (d, *J* = 8.0 Hz, 1H)	7.93 (d, *J* = 8.0 Hz, 1H)	7.96 (d, *J* = 8.0 Hz, 1H)
7.96 (s, 1H)	7.93 (s, 1H)	7.95 (s, 1H)
7.34 (d, *J* = 8.0 Hz, 1H)	7.32 (d, *J* = 8.0 Hz, 1H)	7.34 (d, *J* = 8.0 Hz, 1H)
7.28 (t, *J* = 7.6 Hz, 1H)	7.25 (dt, *J* = 8.1, 1.4 Hz, 1H)	7.28 (t, *J* = 7.6 Hz, 1H)
7.08 (d, *J* = 7.6 Hz, 1H)	7.05 (dt, *J* = 8.1, 1.4 Hz, 1H)	7.08 (d, *J* = 7.6 Hz, 1H)
7.07 (s, 1H)	7.03 (s, 1H)	7.05 (s, 1H)
3.26 (d, *J* = 11.5 Hz, 1H)	3.22 (dd, *J* = 12.2, 4.6 Hz, 1H)	3.24 (dd, *J* = 12.1, 4.3 Hz, 1H)
3.10 (dd, *J* = 16.2, 4.6 Hz, 1H)	3.06 (ddd, *J* = 16.3, 5.4, 2.3, 1H)	3.08 (dd, *J* = 16.5. 4.0, 1H)
2.98 (dd, *J* = 16.5, 4.6 Hz, 1H)	2.94 (ddd, *J* = 16.3, 5.4, 2.3, 1H)	3.01–2.89 (m, 1H)
2.60 (dd, *J* = 13.2, 2.0 Hz, 1H)	2.57 (dt, *J* = 13.6, 3.6 Hz, 1H)	2.59 (dd, *J* = 13.2, 2.0, 1H)

2.38–2.31 (m, 1H)	2.30 (dq, *J* = 12.6, 2.3 Hz, 1H)	2.38–2.26 (m, 1H)
2.25 (dd, *J* = 13.9, 6.0 Hz, 1H)	2.23 (m, 1H)	2.25–2.19 (m, 1H)
2.20–2.15 (m, 1H)	2.09 (dt, *J* = 12.7, 5.4, 1H)	2.19–2.06 (m, 1H)
1.98–1.92 (m, 1H)	1.90 (qd, *J* = 13.6, 3.6 Hz, 1H)	1.97–1.89 (m, 1H)
1.65–1.60 (m, 1H)	1.58 (dt, *J* = 13.6, 4.1 Hz, 1H)	1.59 (ddd, *J* = 13.6, 13.6, 3.5 1H)
1.57–1.45 (m, 4H)	1.56 (m, 1H) 1.48 (s, 3H)	1.54 (dd, *J* = 13.0, 7.2 Hz, 1H) 1.49 (s, 3H)
1.29 (s, 3H)	1.26 (s, 3H)	1.27 (s, 3H)

Chemical Shifts of ^{13}C-NMR for Natural and Synthetic Oridamycin A (2-2)

Sarpong **(176 MHz, CD_3OD)**	**Natural[1b]** **(151 MHz, CD_3OD)**	**Ang Li[2a]** **(101 MHz, CD_3OD)**
181.0	181.0	181.0
142.0	142.0	142.1
140.3	140.3	140.4
140.1	140.1	140.1
134.5	134.5	134.5
126.0	126.1	126.1
124.6	124.6	124.6
123.2	123.2	123.3

120.6	120.6	120.6
119.3	119.3	119.4
117.5	117.5	117.5
111.4	111.4	111.4
110.7	110.7	110.7
79.0	79.1	79.1
54.0	54.1	54.1
49.8	49.8	49.8
39.9	40.0	40.0
39.6	39.6	39.6
34.0	34.0	34.0
30.2	30.3	30.3
24.8	24.8	24.8
24.5	24.6	24.6
22.5	22.5	22.5

Chemical Shifts of ^{1}H-NMR for Omura/Nagamitsu and Sarpong's *trans*-diol

Sarpong (600 MHz, $CDCl_3$)	**Omura/Nagamitsu[9a]** (400 MHz, $CDCl_3$)
6.64 (d, *J* = 4.8 Hz, 1H)	6.82–6.79 (m, 1H)
3.68–3.58 (m, 2H)	3.62–3.58 (m, 1H)
3.39 (d, *J* = 10.6 Hz, 1H)	3.53 (d, *J*=11.2 Hz, 1H)
3.04 (br s, 2H)	3.27 (d, *J*=11.2 Hz, 1H)
2.39–2.29 (m, 1H)	2.43–2.27 (m, 2H)
2.18 (d, *J* = 19.1 Hz, 1H)	2.01 (dd, *J*=10.9, 4.8 Hz, 1H)
1.91 (d, *J* = 14.3 Hz, 1H)	1.86 (dt, *J*=13.9, 3.4 Hz, 1H)
1.79 (dd, *J* = 11.5, 4.2 Hz, 1H), 1.75 (d, *J* = 4.0 Hz, 1H)	1.76–1.68 (m, 2H)
1.72 (s, 3H)	1.72–1.70 (m, 3H)
1.70–1.60 (m, 1H)	
1.47 (td, *J* = 13.9, 3.3 Hz, 1H)	1.47–1.39 (m, 1H)
1.06 (s, 3H)	1.07 (s, 3H)
0.99 (s, 3H)	0.85 (s, 3H)

Chemical Shifts of ^{13}C-NMR for for Nagamitsu and Sarpong *trans*-diol

Sarpong (156 MHz, $CDCl_3$)	**Omura/Nagamitsu [9a]** (101 MHz, $CDCl_3$)
205.4	207.7
143.4	146.3
133.2	133.7
75.4	72.5
69.6	65.5
44.4	45.5
42.9	44.0
42.5	42.6
31.4	32.7
26.6	27.2
24.1	24.9
17.9	18.2
16.4	16.4
11.9	12.9

Fungitoxicity assessment

The technical materials were evaluated for antifungal activity against three plant pathogens *Ustilago maydis*, *Zymoseptoria tritici* and *Magnaporthe oryzae* in 96-well microtitre plate-based growth inhibition assays. Test materials were prepared as 1 mg/ml stock solutions in DMSO and a five-fold dilution series was prepared. 2 µl of the diluted compounds were added to two replicate wells to deliver a final test concentration of 10 ppm once inoculated. Wells then received 200 µl of cells in minimal growth media containing 20 g glucose, 3 g K_2HPO_4 , 3 g KH_2PO_4 and 6.7 g yeast nitrogen base without amino acids (BD Difco, BD291920) per liter. *Z. tritici* spores were collected from a 3-day old yeast malt agar plate that is maintained at 18°C under black light for 12 hours and dark for 12 hours. *M. oryzae* spores were collected from 12 to18-day old potato dextrose agar plates supplemented with 16 g per liter rice flour and maintained at 22°C under 12 hours white fluorescent light and 12 hours dark. *U. maydis* spores were taken from a 24-hour shake flask culture in potato dextrose broth maintained at 24°C and 120 rpm. Final cell densities were 1 X 10^5 cells ml^{-1} (*Z. tritici*), 4 X 10^4 cells ml^{-1} (*M. oryzae*) and 5 X 10^4 cells ml^{-1} (*U. maydis*). Test plates were incubated in the dark for 48 hr (*U. maydis*) or 72 hr (*M. oryzae* and *Z. tritici*) at 22^{o}C (M. oryzae and Z. tritici) or 24^{o}C (*U. maydis*), and initial and final cell density readings determined using a NepheloStar nephelometer (BMG LABTECH Gmb, D-77799 Ortenberg, Germany). Percentage growth inhibition was calculated by reference to control wells containing only growth media, amended with 2 ul DMSO, and inoculum.

Summary of bioactivity

Compound	Wheat leaf blotch % Growth Inhibition (10 ppm)	Rice blast % Growth Inhibition (10 ppm)	Corn smut % Growth Inhibition (10 ppm)
Xiamycin H (**5**)	100	50	40
25	40	0	30
19Epi-Xiamycin C (**3**)	20	10	10
8a	20	0	30
20	10	10	0
21	10	0	30
7	10	10	50
15 major	5	35	15
8b	5	5	0
Xiamycin F (**4**)	0	10	10
Xiamycin C (**3**)	0	10	10
Min triene diol	0	30	0
16	0	30	0
Xiamycin A (**1)**	0	15	5
27	0	5	5
13	0	30	20
23	0	50	0

UV Absorption

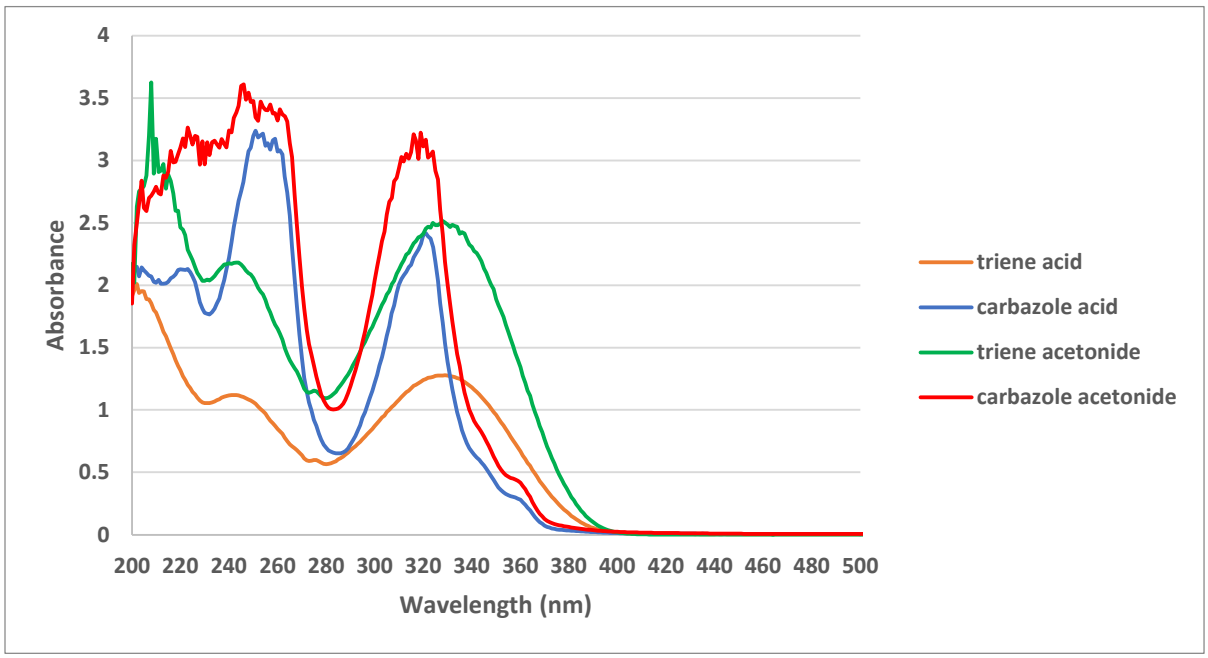

Crystallographic Data

Table 1. Crystal data and structure refinement for mp001 (CCDC 1831586)

Identification code	mp001	
Empirical formula	C14 H22 O3	
Formula weight	238.31	
Temperature	100(2) K	
Wavelength	1.54178 Å	
Crystal system	Orthorhombic	
Space group	P 21 21 21	
Unit cell dimensions	a = 7.2602(5) Å	α= 90°.
	b = 8.3489(6) Å	= 90°.
	c = 20.4643(15) Å	= 90°.
Volume	1240.44(15) $Å^3$	
Z	4	
Density (calculated)	1.276 Mg/m^3	
Absorption coefficient	0.705 mm^{-1}	
F(000)	520	
Crystal size	0.100 x 0.040 x 0.040 mm^3	
Theta range for data collection	4.321 to 68.329°.	
Index ranges	-8<=h<=8, -10<=k<=9, -24<=l<=24	
Reflections collected	18197	
Independent reflections	2259 [R(int) = 0.0248]	

Completeness to theta = 67.000°	100.0 %
Absorption correction	Semi-empirical from equivalents
Max. and min. transmission	0.753 and 0.708
Refinement method	Full-matrix least-squares on F^2
Data / restraints / parameters	2259 / 0 / 165
Goodness-of-fit on F^2	1.080
Final R indices [I>2sigma(I)]	R1 = 0.0260, wR2 = 0.0722
R indices (all data)	R1 = 0.0263, wR2 = 0.0724
Absolute structure parameter	0.06(3)
Extinction coefficient	n/a
Largest diff. peak and hole	0.217 and -0.160 e.$Å^{-3}$

Table 2. Atomic coordinates (x 10^4) and equivalent isotropic displacement parameters ($Å^2$x 10^3) for mp001. U(eq) is defined as one third of the trace of the orthogonalized U^{ij} tensor.

	x	y	z	U(eq)
C(1)	5288(2)	5140(2)	5101(1)	15(1)
C(2)	7066(2)	5306(2)	5448(1)	18(1)
C(3)	7040(2)	5137(2)	6180(1)	24(1)
C(4)	8604(2)	5575(2)	5108(1)	16(1)
C(5)	8691(2)	5723(2)	4381(1)	16(1)

C(6)	6795(2)	5938(2)	4064(1)	13(1)
C(7)	5368(2)	4775(2)	4368(1)	14(1)
C(8)	5893(2)	2982(2)	4326(1)	18(1)
C(9)	3470(2)	5050(2)	4062(1)	16(1)
C(10)	3543(2)	4956(2)	3315(1)	17(1)
C(11)	4886(2)	6175(2)	3040(1)	16(1)
C(12)	6867(2)	5959(2)	3302(1)	14(1)
C(13)	7785(2)	4479(2)	2993(1)	18(1)
C(14)	8024(2)	7410(2)	3077(1)	17(1)
O(1)	3819(2)	5228(2)	5395(1)	20(1)
O(2)	4922(2)	6145(2)	2340(1)	20(1)
O(3)	7397(2)	8923(1)	3316(1)	20(1)

Table 3. Bond lengths [Å] and angles [°] for mp001.

C(1)-O(1)	1.227(2)
C(1)-C(2)	1.481(2)
C(1)-C(7)	1.530(2)
C(2)-C(4)	1.335(2)
C(2)-C(3)	1.504(2)
C(3)-H(3A)	0.9800
C(3)-H(3B)	0.9800
C(3)-H(3C)	0.9800
C(4)-C(5)	1.494(2)
C(4)-H(4)	0.9500
C(5)-C(6)	1.532(2)
C(5)-H(5A)	0.9900

C(5)-H(5B)	0.9900
C(6)-C(7)	1.550(2)
C(6)-C(12)	1.5598(19)
C(6)-H(6)	1.0000
C(7)-C(9)	1.531(2)
C(7)-C(8)	1.547(2)
C(8)-H(8A)	0.9800
C(8)-H(8B)	0.9800
C(8)-H(8C)	0.9800
C(9)-C(10)	1.531(2)
C(9)-H(9A)	0.9900
C(9)-H(9B)	0.9900
C(10)-C(11)	1.518(2)
C(10)-H(10A)	0.9900
C(10)-H(10B)	0.9900
C(11)-O(2)	1.4324(18)
C(11)-C(12)	1.546(2)
C(11)-H(11)	1.0000
C(12)-C(13)	1.540(2)
C(12)-C(14)	1.545(2)
C(13)-H(13A)	0.9800
C(13)-H(13B)	0.9800
C(13)-H(13C)	0.9800
C(14)-O(3)	1.429(2)
C(14)-H(14A)	0.9900
C(14)-H(14B)	0.9900
O(2)-H(2)	0.88(3)

O(3)-H(3)	0.84(2)
O(1)-C(1)-C(2)	121.06(13)
O(1)-C(1)-C(7)	121.75(14)
C(2)-C(1)-C(7)	117.12(13)
C(4)-C(2)-C(1)	119.58(14)
C(4)-C(2)-C(3)	123.13(15)
C(1)-C(2)-C(3)	117.28(14)
C(2)-C(3)-H(3A)	109.5
C(2)-C(3)-H(3B)	109.5
H(3A)-C(3)-H(3B)	109.5
C(2)-C(3)-H(3C)	109.5
H(3A)-C(3)-H(3C)	109.5
H(3B)-C(3)-H(3C)	109.5
C(2)-C(4)-C(5)	124.71(15)
C(2)-C(4)-H(4)	117.6
C(5)-C(4)-H(4)	117.6
C(4)-C(5)-C(6)	113.13(13)
C(4)-C(5)-H(5A)	109.0
C(6)-C(5)-H(5A)	109.0
C(4)-C(5)-H(5B)	109.0
C(6)-C(5)-H(5B)	109.0
H(5A)-C(5)-H(5B)	107.8
C(5)-C(6)-C(7)	110.92(12)
C(5)-C(6)-C(12)	113.20(12)
C(7)-C(6)-C(12)	115.52(12)
C(5)-C(6)-H(6)	105.4

C(7)-C(6)-H(6)	105.4
C(12)-C(6)-H(6)	105.4
C(1)-C(7)-C(9)	109.64(12)
C(1)-C(7)-C(8)	104.86(13)
C(9)-C(7)-C(8)	110.12(13)
C(1)-C(7)-C(6)	107.11(12)
C(9)-C(7)-C(6)	110.08(12)
C(8)-C(7)-C(6)	114.79(13)
C(7)-C(8)-H(8A)	109.5
C(7)-C(8)-H(8B)	109.5
H(8A)-C(8)-H(8B)	109.5
C(7)-C(8)-H(8C)	109.5
H(8A)-C(8)-H(8C)	109.5
H(8B)-C(8)-H(8C)	109.5
C(7)-C(9)-C(10)	111.66(12)
C(7)-C(9)-H(9A)	109.3
C(10)-C(9)-H(9A)	109.3
C(7)-C(9)-H(9B)	109.3
C(10)-C(9)-H(9B)	109.3
H(9A)-C(9)-H(9B)	107.9
C(11)-C(10)-C(9)	111.04(12)
C(11)-C(10)-H(10A)	109.4
C(9)-C(10)-H(10A)	109.4
C(11)-C(10)-H(10B)	109.4
C(9)-C(10)-H(10B)	109.4
H(10A)-C(10)-H(10B)	108.0
O(2)-C(11)-C(10)	111.80(13)

O(2)-C(11)-C(12)	109.17(12)
C(10)-C(11)-C(12)	112.95(12)
O(2)-C(11)-H(11)	107.6
C(10)-C(11)-H(11)	107.6
C(12)-C(11)-H(11)	107.6
C(13)-C(12)-C(14)	105.72(12)
C(13)-C(12)-C(11)	110.71(12)
C(14)-C(12)-C(11)	108.07(12)
C(13)-C(12)-C(6)	114.63(12)
C(14)-C(12)-C(6)	108.99(12)
C(11)-C(12)-C(6)	108.51(11)
C(12)-C(13)-H(13A)	109.5
C(12)-C(13)-H(13B)	109.5
H(13A)-C(13)-H(13B)	109.5
C(12)-C(13)-H(13C)	109.5
H(13A)-C(13)-H(13C)	109.5
H(13B)-C(13)-H(13C)	109.5
O(3)-C(14)-C(12)	114.69(13)
O(3)-C(14)-H(14A)	108.6
C(12)-C(14)-H(14A)	108.6
O(3)-C(14)-H(14B)	108.6
C(12)-C(14)-H(14B)	108.6
H(14A)-C(14)-H(14B)	107.6
C(11)-O(2)-H(2)	109.6(14)
C(14)-O(3)-H(3)	109.0(17)

Symmetry transformations used to generate equivalent atoms:

Table 4. Anisotropic displacement parameters ($Å^2 x\ 10^3$)for mp001. The anisotropic displacement factor exponent takes the form: $-2\pi^2[h^2 a^{*2} U^{11} + ... + 2\ h\ k\ a^*\ b^*\ U^{12}]$

	U^{11}	U^{22}	U^{33}	U^{23}	U^{13}	U^{12}
C(1)	20(1)	9(1)	16(1)	1(1)	0(1)	0(1)
C(2)	23(1)	13(1)	16(1)	-2(1)	-4(1)	2(1)
C(3)	28(1)	28(1)	16(1)	0(1)	-4(1)	4(1)
C(4)	19(1)	12(1)	18(1)	-1(1)	-6(1)	1(1)
C(5)	15(1)	16(1)	18(1)	1(1)	-1(1)	1(1)
C(6)	14(1)	12(1)	13(1)	-1(1)	0(1)	1(1)
C(7)	14(1)	13(1)	14(1)	0(1)	0(1)	0(1)
C(8)	21(1)	13(1)	19(1)	-1(1)	-1(1)	-2(1)
C(9)	14(1)	20(1)	16(1)	-1(1)	0(1)	-1(1)
C(10)	14(1)	21(1)	17(1)	-2(1)	-3(1)	-1(1)
C(11)	17(1)	18(1)	13(1)	-2(1)	-2(1)	1(1)
C(12)	15(1)	14(1)	12(1)	0(1)	0(1)	-1(1)
C(13)	18(1)	20(1)	17(1)	-3(1)	1(1)	2(1)
C(14)	20(1)	17(1)	14(1)	2(1)	-1(1)	-2(1)
O(1)	21(1)	22(1)	16(1)	-2(1)	4(1)	-3(1)
O(2)	23(1)	22(1)	13(1)	1(1)	-4(1)	-5(1)
O(3)	27(1)	16(1)	18(1)	1(1)	-7(1)	-1(1)

Table 5. Hydrogen coordinates ($x\ 10^4$) and isotropic displacement parameters ($Å^2 x\ 10^3$)

for mp001.

	x	y	z	U(eq)
H(3A)	8305	5050	6343	36
H(3B)	6350	4171	6300	36
H(3C)	6446	6078	6374	36
H(4)	9723	5678	5344	19
H(5A)	9280	4751	4199	19
H(5B)	9475	6652	4266	19
H(6)	6380	7035	4194	16
H(8A)	5098	2361	4619	26
H(8B)	7182	2844	4457	26
H(8C)	5732	2605	3876	26
H(9A)	3004	6116	4194	20
H(9B)	2600	4233	4229	20
H(10A)	3927	3866	3182	21
H(10B)	2300	5158	3135	21
H(11)	4452	7261	3176	19
H(13A)	8082	4707	2535	27
H(13B)	6939	3566	3015	27
H(13C)	8918	4224	3231	27
H(14A)	9313	7249	3220	20
H(14B)	8022	7442	2593	20
H(2)	4200(30)	5370(30)	2196(11)	33(6)

H(3)	7900(30)	9110(30)	3677(12)	34(6)

Table 1 Crystal data and structure refinement for IB001 (CCDC 1831587)

Identification code	IB001
Empirical formula	$C_{14}H_{24}O_4$
Formula weight	256.33
Temperature/K	100(2)
Crystal system	orthorhombic
Space group	$P2_12_12_1$
a/Å	7.21010(10)
b/Å	11.2298(3)
c/Å	16.4264(3)
α/°	90
β/°	90
γ/°	90
Volume/Å^3	1330.01(5)
Z	4
ρ_{calc}g/cm^3	1.280
μ/mm^{-1}	0.749
F(000)	560.0
Crystal size/mm^3	0.05 × 0.05 × 0.03
Radiation	CuKα (λ = 1.54184)
2Θ range for data collection/°	9.54 to 157.698
Index ranges	-9 ≤ h ≤ 9, -14 ≤ k ≤ 14, -20 ≤ l ≤ 12

Reflections collected	14075
Independent reflections	2801 [R_{int} = 0.0452, R_{sigma} = 0.0303]
Data/restraints/parameters	2801/0/182
Goodness-of-fit on F^2	1.062
Final R indexes [I>=2σ (I)]	R_1 = 0.0353, wR_2 = 0.0923
Final R indexes [all data]	R_1 = 0.0386, wR_2 = 0.0961
Largest diff. peak/hole / e $Å^{-3}$	0.20/-0.18
Flack parameter	-0.11(10)

Table 2 Fractional Atomic Coordinates (×10^4) and Equivalent Isotropic Displacement Parameters ($Å^2$×10^3) for IB001. U_{eq} is defined as 1/3 of of the trace of the orthogonalised U_{IJ} tensor.

Atom	*x*	*y*	*z*	U(eq)
O2	4401(2)	6426.1(13)	5729.1(9)	22.0(3)
O1	5088(2)	912.8(14)	6645.0(9)	24.1(3)
O3	1109(2)	6680.5(13)	6529.7(9)	23.6(3)
O4	7943(2)	7212.0(16)	5574.0(11)	28.8(4)
C4	3698(3)	2854.7(18)	6658.0(12)	17.7(4)
C5	2253(3)	3393.7(19)	6065.1(12)	17.6(4)
C14	1511(3)	5454.0(18)	6698.2(12)	20.0(4)
C7	329(3)	1559.2(19)	6301.8(13)	23.0(4)
C6	322(3)	2889.5(19)	6243.5(13)	22.2(4)
C3	3673(3)	1496.9(19)	6553.2(12)	20.8(4)
C11	4313(3)	5145.0(18)	5775.2(12)	19.2(4)
C12	2290(3)	4776.7(18)	5950.4(12)	17.6(4)
C10	5683(3)	4679.7(19)	6402.4(13)	20.7(4)

C8	3292(3)	3048.8(18)	7570.9(12)	22.0(4)
C13	1114(3)	5069(2)	5193.7(12)	22.1(4)
C9	5629(3)	3321.0(19)	6442.2(13)	20.5(4)
C2	1862(3)	902(2)	6411.6(12)	23.4(4)
C1	1844(4)	-435(2)	6422.8(15)	28.5(5)

Table 3 Anisotropic Displacement Parameters ($Å^2×10^3$) for IB001. The Anisotropic displacement factor exponent takes the form: $-2\pi^2[h^2a^{*2}U_{11}+2hka^*b^*U_{12}+\ldots]$.

Atom	U_{11}	U_{22}	U_{33}	U_{23}	U_{13}	U_{12}
O2	19.4(8)	20.2(7)	26.4(8)	4.6(6)	-1.7(6)	-2.4(6)
O1	23.0(7)	23.1(7)	26.3(7)	1.3(6)	1.9(6)	4.3(6)
O3	22.0(7)	19.3(7)	29.6(8)	0.5(6)	2.1(6)	2.8(6)
O4	22.0(8)	33.9(9)	30.4(8)	11.3(7)	-0.4(7)	0.9(7)
C4	14.8(9)	19.0(9)	19.3(9)	0.5(7)	1.3(8)	-0.3(7)
C5	15.3(9)	18.2(9)	19.2(9)	-2.3(8)	-1.0(7)	-0.2(7)
C14	19.2(9)	19.4(10)	21.4(9)	0.3(8)	0.7(8)	1.0(7)
C7	20.8(10)	23.6(10)	24.7(10)	-1.7(8)	0.8(8)	-6.3(8)
C6	17.2(10)	22.5(10)	26.8(10)	-0.4(8)	-0.7(8)	-1.5(8)
C3	21.4(10)	21.4(10)	19.7(9)	0.5(8)	1.9(8)	2.7(8)
C11	20.2(10)	18.1(9)	19.3(9)	1.9(8)	0.0(8)	-0.7(7)
C12	16.4(9)	19.6(10)	16.9(9)	-0.1(7)	-1.8(7)	0.2(8)
C10	16.0(9)	22.3(10)	23.7(10)	2.5(8)	-0.6(7)	-0.8(7)
C8	24.3(10)	22.2(10)	19.5(9)	1.1(8)	0.0(8)	-0.4(8)
C13	18.7(9)	25.2(10)	22.4(10)	2.8(8)	-3.7(8)	-0.8(8)
C9	17.5(9)	20.9(10)	23.1(10)	1.2(8)	0.3(8)	2.9(8)
C2	29.2(11)	20.9(10)	20(1)	-1.0(8)	1.8(8)	-4.2(9)

C1	36.5(12)	19.4(10)	29.7(11)	-0.1(9)	0.7(10)	-3.8(9)

Table 4 Bond Lengths for IB001.

Atom	Atom	Length/Å	Atom	Atom	Length/Å
O2	C11	1.442(2)	C14	C12	1.550(3)
O1	C3	1.222(2)	C7	C6	1.497(3)
O3	C14	1.434(2)	C7	C2	1.341(3)
C4	C5	1.550(3)	C3	C2	1.485(3)
C4	C3	1.535(3)	C11	C12	1.543(3)
C4	C8	1.543(3)	C11	C10	1.520(3)
C4	C9	1.529(3)	C12	C13	1.540(3)
C5	C6	1.532(3)	C10	C9	1.528(3)
C5	C12	1.565(3)	C2	C1	1.502(3)

Table 5 Bond Angles for IB001.

Atom	Atom	Atom	Angle/˚	Atom	Atom	Atom	Angle/˚
C3	C4	C5	108.04(16)	O2	C11	C12	108.59(16)
C3	C4	C8	104.31(16)	O2	C11	C10	110.48(16)
C8	C4	C5	115.33(16)	C10	C11	C12	113.32(16)
C9	C4	C5	109.43(16)	C14	C12	C5	112.68(16)
C9	C4	C3	108.97(16)	C11	C12	C5	107.72(16)
C9	C4	C8	110.48(17)	C11	C12	C14	111.02(16)
C4	C5	C12	116.88(16)	C13	C12	C5	107.43(16)
C6	C5	C4	110.30(16)	C13	C12	C14	109.61(16)
C6	C5	C12	113.90(16)	C13	C12	C11	108.22(16)
O3	C14	C12	113.05(16)	C11	C10	C9	110.84(16)

C2	C7	C6	124.08(19)	C10	C9	C4	112.04(16)
C7	C6	C5	112.21(17)	C7	C2	C3	119.92(19)
O1	C3	C4	120.65(18)	C7	C2	C1	123.0(2)
O1	C3	C2	120.79(19)	C3	C2	C1	117.1(2)
C2	C3	C4	118.33(17)				

Table 6 Hydrogen Atom Coordinates (Å×10^4) and Isotropic Displacement Parameters (Å^2×10^3) for IB001.

Atom	***x***	***y***	***z***	**U(eq)**
H5	2590.14	3063.95	5519.3	21
H14A	362	5054.92	6883.89	24
H14B	2424.66	5410.92	7147.05	24
H7	-824.52	1155.06	6258.24	28
H6A	-139.39	3227.14	6762.13	27
H6B	-540.35	3136.55	5805.74	27
H11	4669.65	4815.74	5231.66	23
H10A	5375.54	5012.91	6943.82	25
H10B	6950.36	4944.02	6257.08	25
H8A	3463.11	3891.5	7706.5	33
H8B	4143.69	2563.95	7896.86	33
H8C	2010.59	2814.25	7688.92	33
H13A	1500.83	4560.2	4739.71	33
H13B	1291.47	5906.6	5045.42	33
H13C	-198.36	4926.25	5314.39	33
H9A	6528.44	3041.79	6855.58	25
H9B	6008.65	2991.02	5908.75	25
H1A	567.49	-720.16	6360.58	43

H1B	2349.47	-719.42	6941.4	43
H1C	2604.35	-738.12	5973.69	43
H3	2110(50)	6990(30)	6336(18)	33(8)
H4A	8850(50)	7070(30)	5870(20)	42(9)
H2	5600(60)	6610(30)	5690(20)	59(11)
H4B	8370(50)	7720(40)	5190(20)	56(10)

Crystal structure determination of [IB001]

Crystal Data for $C_{14}H_{24}O_4$ (*M* =256.33 g/mol): orthorhombic, space group $P2_12_12_1$ (no. 19), *a* = 7.21010(10) Å, *b* = 11.2298(3) Å, *c* = 16.4264(3) Å, *V* = 1330.01(5) Å^3, *Z* = 4, *T* = 100(2) K, μ(CuKα) = 0.749 mm^{-1}, *Dcalc* = 1.280 g/cm^3, 14075 reflections measured (9.54° ≤ 2Θ ≤ 157.698°), 2801 unique (R_{int} = 0.0452, R_{sigma} = 0.0303) which were used in all calculations. The final R_1 was 0.0353 (I > 2σ(I)) and wR_2 was 0.0961 (all data).

Refinement model description

Number of restraints - 0, number of constraints - unknown.

Copies of NMR Spectra

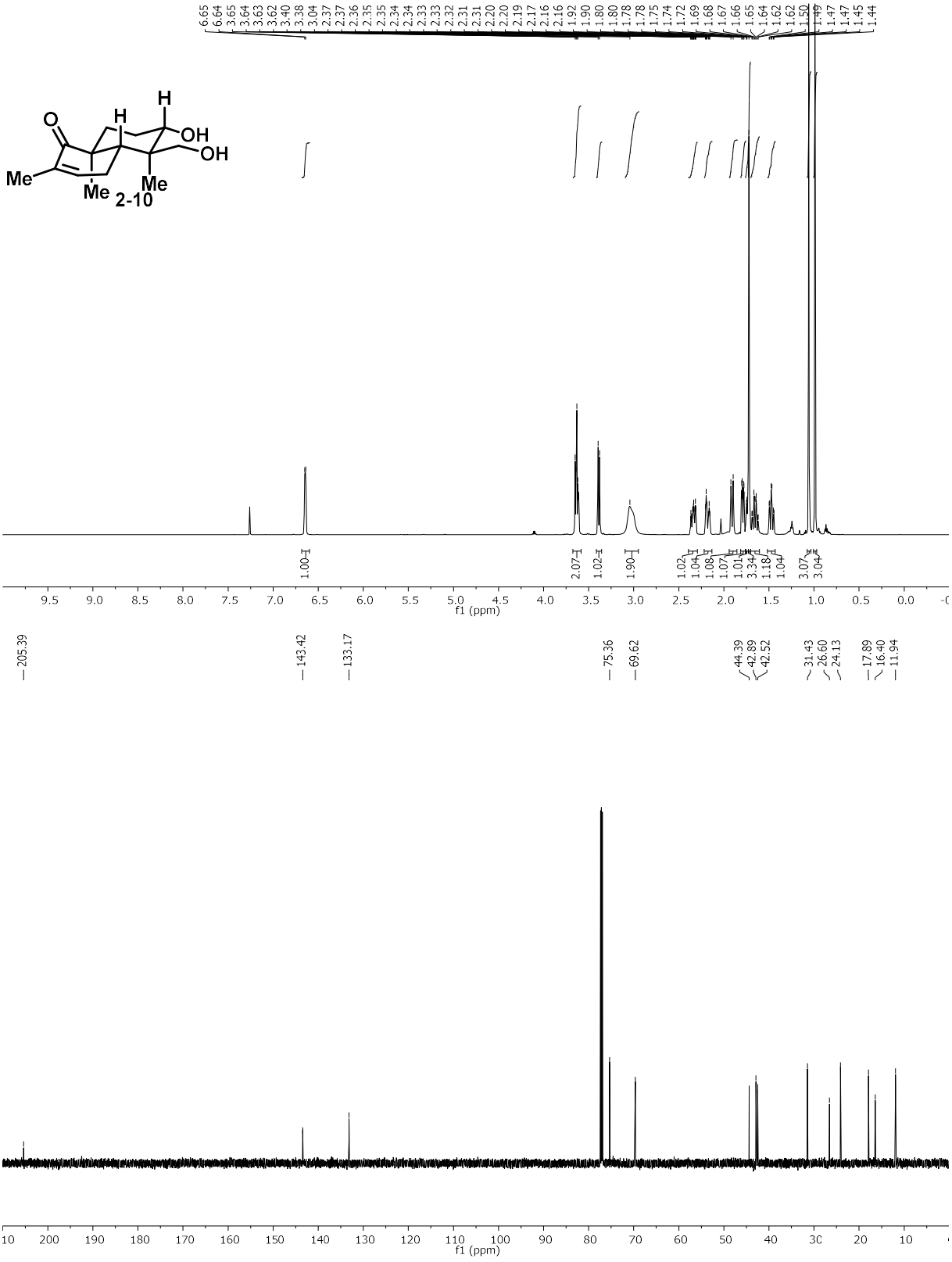

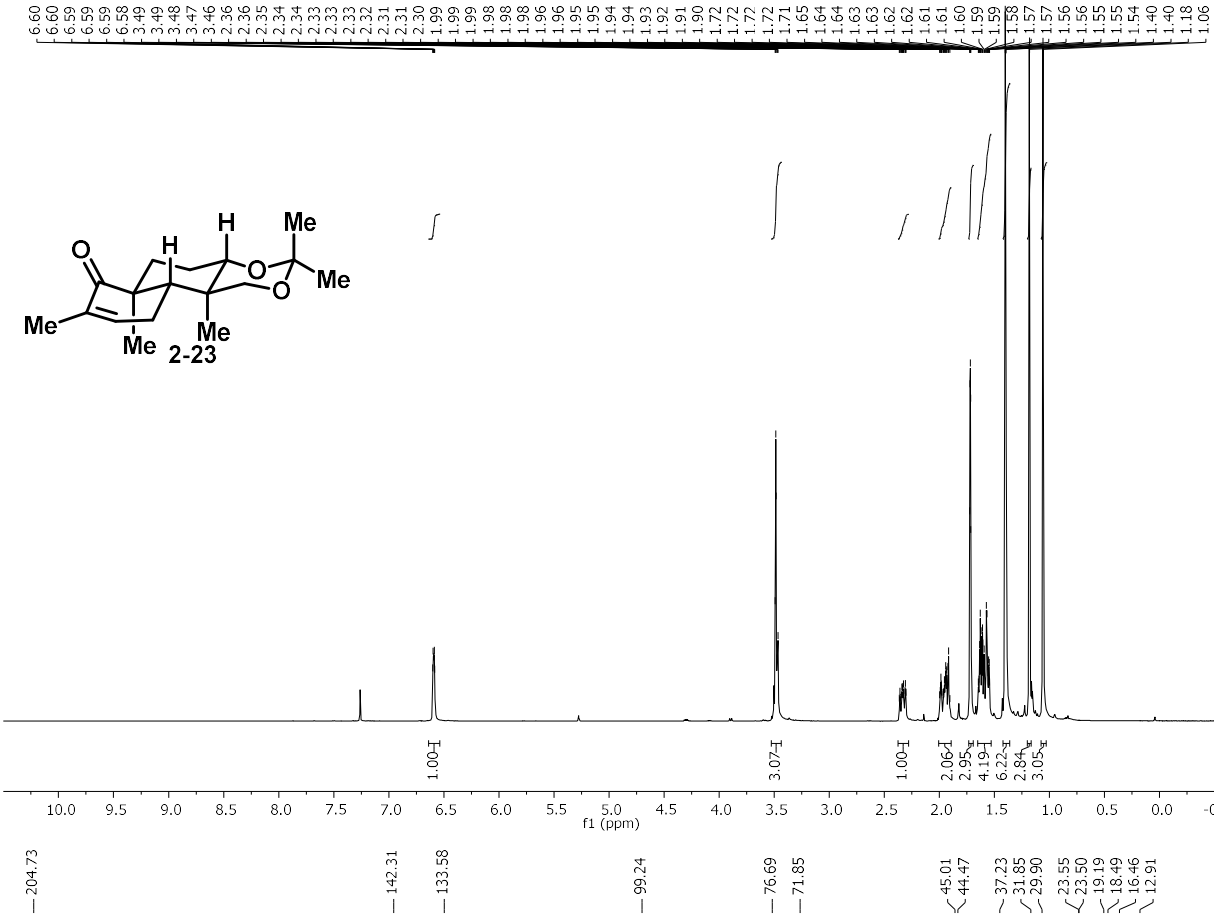
H
Me
O
H
O
Me
O
Me
Me
Me
2-23
1.00
3.07
1.00
2.06
2.95
4.19
6.22
2.84
3.05
f1 (ppm)

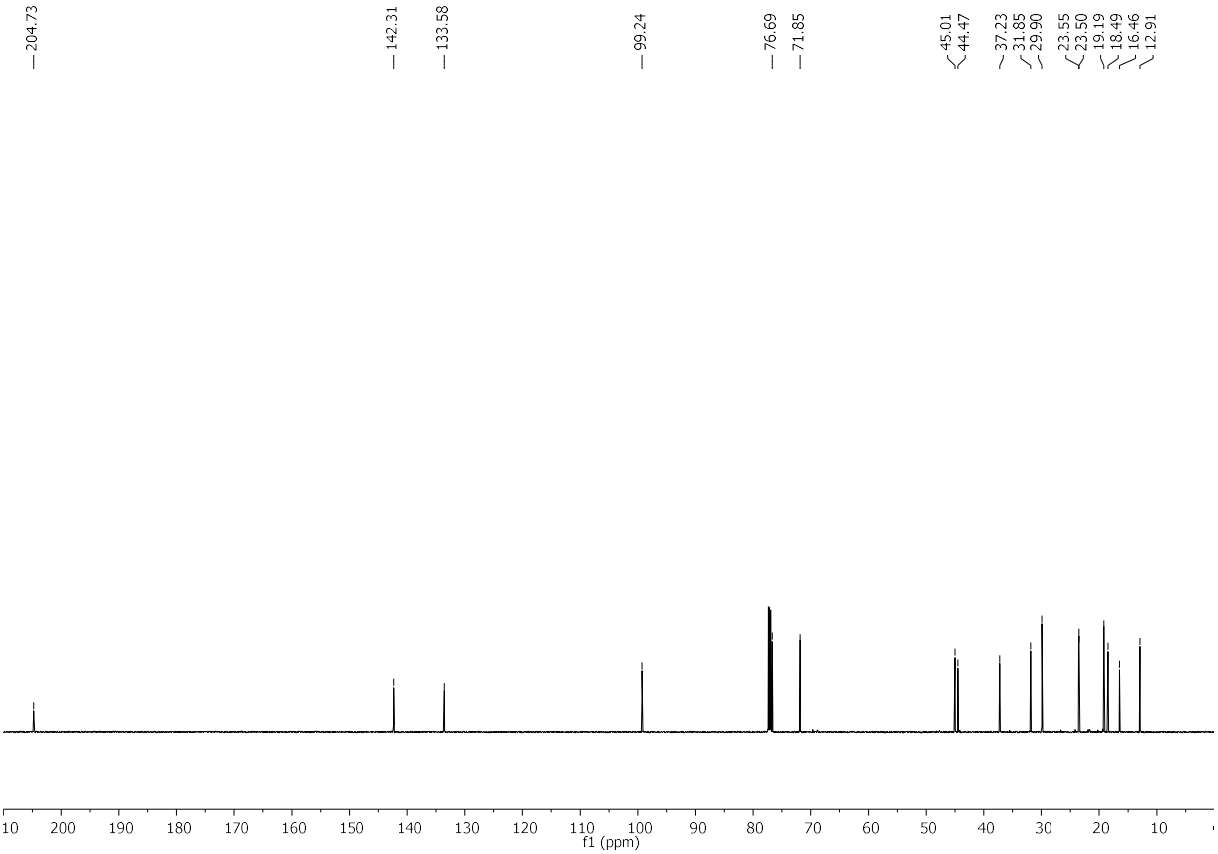
204.73
142.31
133.58
99.24
76.69
71.85
45.01
44.47
37.23
31.85
29.90
23.55
23.50
19.19
18.49
16.46
12.91
f1 (ppm)

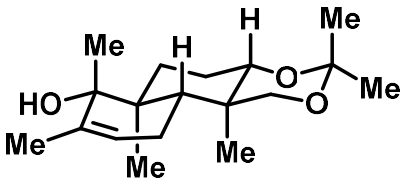
Me
H
H
Me
HO
O
O
Me
Me
Me
Me

2-20

5.29
5.29
3.51
3.51
3.49
3.48
3.46
2.00
1.99
1.98
1.97
1.97
1.96
1.94
1.94
1.93
1.70
1.70
1.68
1.68
1.67
1.65
1.64
1.63
1.62
1.55
1.54
1.52
1.51
1.51
1.45
1.42
1.30
1.23
1.18
1.03
1.00
1.07
2.01
1.02
3.46
3.84
2.21
3.09
3.13
3.09
1.04
3.17
3.05
f1 (ppm)

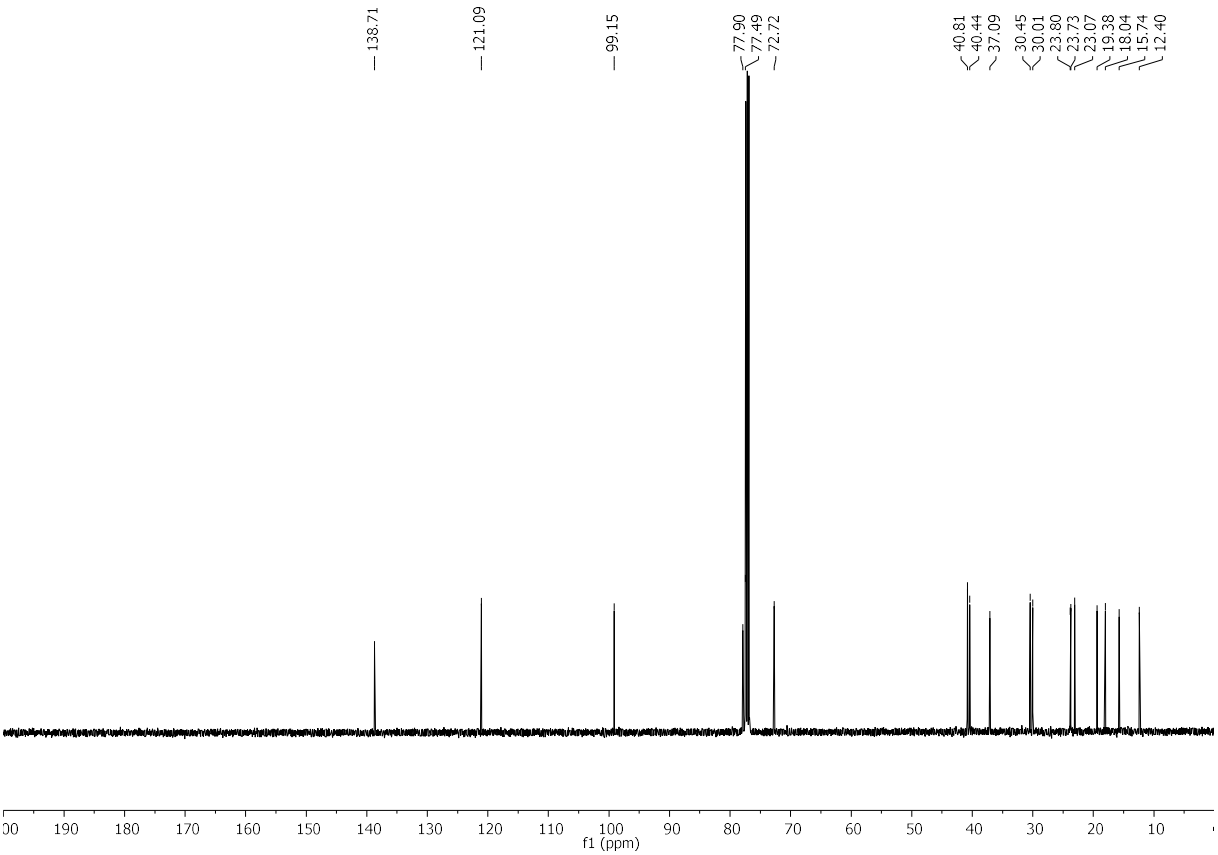
138.71
121.09
99.15
77.90
77.49
72.72
40.81
40.44
37.09
30.45
30.01
23.80
23.73
23.07
19.38
18.04
15.74
12.40
f1 (ppm)

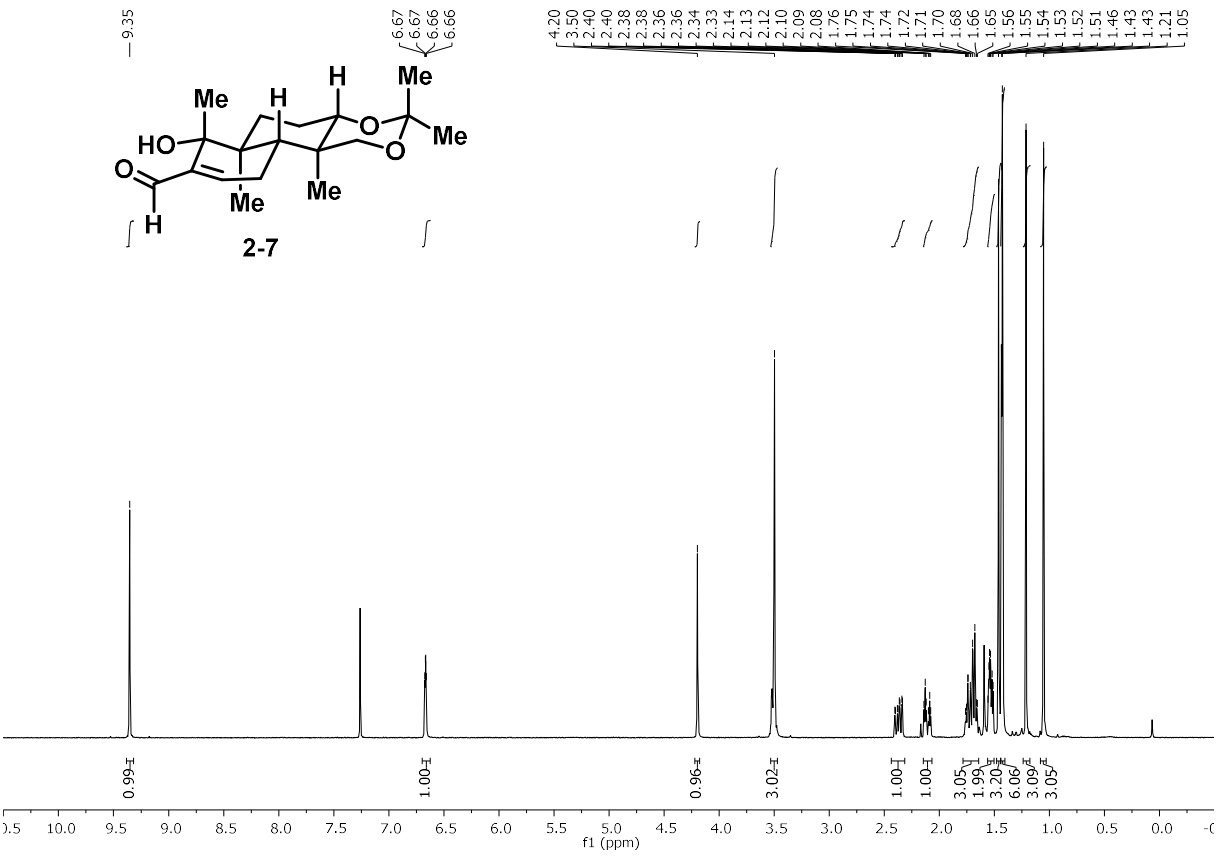
9.35
6.67
6.67
6.66
6.66
4.20
3.50
2.40
2.40
2.38
2.38
2.36
2.36
2.34
2.33
2.14
2.13
2.12
2.10
2.09
2.08
1.76
1.75
1.74
1.74
1.72
1.71
1.70
1.68
1.66
1.65
1.56
1.55
1.54
1.53
1.52
1.51
1.46
1.43
1.43
1.21
1.05
Me
H
Me
HO
O
O
Me
Me
Me
H
2-7
0.99
1.00
0.96
3.02
1.00
1.00
3.05
1.99
3.20
6.06
3.09
3.05
f1 (ppm)

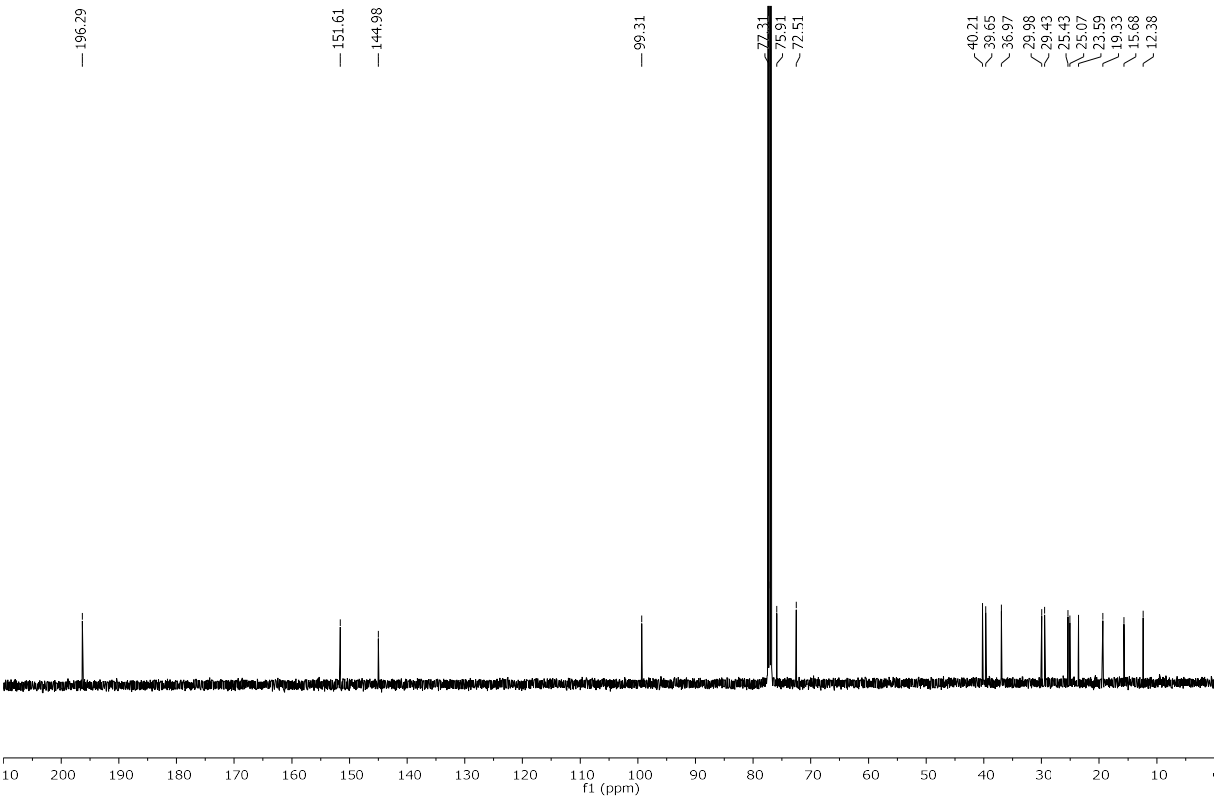
196.29
151.61
144.98
99.31
77.31
75.91
72.51
40.21
39.65
36.97
29.98
29.43
25.43
25.07
23.59
19.33
15.68
12.38
f1 (ppm)

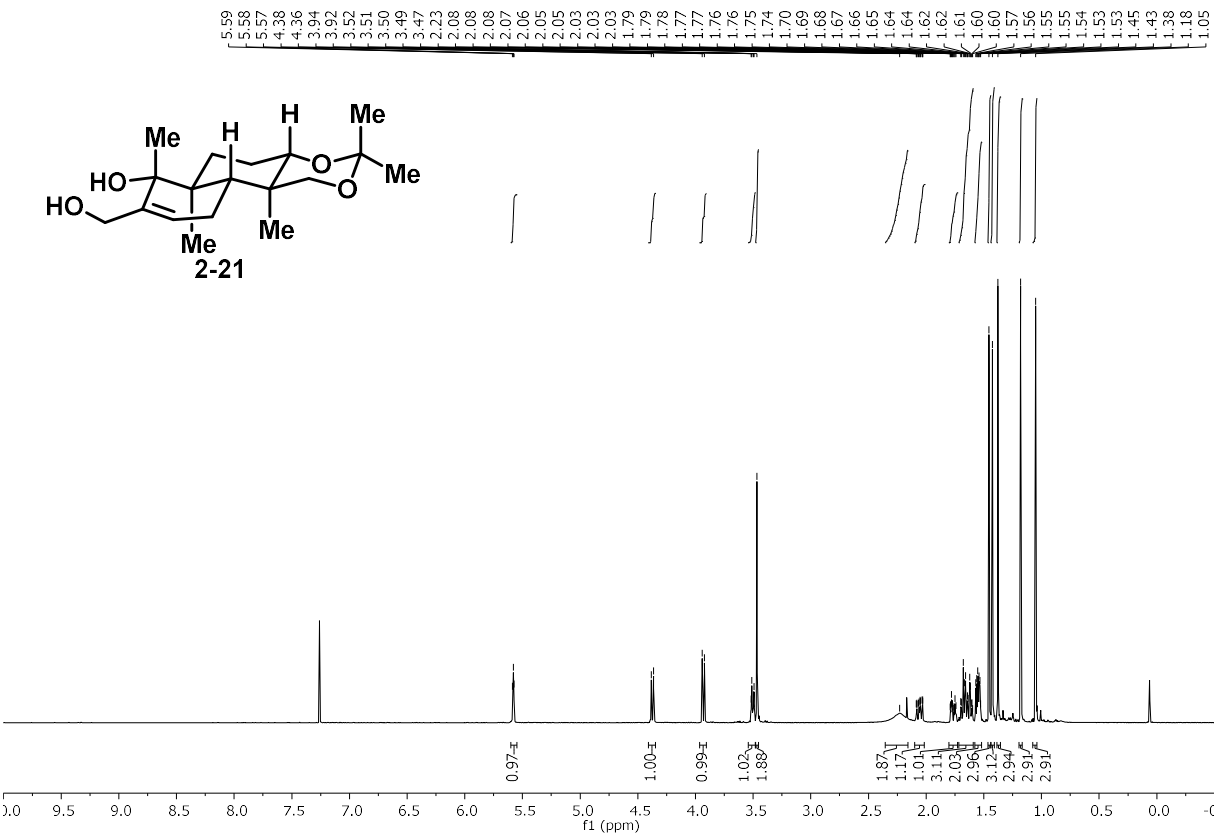
Me
H
H
Me
HO
O
Me
HO
O
Me
Me
2-21
f1 (ppm)

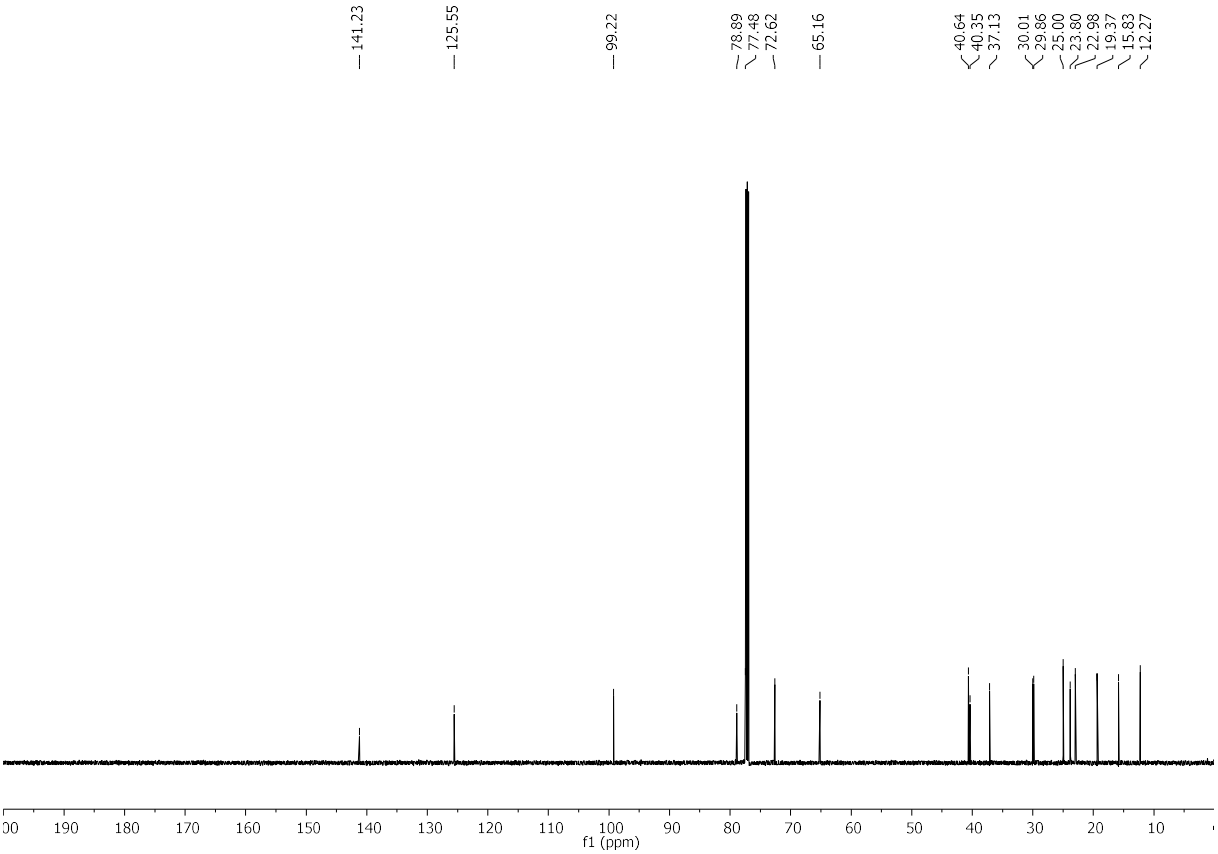
f1 (ppm)

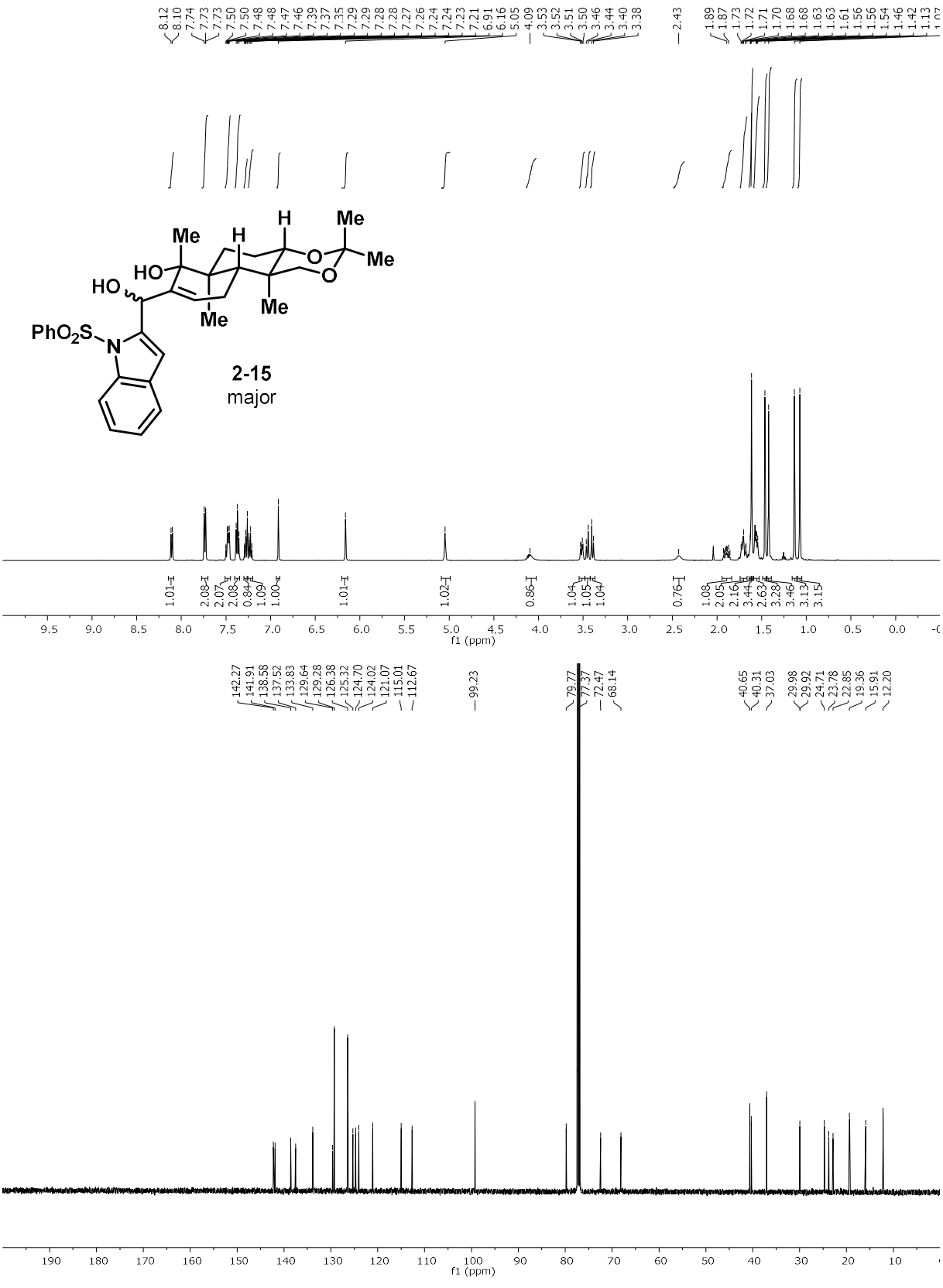
Me
H
H
Me
HO
HO
O
O
Me
Me
Me
PhO2S
N
2-15
major
f1 (ppm)
f1 (ppm)

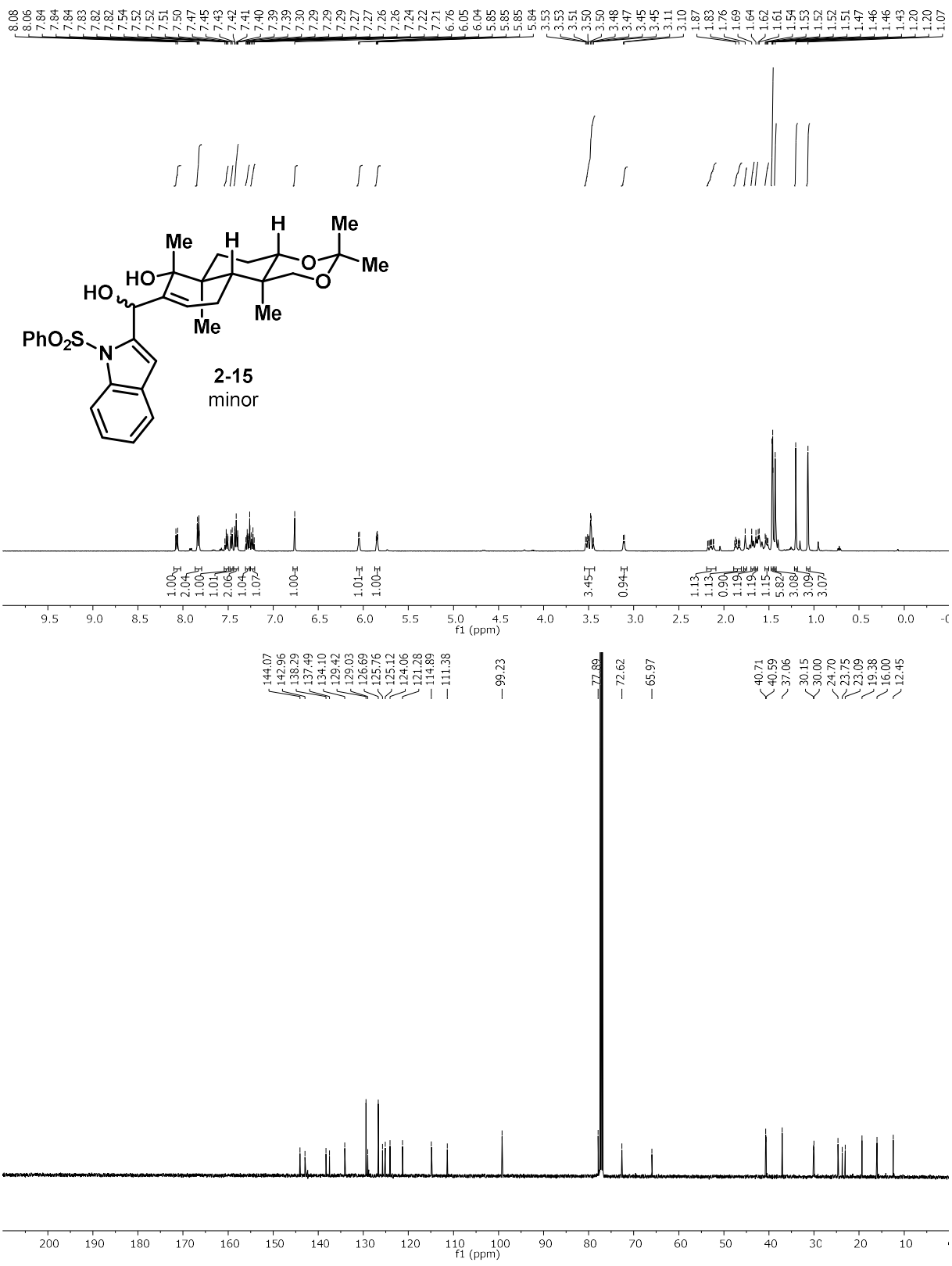
Me
H
H
Me
HO
O
Me
HO
O
Me
Me
PhO2S
N
2-15
minor
f1 (ppm)
f1 (ppm)

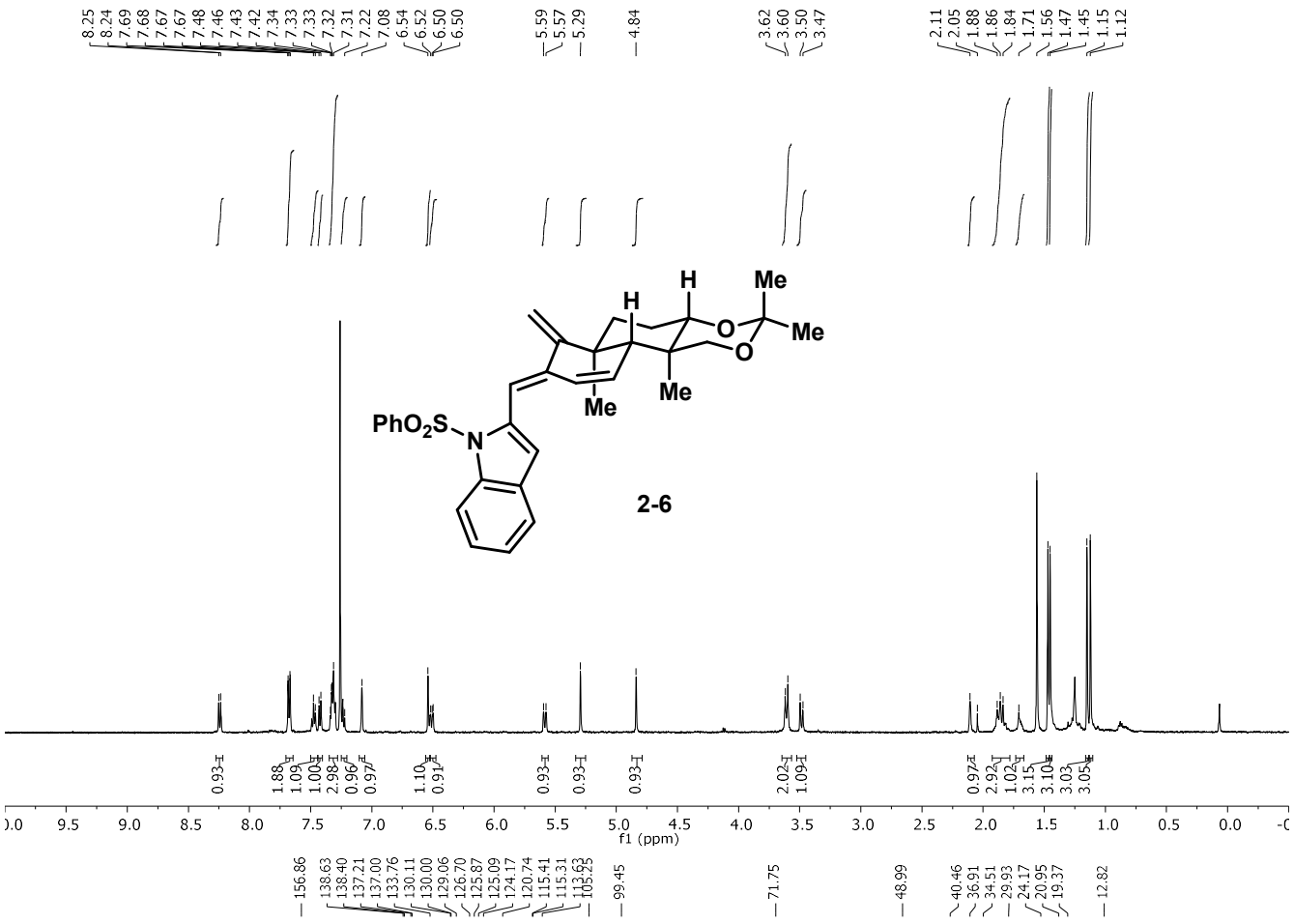
8.25
8.24
7.69
7.68
7.67
7.67
7.48
7.46
7.43
7.42
7.34
7.33
7.33
7.32
7.31
7.22
7.08
6.54
6.52
6.50
6.50
5.59
5.57
5.29
4.84
3.62
3.60
3.50
3.47
2.11
2.05
1.88
1.86
1.84
1.71
1.56
1.47
1.45
1.15
1.12
H
Me
H
O
Me
O
Me
Me
PhO2S
N
2-6
0.93
1.88
1.09
1.00
2.98
0.96
0.97
1.10
0.91
0.93
0.93
0.93
2.02
1.09
0.97
2.92
1.02
3.15
3.10
3.03
3.05
f1 (ppm)

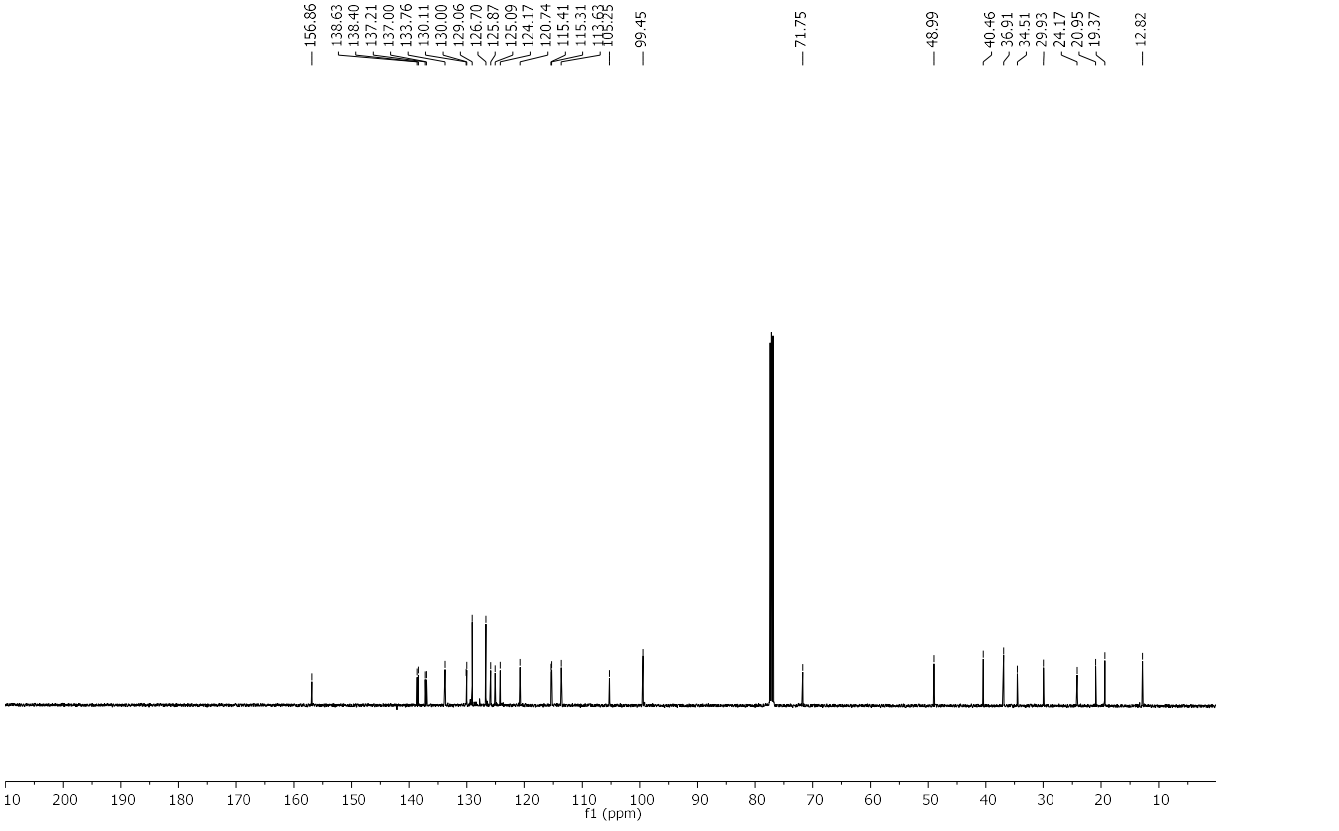
156.86
138.63
138.40
137.21
137.00
133.76
130.11
130.00
129.06
126.70
125.87
125.09
124.17
120.74
115.41
115.31
113.63
105.25
99.45
71.75
48.99
40.46
36.91
34.51
29.93
24.17
20.95
19.37
12.82
f1 (ppm)

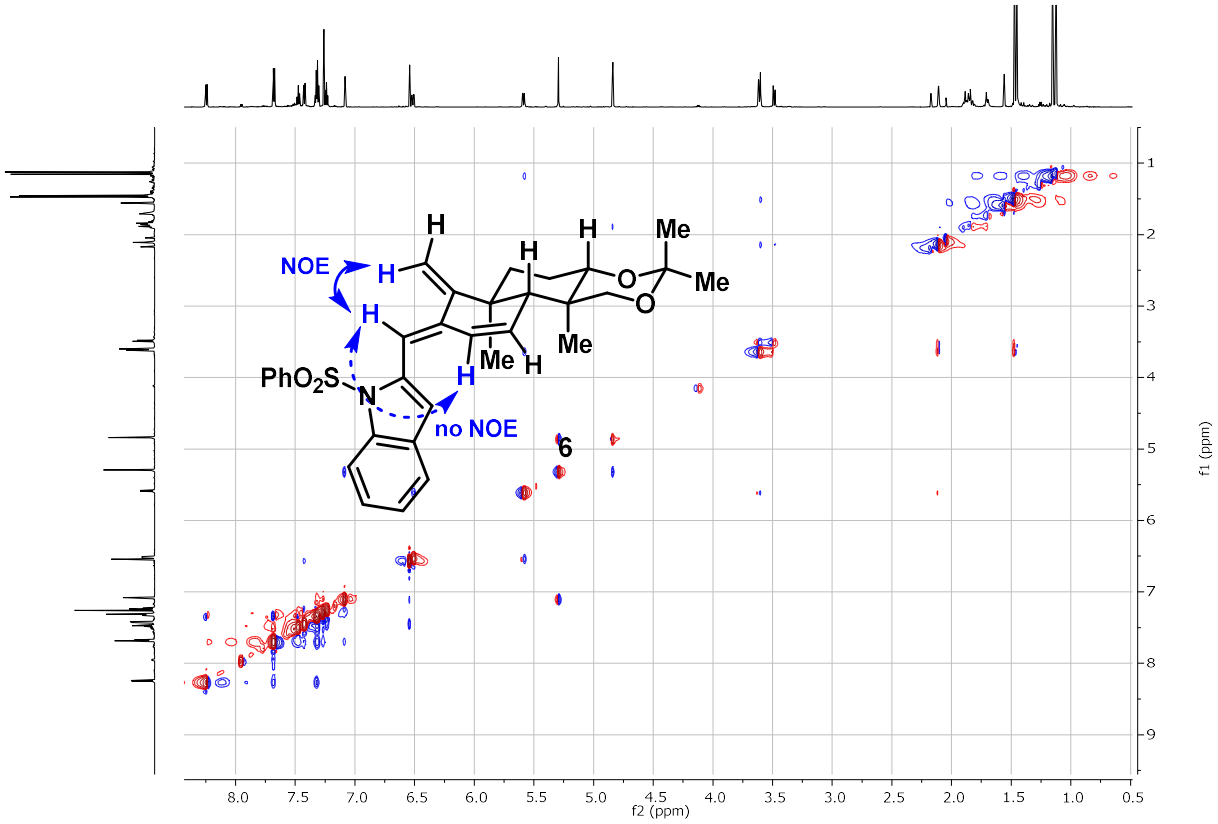
NOE
H
H
H
H
Me
Me
O
O
Me
Me
H
H
PhO2S
N
H
no NOE
6
f2 (ppm)
f1 (ppm)

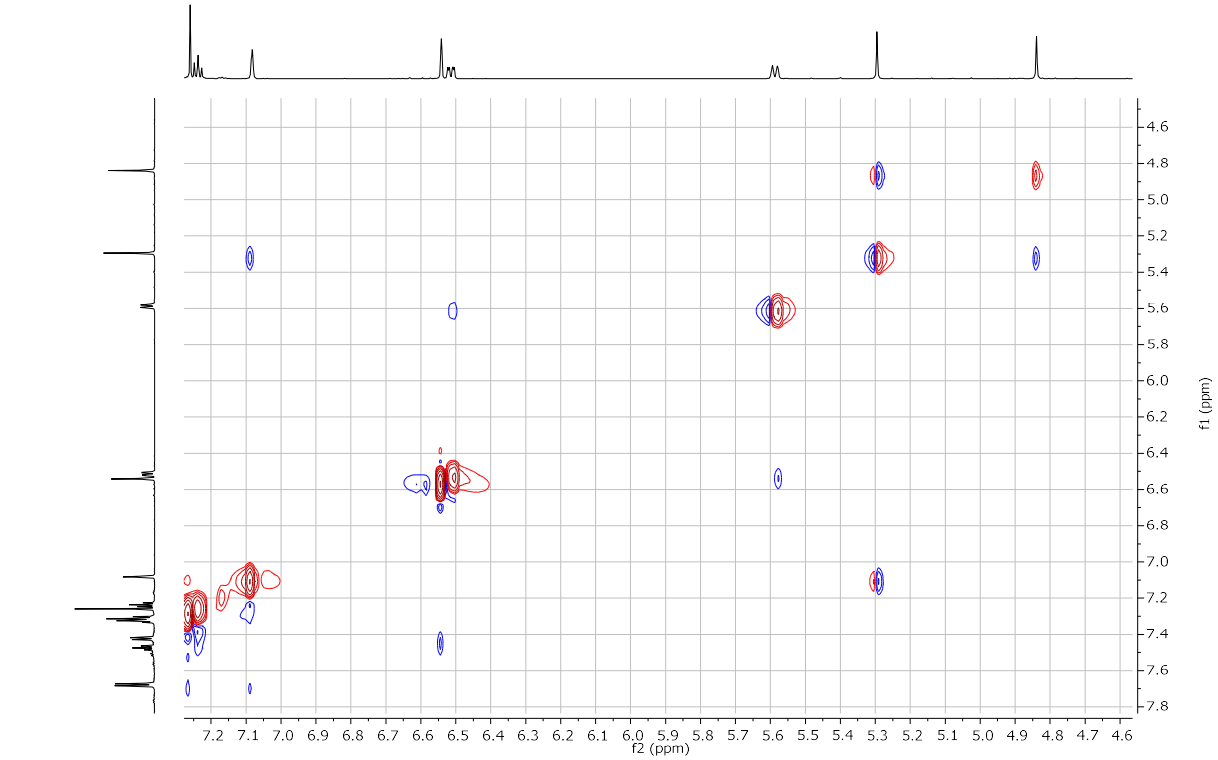
f2 (ppm)
f1 (ppm)

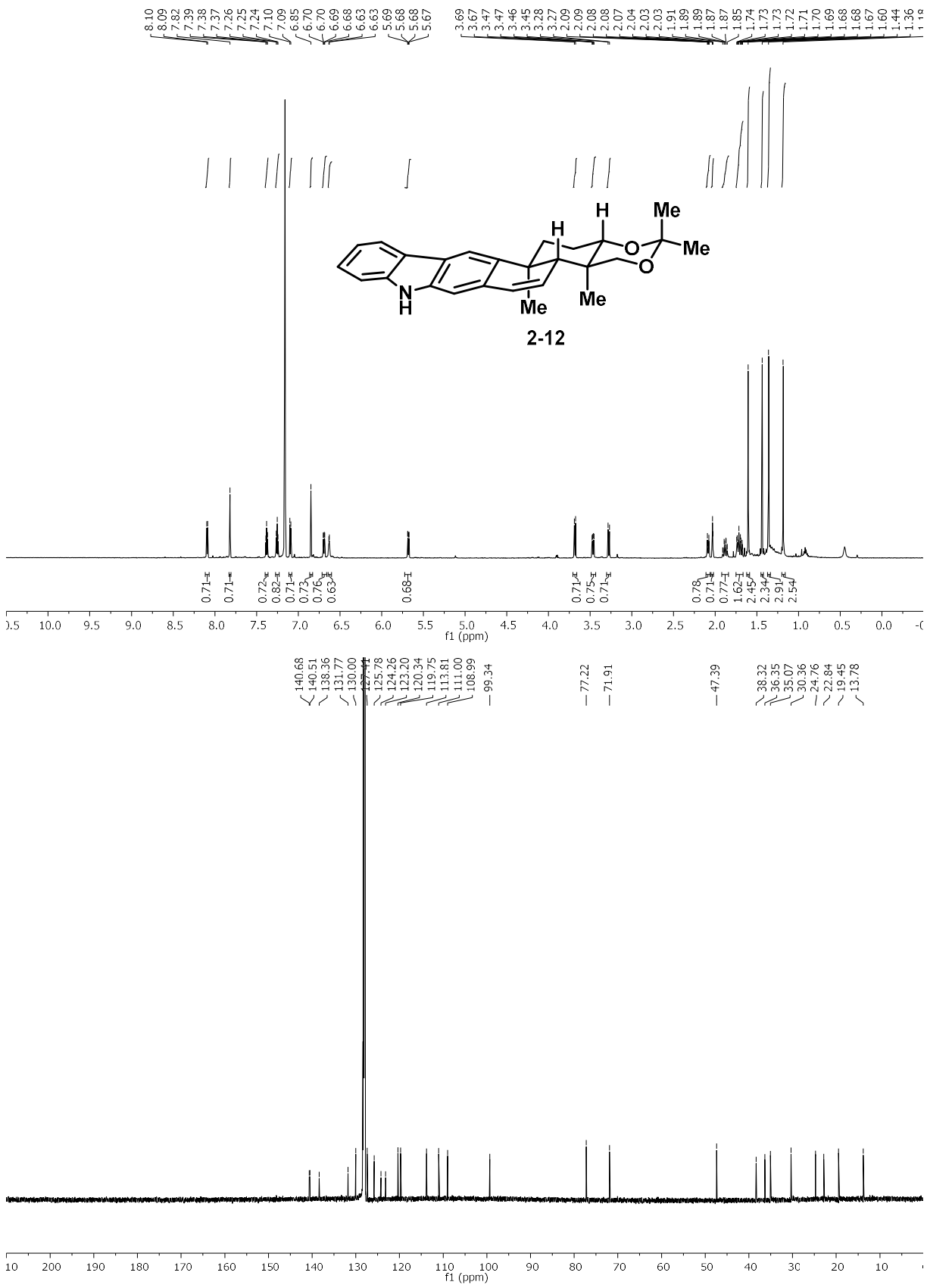
H
Me
H
O
Me
O
N
H
Me
Me
2-12
f1 (ppm)
f1 (ppm)

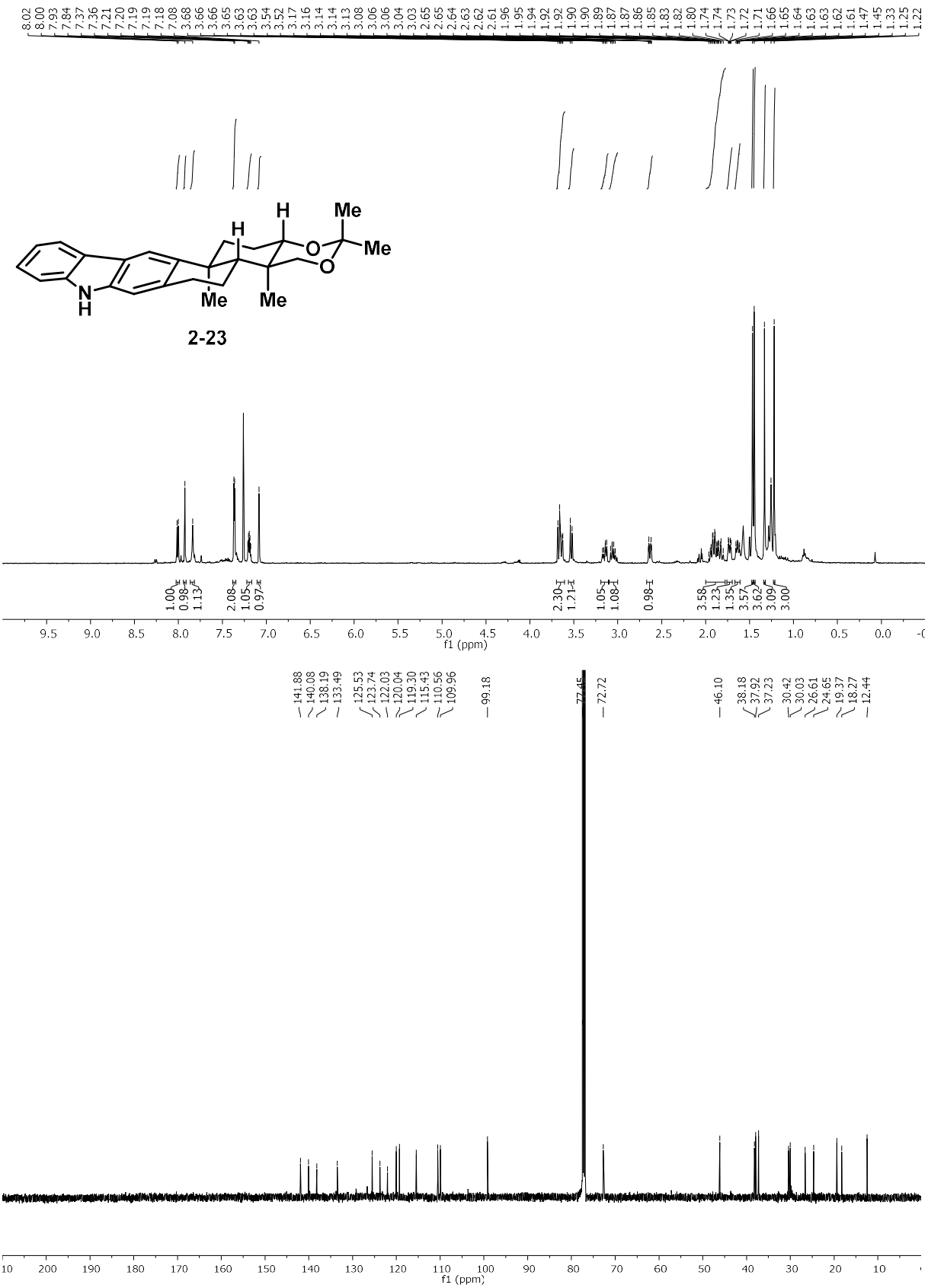
8.02 8.00 7.93 7.84 7.37 7.36 7.21 7.20 7.19 7.19 7.18 7.08 3.68 3.66 3.66 3.65 3.63 3.63 3.54 3.52 3.17 3.16 3.14 3.14 3.13 3.08 3.06 3.06 3.04 3.03 2.65 2.65 2.64 2.63 2.62 2.61 1.96 1.95 1.94 1.92 1.92 1.90 1.90 1.89 1.87 1.87 1.86 1.85 1.83 1.82 1.80 1.74 1.74 1.73 1.72 1.71 1.66 1.65 1.64 1.63 1.63 1.62 1.61 1.47 1.45 1.33 1.25 1.22
H
Me
H
O
Me
O
N
H
Me
Me
2-23
1.00 0.98 1.13 2.08 1.05 0.97 2.30 1.21 1.05 1.08 0.98 3.58 1.23 1.35 3.57 3.62 3.09 3.00
f1 (ppm)
141.88 140.08 138.19 133.49 125.53 123.74 122.03 120.04 119.30 115.43 110.56 109.96 99.18 77.45 72.72 46.10 38.18 37.92 37.23 30.42 30.03 26.61 24.65 19.37 18.27 12.44
f1 (ppm)

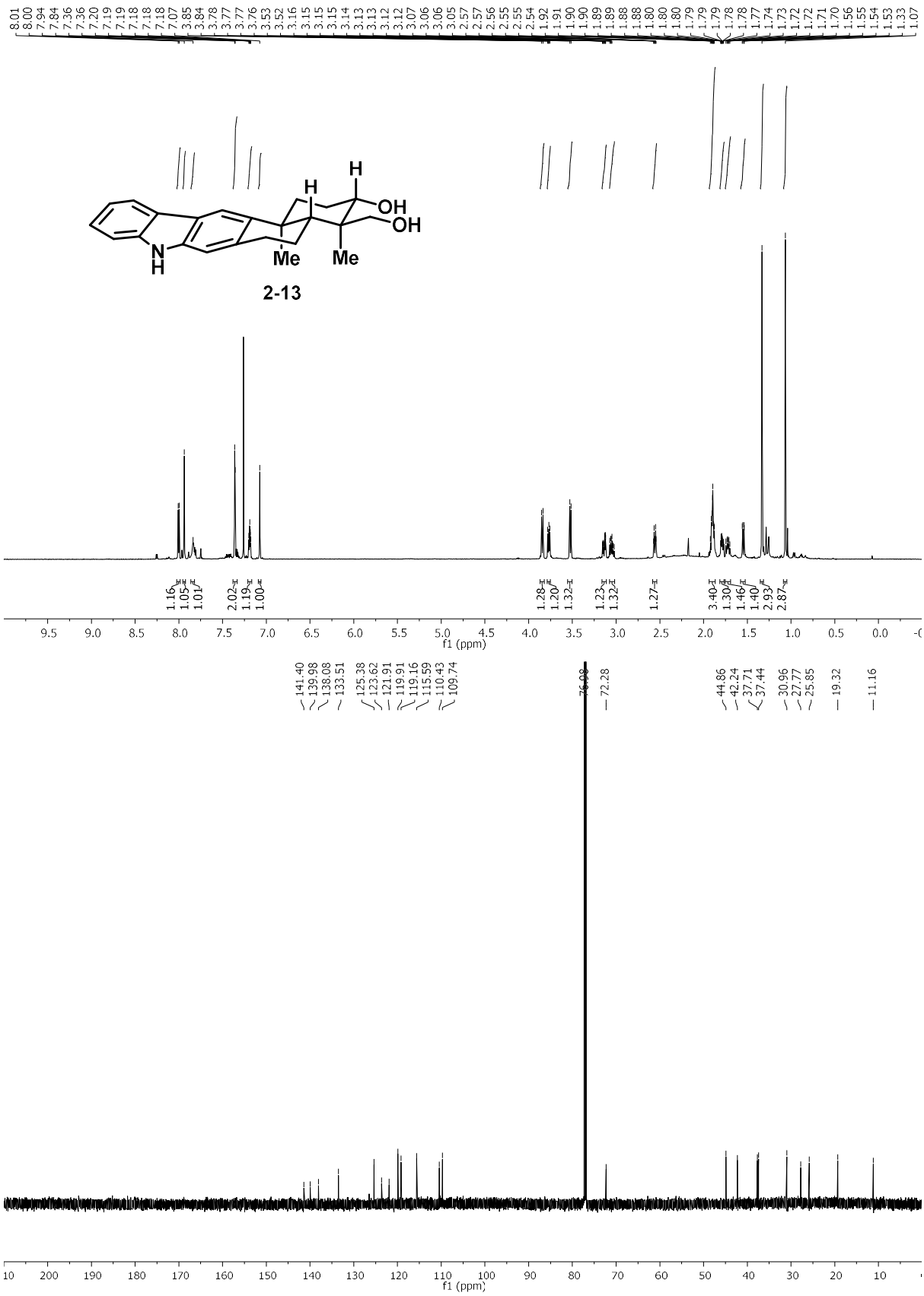
8.01 8.00 7.94 7.84 7.36 7.36 7.20 7.19 7.19 7.18 7.18 7.18 7.07 3.85 3.84 3.78 3.77 3.77 3.76 3.53 3.52 3.16 3.15 3.15 3.15 3.14 3.13 3.13 3.12 3.12 3.07 3.06 3.06 3.05 2.57 2.57 2.56 2.55 2.55 2.54 1.92 1.91 1.90 1.90 1.89 1.89 1.88 1.88 1.80 1.80 1.79 1.79 1.79 1.78 1.78 1.77 1.74 1.73 1.72 1.72 1.71 1.70 1.56 1.55 1.54 1.53 1.33 1.07
H
H
OH
OH
N
H
Me
Me
2-13
1.16
1.05
1.01
2.02
1.19
1.00
1.28
1.20
1.32
1.23
1.32
1.27
3.40
1.30
1.46
1.40
2.93
2.87
f1 (ppm)
141.40 139.98 138.08 133.51 125.38 123.62 121.91 119.91 119.16 115.59 110.43 109.74
76.99
72.28
44.86 42.24 37.71 37.44 30.96 27.77 25.85 19.32 11.16
f1 (ppm)

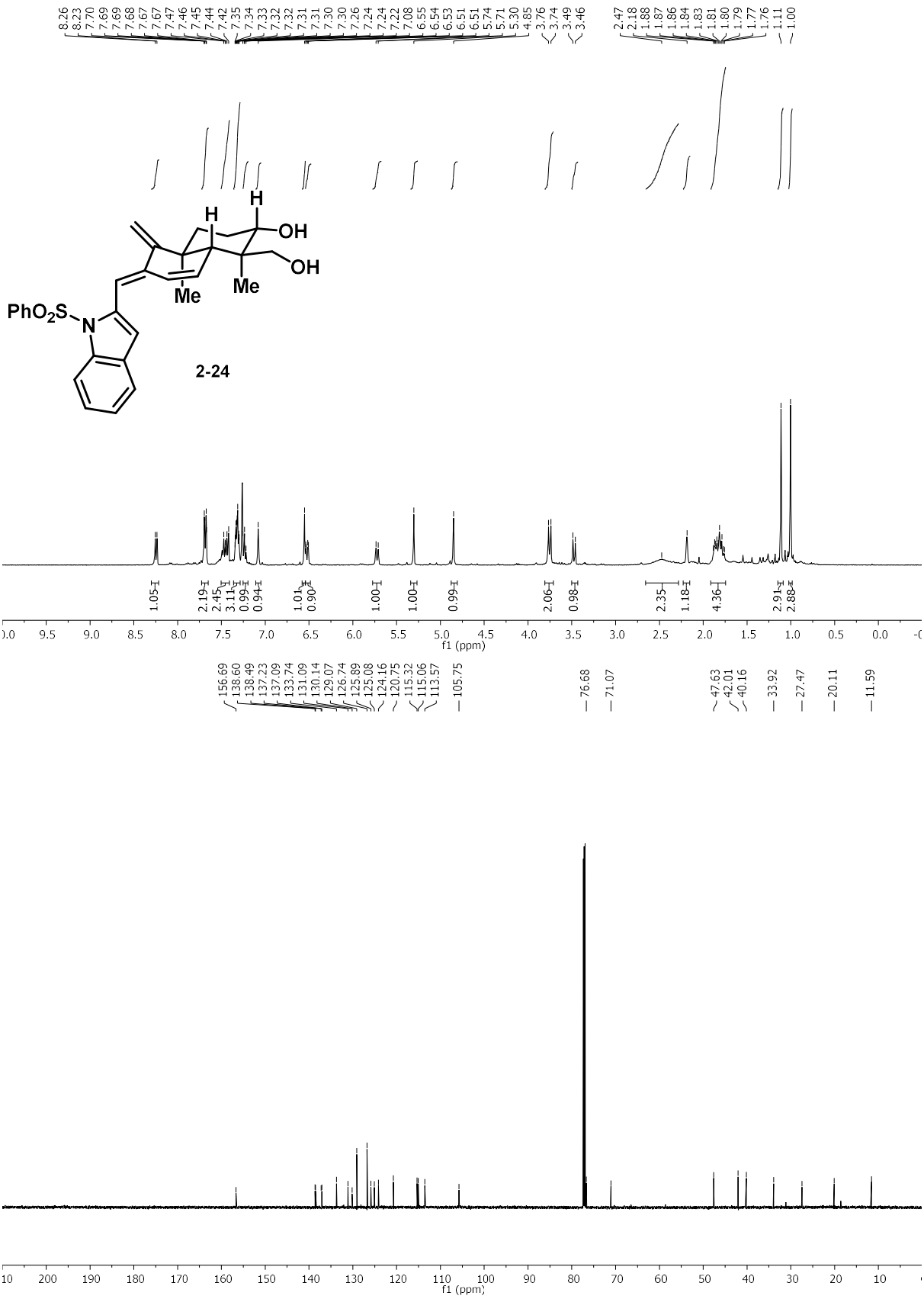
8.26 8.23 7.70 7.69 7.69 7.68 7.67 7.67 7.47 7.46 7.45 7.44 7.42 7.35 7.34 7.33 7.32 7.32 7.31 7.31 7.30 7.30 7.26 7.24 7.24 7.22 7.08 6.55 6.54 6.53 6.51 6.51 5.74 5.71 5.30 4.85 3.76 3.74 3.49 3.46
2.47 2.18 1.88 1.87 1.86 1.84 1.83 1.81 1.80 1.79 1.77 1.76 1.11 1.00
H
H
OH
OH
Me
Me
PhO2S
N
2-24
1.05 2.19 2.45 3.11 0.99 0.94 1.01 0.90 1.00 1.00 0.99 2.06 0.98 2.35 1.18 4.36 2.91 2.88
f1 (ppm)
156.69 138.60 138.49 137.23 137.09 133.74 131.09 130.14 129.07 126.74 125.89 125.08 124.16 120.75 115.32 115.06 113.57 105.75 76.68 71.07 47.63 42.01 40.16 33.92 27.47 20.11 11.59
f1 (ppm)

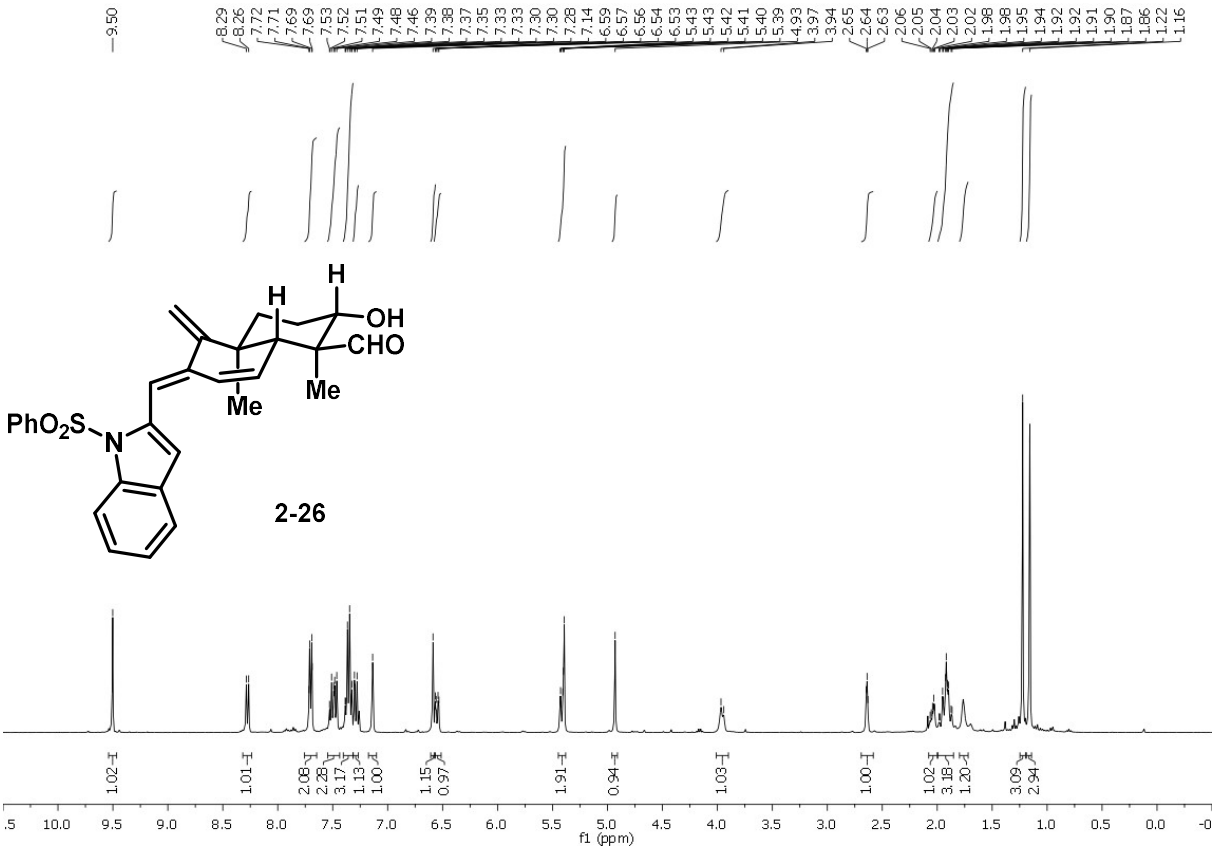
H
H
OH
CHO
Me
Me
PhO2S
N
2-26
f1 (ppm)

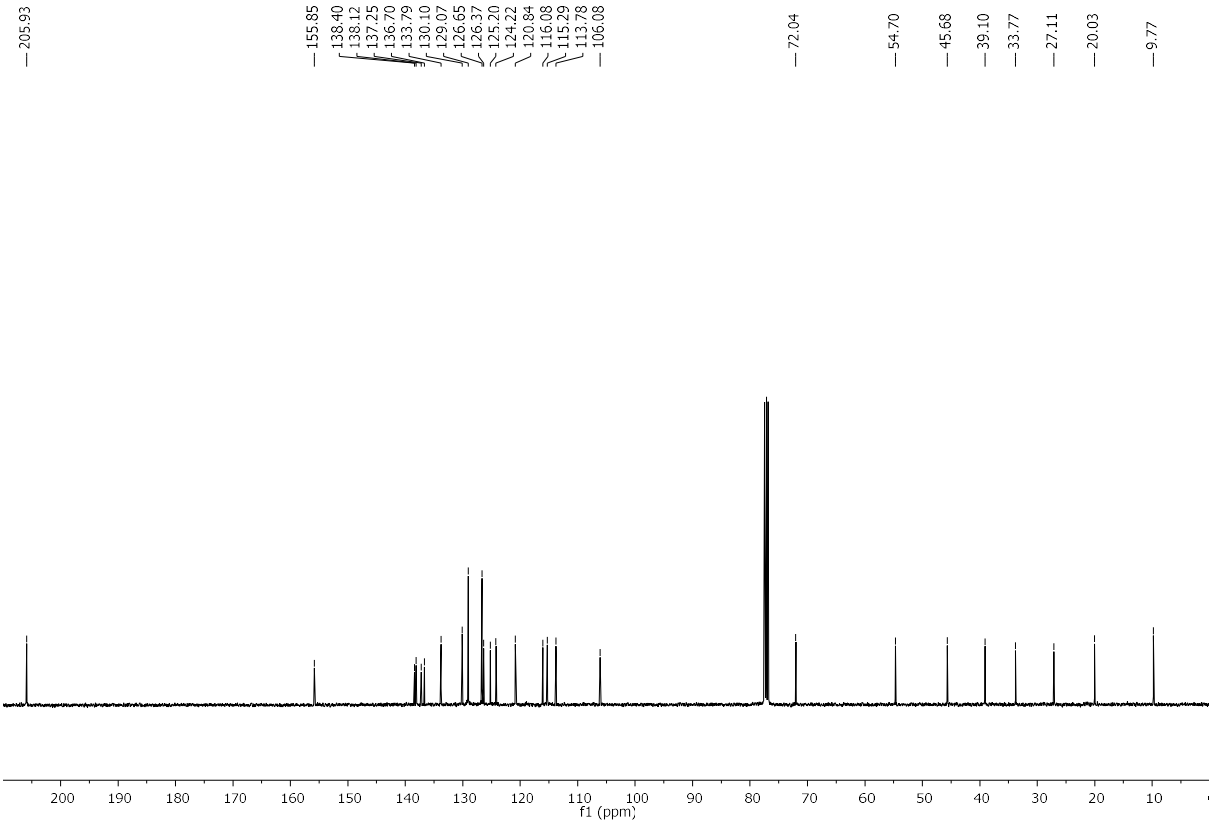
f1 (ppm)

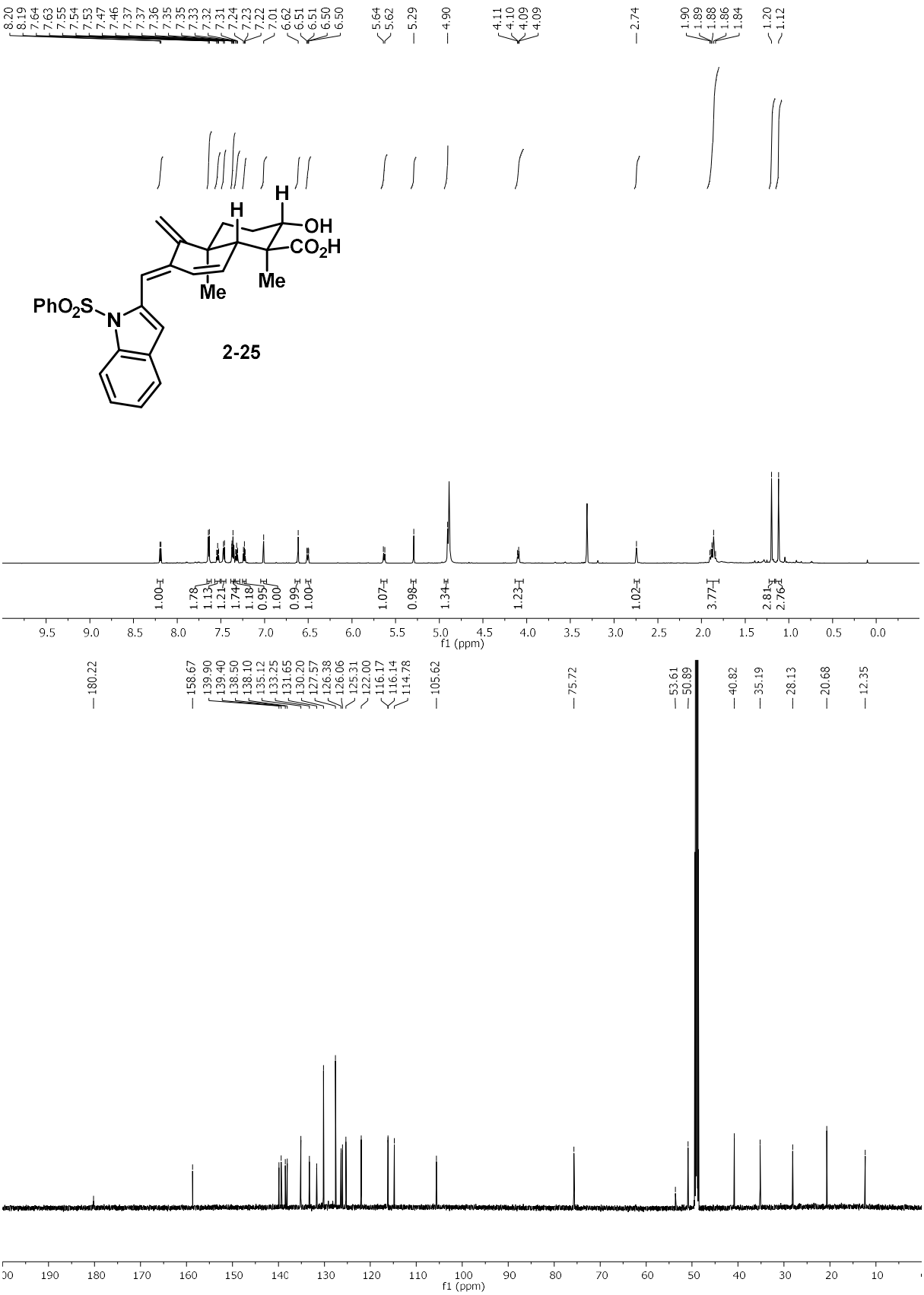
8.20
8.19
7.64
7.63
7.55
7.54
7.53
7.47
7.46
7.37
7.37
7.36
7.35
7.35
7.33
7.32
7.31
7.24
7.23
7.22
7.01
6.62
6.51
6.51
6.50
6.50
5.64
5.62
5.29
4.90
4.11
4.10
4.09
4.09
2.74
1.90
1.89
1.88
1.86
1.84
1.20
1.12
H
H
OH
CO2H
Me
Me
PhO2S
N
2-25
1.00
1.78
1.13
1.21
1.74
1.18
0.95
1.00
0.99
1.00
1.07
0.98
1.34
1.23
1.02
3.77
2.81
2.76
f1 (ppm)
180.22
158.67
139.90
139.40
138.50
138.10
135.12
133.25
131.65
130.20
127.57
126.38
126.06
125.31
122.00
116.17
116.14
114.78
105.62
75.72
53.61
50.89
40.82
35.19
28.13
20.68
12.35
f1 (ppm)

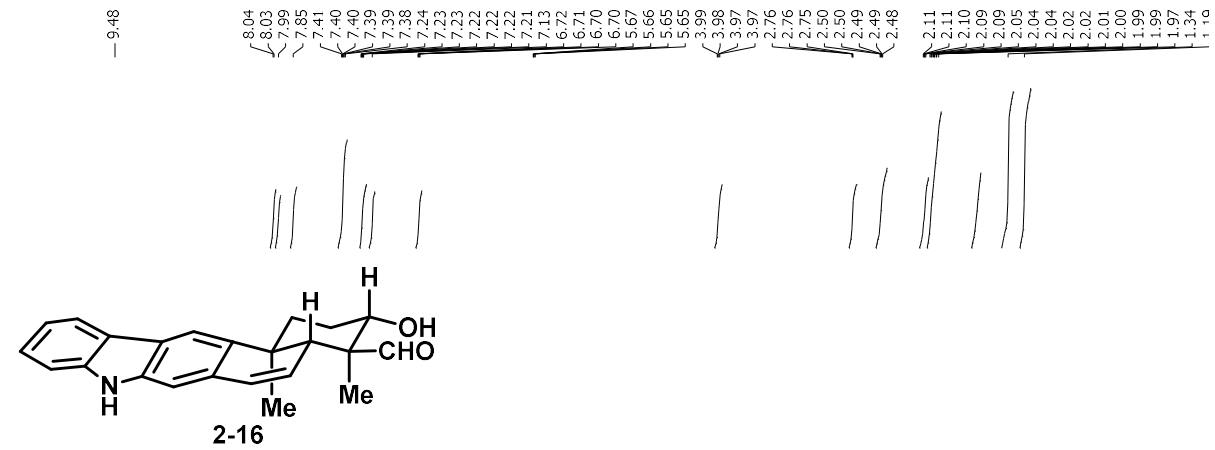
9.48
8.04
8.03
7.99
7.85
7.41
7.40
7.40
7.39
7.39
7.38
7.24
7.23
7.23
7.22
7.22
7.22
7.21
7.13
6.72
6.71
6.70
6.70
5.67
5.66
5.65
5.65
3.99
3.98
3.97
3.97
2.76
2.76
2.75
2.50
2.50
2.49
2.49
2.48
2.11
2.11
2.10
2.09
2.09
2.05
2.04
2.04
2.02
2.02
2.01
2.00
1.99
1.99
1.97
1.34
H
H
OH
CHO
N
H
Me
Me

2-16

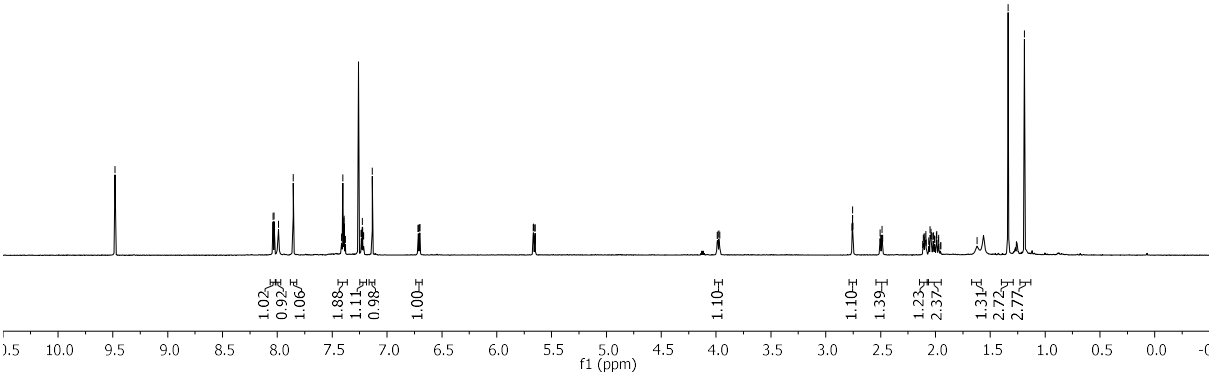
1.02
0.92
1.06
1.88
1.11
0.98
1.00
1.10
1.10
1.39
1.23
2.37
1.31
2.72
2.77
f1 (ppm)

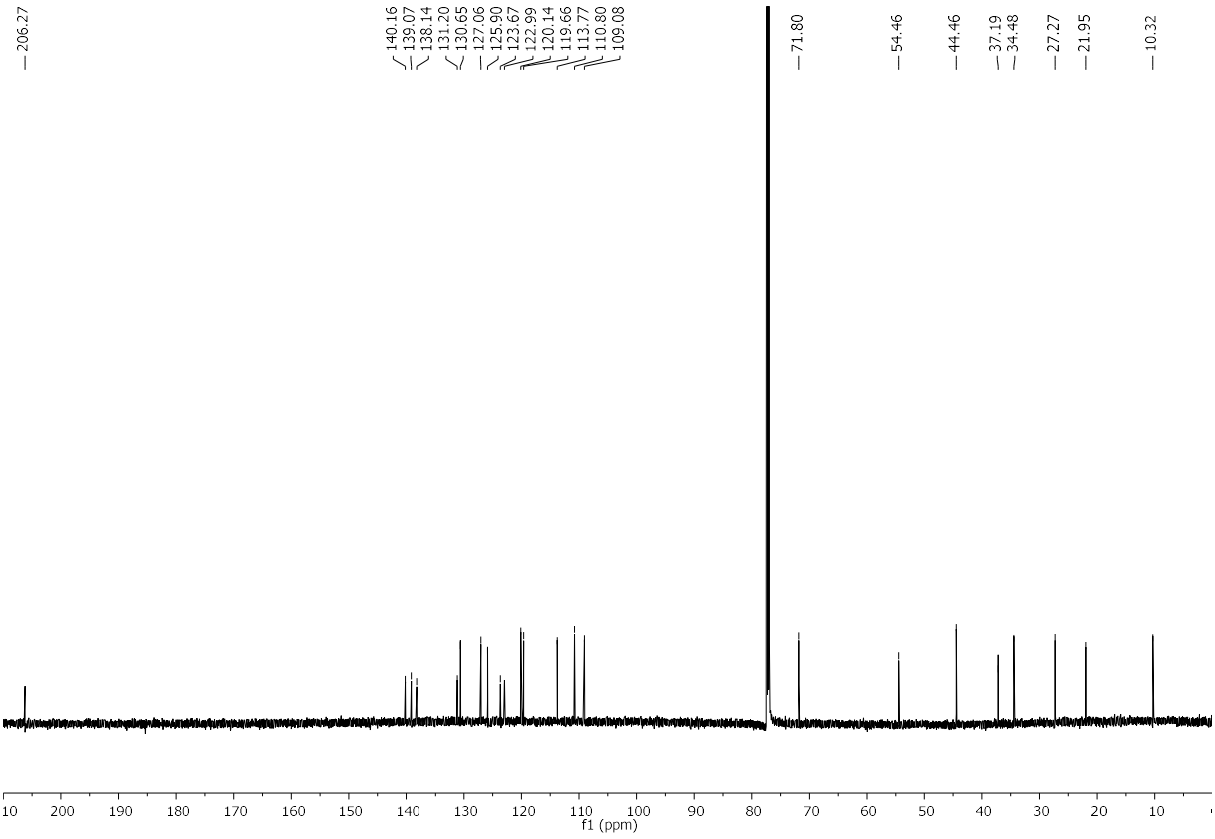
206.27
140.16
139.07
138.14
131.20
130.65
127.06
125.90
123.67
122.99
120.14
119.66
113.77
110.80
109.08
71.80
54.46
44.46
37.19
34.48
27.27
21.95
10.32
f1 (ppm)

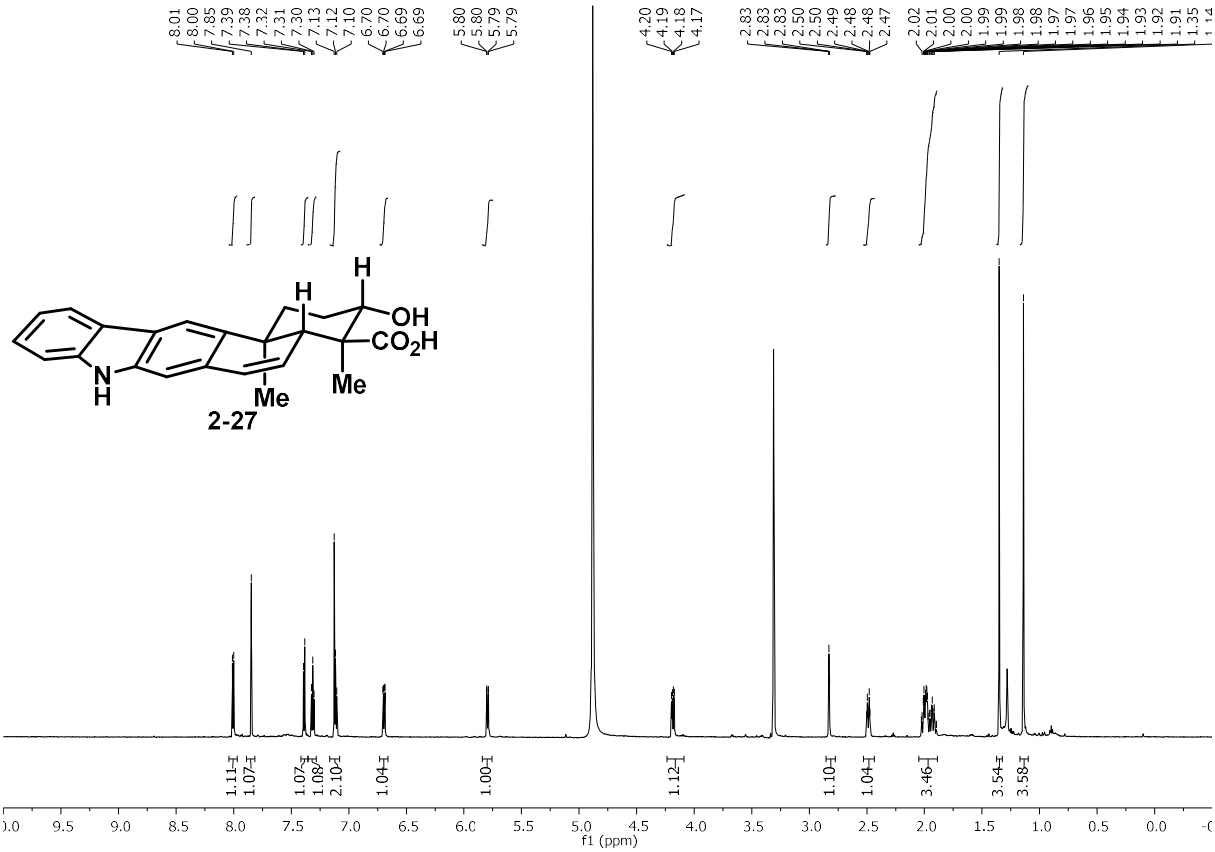
8.01
8.00
7.85
7.39
7.38
7.32
7.31
7.30
7.13
7.12
7.10
6.70
6.70
6.69
6.69
5.80
5.80
5.79
5.79
4.20
4.19
4.18
4.17
2.83
2.83
2.83
2.50
2.50
2.49
2.48
2.48
2.47
2.02
2.01
2.00
2.00
1.99
1.99
1.98
1.98
1.97
1.97
1.96
1.95
1.94
1.93
1.92
1.91
1.35
H
H
OH
CO2H
N
H
Me
Me
2-27
1.11
1.07
1.07
1.08
2.10
1.04
1.00
1.12
1.10
1.04
3.46
3.54
3.58
f1 (ppm)

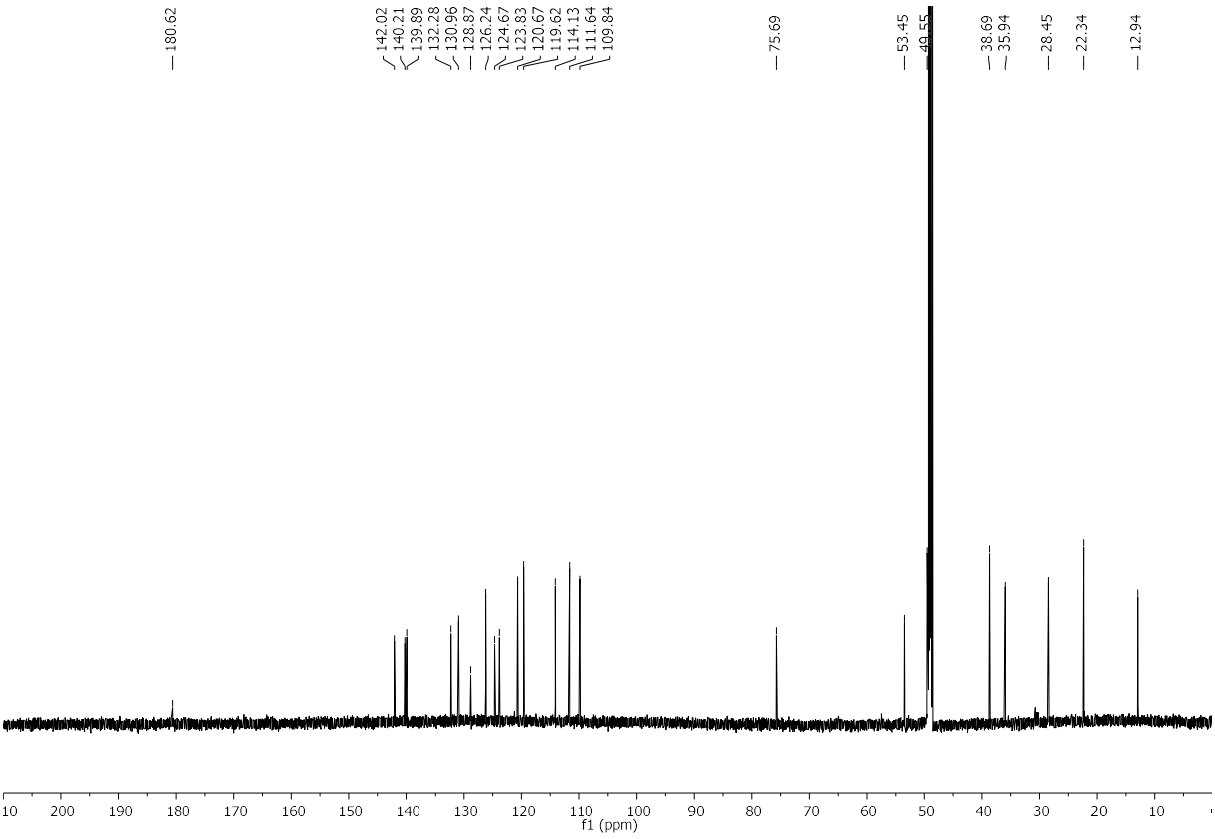
180.62
142.02
140.21
139.89
132.28
130.96
128.87
126.24
124.67
123.83
120.67
119.62
114.13
111.64
109.84
75.69
53.45
49.55
38.69
35.94
28.45
22.34
12.94
f1 (ppm)

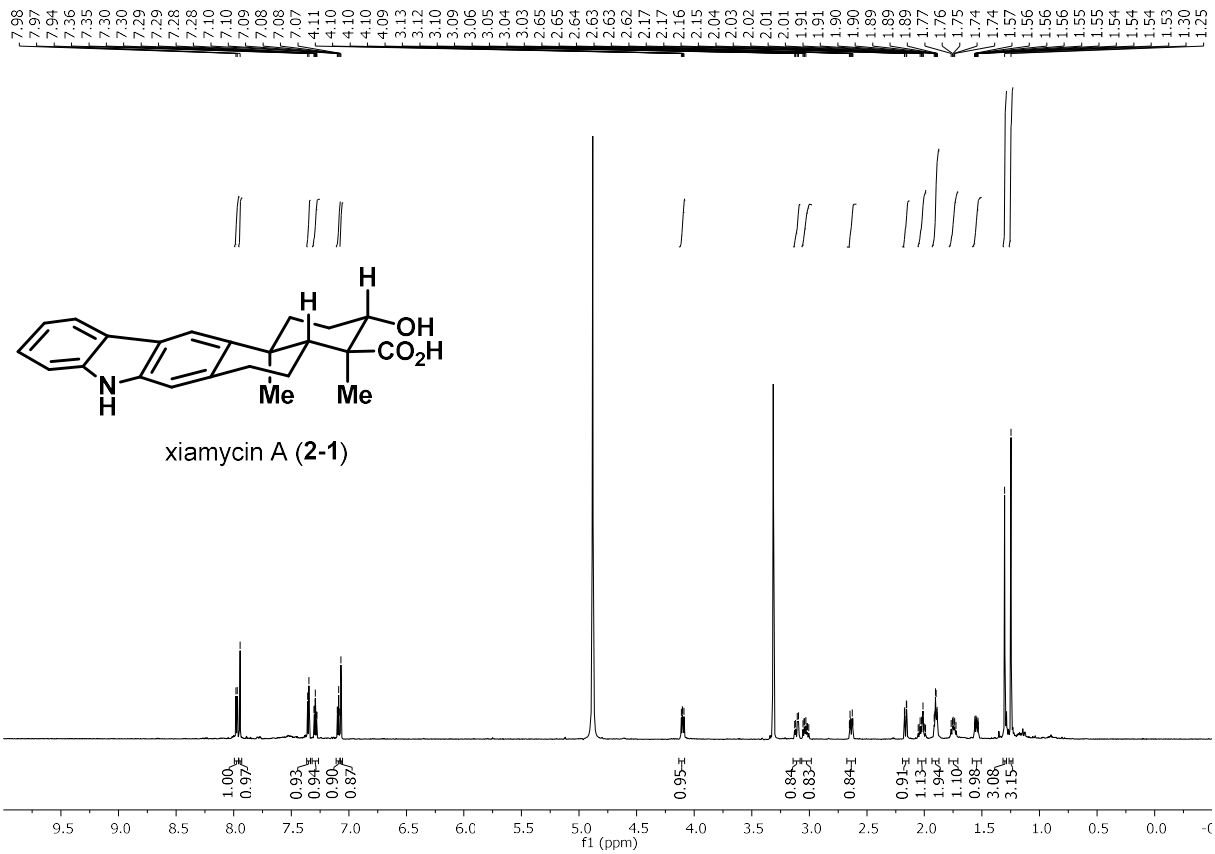

xiamycin A (**2-1**)

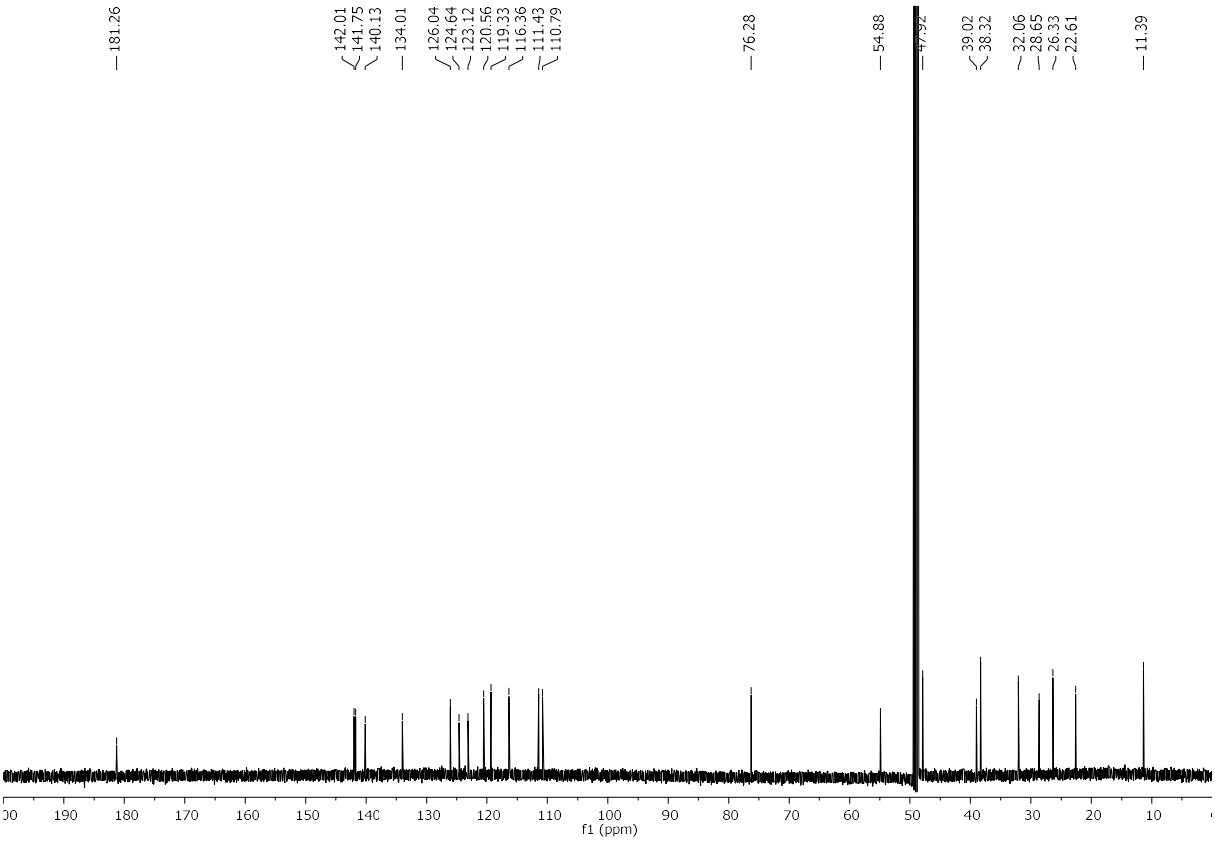

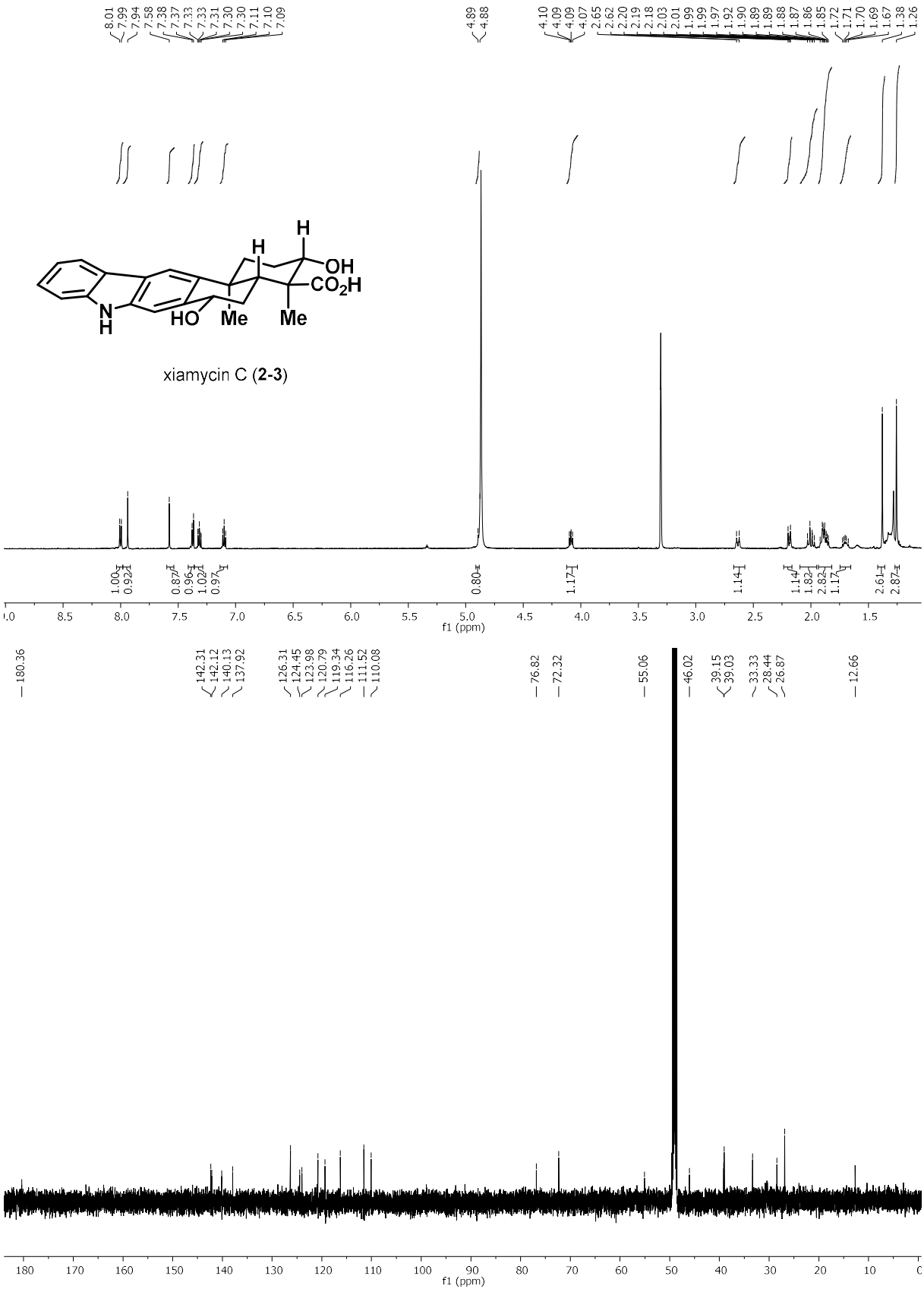
8.01
7.99
7.94
7.58
7.38
7.37
7.33
7.33
7.31
7.30
7.30
7.11
7.10
7.09
4.89
4.88
4.10
4.09
4.09
4.07
2.65
2.62
2.20
2.19
2.18
2.03
2.01
1.99
1.99
1.97
1.92
1.90
1.89
1.89
1.88
1.87
1.86
1.85
1.72
1.71
1.70
1.69
1.67
1.38
1.26
H
H
OH
CO2H
N
H
HO
Me
Me
xiamycin C (2-3)
1.00
0.92
0.87
0.96
1.02
0.97
0.80
1.17
1.14
1.14
1.82
2.82
1.17
2.61
2.87
f1 (ppm)
180.36
142.31
142.12
140.13
137.92
126.31
124.45
123.98
120.79
119.34
116.26
111.52
110.08
76.82
72.32
55.06
46.02
39.15
39.03
33.33
28.44
26.87
12.66
f1 (ppm)

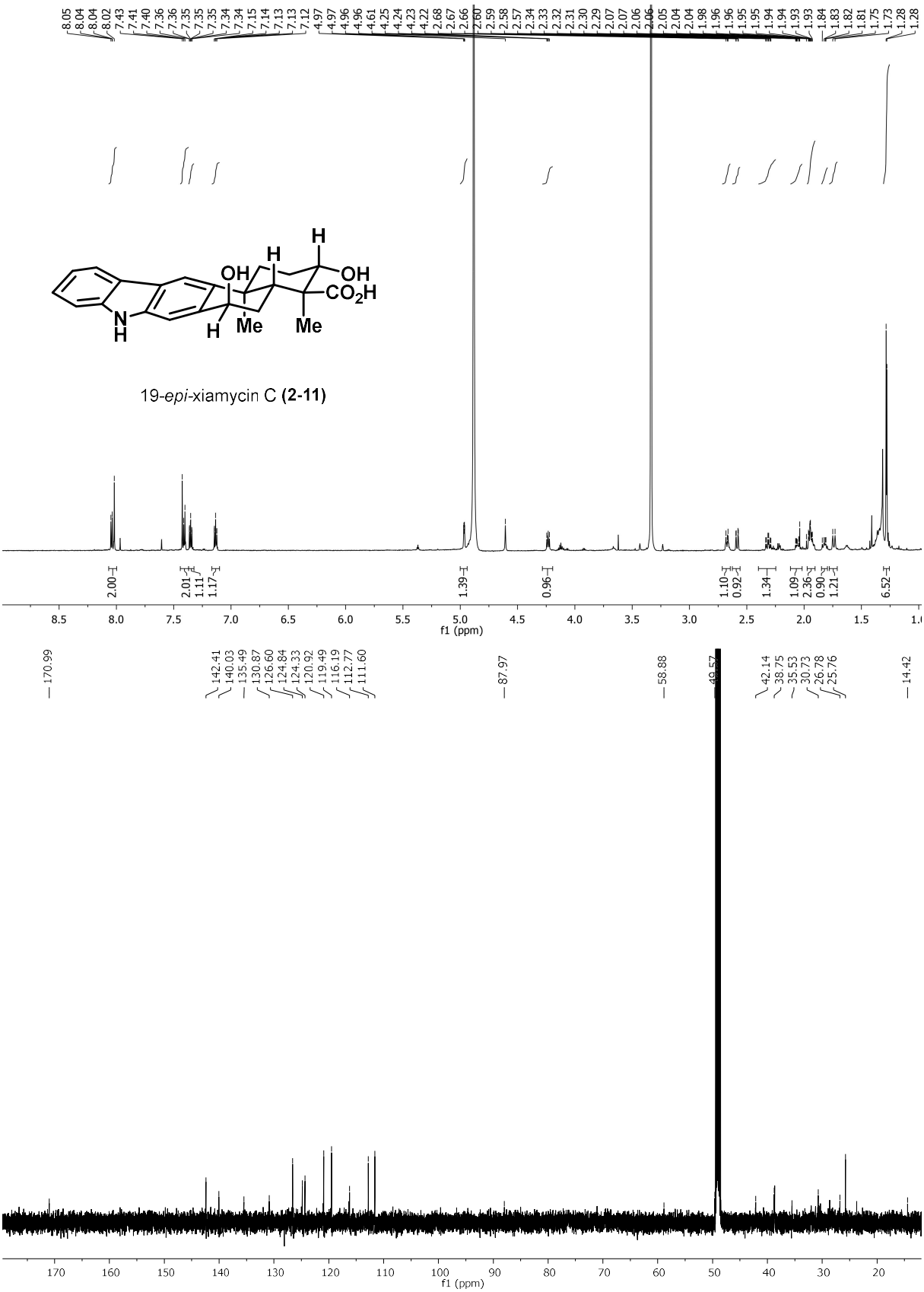
19-epi-xiamycin C (2-11)
f1 (ppm)
f1 (ppm)

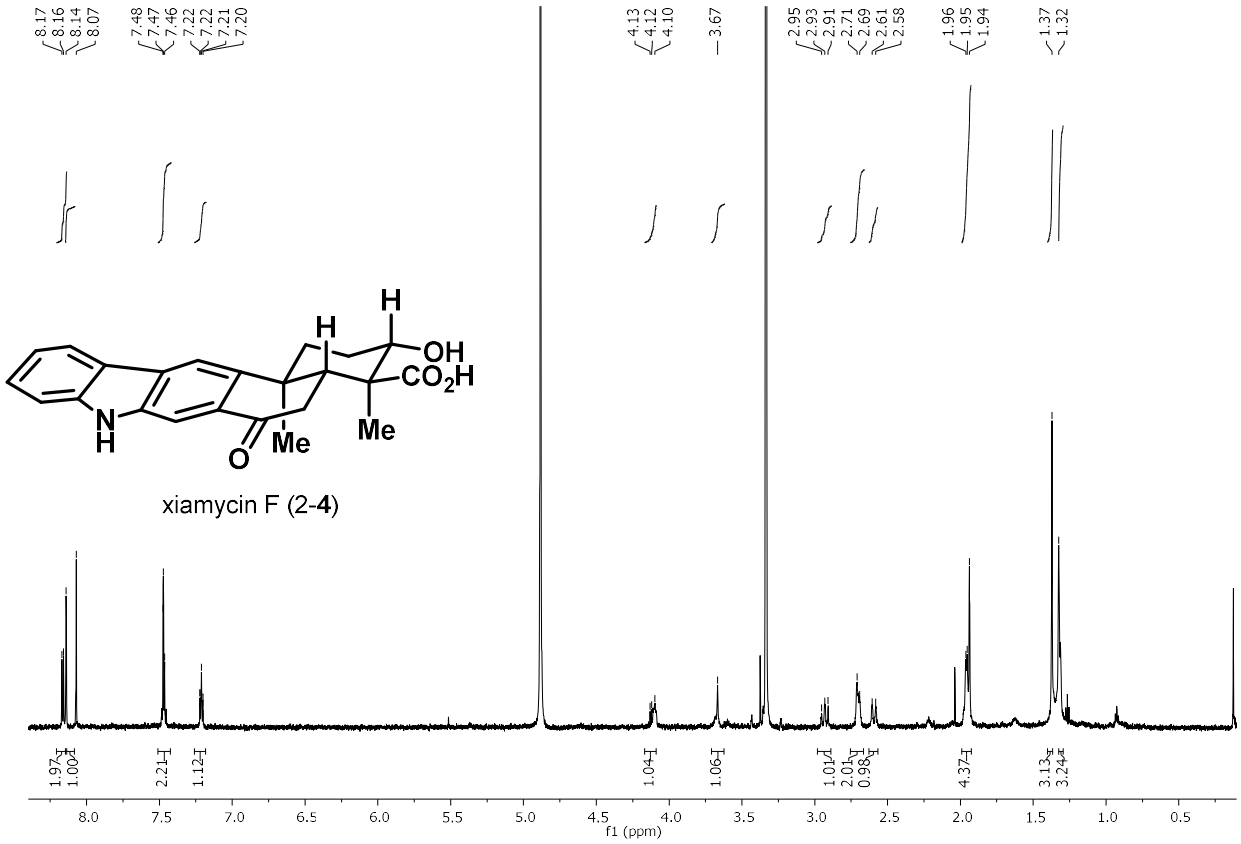

xiamycin F (2-**4**)

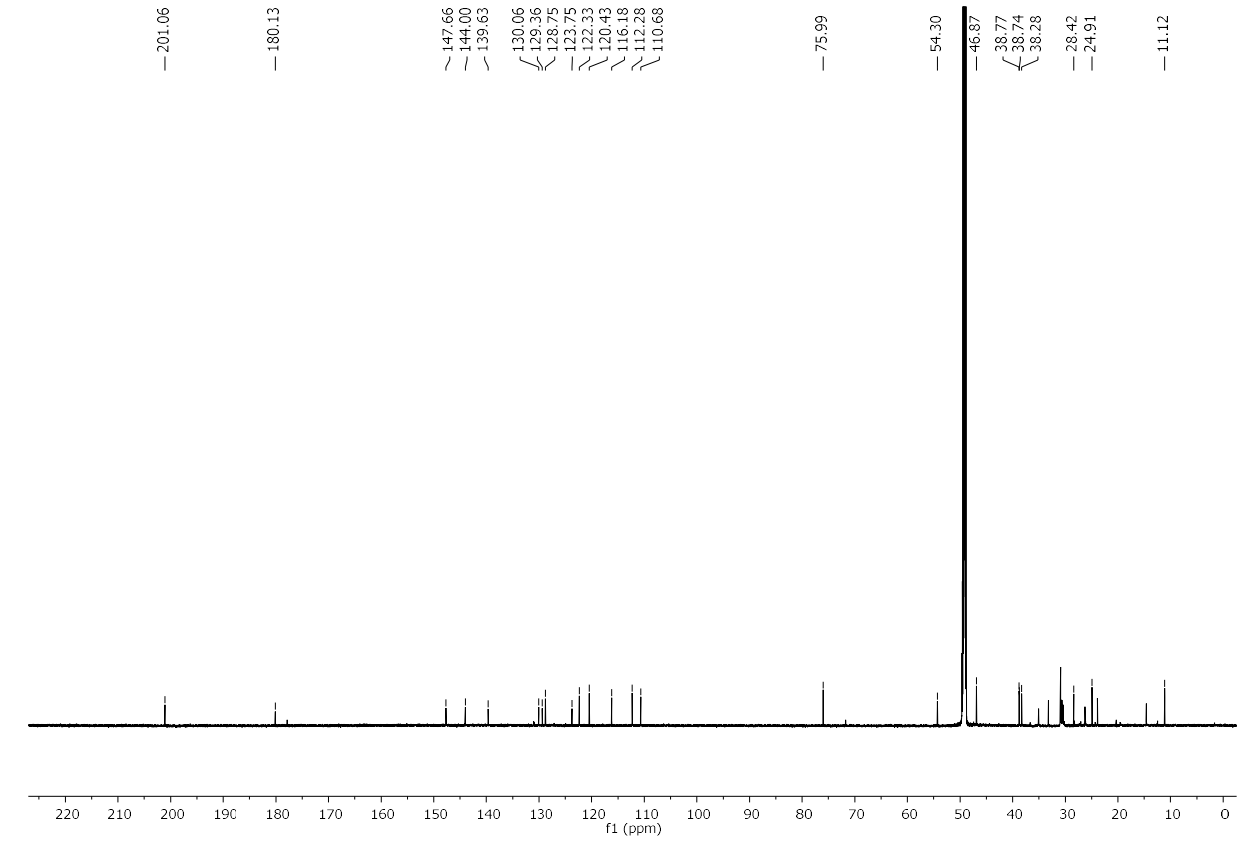

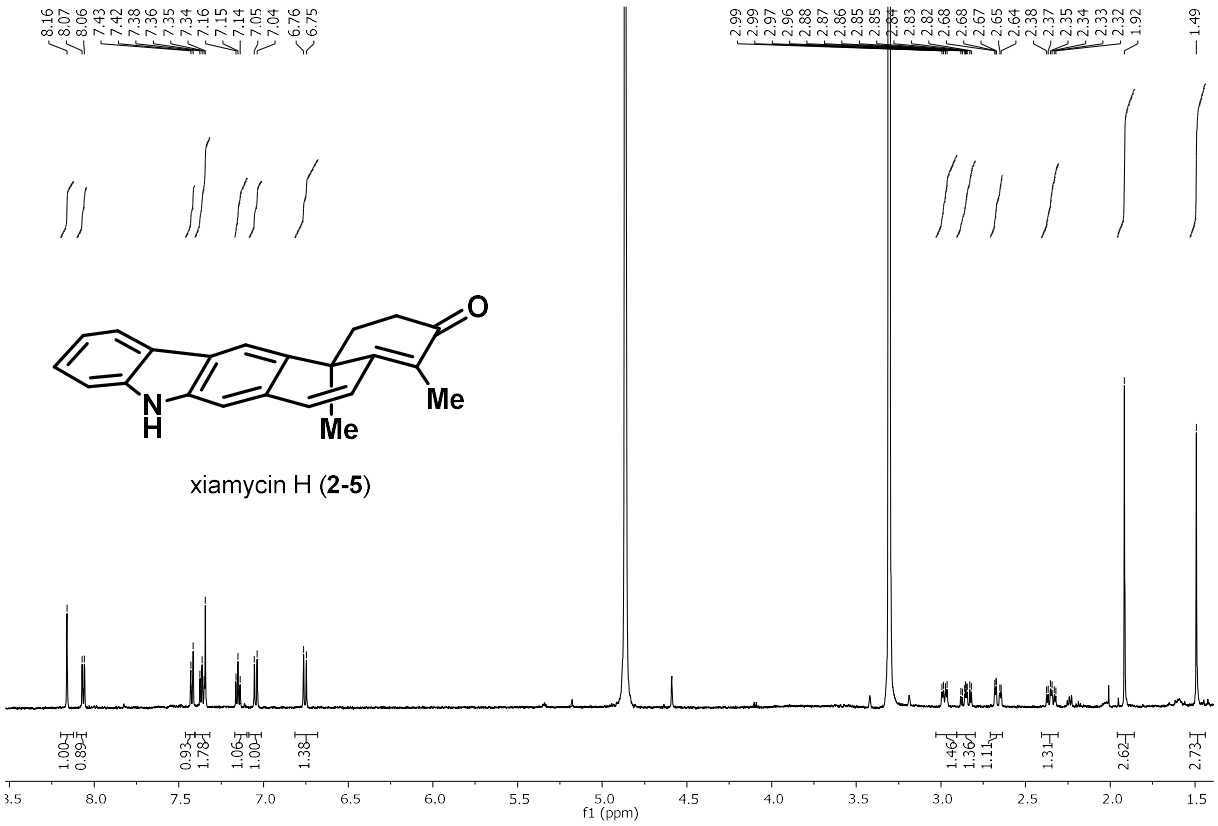

xiamycin H (**2-5**)

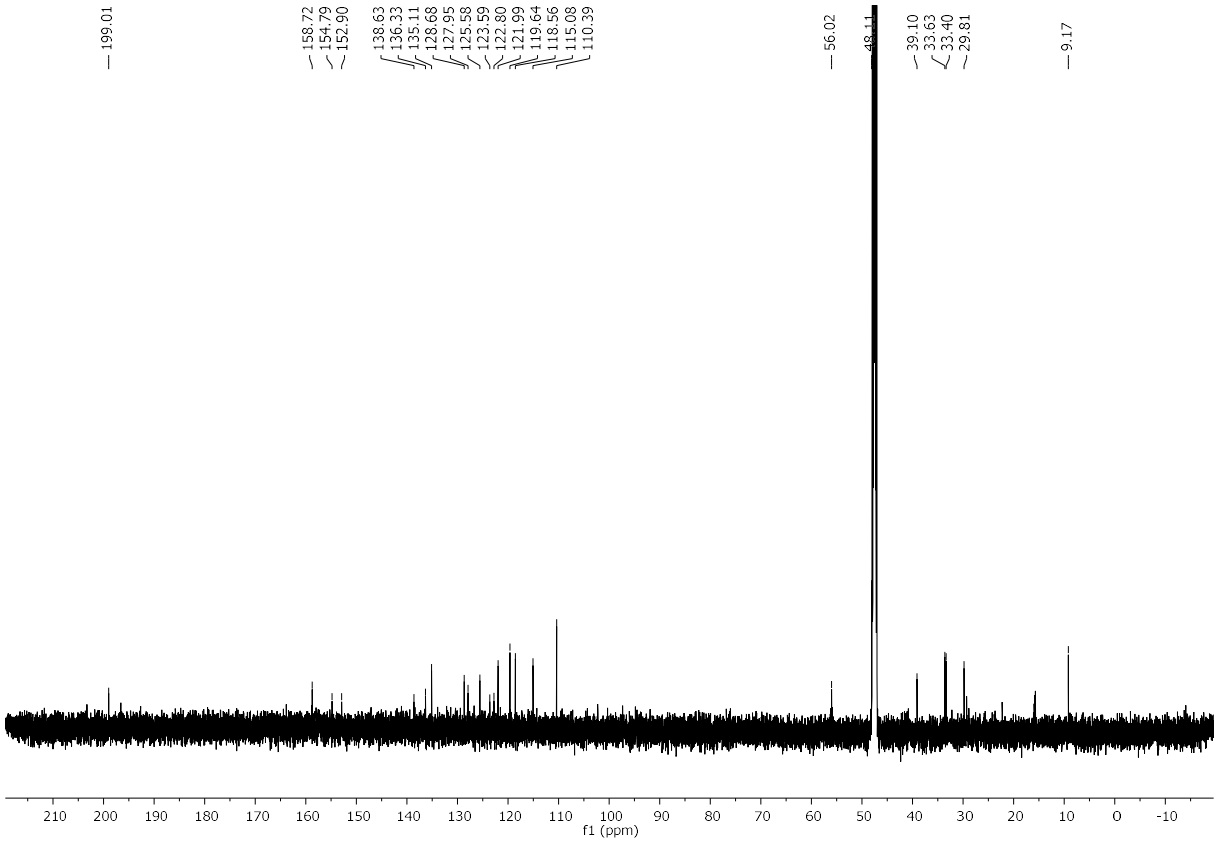

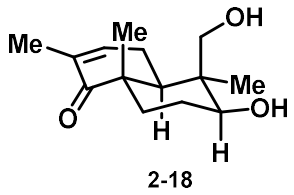
Me
Me
OH
Me
O
OH
H
H

2-18

7.26
6.68
6.67
6.67
6.66
6.66
6.65
4.27
4.24
3.72
3.69
3.49
3.46
3.42
3.40
3.38
1.93
1.90
1.83
1.83
1.81
1.81
1.80
1.70
1.70
1.70
1.69
1.69
1.66
1.65
1.63
1.62
1.49
1.47
1.46
1.45
1.44
1.43
1.41
1.21
0.95
1.00
1.04
1.88
1.09
1.11
1.01
1.03
1.08
2.12
3.07
1.16
1.11
3.18
3.06
f1 (ppm)

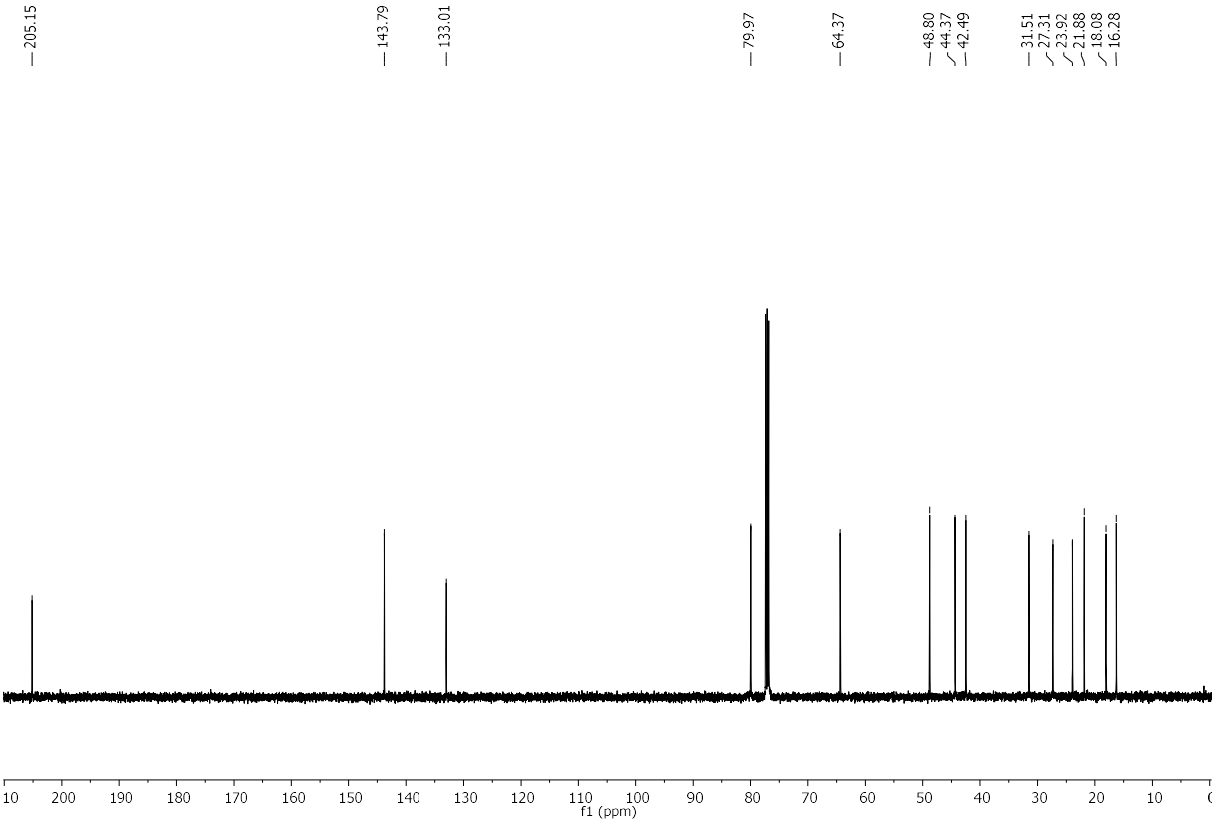
205.15
143.79
133.01
79.97
64.37
48.80
44.37
42.49
31.51
27.31
23.92
21.88
18.08
16.28
f1 (ppm)

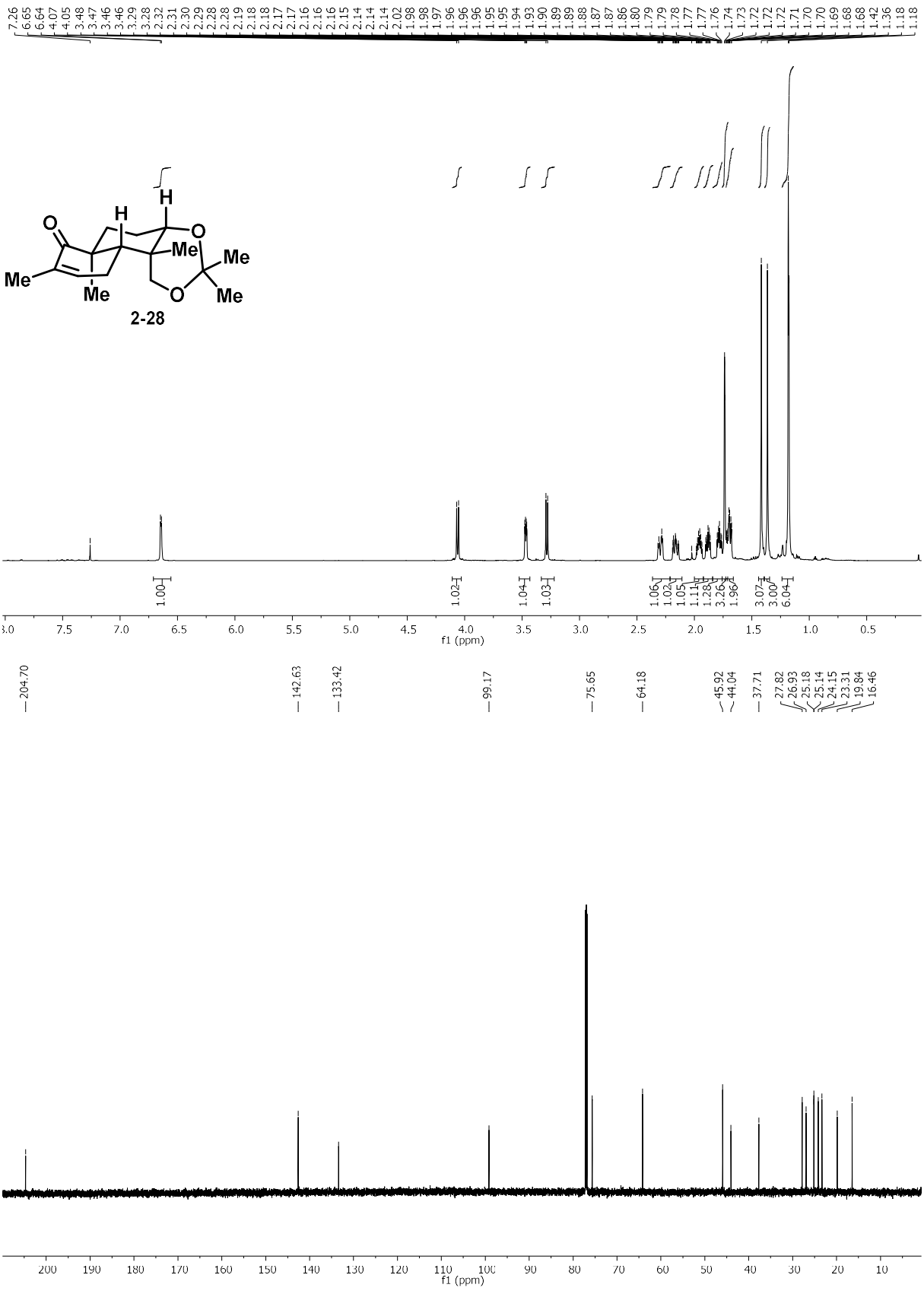
7.26 6.65 6.64 4.07 4.05 3.48 3.47 3.46 3.46 3.29 3.28 2.32 2.31 2.30 2.29 2.28 2.28 2.19 2.18 2.18 2.17 2.17 2.16 2.16 2.16 2.15 2.14 2.14 2.14 2.02 1.98 1.98 1.97 1.96 1.96 1.96 1.95 1.95 1.94 1.93 1.90 1.89 1.89 1.88 1.87 1.87 1.86 1.80 1.79 1.79 1.78 1.77 1.77 1.76 1.74 1.73 1.72 1.72 1.72 1.71 1.70 1.70 1.69 1.68 1.68 1.42 1.36 1.18 1.18
H
H
O
O
Me
Me
Me
Me
O
Me
2-28
1.00 1.02 1.04 1.03 1.06 1.02 1.05 1.14 1.28 3.26 1.96 3.07 3.00 6.04
f1 (ppm)
204.70 142.63 133.42 99.17 75.65 64.18 45.92 44.04 37.71 27.82 26.93 25.18 25.14 24.15 23.31 19.84 16.46
f1 (ppm)

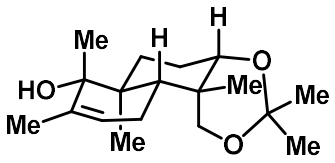

2-29

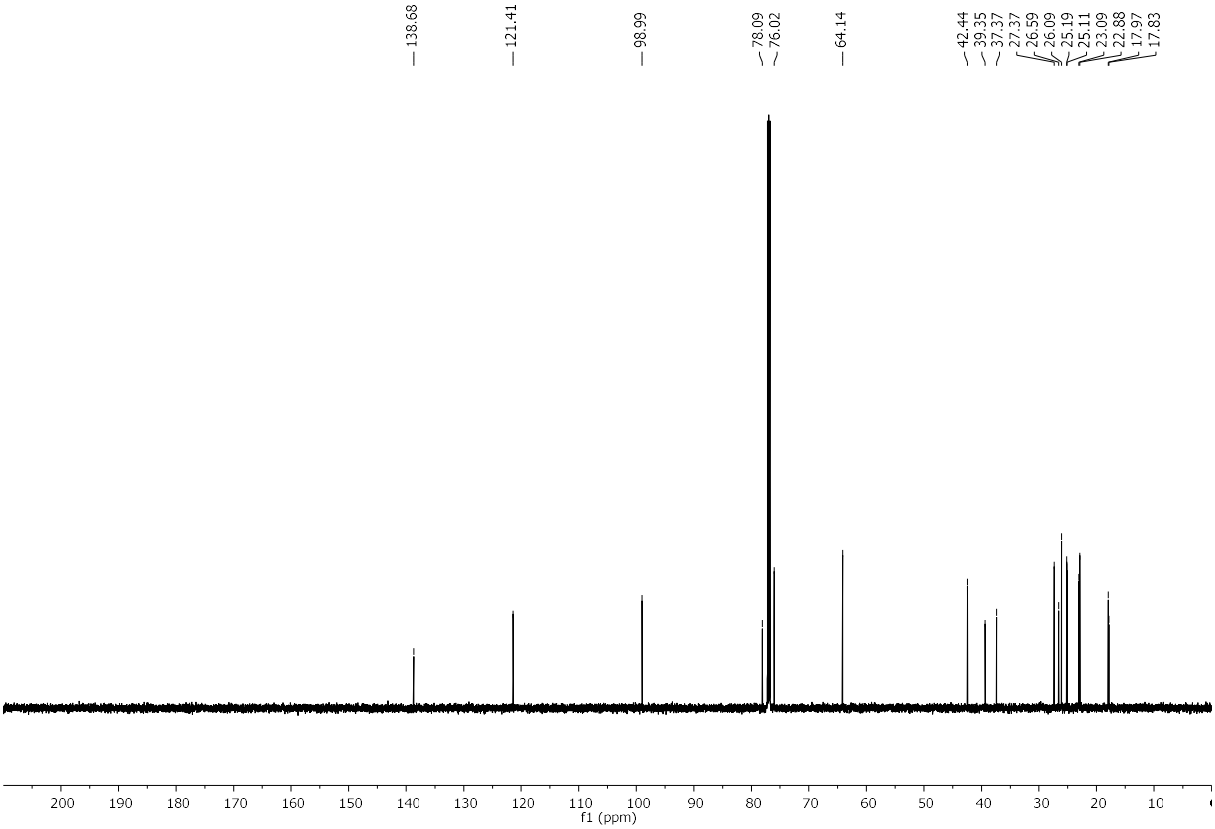

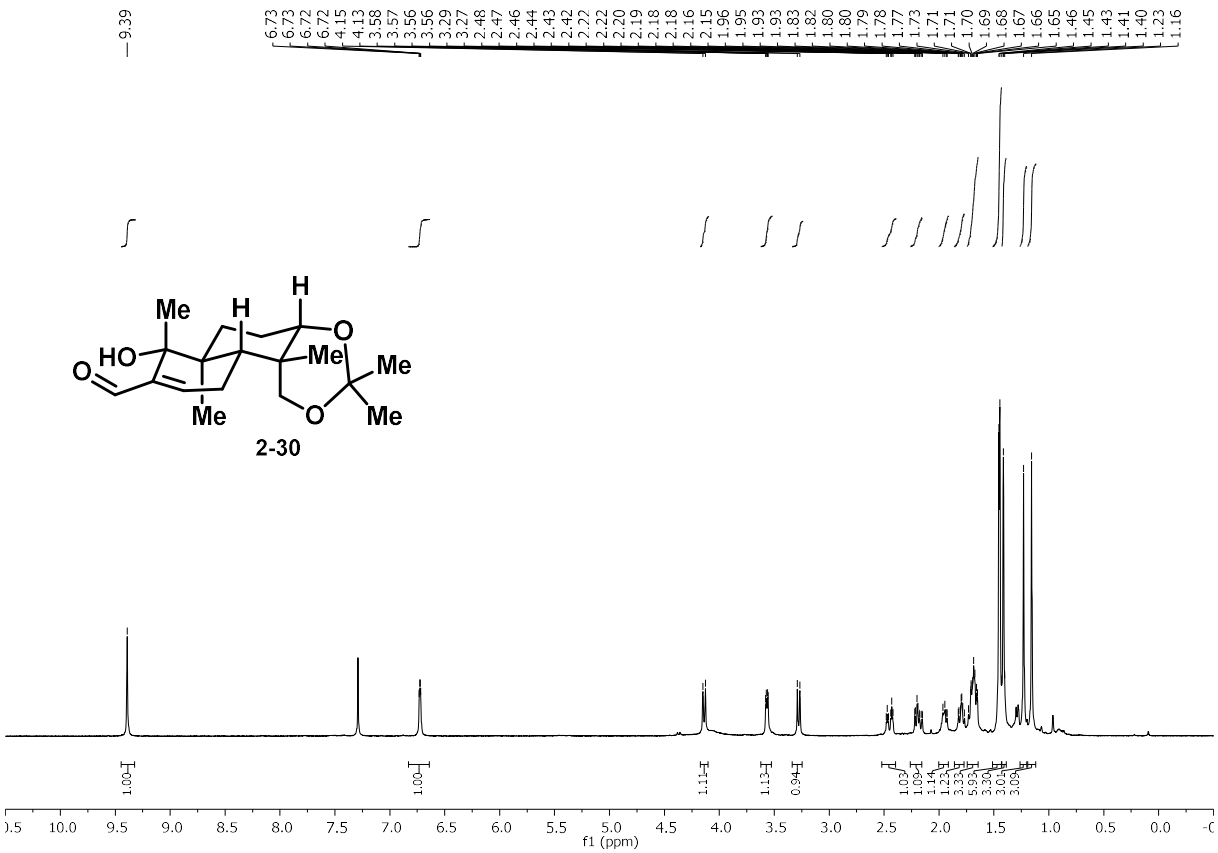
9.39
6.73
6.73
6.72
6.72
4.15
4.13
3.58
3.57
3.56
3.56
3.29
3.27
2.48
2.47
2.46
2.44
2.43
2.42
2.22
2.22
2.20
2.19
2.18
2.18
2.16
2.15
1.96
1.95
1.93
1.93
1.83
1.82
1.80
1.80
1.79
1.78
1.77
1.73
1.71
1.71
1.70
1.69
1.68
1.67
1.66
1.65
1.46
1.45
1.43
1.41
1.40
1.23
1.16
Me
H
H
HO
O
Me
O
Me
Me
O
Me
1.00
1.00
1.11
1.13
0.94
1.03
1.09
1.14
1.23
3.33
5.93
3.30
3.01
3.09
f1 (ppm)

2-30

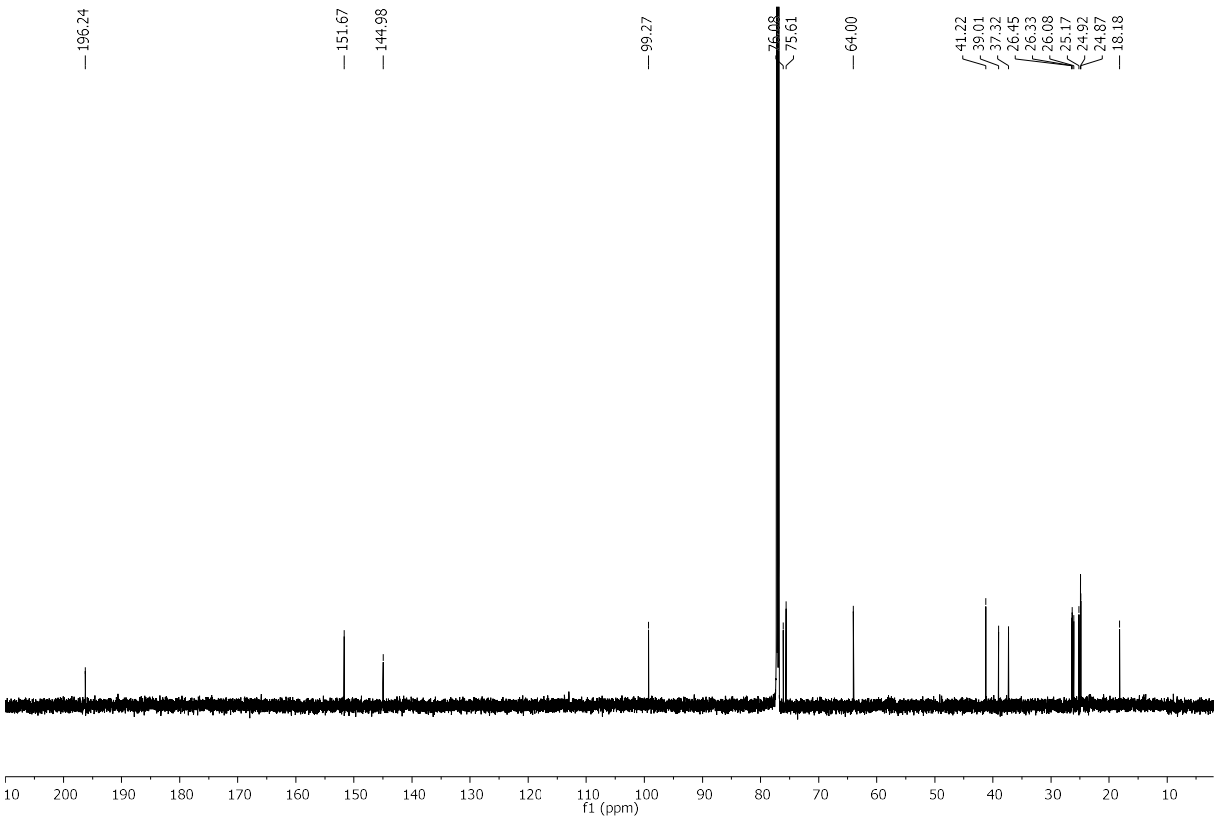
196.24
151.67
144.98
99.27
76.08
75.61
64.00
41.22
39.01
37.32
26.45
26.33
26.08
25.17
24.92
24.87
18.18
f1 (ppm)

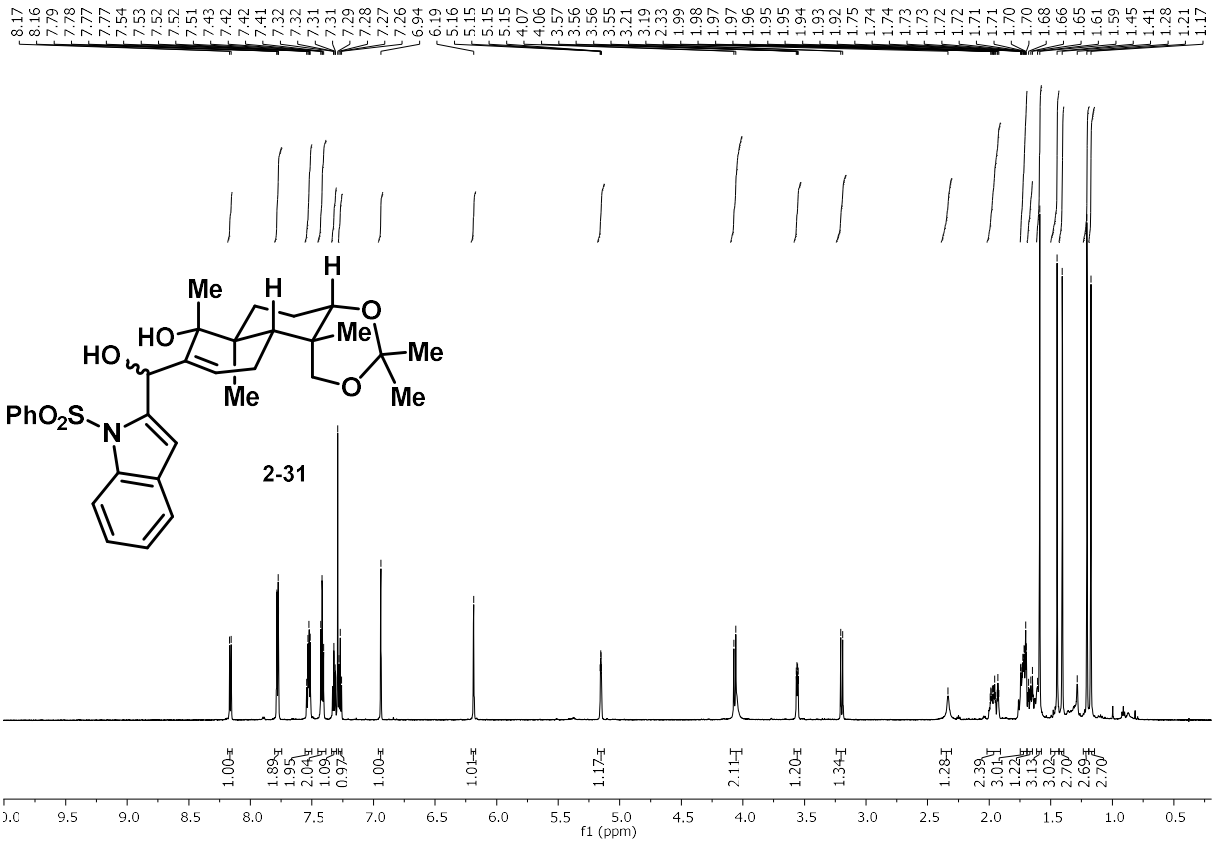
Me
H
H
O
HO
Me
HO
Me
Me
PhO2S
N
O
Me
2-31
f1 (ppm)

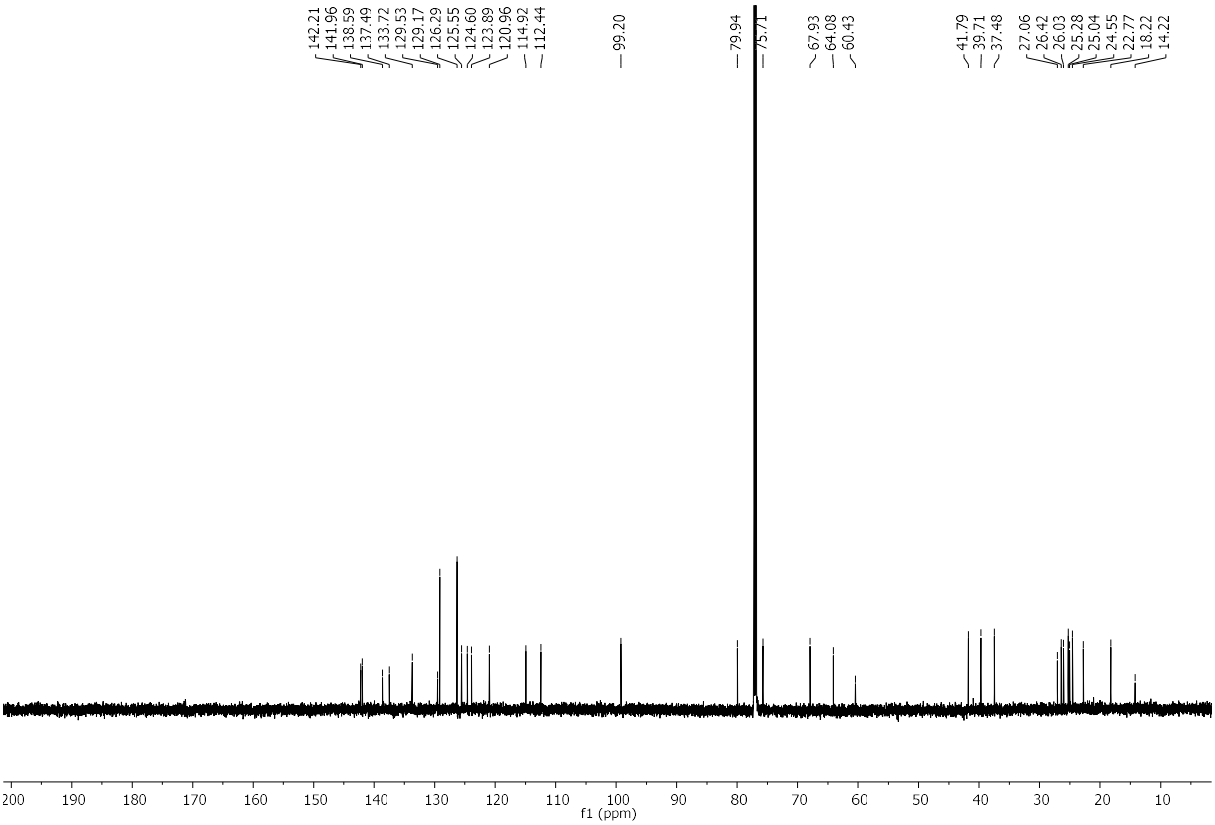
f1 (ppm)

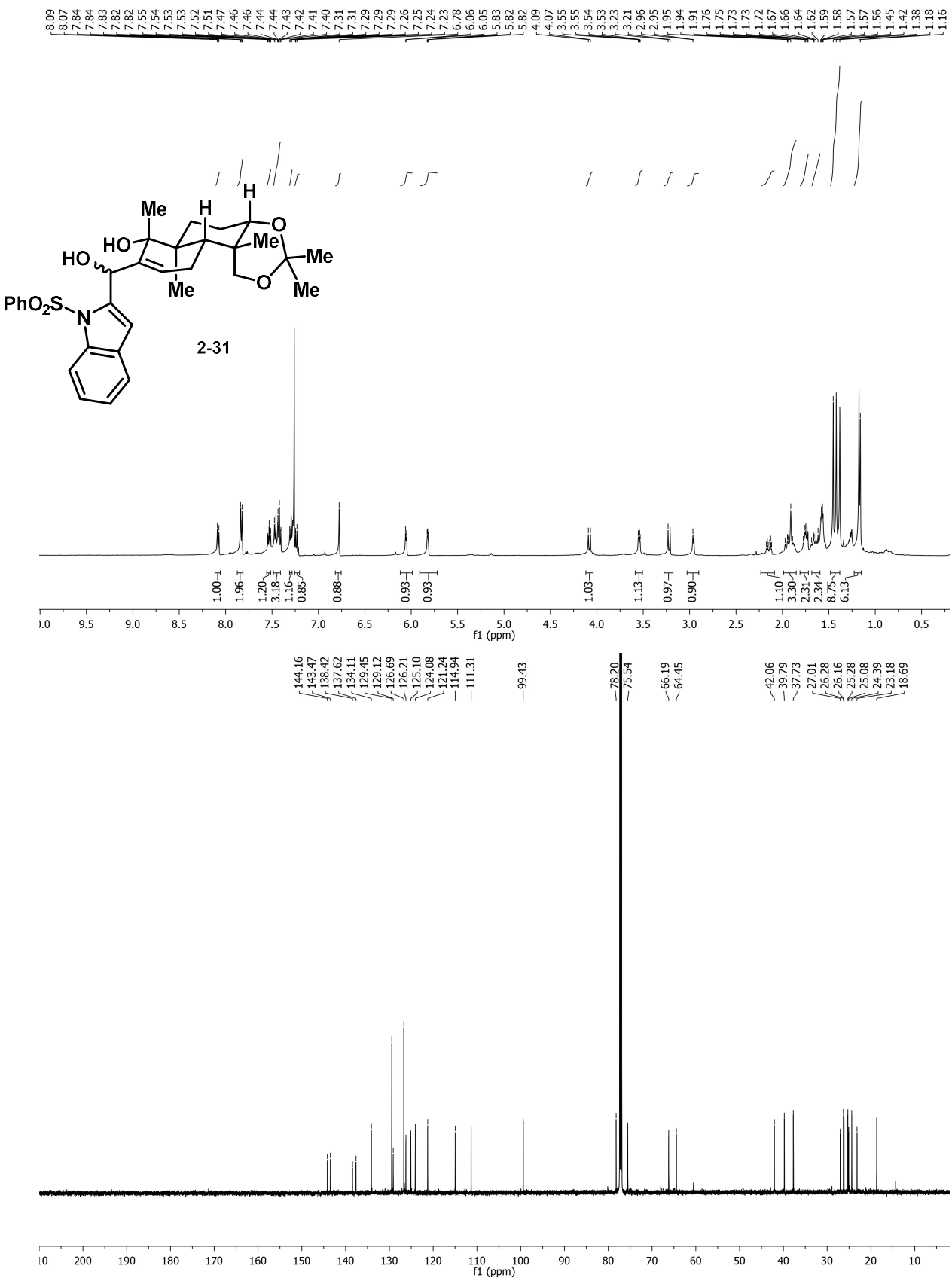
Me
H
H
O
Me
HO
HO
Me
Me
Me
O
Me
PhO2S
N
2-31
f1 (ppm)
f1 (ppm)

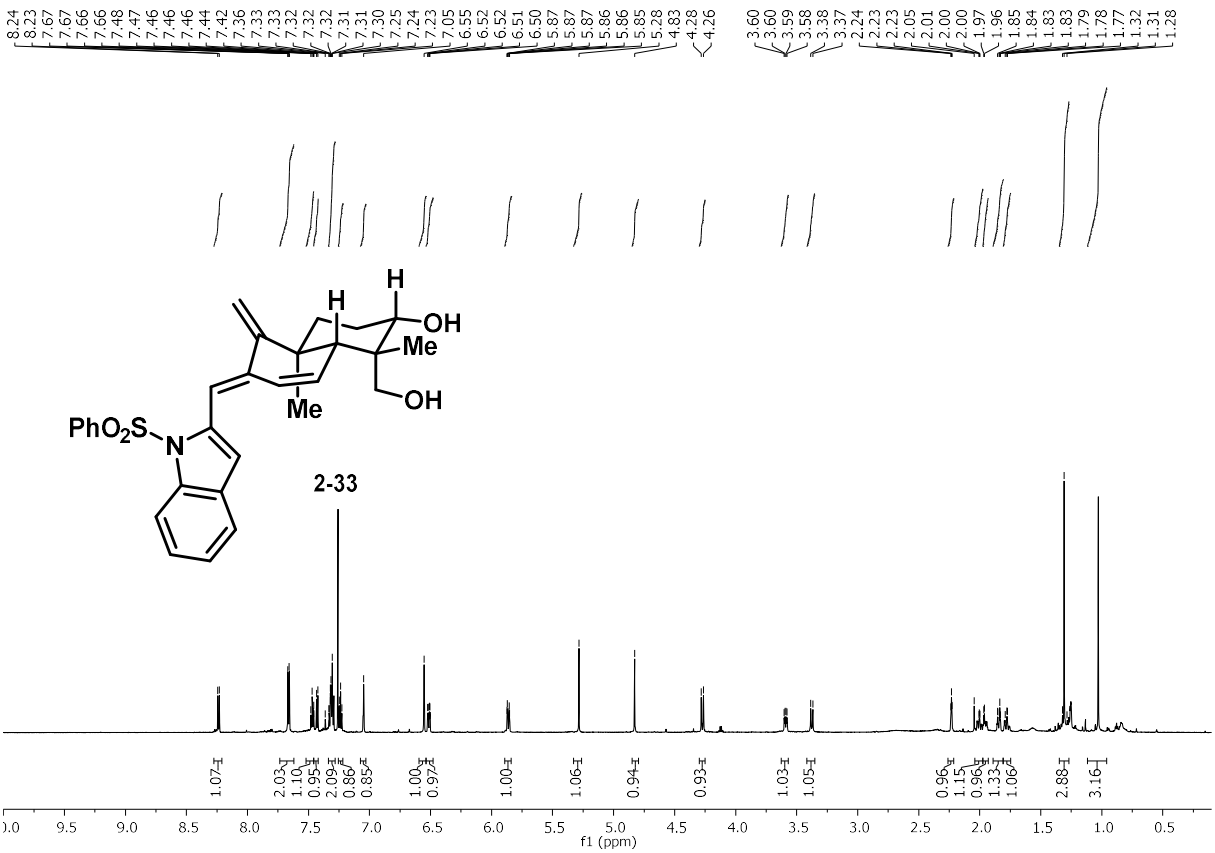
H
H
OH
Me
OH
Me
PhO2S
N
2-33
f1 (ppm)

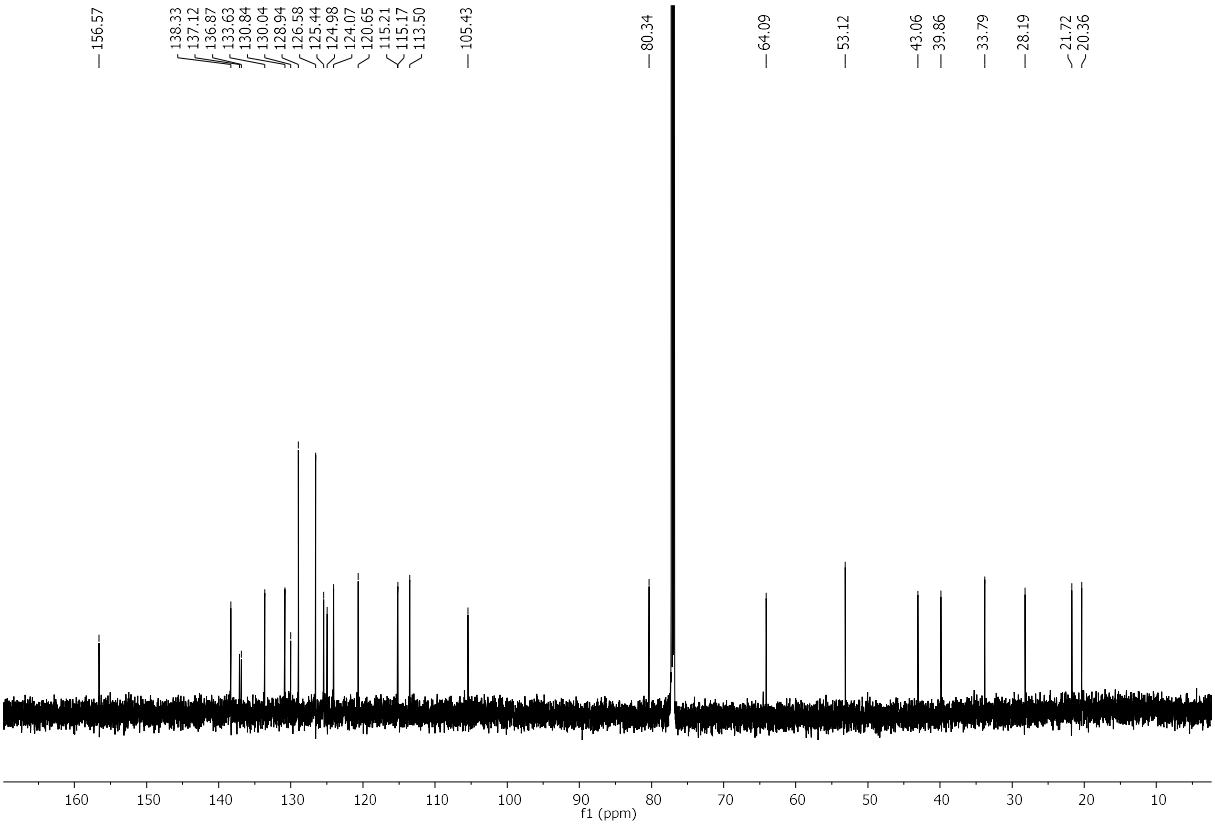
156.57
138.33
137.12
136.87
133.63
130.84
130.04
128.94
126.58
125.44
124.98
124.07
120.65
115.21
115.17
113.50
105.43
80.34
64.09
53.12
43.06
39.86
33.79
28.19
21.72
20.36
f1 (ppm)

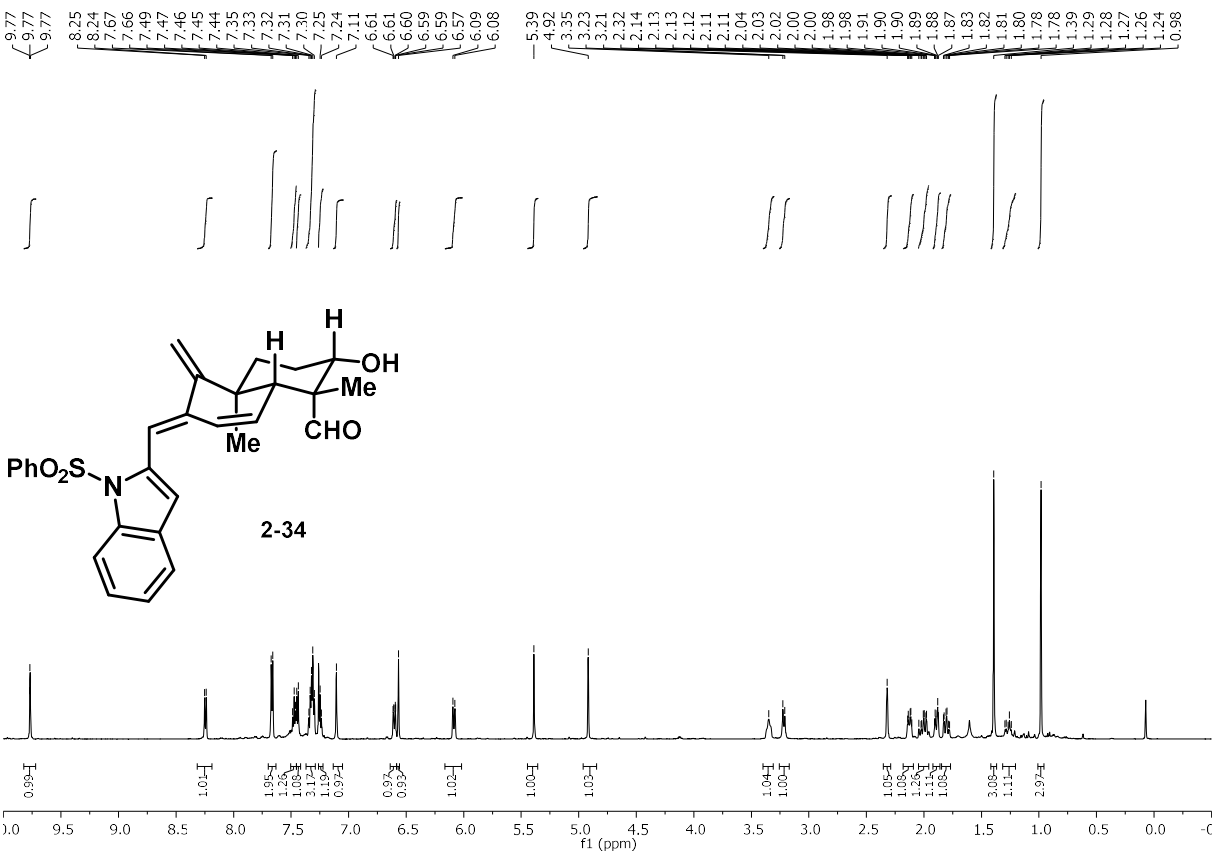

2-34

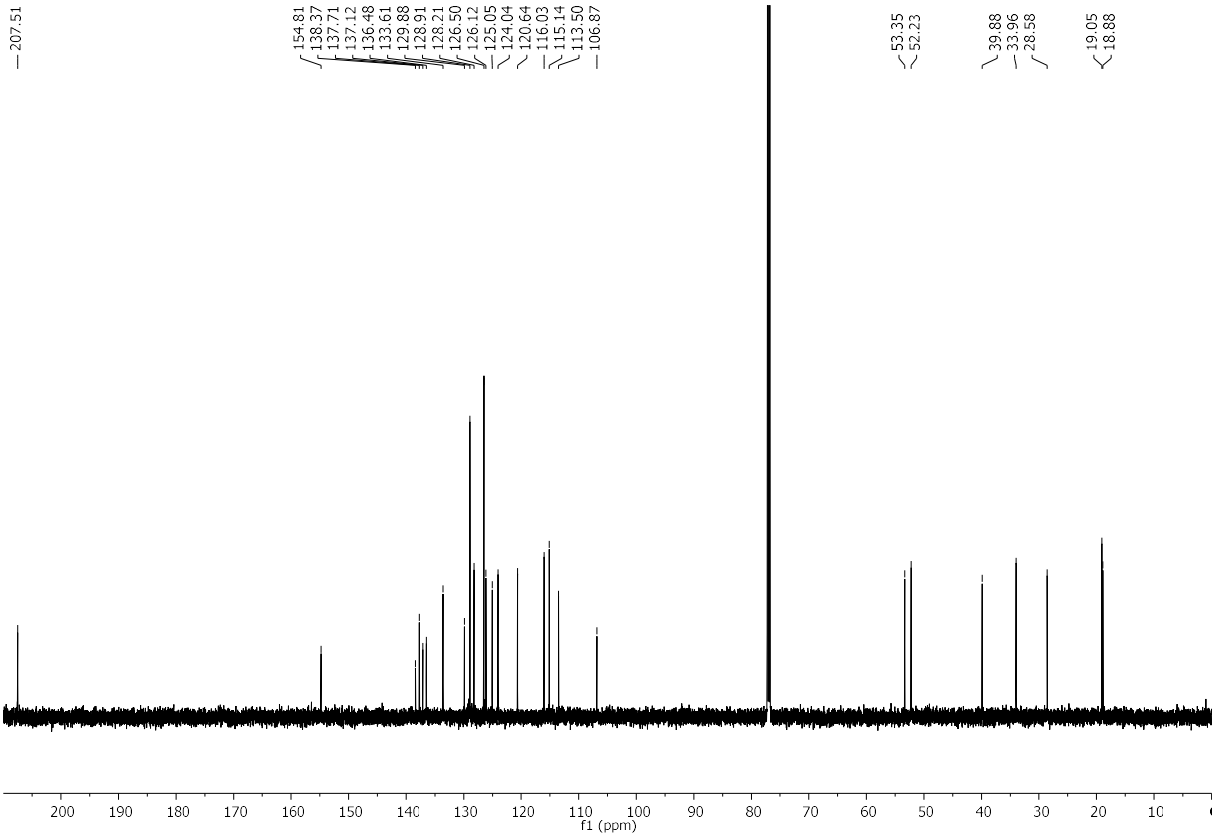

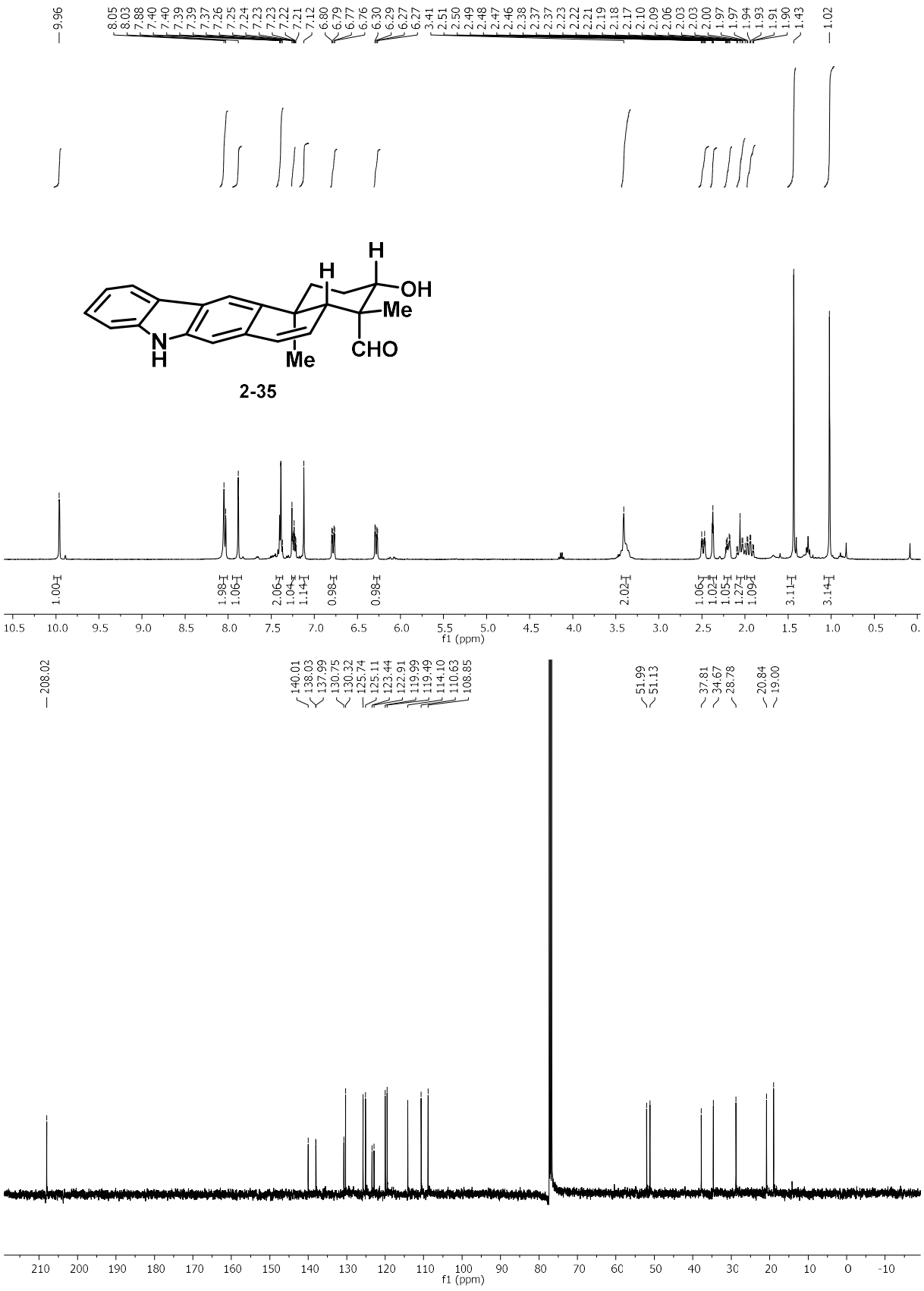
9.96
8.05
8.03
7.88
7.40
7.40
7.39
7.39
7.37
7.26
7.25
7.24
7.23
7.23
7.22
7.21
7.12
6.80
6.79
6.77
6.76
6.30
6.29
6.27
6.27
3.41
2.51
2.50
2.49
2.48
2.47
2.46
2.38
2.37
2.37
2.23
2.22
2.21
2.19
2.18
2.17
2.10
2.09
2.06
2.03
2.03
2.00
1.97
1.97
1.94
1.93
1.91
1.90
1.43
1.02
H
H
OH
Me
CHO
N
H
Me
2-35
1.00
1.98
1.06
2.06
1.04
1.14
0.98
0.98
2.02
1.06
1.02
1.05
1.27
1.09
3.11
3.14
f1 (ppm)
208.02
140.01
138.03
137.99
130.75
130.32
125.74
125.11
123.44
122.91
119.99
119.49
114.10
110.63
108.85
51.99
51.13
37.81
34.67
28.78
20.84
19.00
f1 (ppm)

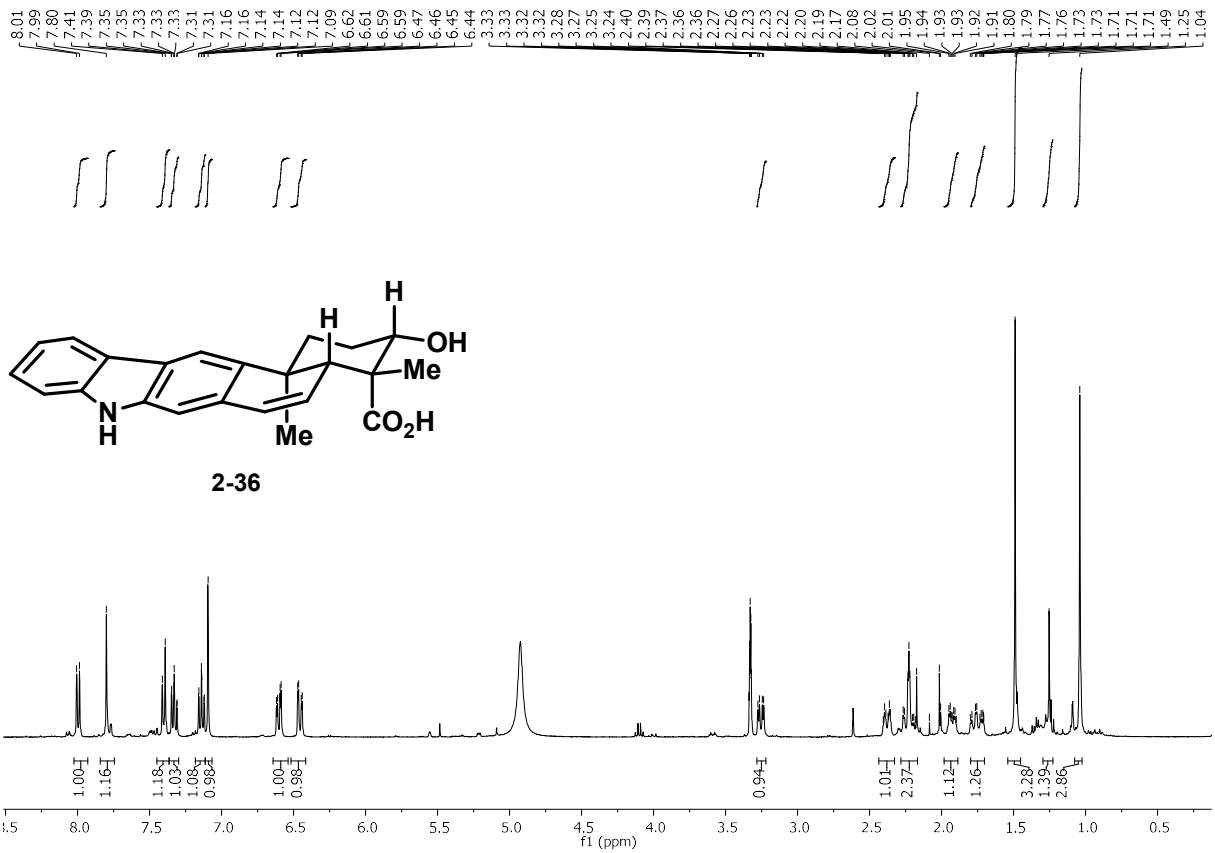
8.01 7.99 7.80 7.41 7.39 7.35 7.35 7.33 7.33 7.33 7.31 7.31 7.16 7.16 7.14 7.14 7.12 7.12 7.09 6.62 6.61 6.59 6.59 6.47 6.46 6.45 6.44
3.33 3.33 3.32 3.32 3.28 3.27 3.25 3.24 2.40 2.39 2.37 2.36 2.36 2.27 2.26 2.23 2.22 2.20 2.19 2.17 2.08 2.02 2.01 1.95 1.94 1.93 1.93 1.92 1.91 1.80 1.79 1.77 1.76 1.73 1.73 1.71 1.71 1.71 1.49 1.25 1.04
H
H
OH
Me
N
H
Me
CO2H
1.00 1.16 1.18 1.03 1.08 0.98 1.00 0.98 0.94 1.01 2.37 1.12 1.26 3.28 1.39 2.86
f1 (ppm)

2-36

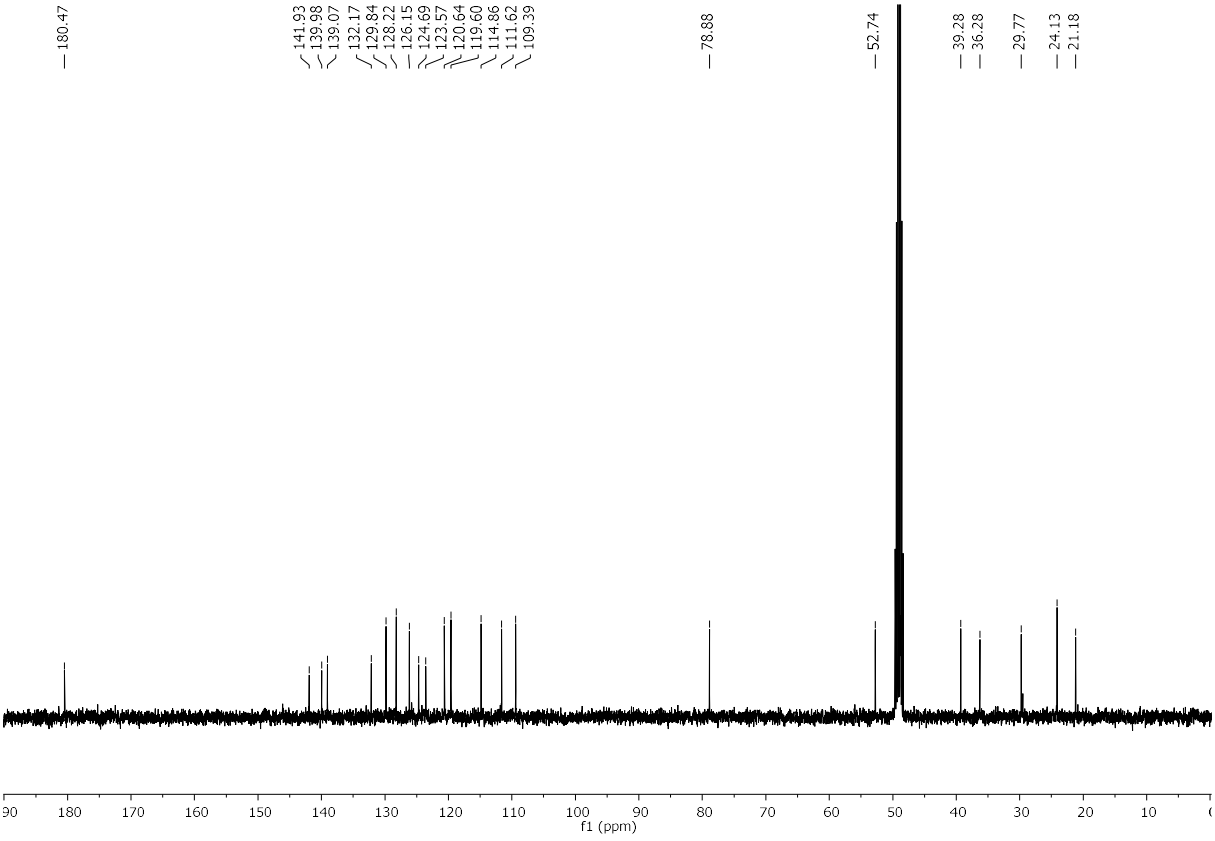
180.47
141.93 139.98 139.07 132.17 129.84 128.22 126.15 124.69 123.57 120.64 119.60 114.86 111.62 109.39
78.88
52.74
39.28 36.28 29.77 24.13 21.18
f1 (ppm)

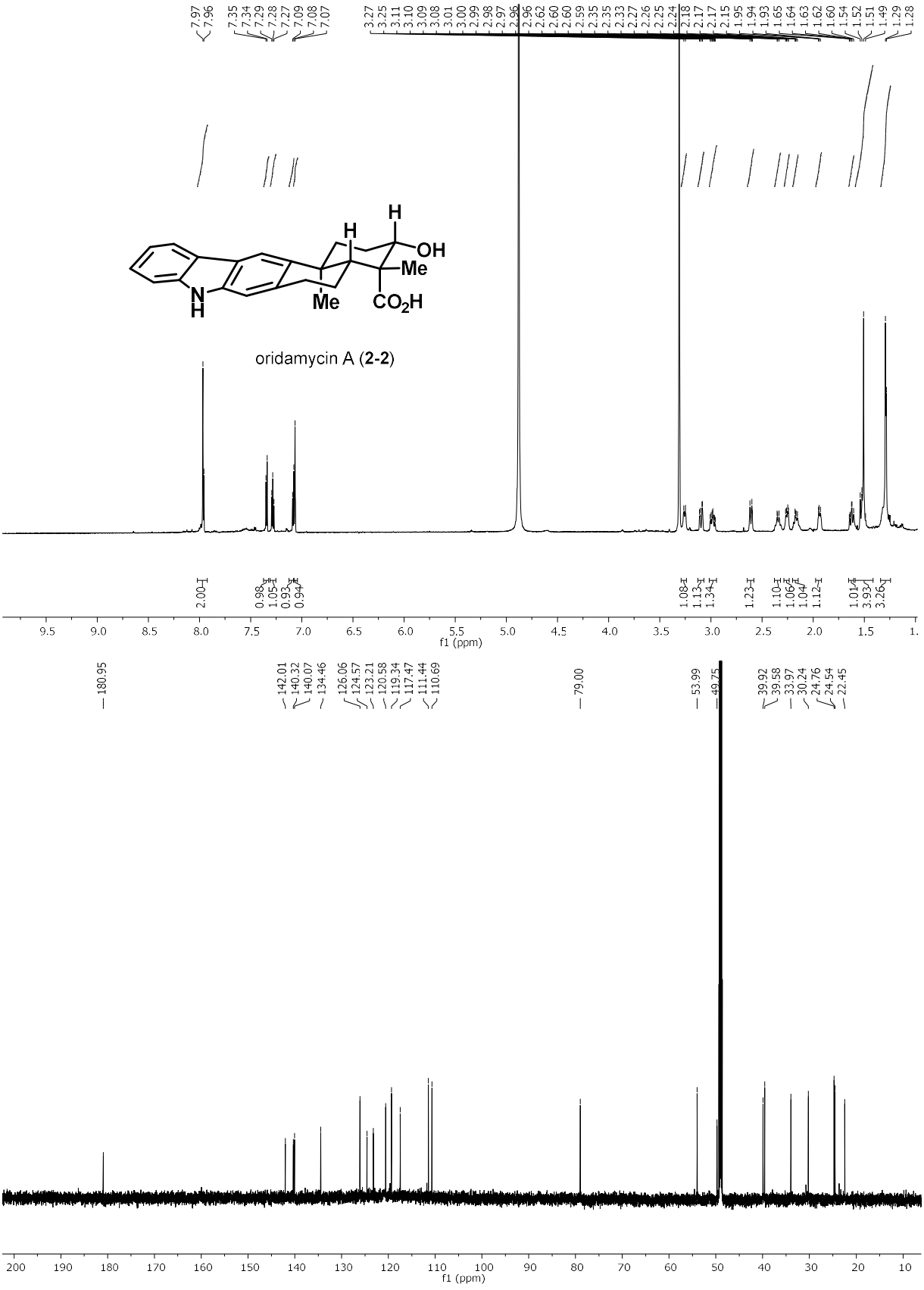
7.97
7.96
7.35
7.34
7.29
7.28
7.27
7.09
7.08
7.07
3.27
3.25
3.11
3.10
3.09
3.08
3.01
3.00
2.99
2.98
2.97
2.96
2.96
2.62
2.60
2.60
2.59
2.35
2.35
2.33
2.27
2.26
2.25
2.24
2.18
2.17
2.17
2.15
1.95
1.94
1.93
1.65
1.64
1.63
1.62
1.60
1.54
1.52
1.51
1.49
1.29
1.28
H
H
OH
Me
N
H
Me
CO2H
oridamycin A (2-2)
2.00
0.98
1.05
0.93
0.94
1.08
1.13
1.34
1.23
1.10
1.06
1.04
1.12
1.01
3.93
3.26
f1 (ppm)
180.95
142.01
140.32
140.07
134.46
126.06
124.57
123.21
120.58
119.34
117.47
111.44
110.69
79.00
53.99
49.75
39.92
39.58
33.97
30.24
24.76
24.54
22.45
f1 (ppm)

2.6 References

(1) (a) Ding, L.; Münch, J.; Goerls, H.; Maier, A.; Fiebig, H.-H.; Lin, W.-H.; Hertweck, C. Xiamycin, a Pentacyclic Indolosesquiterpene with Selective Anti-HIV Activity from a Bacterial Mangrove Endophyte. *Bioorg. Med. Chem. Lett.* **2010**, *20*, 6685–6687. (b) Takada, K.; Kajiwara, H.; Imamura, N. Oridamycins A and B, Anti-Saprolegnia Parasitica Indolosesquiterpenes Isolated from Streptomyces Sp. KS84. *J. Nat. Prod.* **2010**, *73*, 698–701. (c) Ding, L.; Maier, A.; Fiebig, H.-H.; Lin, W.-H.; Hertweck, C. A Family of Multicyclic Indolosesquiterpenes from a Bacterial Endophyte. *Org. Biomol. Chem.* **2011**, *9*, 4029–4031. (d) Kim, S.-H.; Ha, T.-K.-Q.; Oh, W. K.; Shin, J.; Oh, D.-C. Antiviral Indolosesquiterpenoid Xiamycins C–E from a Halophilic Actinomycete. *J. Nat. Prod.* **2016**, *79*, 51–58. (e) Zhang, Q.; Li, H.; Yu, L.; Sun, Y.; Zhu, Y.; Zhu, H.; Zhang, L.; Li, S.-M.; Shen, Y.; Tian, C.; Li, A.; Liu, H.; Zhang, C. Characterization of the Flavoenzyme XiaK as an N-Hydroxylase and Implications in Indolosesquiterpene Diversification. *Chem. Sci.* **2017**, *8*, 5067–5077.

(2) (a) Meng, Z.; Yu, H.; Li, L.; Tao, W.; Chen, H.; Wan, M.; Yang, P.; Edmonds, D. J.; Zhong, J.; Li, A. Total Synthesis and Antiviral Activity of Indolosesquiterpenoids from the Xiamycin and Oridamycin Families. *Nat. Commun* **2015**, *6*, 6096. (b) Rosen, B. R.; Werner, E. W.; O'Brien, A. G.; Baran, P. S. Total Synthesis of Dixiamycin B by Electrochemical Oxidation. *J. Am. Chem. Soc.* **2014**, *136*, 5571–5574. (c) Feng, J.; Noack, F.; Krische, M. J. Modular Terpenoid Construction via Catalytic Enantioselective Formation of All-Carbon Quaternary Centers: Total Synthesis of Oridamycin A, Triptoquinones B and C, and Isoiresin. *J. Am. Chem. Soc.* **2016**, *138*, 12364–12367. (d) Trotta, A. H. Total Synthesis of Oridamycins A and B. *Org. Lett.* **2015**, *17*, 3358–3361. (e) Trotta, A. H. Toward a Unified Total Synthesis of the Xiamycin and Oridamycin Families of Indolosesquiterpenes. *J. Org. Chem.* **2017**, *82*, 13500–13516. (f) Dethe, D. H.; Shukla, M. Enantioselective First Total Syntheses of the Antiviral Natural Products Xiamycins D and E. *Chem. Commun.* **2021**, *57*, 10644–10646.

(3) (a)Fones, H.; Gurr, S. The Impact of Septoria Tritici Blotch Disease on Wheat: An EU Perspective. *Fun. Gen. Biol.* **2015**, *79*, 3–7. (b) Poole, N. F.; Arnaudin, M. E. The Role of Fungicides for Effective Disease Management in Cereal Crops. *Can. J. Plant Path.y* **2014**, *36*, 1–11.

(4) Boger, D. L.; Brotherton, C. E. Total Synthesis of Azafluoranthene Alkaloids: Rufescine and Imeluteine. *J. Org. Chem.* **1984**, *49*, 4050–4055.

(5)(a) Leger, P. R.; Kuroda, Y.; Chang, S.; Jurczyk, J.; Sarpong, R. C–C Bond Cleavage Approach to Complex Terpenoids: Development of a Unified Total Synthesis of the Phomactins. *J. Am. Chem. Soc.* **2020**, *142*, 15536–15547. (b) Lusi, R. F.; Perea, M. A.; Sarpong, R. C–C Bond Cleavage of α-Pinene Derivatives Prepared from Carvone as a General Strategy for Complex Molecule Synthesis. *Acc. Chem. Res.* **2022**, *55*, 746–758. (c) Weber, M.; Owens, K.; Masarwa, A.; Sarpong, R. Construction of Enantiopure Taxoid and Natural Product-like Scaffolds Using a C–C Bond Cleavage/Arylation Reaction. *Org. Lett.* **2015**, *17*, 5432–5435. (d) Na, C. G.; Kang, S. H.; Sarpong, R. Development of a C–C Bond Cleavage/Vinylation/Mizoroki–Heck Cascade Reaction: Application to the Total Synthesis of 14- and 15-Hydroxypatchoulol. *J. Am. Chem. Soc.* **2022**, *144*,

19253–19257. (e) Nagasawa, S.; Jones, K. E.; Sarpong, R. Enantiospecific Entry to a Common Decalin Intermediate for the Syntheses of Highly Oxygenated Terpenoids. *J. Org. Chem.* **2019**, *84*, 12209–12215. (f) Perea, M. A.; Wang, B.; Wyler, B. C.; Ham, J. S.; O'Connor, N. R.; Nagasawa, S.; Kimura, Y.; Manske, C.; Scherübl, M.; Nguyen, J. M.; Sarpong, R. General Synthetic Approach to Diverse Taxane Cores. *J. Am. Chem. Soc.* **2022**. (g) Kuroda, Y.; Nicacio, K. J.; da Silva-Jr, I. A.; Leger, P. R.; Chang, S.; Gubiani, J. R.; Deflon, V. M.; Nagashima, N.; Rode, A.; Blackford, K.; Ferreira, A. G.; Sette, L. D.; Williams, D. E.; Andersen, R. J.; Jancar, S.; Berlinck, R. G. S.; Sarpong, R. Isolation, Synthesis and Bioactivity Studies of Phomactin Terpenoids. *Nat. Chem* **2018**, *10*, 938–945. (h) Blümel, M.; Nagasawa, S.; Blackford, K.; Hare, S. R.; Tantillo, D. J.; Sarpong, R. Rearrangement of Hydroxylated Pinene Derivatives to Fenchone-Type Frameworks: Computational Evidence for Dynamically-Controlled Selectivity. *J. Am. Chem. Soc.* **2018**, *140*, 9291–9298. (i) Masarwa, A.; Weber, M.; Sarpong, R. Selective C–C and C–H Bond Activation/Cleavage of Pinene Derivatives: Synthesis of Enantiopure Cyclohexenone Scaffolds and Mechanistic Insights. *J. Am. Chem. Soc.* **2015**, *137*, 6327–6334. (j) Lusi, R. F.; Sennari, G.; Sarpong, R. Strategy Evolution in a Skeletal Remodeling and C–H Functionalization-Based Synthesis of the Longiborneol Sesquiterpenoids. *J. Am. Chem. Soc.* **2022**, *144*, 17277–17294. (k) Kerschgens, I.; Rovira, A. R.; Sarpong, R. Total Synthesis of (−)-Xishacorene B from (R)-Carvone Using a C–C Activation Strategy. *J. Am. Chem. Soc.* **2018**, *140*, 9810–9813. (l) Lusi, R. F.; Sennari, G.; Sarpong, R. Total Synthesis of Nine Longiborneol Sesquiterpenoids Using a Functionalized Camphor Strategy. *Nat. Chem.* **2022**, *14*, 450–456. (m) Finkbeiner, P.; Murai, K.; Röpke, M.; Sarpong, R. Total Synthesis of Terpenoids Employing a "Benzannulation of Carvone" Strategy: Synthesis of (−)-Crotogoudin. *J. Am. Chem. Soc.* **2017**, *139*, 11349–11352.

(6)(a) Gaich, T.; Mulzer, J. 2.7 Chiral Pool Synthesis: Starting from Terpenes. In *Comprehensive Chirality*; Carreira, E. M., Yamamoto, H., Eds.; Elsevier: Amsterdam, 2012; pp 163–206.

(b) Brill, Z. G.; Condakes, M. L.; Ting, C. P.; Maimone, T. J. Navigating the Chiral Pool in the Total Synthesis of Complex Terpene Natural Products. *Chem. Rev.* **2017**, *117*, 11753–11795.

(7)(a) Brocksom, T. J.; Desiderá, A. L.; Alves, L. de C.; Oliveira, K. T. de. The New Directions of Organic Synthesis. Current Organic Synthesis 12, 496–522.

(8) Binkley, R. W.; Flechtner, T. W. Photoremovable Protecting Groups. In *Synthetic Organic Photochemistry*; Horspool, W. M., Ed.; Springer US: Boston, MA, 1984; pp 375–423.

(9) (a)Odani, A.; Ishihara, K.; Ohtawa, M.; Tomoda, H.; Omura, S.; Nagamitsu, T. Total Synthesis of Pyripyropene A. *Tetrahedron* **2011**, *67*, 8195–8203. (b) Zhong, Z.; Zhao, G.; Xu, D.; Dong, B.; Song, D.; Xie, X.; She, X. Bioinspired Total Syntheses of Isospongian-Type Diterpenoids (−)-Kravanhins A and C. *Chem. Asian J.* **2016**, *11*, 1542–1547.

(10)(a) Evans, D. A.; Chapman, K. T. The Directed Reduction of β-Hydroxy Ketones Employing $Me_4NHB(OAc)_3$. *Tetrahedron Lett.* **1986**, *27*, 5939–5942. (b) Reisman, S. E.; Ready, J. M.; Weiss, M. M.; Hasuoka, A.; Hirata, M.; Tamaki, K.; Ovaska, T. V.; Smith, C. J.; Wood, J. L. Evolution of a

Synthetic Strategy: Total Synthesis of (±)-Welwitindolinone A Isonitrile. *J. Am. Chem. Soc.* **2008**, *130*, 2087–2100.

(11) NMR comparison to known compound **7** (reference 9) showed several discrepancies (see supporting information for details) which led us to unambiguously confirm our result by X-ray analysis.

(12) Paul, A.; Seidel, D. α-Functionalization of Cyclic Secondary Amines: Lewis Acid Promoted Addition of Organometallics to Transient Imines. *J. Am. Chem. Soc.* **2019**, *141*, 8778–8782.

(13) a) For a review on electrocyclization as a benzannulation strategy, see: Trauner D.; Webster, R.; In *Comprehensive Organic Synthesis: Second Edition*. Vol. 5, Elsevier Ltd., 2014, pp 783–826. (b) Roy, J.; Jana, A. K.; Mal, D. Recent Trends in the Synthesis of Carbazoles: An Update. *Tetrahedron* **2012**, *68*, 6099–6121.

(14) (1) Bach, T.; Hehn, J. P. Photochemical Reactions as Key Steps in Natural Product Synthesis. *Angew. Chem. Int. Ed.* **2011**, *50*, 1000–1045.

(15) (a) Hernandez-Perez, A. C.; Collins, S. K. A Visible-Light-Mediated Synthesis of Carbazoles. *Angew. Chem. Int. Ed.* **2013**, *52*, 12696–12700. (b) Hernandez-Perez, A. C.; Caron, A.; Collins, S. K. Photochemical Synthesis of Complex Carbazoles: Evaluation of Electronic Effects in Both UV- and Visible-Light Methods in Continuous Flow. *Chemistry – A European Journal* **2015**, *21*, 16673–16678. (c) Choi, S.; Chatterjee, T.; Choi, W. J.; You, Y.; Cho, E. J. Synthesis of Carbazoles by a Merged Visible Light Photoredox and Palladium-Catalyzed Process. *ACS Catal.* **2015**, *5*, 4796–4802.

(16) In general, full consumption of the starting material was observed. Broadened NMR-signals indicate the potential formation of unidentified polymerization side-products.

(17) (a) Kageyama, Y.; Ohshima, R.; Sakurama, K.; Fujiwara, Y.; Tanimoto, Y.; Yamada, Y.; Aoki, S. Photochemical Cleavage Reactions of 8-Quinolinyl Sulfonates in Aqueous Solution. *Chemical and Pharmaceutical Bulletin* **2009**, *57*, 1257–1266. (b) Hong, X.; Mejía-Oneto, J. M.; France, S.; Padwa, A. Photodesulfonylation of Indoles Initiated by Electron Transfer from Triethylamine. *Tetrahedron Letters* **2006**, *47*, 2409–2412. (c) Art, J. F.; Kestemont, J. P.; Soumillion, J. Ph. Photodetosylation of Sulfonamides Initiated by Electron Transfer from an Anionic Sensitizer. *Tetrahedron Letters* **1991**, *32*, 1425–1428. (d) Hamada, Tatsuo.; Nishida, Atsushi.; Yonemitsu, Osamu. Selective Removal of Electron-Accepting p-Toluene- and Naphthalenesulfonyl Protecting Groups for Amino Function via Photoinduced Donor Acceptor Ion Pairs with Electron-Donating Aromatics. *J. Am. Chem. Soc.* **1986**, *108*, 140–145.

(18) The UV/vis absorption spectrum of triene **6** and carbazole **12** showed absorption maxima at 328 and 320 nm, respectively. Product **12** was found stable under prolonged irradiation and was fully recovered.

(19) We also found that the photocyclization also works on the stage of the α-hydroxy acid, forming the corresponding carbazole in 32% yield.

(20) Bal, B. S.; Childers, W. E.; Pinnick, H. W. Oxidation of α,β-Un Saturated Aldehydes. *Tetrahedron* **1981**, *37*, 2091–2096.

(21) Chen, K.-M.; Gunderson, K. G.; Hardtmann, G. E.; Prasad, K.; Repic, O.; Shapiro, M. J. A Novel Method for the In Situ Generation of Alkoxydialkylboranes and Their Use in the Selective Preparation of 1,3-Syn Diols. *Chem. Lett.* **1987**, *16*, 1923–1926.

2.7 Experimental contributors

This chapter includes content reproduced, with permission, from: Pfaffenbach, M. Bakanas, I., O'Connor, N. R., Herrick, J., Sarpong, R. Total Syntheses of Xiamycins A, C, F, H and Oridamycin A and Preliminary Evaluation of their Anti-Fungal Properties, *Angew. Chem. Int. Ed.* **2019**, *58*, 15304–15308. Initial experimental work performed by M.P. and N.R.O, family synthesis performed by I.B. written by I.B. with guidance from M.P and R. S. Biological activity studies led by J.H.

Chapter 3
Progress Toward a Unified Syntheses of Paspaline-type Indole Diterpenoids and Xiamycin-type Indolosesquiterpenoids

3.1 Introduction to paspaline and xiamycin natural products and unified plan

Strategies that unify the syntheses of distinct natural product families can expedite access to a wide area of chemical space for exploration.[1] The logic here is that until the point of divergence, only one synthesis route needs to be executed en route to many natural product targets. Our laboratory has had a broad interest in the synthesis of indoloterpene natural products as part of an ongoing collaboration with Corteva in the study of their anti-feedant bioactivities.[2] Our studies focused on the indole diterpenoid (IDT) paspaline[3] (**3-1**) and the indolosesquiterpenoid (IST) xiamycin A[4] (**3-2**), which have displayed a variety of interesting bioactivities (Figure 3-1). Proposed to be the biogenetic precursor to many IDTs, paspaline (**3-1**) was first isolated from the terrestrial fungal endophyte *Claviceps paspali* in 1966. This fungus is known for causing 'Paspalum Staggers',[5] which is a neurotoxic outcome that is attributed to tremorgenic IDTs. Interestingly, paspaline itself is not tremorgenic, but its downstream congeners are. In addition, xiamycin A (**3-2**) displays antibiotic and modest anti-HIV activity.[6]

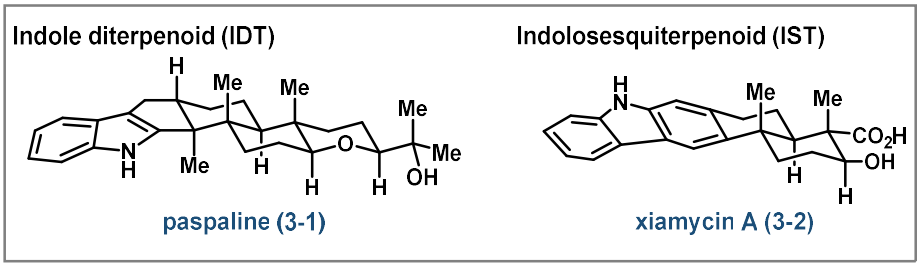

Figure 3.1. Targeted representatives of the indole diterpenoid and indolosesquiterpenoid families, paspaline and xiamycin A, respectively.

Given that both **3-1** and **3-2** are low-oxidation level members of their respective families, we hypothesized that late-stage oxidations could enable access to other congeners and the broad profiling of the biological activity of IDTs and ISTs.[7] Herein, we disclose our progress toward the unified syntheses of these indole alkaloids, culminating in a synthesis of xiamycin A (**3-2** Chapter 2).[8]

While there have been several elegant syntheses of both paspaline[9] (**3-1**) and xiamycin A[10] (**3-2**), a unified synthesis of these compounds is yet to be achieved. We recognized that **3-1**

and **3-2** had similar structural elements in that they consist of terpene units that are differentially fused to an indole unit (Figure 3-2). These structural elements also point to their biosynthetic origin. Taking advantage of this recognition in our retrosynthesis, we hypothesized that the coupling for the indole and terpene fragments to serve as the strategic point of divergence. Paspaline (**3-1**) was retrosynthetically disconnected back to 3-magnesio indole nucleophile **3-3** and terpenoid electrophile **3-4**. Alternatively, xiamycin A was proposed to arise from 2-lithio indole nucleophile **3-5** and **3-4**. We envisioned that **3-4** could be accessed from the chiral-pool terpene (*R*)-carvone (**3-6**), which our laboratory has employed as a versatile starting material in various synthesis.[11] On the basis of this strategy, our synthesis commenced with the common intermediate, aldehyde **3-4**, as the first goal.

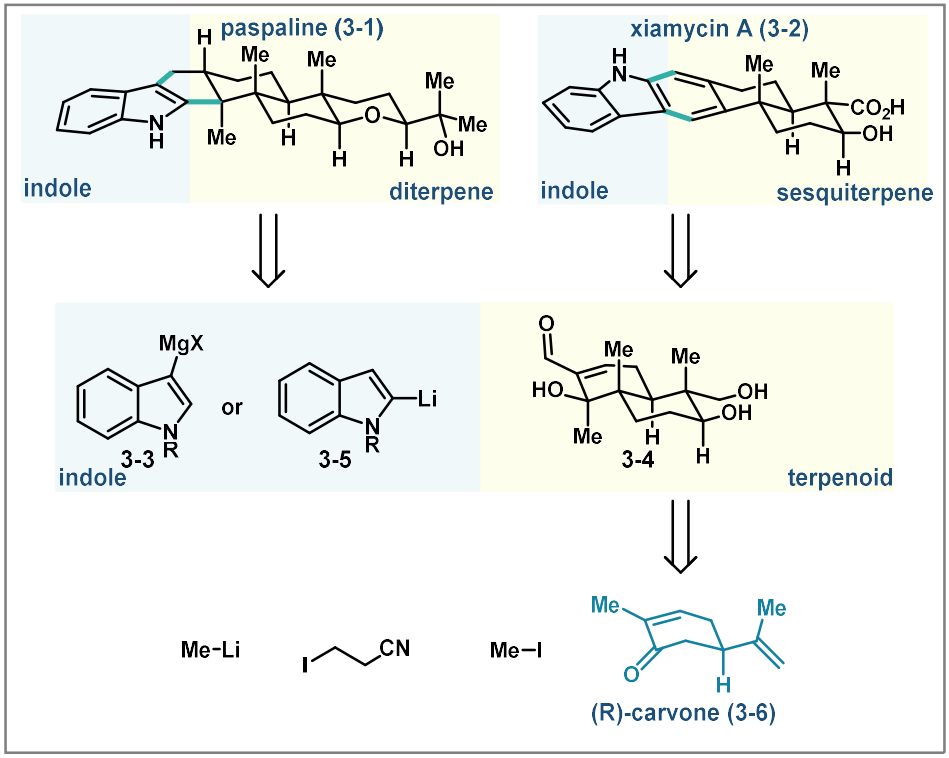

Figure 3.2. Unified retrosynthesis of paspaline (**3-1**) and xiamycin A (**3-2**) starting from carvone (**3-6**)

3.2 Forward Synthesis

(*R*)-carvone (**3-6**) was elaborated using a sequence disclosed by Omura and Nagamitsu[12] to *trans*-decalin **3-7** in 47% over four steps (Scheme 3-1). The primary hydroxy group of **3-7** directed the chemo- and diastereoselective reduction of the β-disposed ketone group using tetramethylammonium triacetoxyborohydride to give diol **3-8**.[13] Subsequent protection of the diol with dimethoxypropane, followed by 1,2-addition of MeLi into the carbonyl of the enone moiety, and allylic alcohol group oxidation selective for the primary hydroxy group yielded

aldehyde **3-4** in 61% over 4 steps. This sequence was amenable to multigram synthesis enabling preparation of over 3 grams of **3-4** in a single pass. Ready access to common synthetic intermediate **3-4** set the stage for the planned syntheses of paspaline (**3-1**) and xiamycin A (**3-2**).

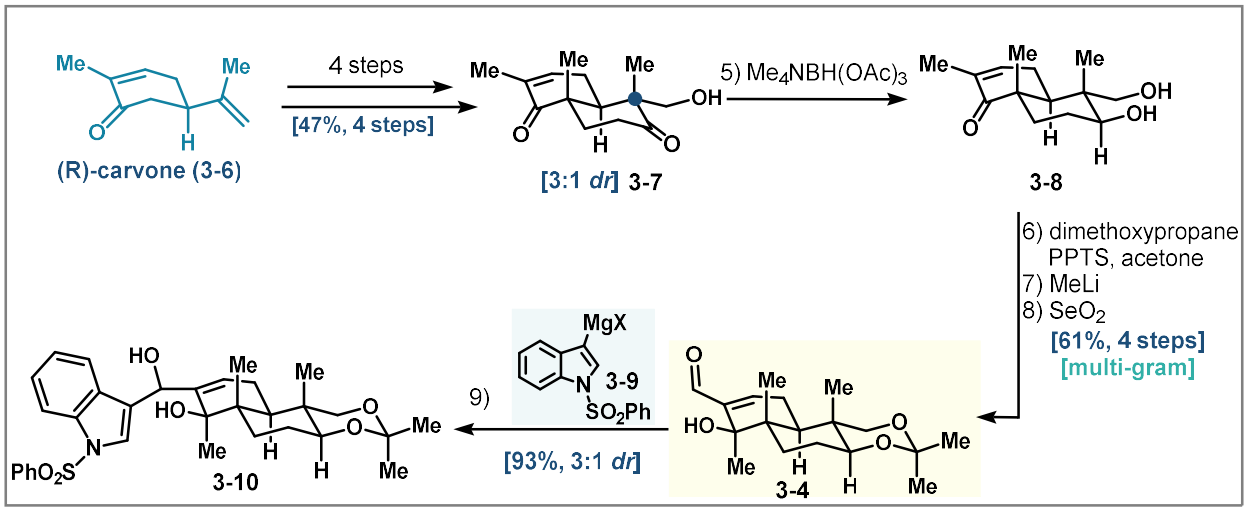

Scheme 3.1. Synthesis of common intermediate **3-4** and coupling of an indole fragment at C3

First targeting paspaline (**3-1**), 3-magnesio indole nucleophile **3-9** was added into aldehyde **3-4** to give secondary alcohol **3-10** as an inconsequential mixture of diastereomers. With access to sufficient quantities of **3-10** in hand, we planned construction of the *trans*-hydrindane ring of paspaline (**3-1**) through reductive closure to arrive at the 5-membered ring. This transformation would entail formation of a bond between C-2 of the indole and the carbon bearing the tertiary hydroxy group (Scheme 3-2), that we envisioned could be constructed through a Friedel–Crafts type cyclization followed by reduction. We hypothesized that by virture of being allylic, ionization of the tertiary hydroxy group would occur easily to aid in the desired cyclization. However, this strategy would first require cleavage of the electron-withdrawing group on the indole nitrogen to render the indole fragment suitably nucleophilic for the planned cyclization. Treatment of **3-10** with tetrabutylammonium fluoride led to a one-pot cleavage of the phenylsulfonyl group as well as elimination of the pseudobenzylic hydroxy group to give diene **3-11** in 80% yield. We found that treatment of **3-11** with aluminium trichloride ($AlCl_3$) led to the desired cyclization and concurrent acetonide cleavage yielding hydrindene **3-12**. However, **3-12** was found to be highly unstable, decomposing under most subsequent reaction conditions and upon silica gel chromatography. We were able to reduce the double bonds of **3-12** with palladium on carbon (Pd/C) under an atmosphere of hydrogen. However, hydrogenation proceeded on the undesired face—likely steered by the 1,3-axial methyl groups of the trans-decalin—to give *cis*-hydrindane **3-13**. The facial selectivity observed in this hydrogenation, combined with the inherent thermodynamic preference[14] for *cis*- over *trans*-hydrindanes, led us to revise our synthetic strategy to set the crucial C-6 stereocenter prior to cyclization.

Aldehyde **3-4** was reduced with Pd/C under an atmosphere of hydrogen to give axially disposed aldehyde **3-14** (Scheme 3-2). Notably, the diastereoselectivity of this reaction was found to be highly dependent on the source of the Pd/C. Epimerization with DBU and heating exclusively gave the equatorially disposed aldehyde. However, treatment of aldehyde **3-14** with an excess of Grignard **3-9** led to formation of adduct **3-15** as a 4:1 mixture of diastereomers at C7 (bearing the exocyclic hydroxy group), with full epimerization at C-6. We hypothesize that this outcome arises because of rapid epimerization alpha to the aldehyde group prior to addition of

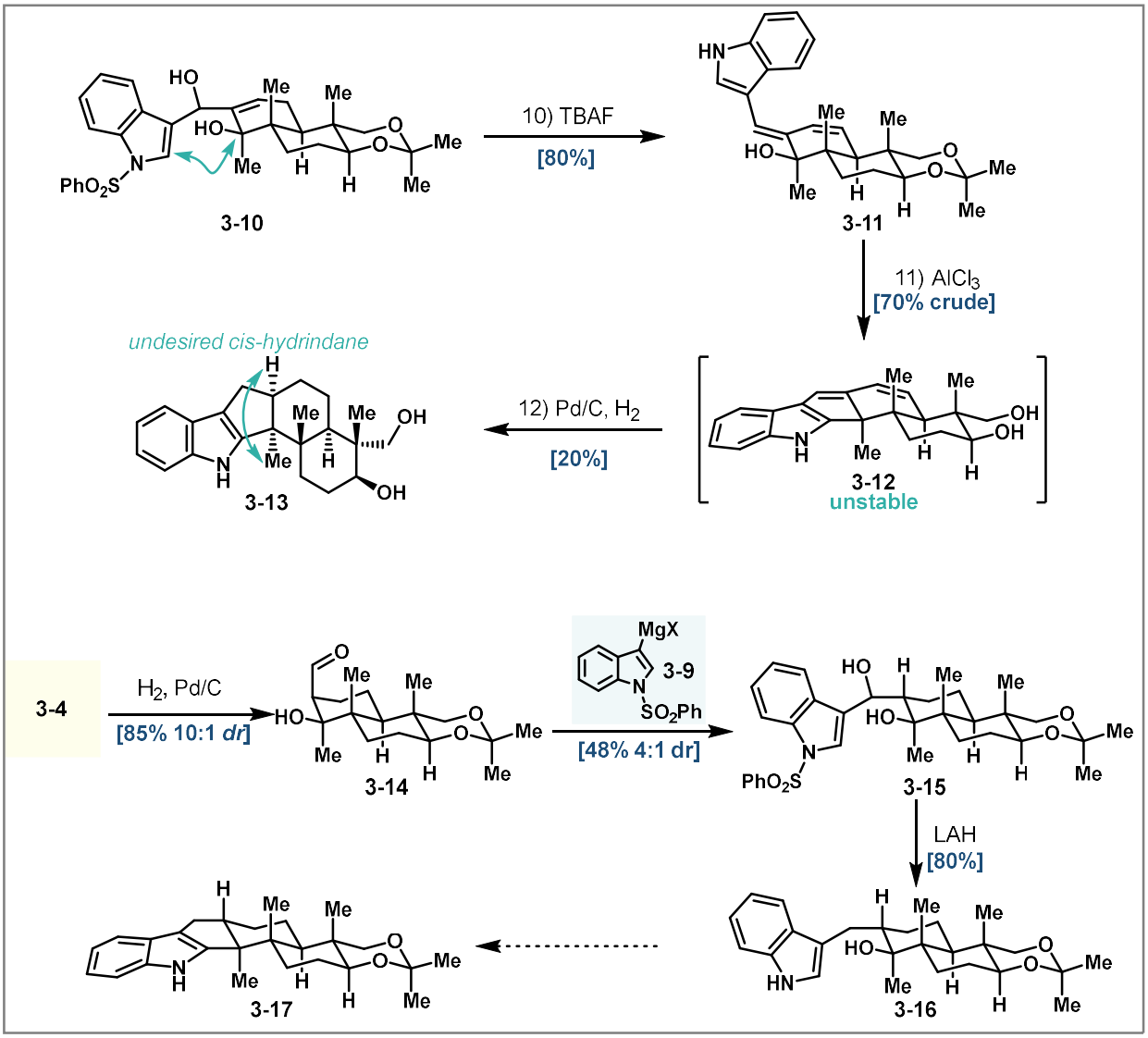

Scheme 3.2 A. Synthesis of the epi-paspaline skeleton, *cis*-hydrindane **B.** Attempted Friedel–Crafts cyclization from lower oxidation level.

the nucleophile, either via a retro-aldol reaction pathway or direct deprotonation. Additionally, the tertiary hydroxy group may direct the Grignard reagent toward an equatorial approach, such that only the equatorially disposed epimer participates in the nucleophilic addition. Nevertheless, this surprising finding obviated any need for epimerization in a separate step and allowed us to

investigate the key cyclization with the stereochemistry at C-6 correctly set beforehand. Reduction of **3-15** with lithium aluminum hydride ($LiAlH_4$) led to cleavage of the phenyl sulfonyl group and reduction of the pseudo-benzylic hydroxy group to give indole **3-16**. We then investigated the cyclization of **3-16** to give *trans*-hydrindane **3-17**. However, treatment with a variety of Lewis acids did not result in the desired cyclization, but instead no reaction or cleavage of the acetonide was observed. This is in stark contrast to the findings of Newhouse[9f] and coworkers in their synthesis of paspaline (**3-1**), wherein they attempted a similar transformation that proceeded in low, but appreciable yield. The major difference in our system is the arrangement of protecting groups, which, though distal, appears to have a profound effect on the stereoelectronic properties of the system. Radical cyclization and anionic cyclizations were also attempted, but none resulted in any productive reactivity. This is likely due to the pronounced steric congestion of the system, posing a significant challenge for formation of the vicinal quaternary centers.

At this stage, transition metal-mediated cyclizations were also attempted. The desired cyclization precursor was obtained from aldehyde **3-14** upon treatment with Grignard **3-18** to give adduct **3-19,** containing a bromine at the C-2 position of the indole (Scheme 3-3). The pseudobenzylic hydroxy group was protected as the TBS ether and the tertiary hydroxy group was eliminated with thionyl bromide to give exomethylene **3-20**. Treatment of **3-20** with $Pd(PPh_3)_4$ led to exclusive formation of carbazole **3-21**, presumably through the undesired 6-*endo* cyclization followed by β-hydride elimination and subsequent elimination of the silyloxy group. The carbazole nucleus is found in the family of IDTs represented in the more recently isolated shearilicine[15], a potential application of these findings.

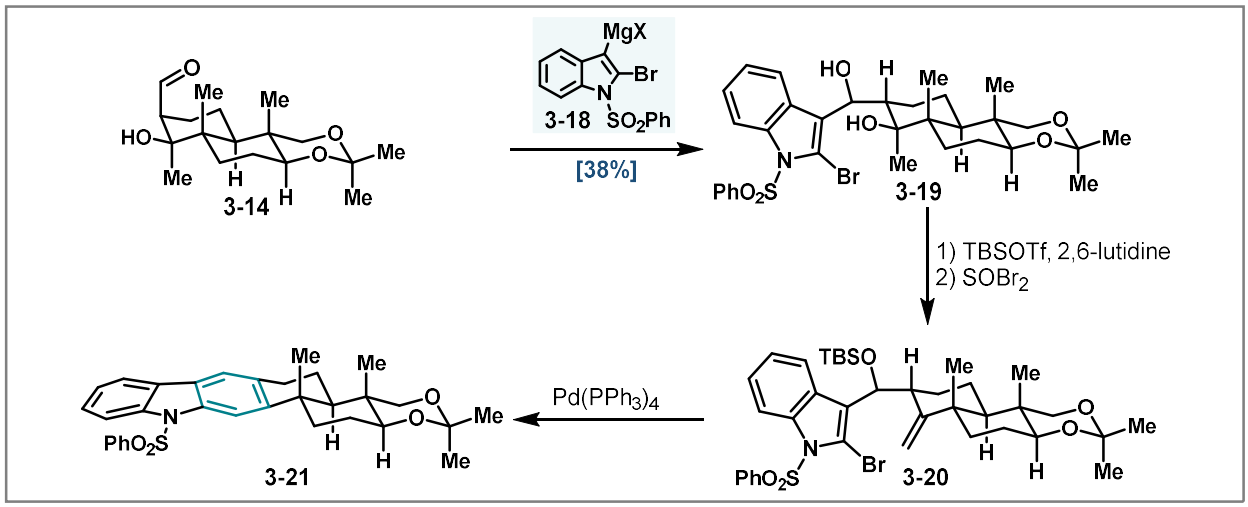

Scheme 3-3. Palladium-mediated cyclization to give carbazole **3-21** through undesired 6-*endo* cyclization mode.

At this point, we aimed to apply the insights we had gained from our investigations toward paspaline to the synthesis of xiamycin A (**3-2**).[8] Aldehyde **3-4** was coupled with 2-lithiosulfonylindole **3-22** to give adduct **3-23** in nearly quantitative yield as an inconsequential 1:1

mixture of diastereomers. Diol **3-23** underwent double dehydration with Martin sulfurane, followed by one-pot cleavage of the acetonide with 6 M aqueous hydrogen chloride solution (HCl). Selective oxidation of the resulting primary hydroxy group yielded triene aldehyde **3-24**. This conjugated system was primed to undergo 6π-electrocyclization, which proceeded upon irradiation with 350 nm light in degassed benzene. This reaction involved a photo-cascade beginning with alkene isomerization (to **3-25**), 6π-electrocyclization (to **3-26**), and a surprising photo-desulfonylation of the indole to give free carbazole **3-27** in 21% yield over three steps from **3-23**. Hydrogenation of the benzylic double bond and Pinnick oxidation of the aldehyde completed the synthesis of xiamycin A in 14 steps from commercially available starting materials, and in just 6 steps from our common synthetic intermediate. We were able to expand this synthesis to other members of the xiamycin family and test their antifeedant activities identifying three inhibitors of three agrochemically relevant fungal pathogens.

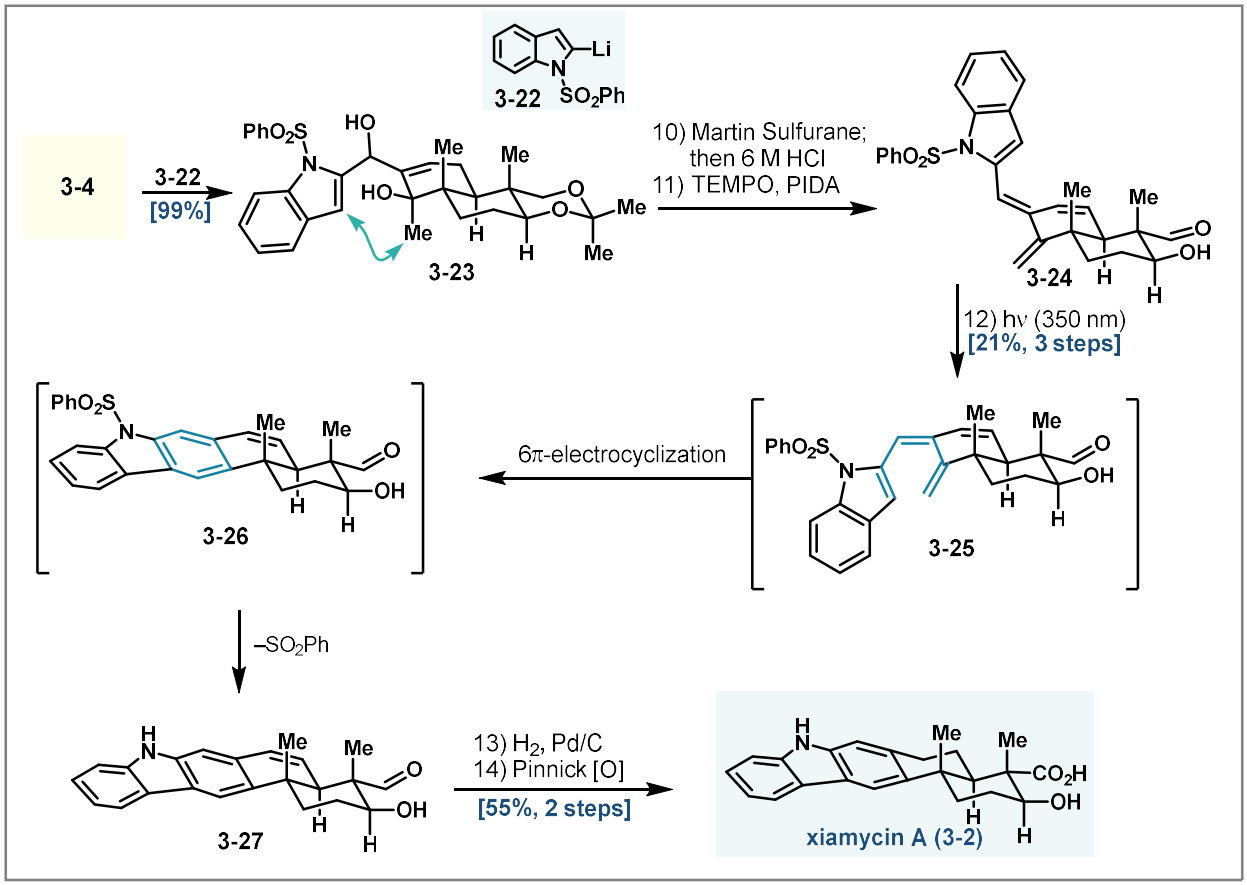

Scheme 3-4: Total Synthesis of xiamycin A (**3-2**)

3.3 Conclusion and outlook

In summary, we have developed a unified strategy for the synthesis of paspaline-type IDTs and xiamycin-type ISTs. While we were able to construct the core of paspaline (**3-13**), the

undesired stereochemistry at the hydrindane ring junction was obtained. However, insights gained from our unified approach informed our synthesis of xiamycin A (**3-2**) and allowed us to access the natural product from the common intermediate in rapid fashion. The expedience of this strategic approach is a testament to the utility of unified approaches. Our approach commenced from the chiral-pool terpene (*R*)-carvone (**3-6**), which was elaborated to the common synthetic intermediate **3-4** in 8 steps. From there the judicious choice of indole nucleophile provided selective access to either family. These studies enabled the biological profiling of xiamycin natural products which may enable further exploration of IST anti-feedants.

3.4 Experimental

General Considerations

Unless otherwise noted, all reactions were performed in flame or oven-dried glassware fitted with rubber septa under a positive pressure of nitrogen using standard Schlenk techniques. Air- and moisture-sensitive liquids were transferred via syringe or stainless-steel cannula through rubber septa. Solids were added under inert gas or were dissolved in appropriate solvents. Low temperature-reactions were carried out in a Dewar vessel filled with a cooling agent: acetone/dry ice (−78 °C), H_2O/ice (0 °C). Reaction temperatures above 23 °C were conducted in an oil bath or in a heated metal block (reactions conducted in vials). The reactions were magnetically stirred and monitored by NMR spectroscopy or analytical thin-layer chromatography (TLC), using glass plates precoated with silica gel (Silicycle Siliaplates, glass backed, extra hard layer, 60 Å, 250 µm thickness, F254 indicator). TLC plates were visualized by exposure to ultraviolet light (254 nm), were stained by submersion in aqueous potassium permanganate solution (KMnO4), p-anisaldehyde, or ceric ammonium molybdate solution (CAM), and were developed by heating with a heat gun. Flash-column chromatography on silica gel was performed as described by Still et al.,1 employing silica gel (Silicycle silica gel, 40–63 µm particle size). Organic solutions were concentrated under reduced pressure on a temperature-controlled rotary evaporator equipped with a dry ice/isopropanol condenser. The yields refer to chromatographically and spectroscopically (^{1}H and ^{13}C NMR) pure material.

Materials

Unless noted below, commercial reagents were purchased from Sigma Aldrich, Acros Organics, ChemImpex, Oakwood Chemical, Combi-blocks, TCI, and/or Alfa Aesar, and used without additional purification. Solvents were purchased from Fisher Scientific, Acros Organics, Alfa Aesar, and Sigma Aldrich. Tetrahydrofuran (THF), diethyl ether (Et_2O), acetonitrile (CH_3CN), benzene, toluene (PhMe), methanol (MeOH), and triethylamine (Et_3N) were sparged with argon and dried by passing through alumina columns using argon in a Glass Contour solvent purification system. Dichloromethane (CH_2Cl_2, DCM) was freshly distilled over calcium hydride under a N_2 atmosphere prior to each use.

NMR spectroscopy

NMR spectral data were obtained using deuterated solvents, obtained from Cambridge Isotope Laboratories, Inc. ^{1}H NMR and ^{13}C NMR data were recorded on Bruker AVB-400, AVQ-400, AV-500, NEO-500, AV-600 or AV-700 spectrometers operating at 400 MHz, 400 MHz, 500 MHz, 500 MHz, 600 MHz, 700 MHz for proton nuclei (100 MHz, 100 MHz, 125 MHz, 125 MHz, 150 MHz, 175 MHz for carbon nuclei), respectively. Proton chemical shifts are expressed in parts per million (ppm, δ scale) and are referenced to residual protium in the NMR solvent ($CHCl_3$: δ 7.26). Carbon chemical shifts are expressed in parts per million (δ scale, assigned carbon atom) and are referenced to the carbon resonance of the NMR solvent ($CDCl_3$: δ 77.16). ^{1}H NMR spectroscopic

data are reported as follows: Chemical shift in ppm (multiplicity, coupling constants J (Hz), integration) (e.g. "5.21 (t, 3 J = 7.3 Hz, ^{1}H)"). The multiplicities are abbreviated with s (singlet), br s (broad singlet), d (doublet), t (triplet), q (quartet), p (pentet), se (sextet), h (heptet), m (multiplet) and app (apparent multiplicity). In case of combined multiplicities, the multiplicity with the larger coupling constant is stated first. Except for multiplets, the chemical shift of all signals, as well for centrosymmetric multiplets, is reported as the center of the resonance range. Data for ^{13}C spectroscopy are reported in terms of chemical shift (δ ppm). Additionally to 1D NMR experiments, 2D NMR techniques such as homonuclear correlation spectroscopy (COSY), heteronuclear single quantum coherence (HSQC), heteronuclear multiple bond coherence (HMBC) and nuclear Overhauser enhancement spectroscopy (NOESY) were used to assist structure elucidation. All raw FID files were processed and the spectra analyzed using the program MestReNOVA 11.0 from Mestrelab Research S. L.

Note: The AVB-400, AVQ-400, AV-500, DRX-500 and AV-600 instruments were partially supported by NIH grants SRR023679A, RR02424A-01, S10RR03353-01 and 1S10RR016634-01, and NSF grants CHE-9633007, CHE-8208992, CHE-0130862, and CHE-8703048. The AV-700 instrument was supported by the Berkeley College of Chemistry NMR facility.

Mass spectrometry

Mass spectral data were obtained from the Mass Spectral Facility at the University of California, Berkeley, on a Finnigan/Thermo LTQ-FT instrument (ESI). Data acquisition and processing were performed using the XcaliburTM software.

IR spectroscopy

IR spectroscopic data were recorded on a Bruker ALPHA FT-IR spectrophotometer using a diamond attenuated total reflectance (ATR) accessory. If required, substances were dissolved in dichloromethane prior to direct application on the ATR unit. Data are represented as follows: frequency of absorption (cm^{-1}), and intensity of absorption (s = strong, m = medium, w = weak, br = broad).

X-ray analysis

Single-crystal X-ray diffraction experiments were performed at the UC Berkeley CHEXRAY crystallographic facility. Measurements of all compounds were performed on a Rigaku XtaLAB P200 rotating anode equipped with a Pilatus 200K hybrid pixel array detector. Data were collected using Cu Kα radiation (λ = 1.54184 Å). Crystals were kept at 100(2) K throughout collection. Data collection was performed with CrysAlisPro. 2 Data processing was done using CrysAlisPro and included either a multi-scan absorption or faceindexed absorption correction applied using the SCALE3 ABSPACK scaling algorithm within CrysAlisPro. All structures were solved with SHELXT.3 Structures were refined with SHELXL.4 All non-hydrogen atoms were refined anisotropically, and hydrogen atoms were either included at the geometrically calculated positions and refined using a riding model or located as Q peaks in the Fourier difference map.

Synthetic procedures and analytical data[15]

Synthesis of indole adduct 3-10

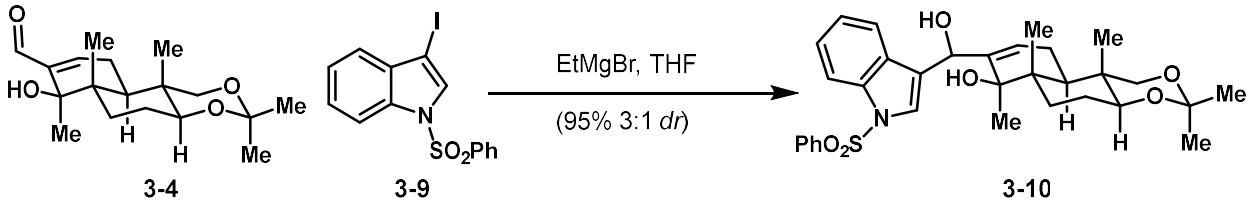

3-4 3-9 3-10

Trace water was removed from 3-iodo-1-(phenylsulfonyl)-1*H*-indole **3-9**[16] (6.31 g, 16.46 mmol, 7.0 equiv) via azeotropic distillation with benzene. Then, it was dissolved in THF (54 mL) and cooled to 0 °C. A solution of EtMgBr (5.5 ml of a 3.0 M in Et_2O, 16.34 mmol, 6.95 equiv) was added dropwise. The yellow solution was stirred at 0 °C for 20 min, then at room temperature for 30 min. During this time, trace water was removed from aldehyde **3-4** (728 mg, 2.35 mmol, 1.0 equiv) via azeotropic distillation with benzene. Then it was dissolved in THF (39 mL) and cooled to 0 °C. The solution of **3-9** and EtMgBr was re-cooled to 0 °C, then cannulated into the solution containing aldehyde **3-4** over the course of 5 minutes at 0 °C. The resulting solution was allowed to stir at 0 °C for 20 min before being quenched with sat. aq. NH_4Cl. The aq. layer was extracted three times with EtOAc and the combined organic layers were washed with sat. aq. NaCl, dried over $MgSO_4$, filtered, and concentrated. The residue was purified via gradient flash chromatography (Yamazen, eluting with 39-60% EtOAc in hexanes) to yield a mixture of diastereomers of **3-10** as a yellow foam (1.26 g, 95% combined yield, dr = 3:1) which was used in the next reaction.

Major isomer:

R_f = 0.36 (Hexane:EtOAc = 1:1), UV-active, blue spot (CAM).

^{1}H-NMR (600 MHz, $CDCl_3$): δ = 8.00 (d, *J* = 8.3 Hz, 1H), 7.90 (d, *J* = 7.6 Hz, 2H), 7.67 (s, 1H), 7.56–7.49 (m, 1H), 7.47–7.40 (m, 2H), 7.33–7.27 (m, 1H), 7.26–7.22 (m, 1H), 7.21–7.14 (m, 1H), 5.69 (s, 1H), 5.11 (br s, 1H), 3.54–3.34 (m, 4H), 2.35 (s, 1H), 1.95–1.82 (m, 1H), 1.74–1.64 (m, 3H), 1.63–1.59 (m, 2H), 1.58 (s, 3H), 1.44 (s, 3H), 1.41 (s, 3H), 1.14 (s, 3H), 1.08 (s, 3H) ppm.

^{13}C-NMR (150 MHz, $CDCl_3$): δ = 141.7, 138.3, 135.6, 133.9, 129.4 (2x), 129.1, 126.9 (2x), 125.4, 124.8, 124.4, 124.2, 123.3, 120.4, 113.9, 99.2, 79.3, 77.4, 72.4, 67.2, 40.6, 40.5, 37.1, 30.0, 29.9, 25.4, 23.8, 22.7, 19.3, 15.9, 12.2 ppm.

IR (neat): ν = 3423, 2989, 2944, 2902, 1446, 1370, 1082, 1035, 787, 597, 552 cm^{-1}.

HRMS (ESI, *m*/*z*): $[M-H]^-$ calcd. for $C_{32}H_{38}NO_6S$, 564.2425; found 564.2426.

$[\alpha]_D^{22}$ –239 (c = 1.00, $CHCl_3$)

Minor isomer:

^{1}H-NMR (600 MHz, $CDCl_3$): δ = 7.99 (d, J = 8.1 Hz, 1H), 7.87 (d, J = 7.7 Hz, 2H), 7.58 (s, 1H), 7.55–7.50 (m, 1H), 7.47 (d, J = 7.7 Hz, 1H), 7.44-7.40 (m, 2H), 7.31(t, J = 7.7 Hz, 1H), 7.20 (t, J = 7.3 Hz, 1H), 5.67 (br s, 1H), 5.53 (br s, 1H), 3.49–3.39 (m, 4H), 2.10–2.00 (m, 1H), 1.86–1.80 (m, 1H), 1.71–1.61 (m, 2H), 1.56–1.50 (m, 3H), 1.43 (s, 3H), 1.42 (s, 3H), 1.16 (s, 3H), 1.15 (s, 3H), 1.04 (s, 3H) ppm.

^{13}C-NMR (150 MHz, $CDCl_3$): δ = 142.5, 138.4, 135.8, 133.9, 129.4 (2x), 129.3, 126.9 (2x), 126.3, 125.4, 125.0, 123.7, 123.5, 120.6, 113.9, 99.2, 79.3, 72.5, 70.9, 40.8, 40.3, 37.1, 30.0, 29.4, 25.7, 23.8, 23.1, 19.3, 16.0, 12.2 ppm.

IR (neat): ν = 3423, 2990, 2946, 2902, 1448, 1370, 1085, 1035, 787, 594, 552 cm^{-1}.

HRMS (ESI, *m*/*z*): $[M-H]^-$ calcd. for $C_{32}H_{38}NO_6S$, 564.2425; found 564.2426.

R_f = 0.32 (Hexane:EtOAc = 1:1), UV-active, blue spot (CAM).

$[\alpha]_D^{22}$ –210 (c = 0.5, $CHCl_3$)

Synthesis of diene S3-1

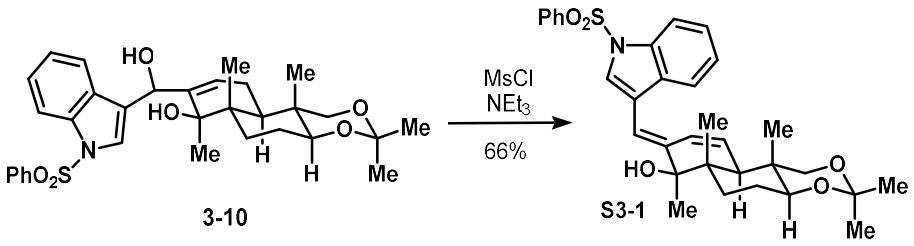

NEt_3 (0.4 mL, 2.81 mmol, 9.0 equiv), followed by MsCl (41µL, 0.53 mmol, 1.7 equiv) was added dropwise to a solution of **3-10** (177 mg, 0.31 mmol, 1.0 equiv) in DCM (10.4 mL, 0.03 M) at 0 °C. After stirring for 2 h at 0 °C, the pale yellow solution was stirred at room temperature for additional 2 h and then quenched by the addition of sat. aq. $NaHCO_3$. The aq. layer was extracted three times with DCM and the combined org. layers were washed with sat. aq. NaCl solution and dried over $MgSO_4$. After removal of the solvent *in vacuo*, the residue was purified by gradient flash chromatography (Yamazen, eluting with 33-53% EtOAc in hexanes) to afford 112 mg (66%) of compound **S3-1** as a yellow solid. Suitable crystals for X-ray analysis were obtained after crystallization from a Hexane/EtOAc (1:1) solution.

^{1}H-NMR (600 MHz, $CDCl_3$): δ = 7.99 (d, *J* = 8.3 Hz, 1H), 7.90 (d, *J* = 7.7 Hz, 2H), 7.56–7.51 (m, 3H), 7.47–7.42 (m, 2H), 7.34 (t, *J* = 7.9 Hz, 1H), 7.28–7.24 (m, 1H), 6.68 (s, 1H), 6.62 (dd, *J* = 10.3, 2.9 Hz, 1H), 5.55 (d, *J* = 10.3 Hz, 1H), 3.7 (d, *J* = 10.6 Hz, 1H), 3.61 (dd, *J* = 11.6, 3.5 Hz, 1H), 3.56 (d, *J* = 10.6 Hz, 1H), 2.04 (s, 1H), 1.78–1.71 (m, 1H), 1.69-1.61 (m, 3H), 1.50 (s, 3H), 1.46 (s, 3H), 1.33 (s, 3H), 1.18 (s, 3H), 0.97 (s, 3H) ppm.

^{13}C-NMR (150 MHz, $CDCl_3$): δ = 145.3, 138.3, 134.9, 134.0, 131.1, 129.4 (2x), 127.3, 126.9 (2x), 126.4, 125.2, 123.9, 123.5, 120.1, 119.3, 113.7, 112.6, 99.5, 77.7, 77.5, 72.2, 47.4, 42.5, 36.7, 30.0, 29.4, 23.9, 23.8, 19.5, 16.2, 13.6 ppm.

R_f = 0.48 (Hexane:EtOAc = 1:1), UV-active, blue spot (CAM).

Synthesis of cyclization precursor 3-11

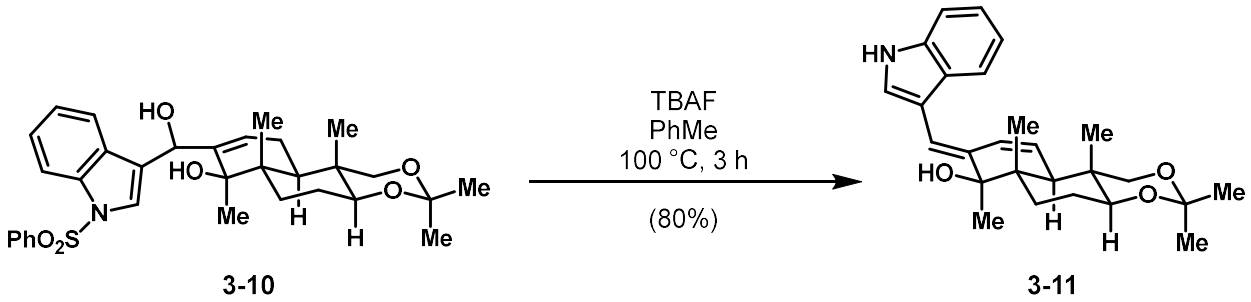

3-10 **3-11**

TBAF (0.96 mL of a 1.0 M THF solution, 0.96 mmol, 4.5 equiv) was added dropwise to a solution of indole **3-10** (120 mg, 0.21 mmol, 1.0 equiv) in PhMe (5.1 mL, 0.04 M) at room temperature. The flask was placed in a preheated oil bath and stirred at 100 °C for 3 h. The resulting brown solution was cooled to 0 °C and then quenched by the addition of sat. aq. $NaHCO_3$. Solid NaCl and EtOAc were added and the aq. layer was extracted three times with EtOAc. The combined org. layers were washed with sat. aq. NaCl solution and dried over $MgSO_4$. After removal of the solvent *in vacuo*, the residue was purified by gradient flash chromatography (Yamazen, eluting with 33-53% EtOAc in hexanes) to afford 69 mg (80%) of compound **3-11** as a yellow oil.

R_f = 0.45 (Hexane:EtOAc = 1:1), UV-active, blue spot (CAM).

^{1}H-NMR (500 MHz, CD_3OD): δ = 7.59 (d, *J* = 7.6 Hz, 1H), 7.35 (d, *J* = 8.2 Hz, 1H), 7.26 (s, 1H), 7.14–7.08 (m, 1H), 7.06–7.01 (m, 1H), 6.86 (s, 1H), 6.80 (dd, *J* = 10.1, 2.7 Hz, 1H), 5.47, (d, *J* = 10.1 Hz, 1H), 3.75–3.60 (m, 3H), 2.13 (s, 1H), 1.75–1.65 (m, 3H), 1.60–1.55 (m, 1H), 1.49 (s, 3H), 1.38 (s, 3H), 1.33 (s, 3H), 1.14 (s, 3H), 0.99 (s, 3H) ppm.

^{13}C-NMR (125 MHz, CD_3OD): δ = 141.2, 137.6, 129.0, 128.5, 125.2, 124.6, 122.7, 120.1, 119.8, 116.4, 113.7, 112.2, 100.6, 78.7, 78.5, 73.0, 48.3, 43.3, 37.7, 30.4, 30.1, 25.0, 24.2, 19.7, 16.7, 13.8 ppm.

IR (neat): ν = 3417, 3303, 2990, 2940, 2869, 1457, 1380, 1253, 1149, 759, 739 cm^{-1}.

HRMS (ESI, *m*/*z*): $[M-H]^-$ calcd. for $C_{26}H_{32}NO_3$, 406.2388; found 406.2385.

M.p. = 148 °C

$[\alpha]_D^{22}$ +140.6 (c = 1.00, $CHCl_3$)

Friedel–Crafts cyclization to form 3-12

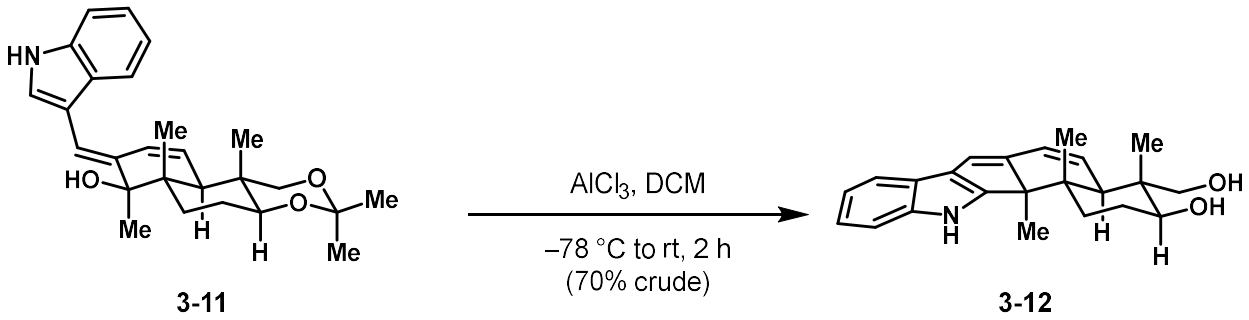

3-11 **3-12**

$AlCl_3$ (26 mg, 0.19 mmol, 4.0 equiv, dissolved in 2x 0.3 mL MeCN) was added dropwise to a solution of diene **3-11** (20 mg, 0.049 mmol, 1.0 equiv) in DCM (2.5 mL, 0.02 M) at –78 °C. After 5 min, the solution was warmed to room temperature and stirred for 2 h. The resulting red-brown solution was then quenched by the addition of sat. aq. NaCl and the aq. layer was extracted three times with EtOAc. The combined org. layers were washed 4 timeswith sat. aq. $NaHCO_3$ solution, dried over $MgSO_4$, and concentrated to afford 12 mg (70%) of crude diol **3-12**. The cyclized product proved unstable to silica and was immediately used in the next reaction.

^{1}H-NMR (500 MHz, CD_3OD): δ = 7.49 (d, *J* = 7.3 Hz, 1H), 7.35 (d, *J* = 7.9 Hz, 1H), 7.05–6.97 (m, 2H), 6.51 (s, 1H), 6.48 (d, *J* = 12.6 Hz, 1H), 5.59 (d, *J* = 10.1 Hz, 1H), 3.78 (dd, *J* = 11.2, 5.2 Hz, 1H), 3.65 (d, *J* = 11.3 Hz, 1H), 3.47 (d, *J* = 11.0 Hz, 1H), 2.71 (br s, 1H), 2.12–2.03 (m, 1H), 1.83–1.72 (m, 3H), 1.20 (s, 3H), 0.77 (s, 3H), 0.48 (s, 3H) ppm.

^{13}C-NMR (125 MHz, CD_3OD): δ = 154.5, 149.3, 142.5, 125.7, 124.5, 123.4, 123.1, 121.2, 120.3, 119.4, 119.3, 112.9, 73.2, 66.8, 56.3, 43.5, 43.4, 42.5, 32.3, 27.8, 18.7, 17.4, 13.8 ppm.

R_f = 0.25 (EtOAc), UV-active, blue spot (CAM).

Synthesis of cis-hydrindane 3-13

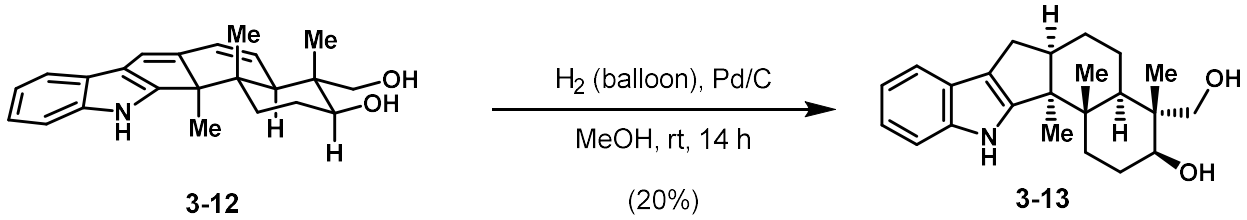

3-12 **3-13**

Hydrogen from a balloon was bubbled through a mixture of crude diene **3-12** (4 mg, 0.011 mmol, 1.0 equiv) and 5% Pd/C (4 mg, 0.03 mmol, 3.3 equiv) in MeOH (1.3 mL) for 1 min. The mixture was then vigorously stirred under an atmosphere of hydrogen (balloon) for 14 h at room temperature. After filtering the mixture through celite (EtOAc/MeOH eluent), the solution was concentrated *in vacuo* and the crude material was purified by pTLC to afford 1 mg (25%) of *cis*-hydridane **3-13** as a yellow oil.

R_f = 0.29 (EtOAc), UV-active, blue spot (CAM).

^{1}H-NMR (500 MHz, CD_3OD): δ = 7.31 (d, *J* = 7.5 Hz, 1H), 7.27 (d, *J* = 8.0 Hz, 1H), 6.99–6.90 (m, 2H), 3.68–3.62 (m, 1H), 3.55 (d, *J* = 11.1 Hz, 1H), 3.36–3.32 (m, 1H), 2.75–2.71 (m, 1H), 2.70–2.66 (m, 1H), 2.59–2.56 (m, 1H), 1.94–1.83 (m, 2H), 1.82–1.73 (m, 2H), 1.64–1.52 (m, 4H), 1.49–1.46 (m, 1H), 1.45 (s, 3H), 0.72 (s, 3H), 0.48 (s, 3H) ppm.

^{13}C NMR (151 MHz, MeOD) δ 150.11, 142.87, 125.68, 120.95, 119.64, 118.96, 117.01, 112.46, 73.73, 67.95, 67.77, 52.16, 49.80, 47.34, 44.77, 40.46, 39.19, 35.84, 33.05, 27.67, 25.07, 21.76 ppm.

HRMS (ESI, *m*/*z*): $[M–2H]^-$ calcd. for $C_{23}H_{30}NO_3$, 352.2269; found 352.2271.

IR (neat): ν = 3399, 2951, 2927, 1660, 1453, 1299, 1076, 1031, 743 cm^{-1}.

$[\alpha]_D^{22}$ –25 (c = 1.00, MeOH)

Synthesis of aldehyde 3-14

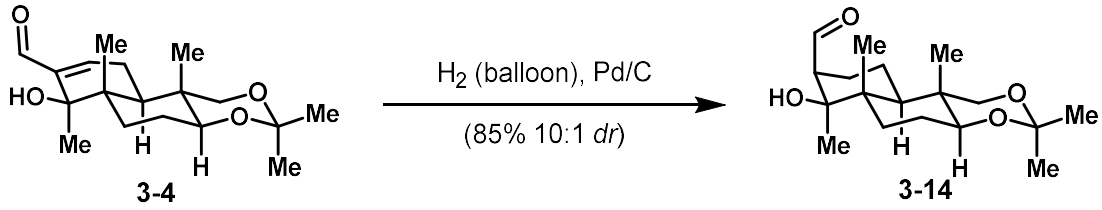

Hydrogen from a balloon was bubbled through a mixture of aldehyde **3-4** (107 mg, 0.347 mmol, 1.0 equiv) and 10% Pd/C (50 mg, 0.47 mmol, 1.35 equiv) in MeOH (17.4 mL) for 1 min. The mixture was then vigorously stirred under an atmosphere of hydrogen (balloon) for 35 minutes at room temperature. After filtering the mixture through celite (EtOAc/MeOH eluent), the solution was concentrated *in vacuo* and the crude material was purified by silica gel flash chromatography (Yamazen 20% to 48% hexanes:EtOAc) to yield **3-14** as a white solid (92 mg, 85%, 10:1 *dr*).

R_f = 0.25 (Hexane:EtOAc = 7:3), UV-active, blue spot (CAM).

^{1}H NMR (600 MHz, $CDCl_3$) δ 10.06 (d, *J* = 0.9 Hz, 1H), 3.49 (d, *J* = 10.6 Hz, 1H), 3.47 – 3.42 (m, 2H), 2.31 (ddd, *J* = 9.3, 4.8, 2.0 Hz, 2H), 2.25 – 2.22 (m, 1H), 1.64 – 1.58 (m, 2H), 1.57 – 1.53 (m, 1H), 1.50 (s, 3H), 1.48 – 1.45 (m, 1H), 1.44 (s, 3H), 1.41 (s, 4H), 1.21 (dd, *J* = 12.2, 3.0 Hz, 1H), 1.19 (s, 1H), 1.03 (d, *J* = 1.0 Hz, 3H), 0.92 (d, *J* = 0.9 Hz, 3H) ppm.

^{13}C NMR (151 MHz, $CDCl_3$) δ 205.2, 99.1, 78.2, 72.9, 57.8, 44.2, 43.0, 37.1, 30.7, 29.9, 26.7, 23.7, 22.0, 19.4, 18.0, 16.30, 12.3.
IR (neat): ν = 3452, 2938, 2872, 1698, 1453, 1372, 1202, 1102, 862 cm^{-1}.

HRMS (ESI, *m/z*): $[M-H]^-$ calcd. for $C_{18}H_{29}O_4$, 309.2071; found 309.2072.

M.p. = 140 °C

$[\alpha]_D^{22}$ +16 (c = 1.00, $CHCl_3$)

Synthesis of indole adduct 3-15

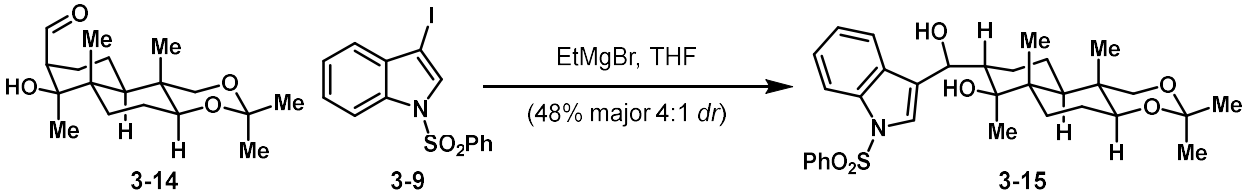

Trace water was removed from 3-iodo-1-(phenylsulfonyl)-1*H*-indole **3-9**[16] (432 mg, 1.13 mmol, 7 equiv) via azeotropic distillation with benzene. Then, it was dissolved in THF (3.8 mL) and cooled to 0 °C. A solution of EtMgBr (1.1 ml of a 1.0 M in Et_2O, 1.1 mmol, 6.95 equiv) was added dropwise. The yellow solution was stirred at 0 °C for 20 min, then at room temperature for 30 min. During this time, trace water was removed from aldehyde **3-14** (50 mg, 2.35 mmol, 1 equiv) via azeotropic distillation with benzene. Then it was dissolved in THF (1.2 mL) and cooled to 0 °C. The solution of **3-9** and EtMgBr was re-cooled to 0 °C, then cannulated into the solution containing aldehyde **3-14** over the course of 5 minutes at 0 °C. The resulting solution was allowed to stir at 0 °C for 20 min before being quenched with sat. aq. NH_4Cl. The aq. layer was extracted three times with EtOAc and the combined organic layers were washed with sat. aq. NaCl, dried over $MgSO_4$, filtered, and concentrated. The residue was purified via gradient flash chromatography (Yamazen, eluting with 39-60% EtOAc in hexanes) to yield a 4:1 mixture of diastereomers of **3-15** as an orange foam (43 mg, 48%) the major of which was used in the next reaction.

Major isomer:

R_f = 0.10 (Hexane:EtOAc = 7:3), UV-active, (CAM).

^{1}H NMR (700 MHz, $CDCl_3$) δ 7.98 (d, *J* = 8.4 Hz, 1H), 7.90 – 7.82 (m, 2H), 7.74 (d, *J* = 7.9 Hz, 1H), 7.57 – 7.50 (m, 1H), 7.48 (s, 1H), 7.43 (t, *J* = 7.9 Hz, 2H), 7.32 (t, *J* = 7.8 Hz, 1H), 7.24 (t, *J* = 7.7 Hz, 1H), 4.86 (dd, *J* = 9.9, 1.5 Hz, 1H), 4.29 – 4.17 (m, 1H), 3.49 – 3.45 (m, 1H), 3.40 (t, *J* = 9.7 Hz, 2H), 2.37 (ddd, *J* = 13.6, 9.9, 4.1 Hz, 1H), 1.70 – 1.64 (m, 2H), 1.60 (dt, *J* = 7.4, 3.9 Hz, 2H), 1.53 (d, *J* = 9.7 Hz, 1H), 1.46 (d, *J* = 1.8 Hz, 3H), 1.44 (s, 3H), 1.40 (s, 3H), 1.26 – 1.22 (m, 2H), 1.15 (s, 4H), 1.01 (s, 3H) ppm.

^{13}C NMR (176 MHz, $CDCl_3$) δ 138.2, 135.8, 134.1, 129.4, 129.1, 126.9, 125.1, 124.8, 124.0, 123.5, 121.2, 114.0, 99.1, 79.9, 72.8, 72.0, 44.7, 43.3, 43.0, 36.9, 30.0, 29.9, 26.7, 23.7, 20.1, 19.4, 17.3, 15.6, 12.3 ppm.

IR (neat): ν = 3346, 2988, 2944, 2834, 1655, 1447, 1373, 1176, 1120, 1019, 728, 599, 571 cm^{-1}.

HRMS (ESI, *m/z*): $[M-H]^-$ calcd. for $C_{32}H_{40}NO_6S$, 566.2582; found 566.2577.

$[\alpha]_D^{22}$ –32.7 (c = 1.00, $CHCl_3$)

Synthesis of cyclization precursor 3-16

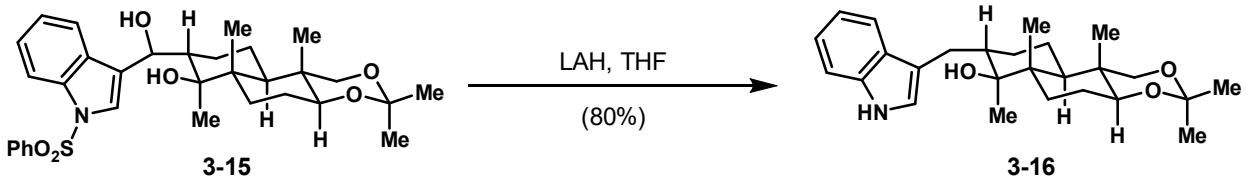

$LiAlH_4$ (0.54 mL of a 2.0 M THF solution, 1.08 mmol, 6.5 equiv) was added dropwise to a solution of indole **3-15** (94 mg, 0.17 mmol, 1.0 equiv) in THF (5.5 mL, 0.03 M) at room temperature. The flask was placed in a preheated oil bath and stirred at 55 °C for 4 h. The resulting yellow mixture was cooled to 0 °C and then quenched carefully by the addition of sat. aq. NaCl. Solid NaCl and EtOAc were added and the mixture was stirred at room temperature for 15 min. The aq. layer was extracted three times with EtOAc, then the combined org. layers were washed with sat. aq. NaCl solution and dried over $MgSO_4$. After removal of the solvent *in vacuo*, the residue was purified by gradient flash chromatography (Yamazen, eluting with 25-46% EtOAc in hexanes) to afford 62 mg (80%) of compound **3-16** as a white solid.

R_f = 0.6 (Hexane:EtOAc = 1:1), UV-active, blue spot (CAM).

^{1}H NMR (700 MHz, $CDCl_3$) δ 7.93 (s, 1H), 7.64 (d, *J* = 7.9 Hz, 1H), 7.36 (d, *J* = 8.0 Hz, 1H), 7.19 (t, *J* = 7.5 Hz, 1H), 7.11 (t, *J* = 7.4 Hz, 1H), 6.98 (s, 1H), 3.51 – 3.45 (m, 2H), 3.43 (d, *J* = 10.6 Hz, 1H), 3.20 (dd, *J* = 13.9, 2.9 Hz, 1H), 2.28 (dd, *J* = 14.0, 10.1 Hz, 1H), 2.07 – 2.01 (m, 1H), 1.81 – 1.74 (m, 1H), 1.69 – 1.61 (m, 3H), 1.51 (s, 1H), 1.45 (s, 3H), 1.41 (s, 3H), 1.30 (s, 3H), 1.26 (d, *J* = 4.4 Hz, 3H), 1.22 (d, *J* = 3.0 Hz, 2H), 1.15 (d, *J* = 5.1 Hz, 1H), 1.07 (s, 3H), 1.03 (s, 3H) ppm.

^{13}C NMR (176 MHz, $CDCl_3$) δ 136.5, 127.9, 122.1, 122.0, 119.4, 119.4, 119.3, 116.0, 111.2, 99.0, 78.2, 77.7, 73.0, 44.2, 43.2, 42.9, 37.1, 30.6, 30.0, 29.9, 29.3, 26.1, 23.9, 20.7, 19.4, 17.0, 15.4, 12.4 ppm.

IR (neat): ν = 3298, 2990, 2929, 2867, 1456, 1377, 1233, 1095, 1066, 1056, 855, 739, 668 cm^{-1}.

HRMS (ESI, *m*/*z*): $[M-H]^-$ calcd. for $C_{26}H_{36}NO_3$, 410.2701; found 410.2697.

M.p. = 165 °C

$[\alpha]_D^{22}$ –49.3 (c = 1.40, $CHCl_3$)

X-ray structure:

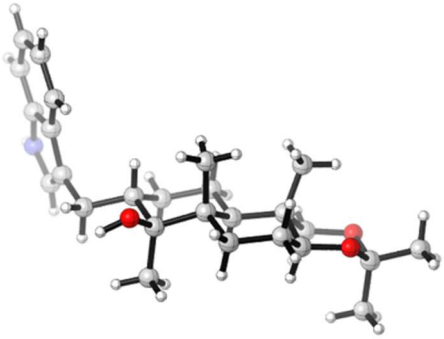

Synthesis of 2-bromo indole adduct 3-19

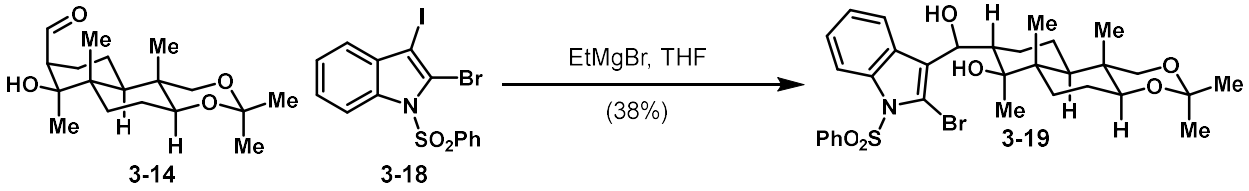

Trace water was removed from 3-iodo-1-(phenylsulfonyl)-1*H*-indole **3-9**[17] (953 mg, 2.06 mmol, 7.0 equiv) via azeotropic distillation with benzene. Then, it was dissolved in THF (7.4 mL) and cooled to 0 °C. A solution of EtMgBr (2.1 ml of a 1.0 M in Et_2O, 2.05 mmol, 6.95 equiv) was added dropwise. The yellow solution was stirred at 0 °C for 20 min, then at room temperature for 30 min. During this time, trace water was removed from aldehyde **3-14** (92 mg, 0.295 mmol, 1.0 equiv) via azeotropic distillation with benzene. Then it was dissolved in THF (2 mL) and cooled to 0 °C. The solution of **3-18** and EtMgBr was re-cooled to 0 °C, then cannulated into the solution containing aldehyde **3-14** over the course of 5 minutes at 0 °C. The resulting solution was allowed to stir at 0 °C for 20 min before being quenched with sat. aq. NH_4Cl. The aq. layer was extracted three times with EtOAc and the combined organic layers were washed with sat. aq. NaCl, dried over $MgSO_4$, filtered, and concentrated. The residue was purified via silica gel column chromatography (80% hexanes:EtOAc) to yield adduct **3-19** as a yellow foam (72 mg, 38%)

R_f = 0.13 (Hexane:EtOAc = 7:3), UV-active, (CAM).

^{1}H NMR (600 MHz, $CDCl_3$) δ 8.31 (d, *J* = 8.4 Hz, 1H), 7.84 (d, *J* = 7.3 Hz, 2H), 7.58 – 7.52 (m, 1H), 7.45 – 7.39 (m, 2H), 7.36 (ddd, *J* = 8.6, 7.3, 1.3 Hz, 1H), 7.31 – 7.26 (m, 2H), 5.30 (s, 1H), 5.04 (d, *J* = 10.0 Hz, 1H), 3.41 (td, *J* = 20.0, 19.1, 11.1 Hz, 4H), 2.52 – 2.45 (m, 1H), 1.70 – 1.57 (m, 3H), 1.49 (s, 3H), 1.44 (s, 3H), 1.40 (s, 3H), 1.22 – 1.15 (m, 2H), 1.13 (s, 3H), 1.08 – 1.03 (m, 1H), 1.00 (s, 3H), 0.95 – 0.91 (m, 1H), 0.91 – 0.88 (m, 1H) ppm.

IR (neat): ν = 3323, 2941, 2875, 2831, 1654, 1558, 1444, 1377, 1215, 1022, 750, 727, 571 cm^{-1}.

HRMS (ESI, *m*/*z*): $[M-H]^-$ calcd. for $C_{32}H_{39}BrNO_6S$, 644.1687; found 644.1683.

Synthesis of silyl ether S3-4

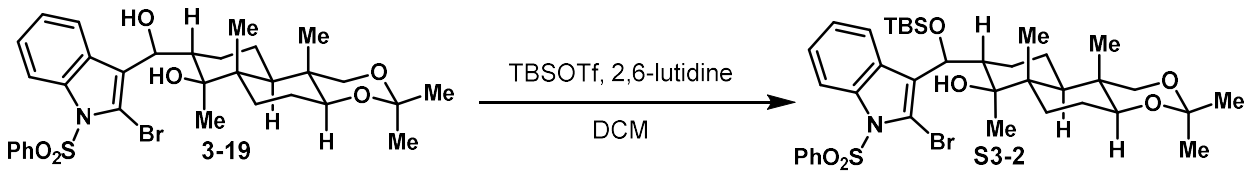

Alcohol **3-19** (8 mg, 0.0124 mmol, 1 equiv) was dissolved in DCM (0.2 mL) and moved to an ice bath to cool the solution to 0 °C. To this stirring solution was added 2,6-lutidine (8.6 µL, 0.074 mmol, 6 equiv) followed by TBSOTf (8.5 µL, 0.037 mmol, 3 equiv). The reaction was stirred at this temperature for 3 h, then quenched by the addition of sat. aq. NaCl. The aqueous layer was extracted with EtOAc two times, washed further with sat. aq. NaCl, dried over Na_2SO_4, filtered and concentrated *in vacuo*. The crude residue was purified by preparatory thin layer chromatography (hexanes:EtOAc 4:1) to give **S3-2** as a clear oil (3.8 mg, 40%).

R_f = 0.63 (Hexane:EtOAc = 7:3), UV-active, (CAM).

^{1}H NMR (600 MHz, CDCl3) δ 8.37 (d, J = 8.5 Hz, 1H), 7.86 (d, J = 8.4 Hz, 2H), 7.80 (d, J = 5.9 Hz, 1H), 7.56 (t, J = 7.5 Hz, 1H), 7.44 – 7.39 (m, 3H), 7.34 – 7.30 (m, 1H), 4.99 (s, 1H), 4.94 (d, J = 10.1 Hz, 1H), 3.50 – 3.45 (m, 1H), 3.45 – 3.39 (m, 2H), 2.46 (ddd, J = 12.1, 10.2, 4.6 Hz, 1H), 1.72 (dd, J = 9.5, 3.1 Hz, 1H), 1.63 (d, J = 9.4 Hz, 2H), 1.52 – 1.49 (m, 1H), 1.46 (s, 3H), 1.42 (s, 3H), 1.38 (s, 3H), 1.11 (s, 3H), 1.00 (s, 3H), 0.91 (d, J = 3.7 Hz, 2H), 0.89 – 0.84 (m, 2H), 0.76 (s, 9H), 0.05 (s, 3H), -0.81 (s, 3H) ppm.

^{13}C-NMR (150 MHz, CDCl3): δ = 138.3, 138.2, 134.3, 129.3 (2x), 128.1, 127.2 (2x), 126.7, 125.7, 124.3, 121.1, 116.0, 109.6, 99.0, 78.0, 77.6, 74.1, 72.9, 44.9, 43.1, 42.7, 36.9, 30.3, 30.0, 25.9 (3x), 25.8, 23.8, 20.1, 19.4, 17.9, 17.6, 15.5, 12.3, –4.9, –5.3 ppm.

IR (neat): ν = 3488, 2990, 2952, 2936, 2860, 1445, 1370, 1203, 1087, 837, 752, 723, 573 cm-1.

HRMS (ESI, m/z): $[M-H]^-$ calcd. for C38H53BrNO6SSi, 758.2552; found 758.2545.

Synthesis of exomethylene 3-20

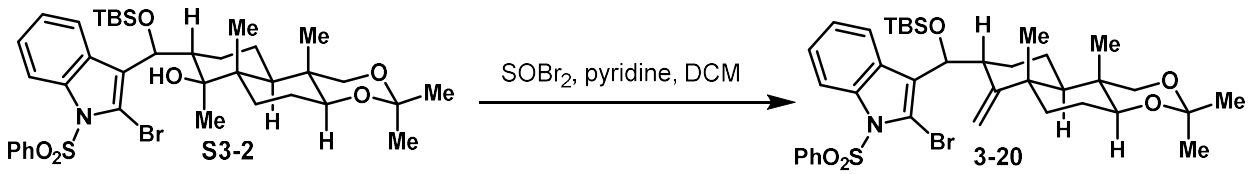

Silyl ether **S3-2** (9 mg, 0.012 mmol, 1 equiv) was dissolved in DCM (0.2 mL) and moved to an ice bath to cool the solution to 0 °C. To this stirring solution was added pyridine (0.02 mL) followed by $SOBr_2$ (4.5 µL, 0.070 mmol, 5 equiv). The reaction was stirred at this temperature for 3 h, then quenched by the addition of sat. aq. NaCl. The aqueous layer was extracted with EtOAc two times, washed further with sat. aq. NaCl, dried over Na_2SO_4, filtered and concentrated *in vacuo*. The crude residue was purified by preparatory thin layer chromatography (hexanes:EtOAc 4:1) to give **S3-2** as a clear oil (4.9 mg, 54%).

R_f = 0.50 (Hexane:EtOAc = 8:2), UV-active, (*p*-anisaldehyde).

^{1}H NMR (700 MHz, $CDCl_3$) δ 8.05 (d, *J* = 8.3 Hz, 1H), 7.89 – 7.85 (m, 2H), 7.67 (d, *J* = 7.9 Hz, 1H), 7.53 (t, *J* = 7.4 Hz, 1H), 7.45 – 7.39 (m, 4H), 7.35 (t, *J* = 7.7 Hz, 1H), 7.25 (t, *J* = 7.5 Hz, 1H), 4.95 (d, *J* = 8.0 Hz, 1H), 4.83 (d, *J* = 6.7 Hz, 2H), 3.52 (d, *J* = 7.5 Hz, 1H), 3.45 – 3.38 (m, 2H), 2.80 (s, 1H), 2.25 (t, *J* = 7.6 Hz, 2H), 2.04 (d, *J* = 6.7 Hz, 2H), 1.76 (d, *J* = 9.0 Hz, 2H), 1.68 (d, *J* = 6.0 Hz, 2H), 1.44 (d, *J* = 4.9 Hz, 6H), 1.10 (s, 4H), 1.06 (s, 3H), 0.78 (s, 9H), 0.09 – -0.06 (m, 6H) ppm.

HRMS (ESI, *m*/*z*): $[M-H]^-$ calcd. for $C_{38}H_{51}BrNO_5SSi$, 740.2446; found 740.2441.

Unexpected synthesis of carbazole 3-21

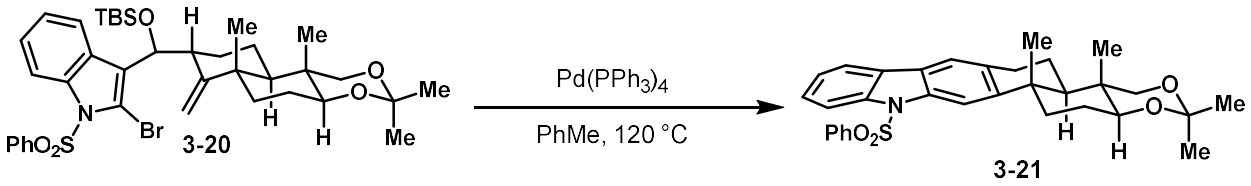

Alkene **3-20** (4 mg, 0.005 mmol, 1 equiv) was dissolved in degassed PhMe (0.1 mL) within a glove box. $Pd(PPh)_3$ (5.8 mg, 0.005 mmol, 1 equiv) was added, the reaction vessel was sealed and moved to a preheated vial block at 120 °C. The brown reaction mixture was allowed to stir 14 h at this temperature wherein a black precipitate formed. The crude reaction mixture was purified by preparatory TLC, concentrated *in vacuo* and evaluated by ^{1}HNMR. The resulting impure mixture showed diagnostic signals of carbazole **3-21** as the sole product.

Synthesis of trisubstituted alkene S3-2

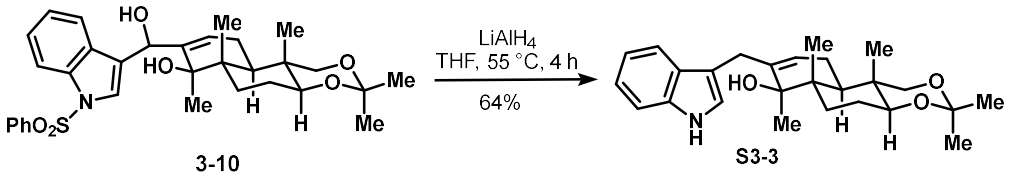

$LiAlH_4$ (0.85 mL of a 2.0 M THF solution, 1.69 mmol, 6.0 equiv) was added dropwise to a solution of indole **3-10** (160 mg, 0.29 mmol, 1.0 equiv) in THF (9.4 mL, 0.03 M) at room temperature. The flask was placed in a preheated oil bath and stirred at 55 °C for 4 h. The resulting yellow mixture was cooled to 0 °C and then quenched carefully by the addition of sat. aq. NaCl. Solid NaCl and EtOAc were added and the mixture was stirred at room temperature for 15 min. The aq. layer was extracted three times with EtOAc, then the combined org. layers were washed with sat. aq. NaCl solution and dried over $MgSO_4$. After removal of the solvent *in vacuo*, the residue was purified by gradient flash chromatography (Yamazen, eluting with 25-46% EtOAc in hexanes) to afford 74 mg (64%) of compound **S3-3** as a white solid.

R_f = 0.55 (Hexane:EtOAc = 1:1), UV-active, blue spot (CAM).

^{1}H-NMR (500 MHz, $CDCl_3$): δ = 7.98 (br s, 1H), 7.56 (d, *J* = 7.9 Hz, 1H), 7.36 (d, *J* = 8.2 Hz, 1H), 7.18 (t, *J* = 7.5 Hz, 1H), 7.12–7.09 (m, 1H), 7.03 (s, 1H), 5.29 (br s, 1H), 3.66–3.60 (m, 1H), 3.55–3.47 (m, 2H), 3.47–3.44 (m, 2H), 2.03–1.94 (m, 1H), 1.75–1.58 (m, 4H), 1.46 (s, 3H), 1.42 (s, 6H), 1.16 (s, 3H), 1.01 (s, 3H) ppm.

^{13}C-NMR (125 MHz, $CDCl_3$): δ = 141.4, 136.7, 127.6, 122.6, 122.2, 122.0, 119.6, 119.5, 115.2, 111.2, 99.2, 78.7, 77.6, 72.7, 40.8, 40.6, 37.1, 30.3, 30.0, 29.9, 27.2, 24.4, 23.9, 23.0, 19.4, 15.9, 12.3 ppm.

IR (neat): ν = 3412, 2988, 2941, 2898, 1455, 1379, 1226, 1089, 859, 737, 423 cm^{-1}.

HRMS (ESI, *m/z*): $[M-H]^-$ calcd. for $C_{26}H_{34}NO_3$, 408.2544; found 408.2547.

M.p. = 196 °C

$[\alpha]_D^{22}$ –49.1 (c = 1.00, $CHCl_3$)

Synthesis of branched indole S3-3

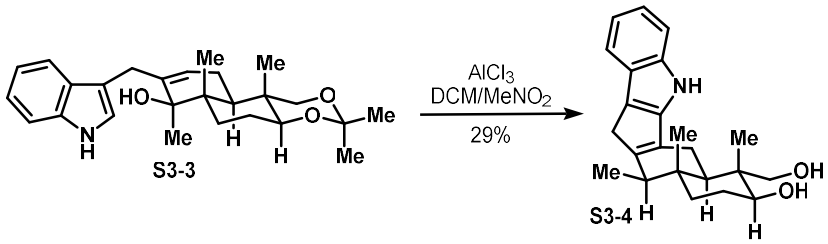

Compound **S3-3** (8 mg, 0.02 mmol, 1.0 equiv, dissolved in 2x 0.2 mL of DCM) was added dropwise to a solution of $AlCl_3$ (10 mg, 0.08 mmol, 4.0 equiv) in DCM/$MeNO_2$ (1:1, 1.2 mL, 0.02 M) at –78 °C. The resulting orange-brown solution was then stirred at room temperature for 1.5 h before being quenched by the addition of sat. aq. NaCl. The aq. layer was extracted three times with EtOAc and the combined org. layers were washed 2x with sat. aq. $NaHCO_3$ solution and dried over $MgSO_4$. After removal of the solvent *in vacuo*, the residue was purified by pTLC to afford 2 mg (29%) of compound **S3-4** as a yellow oil.

R_f = 0.25 (Hexane:EtOAc = 1:5), UV-active, blue spot (CAM).

^{1}H-NMR (700 MHz, CD_3OD): δ = 7.37 (d, *J* = 7.5 Hz, 1H), 7.31 (d, *J* = 7.5 Hz, 1H), 6.96–6.90 (m, 2H), 3.70 (dd, *J* = 11.7, 4.2 Hz, 1H), 3.61 (d, *J* = 11.1 Hz, 1H), 3.41 (d, *J* = 11.1 Hz, 1H), 3.13–3.08 (m, 1H), 3.03–2.98 (m, 1H), 2.57 (d, *J* = 16.4 Hz, 1H), 2.45–2.38 (m, 2H), 1.94–1.87 (m, 2H), 1.80–1.72 (m, 1H), 1.70–1.66 (m, 1H), 1.28–1.24 (m, 1H), 1.10 (d, *J* = 7.1 Hz, 3H), 0.92 (s, 3H), 0.88 (s, 3H) ppm.

^{13}C-NMR (175 MHz, CD_3OD): δ = 149.4, 147.3, 141.2, 129.3, 126.1, 120.0, 119.7, 117.9, 117.6, 112.8, 73.8, 66.7, 48.3, 44.0, 43.9, 38.0, 37.3, 32.3, 27.8, 21.5, 14.3, 12.8, 12.6 ppm.

IR (neat): ν = 3408, 2922, 2918, 1639, 1480, 1262, 1055, 1040, 738 cm^{-1}.

HRMS (ESI, *m*/*z*): $[M–H]^-$ calcd. for $C_{23}H_{29}NO_2$, 350.2126; found 350.2123.

$[\alpha]_D^{22}$ –23.7 (c = 0.5, MeOH)

Synthesis of exomethylene S3-5

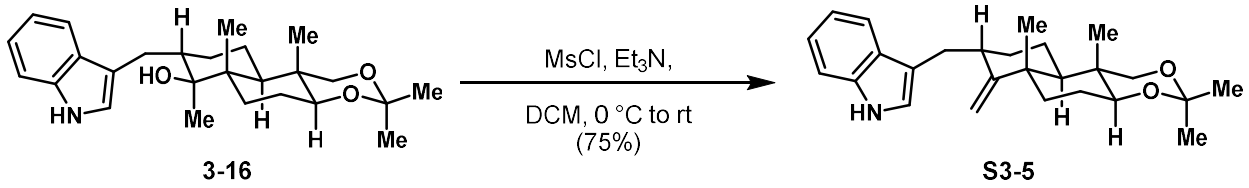

3-16 **S3-5**

Alcohol **3-16** (50 mg, 0.12 mmol, 1 equiv) was dissolved in DCM (1.2 mL) and moved to an ice bath to cool the solution to 0 °C. To this stirring solution was added Et_3N (68 μL, 0.48 mmol, 4 equiv) followed by MsCl (10 μL, 0.013 mmol, 1 equiv). The reaction was allowed to warm to room temperature and stirred for 3 hours. It was then quenched by the addition of sat. aq. NH_4Cl. The aqueous layer was extracted with EtOAc two times, washed with sat. aq. NaCl, dried over Na_2SO_4, filtered and concentrated *in vacuo*. The crude residue was purified by preparatory thin layer chromatography (hexanes:EtOAc 4:1) to give **S3-5** as a yellow solid (35.5 mg, 75%).

R_f = 0.3 (Hexane:EtOAc = 2:1), UV-active, blue spot (CAM).

^{1}H NMR (500 MHz, $CDCl_3$) δ 7.60 – 7.54 (m, 1H), 7.22 – 7.17 (m, 1H), 7.11 (ddd, *J* = 8.0, 7.0, 1.0 Hz, 1H), 6.96 (d, *J* = 2.3 Hz, 1H), 4.75 (d, *J* = 7.2 Hz, 1H), 3.53 (dd, *J* = 7.1, 4.2 Hz, 1H), 3.47 (d, *J* = 10.7 Hz, 1H), 3.41 (s, 1H), 3.11 (d, *J* = 10.0 Hz, 1H), 2.63 – 2.54 (m, 1H), 1.90 (dd, *J* = 12.8, 3.4 Hz, 1H), 1.80 – 1.68 (m, 2H), 1.61 (dd, *J* = 7.9, 3.6 Hz, 1H), 1.42 (d, *J* = 6.5 Hz, 3H), 1.14 (s, 2H), 1.06 (d, *J* = 0.8 Hz, 2H), 1.01 (dd, *J* = 12.7, 3.1 Hz, 1H) ppm.

^{13}C NMR (151 MHz, $CDCl_3$) δ 162.6, 136.4, 128.0, 122.0, 119.3, 119.1, 115.5, 111.2, 100.8, 99.1, 77.6, 72.7, 50.0, 40.6, 39.1, 37.6, 36.2, 34.6, 30.0, 29.0, 24.4, 22.1, 21.4, 19.4, 12.4 ppm.

IR (neat): ν = 3409, 3355, 2930, 2870, 1709, 1621, 1457, 1080, 1042, 742 cm^{-1}.

X-ray crystallographic details

Table 1. Crystal data and structure refinement for mp001 (CCDC 1831586)

Identification code	mp001	
Empirical formula	C14 H22 O3	
Formula weight	238.31	
Temperature	100(2) K	
Wavelength	1.54178 Å	
Crystal system	Orthorhombic	
Space group	P 21 21 21	
Unit cell dimensions	a = 7.2602(5) Å	$\alpha = 90°$.
	b = 8.3489(6) Å	$\beta = 90°$.
	c = 20.4643(15) Å	$\gamma = 90°$.
Volume	1240.44(15) $Å^3$	
Z	4	
Density (calculated)	1.276 Mg/m^3	
Absorption coefficient	0.705 mm^{-1}	
F(000)	520	
Crystal size	0.100 x 0.040 x 0.040 mm^3	
Theta range for data collection	4.321 to 68.329°.	

Index ranges	-8<=h<=8, -10<=k<=9, -24<=l<=24
Reflections collected	18197
Independent reflections	2259 [R(int) = 0.0248]
Completeness to theta = 67.000°	100.0 %
Absorption correction	Semi-empirical from equivalents
Max. and min. transmission	0.753 and 0.708
Refinement method	Full-matrix least-squares on F^2
Data / restraints / parameters	2259 / 0 / 165
Goodness-of-fit on F^2	1.080
Final R indices [I>2sigma(I)]	R1 = 0.0260, wR2 = 0.0722
R indices (all data)	R1 = 0.0263, wR2 = 0.0724
Absolute structure parameter	0.06(3)
Extinction coefficient	n/a
Largest diff. peak and hole	0.217 and -0.160 e.$Å^{-3}$

Table 2. Atomic coordinates (x 10^4) and equivalent isotropic displacement parameters ($Å^2$x 10^3)

for mp001. U(eq) is defined as one third of the trace of the orthogonalized U^{ij} tensor.

---

	x	y	z	U(eq)
C(1)	5288(2)	5140(2)	5101(1)	15(1)
C(2)	7066(2)	5306(2)	5448(1)	18(1)
C(3)	7040(2)	5137(2)	6180(1)	24(1)
C(4)	8604(2)	5575(2)	5108(1)	16(1)
C(5)	8691(2)	5723(2)	4381(1)	16(1)
C(6)	6795(2)	5938(2)	4064(1)	13(1)
C(7)	5368(2)	4775(2)	4368(1)	14(1)
C(8)	5893(2)	2982(2)	4326(1)	18(1)
C(9)	3470(2)	5050(2)	4062(1)	16(1)
C(10)	3543(2)	4956(2)	3315(1)	17(1)
C(11)	4886(2)	6175(2)	3040(1)	16(1)
C(12)	6867(2)	5959(2)	3302(1)	14(1)
C(13)	7785(2)	4479(2)	2993(1)	18(1)
C(14)	8024(2)	7410(2)	3077(1)	17(1)
O(1)	3819(2)	5228(2)	5395(1)	20(1)
O(2)	4922(2)	6145(2)	2340(1)	20(1)
O(3)	7397(2)	8923(1)	3316(1)	20(1)

Table 3. Bond lengths [Å] and angles [°] for mp001.

C(1)-O(1)	1.227(2)
C(1)-C(2)	1.481(2)
C(1)-C(7)	1.530(2)

C(2)-C(4)	1.335(2)
C(2)-C(3)	1.504(2)
C(3)-H(3A)	0.9800
C(3)-H(3B)	0.9800
C(3)-H(3C)	0.9800
C(4)-C(5)	1.494(2)
C(4)-H(4)	0.9500
C(5)-C(6)	1.532(2)
C(5)-H(5A)	0.9900
C(5)-H(5B)	0.9900
C(6)-C(7)	1.550(2)
C(6)-C(12)	1.5598(19)
C(6)-H(6)	1.0000
C(7)-C(9)	1.531(2)
C(7)-C(8)	1.547(2)
C(8)-H(8A)	0.9800
C(8)-H(8B)	0.9800
C(8)-H(8C)	0.9800
C(9)-C(10)	1.531(2)
C(9)-H(9A)	0.9900
C(9)-H(9B)	0.9900
C(10)-C(11)	1.518(2)
C(10)-H(10A)	0.9900
C(10)-H(10B)	0.9900
C(11)-O(2)	1.4324(18)
C(11)-C(12)	1.546(2)

C(11)-H(11)	1.0000
C(12)-C(13)	1.540(2)
C(12)-C(14)	1.545(2)
C(13)-H(13A)	0.9800
C(13)-H(13B)	0.9800
C(13)-H(13C)	0.9800
C(14)-O(3)	1.429(2)
C(14)-H(14A)	0.9900
C(14)-H(14B)	0.9900
O(2)-H(2)	0.88(3)
O(3)-H(3)	0.84(2)

O(1)-C(1)-C(2)	121.06(13)
O(1)-C(1)-C(7)	121.75(14)
C(2)-C(1)-C(7)	117.12(13)
C(4)-C(2)-C(1)	119.58(14)
C(4)-C(2)-C(3)	123.13(15)
C(1)-C(2)-C(3)	117.28(14)
C(2)-C(3)-H(3A)	109.5
C(2)-C(3)-H(3B)	109.5
H(3A)-C(3)-H(3B)	109.5
C(2)-C(3)-H(3C)	109.5
H(3A)-C(3)-H(3C)	109.5
H(3B)-C(3)-H(3C)	109.5
C(2)-C(4)-C(5)	124.71(15)
C(2)-C(4)-H(4)	117.6

C(5)-C(4)-H(4)	117.6
C(4)-C(5)-C(6)	113.13(13)
C(4)-C(5)-H(5A)	109.0
C(6)-C(5)-H(5A)	109.0
C(4)-C(5)-H(5B)	109.0
C(6)-C(5)-H(5B)	109.0
H(5A)-C(5)-H(5B)	107.8
C(5)-C(6)-C(7)	110.92(12)
C(5)-C(6)-C(12)	113.20(12)
C(7)-C(6)-C(12)	115.52(12)
C(5)-C(6)-H(6)	105.4
C(7)-C(6)-H(6)	105.4
C(12)-C(6)-H(6)	105.4
C(1)-C(7)-C(9)	109.64(12)
C(1)-C(7)-C(8)	104.86(13)
C(9)-C(7)-C(8)	110.12(13)
C(1)-C(7)-C(6)	107.11(12)
C(9)-C(7)-C(6)	110.08(12)
C(8)-C(7)-C(6)	114.79(13)
C(7)-C(8)-H(8A)	109.5
C(7)-C(8)-H(8B)	109.5
H(8A)-C(8)-H(8B)	109.5
C(7)-C(8)-H(8C)	109.5
H(8A)-C(8)-H(8C)	109.5
H(8B)-C(8)-H(8C)	109.5
C(7)-C(9)-C(10)	111.66(12)

C(7)-C(9)-H(9A)	109.3
C(10)-C(9)-H(9A)	109.3
C(7)-C(9)-H(9B)	109.3
C(10)-C(9)-H(9B)	109.3
H(9A)-C(9)-H(9B)	107.9
C(11)-C(10)-C(9)	111.04(12)
C(11)-C(10)-H(10A)	109.4
C(9)-C(10)-H(10A)	109.4
C(11)-C(10)-H(10B)	109.4
C(9)-C(10)-H(10B)	109.4
H(10A)-C(10)-H(10B)	108.0
O(2)-C(11)-C(10)	111.80(13)
O(2)-C(11)-C(12)	109.17(12)
C(10)-C(11)-C(12)	112.95(12)
O(2)-C(11)-H(11)	107.6
C(10)-C(11)-H(11)	107.6
C(12)-C(11)-H(11)	107.6
C(13)-C(12)-C(14)	105.72(12)
C(13)-C(12)-C(11)	110.71(12)
C(14)-C(12)-C(11)	108.07(12)
C(13)-C(12)-C(6)	114.63(12)
C(14)-C(12)-C(6)	108.99(12)
C(11)-C(12)-C(6)	108.51(11)
C(12)-C(13)-H(13A)	109.5
C(12)-C(13)-H(13B)	109.5
H(13A)-C(13)-H(13B)	109.5

C(12)-C(13)-H(13C)	109.5
H(13A)-C(13)-H(13C)	109.5
H(13B)-C(13)-H(13C)	109.5
O(3)-C(14)-C(12)	114.69(13)
O(3)-C(14)-H(14A)	108.6
C(12)-C(14)-H(14A)	108.6
O(3)-C(14)-H(14B)	108.6
C(12)-C(14)-H(14B)	108.6
H(14A)-C(14)-H(14B)	107.6
C(11)-O(2)-H(2)	109.6(14)
C(14)-O(3)-H(3)	109.0(17)

Symmetry transformations used to generate equivalent atoms:

Table 4. Anisotropic displacement parameters ($Å^2 x\ 10^3$)for mp001. The anisotropic displacement factor exponent takes the form: $-2\pi^2[\ h^2 a^{*2} U^{11} + ... + 2\ h\ k\ a^*\ b^*\ U^{12}\ ]$

	U^{11}	U^{22}	U^{33}	U^{23}	U^{13}	U^{12}
C(1)	20(1)	9(1)	16(1)	1(1)	0(1)	0(1)
C(2)	23(1)	13(1)	16(1)	-2(1)	-4(1)	2(1)
C(3)	28(1)	28(1)	16(1)	0(1)	-4(1)	4(1)
C(4)	19(1)	12(1)	18(1)	-1(1)	-6(1)	1(1)

C(5)	15(1)	16(1)	18(1)	1(1)	-1(1)	1(1)
C(6)	14(1)	12(1)	13(1)	-1(1)	0(1)	1(1)
C(7)	14(1)	13(1)	14(1)	0(1)	0(1)	0(1)
C(8)	21(1)	13(1)	19(1)	-1(1)	-1(1)	-2(1)
C(9)	14(1)	20(1)	16(1)	-1(1)	0(1)	-1(1)
C(10)	14(1)	21(1)	17(1)	-2(1)	-3(1)	-1(1)
C(11)	17(1)	18(1)	13(1)	-2(1)	-2(1)	1(1)
C(12)	15(1)	14(1)	12(1)	0(1)	0(1)	-1(1)
C(13)	18(1)	20(1)	17(1)	-3(1)	1(1)	2(1)
C(14)	20(1)	17(1)	14(1)	2(1)	-1(1)	-2(1)
O(1)	21(1)	22(1)	16(1)	-2(1)	4(1)	-3(1)
O(2)	23(1)	22(1)	13(1)	1(1)	-4(1)	-5(1)
O(3)	27(1)	16(1)	18(1)	1(1)	-7(1)	-1(1)

Table 5. Hydrogen coordinates (x 10^4) and isotropic displacement parameters (Å^{2}x 10^3) for mp001.

	x	y	z	U(eq)
H(3A)	8305	5050	6343	36
H(3B)	6350	4171	6300	36
H(3C)	6446	6078	6374	36

H(4)	9723	5678	5344	19
H(5A)	9280	4751	4199	19
H(5B)	9475	6652	4266	19
H(6)	6380	7035	4194	16
H(8A)	5098	2361	4619	26
H(8B)	7182	2844	4457	26
H(8C)	5732	2605	3876	26
H(9A)	3004	6116	4194	20
H(9B)	2600	4233	4229	20
H(10A)	3927	3866	3182	21
H(10B)	2300	5158	3135	21
H(11)	4452	7261	3176	19
H(13A)	8082	4707	2535	27
H(13B)	6939	3566	3015	27
H(13C)	8918	4224	3231	27
H(14A)	9313	7249	3220	20
H(14B)	8022	7442	2593	20
H(2)	4200(30)	5370(30)	2196(11)	33(6)
H(3)	7900(30)	9110(30)	3677(12)	34(6)

A colorless block 0.41 x 0.28 x 0.19 mm in size was mounted on a Cryoloop with Paratone oil. Data were collected in a nitrogen gas stream at 100(2) K using omega scans. Crystal-to-detector distance was 35.00 mm and exposure time was 0.50 seconds per frame at low and high angles using a scan width of 0.5°. Data collection was 100% complete to 74.000° in θ. A total of 50378 reflections were collected covering the indices -11<=h<=11, -10<=k<=11, -65<=l<=66. 4662 reflections were founded to be symmetry independent, with an R_{int} of 0.0452. Indexing and unit cell refinement indicated a primitive, tetragonal lattice. The space group was found to be P 41 21 2 (No. 92). The data were integrated using the CrysAlis^{Pro} 1.171.39.46e software program and scaled using the SCALE3 ABSPACK scaling algorithm. Solution by intrinsic phasing (SHELXT-2015) produced a heavy-atom phasing model consistent with the proposed structure. All non-hydrogen atoms were refined anisotropically by full-matrix least-squares (SHELXL-2014). All hydrogen atoms were placed using a riding model. Their positions were constrained relative to their parent atom using the appropriate HFIX command in SHELXL-2014.

Table 1. Crystal data and structure refinement for IB002_Sarpong.

Identification code	IB002_Sarpong	
Empirical formula	C26 H37 N O3	
Formula weight	411.56	
Temperature	100(2) K	
Wavelength	1.54184 Å	
Crystal system	Tetragonal	
Space group	P 41 21 2	
Unit cell dimensions	a = 9.27318(4) Å	a= 90°.
	b = 9.27318(4) Å	b= 90°.
	c = 52.9739(4) Å	g = 90°.
Volume	4555.33(5) Å^3	
Z	8	
Density (calculated)	1.200 Mg/m^3	
Absorption coefficient	0.605 mm^{-1}	
F(000)	1792	
Crystal size	0.410 x 0.280 x 0.190 mm^3	

Theta range for data collection	3.337 to 74.499°.
Index ranges	-11<=h<=11, -10<=k<=11, -65<=l<=66
Reflections collected	50378
Independent reflections	4662 [R(int) = 0.0452]
Completeness to theta = 74.000°	99.9 %
Absorption correction	Semi-empirical from equivalents
Max. and min. transmission	1.00000 and 0.71681
Refinement method	Full-matrix least-squares on F^2
Data / restraints / parameters	4662 / 0 / 284
Goodness-of-fit on F^2	1.094
Final R indices [I>2sigma(I)]	R1 = 0.0346, wR2 = 0.0881
R indices (all data)	R1 = 0.0349, wR2 = 0.0884
Absolute structure parameter	0.00(7)
Extinction coefficient	n/a
Largest diff. peak and hole	0.135 and -0.162 e.$Å^{-3}$

Table 2. Atomic coordinates (x 10^4) and equivalent isotropic displacement parameters ($Å^2$x 10^3)

for ib002_sarpong. U(eq) is defined as one third of the trace of the orthogonalized U^{ij} tensor.

	x	y	z	U(eq)
C(1)	6288(2)	5573(2)	3724(1)	31(1)
C(2)	5382(2)	6538(2)	3604(1)	37(1)
C(3)	3881(3)	6400(2)	3619(1)	38(1)
C(4)	3245(2)	5297(2)	3755(1)	33(1)
C(5)	4133(2)	4307(2)	3882(1)	27(1)
C(6)	5644(2)	4469(2)	3862(1)	26(1)
C(7)	5201(2)	2538(2)	4103(1)	29(1)
C(8)	3879(2)	3060(2)	4040(1)	28(1)
C(9)	2453(2)	2489(2)	4125(1)	31(1)
C(10)	1662(2)	3487(2)	4313(1)	27(1)
C(11)	98(2)	2986(2)	4371(1)	28(1)
C(12)	53(2)	1417(2)	4462(1)	35(1)
C(13)	-648(2)	4090(2)	4556(1)	26(1)
C(14)	-732(2)	5573(2)	4423(1)	32(1)
C(15)	-2208(2)	3621(2)	4619(1)	31(1)
C(16)	-2899(2)	4465(2)	4838(1)	30(1)
C(17)	-1940(2)	4292(2)	5067(1)	28(1)
C(18)	-1837(2)	4675(2)	5514(1)	32(1)
C(19)	-2510(3)	5665(3)	5706(1)	44(1)
C(20)	-1898(2)	3111(2)	5600(1)	36(1)
C(21)	367(2)	4593(2)	5273(1)	29(1)
C(22)	-439(2)	4954(2)	5028(1)	26(1)
C(23)	-484(2)	6599(2)	5002(1)	33(1)
C(24)	265(2)	4136(2)	4804(1)	24(1)
C(25)	1824(2)	4605(2)	4753(1)	27(1)

C(26)	2544(2)	3656(2)	4556(1)	29(1)
N(1)	6274(2)	3365(2)	3997(1)	30(1)
O(1)	-734(2)	3044(2)	4138(1)	35(1)
O(2)	-2625(2)	4901(2)	5285(1)	32(1)
O(3)	-381(2)	5156(2)	5488(1)	32(1)

Table 3. Bond lengths [Å] and angles [°] for ib002_sarpong.

C(1)-C(2)	1.381(3)
C(1)-C(6)	1.393(3)
C(1)-H(1B)	0.9500
C(2)-C(3)	1.400(3)
C(2)-H(2)	0.9500
C(3)-C(4)	1.385(3)
C(3)-H(3)	0.9500
C(4)-C(5)	1.404(3)
C(4)-H(4)	0.9500
C(5)-C(6)	1.413(3)
C(5)-C(8)	1.445(3)
C(6)-N(1)	1.379(2)
C(7)-C(8)	1.359(3)
C(7)-N(1)	1.376(3)
C(7)-H(7)	0.9500
C(8)-C(9)	1.496(3)
C(9)-C(10)	1.543(3)
C(9)-H(9A)	0.9900
C(9)-H(9B)	0.9900
C(10)-C(26)	1.533(2)
C(10)-C(11)	1.554(3)
C(10)-H(10)	1.0000
C(11)-O(1)	1.456(2)
C(11)-C(12)	1.533(3)
C(11)-C(13)	1.576(3)
C(12)-H(12A)	0.9800
C(12)-H(12B)	0.9800
C(12)-H(12C)	0.9800

C(13)-C(14)	1.546(3)
C(13)-C(15)	1.547(3)
C(13)-C(24)	1.564(2)
C(14)-H(14A)	0.9800
C(14)-H(14B)	0.9800
C(14)-H(14C)	0.9800
C(15)-C(16)	1.540(2)
C(15)-H(15A)	0.9900
C(15)-H(15B)	0.9900
C(16)-C(17)	1.513(2)
C(16)-H(16A)	0.9900
C(16)-H(16B)	0.9900
C(17)-O(2)	1.433(2)
C(17)-C(22)	1.534(3)
C(17)-H(17)	1.0000
C(18)-O(3)	1.428(2)
C(18)-O(2)	1.431(2)
C(18)-C(19)	1.506(3)
C(18)-C(20)	1.522(3)
C(19)-H(19A)	0.9800
C(19)-H(19B)	0.9800
C(19)-H(19C)	0.9800
C(20)-H(20A)	0.9800
C(20)-H(20B)	0.9800
C(20)-H(20C)	0.9800
C(21)-O(3)	1.430(2)
C(21)-C(22)	1.536(2)
C(21)-H(21A)	0.9900
C(21)-H(21B)	0.9900
C(22)-C(23)	1.532(3)
C(22)-C(24)	1.553(2)
C(23)-H(23A)	0.9800
C(23)-H(23B)	0.9800
C(23)-H(23C)	0.9800
C(24)-C(25)	1.533(2)

C(24)-H(24)	1.0000
C(25)-C(26)	1.522(2)
C(25)-H(25A)	0.9900
C(25)-H(25B)	0.9900
C(26)-H(26A)	0.9900
C(26)-H(26B)	0.9900
N(1)-H(1A)	0.93(3)
O(1)-H(1)	0.92(3)

C(2)-C(1)-C(6)	117.14(19)
C(2)-C(1)-H(1B)	121.4
C(6)-C(1)-H(1B)	121.4
C(1)-C(2)-C(3)	121.4(2)
C(1)-C(2)-H(2)	119.3
C(3)-C(2)-H(2)	119.3
C(4)-C(3)-C(2)	121.28(19)
C(4)-C(3)-H(3)	119.4
C(2)-C(3)-H(3)	119.4
C(3)-C(4)-C(5)	118.90(19)
C(3)-C(4)-H(4)	120.6
C(5)-C(4)-H(4)	120.6
C(4)-C(5)-C(6)	118.38(18)
C(4)-C(5)-C(8)	134.70(18)
C(6)-C(5)-C(8)	106.91(16)
N(1)-C(6)-C(1)	129.56(18)
N(1)-C(6)-C(5)	107.53(17)
C(1)-C(6)-C(5)	122.91(18)
C(8)-C(7)-N(1)	110.66(17)
C(8)-C(7)-H(7)	124.7
N(1)-C(7)-H(7)	124.7
C(7)-C(8)-C(5)	106.27(17)
C(7)-C(8)-C(9)	126.62(18)
C(5)-C(8)-C(9)	127.06(18)
C(8)-C(9)-C(10)	113.82(16)
C(8)-C(9)-H(9A)	108.8

C(10)-C(9)-H(9A)	108.8
C(8)-C(9)-H(9B)	108.8
C(10)-C(9)-H(9B)	108.8
H(9A)-C(9)-H(9B)	107.7
C(26)-C(10)-C(9)	110.39(15)
C(26)-C(10)-C(11)	111.28(14)
C(9)-C(10)-C(11)	113.06(15)
C(26)-C(10)-H(10)	107.3
C(9)-C(10)-H(10)	107.3
C(11)-C(10)-H(10)	107.3
O(1)-C(11)-C(12)	106.72(16)
O(1)-C(11)-C(10)	108.39(14)
C(12)-C(11)-C(10)	111.79(16)
O(1)-C(11)-C(13)	105.65(14)
C(12)-C(11)-C(13)	114.12(15)
C(10)-C(11)-C(13)	109.78(15)
C(11)-C(12)-H(12A)	109.5
C(11)-C(12)-H(12B)	109.5
H(12A)-C(12)-H(12B)	109.5
C(11)-C(12)-H(12C)	109.5
H(12A)-C(12)-H(12C)	109.5
H(12B)-C(12)-H(12C)	109.5
C(14)-C(13)-C(15)	107.52(15)
C(14)-C(13)-C(24)	112.62(15)
C(15)-C(13)-C(24)	109.46(13)
C(14)-C(13)-C(11)	108.52(14)
C(15)-C(13)-C(11)	111.20(15)
C(24)-C(13)-C(11)	107.56(14)
C(13)-C(14)-H(14A)	109.5
C(13)-C(14)-H(14B)	109.5
H(14A)-C(14)-H(14B)	109.5
C(13)-C(14)-H(14C)	109.5
H(14A)-C(14)-H(14C)	109.5
H(14B)-C(14)-H(14C)	109.5
C(16)-C(15)-C(13)	114.13(16)

C(16)-C(15)-H(15A)	108.7
C(13)-C(15)-H(15A)	108.7
C(16)-C(15)-H(15B)	108.7
C(13)-C(15)-H(15B)	108.7
H(15A)-C(15)-H(15B)	107.6
C(17)-C(16)-C(15)	107.82(15)
C(17)-C(16)-H(16A)	110.1
C(15)-C(16)-H(16A)	110.1
C(17)-C(16)-H(16B)	110.1
C(15)-C(16)-H(16B)	110.1
H(16A)-C(16)-H(16B)	108.5
O(2)-C(17)-C(16)	110.08(14)
O(2)-C(17)-C(22)	110.65(15)
C(16)-C(17)-C(22)	112.53(15)
O(2)-C(17)-H(17)	107.8
C(16)-C(17)-H(17)	107.8
C(22)-C(17)-H(17)	107.8
O(3)-C(18)-O(2)	110.87(14)
O(3)-C(18)-C(19)	105.41(18)
O(2)-C(18)-C(19)	105.80(15)
O(3)-C(18)-C(20)	111.19(16)
O(2)-C(18)-C(20)	112.04(17)
C(19)-C(18)-C(20)	111.20(17)
C(18)-C(19)-H(19A)	109.5
C(18)-C(19)-H(19B)	109.5
H(19A)-C(19)-H(19B)	109.5
C(18)-C(19)-H(19C)	109.5
H(19A)-C(19)-H(19C)	109.5
H(19B)-C(19)-H(19C)	109.5
C(18)-C(20)-H(20A)	109.5
C(18)-C(20)-H(20B)	109.5
H(20A)-C(20)-H(20B)	109.5
C(18)-C(20)-H(20C)	109.5
H(20A)-C(20)-H(20C)	109.5
H(20B)-C(20)-H(20C)	109.5

O(3)-C(21)-C(22)	110.90(14)
O(3)-C(21)-H(21A)	109.5
C(22)-C(21)-H(21A)	109.5
O(3)-C(21)-H(21B)	109.5
C(22)-C(21)-H(21B)	109.5
H(21A)-C(21)-H(21B)	108.0
C(23)-C(22)-C(17)	112.67(16)
C(23)-C(22)-C(21)	107.73(15)
C(17)-C(22)-C(21)	103.92(14)
C(23)-C(22)-C(24)	115.49(15)
C(17)-C(22)-C(24)	106.79(14)
C(21)-C(22)-C(24)	109.61(14)
C(22)-C(23)-H(23A)	109.5
C(22)-C(23)-H(23B)	109.5
H(23A)-C(23)-H(23B)	109.5
C(22)-C(23)-H(23C)	109.5
H(23A)-C(23)-H(23C)	109.5
H(23B)-C(23)-H(23C)	109.5
C(25)-C(24)-C(22)	113.04(14)
C(25)-C(24)-C(13)	111.85(14)
C(22)-C(24)-C(13)	115.33(14)
C(25)-C(24)-H(24)	105.2
C(22)-C(24)-H(24)	105.2
C(13)-C(24)-H(24)	105.2
C(26)-C(25)-C(24)	111.69(15)
C(26)-C(25)-H(25A)	109.3
C(24)-C(25)-H(25A)	109.3
C(26)-C(25)-H(25B)	109.3
C(24)-C(25)-H(25B)	109.3
H(25A)-C(25)-H(25B)	107.9
C(25)-C(26)-C(10)	113.71(15)
C(25)-C(26)-H(26A)	108.8
C(10)-C(26)-H(26A)	108.8
C(25)-C(26)-H(26B)	108.8
C(10)-C(26)-H(26B)	108.8

H(26A)-C(26)-H(26B)	107.7
C(7)-N(1)-C(6)	108.63(16)
C(7)-N(1)-H(1A)	127.0(17)
C(6)-N(1)-H(1A)	123.7(17)
C(11)-O(1)-H(1)	109.1(19)
C(18)-O(2)-C(17)	113.47(14)
C(18)-O(3)-C(21)	114.84(14)

Symmetry transformations used to generate equivalent atoms:

Table 4. Anisotropic displacement parameters ($Å^2 x\ 10^3$)for ib002_sarpong. The anisotropic displacement factor exponent takes the form: $-2p^2[\ h^2 a^{*2} U^{11} + ... + 2\ h\ k\ a^*\ b^*\ U^{12}\ ]$

	U^{11}	U^{22}	U^{33}	U^{23}	U^{13}	U^{12}
C(1)	32(1)	37(1)	24(1)	-4(1)	5(1)	-1(1)
C(2)	49(1)	33(1)	27(1)	0(1)	7(1)	1(1)
C(3)	46(1)	36(1)	31(1)	2(1)	1(1)	11(1)
C(4)	31(1)	39(1)	29(1)	-2(1)	-1(1)	7(1)
C(5)	29(1)	31(1)	20(1)	-4(1)	1(1)	2(1)
C(6)	29(1)	33(1)	17(1)	-4(1)	1(1)	2(1)
C(7)	30(1)	36(1)	21(1)	1(1)	2(1)	2(1)
C(8)	30(1)	32(1)	21(1)	-5(1)	2(1)	0(1)
C(9)	31(1)	32(1)	30(1)	-5(1)	3(1)	-2(1)
C(10)	26(1)	29(1)	25(1)	-2(1)	1(1)	1(1)
C(11)	25(1)	36(1)	22(1)	-4(1)	-1(1)	-1(1)
C(12)	35(1)	34(1)	36(1)	-7(1)	6(1)	-2(1)
C(13)	23(1)	35(1)	21(1)	2(1)	-1(1)	2(1)
C(14)	33(1)	39(1)	24(1)	4(1)	3(1)	10(1)
C(15)	24(1)	47(1)	21(1)	-2(1)	-1(1)	2(1)
C(16)	24(1)	45(1)	21(1)	4(1)	2(1)	5(1)
C(17)	28(1)	34(1)	20(1)	1(1)	2(1)	6(1)
C(18)	32(1)	44(1)	20(1)	3(1)	0(1)	6(1)

C(19)	49(1)	59(1)	24(1)	-2(1)	4(1)	15(1)
C(20)	40(1)	45(1)	24(1)	7(1)	-3(1)	0(1)
C(21)	30(1)	33(1)	22(1)	-2(1)	-1(1)	3(1)
C(22)	29(1)	28(1)	21(1)	1(1)	0(1)	4(1)
C(23)	42(1)	29(1)	29(1)	0(1)	4(1)	6(1)
C(24)	26(1)	24(1)	21(1)	1(1)	-1(1)	2(1)
C(25)	27(1)	30(1)	24(1)	-2(1)	-1(1)	-1(1)
C(26)	23(1)	34(1)	29(1)	-3(1)	-1(1)	1(1)
N(1)	24(1)	45(1)	22(1)	2(1)	1(1)	4(1)
O(1)	26(1)	55(1)	24(1)	-9(1)	-2(1)	1(1)
O(2)	32(1)	45(1)	19(1)	3(1)	2(1)	12(1)
O(3)	36(1)	38(1)	22(1)	-4(1)	0(1)	2(1)

Table 5. Hydrogen coordinates (x 10^4) and isotropic displacement parameters (Å^{2}x 10^3) for ib002_sarpong.

	x	y	z	U(eq)
H(1B)	7307	5658	3712	37
H(2)	5786	7312	3511	44
H(3)	3286	7077	3533	45
H(4)	2225	5211	3763	40
H(7)	5361	1716	4206	35
H(9A)	2603	1538	4206	37
H(9B)	1830	2340	3976	37
H(10)	1596	4461	4233	32
H(12A)	-951	1127	4490	52
H(12B)	590	1332	4621	52
H(12C)	491	791	4335	52
H(14A)	-1435	6184	4510	47
H(14B)	-1032	5439	4247	47

H(14C)	218	6035	4428	47
H(15A)	-2813	3744	4466	37
H(15B)	-2206	2582	4662	37
H(16A)	-2988	5497	4793	37
H(16B)	-3875	4083	4874	37
H(17)	-1811	3237	5098	33
H(19A)	-2367	6669	5654	66
H(19B)	-2057	5507	5871	66
H(19C)	-3545	5462	5718	66
H(20A)	-2901	2844	5635	54
H(20B)	-1319	2995	5753	54
H(20C)	-1514	2486	5467	54
H(21A)	459	3534	5290	34
H(21B)	1350	5009	5267	34
H(23A)	475	6956	4957	50
H(23B)	-780	7026	5164	50
H(23C)	-1177	6868	4871	50
H(24)	335	3110	4861	29
H(25A)	1831	5619	4695	33
H(25B)	2381	4556	4913	33
H(26A)	2714	2689	4630	35
H(26B)	3495	4074	4513	35
H(1)	-460(30)	2280(30)	4035(6)	66(9)
H(1A)	7260(30)	3300(30)	4028(5)	50(7)

Table 6. Torsion angles [°] for ib002_sarpong.

C(6)-C(1)-C(2)-C(3)	-0.9(3)
C(1)-C(2)-C(3)-C(4)	0.6(3)
C(2)-C(3)-C(4)-C(5)	0.3(3)
C(3)-C(4)-C(5)-C(6)	-0.9(3)
C(3)-C(4)-C(5)-C(8)	179.59(19)
C(2)-C(1)-C(6)-N(1)	179.63(17)
C(2)-C(1)-C(6)-C(5)	0.2(3)
C(4)-C(5)-C(6)-N(1)	-178.84(15)
C(8)-C(5)-C(6)-N(1)	0.77(19)

C(4)-C(5)-C(6)-C(1)	0.7(3)
C(8)-C(5)-C(6)-C(1)	-179.71(16)
N(1)-C(7)-C(8)-C(5)	0.0(2)
N(1)-C(7)-C(8)-C(9)	-177.68(17)
C(4)-C(5)-C(8)-C(7)	179.1(2)
C(6)-C(5)-C(8)-C(7)	-0.4(2)
C(4)-C(5)-C(8)-C(9)	-3.3(3)
C(6)-C(5)-C(8)-C(9)	177.18(17)
C(7)-C(8)-C(9)-C(10)	109.2(2)
C(5)-C(8)-C(9)-C(10)	-67.9(2)
C(8)-C(9)-C(10)-C(26)	-62.6(2)
C(8)-C(9)-C(10)-C(11)	171.98(15)
C(26)-C(10)-C(11)-O(1)	172.06(15)
C(9)-C(10)-C(11)-O(1)	-63.0(2)
C(26)-C(10)-C(11)-C(12)	-70.58(19)
C(9)-C(10)-C(11)-C(12)	54.3(2)
C(26)-C(10)-C(11)-C(13)	57.12(19)
C(9)-C(10)-C(11)-C(13)	-177.98(15)
O(1)-C(11)-C(13)-C(14)	-54.50(19)
C(12)-C(11)-C(13)-C(14)	-171.43(16)
C(10)-C(11)-C(13)-C(14)	62.18(18)
O(1)-C(11)-C(13)-C(15)	63.57(18)
C(12)-C(11)-C(13)-C(15)	-53.4(2)
C(10)-C(11)-C(13)-C(15)	-179.75(14)
O(1)-C(11)-C(13)-C(24)	-176.60(14)
C(12)-C(11)-C(13)-C(24)	66.5(2)
C(10)-C(11)-C(13)-C(24)	-59.92(18)
C(14)-C(13)-C(15)-C(16)	-73.07(19)
C(24)-C(13)-C(15)-C(16)	49.6(2)
C(11)-C(13)-C(15)-C(16)	168.27(15)
C(13)-C(15)-C(16)-C(17)	-57.1(2)
C(15)-C(16)-C(17)-O(2)	-172.59(16)
C(15)-C(16)-C(17)-C(22)	63.5(2)
O(2)-C(17)-C(22)-C(23)	-57.09(19)
C(16)-C(17)-C(22)-C(23)	66.5(2)

O(2)-C(17)-C(22)-C(21)	59.25(18)
C(16)-C(17)-C(22)-C(21)	-177.14(15)
O(2)-C(17)-C(22)-C(24)	175.09(13)
C(16)-C(17)-C(22)-C(24)	-61.30(19)
O(3)-C(21)-C(22)-C(23)	62.2(2)
O(3)-C(21)-C(22)-C(17)	-57.56(19)
O(3)-C(21)-C(22)-C(24)	-171.41(15)
C(23)-C(22)-C(24)-C(25)	58.0(2)
C(17)-C(22)-C(24)-C(25)	-175.89(14)
C(21)-C(22)-C(24)-C(25)	-63.91(19)
C(23)-C(22)-C(24)-C(13)	-72.5(2)
C(17)-C(22)-C(24)-C(13)	53.66(19)
C(21)-C(22)-C(24)-C(13)	165.64(15)
C(14)-C(13)-C(24)-C(25)	-60.10(19)
C(15)-C(13)-C(24)-C(25)	-179.64(15)
C(11)-C(13)-C(24)-C(25)	59.42(19)
C(14)-C(13)-C(24)-C(22)	70.93(19)
C(15)-C(13)-C(24)-C(22)	-48.6(2)
C(11)-C(13)-C(24)-C(22)	-169.55(14)
C(22)-C(24)-C(25)-C(26)	172.72(14)
C(13)-C(24)-C(25)-C(26)	-55.10(19)
C(24)-C(25)-C(26)-C(10)	51.1(2)
C(9)-C(10)-C(26)-C(25)	-178.94(16)
C(11)-C(10)-C(26)-C(25)	-52.6(2)
C(8)-C(7)-N(1)-C(6)	0.5(2)
C(1)-C(6)-N(1)-C(7)	179.72(18)
C(5)-C(6)-N(1)-C(7)	-0.8(2)
O(3)-C(18)-O(2)-C(17)	53.1(2)
C(19)-C(18)-O(2)-C(17)	166.91(17)
C(20)-C(18)-O(2)-C(17)	-71.8(2)
C(16)-C(17)-O(2)-C(18)	175.13(17)
C(22)-C(17)-O(2)-C(18)	-59.9(2)
O(2)-C(18)-O(3)-C(21)	-52.0(2)
C(19)-C(18)-O(3)-C(21)	-166.05(15)
C(20)-C(18)-O(3)-C(21)	73.34(18)

C(22)-C(21)-O(3)-C(18)	57.0(2)

Symmetry transformations used to generate equivalent atoms:

Copies of NMR spectra

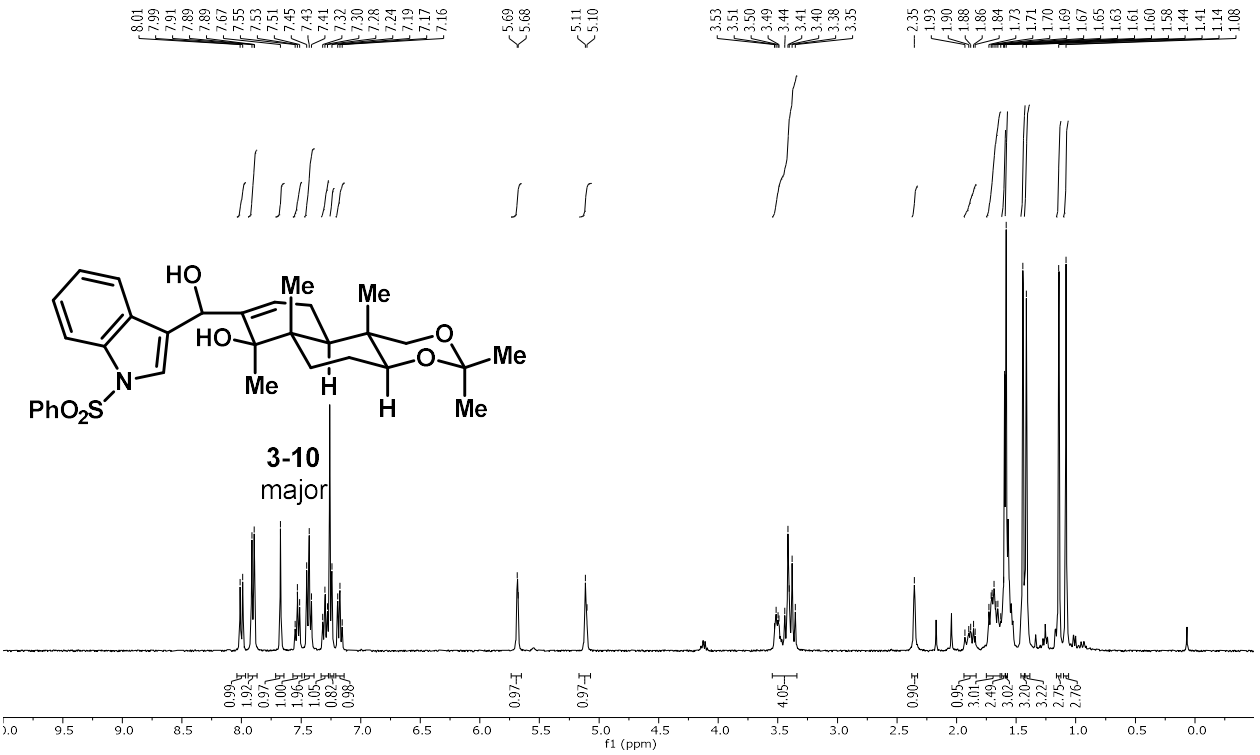

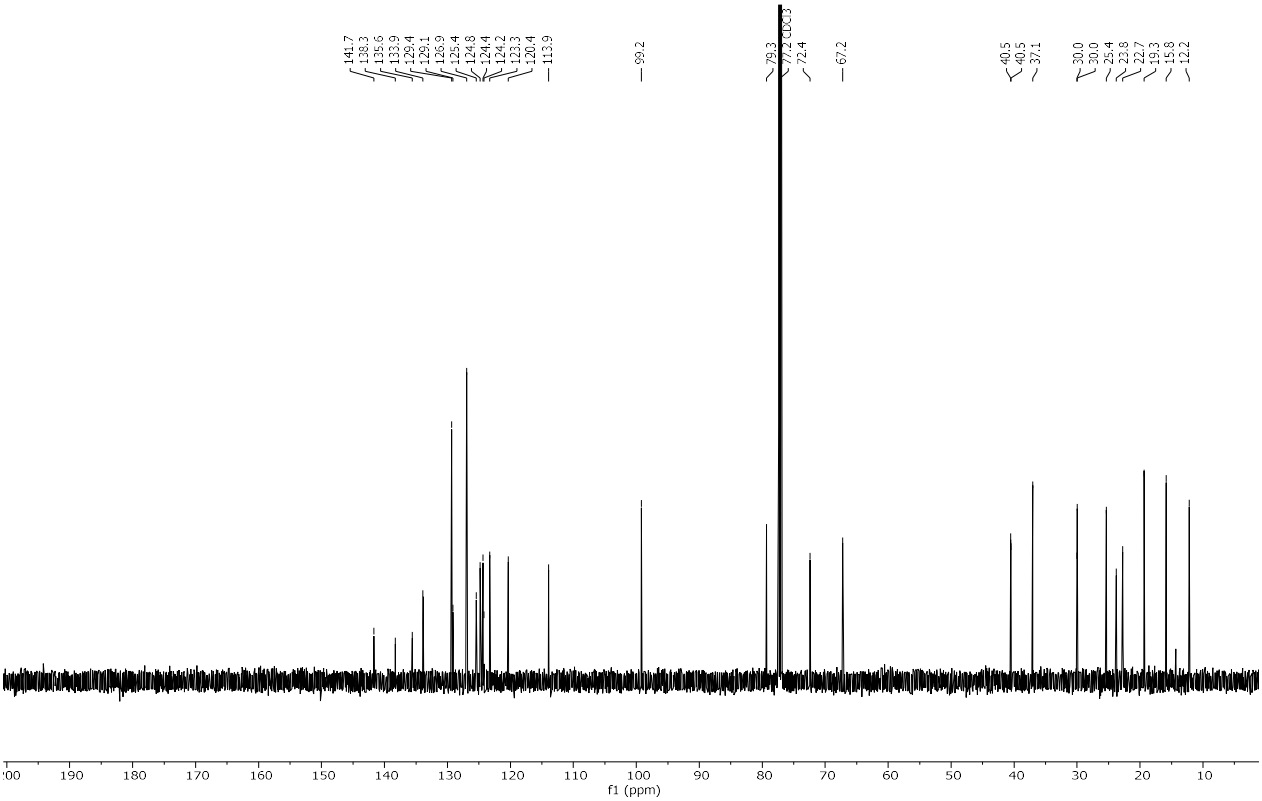

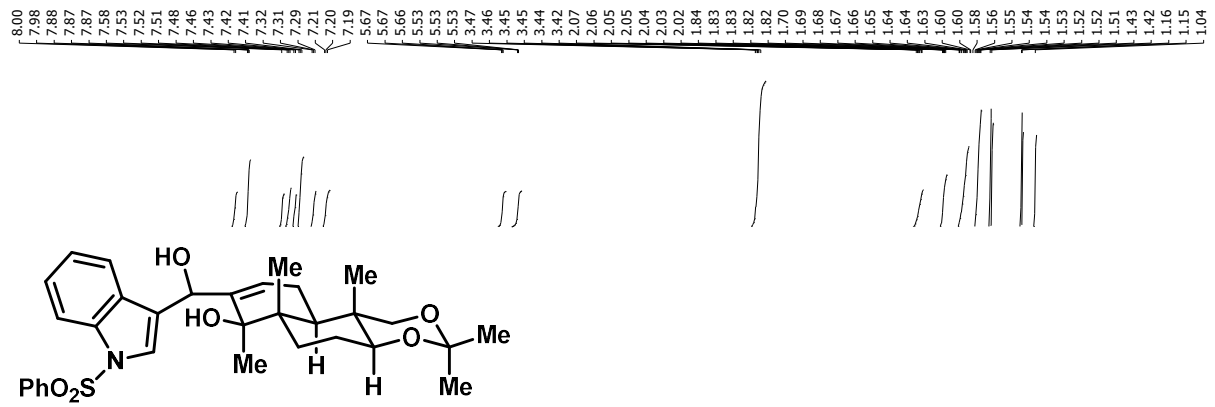

3-10
minor

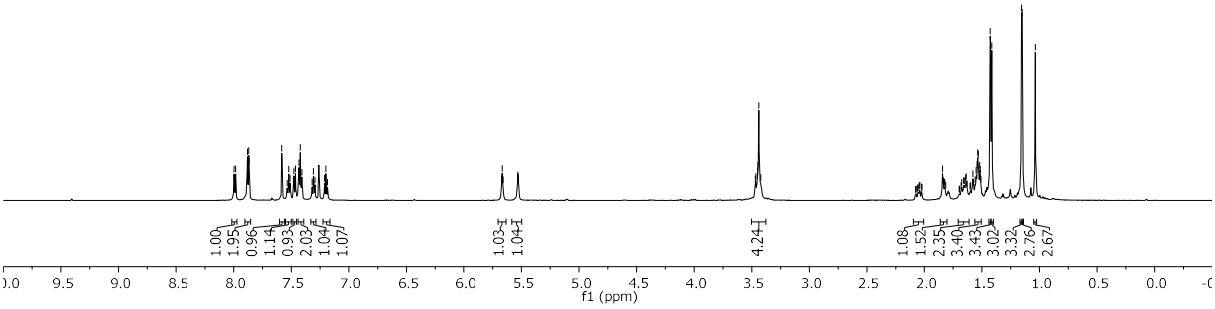

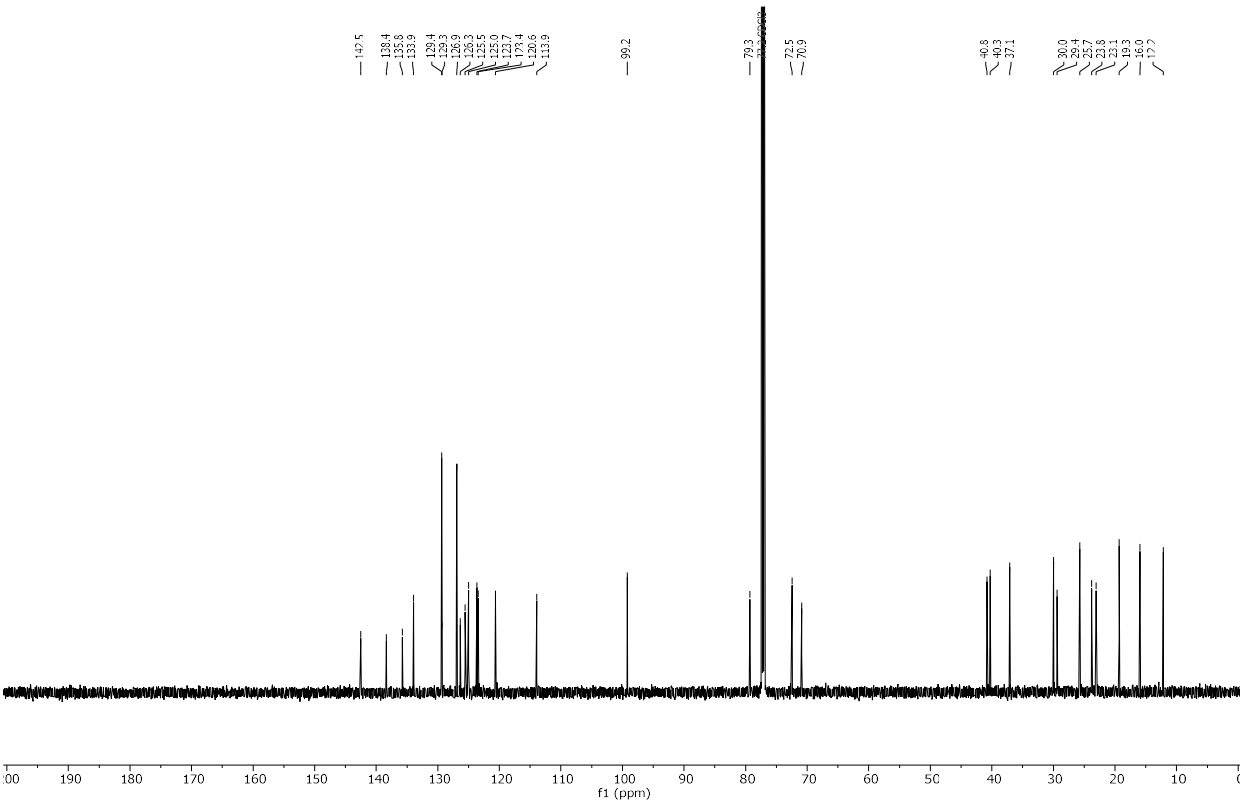

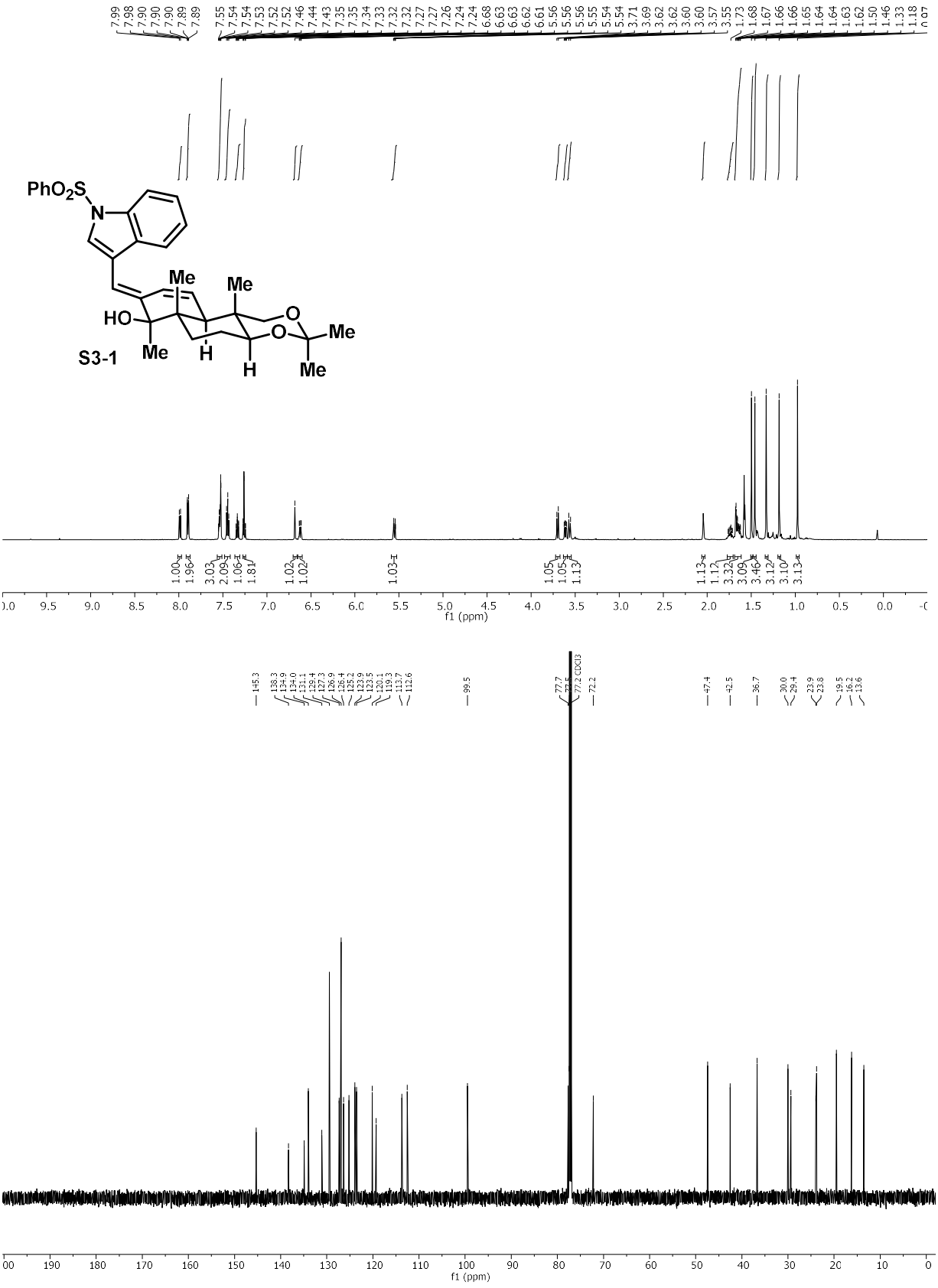
PhO2S
N
Me
Me
HO
Me
H
O
O
Me
H
Me
S3-1
f1 (ppm)
f1 (ppm)

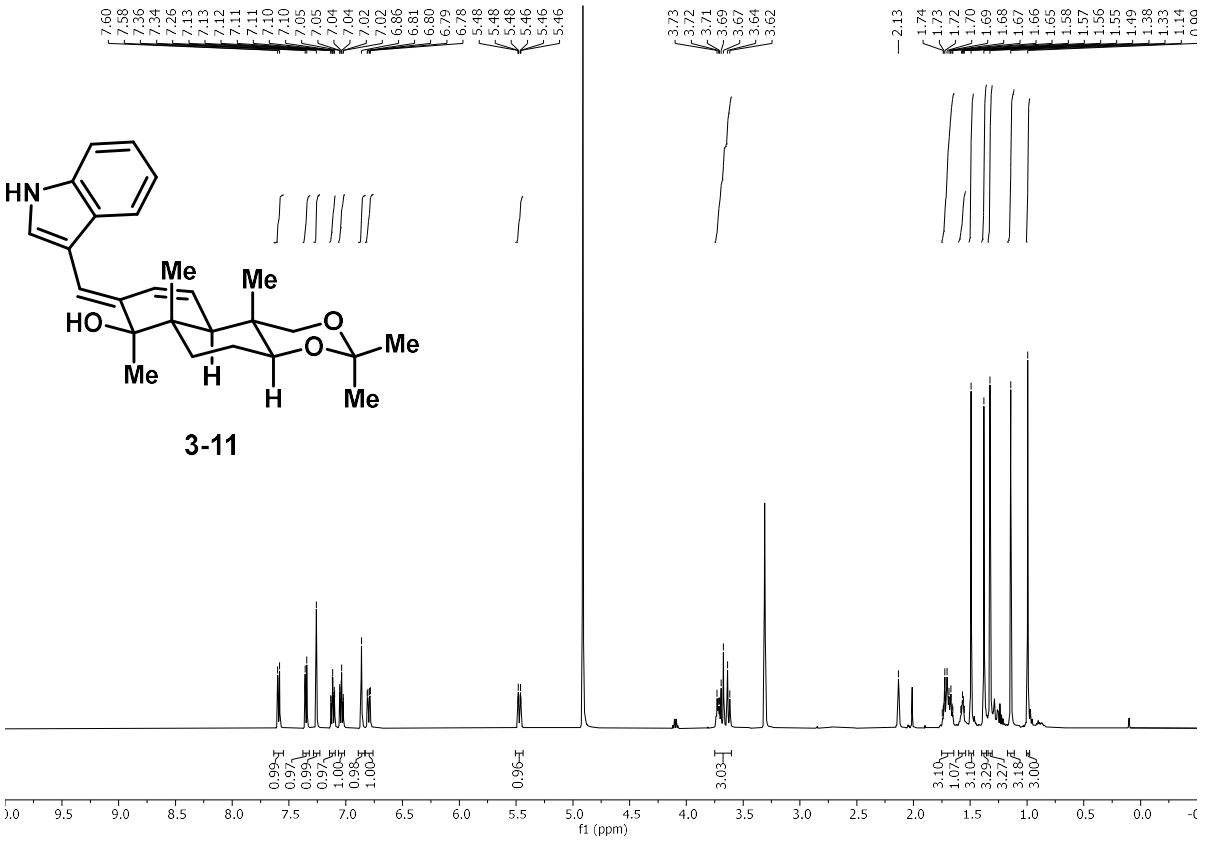
HN
Me
Me
HO
Me
H
H
O
O
Me
Me
3-11
f1 (ppm)

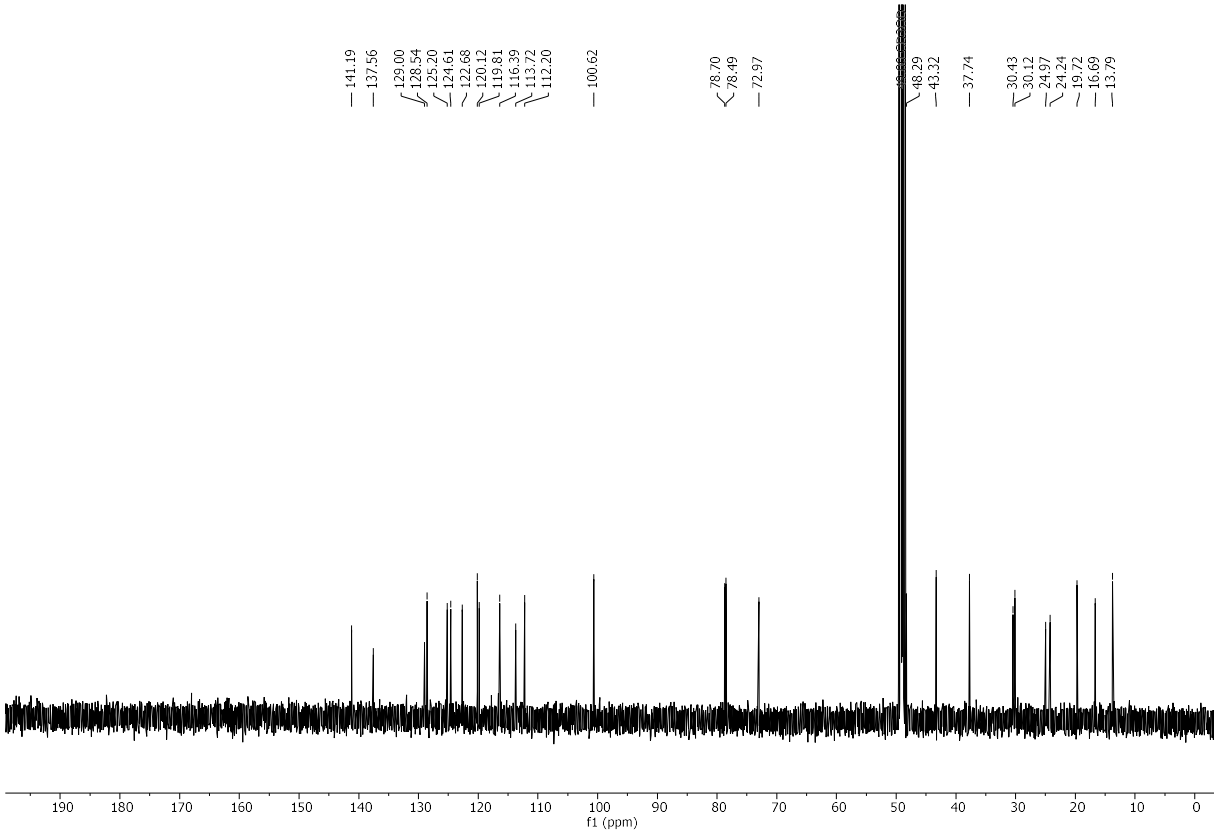
f1 (ppm)

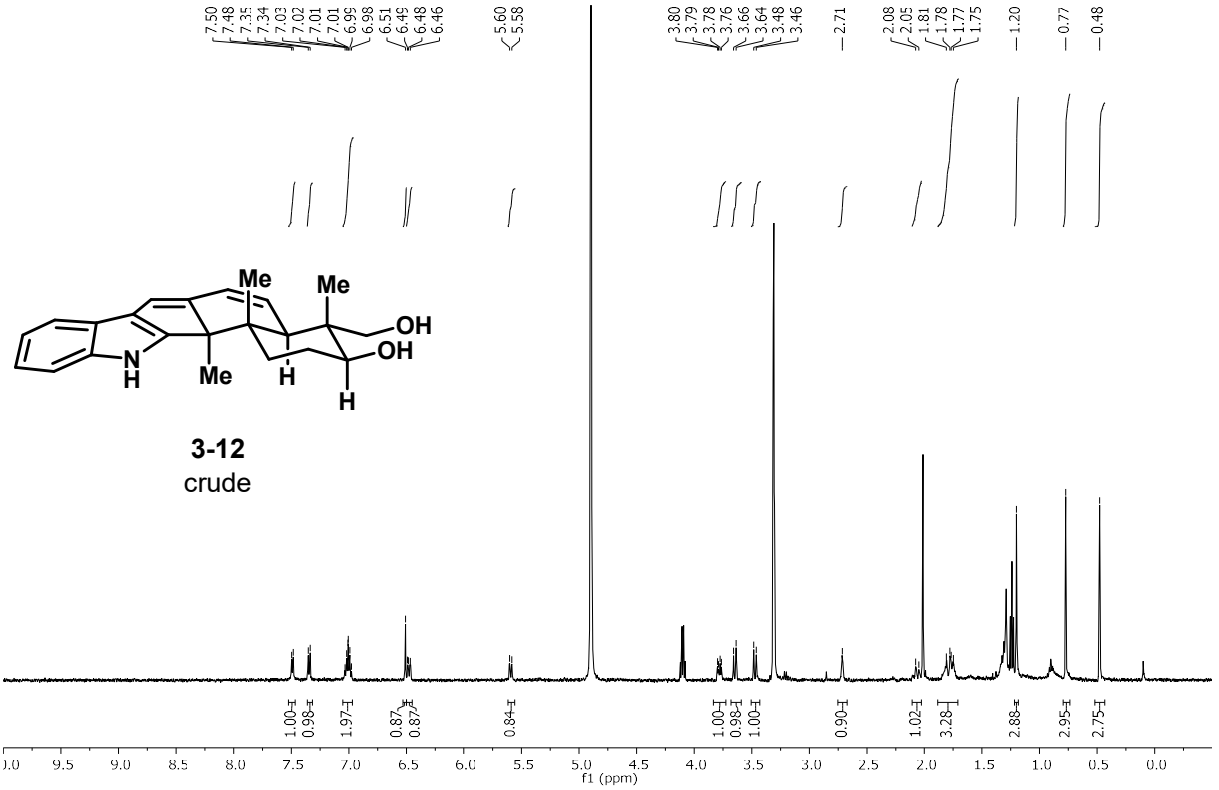
Me
Me
OH
OH
N
H
Me
H
H

3-12
crude

7.50
7.48
7.34
7.03
7.02
7.01
7.01
6.99
6.98
6.51
6.49
6.48
6.46
5.60
5.58
3.80
3.79
3.78
3.76
3.66
3.64
3.48
3.46
2.71
2.08
2.05
1.81
1.78
1.77
1.75
1.20
0.77
0.48
1.00
0.98
1.97
0.87
0.87
0.84
1.00
0.98
1.00
0.90
1.02
3.28
2.88
2.95
2.75
f1 (ppm)

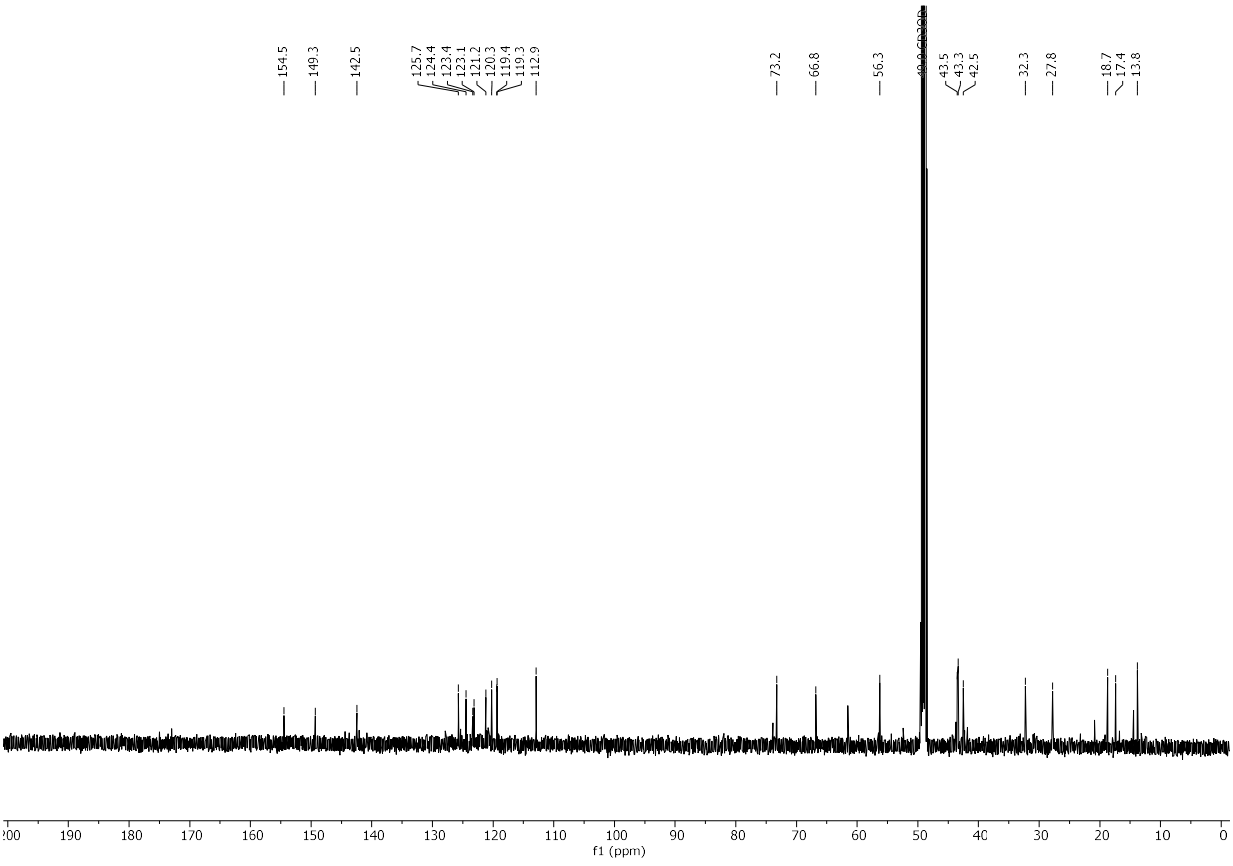
154.5
149.3
142.5
125.7
124.4
123.4
123.1
121.2
120.3
119.4
119.3
112.9
73.2
66.8
56.3
43.5
43.3
42.5
32.3
27.8
18.7
17.4
13.8
f1 (ppm)

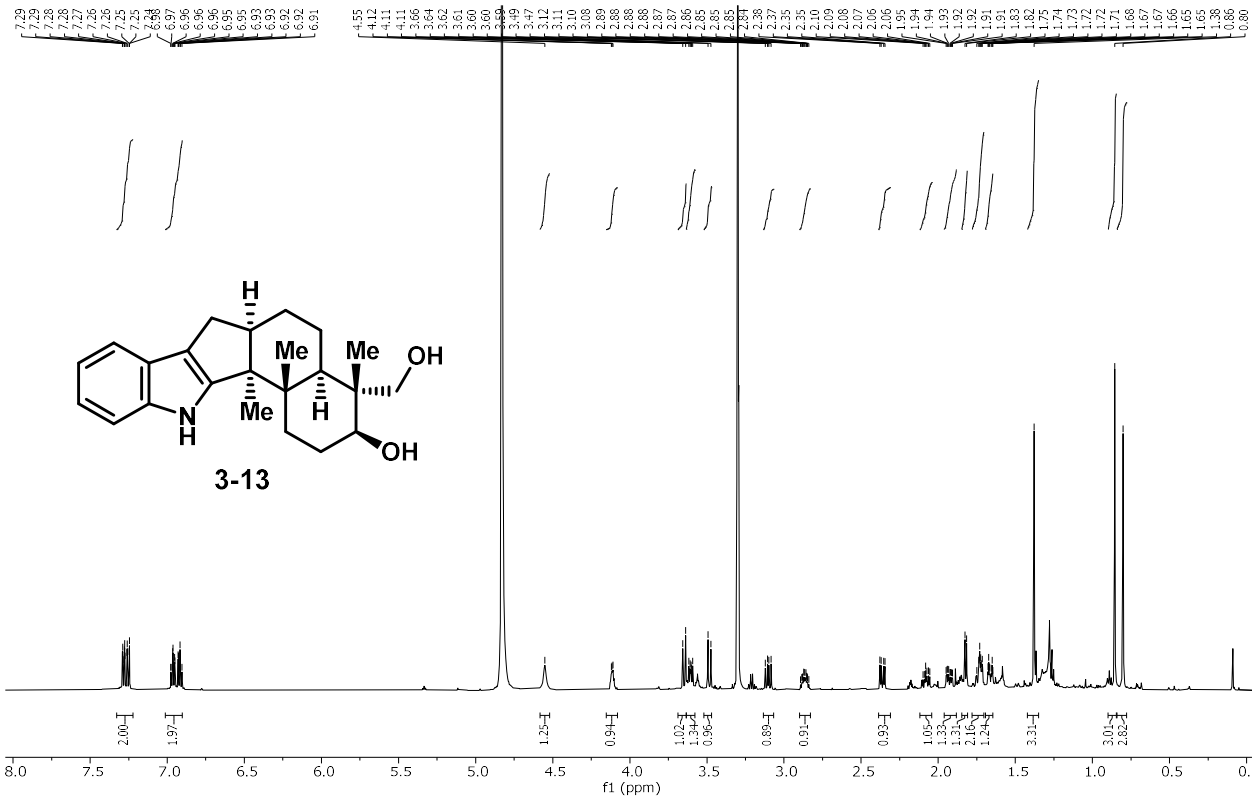

3-13

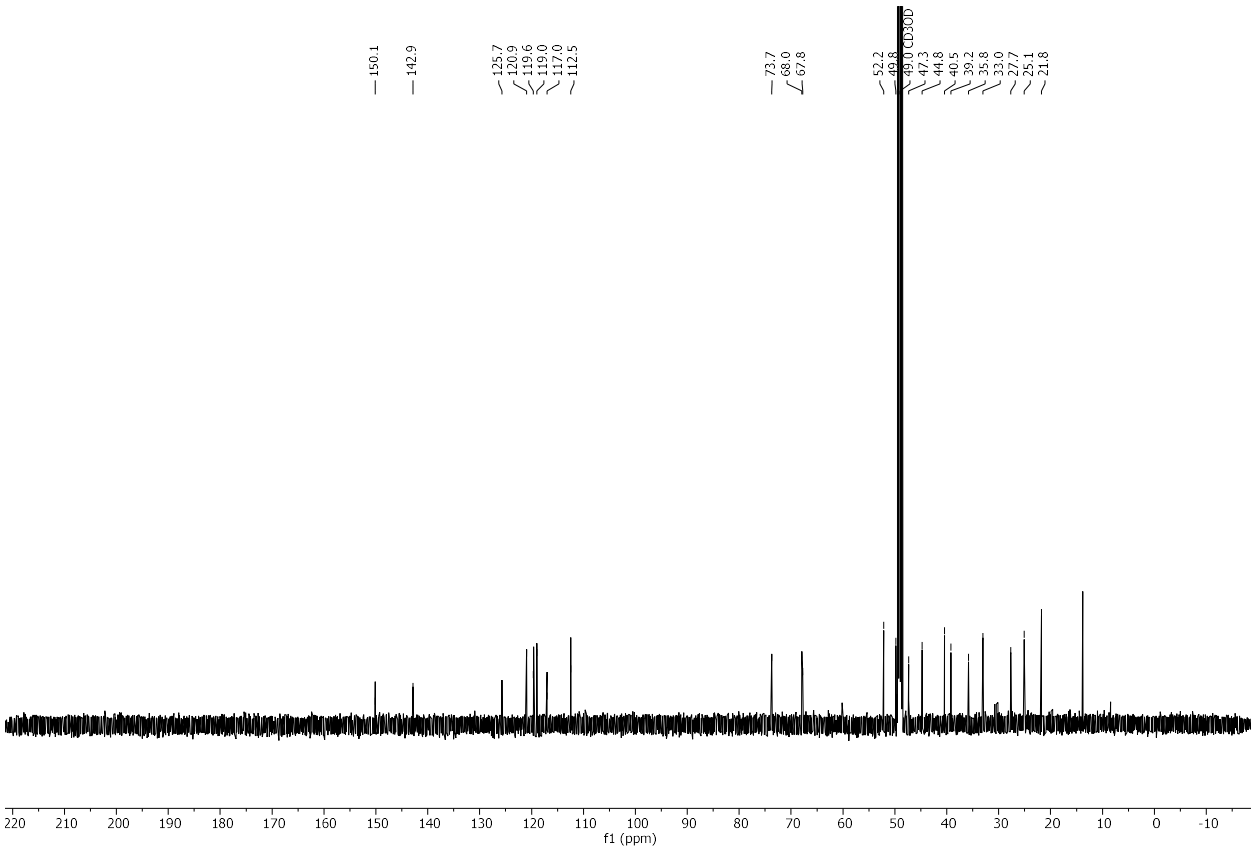

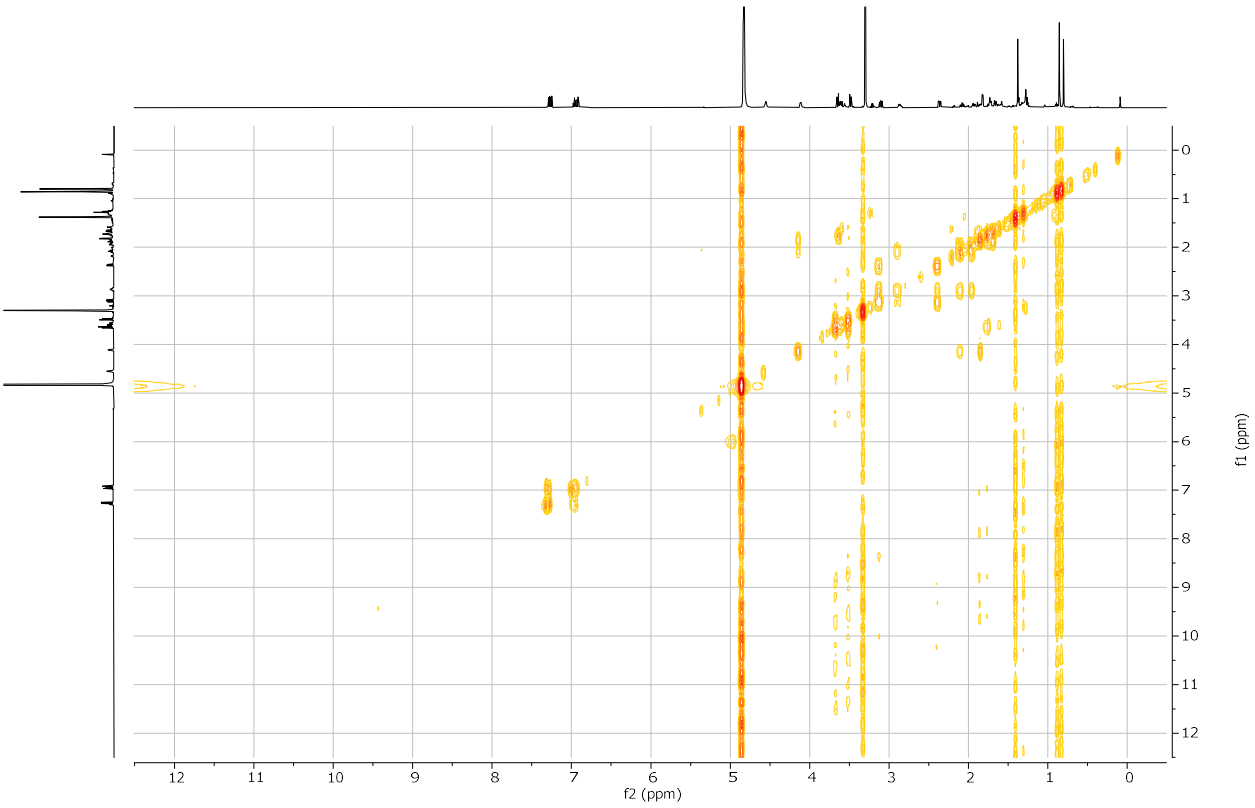
f2 (ppm)
f1 (ppm)

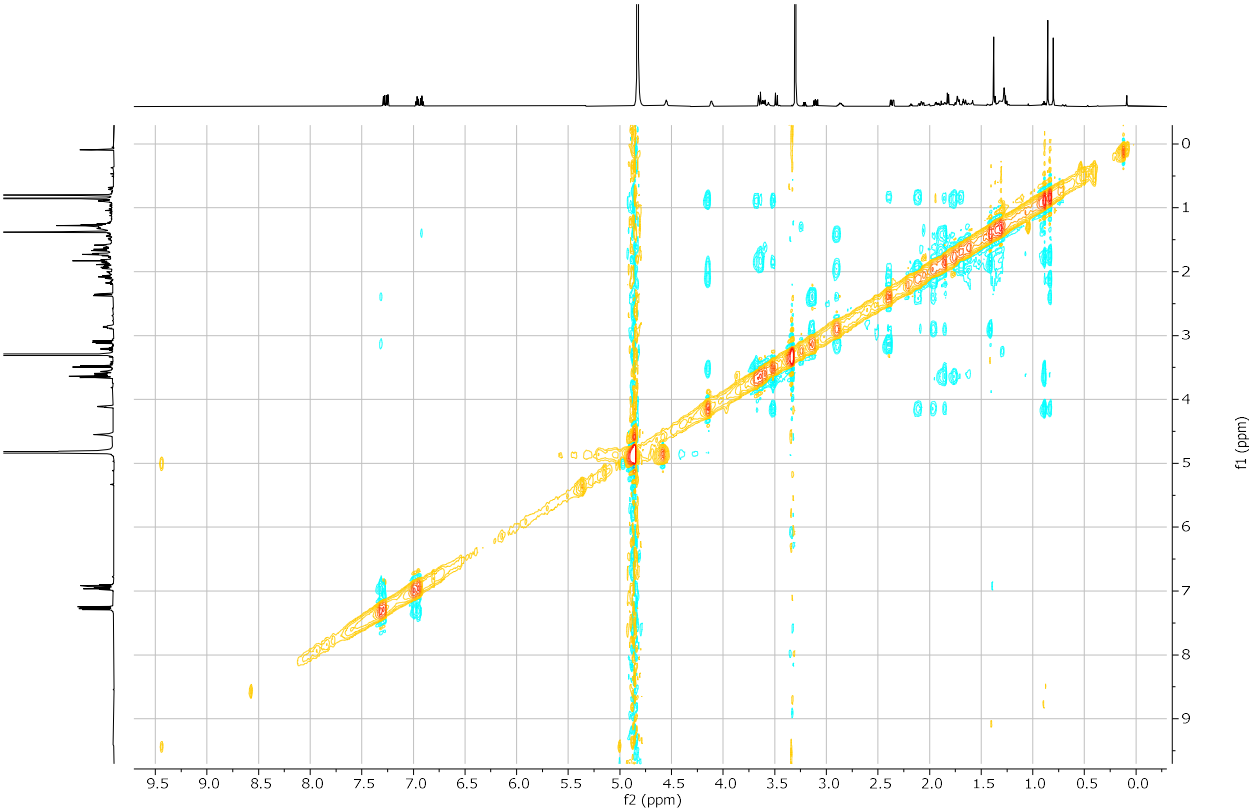
f2 (ppm)
f1 (ppm)

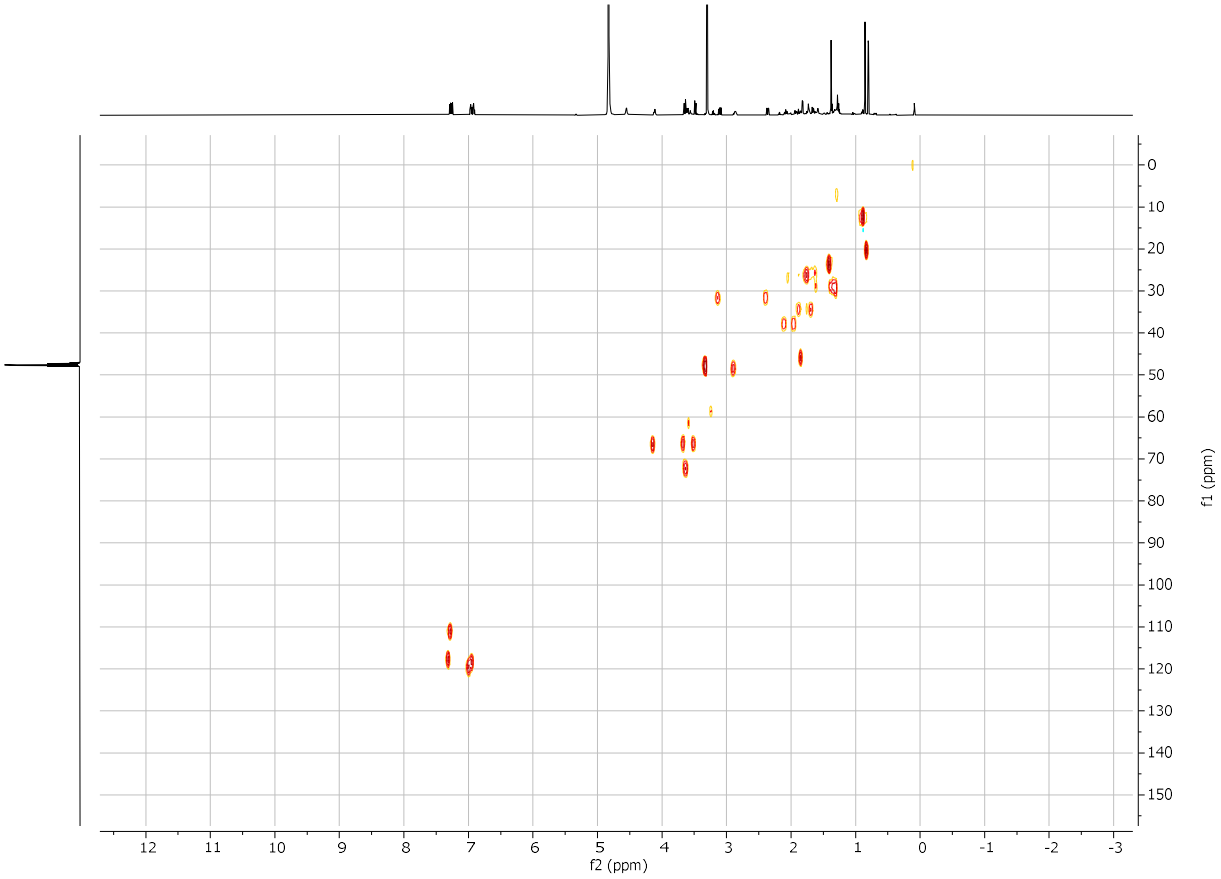
0
10
20
30
40
50
60
70
80
90
100
110
120
130
140
150
f1 (ppm)
12
11
10
9
8
7
6
5
4
3
2
1
0
-1
-2
-3
f2 (ppm)

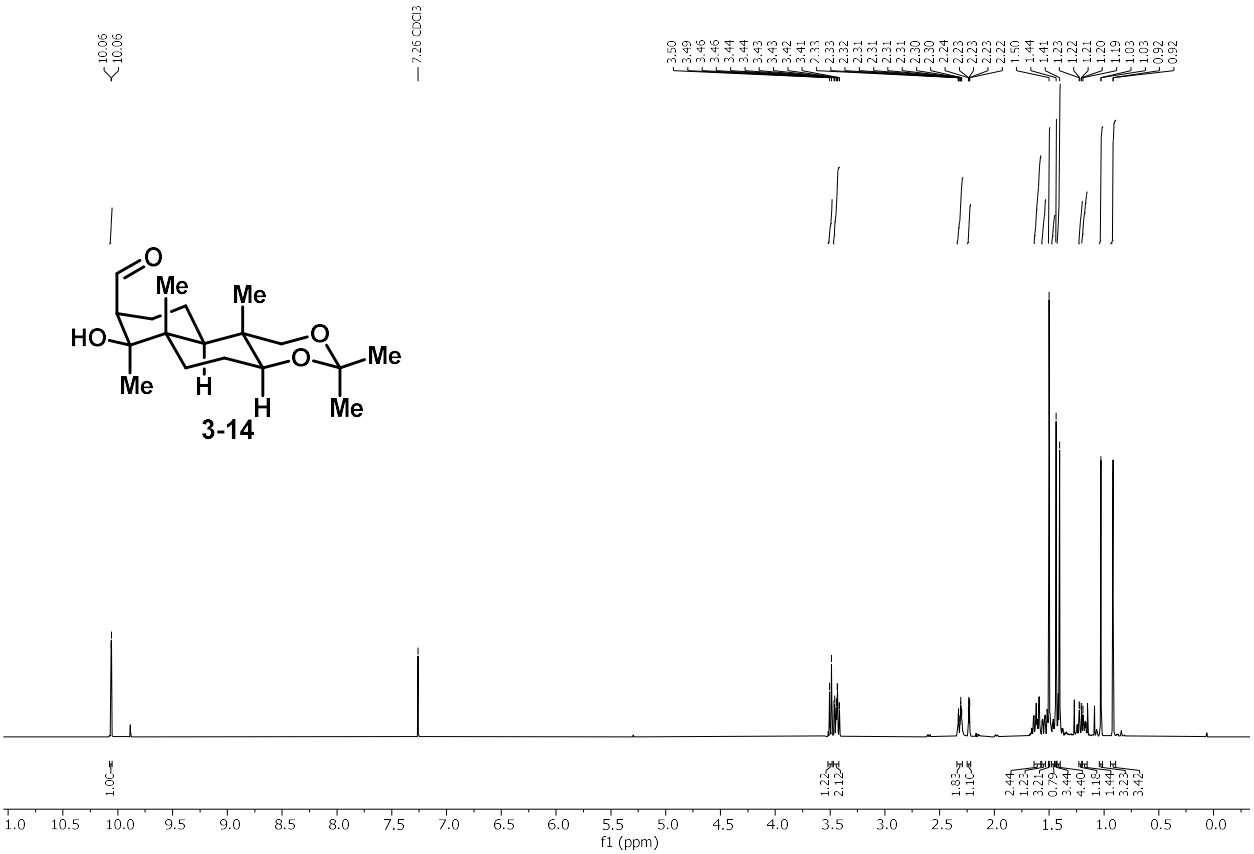
10.06
10.06
7.26 CDCl3
3.50
3.49
3.46
3.46
3.44
3.44
3.43
3.43
3.42
3.41
2.33
2.32
2.31
2.31
2.31
2.30
2.30
2.24
2.23
2.23
2.23
2.22
1.50
1.44
1.41
1.23
1.22
1.21
1.20
1.19
1.03
1.03
0.92
0.92
O
Me
Me
HO
O
O
Me
Me
H
H
Me
3-14
1.00
1.22
2.12
1.83
1.10
2.44
1.23
3.21
0.79
3.44
4.40
1.18
1.44
3.23
3.42
1.0 10.5 10.0 9.5 9.0 8.5 8.0 7.5 7.0 6.5 6.0 5.5 5.0 4.5 4.0 3.5 3.0 2.5 2.0 1.5 1.0 0.5 0.0
f1 (ppm)

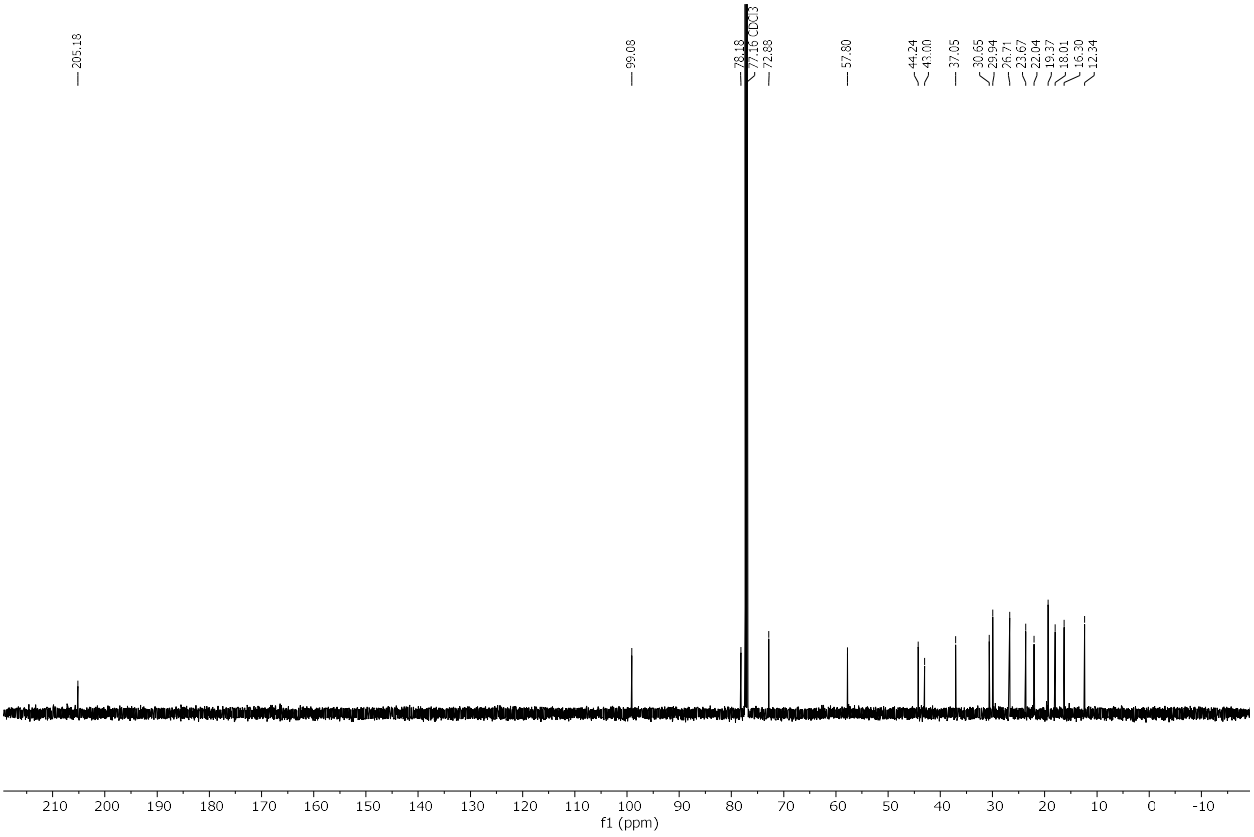
205.18
99.08
78.48
77.16 CDCl3
72.88
57.80
44.24
43.00
37.05
30.65
29.94
26.71
23.67
22.04
19.37
18.01
16.30
12.34
210 200 190 180 170 160 150 140 130 120 110 100 90 80 70 60 50 40 30 20 10 0 -10
f1 (ppm)

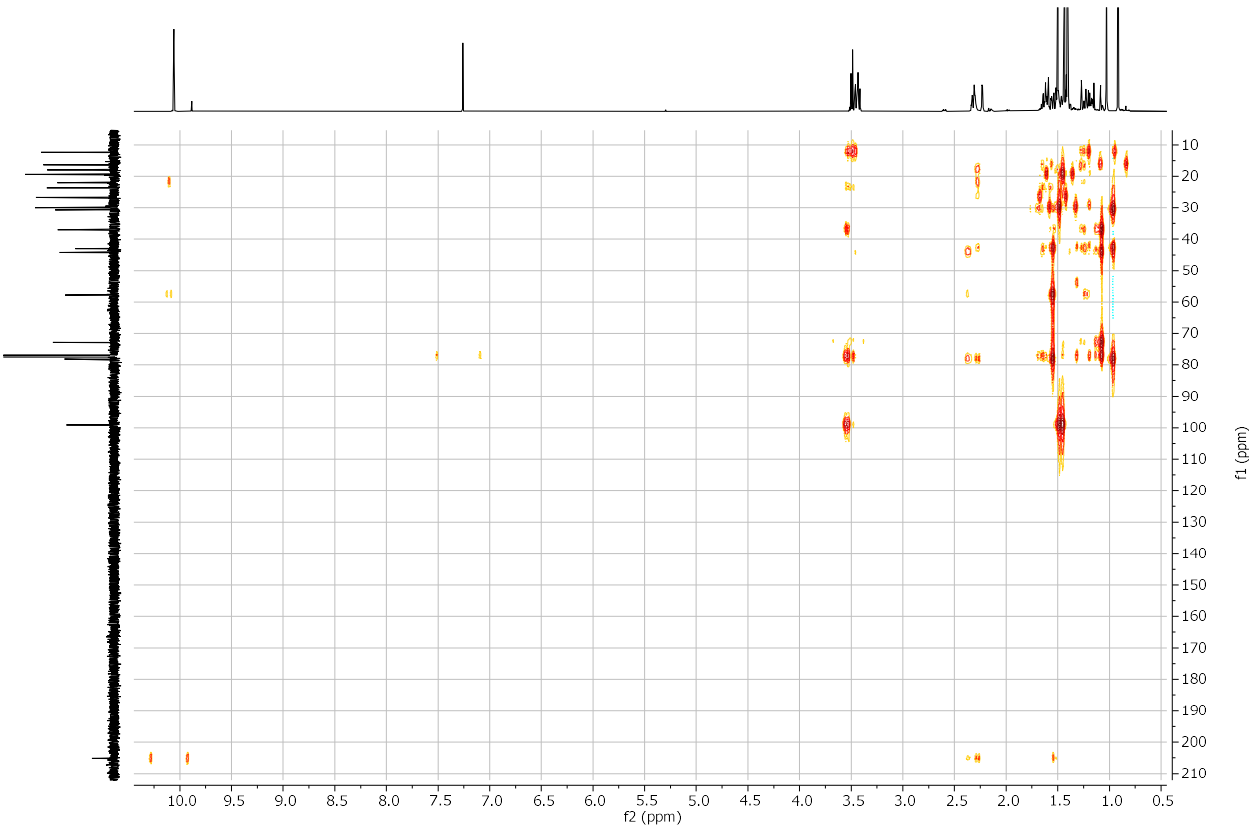
f2 (ppm)
f1 (ppm)

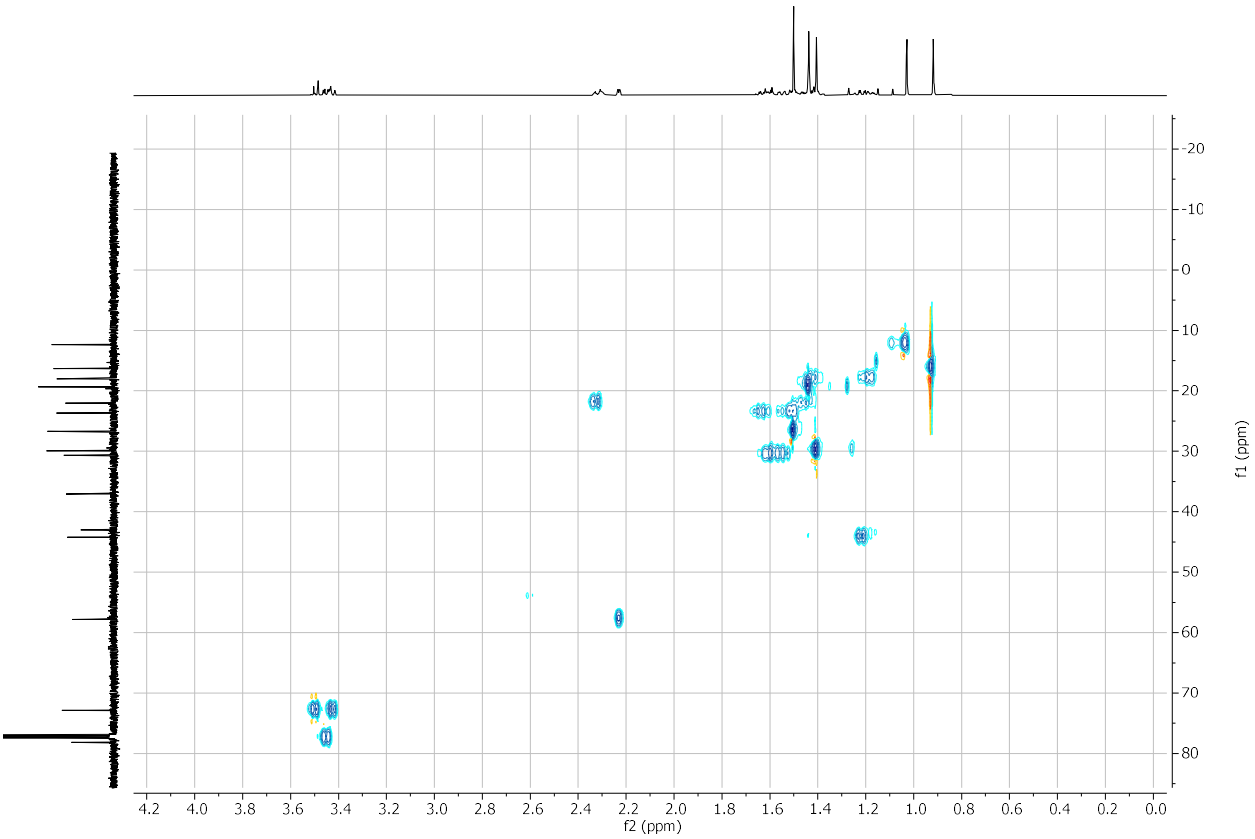
f2 (ppm)
f1 (ppm)

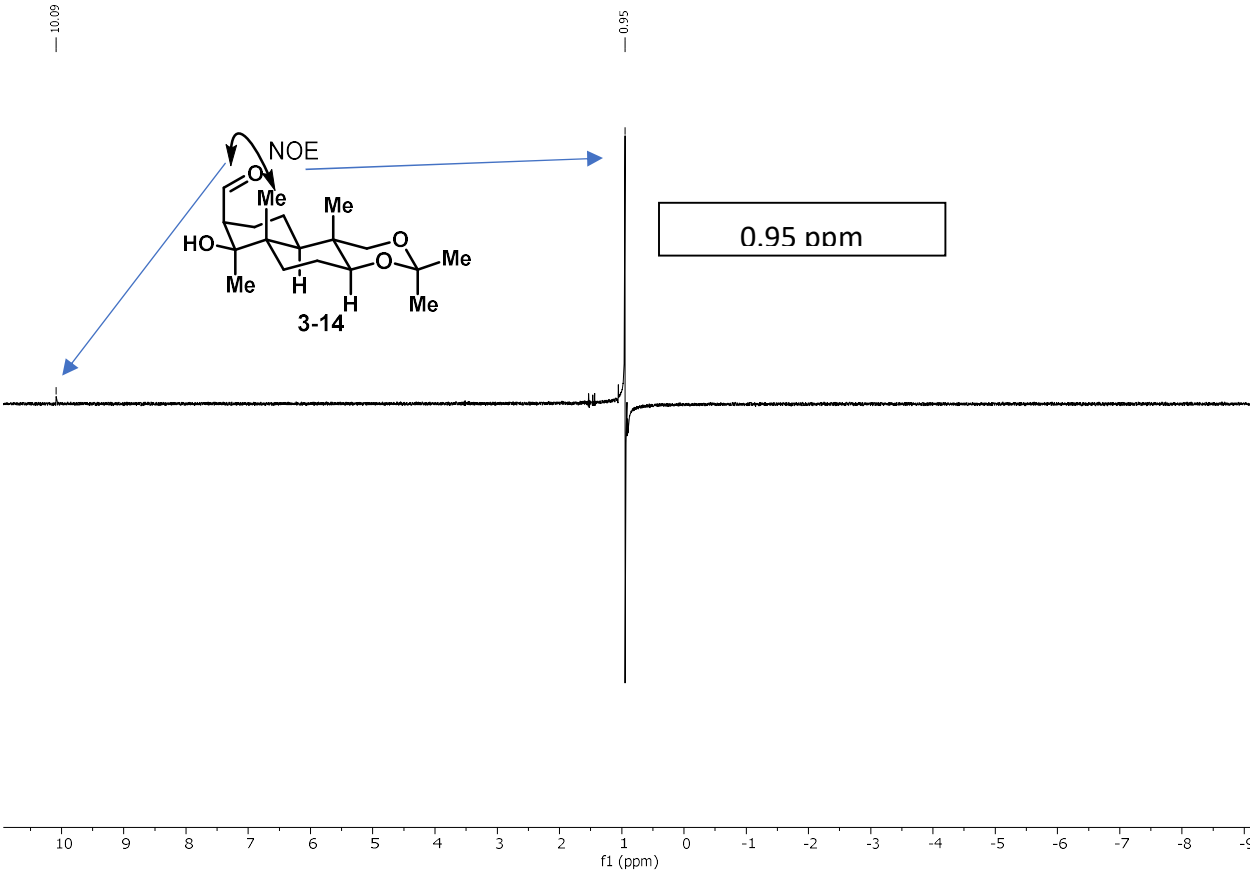
10.09
0.95
NOE
O
Me
Me
HO
O
Me
Me
H
O
H
Me
3-14
0.95 ppm
10
9
8
7
6
5
4
3
2
1
0
-1
-2
-3
-4
-5
-6
-7
-8
f1 (ppm)

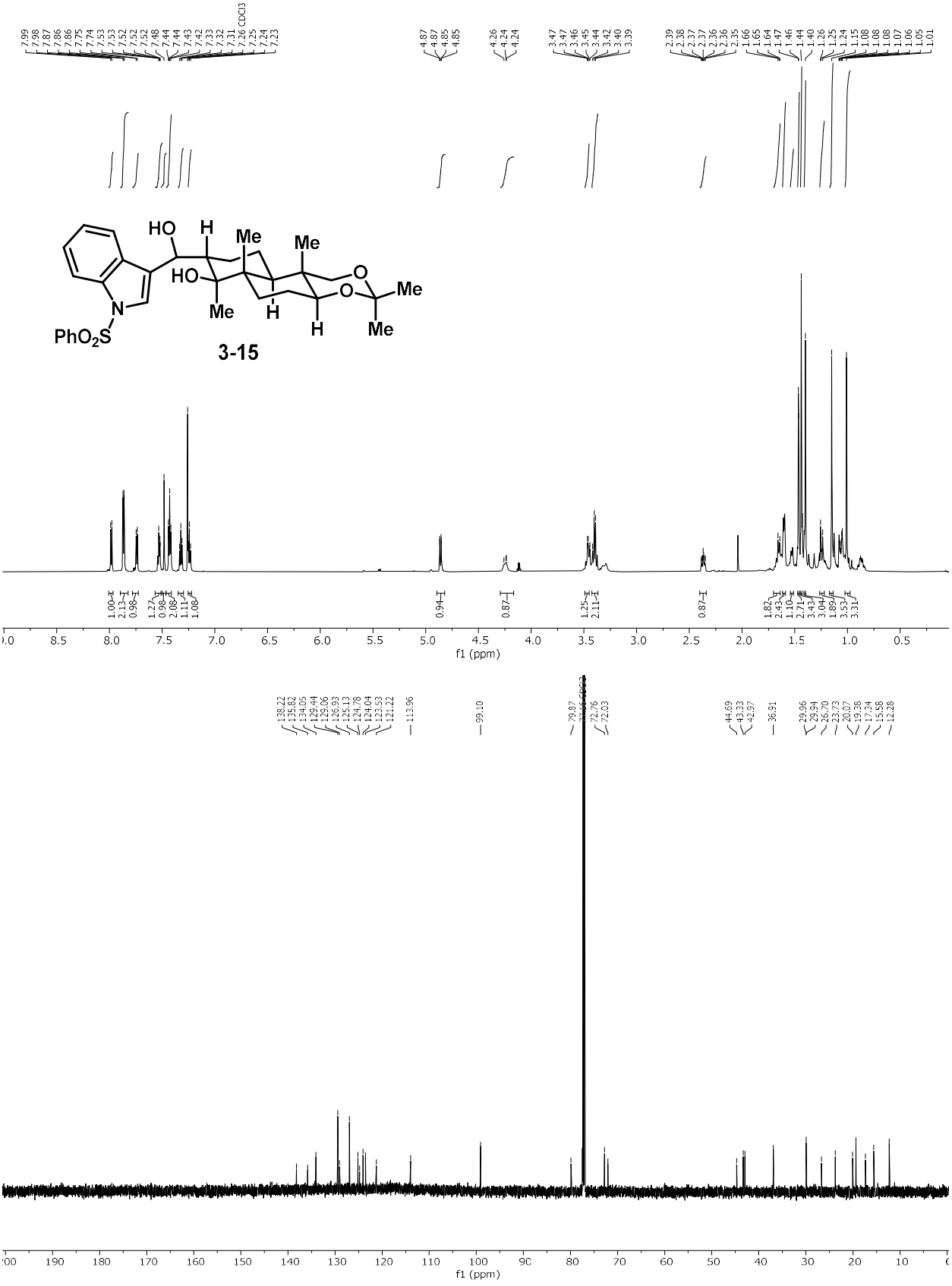
HO
H
Me
Me
HO
O
O
Me
Me
H
N
H
Me
PhO2S
3-15
f1 (ppm)
f1 (ppm)

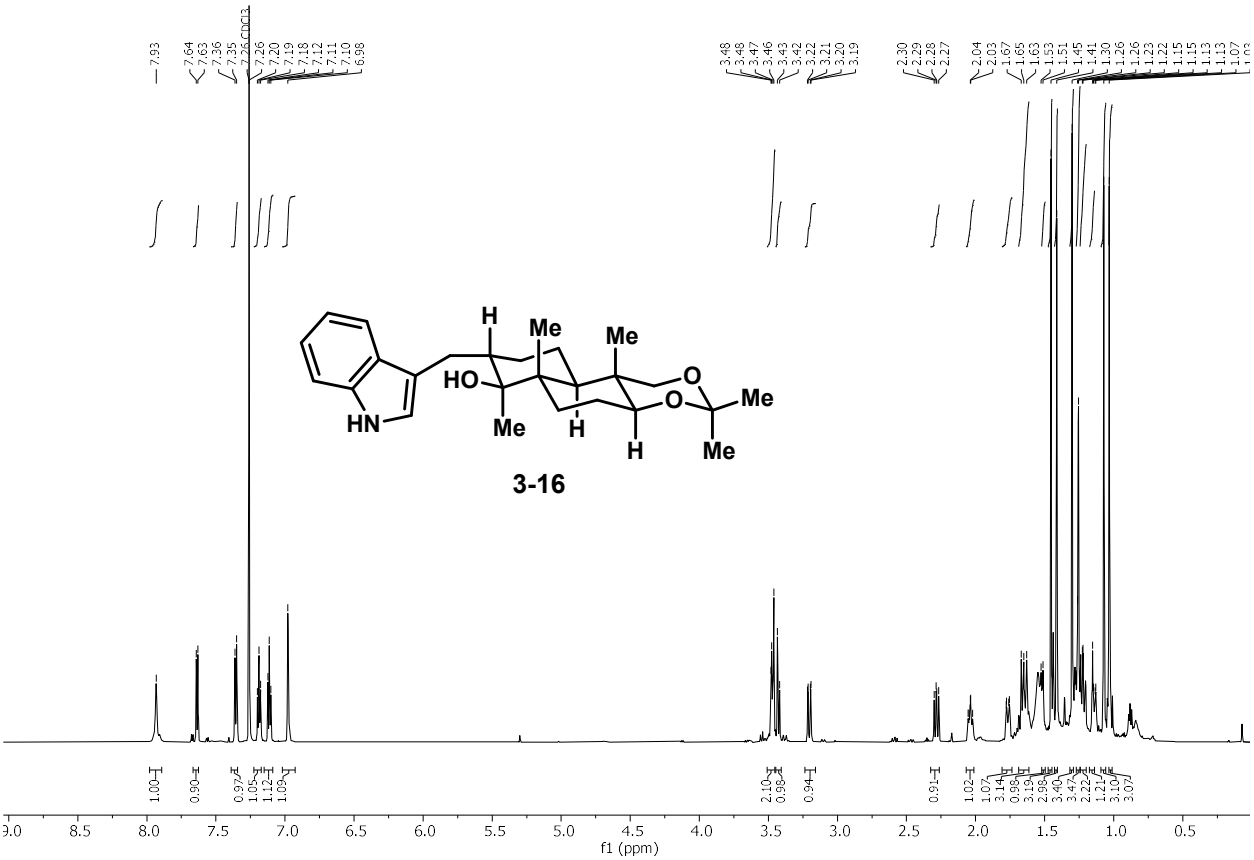
HO
HN
Me
O
H
3-16
f1 (ppm)

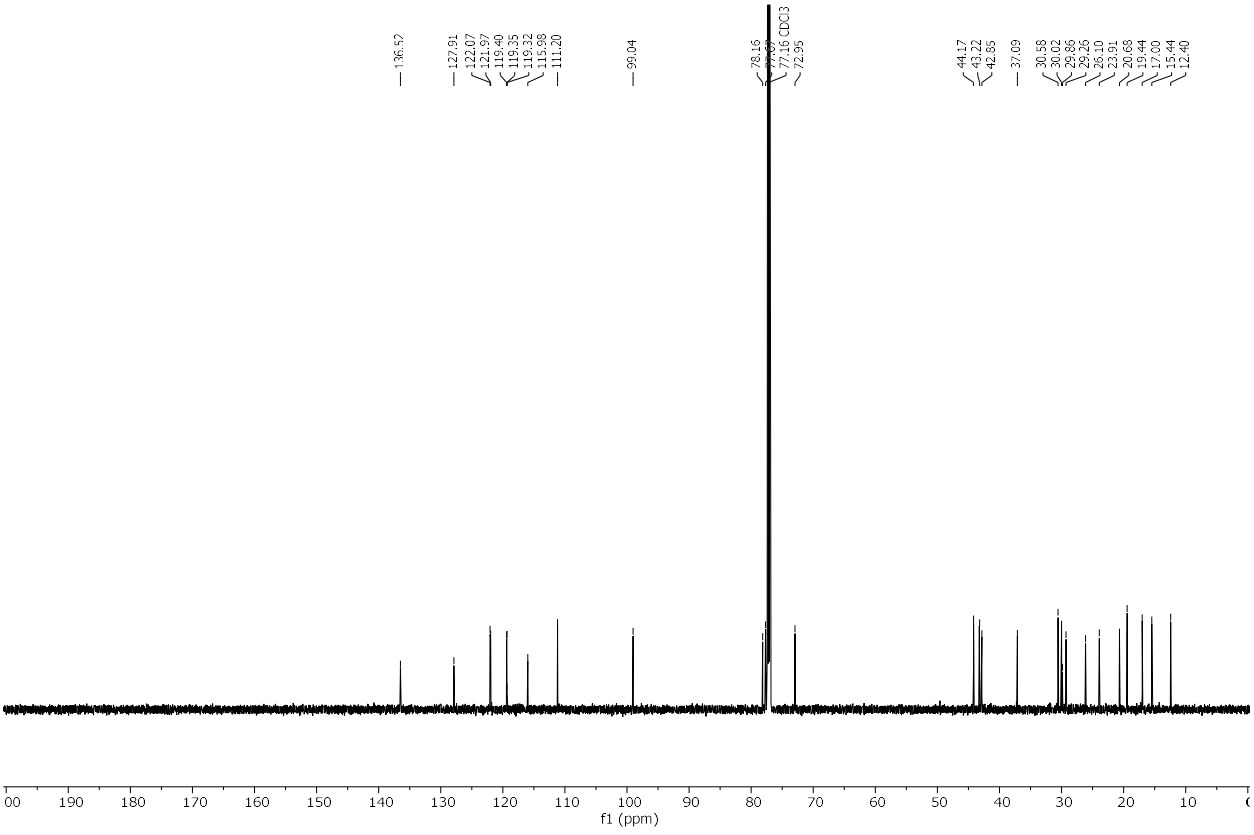
f1 (ppm)

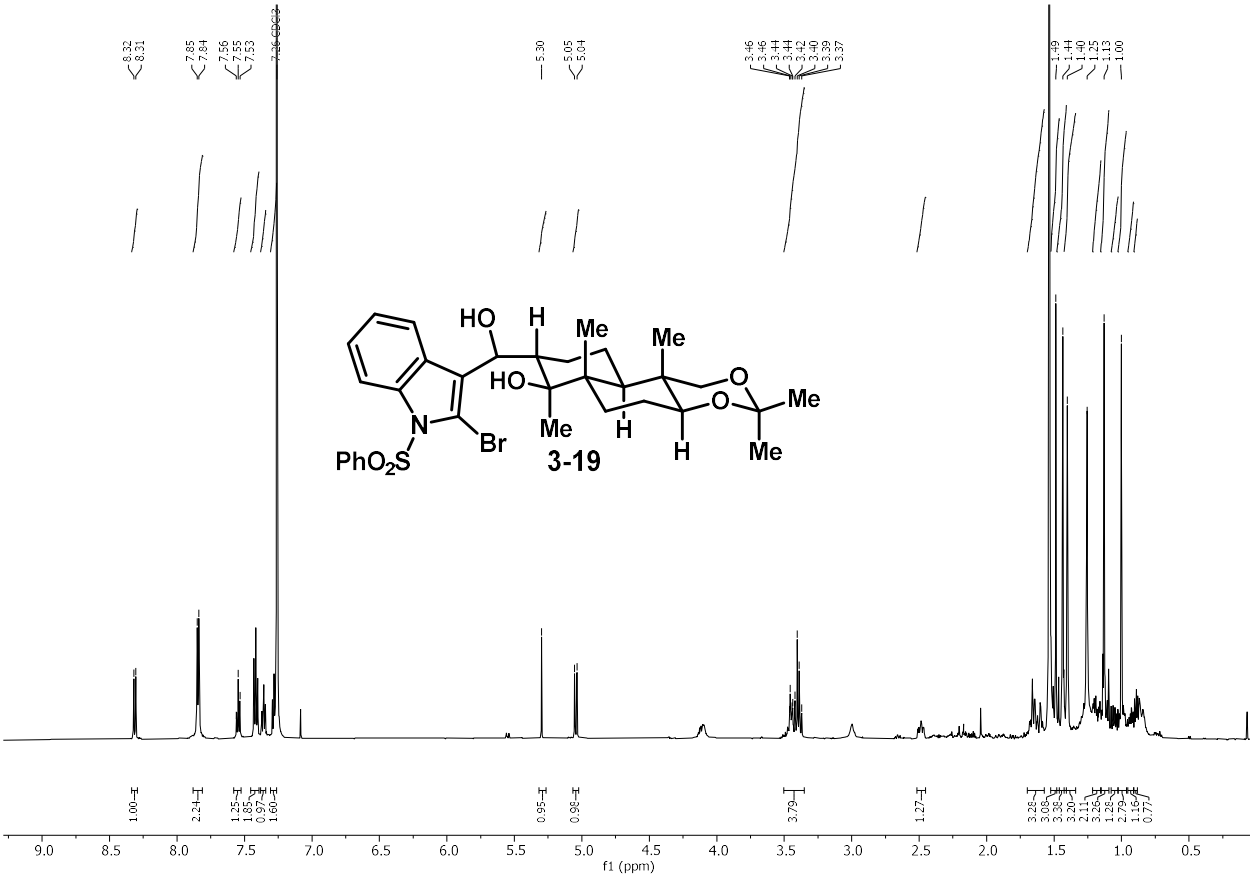
HO
H
Me
Me
HO
O
O
Me
N
Br
Me
H
H
Me
PhO2S
3-19
f1 (ppm)

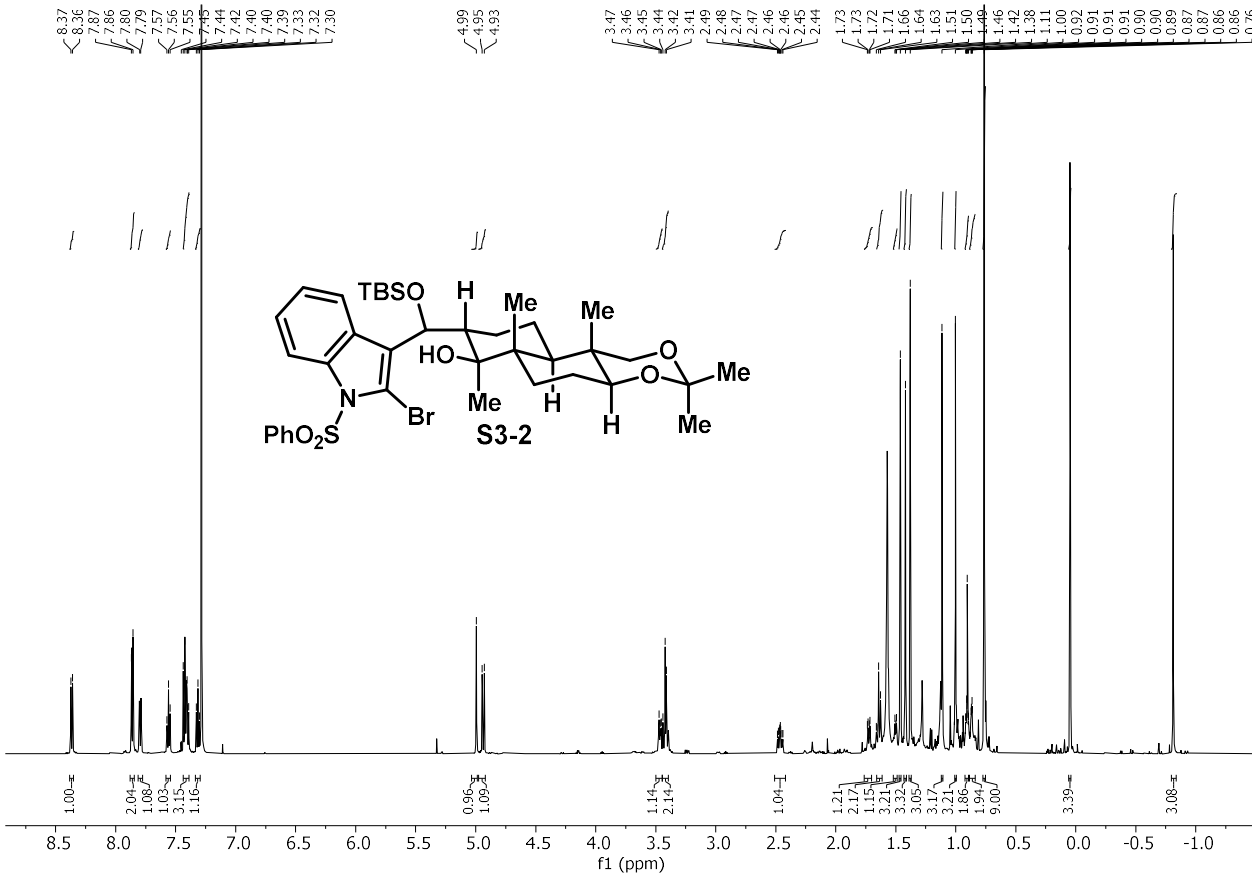
TBSO
H
Me
Me
HO
O
O
Me
N
Br
Me
H
H
Me
PhO2S
S3-2
f1 (ppm)

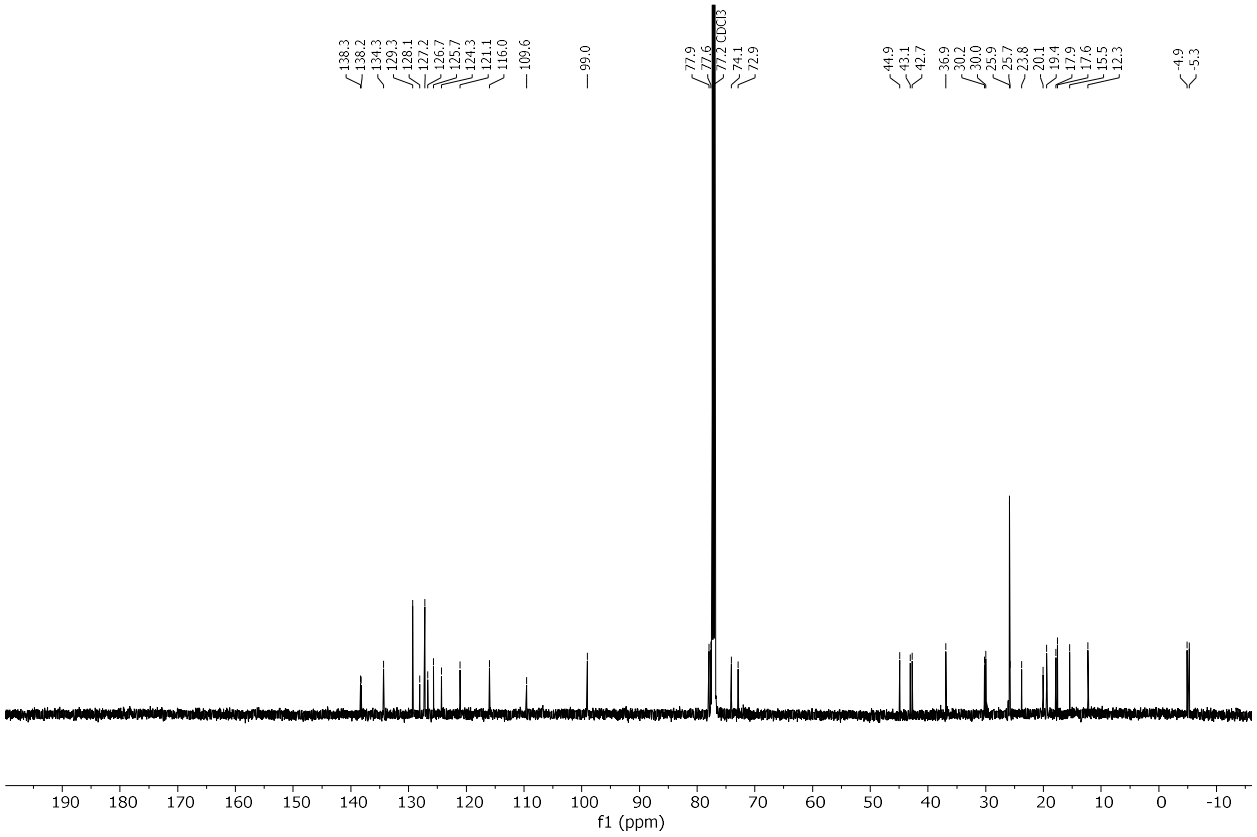
CDCl3
f1 (ppm)

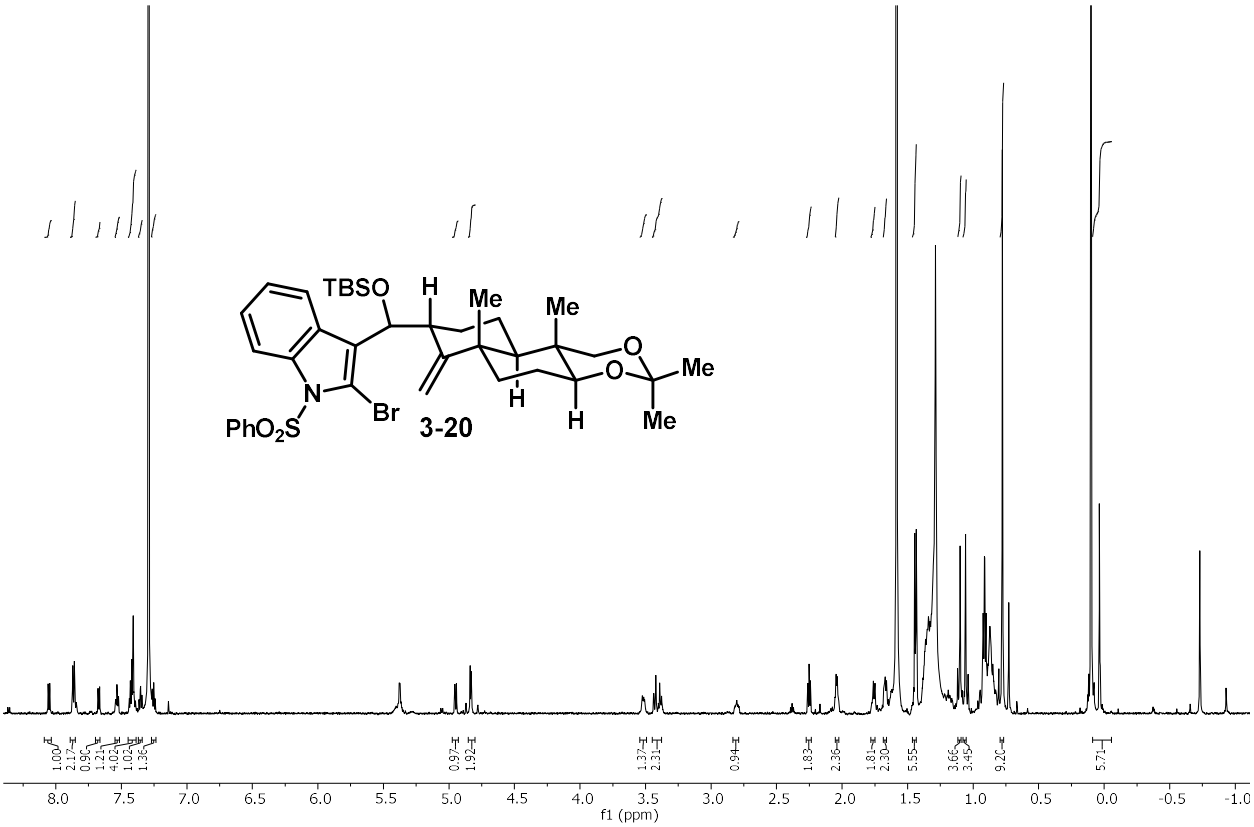
TBSO
H
Me
Me
O
O
Me
N
Br
PhO2S
H
H
Me
3-20
f1 (ppm)

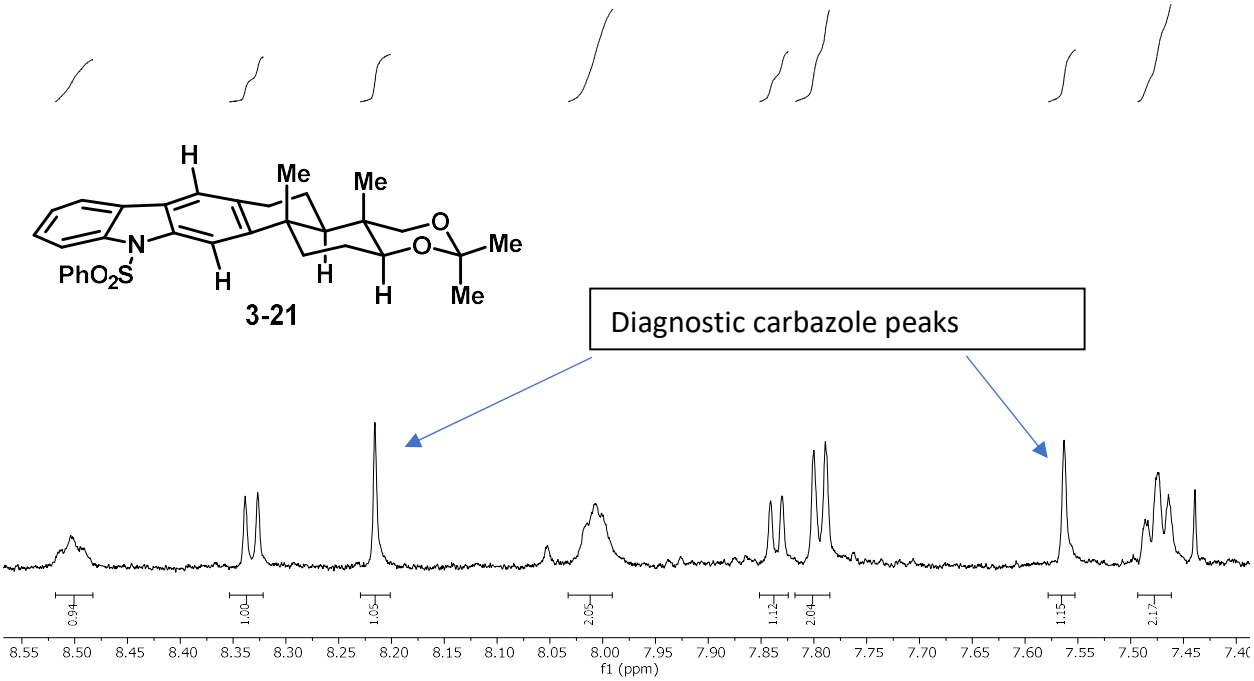
H
Me
Me
O
N
O
Me
PhO2S
H
H
H
Me
3-21
Diagnostic carbazole peaks
f1 (ppm)

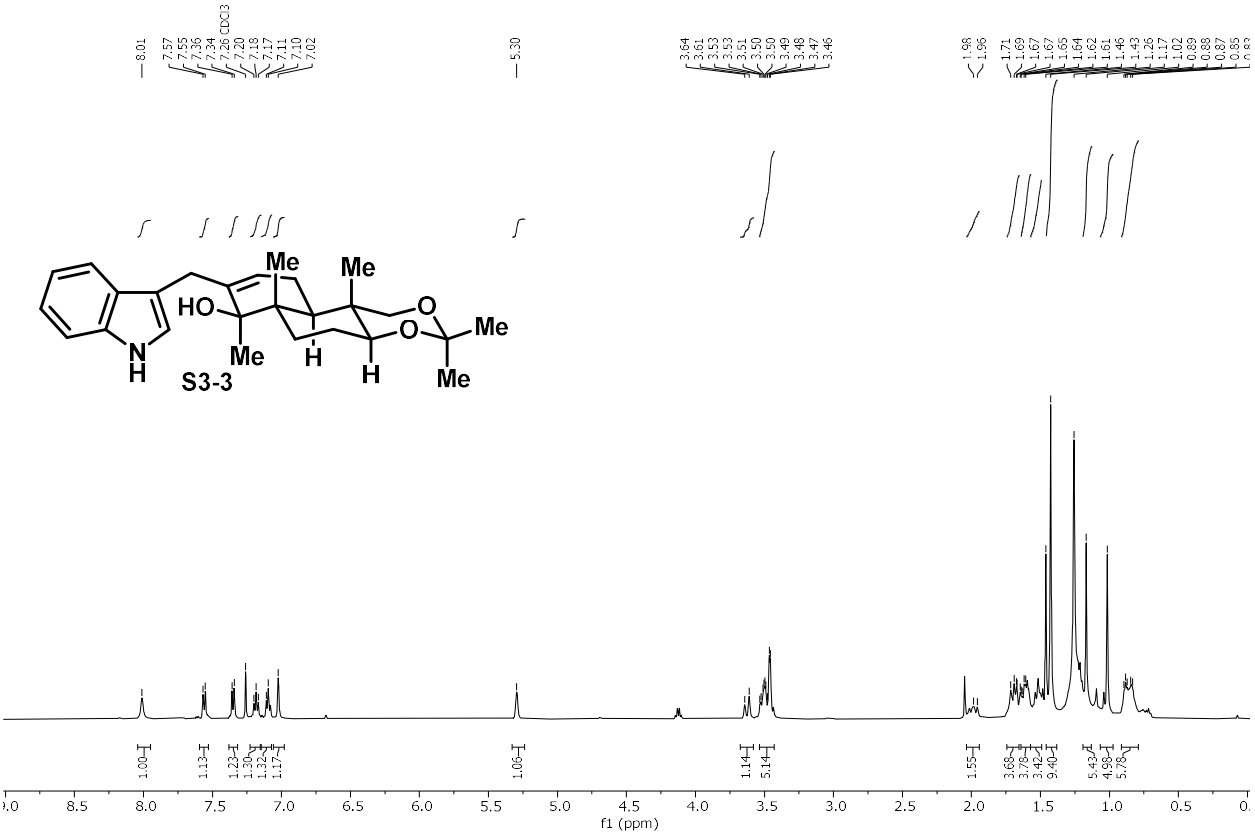
Me
Me
HO
O
O
Me
Me
H
H
Me
N
H
S3-3
f1 (ppm)

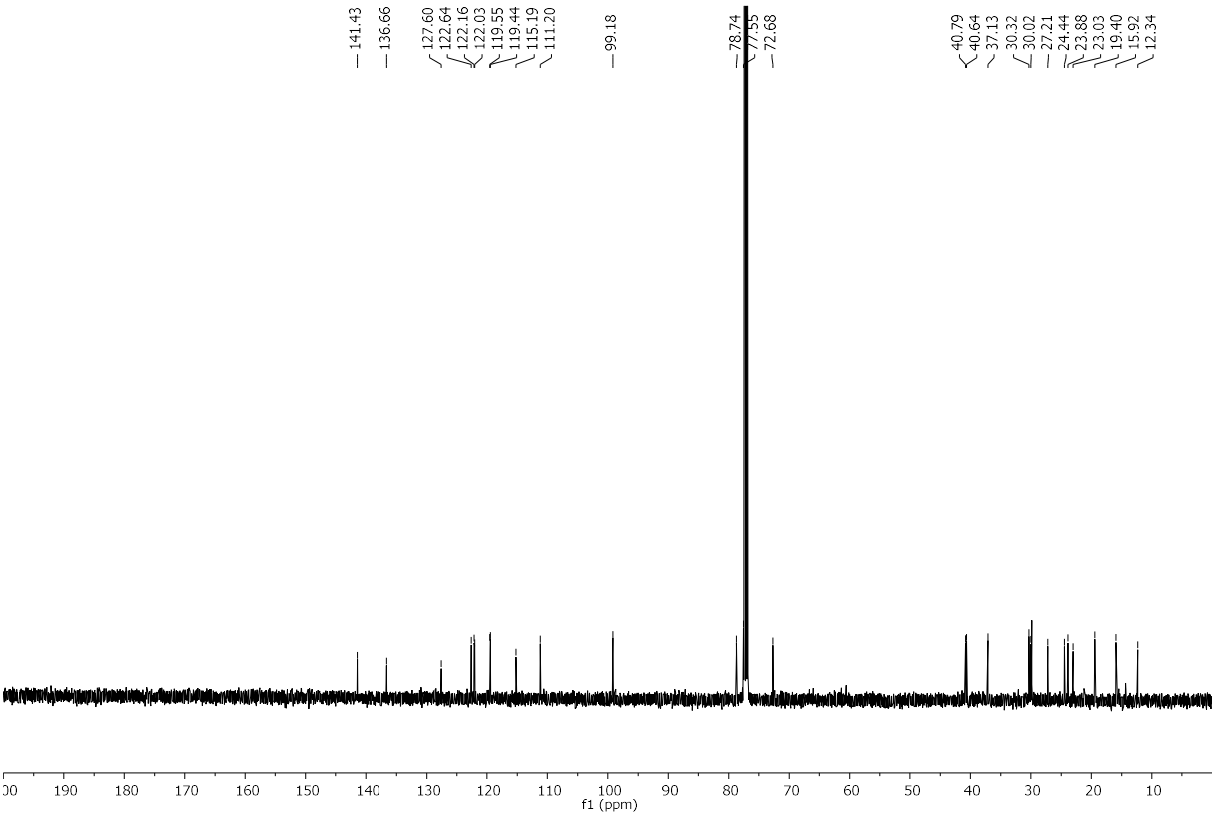
f1 (ppm)

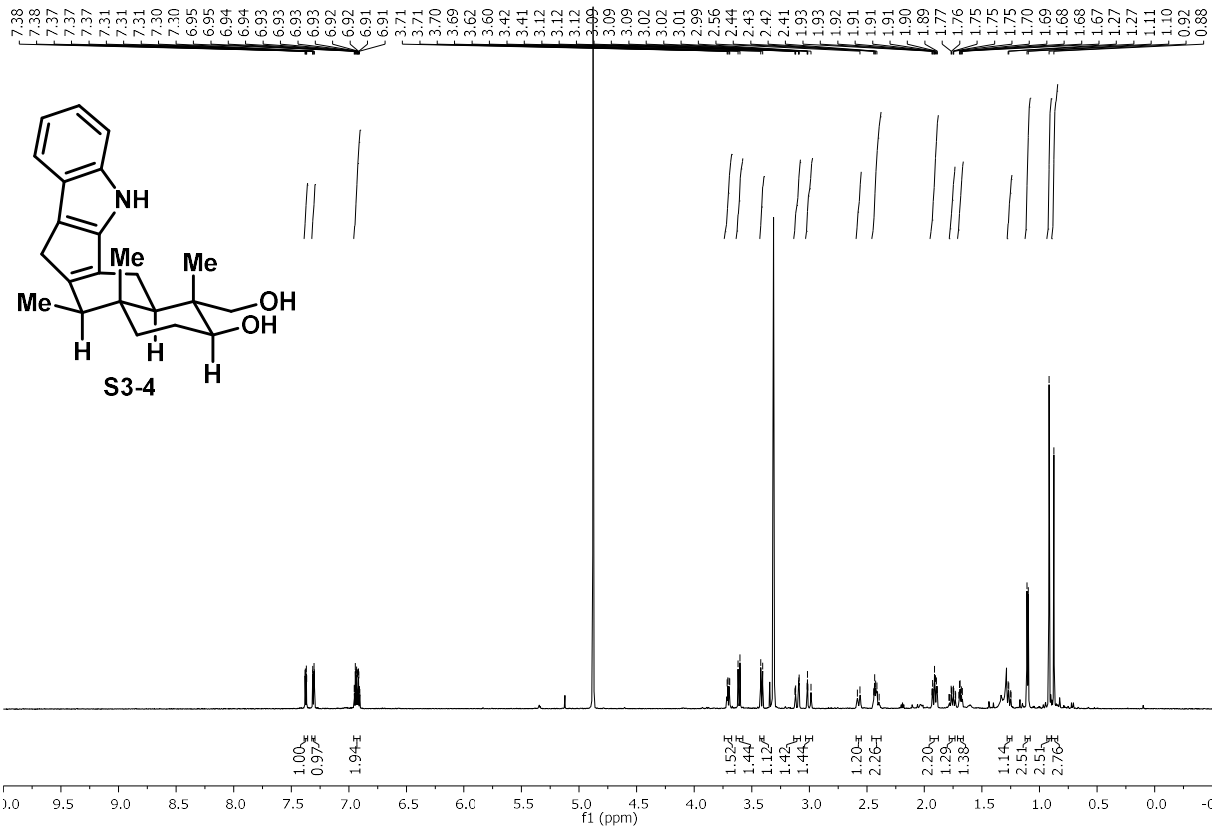
NH
Me
Me
Me
OH
OH
H
H
H
S3-4
f1 (ppm)

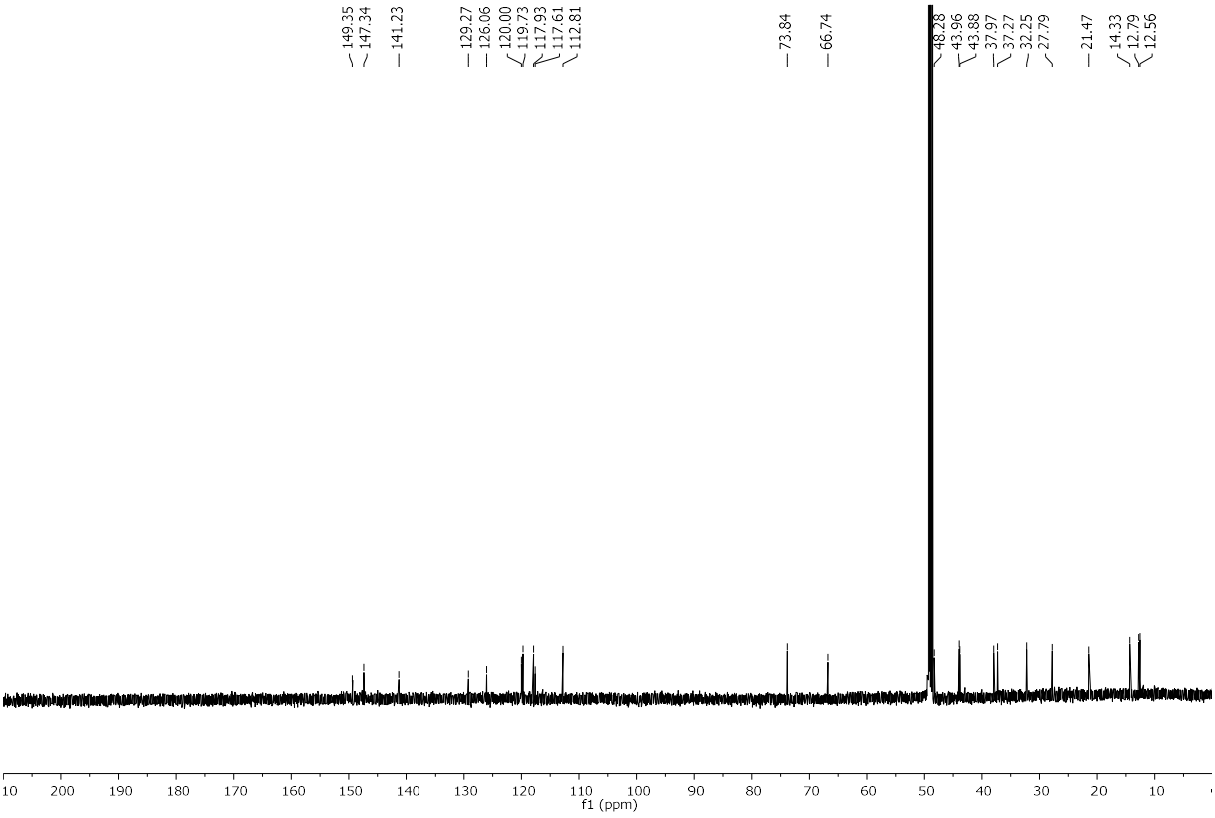
f1 (ppm)

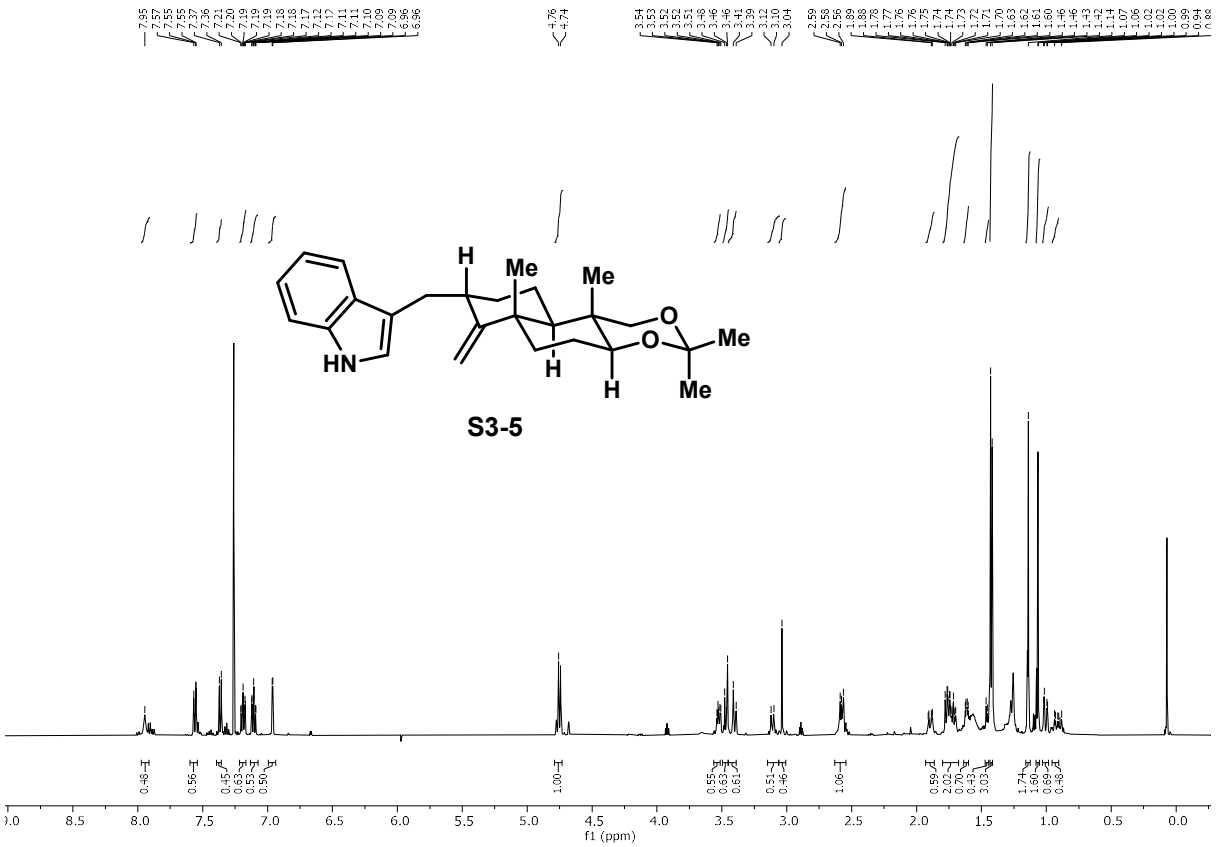
H
Me
Me
O
O
Me
HN
H
H
Me
f1 (ppm)

S3-5

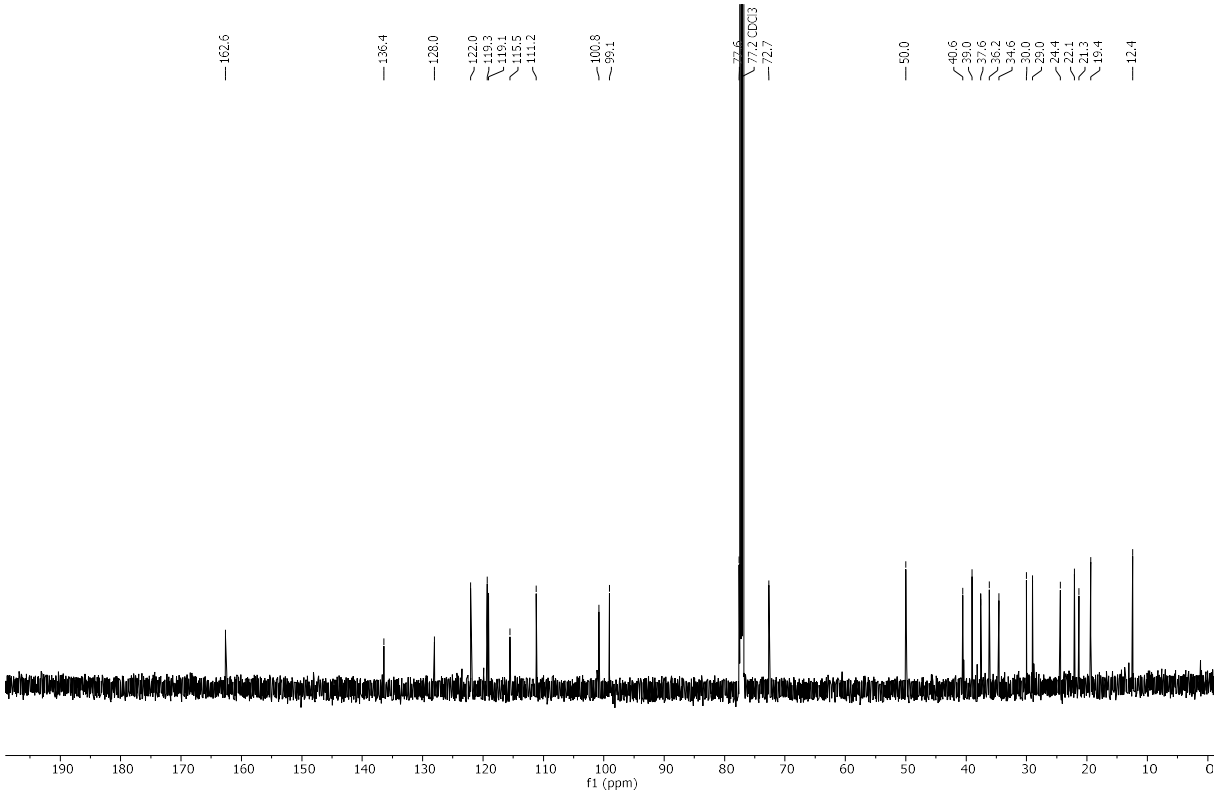
162.6
136.4
128.0
122.0
119.3
119.1
115.5
111.2
100.8
98.1
77.6
77.2 CDCl3
72.7
50.0
40.6
39.0
37.6
36.2
34.6
30.0
29.0
24.4
22.1
21.3
19.4
12.4
f1 (ppm)

3.5 References

(1) (a) Jones, S. B.; Simmons, B.; Mastracchio, A.; MacMillan, D. W. C. Collective Synthesis of Natural Products by Means of Organocascade Catalysis. *Nature* **2011**, *475*, 183–188. (b) Anagnostaki, E. E.; Zografos, A. L. "Common Synthetic Scaffolds" in the Synthesis of Structurally Diverse Natural Products. *Chem. Soc. Rev.* **2012**, *41*, 5613–5625. (c) Li, L.; Chen, Z.; Zhang, X.; Jia, Y. Divergent Strategy in Natural Product Total Synthesis. *Chem. Rev.* **2018**, *118*, 3752–3832. (d) Serba, C.; Winssinger, N. Following the Lead from Nature: Divergent Pathways in Natural Product Synthesis and Diversity-Oriented Synthesis. *Eur. J. Org. Chem.* **2013**, *2013*, 4195–4214.

(2) (a) Loiseleur, O. Natural Products in the Discovery of Agrochemicals. *CHIMIA* **2017**, *71*, 810–810. (b) Fones, H.; Gurr, S. The Impact of Septoria Tritici Blotch Disease on Wheat: An EU Perspective. *Fungal Genet. Biol.* **2015**, *79*, 3–7. (c) Poole, N. F.; Arnaudin, M. E. The Role of Fungicides for Effective Disease Management in Cereal Crops. *Can. J. Plant Pathol.* **2014**, *36*, 1–11.

(3) (a) Fueki, S.; Tokiwano, T.; Toshima, H.; Oikawa, H. Biosynthesis of Indole Diterpenes, Emindole, and Paxilline: Involvement of a Common Intermediate. *Org. Lett.* **2004**, *6*, 2697–2700. (b) Fehr, Th.; Acklin, W. Die Isolierung zweier neuartiger Indol-Derivate aus dem Mycel von Claviceps paspali. *Helv. Chim. Acta* **1966**, *49*, 1907–1910. (c)Munday-Finch, S. C.; Wilkins, A. L.; Miles, C. O. Isolation of Paspaline B, an Indole-Diterpenoid from Penicilium Paxilli. *Phytochemistry* **1996**, *41*, 327–332. (d) Springer, J. P.; Clardy, J. Paspaline and Paspalicine, Two Indole-Mevalonate Metabolites from Claviceps Paspali. *Tetrahedron Lett.* **1980**, *21*, 231–234. (e) Saikia, S.; Nicholson, M. J.; Young, C.; Parker, E. J.; Scott, B. The Genetic Basis for Indole-Diterpene Chemical Diversity in Filamentous Fungi. *Mycol. Res.* **2008**, *112*, 184–199. (f) Mantle, P. G. The Role of Tryptophan as a Biosynthetic Precursor of Indole-Diterpenoid Fungal Metabolites: Continuing a Debate. *Phytochemistry* **2009**, *70*, 7–10.

(4) A) Ding, L.; Maier, A.; Fiebig, H.-H.; Lin, W.-H.; Hertweck, C. A Family of Multicyclic Indolosesquiterpenes from a Bacterial Endophyte. *Org. Biomol. Chem.* **2011**, *9*, 4029–4031; B) Zhang, Q.; Li, H.; Yu, L.; Sun, Y.; Zhu, Y.; Zhu, H.; Zhang, L.; Li, S.-M.; Shen, Y.; Tian, C.; Li, A.; Liu, H.; Zhang, C. Characterization of the Flavoenzyme XiaK as an N-Hydroxylase and Implications in Indolosesquiterpene Diversification. *Chem. Sci.* **2017**, *8*, 5067–5077. (c) Ding, L.; Münch, J.; Goerls, H.; Maier, A.; Fiebig, H.-H.; Lin, W.-H.; Hertweck, C. Xiamycin, a Pentacyclic Indolosesquiterpene with Selective Anti-HIV Activity from a Bacterial Mangrove Endophyte. *Bioorg. Med. Chem. Lett.***2010**, *20*, 6685–6687.

(5) A) Shymanovich, T.; Saari, S.; Lovin, M. E.; Jarmusch, A. K.; Jarmusch, S. A.; Musso, A. M.; Charlton, N. D.; Young, C. A.; Cech, N. B.; Faeth, S. H. Alkaloid Variation Among Epichloid Endophytes of Sleepygrass (Achnatherum Robustum) and Consequences for Resistance to Insect

Herbivores. *J. Chem. Ecol.* **2015**, *41*, 93–104. (b) Shymanovich, T.; Faeth, S. H. Anti-Insect Defenses of Achnatherum Robustum (Sleepygrass) Provided by Two Epichloë Endophyte Species. *Entomol. Exp. Appl.* **2018**, *166*, 474–482. (c) Selala, M. I.; Daelemans, F.; Schepens, P. J. C. Fungal Tremorgens: The Mechanism Of Action Of Single Nitrogen Containing Toxins - A Hypothesis. *Drug Chem. Toxicol.* **1989**, *12*, 237–257. (d) Cole, R. J.; Dorner, J. W.; Lansden, J. A.; Cox, R. H.; Pape, C.; Cunfer, B.; Nicholson, S. S.; Bedell, D. M. Paspalum Staggers: Isolation and Identification of Tremorgenic Metabolites from Sclerotia of Claviceps Paspali. *J. Agric. Food Chem.* **1977**, *25*, 1197–1201. (e) Cole, R. J.; Dorner, J. W.; Lansden, J. A.; Cox, R. H.; Pape, C.; Cunfer, B.; Nicholson, S. S.; Bedell, D. M. Paspalum Staggers: Isolation and Identification of Tremorgenic Metabolites from Sclerotia of Claviceps Paspali. *J. Agric. Food Chem.* **1977**, *25*, 1197–1201. (f) Kozák, L.; Szilágyi, Z.; Tóth, L.; Pócsi, I.; Molnár, I. Tremorgenic and Neurotoxic Paspaline-Derived Indole-Diterpenes: Biosynthetic Diversity, Threats and Applications. *Appl Microbiol. Biotechnol.* **2019**, *103*, 1599–1616.

(6) Meng, Z.; Yu, H.; Li, L.; Tao, W.; Chen, H.; Wan, M.; Yang, P.; Edmonds, D. J.; Zhong, J.; Li, A. Total Synthesis and Antiviral Activity of Indolosesquiterpenoids from the Xiamycin and Oridamycin Families. *Nat. Commun.* **2015**, *6*, 6096.

(7) (a) Hong, B.; Luo, T.; Lei, X. Late-Stage Diversification of Natural Products. *ACS Cent. Sci.* **2020**, *6*, 622–635. (b) Kim, K. E.; Kim, A. N.; McCormick, C. J.; Stoltz, B. M. Late-Stage Diversification: A Motivating Force in Organic Synthesis. *J. Am. Chem. Soc.* **2021**, *143*, 16890–16901.

(8) Pfaffenbach, M.; Bakanas, I.; O'Connor, N. R.; Herrick, J. L.; Sarpong, R. Total Syntheses of Xiamycins A, C, F, H and Oridamycin A and Preliminary Evaluation of Their Anti-Fungal Properties. *Angew. Chem. Int. Ed.* **2019**, *58*, 15304–15308.

(9) (a) George, D. T.; Kuenstner, E. J.; Pronin, S. V. A Concise Approach to Paxilline Indole Diterpenes. *J. Am. Chem. Soc.* **2015**, *137*, 15410–15413. (b) Sharpe, R. J.; Johnson, J. S. A Global and Local Desymmetrization Approach to the Synthesis of Steroidal Alkaloids: Stereocontrolled Total Synthesis of Paspaline. *J. Am. Chem. Soc.* **2015**, *137*, 4968–4971. (c) Sharpe, R. J.; Johnson, J. S. Asymmetric Total Synthesis of the Indole Diterpene Alkaloid Paspaline. *J. Org. Chem.* **2015**, *80*, 9740–9766. (d) Smith, A. B. I.; Leenay, T. L. Indole Diterpene Synthetic Studies. 5. Development of a Unified Synthetic Strategy; a Stereocontrolled, Second-Generation Synthesis of (-)-Paspaline. *J. Am. Chem. Soc.* **1989**, *111*, 5761–5768. (e) Smith, A. B. I.; Mewshaw, R. Total Synthesis of (-)-Paspaline. *J. Am. Chem. Soc.* **1985**, *107*, 1769–1771. (f) Kim, D. E.; Zweig, J. E.; Newhouse, T. R. Total Synthesis of Paspaline A and Emindole PB Enabled by Computational Augmentation of a Transform-Guided Retrosynthetic Strategy. *J. Am. Chem. Soc.* **2019**, *141*, 1479–1483. Partial syntheses and related syntheses: (g) Churruca, F.; Fousteris, M.; Ishikawa, Y.; von Wantoch Rekowski, M.; Hounsou, C.; Surrey, T.; Giannis, A. A Novel Approach to Indoloditerpenes by Nazarov Photocyclization: Synthesis and Biological Investigations of Terpendole E Analogues. *Org. Lett.* **2010**, *12*, 2096–2099. (h) Oikawa, M.; Hashimoto, R.; Sasaki, M. Asymmetric Synthesis and in Vivo Biological Inactivity of the Right-Hand Terpenoid Fragment

of Terpendole E. *Eur. J. Org. Chem.* **2011**, *2011*, 538–546. l) Guo, L.-D.; Xu, Z.; Tong, R. Asymmetric Total Synthesis of Indole Diterpenes Paspalicine, Paspalinine, and Paspalinine-13-Ene. *Angew. Chem. Int. Ed*. **2022**, *61*, e202115384. (j) Isaka, T.; Hasegawa, M.; Toshima, H. Biomimetic Cyclization of Epoxide Precursors of Indole Mono-, Sesqui- and Diterpene Alkaloids by Lewis Acids. *Biosci. Biotechnol. Biochem.* **2011**, *75*, 2213–2222. (k) Schatz, D. J.; Li, W.; Pronin, S. V. Catalytic Enantioselective Conjugate Addition En Route to Paxilline Indoloterpenoids. *Tetrahedron* **2019**, *75*, 3361–3365. (l) Smith, A. B.; Kürti, L.; Davulcu, A. H.; Cho, Y. S. Development of a Scalable Synthesis of a Common Eastern Tricyclic Lactone for Construction of the Nodulisporic Acids. *Org. Process Res. Dev.* **2007**, *11*, 19–24. (m) Smith, A. B.; Kürti, L.; Davulcu, A. H.; Cho, Y. S.; Ohmoto, K. Indole Diterpene Synthetic Studies: Development of a Second-Generation Synthetic Strategy for (+)-Nodulisporic Acids A and B. *J. Org. Chem.* **2007**, *72*, 4611–4620. (n) Smith, A. B.; Davulcu, A. H.; Cho, Y. S.; Ohmoto, K.; Kürti, L.; Ishiyama, H. Indole Diterpene Synthetic Studies. Total Synthesis of (+)-Nodulisporic Acid F and Construction of the Heptacyclic Cores of (+)-Nodulisporic Acids A and B and (−)-Nodulisporic Acid D. *J. Org. Chem.* **2007**, *72*, 4596–4610. (o) Smith, A. B.; Davulcu, A. H.; Kürti, L. Indole Diterpenoid Synthetic Studies. The Total Synthesis of (+)-Nodulisporic Acid F. *Org. Lett.* **2006**, *8*, 1665–1668. (p) Clark, J. S.; Myatt, J.; Roberts, L.; Walshe, N. Investigation of the Biomimetic Synthesis of Emindole SB Using a Fluorinated Polyene Cyclisation Precursor. *Synlett* **2005**, No. 4, 697–699. (q) Rainier, J. D.; Smith, A. B. Polyene Cyclizations to Indole Diterpenes. The First Synthesis of (+)-Emindole SA Using a Biomimetic Approach. *Tetrahedron Lett.* **2000**, *41*, 9419–9423. (r) Adachi, M.; Higuchi, K.; Thasana, N.; Yamada, H.; Nishikawa, T. Stereocontrolled Synthesis of an Indole Moiety of Sespendole and Stereochemical Assignment of the Side Chain. *Org. Lett.* **2012**, *14*, 114–117. (s) Teranishi, T.; Murokawa, T.; Enomoto, M.; Kuwahara, S. Synthesis of (±)-Terpendole E. *Biosci. Biotechnol. Biochem.* **2015**, *79*, 11–15. (t) Tokuyama, H.; Okano, K.; Yoshii, Y. Synthetic Studies on Paspaline: Lewis Acid-Mediated Sequential Construction of A-E Ring Skeleton. *Heterocycles* **2012**, *84*, 1325. (u) Guile, S. D.; Saxton, J. E.; Thornton-Pett, M. Synthetic Studies towards Paspalicine. Part 2. An Alternative Approach to the Synthesis of the C/D Ring System. *J. Chem. Soc., Perkin Trans. 1* **1992**, No. 14, 1763–1767. (v) Smith, A. B.; Sunazuka, T.; Leenay, T. L.; Kingery-Wood, J. Total Syntheses of (+)-Paspalicine and (+)-Paspalinine. *J. Am. Chem. Soc.* **1990**, *112*, 8197–8198. (w) Smith, A. B.; Cui, H. Total Synthesis of (−)-21-Isopentenylpaxilline. *Org. Lett.* **2003**, *5*, 587–590. (x) Zou, Y.; Melvin, J. E.; Gonzales, S. S.; Spafford, M. J.; Smith, A. B. I. Total Synthesis of (−)-Nodulisporic Acid D. *J. Am. Chem. Soc.* **2015**, *137*, 7095–7098. (y) Zou, Y.; Li, X.; Yang, Y.; Berritt, S.; Melvin, J.; Gonzales, S.; Spafford, M.; Smith, A. B. I. Total Synthesis of (−)-Nodulisporic Acids D, C, and B: Evolution of a Unified Synthetic Strategy. *J. Am. Chem. Soc.* **2018**, *140*, 9502–9511. (z) Hauser, N.; Imhof, M. A.; Eichenberger, S. S.; Kündig, T.; Carreira, E. M. Total Synthesis of Shearinines D and G: A Convergent Approach to Indole Diterpenoids. *Angew. Chem. Int. Ed.* **2022**, *61*, e202112838. (aa) Enomoto, M.; Morita, A.; Kuwahara, S. Total Synthesis of the Tremorgenic Indole Diterpene Paspalinine. *Angew. Chem. Int. Ed.* **2012**, *51*, 12833–12836l. (ab) Hayakawa, I.; Matsumaru, N.; Sakakura, A. Toward the Synthesis of Paspaline-Type Indole-Terpenes: Stereoselective Construction of Core Scaffold with Contiguous Asymmetric Quaternary Carbon Centers. *J. Org. Chem.* **2021**, *86*, 9802–9810. (ac) Ali, A.; Saxton, J. E. Towards Paspalicine :

Synthesis of Rings D-G. *Tetrahedron Lett.* **1989**, *30*, 3197–3200. (ad) Smith, A. B.; Kanoh, N.; Ishiyama, H.; Minakawa, N.; Rainier, J. D.; Hartz, R. A.; Cho, Y. S.; Cui, H.; Moser, W. H. Tremorgenic Indole Alkaloids. The Total Synthesis of (−)-Penitrem D. *J. Am. Chem. Soc.* **2003**, *125*, 8228–8237.

(10) (a) Dethe, D. H.; Shukla, M. Enantioselective First Total Syntheses of the Antiviral Natural Products Xiamycins D and E. *Chem. Commun.* **2021**, *57*, 10644–10646. (b) Feng, J.; Noack, F.; Krische, M. J. Modular Terpenoid Construction via Catalytic Enantioselective Formation of All-Carbon Quaternary Centers: Total Synthesis of Oridamycin A, Triptoquinones B and C, and Isoiresin. *J. Am. Chem. Soc.* **2016**, *138*, 12364–12367. (c) Rosen, B. R.; Werner, E. W.; O'Brien, A. G.; Baran, P. S. Total Synthesis of Dixiamycin B by Electrochemical Oxidation. *J. Am. Chem. Soc.* **2014**, *136*, 5571–5574. (d) Trotta, A. H. Total Synthesis of Oridamycins A and B. *Org. Lett.* **2015**, *17*, 3358–3361. E) Trotta, A. H. Toward a Unified Total Synthesis of the Xiamycin and Oridamycin Families of Indolosesquiterpenes. *J. Org. Chem.* **2017**, *82*, 13500–13516.

(11) (a)Leger, P. R.; Kuroda, Y.; Chang, S.; Jurczyk, J.; Sarpong, R. C–C Bond Cleavage Approach to Complex Terpenoids: Development of a Unified Total Synthesis of the Phomactins. *J. Am. Chem. Soc.* **2020**, *142*, 15536–15547. (b) Lusi, R. F.; Perea, M. A.; Sarpong, R. C–C Bond Cleavage of α-Pinene Derivatives Prepared from Carvone as a General Strategy for Complex Molecule Synthesis. *Acc. Chem. Res.* **2022**, *55*, 746–758. (c) Weber, M.; Owens, K.; Masarwa, A.; Sarpong, R. Construction of Enantiopure Taxoid and Natural Product-like Scaffolds Using a C–C Bond Cleavage/Arylation Reaction. *Org. Lett.* **2015**, *17*, 5432–5435. (d) Na, C. G.; Kang, S. H.; Sarpong, R. Development of a C–C Bond Cleavage/Vinylation/Mizoroki–Heck Cascade Reaction: Application to the Total Synthesis of 14- and 15-Hydroxypatchoulol. *J. Am. Chem. Soc.* **2022**, *144*, 19253–19257. (e) Nagasawa, S.; Jones, K. E.; Sarpong, R. Enantiospecific Entry to a Common Decalin Intermediate for the Syntheses of Highly Oxygenated Terpenoids. *J. Org. Chem.* **2019**, *84*, 12209–12215. (f) Perea, M. A.; Wang, B.; Wyler, B. C.; Ham, J. S.; O'Connor, N. R.; Nagasawa, S.; Kimura, Y.; Manske, C.; Scherübl, M.; Nguyen, J. M.; Sarpong, R. General Synthetic Approach to Diverse Taxane Cores. *J. Am. Chem. Soc.* **2022**. (g) Kuroda, Y.; Nicacio, K. J.; da Silva-Jr, I. A.; Leger, P. R.; Chang, S.; Gubiani, J. R.; Deflon, V. M.; Nagashima, N.; Rode, A.; Blackford, K.; Ferreira, A. G.; Sette, L. D.; Williams, D. E.; Andersen, R. J.; Jancar, S.; Berlinck, R. G. S.; Sarpong, R. Isolation, Synthesis and Bioactivity Studies of Phomactin Terpenoids. *Nat. Chem.* **2018**, *10*, 938–945. (h) Blümel, M.; Nagasawa, S.; Blackford, K.; Hare, S. R.; Tantillo, D. J.; Sarpong, R. Rearrangement of Hydroxylated Pinene Derivatives to Fenchone-Type Frameworks: Computational Evidence for Dynamically-Controlled Selectivity. *J. Am. Chem. Soc.* **2018**, *140*, 9291–9298. (i) Masarwa, A.; Weber, M.; Sarpong, R. Selective C–C and C–H Bond Activation/Cleavage of Pinene Derivatives: Synthesis of Enantiopure Cyclohexenone Scaffolds and Mechanistic Insights. *J. Am. Chem. Soc.* **2015**, *137*, 6327–6334; J) Lusi, R. F.; Sennari, G.; Sarpong, R. Strategy Evolution in a Skeletal Remodeling and C–H Functionalization-Based Synthesis of the Longiborneol Sesquiterpenoids. *J. Am. Chem. Soc.* **2022**, *144*, 17277–17294. (k) Kerschgens, I.; Rovira, A. R.; Sarpong, R. Total Synthesis of (−)-Xishacorene B from (R)-Carvone Using a C–C Activation Strategy. *J. Am. Chem. Soc.* **2018**, *140*, 9810–9813. (l) Lusi, R. F.; Sennari, G.; Sarpong, R. Total Synthesis of Nine

Longiborneol Sesquiterpenoids Using a Functionalized Camphor Strategy. *Nat. Chem.* **2022**, *14*, 450–456. (m) Finkbeiner, P.; Murai, K.; Röpke, M.; Sarpong, R. Total Synthesis of Terpenoids Employing a "Benzannulation of Carvone" Strategy: Synthesis of (−)-Crotogoudin. *J. Am. Chem. Soc.* **2017**, *139*, 11349–11352.

(12) Odani, A.; Ishihara, K.; Ohtawa, M.; Tomoda, H.; Omura, S.; Nagamitsu, T. Total Synthesis of Pyripyropene A. *Tetrahedron* **2011**, *67*, 8195–8203.

(13) Saksena, A. K.; Mangiaracina, P. Recent Studies on Veratrum Alkaloids: A New Reaction of Sodium Triacetoxyborohydride [NaBH(OAc)3]. *Tetrahedron Lett.* **1983**, *24*, 273–276.

(14) Ariantari, N. P.; Ancheeva, E.; Wang, C.; Mándi, A.; Knedel, T.-O.; Kurtán, T.; Chaidir, C.; Müller, W. E. G.; Kassack, M. U.; Janiak, C.; Daletos, G.; Proksch, P. Indole Diterpenoids from an Endophytic Penicillium Sp. *J. Nat. Prod.* **2019**, *82*, 1412–1423.

(15) Aldehyde **3-4** was prepared according to Pfaffenbach, M.; Bakanas, I.; O'Connor, N. R.; Herrick, J. L.; Sarpong, R. Total Syntheses of Xiamycins A, C, F, H and Oridamycin A and Preliminary Evaluation of Their Anti-Fungal Properties. *Angew. Chem. Int. Ed.* **2019**, *58*, 15304–15308. (also Chapter 2 experimental)

(16) Abbiati, G.; Canevari, V.; Rossi, E.; Ruggeri, A. Facile and Inexpensive Entry to Indeno[2,1-b]Indol-6-one Nucleus. *Synth. Commun.* **2005**, *35*, 1845–1850.

(17) Liu, Y.; Gribble, G. W. Bis-Suzuki Reactions of 2,3-Dihaloindoles. A Convenient Synthesis of 2,3-Diarylindoles. *Tetrahedron Lett.* **2000**, *41*, 8717–8721.

3.6 Experimental contributors

This chapter includes content reproduced, with permission, from: Bakanas, I., Pfaffenbach, M., Miaskewicz, S. O'Connor, Sarpong, R. Progress Toward a Unified Syntheses of Paspaline-type Indole Diterpenoids and Xiamycin-type Indolosesquiterpenoids Initial experimental work performed by M.P. and N.R.O, family synthesis performed by I.B. and S.M. written by I.B. with guidance from R. S.

Chapter 4
Symmetry Strategies and Tactics in Synthesis

4.1 Introduction

Natural product total synthesis has been described as not only a precise science, but a fine art as well.[1] The complex structures of natural products and the methods for their construction have drawn interest and comparisons to architecture and other beautiful human-made constructions.[2] The art of synthesis planning also shares elements with that of classical games, like chess, comprising elements of strategies and tactics.[3] To solve problems in chemical synthesis we look for *tactics* that lead to success in each step—not on a chess board but in the bonds and atoms of our molecule—and we are inspired by tactics used previously in the literature. This contrasts with *strategies* which are planned from the outset and are broader in scope. Though sometimes used interchangeably in the literature, tactics and strategies are distinct but intertwined and using definitions from the chess literature they can be defined as follows:

Strategy *the overall objectives of a player, which [they] will attempt to carry out throughout the game…The extent to which this overall plan will be carried out will depend upon the strength of resistance and the existence of any opportunities arising in the short term*

Tactics *maneuvers to take advantage of opportunities arising in the short term... they gain immediate advantage if correct .*[4]

Classically, strategies in synthesis are displayed in retrosynthesis planning (Figure 4-1A): bond network analysis to guide disconnections,[5] fragment recognition (find-the-carvone strategies that our laboratory has pursued),[6] two-phase synthesis,[7] bioinspired synthesis,[8] and hidden symmetry recognitions[9] to name a few are all tried and tested synthetic strategies. The possibilities in retrosynthesis planning are myriad, and a good strategy allows one to cut through the noise and select the most effective disconnections.

Tactics are less obvious in their comparison to chess for the simple reason that synthesis is an experimental science. Whilst in chess one can guarantee a checkmate in 3, in the laboratory it is not possible to know if a new reaction will work. One exception, however, is intercepting a previous synthesis to complete a formal synthesis, much like hitting upon a known checkmate sequence, this is the exact set of moves that will take one to the target. We can recognize the simplifying nature of this tactic, why solve the endgame when you can utilize a prescribed set of guaranteed moves? Suffice to say there are many tactics in synthesis, including, but not limited to, directed C–H oxidation,[10] protecting group manipulation,[11] and use of chiral auxiliaries (Figure 4-1B).[12]

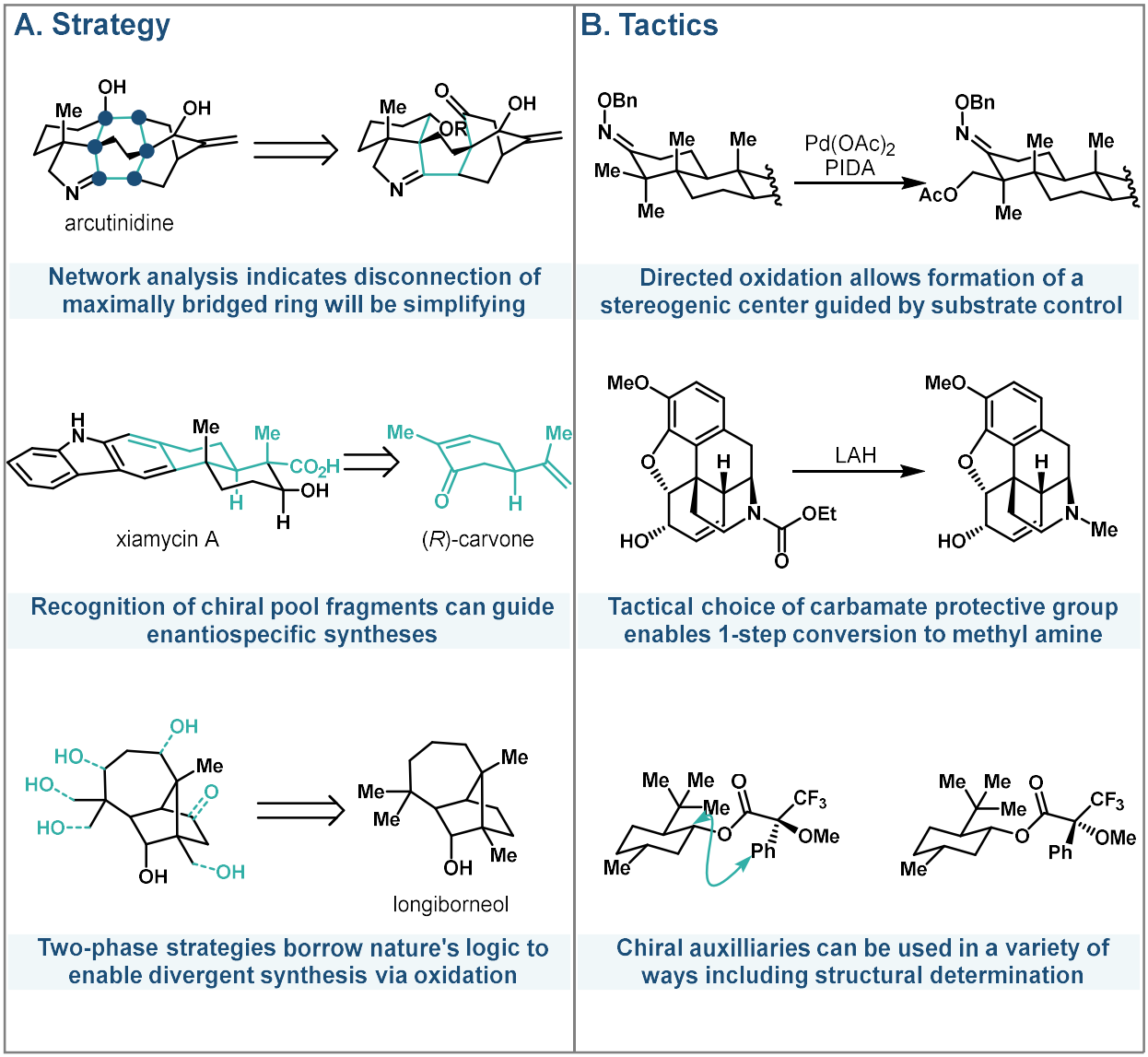

Figure 4.1 A. Examples of strategies in natural product synthesis. **B.** Examples of tactics

One key interest of my doctoral studies has been the use of symmetry in synthesis, which as discussed above, is a classic strategy. However, the exploitation of symmetry is also present in synthesis tactics and can be helpful when navigating a synthesis campaign. This chapter aims to highlight syntheses where recognition of symmetry guides the major disconnections (strategy) and where it is employed to solve a specific problem in the synthesis (tactics). Through analysis and discussion, I hope to illuminate the different use-cases of symmetry and help guide future synthesis planning. The highlighted examples are all recent, however, the reader is directed toward the synthesis of paspaline from Johnson and coworkers where they define “local” and “global” desymmetrization methods.[13] This classification was an inspiration for the following discussion.

4.2 A showcase of strategy: Sarpong total synthesis of delavatine A

Finding hidden symmetry elements within a natural product can be greatly simplifying, especially when combined with other strategies. In their total synthesis of delavatine A (Scheme 4.1, **4-1**),[14] Sarpong and coworkers retrosynthetically disconnected this tetracyclic alkaloid back to its biosynthetic precursor, trialdehyde **4-2**. The benzenoid core of **4-2** is flanked by two 5-membered rings bearing a stereogenic methyl group but differing in connectivity. The key recognition was that these fragments could result from the same precursors—an element of functional group symmetry. Thus **4-2** could be formed from 3,5-biscoupled pyrone **4-3** through a ring opening 6π-electrocyclization cascade. Notably, pyrone **4-3** contains this effective element of symmetry about the central axis of the pyrone, thus **4-3** could be taken back to 3,5-dibromopyrone (**4-4**) and nucleophilic coupling partners **4-5**, which would allow for rapid build-up of the system.

The synthesis commenced from 3,5-dibromopyrone (Scheme 4.1B **4-4**) which underwent sequential positional selective cross-coupling[15] with fragment **4-6** to give intermediate **4-7**, followed by coupling with **4-8** (**4-6** and **4-8** were each derived from pulegone[16] with differing oxidation states for ease of downstream reactions). In the same pot, they added NaCN to ring-open the pyrone and then MeI to give methylated adduct **4-9** in 32% yield. Remarkably, this introduces all of the carbons of the natural product in a single pot, and 14 of those carbons are derived from the same feedstock owing to their recognition of symmetry. The key 6π-electrocyclization was effected by soft enolization (**4-10**) with TBSOTf and Et_3N followed by heating in the presence of DBU to give diester **4-11** as an inconsequential mixture of diastereomers. Diester **4-11** contains the complete carbon skeleton of the natural product—formed in just two pots from 3,5-dibromopyrone. The synthesis was completed through reduction of the diester with LAH, Swern oxidation to give the biosynthetic intermediate, trialdehyde **4-2**, followed by treatment with NH_4OAc with heating to give delavatine A (**4-1**). The expedient nature of this synthesis is due in large part to the recognition of latent symmetry, which allowed assemblage of the carbon skeleton in a single step through the sequential one pot cross-coupling reaction. While no intermediate was overtly symmetrical, the researchers were able recognize pseudosymmetric functional groups that led them toward an efficient synthesis. Thus, their overall objective of a symmetry-guided synthesis was realized.

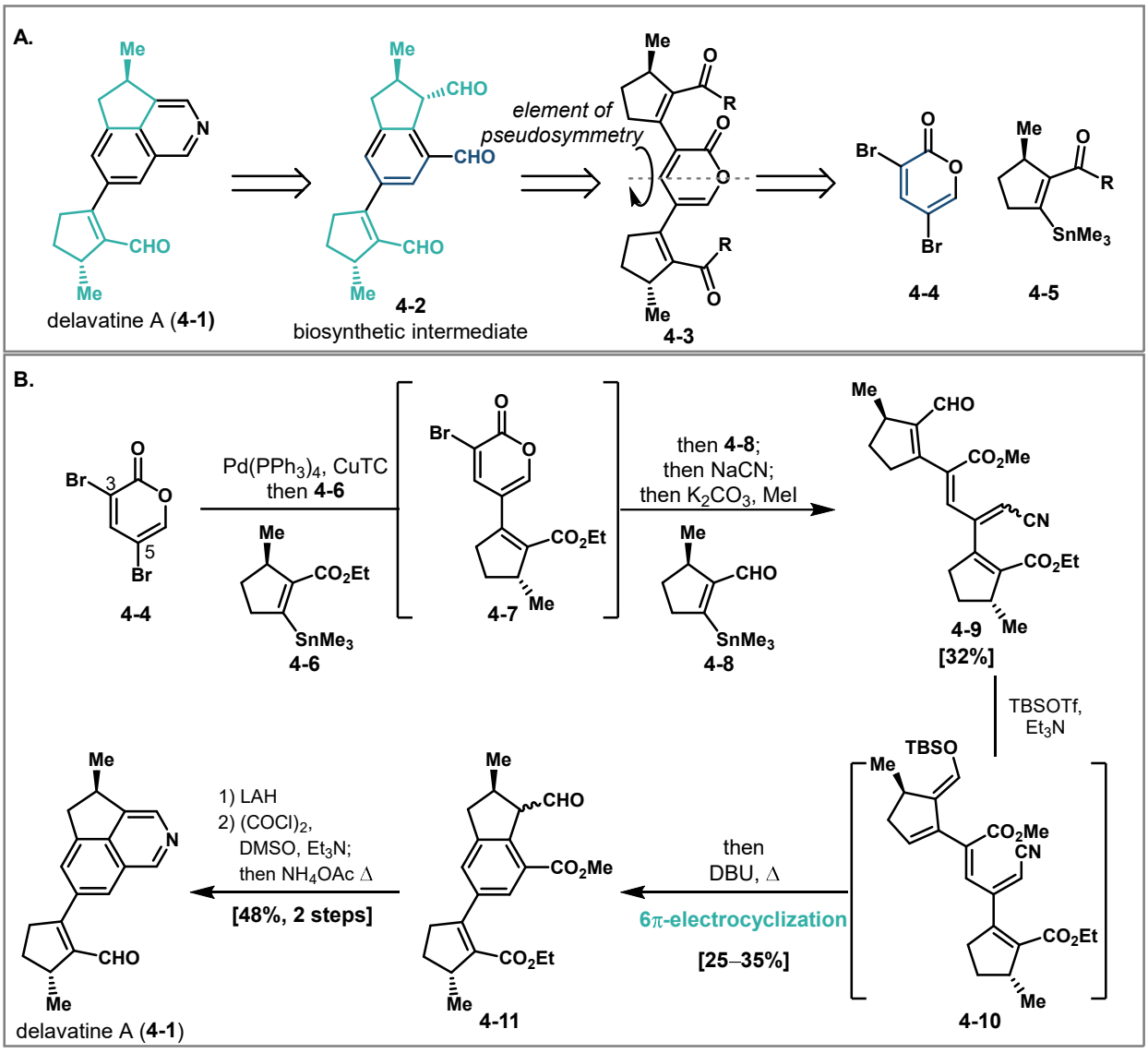

Scheme 4.1 A. Sarpong and coworkers' retrosynthesis of delavatine A. **B.** Summary of the total synthesis of delavatine A

4.3 Highlights in tactics: Luo batrachotoxinin A and Dai pyracurcasone syntheses

Luo and coworkers displayed an exquisite use of symmetry as a problem-solving tactic en route to their synthesis of the steroidal alkaloid batrachotoxinin A (Scheme 4.2 **4-12**).[17] In their original synthesis plan (Scheme 4.2A from the Supporting Information of their communication) bromoketone **4-13** underwent photoredox radical coupling[18] with ketoester **4-14** in the presence of chiral amine **4-15** to give coupled adduct **4-16** in 30% yield. They then planned to effect an intramolecular lithiate addition of **4-16** to give the 6,5-fused rings of the steroidal natural product. However, treatment of **4-16** with *t*-BuLi gave undesired ester migration product **4-17** as a 1:1 mixture of diastereomers.

Here they faced a real challenge: the intramolecular lithiate addition was selective for the undesired electrophile, but the electron-withdrawing ester of **4-14** was necessary in order to achieve selective radical coupling. Their elegant solution was to switch the coupling partner from ketoester **4-14** to bicyclo[3.2.0]octane diketone **4-18** (Scheme 4-2B). The same photoredox radical coupling could now be performed with an achiral amine mediator to give adduct **4-19** in a much-improved 70% yield. The benefit of using a symmetrical coupling partner here was two-fold. First, the newly formed all-carbon quaternary center is not stereogenic, so there was no need to use a chiral amine mediator to control diastereoselectivity. Second, absent the ester, the reaction with *t*-BuLi proceeded smoothly and after treatment with TMSOTf and Et_3N, gave the desired 6,5-fused ring system (**4-20**) in 25% over 2 steps. An excess of *t*-BuLi was required for this reaction as they observed deprotonation of the enolate occurred faster than lithium halogen exchange. The subsequent cyclization was then under the control of substrate conformation (described in detail in their Supporting Information). This tactic did leave behind an additional five-membered ring which in a sequence of 6 steps could be opened to give aldehyde **4-21**. Reductive amination and formation of the seven-membered ring proceeded in 61% yield to give **4-22**. Schenck-ene oxidation, addition of MeMgBr, and then reduction of the amide with LAH gave batrachotoxinin A in 12 steps from **4-13**. The synthesis could not have navigated the roadblock of lithiate addition selectivity if not for the clever application of the symmetry tactic. In this case the authors were able to take advantage in the short term of an opportunity to use a symmetrical building block and gained immediate advantage—a symmetry tactic.

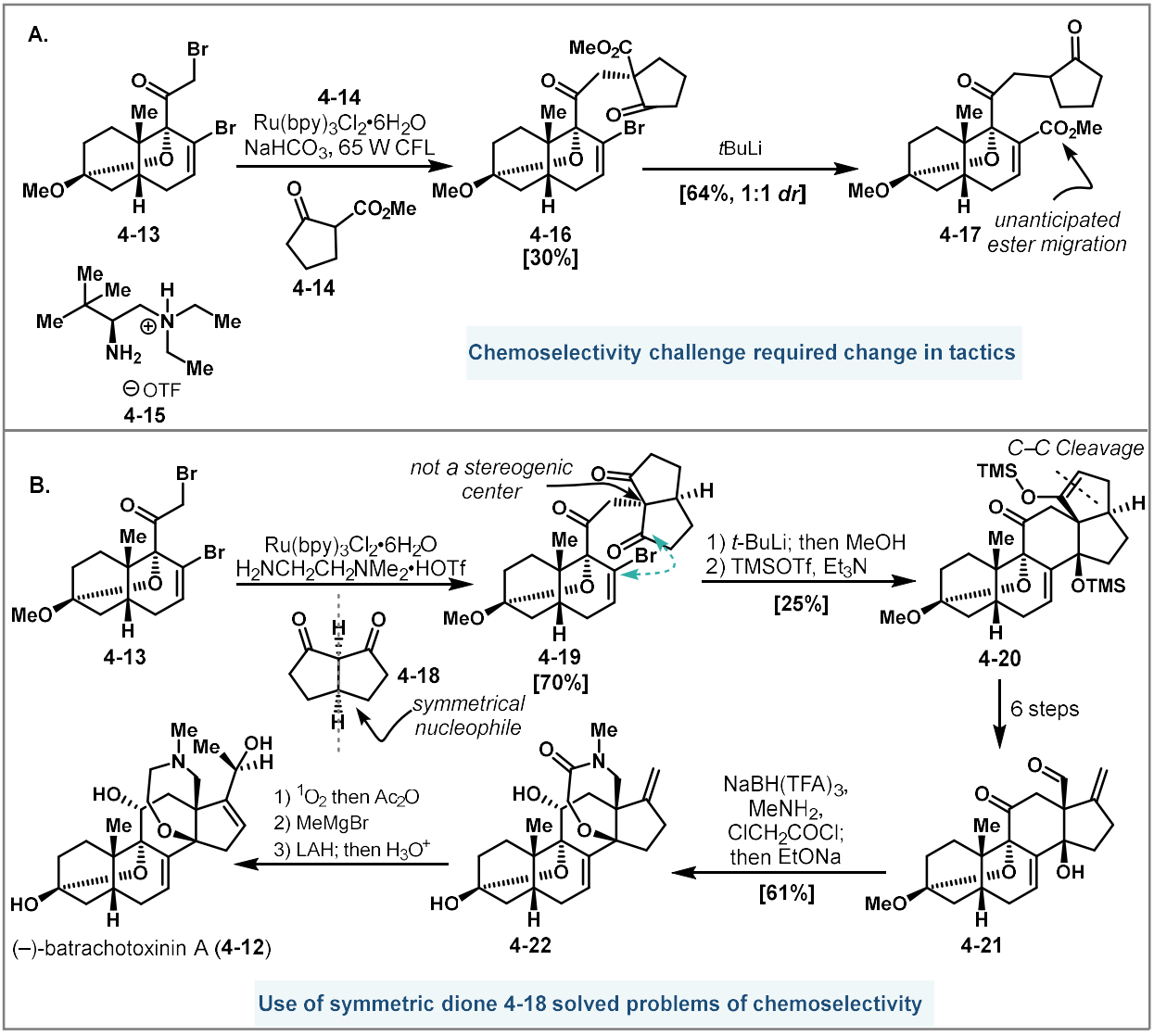

Scheme 4.2 A. Luo and coworkers' initial route toward batrachotoxinin A (**4-12**). **B.** Revised route incorporating symmetrical diketone **4-18** to solve the challenge of chemoselectivity.

Mingji Dai and coworkers have also used symmetry tactics in their recent synthesis of pyracurcasone (**4-23**),[19] also revolving around a five-membered ring. Their synthesis commenced from perillaldehyde which was advanced to allylic alcohol **4-24** in 2 steps. This allylic alcohol could be displaced by simple, symmetrical, nucleophile 1,3-cyclopentanedione (**4-25**) under Mitsonobu conditions to selectively give O-alkylated product **4-26**. Heating of vinylogous ester **4-26** in DMF induced a Claisen rearrangement followed by cyclization onto the acetal to give **4-28** in 48% over 2 steps. Functional group symmetry simplifies any complications in positional selectivity or diastereoselectivity in this system. 1,2-Addition of lithiate **4-29** into the carbonyl group of **4-28** followed by iron-mediated rearrangement (via intermediate **4-30**) gave the key seven-membered ring of the natural product (**4-31**). The back and forth interplay between the carbonyl positions of the original 1,3-cyclopentanedione (**4-25**) highlight the potency of this symmetry tactic. It is

particularly clear when one considers traversing between intermediates **4-27** and **4-30**, the five-membered ring fragment must be symmetrical—otherwise, there would be massive challenges of positional selectivity. In three separate steps, symmetry tactics simplify the challenges that Dai and coworkers faced en route to the synthesis of the natural product, several congeners, and analogues in short order.

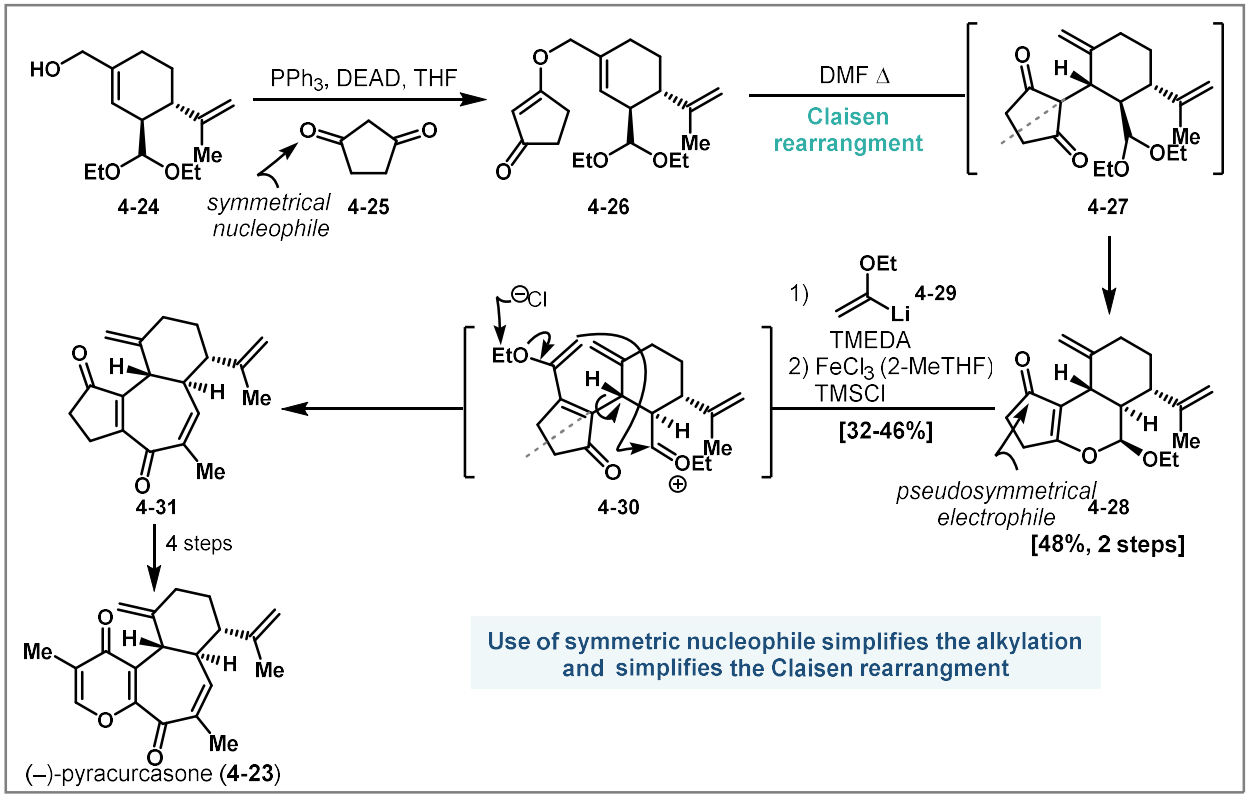

Scheme 4.3 Dai and coworkers' total synthesis of pyracurcasone A (**4-23**) utilizing symmetry tactics

4.4 Conclusion and Outlook

This short chapter highlights the power of hidden symmetry tactics and strategies in simplifying the synthesis of natural products. The delavatine A (**4-1**) synthesis from Sarpong and coworkers relied on a recognition of hidden symmetry to inspire a site-selective sequential cross-coupling that assembled the carbons of the natural product rapidly. Symmetry tactics served the Luo and Dai lab well in their synthesis of batrachotoxinin A (**4-12**) and pyracurcasone (**4-23**) through the addition of symmetric fragments that obviated challenges of site- or chemoselectivity. These considerations were fully on my mind as I devised a symmetry-inspired synthesis of the melicolone natural products (Chapter 6).

4.5 References

(1) (a)Nicolaou, K. C.; Vourloumis, D.; Winssinger, N.; Baran, P. S. The Art and Science of Total Synthesis at the Dawn of the Twenty-First Century. *Angew. Chem. Int. Ed.* **2000**, *39*, 44–122. (b) Molinski, T. F. All Natural: The Renaissance of Natural Products Chemistry. *Org. Lett.* **2014**, *16*, 3849–3855.

(2) Trauner, D. The Chemist and the Architect. *Angew. Chem. Int. Ed.* **2018**, *57*, 4177–4191

(3) *Strategies and Tactics in Organic Synthesis*; Elsevier, 1984

(4) Brace, E. R. *An Illustrated Dictionary of Chess*; New York : David McKay, 1977.

(5) (a) Doering, N. A.; Sarpong, R.; Hoffmann, R. W. A Case for Bond-Network Analysis in the Synthesis of Bridged Polycyclic Complex Molecules: Hetidine and Hetisine Diterpenoid Alkaloids. *Angew. Chem. Int. Ed.* **2020**, *59*, 10722–10731. (b) McCowen, S. V.; Doering, N. A.; Sarpong, R. Retrosynthetic Strategies and Their Impact on Synthesis of Arcutane Natural Products. *Chem. Sci.* **2020**, *11*, 7538–7552.

(6) (a) Brill, Z. G.; Condakes, M. L.; Ting, C. P.; Maimone, T. J. Navigating the Chiral Pool in the Total Synthesis of Complex Terpene Natural Products. *Chem. Rev.* **2017**, *117*, 11753–11795. (b)

Pfaffenbach, M.; Bakanas, I.; O'Connor, N. R.; Herrick, J. L.; Sarpong, R. Total Syntheses of Xiamycins A, C, F, H and Oridamycin A and Preliminary Evaluation of Their Anti-Fungal Properties. *Angew. Chem. Int. Ed.* **2019**, *58*, 15304–15308.

(7) (a)Kanda, Y.; Nakamura, H.; Umemiya, S.; Puthukanoori, R. K.; Murthy Appala, V. R.; Gaddamanugu, G. K.; Paraselli, B. R.; Baran, P. S. Two-Phase Synthesis of Taxol. *J. Am. Chem. Soc.* **2020**, *142*, 10526–10533. (b)Two-Phase Total Synthesis of Taxanes: Tactics and Strategies. *J. Org. Chem.* **2020**, *85*, 10293–10320. (c) Ishihara, Y.; Baran, P. S. Two-Phase Terpene Total Synthesis: Historical Perspective and Application to the Taxol® Problem. *Synlett* **2010**, *2010*, 1733–1745.

(8) Heathcock, C. H. The Enchanting Alkaloids of Yuzuriha. *Angew. Chem. Int. Ed.* **1992**, *31*, 665–681.

(9) (a)Bai, W.-J.; Wang, X. Appreciation of Symmetry in Natural Product Synthesis. *Nat. Prod. Rep.* **2017**, *34*, 1345–1358. (b)Horwitz, M. A. Local Desymmetrization as an Engine of Stereochemical Elaboration in Total Synthesis. *Tetrahedron Lett.* **2022**, *97*, 153776. (c) Wang, M.; Feng, M.; Tang, B.; Jiang, X. Recent Advances of Desymmetrization Protocol Applied in Natural Product Total Synthesis. *Tetrahedron Lett.* **2014**, *55*, 7147–7155. (d) Schindler, C. S.; Cala, L.; Gaviria, M. A.; Kim, S. L.; Vogel, T. R. Recognition of Symmetry as a Powerful Tool in Natural Product Synthesis. *Synthesis* **2021**, DOI: 10.1055/a-1702-5062.

(10) Sharpe, R. J.; Johnson, J. S. Asymmetric Total Synthesis of the Indole Diterpene Alkaloid Paspaline. *J. Org. Chem.* **2015**, *80*, 9740–9766.

(11) Taber, D. F.; Neubert, T. D.; Rheingold, A. L. Synthesis of (−)-Morphine. *J. Am. Chem. Soc.* **2002**, *124*, 12416–12417.

(12) (a)Diaz-Muñoz, G.; Miranda, I. L.; Sartori, S. K.; de Rezende, D. C.; Alves Nogueira Diaz, M. Use of Chiral Auxiliaries in the Asymmetric Synthesis of Biologically Active Compounds: A Review. *Chirality* **2019**, *31*, 776–812. (b) Hoye, T. R.; Jeffrey, C. S.; Shao, F. Mosher Ester Analysis for the Determination of Absolute Configuration of Stereogenic (Chiral) Carbinol Carbons. *Nat. Protoc.* **2007**, *2*, 2451–2458.

(13) Sharpe, R. J.; Johnson, J. S. A Global and Local Desymmetrization Approach to the Synthesis of Steroidal Alkaloids: Stereocontrolled Total Synthesis of Paspaline. *J. Am. Chem. Soc.* **2015**, *137*, 4968–4971.

(14) (a) Palani, V.; Hugelshofer, C. L.; Sarpong, R. A Unified Strategy for the Enantiospecific Total Synthesis of Delavatine A and Formal Synthesis of Incarviatone A. *J. Am. Chem. Soc.* **2019**, *141*, 14421–14432. (b) Palani, V.; Hugelshofer, C. L.; Kevlishvili, I.; Liu, P.; Sarpong, R. A Short Synthesis of Delavatine A Unveils New Insights into Site-Selective Cross-Coupling of 3,5-Dibromo-2-Pyrone. *J. Am. Chem. Soc.* **2019**, *141*, 2652–2660.

(15) Palani, V.; Perea, M. A.; Sarpong, R. Site-Selective Cross-Coupling of Polyhalogenated Arenes and Heteroarenes with Identical Halogen Groups. *Chem. Rev.* **2022**, *122*, 10126–10169.

(16) Hugelshofer, C. L.; Magauer, T. A General Entry to Antifeedant Sesterterpenoids: Total Synthesis of (+)-Norleucosceptroid A, (−)-Norleucosceptroid B, and (−)-Leucosceptroid K. *Angew. Chem. Int. Ed.* **2014**, *53*, 11351–11355.

(17) Guo, Y.; Guo, Z.; Lu, J.-T.; Fang, R.; Chen, S.-C.; Luo, T. Total Synthesis of (−)-Batrachotoxinin A: A Local-Desymmetrization Approach. *J. Am. Chem. Soc.* **2020**, *142*, 3675–3679.

(18) (a)Nicewicz, D. A.; MacMillan, D. W. C. Merging Photoredox Catalysis with Organocatalysis: The Direct Asymmetric Alkylation of Aldehydes. *Science* **2008**, *322*, 77–80. (b) Zhu, Y.; Zhang, L.; Luo, S. Asymmetric α-Photoalkylation of β-Ketocarbonyls by Primary Amine Catalysis: Facile Access to Acyclic All-Carbon Quaternary Stereocenters. *J. Am. Chem. Soc.* **2014**, *136*, 14642–14645. (c) Zhang, W.; Zhu, Y.; Zhang, L.; Luo, S. Asymmetric α-Alkylation of β-Ketocarbonyls via Direct Phenacyl Bromide Photolysis by Chiral Primary Amine. *Chin. J. Chem.* **2018**, *36*, 716–722.

(19) Cui, C.; Dwyer, B. G.; Liu, C.; Abegg, D.; Cai, Z.-J.; Hoch, D. G.; Yin, X.; Qiu, N.; Liu, J.-Q.; Adibekian, A.; Dai, M. Total Synthesis and Target Identification of the Curcusone Diterpenes. *J. Am. Chem. Soc.* **2021**, *143*, 4379–4386.

Chapter 5

Strategic Application of C–H Oxidation in Natural Product Total Synthesis

5.1 Introduction

In the opening chapter of this dissertation, I expressed that the ultimate goal of organic synthesis is total, programmable control of reactivity. At this extreme, we would view all bonds as functional groups to be manipulated to our liking. Toward this end, the field of C–H oxidation seeks to render unactivated C–H bonds reactive and on this basis reimagine what is possible in synthesis. Total synthesis is the ultimate testing ground for methodology and as such, C–H oxidation-based strategies for the synthesis of complex natural products have gained a great deal of popularity in recent years.[1]

In our own laboratory, C–H oxidation reactions are proving to be extremely powerful tools for completing various synthesis campaigns (see our recent syntheses of the longiborneol, cephanolide, xishacorene, and lycodine-type natural products).[2] Methodological advancements continue to reshape the ways we make molecules, and in particular, methodologies to oxidize unactivated C–H bonds have developed rapidly in recent years.[3] Lagging behind the methodological developments has been the corresponding applications in synthesis, as is often the case, due to barriers of practicality, and generality.[4] Nonetheless, strategies such as "two-phase" synthesis codified by Baran,[5] where the cores of molecules are constructed rapidly in the "cyclase phase" followed by decoration of the periphery through oxidation reactions in the "oxidase phase", as well as semisynthetic oxidation approaches[6] among others have found significant purchase. C–H oxidation reactions can serve a multitude of purposes within a synthesis and increasingly these reactions are being included in synthesis planning. To help guide the utilization of C–H oxidation in complex molecule synthesis, we propose a framework for classifying different strategic use-cases (Figure 5.1), which captures and organizes these strategies on the basis of how they relate to the target structure.

Type 1: leverages newly installed oxidation to build, rearrange, or break the carbon skeleton.

Type 2: builds a ring using the installed oxidation.

Type 3: installs oxidation on the periphery of the target.

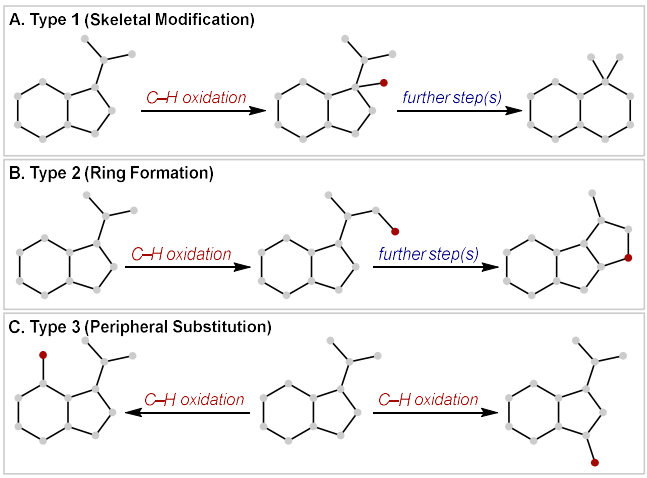

Figure 5.1 Strategic use-cases of C–H oxidation

Use of C–H oxidations may be further classified by whether they are "directed"[7] or "undirected."[8] We, therefore, arrive at six possible strategic classifications for a C–H oxidation reaction deployed in a total synthesis. We will highlight examples in the syntheses of natural products published in the last 3 years that utilize C–H oxidations that fall into the classification scheme illustrated in Figure 5.1 with an eye toward how the oxidation enables uniquely efficient synthesis planning. Finally, we will explore two case studies from our own laboratory where we will provide more insight into the underlying thought processes for planning and navigating syntheses completed in the group.

5.2 Type 1 C–H oxidation

Type 1 C–H oxidations, as defined here, facilitate the formation of core C–C bonds. As such, they have been more frequently deployed earlier in syntheses and have found particular application in bioinspired syntheses. The newly introduced oxidation can allow access to the shallow carbocationic landscape that natural products traverse during biosynthesis by intercepting biosynthesis-like intermediates. In terms of practical synthesis advantages, strategic use of C–H oxidations—and type 1 oxidations in particular—allows for a greatly expanded set of starting materials in synthesis by taking advantage of a larger pool of chiral terpenoids (the "chiral pool")[9] lacking the requisite oxidation. Below we will discuss several examples of Type 1 oxidations, noting how the oxidations allow the user to transform advanced starting materials—steroids and diterpenes—by introducing unnatural oxidation such that little synthetic effort is spent on elaborating the carboskeleton. C–H oxidation opens up distinct new avenues for semisynthesis.

5.2A Undirected Type 1 C–H oxidation

Site-selective undirected C–H oxidation is the ultimate enabler of synthesis planning, because every hydrogen can be a functional group, which opens up numerous strategic

possibilities. The challenge, of course, lies in gaining selectivity.[8] In their synthesis of complex diterpenes (Scheme 5.1), Renata and coworkers leverage enzymatic and chemical methods to selectively oxidize 11 different positions in 4 distinct terpene scaffolds.[10] Through a combination of enzymatic and chemical oxidations, they were able to access 8 diterpenoids in a rapid fashion from abundant, lower oxidation-state, terpene feedstocks. Renata and coworkers recognized the biosynthetic relationships between the diterpenoid families, for example *ent*-beyerane [3.2.1] bicycle and *ent*-atisane [2.2.2] bicycle through a Wagner–Meerwein shift (**5-1** to **5-2**) as well as the relationship between the *ent*-atisane and *ent*-trachylobane [3.2.1.0] tricycle (**5-3** to **5-4**).[11] Their synthesis plan started from the cheap, abundant *ent*-beyerane isosteviol (**5-5**) that was first converted to the *ent*-atisane skeleton and then to the complex *ent*-trachylobane mitrephorone A[12] (**5-11**) through a series of bioinspired carbocationic rearrangements. Key to this strategy was the development of a biocatalytic, site-selective, C-12 oxidation of isosteviol (**5-5**) which could be leveraged to form the desired carbocation.

Biocatalytic C–H oxidations are promising because of the mild conditions that are required in introducing an element of tunable site-selectivity.[13] The enzyme active site enables the catalytic center (often an iron heme) to be turned over with mild oxidants and the secondary ligand sphere of the protein can position substrates for selective oxidation.[13A] That secondary ligand sphere can be optimized and adjusted, a paradigm with which, in theory, a catalyst could be tuned to selectively functionalize any position on any molecule.[14] Several enzymes were identified from the platensimycin biosynthesis, PtmO5, PtmO3, and PtmO6, which promiscuously accept *ent*-kaurane substrates.[15] Among these enzymes, the P450 monooxygenenase (PtmO5) was found to be effective for efficient hydroxylation of C-11 in the *ent*-kaurane scaffold when fused to the reductase domain of $P450_{RhF}$ to give PtmO5-RHFRed. Conversion was further improved upon coexpression with GroES and GroEL chaperone, and the NADPH recycling system Opt13. They then applied these conditions to the oxidation of the *ent*-beyerane isosteviol (**5-5**) which serendipitously underwent selective C-12 oxidation. Renata and coworkers hypothesize that this selectivity arises from the differing positioning of *ent*-kaurane and *ent*-beryane skeletons within the active site. Between PtmO6 and PtmO5, Renata et al. were able to site-selectively and chemoselectively oxidize four different positions on different diterpene feedstocks. Isosteviol (**5-5**) could be selectively oxidized to alcohol **5-6** on preparative scale, setting the stage for the group's synthesis of mitrephorone A (**5-11**).

With sufficient access to alcohol **5-6**, Renata and coworkers initiated their proposed skeletal reorganization through the ionization of **5-6** with TfOH to form the *ent*-atisane skeleton upon 1,2-acyl shift and quenching of the resulting carbocation (**5-7**). Reduction of the *ent*-atisane ketone group with L-selectride gave alcohol **5-8**, which was primed to undergo the second of two skeletal rearrangements. Ionic reduction with BF_3OEt_2 and triethylsilane gave *ent*-trachylobane acid **5-10** in 61% yield over 3 cycles through ionization of the hydroxy group and selective reduction of the resulting non-classical carbocation **5-9**. Acid **5-10** can be elaborated to mitrephorone A (**5-11**) in just 5 additional steps resulting in a synthesis with a total step count of

9. Notably, this is considerably shorter than the previous syntheses (18, and 23 steps)[16] owing in large part to the fact that Renata and coworkers start with a complete carbon skeleton.

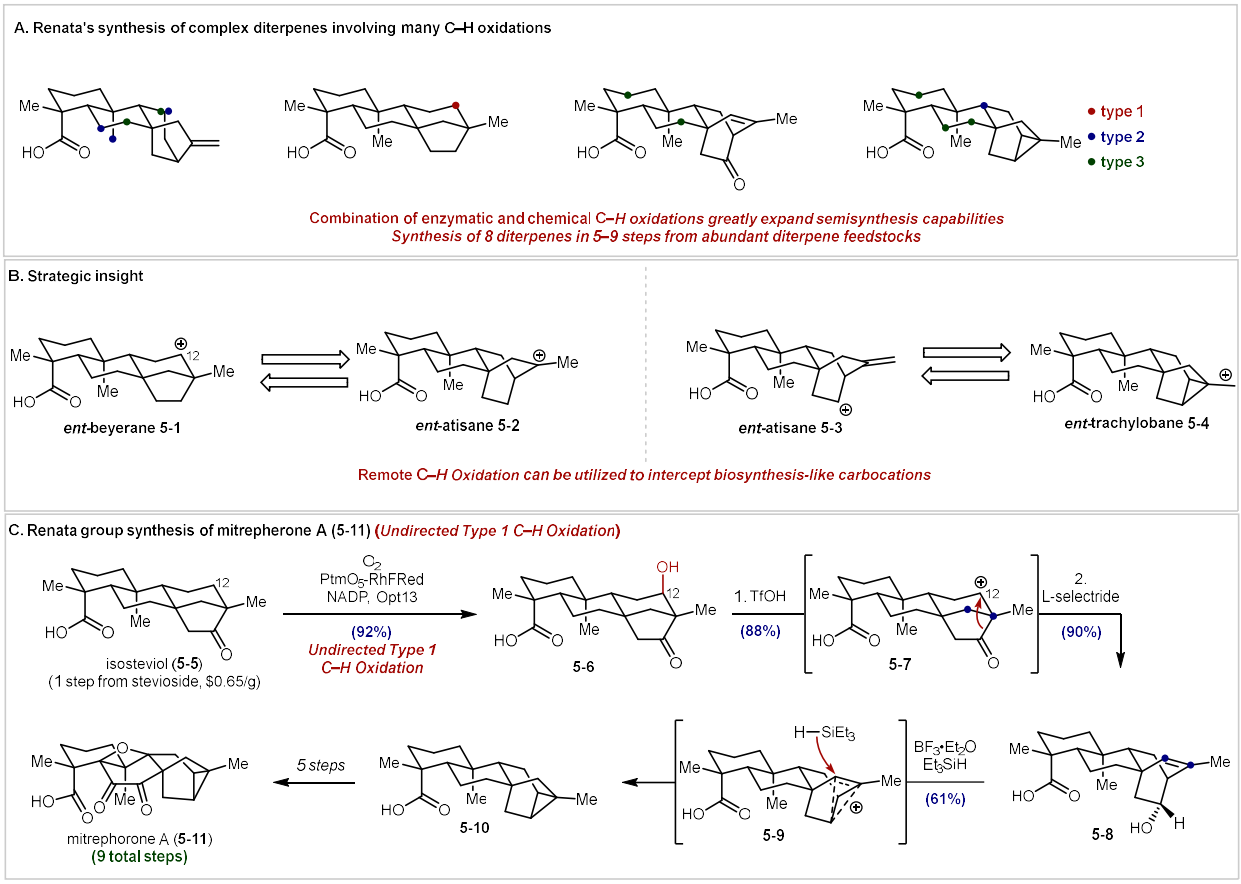

Scheme 5.1A. Renata's syntheses of complex diterpenes featuring multiple C–H oxidations of terpene feedstocks **B**. Carbocationic relationship between bridged diterpenes. **C**. The Renata group's synthesis of mitrephorone A (**5-11**) feature a Type 1 C–H oxidation

It is important to highlight how the available C–H oxidation methodology completely reshaped the optimal way to synthesize mitrephorone A (**5-11**). Isosteviol (**5-5**) is only available as a starting material because it undergoes selective remote C–H oxidation that enables a skeletal reorganization that is only possible because of a Type 1 C–H oxidation. New methodology informed new strategy.

5.2B Directed Type 1 C–H oxidation

In 2022 Heretsch[17] and Deng[18] published nearly simultaneous reports on the synthesis of spirochensilide A[19] (**5-15**) from lanosterol (**5-16**) utilizing a similar strategy (Scheme 5.2). Both groups were inspired, once again, by the biosynthesis of this lanostane triterpenoid. On the basis of analyses of known congeners of lanosterol (**5-16**), they proposed a modified biosynthetic pathway (Scheme 5.2A). Lanosterol undergoes several enzymatic oxidations to give diepoxide **5-12**. Selective ring opening of the northern epoxide gives carbocation **5-13** which undergoes two

successive Wagner–Merweein shifts to give **5-14** bearing the distinctive methyl group patterning. The remaining epoxide then underwent a Meinwald rearrangement to give the eponymous spirocycle found within the core of spirochensilide A (**5-15**).

Both groups targeted the formation of carbocation **5-13** from lanosterol anticipating that they could induce the same carbocationic rearrangements that occur in the biosynthesis en route to the natural product. This strategy would allow for starting the synthesis with all the requisite carbons, but necessitate a C–H oxidation of C-17. One could imagine the difficulties in undirected C–H oxidation at this point; multiple tertiary electron-rich C–H bonds and double bonds would make selectivity extremely challenging. Therefore, both groups opted to use directed C–H oxidations. The Heretsch commences with the cleavage of the prenyl group of lanosterol (**5-16**), taking advantage of this functional group to install the requisite directing group in the form of alcohol **5-17**. Upon treating **5-18** with modified Suarez reaction conditions (NaI, PIDA, and visible-light irradiation),[20] an alkoxy radical is formed that undergoes a 1,5-HAT to abstract the H-atom from C-17. Traditionally, the resulting tertiary radical is further oxidized to either the alkyl halide or carbocation to which the pendent hydroxy group adds. In this case, the oxidation triggers the first of the two bioinspired Wagner–Meerwein shifts, leading to rearranged tetrahydropyran product **5-19** in 34% yield, presumably through **5-18**. The second shift can be effected by ionization of the THP through treatment with $TiCl_4$ yielding diene **5-20** after elimination in excellent yield. The final phase of their skeletal reorganization was achieved by oxidative rearrangement of **5-20** through treatment with NIS and $AgNO_3$ in a THF water mixture. The researchers propose that this transformation proceeds by the formation of the halohydrin which equilibrates to the desired epoxide (similar to **5-14**) which undergoes Meinwald rearrangement. From spirocycle **5-21**, the synthesis was completed in an additional 8 steps, a sequence that is notably shorter than the previous 22 step synthesis,[21] once again owing to the advanced starting position.

The Deng group's synthesis[18] rested on a similarly effective recognition. Instead of triggering the rearrangements in a step-wise fashion, they endeavored to do so in a single operation. As such, their synthesis also commenced from lanosterol (**5-16**) which in 2 steps was cleaved to unveil aldehyde **5-22**. Homologation to trifluoromethyl ketone **5-23** was achieved by addition of $TMSCF_3$, and subsequent DMP oxidation in 80% yield over two steps. Yang and coworkers have shown that these trifluoromethyl ketones can be leveraged for intramolecular C–H oxidation,[22] though Deng and coworkers note that the hydroxylation that they report may be its first application in total synthesis. Treating trifluoromethyl ketone **5-23** with oxone in buffered solution results in the formation of the corresponding dioxirane which undergoes intramolecular C–H insertion at C-17 to give the trifluoromethyl hemiketal which was saponified and methylated to give alcohol **5-24** in 50% over 2 steps. Alcohol **5-24** was converted to diepoxide **5-25** in 3 steps setting the stage for the rearrangement cascade. Treatment of diepoxide **5-25** with an excess of BF_3OEt_2 triggered all three of the bioinspired rearrangements to give spirocycle **5-26** in 35% yield which was taken to spirochensilide A in 7 steps.

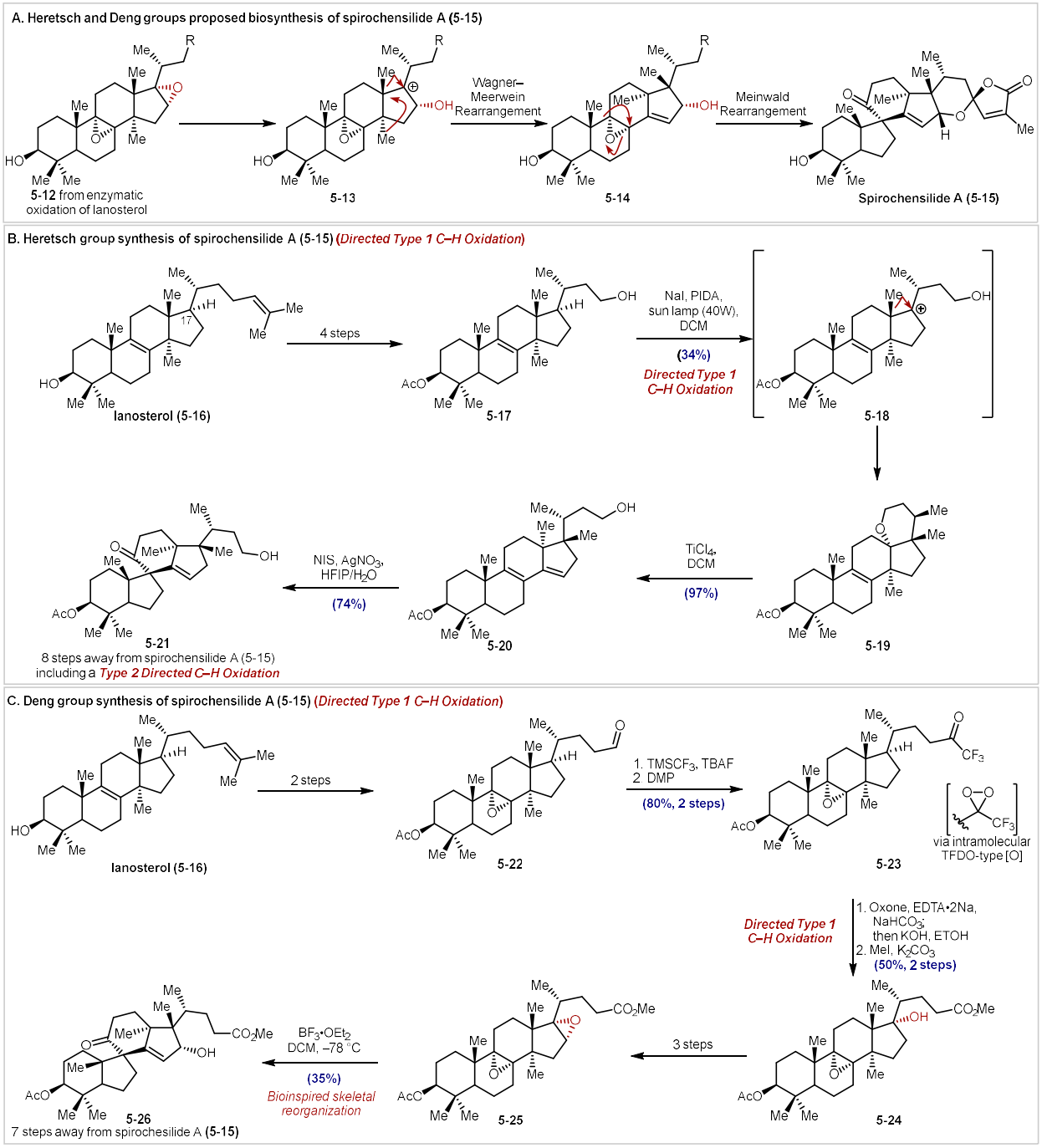

Scheme 5.2A. Proposed biosynthesis of lanostane triterpenoid spirochensilide A (**5-15**) **B**. Heretsch and Deng groups' syntheses of spirochensilide (**5-15**) A using directed type 1 C–H oxidation

When considered together these syntheses show clearly the power of Type 1 C–H oxidation as an entry point into carbocationic rearrangements and rearrangement cascades. In this way the oxidation is leveraged to reshape the carbon skeleton and build target-oriented complexity. While many syntheses using Type 1 C–H oxidations use them to enable such

rearrangement strategies, one could also envision utilizing these reactions to enable the introduction of additional carbon atoms through C–C bond formation. For example, a terpene could be functionalized using C–H oxidation, and the resulting functional handle could be used to synthesize sesquiterpenes or diterpenes through prenylation. In an inverse case, one could envision taking a readily available, larger starting material—higher order terpenoids, steroids etc.—which contain a target relevant subskeleton and using C–H oxidation to enable C–C cleavage reactions which yield a valuable, smaller intermediate. As the collection of oxidation reactions grows, so will the number of strategies in synthesis planning and the complexity of our feedstocks.

5.3 Type 2 C–H oxidation

Type 2 oxidations are defined as those that result in the formation of heterocyclic rings. They have found great use in the synthesis of highly oxidized terpene natural products which feature ether and lactone linkages as major structural elements.[23] Use in this realm has been dominated by directed Suarez oxidations[24] or carboxylate-directed lactonizations with the White-Chen catalyst.[25] These reactions facilitate the oxidative remodeling of terpenes[26] and can greatly simplify functional group manipulation during the synthesis. Undirected Type 2 oxidations are somewhat rare but can be especially effective in a divergent synthesis. Importantly, a single oxidation can be used in a divergent fashion, leading to a variety of oxygenated functional groups. This is especially relevant when targeting families of higher oxidation-level natural products.

5.3A Undirected Type 2 C–H oxidation

In a recent synthesis from Zhang and coworkers, an incisive late-stage desaturation was employed in order to access several high-oxidation state illicium sesquiterpenes.[27] The versatility of the unsaturation is evident in its use as a handle for epoxidation, hydration, and allylic oxidation—all of which are utilized to make natural products. Thus, they targeted late-stage intermediate **5-27** which underwent desaturation[28] to give alkene **5-28**. A strategic feature of this synthesis is the use of a variety of different C–H oxidations to achieve halogenation then elimination, hydroxylation-elimination, and direct desaturation. From a methodological perspective, all of these transformations are possible by targeting an electron-rich tertiary C–H bond.

The Zhang synthesis commences from (R)-pulegone (**5-35**) which underwent Favorskii ring contraction and allylation to give ester **5-34** in 85% yield as a single diastereomer over 2 steps. This set of transformations highlights another value of their late-stage desaturation approach. The unactivated tertiary stereocenter of pulegone allows access to the series in an enantiospecific fashion and is leveraged to control the stereochemistry of the allylation, but is later ablated in the key desaturation step. Much like how the Type 1 oxidations enabled the use of unconventional starting materials, this is a case where Type 2 oxidation enables the use of an enantioenriched starting material where the stereocenter that drives diastereoselectivity is not

directly carried through to the target. Epoxidation of the tetra-substituted alkene with *m*-CPBA and oxidative cleavage of the allyl group with $RuCl_3$ and $NaIO_4$ proceeded with spontaneous lactonization to give bicycle **5-35** in 77% yield. Following a sequence of 4 steps, propargylic alcohol **5-36** was prepared and subjected to palladium-catalyzed borylative-cyclization[29] conditions which yielded alcohol **5-37** after an oxidative work-up. In two additional steps, selenocarbonate **5-38** was prepared and a radical cyclization initiated by AIBN was performed to close the last core ring to give **5-27** in 96% yield.

The key desaturation could then be studied. Initial attempts to achieve C–H bromination (NBS, AIBN, refluxing CCl_4) led not only to the desired C-1 oxidation, but also the undesired oxidation of the C-7 secondary hydroxy group. Calculated bond dissociation energies (BDEs) showed that this alpha-hydroxy bond was weaker than the desired C–H bond. Therefore, Zhang et al. investigated solvent effects, hypothesizing that tuning the electronic and steric environment of the secondary alcohol through H-bonding could affect the BDE and rate of oxidation at C-7.[30]

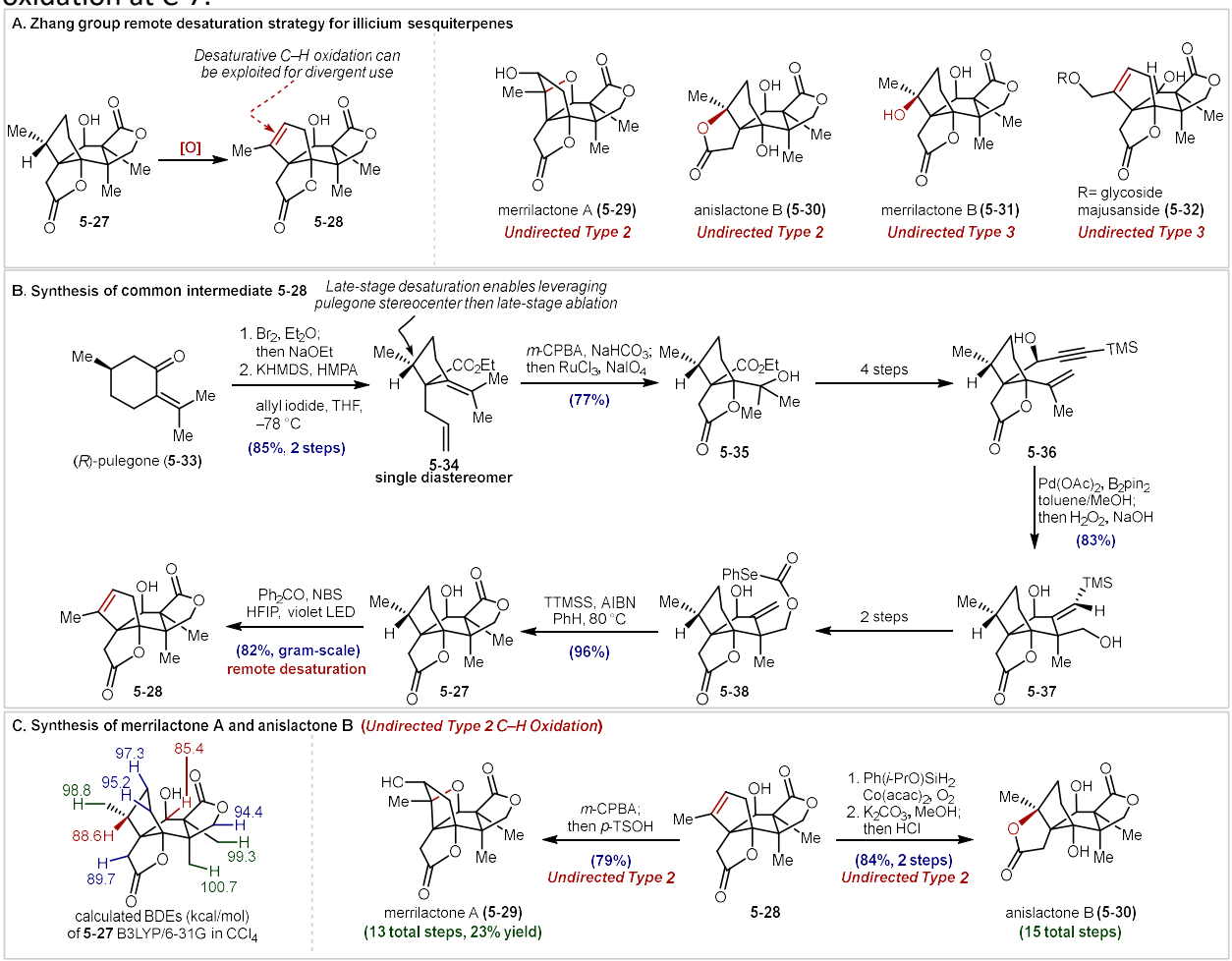

Scheme 5.3A. The Zhang group's plan for remote desaturation to access several illicium sesquiterpenes **B**. Synthesis of the Zhang common intermediate through C–H oxidation **C**.

Completion of merrilactone A (**5-29**) and anislactone B (**5-30**) by leveraging desaturation for undirected Type 2 C–H oxidation.

Use of hexafluoroisopropanol as solvent and 312 nm light initiation immediately suppressed the undesired reactivity, though in moderate yield. Switching to violet LEDs (390 nm) and use of benzophenone as a triplet sensitizer led to the isolation of alkene **5-28** in 82% yield on gram-scale.

This oxidation was parlayed in a Type 2 fashion to synthesize merrilactone A[31] (**5-29**) and anislactone B[32] (**5-30**). First, alkene **5-29** was epoxidized and then treated with *p*-TsOH to induce ether bridge formation to give a heterocycle typical of Type 2 oxidation and complete the synthesis of merrilactone A in 13 steps[33] and an excellent 23% overall yield. Mukaiyama hydration of the alkene group in **5-28** gave merrilactone B[34] (**5-30**) which was converted to anislactone B through trans-lactonization by treatment with K_2CO_3 in MeOH. The late-stage desaturation also enabled the synthesis of two other sesquiterpenes highlighting the utility of this oxidation reaction. The key targeting of an electron-rich tertiary C–H bond in the Zhang synthesis planning was validated, and in the process, a new method for the mild violet light mediated desaturation was developed.

5.3B Directed Type 2 C–H oxidation

Type 2 C–H oxidations have seen the most application when used in the directed manifold owing to the strong history of directed C–H functionalization reactions dating back to classic studies in steroid synthesis.[35] These reactions have been pivotal in many recent syntheses of neurotropic sesquiterpenes.[23] Shenvi and coworkers recently disclosed a synthesis[36] of the sesquiterpene picrotoxinin[37] (**5-39**) that utilizes a Type 2 C–H oxidation to close the C-2 to C-15 lactone. This oxidation-based transform is simplifying when compared to traditional lactonization transforms as it reduces the number of functional groups one must install or carry through the synthesis (Scheme 5.4B).

The Shenvi synthesis commenced with an interesting strategic decision, starting with the aldol reaction of dimethyl carvone (**5-46**) to give **5-48** in 67% yield and high diastereoselectivity for the desired alpha epimer. The superfluous methyl group of dimethyl carvone was necessary for achieving high diastereoselectivity in this addition reaction. However, it needed to be removed later in the synthesis—unusual strategically—but possible through application of C–H oxidation. A two-step annulation sequence delivered bicycle **5-49**. The secondary alcohol and isopropenyl groups were protected in **5-50** through a bromoetherification reaction with NBS in near quantitative yield. Conventional oxidation methodologies were employed to install the lactone moiety in **5-51** where the secondary hydroxy group is axially disposed and primed to oxidize the flanking methyl group which was accomplished using AgOAc, I_2, and visible-light irradiation to give ether **5-52**. A subsequent 3-step oxidation, radical ring opening-halogenation, and dehalogenation sequence deleted the extra methyl group to yield **5-53**. While this deletion sequence required 4 steps, installing the methyl group at the outset of the synthesis enabled the

key diastereoselective annulation. The strategy adopted by Shenvi and coworkers constitutes an unexpected use of Type 1 directed C–H oxidation.

With the extra methyl removed, the synthesis was completed by directed Type 2 C–H oxidation with $Pb(OAc)_2$, $CaCO_3$, and light to effect lactonization followed by reductive cleavage of the bromoether to give picrotoxinin (**5-39**) in 13 total steps—the shortest synthesis of this natural product to date.[38] Key to the efficiency of this synthesis was the use of dimethyl carvone as starting material. The two methyl groups were installed in a single step and enabled the desired diastereoselectivity on the subsequent reaction. However, neither appear at the methyl oxidation state in the natural product. One was deleted through a Type 1 C–H oxidation, and the other was converted into a heterocyclic structural element with a Type 2 C–H oxidation. C–H oxidation strategies expand what is possible from unactivated positions and allowed for this counterintuitive—but highly efficient—plan.

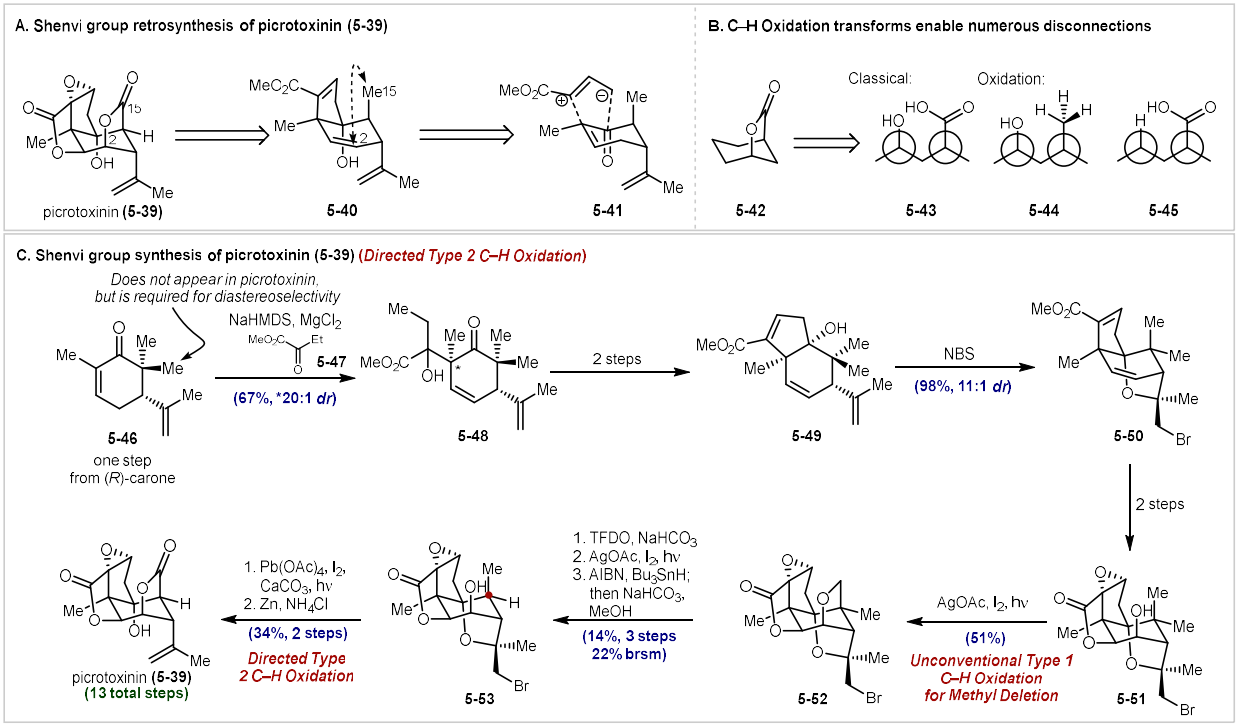

Scheme 5.4 A. The Shenvi group's retrosynthesis of picrotoxinin A **B**. Oxidation-based lactonization disconnections compared to classical disconnection C. Synthesis of picrotoxinin A featuring a Type 2 directed C–H oxidation

5.3 Type 3 C–H Oxidation

Type 3 oxidations perhaps represent the most classical use of C–H oxidation and hold tremendous promise partly due to their reliability at a late-stage.[39] Type 3 oxidation logic intersects smoothly with biosynthetic "two-phase" logic.[5] In natural systems, promiscuous oxygenases are responsible for converting unfunctionalized metabolites to their higher

oxidation-level congeners. There is very sound synthesis logic here; it naturally leads to syntheses that are step-economic without the need for protecting group manipulations or functional group interconversions as one shepherds the oxidation through the synthesis. For the two-phase synthesis to work, however, methods for C–H oxidation must be up to the task and our understanding of principles leading to selectivity must be sound.

5.3a Undirected Type 3 C–H oxidation

Many methods have been employed that target the weakest, most electron-rich (hydridic), C–H bond in the molecule. Some deviation in selectivity is possible using sterically bulky catalysts that select away from tertiary C–H bonds.[40] Other methodologies that target strong C–H bonds[41] and primary selective functionalization[42] have been developed but not used in total synthesis to date. As such, the current methodologies are best employed for targeting tertiary C–H bonds distal from electron-withdrawing groups, or proximal to electron-releasing groups. Several of the syntheses discussed above include examples of undirected Type 3 C–H oxidation. However, we will not be discussing them in detail here. For more information see the full papers from Renata and Zhang.[10,27]

An interesting case of selectivity was explored in the context of the total synthesis of *ent*-trachylobane[43] natural products by Magauer[44] and coworkers. This work stands as a counterpoint to the biocatalytic C–H oxidations explored by Renata and coworkers and highlights the different methodologies that can invert selectivity. The Magauer group set out to investigate the selectivity of chemical methods within the *ent*-trachylobane scaffold. The [3.2.1.0] tricycle of **5-56** was targeted which contains various structural elements that could be oxidized. Thus, they commenced their synthesis from decalin **5-53** which was accessed in 8 steps from commercial material and was crucial in their prior synthesis of mitrephorone A (**5-11**).[16B] A five-step sequence advanced **5-53** to enone **5-54** which underwent Luche reduction and elimination with Burgess reagent to give diene **5-55** in 30% yield over 2 steps. Diene **5-55** was primed for a key Diels–Alder cycloaddition building the [3.2.1.0] tricycle of the family (see **5-56**) in 85% yield upon heating.

With the core of the trachylobanes in hand, Magauer et al. then explored it's oxidation. Use of the electrophilic oxidant TFDO[46] led to selective formation of **5-57** in 43% yield which led to the corresponding natural product after ester saponification. The observed reactivity can be rationalized by the electron-releasing nature of the cyclopropane. Electrochemical oxidation[47] showed similar selectivity, but they were able to isolate 10% of product corresponding to radical ring opening (not shown). Use of Ru(TMP)(CO)[48] also delivered the desired ketone in 27% yield, as well as the lower oxidation level alcohol in 38% yield. Selectivity was changed by using the bulky ((R,R)-Mn(CF_3-PDP) catalyst[49] which resulted in the formation **5-61** containing the [2.2.2] bicycle characteristic of the *ent*-atisane natural products. This is presumably formed from oxidation at C-15 and radical ring opening.

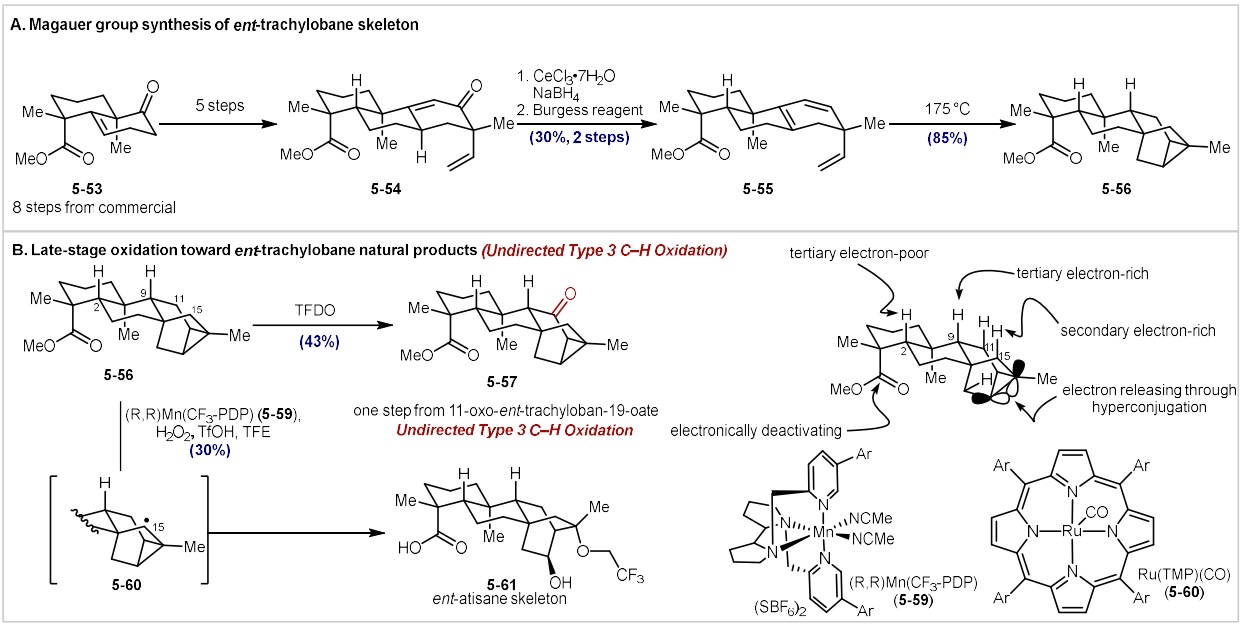

Scheme 5.5 A. Magauer group's synthesis of *ent*-trachylobane skeleton **5-36 B**. Undirected Type 3 C–H oxidation studies toward *ent*-trachylobane natural products

Application of undirected C–H oxidation methodology requires analysis of substrate electronics. Prior studies from Baran and coworkers have shown that ^{13}C-NMR[50] shifts can be reliable predictors of site-selectivity, Zhang and coworkers used BDE calculations to guide their planning (see Section 5.2a), and Magauer and coworkers used the inherent—and atypical—structural features of their target to their advantage.

5.3B Directed Type 3 C–H oxidation

Recently, Luan[51] and coworkers explored the intersection of traditional synthetic logic and C–H oxidation methodology to design an elegant synthesis of dalesconol A[52] (**5-68**). This polyketide natural product contains three aryl ketones with *o*-oxidation lending very naturally to the use of directed C–H oxidation for late-stage manipulations using the ketone—or a derivative thereof—as a directing group.[53] The researchers cleverly planned to do all three oxidations in a single operation,[54] thus rapidly installing the desired oxidation in a step-economic fashion. Thus, they were able to design a two-phase synthesis approach.

The key cyclization event was effected using a Pd(0)-norbornene mediated Catellani-type cascade[55] where aryl iodide **5-62** was coupled with bis-homopropargylic bromide **5-63** through activation of a C–H bond and migratory insertion across the alkyne. The key spiro-tricycle was then formed through a one-pot ketal cleavage/ Michael addition to give **5-64** in 64% yield. This cyclization is remarkably efficient for constructing the core of the molecule. Notably, the choice to push the C–H oxidation to the end of the synthesis allowed for simpler building blocks—additional oxidation did not interfere with the cascade, nor did they have to expend steps to

install it. The wealth of known C–H oxidations directed by ketones provided many options for the subsequent steps, an important strategic consideration.

Benzylic oxidation of diketone **5-64** gave triketone **5-65**. From here, one-step hydroxylation[56] directly from the ketone were unsuccessful. As a result, triketone **5-65** was converted to the trioxime methyl ether **5-66** by treatment with $MeONH_2HCl$. The oxime ether was found to be a suitable directing group for the hydroxylation reaction installing all three hydroxy groups in the product in a single step.[57] The oximes were cleaved upon treatment with HCl giving triol **5-67** in 41% yield, which is a remarkably high yield given the 3 oxidations and directing group cleavages that occurred in a single operation. This rapid increase in oxidation clearly shows how careful synthetic planning can allow for highly efficient multiply-operative reactions. Advanced intermediate **5-67** was converted to dalesconol A (**5-68**) using a palladium catalyzed oxidation developed by Stahl[58] and coworkers to afford the natural product in a longest linear sequence of 8 steps. The reverse order of operations was attempted at this stage, i.e., desaturation prior to hydroxylation. However, no desired reactivity was observed. The researchers also highlighted the power of their strategy for late-stage diversification wherein triketone **5-65** was sulfaminated using iridium catalysis[59] to give trisulfonamide **5-70** in 84% yield. The tosyl groups were cleaved with sulfuric acid to give the aminated analogue of dalesconol A (**5-71**) in 98% yield. The ease with which they were able to prepare these analogues is a strong argument for delaying the oxidation step as late as possible into the synthesis campaign—in this way, diverse libraries can be produced in the fewest possible steps.

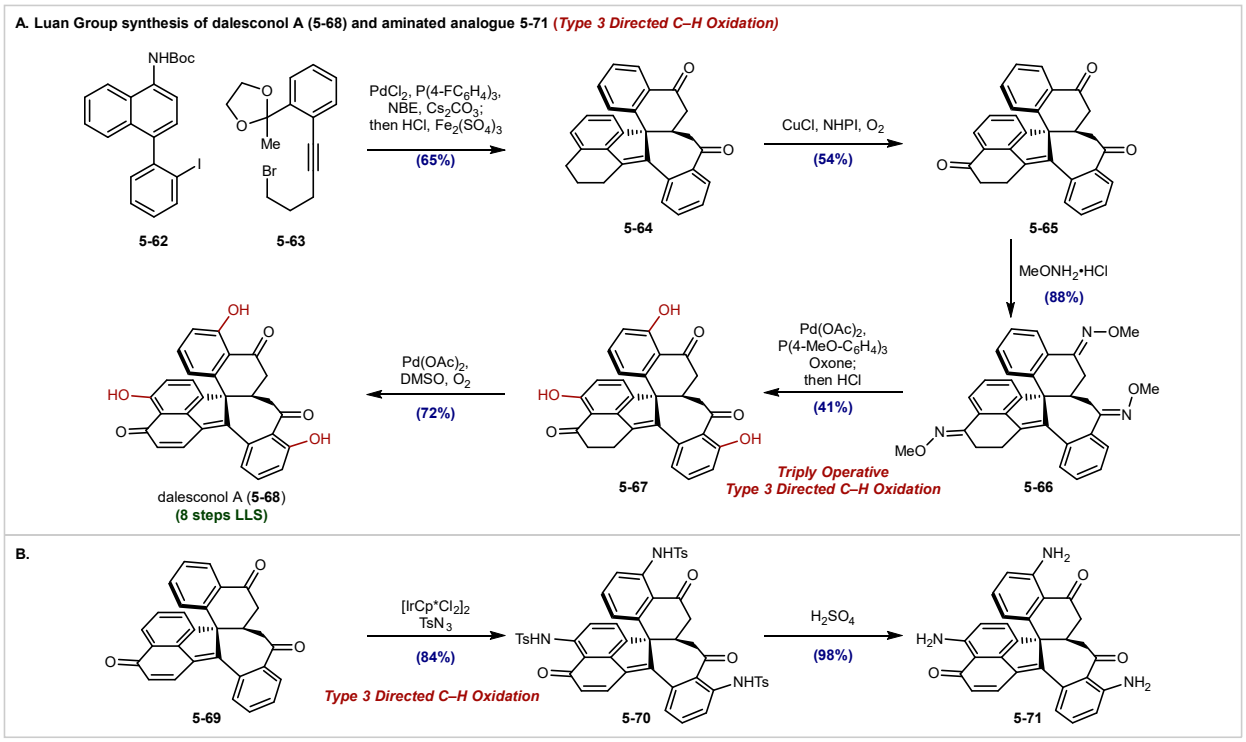

Scheme 5.6A. The Luan group's synthesis of dalesconol A featuring multiple directed Type 3 C–H oxidations in a single pot **B**. Use of Type 3 directed C – H oxidation to access dalesconal A analogues

5.4 Case study: total synthesis of longiborneol sesquiterpenoids

(Written by Dr. Robert Lusi)

A primary goal of our synthetic studies[2F,G] on the longiborneol sesquiterpenoids[60] was to showcase the power of Type 3 C–H oxidations to enable divergent syntheses of related natural products.[3H,8] Use of C–H oxidation methods in complex molecule synthesis aids the continued development of these methods. Such applications can highlight situations in which these methods are ineffective, and factors which may alter their efficacy, bringing focus to areas where further improvements are needed. Applications of these methods in complex molecule synthesis can also serve as proof-of-concept studies which demonstrate how a variety of methods can be employed to functionalize different positions on similar substrates. The longiborneol family was an ideal target for this purpose, because it features 11 natural products which differ only in the oxygenation pattern of a shared carbon scaffold. Our initial retrosynthesis (Scheme 5.7A) relied on a hypothesis that various oxidized congeners could be accessed from the parent natural product longiborneol (**5-74**), or a derivative, by judicious application of directed Type 3 C–H oxidations (see **5-75**). This key strategic decision would be coupled with a concise synthesis of longiborneol from carvone, using functionalized camphor intermediate **5-72** which was accessed with scaffold remodeling chemistry developed by our group.[61] This combination would enable

concise and divergent syntheses of many members of the natural product family. We predicted that using selective Type 3 C–H oxidations for late-stage functionalization of the longiborneol core would uniquely facilitate such a synthesis because it would enable divergence of the individual routes at the latest possible juncture, minimizing total steps. While we were unable to implement every directed Type 3 C–H oxidation depicted in **5-75**, we were able to oxidize every targeted position with a mix of directed and undirected methods.

We commenced with the synthesis of common intermediate **5-76** from (*S*)-carvone (**5-72**) in seven steps. Longiborneol (**5-79**) was synthesized from tricycle **5-76** by hydrogenation of the alkene group and dissolving metal reduction of the carbonyl group. Acetylation of the resulting hydroxy group gave acetyl longiborneol (**5-80**), which we expected would deactivate C8–H toward certain Type 3 C–H oxidations.[45] Specifically, we hypothesized that oxidation of **5-80** with TFDO or the White–Chen catalyst would result primarily in oxidation at C-4, the most sterically accessible methylene group.[40] While that selectivity would not be productive for the synthesis of any of the targeted natural products, we also predicted that we would observe products resulting from oxidation at C-11, due to strain acceleration[46B] and the fact that C-11 is the only other non-neopentyl methylene. In fact, oxidation of **5-80** with TFDO did lead to C-4 and C-11 oxidized products, but yields were low and minor side-products (oxidation at C-5 and C-3) were also observed (not pictured). Despite these shortcomings, the high overall yield of **5-80** from carvone meant that we were still able to obtain synthetically useful amounts of the C-11 oxidized products. Thus, TFDO mediated oxidation of **5-80** followed by cleavage of the acetate group yielded culmorone (**5-84**) and subsequent dissolving metal reduction gave culmorin (**5-88**).

We next investigated whether the installation of additional functionality could enable the use of the TFDO Type 3 C–H oxidation in a more selective synthesis of 5-hydroxyculmorin (**5-91**). Overall, this approach would yield two natural products. Allylic oxidation of **5-81** was used to install a hydroxy group at C-5. While this approach differed from our goal of functionalizing all positions using Type 3 C–H oxidations, we found that such reactions directed from C8 functional groups failed to target C-5 (*vide infra*), and that undirected C–H oxidations led to C-5 oxidized products in very low yield (*vide supra*). Additionally, due to the presence of an alkene group in **5-76** (formed from a Wittig reaction used to install the remainder of the carbon atoms), it was unlikely that any other C–H oxidation would be a superior tactical choice compared to allylic oxidation. Subsequent alkene hydrogenation and carbonyl reduction gave 5-hydroxylongiborneol (**5-85**). Acetylation of both hydroxy groups furnished **5-89** which we predicted would undergo selective TFDO mediated oxidation at C11, due to the inductively electron-withdrawing C-5 acetate deactivating C-5, C-4, and C-3. Indeed, C-11 ketone **5-90** proved to be the only observed product of this undirected Type 3 C–H oxidation, and treatment with dissolving metal conditions cleaved both acetate esters and reduced the carbonyl group to give 5-hydroxyculmorin (**5-91**).

We used directed Type 3 oxidations to target additional positions on the longiborneol skeleton. Hydrogenation of **5-76** followed by reduction of the carbonyl group with $LiAlH_4$ gave C8-*epi*-longiborneol. Treatment with dimethylchlorosilane yielded **5-77**. The (hydrido)silyl ether

group of **5-77** was then used to direct a Hartwig silylation of C12 via iridacycle **5-78**.[62] Tamao–Fleming oxidation of the resulting silacycle gave C-8-*epi*-12-hydroxylongiborneol which was converted to the natural product (**5-79**) by DMP oxidation of both hydroxy groups and reduction of the resulting carbonyls. Attempts to implement a similar synthetic sequence from longiborneol (**5-74**) were ineffective, likely due to an unfavorable geometric relationship between the corresponding (hydrido)silyl ether and the C12 methyl group. This outcome highlights the effects of conformation as well as the relative positions of a directing functional group and the C–H bond being targeted for oxidation,[63] a subtlety which is often not apparent or as pronounced in simpler substrates.

Similarly, our attempts to oxidize C-15 using a Type 3 C–H oxidation directed by a functional group at C-8 were also ineffective. Attempts to employ **5-77** in a Rh-catalyzed Hartwig silylation,[64] known to favor 1,4 functionalization in some cases, led only to C-12 functionalization, likely due to a lack of steric differentiation between C-12 and C-15. An attempted Suarez reaction from C-8-*epi*-longiborneol (not pictured) led to a complex mixture, possibly due to competitive β-scission of the [2.2.1]bicycle.[65] Again, these challenges highlight the need to consider many substrate characteristics—such as relative steric encumbrance and strain energy—when employing C–H oxidation chemistry on complex molecules. As an alternative, we devised a relay oxidation strategy[66] where a functional group installed at C-5 was used to direct the oxidations of C-14 and C-15. To implement this strategy, we synthesized acetyl oxime **5-81** in six steps from common intermediate **5-76**. Treatment of **5-81** with Pd(OAc)2 and sub-stoichiometric quantities of PIDA resulted in a directed Type 3 C–H oxidation of both C-14 and C-15 to give **5-83** as a 2:1 inseparable mixture of diastereomers,[67] favoring the C-14 oxidized product. Reductive cleavage of the oxime,[68] installation of a tosyl hydrazone group, and a $LiAlH_4$ mediated Caglioti reaction led to a separable mixture of the natural products 14-hydroxylongiborneol (**5-86**) and 15-hydroxylongiborneol (**5-87**).

The studies described above provide useful insight into the application of the Sanford acetoxylation chemistry. First, difficulties encountered in installing an oxime on **5-76**, to functionalize C12, indicate that the steric environment of the ketone precursor must be carefully considered. Second, while reactions similar to **5-82** → **5-83** were effective with the methoxime directing group originally employed by Sanford and coworkers[67] we found that methoxime hydrolysis was difficult, leading to degradation and incomplete conversion. Examples of successful methoxime cleavage in complex molecule synthesis generally require harsh, acidic conditions[69] and few other conditions for their cleavage have been reported.[70] Conversely, the one-pot procedure used in our work[2B,I] allows installation of an acetyl oxime in a single step, which can be cleaved under milder conditions.[71] Finally, **5-82** → **5-83** required sub-stoichiometric PIDA to slow the formation of products acetylated at C-14 and C-15. Potential formation of such bis-acetoxylation products must be considered if targeting a single oxidation of a gem-dimethyl group. While conformational rigidity of the substrate may confer selectivity, more flexible substrates could lead to bis-acetoxylation.

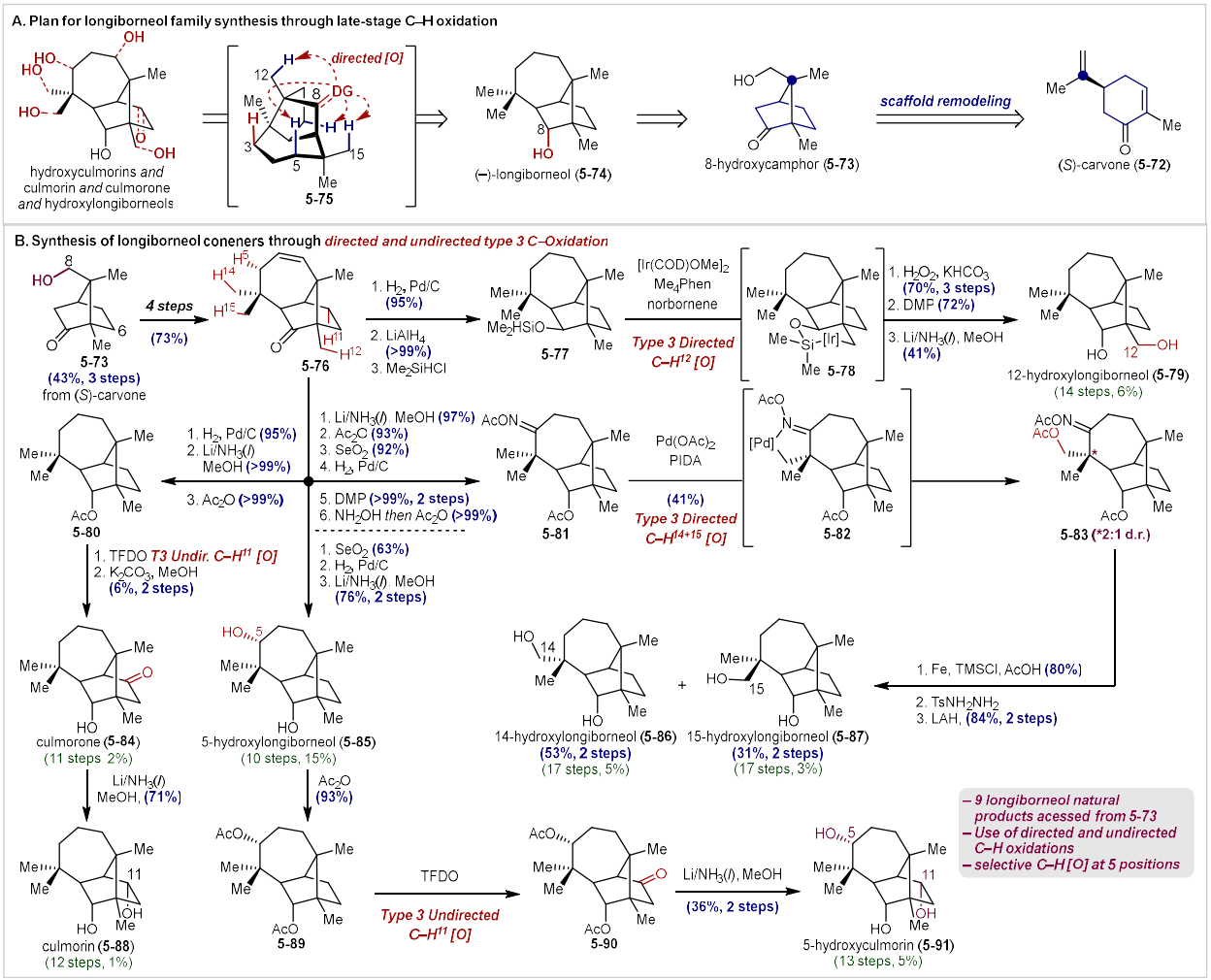

Scheme 5.7A. Two-phase retrosynthesis of longiborneol (**5-74**) sesquiterpenoids **B**. Synthesis of seven congeners using both directed and undirected Type 3 C–H oxidations

In summary, we were able to use a diverse array of Type 3 C–H oxidations to access seven oxidized longiborneol congeners, which collectively feature oxidation at five distinct sites on the natural product skeleton. Our use of C–H oxidation chemistry enabled each of these syntheses to begin from common intermediate **5-76**, which features the complete skeleton and only two functional groups. This strategy of using a minimally functionalized scaffold and applying divergent oxidation reactions to synthesize an array of targets fits squarely into the canon of "two-phase" synthesis and shows its profound utility. In general, this work reflects the synthetic promise of Type 3 oxidations: they can enable the synthesis of diverse targets through the late-stage diversification of synthetically advanced common intermediates with succinct functionalization sequences.

5.6 Conclusion and outlook

Strategies for total synthesis that rely on C–H oxidation are continuing to emerge and are having significant impact. In recent years, there has been an explosion in the number of syntheses that incorporate C–H functionalization at the synthesis planning stage from the outset. We highlighted eight examples just from the last three years that utilize C–H oxidation to build the core of a target molecule. These functionalizations were sub-divided into either carbocyclic (Type 1) or heterocyclic (Type 2) families or those that install oxidation on the periphery (Type 3) of an intermediate en route to a target molecule.

Latent C–H bonds are now routinely viewed as potential functional groups. This emerging consideration has huge implications on how we disconnect molecules. Here, we have proposed a framework that classifies the different strategic uses of oxidation and showed examples of syntheses that leverage oxidation in a variety of ways. Type 1 C–H oxidations have been particularly effective in bioinspired syntheses by facilitating access to biosynthesis-like carbocations that undergo productive rearrangements. The major strategic advantage here, other than mimicking nature's reactions, is the expanded realm of choices of starting materials. Renata, Herestch, and Deng all show examples of efficient syntheses where little to no effort is expended in building the carbon skeleton because of the power of C–H oxidation to advance a readily available advanced intermediate. Beyond their applications in semi-synthesis, Type 1 oxidations will have the power to transform chiral feedstocks into more complex building blocks through oxidation then C–C bond formation or C–C bond deletion.

Directed Type 2 C–H oxidations have possibly seen the most use in recent years owing to the powerful methodologies we have to effect this subset of C–H oxidation. New disconnections for the lactone and ether linkages commonly seen in higher oxidation-level terpenes have been enabled by developments in alcohol and carboxylate directed oxidation. Zhang and coworkers showcased the versatility of desaturation as a means to achieve divergent syntheses. Ultimately, these later-stage oxidations build the structural complexity of the molecule while also minimizing functional group interconversion and protecting group manipulations. Further developments in this area will go hand-in-hand with developments in undirected C–H oxidation as directed oxidations are quite well-developed. Advances in biocatalysis and supramolecular systems can impart site-selectivity that is complementary to that achievable through substrate control. Zhang and coworkers' BDE and solvent effect analysis demonstrated how selectivity in undirected C–H oxidation can be understood and manipulated and showcased how these reactions can be efficiently incorporated into synthesis planning.

Type 3 oxidations hold the ultimate promise of late-stage functionalization. Similar to the subset of oxidation types described above, developments in this area will be contingent on our understanding of undirected C–H oxidation. Methodological advances in remote functionalization have expanded the realm of undirected C–H oxidation considerably, but many of these have yet to be utilized in total synthesis. Advances in the use of transient directing groups

and sophisticated catalyst systems can help obviate some of the step inefficiencies that arise from installing and removing directing groups. Together, these two developments have long-reaching impacts beyond natural product synthesis in the generation of libraries of lead derivatives, for example, in the pharmaceutical industry.

Taken together, we hope this framework for characterizing C–H oxidation reactions in complex molecule synthesis and the accompanying case studies gives the reader some insight into the emerging use of C–H oxidations in total synthesis. Importantly, we hope to have highlighted the reactions that are currently most effectively applied in synthesis, and provided a possible path into their future development.

5.7 References

(1) (a) Abrams, D. J.; Provencher, P. A.; Sorensen, E. J. Recent Applications of C–H Functionalization in Complex Natural Product Synthesis. *Chem. Soc. Rev.* **2018**, *47*, 8925–8967. (b) Chen, D. Y.-K.; Youn, S. W. C–H Activation: A Complementary Tool in the Total Synthesis of Complex Natural Products. *Eur. J. Chem.* **2012**, *18*, 9452–9474. (c) Christmann, M. Selective Oxidation of Aliphatic C–H Bonds in the Synthesis of Complex Molecules. *Angew. Chem. Int. Ed* **2008**, *47*, 2740–2742. (d) Gutekunst, W. R.; Baran, P. S. C–H Functionalization Logic in Total Synthesis. *Chem. Soc. Rev.* **2011**, *40*, 1976–1991. (e)Karimov, R. R.; Hartwig, J. F. Transition-Metal-Catalyzed Selective Functionalization of C(Sp3)−H Bonds in Natural Products. *Angew. Chem. Int. Ed.* **2018**, *57*, 4234–4241. (f) McMurray, L.; O'Hara, F.; Gaunt, M. J. Recent Developments in Natural Product Synthesis Using Metal-Catalysed C–H Bond Functionalisation. *Chem. Soc. Rev.* **2011**, *40*, 1885–1898. (g) Newhouse, T.; Baran, P. S. If C–H Bonds Could Talk: Selective C–H Bond Oxidation. *Angew. Chem. Int. Ed.* **2011**, *50*, 3362–3374. (h) Qiu, Y.; Gao, S. Trends in Applying C–H Oxidation to the Total Synthesis of Natural Products. *Nat. Prod. Rep.* **2016**, *33*, 562–581. (i) Santana, V. C. S.; Fernandes, M. C. V.; Cappuccelli, I.; Richieri, A. C. G.; Jr, E. C. de L. Metal-Catalyzed C–H Bond Oxidation in the Total Synthesis of Natural and Unnatural Products. *Synthesis* **2022**, *54*, 5537–5359.

(2) (a) Fischer, D. F.; Sarpong, R. Total Synthesis of (+)-Complanadine A Using an Iridium-Catalyzed Pyridine C−H Functionalization. *J. Am. Chem. Soc.* **2010**, *132*, 5926–5927. (b) Haider, M.; Sennari, G.; Eggert, A.; Sarpong, R. Total Synthesis of the *Cephalotaxus* Norditerpenoids (±)-Cephanolides A–D. *J. Am. Chem. Soc.* **2021**, *143*, 2710–2715. (c) Haley, H. M. S.; Payer, S. E.; Papidocha, S. M.; Clemens, S.; Nyenhuis, J.; Sarpong, R. Bioinspired Diversification Approach Toward the Total Synthesis of Lycodine-Type Alkaloids. *J. Am. Chem. Soc.* **2021**, *143*, 4732–4740. (d) Jones, K. E.; Park, B.; Doering, N. A.; Baik, M.-H.; Sarpong, R. Rearrangements of the Chrysanthenol Core: Application to a Formal Synthesis of Xishacorene B. *J. Am. Chem. Soc.* **2021**, *143*, 20482–20490. (e) Leal, R. A.; Bischof, C.; Lee, Y. V.; Sawano, S.; McAtee, C. C.; Latimer, L. N.; Russ, Z. N.; Dueber, J. E.; Yu, J.-Q.; Sarpong, R. Application of a Palladium-Catalyzed C−H Functionalization/Indolization Method to Syntheses of Cis-Trikentrin A and Herbindole B. *Angew.*

Chem. Int. Ed. **2016**, *55*, 11824–11828. (f) Lusi, R. F.; Sennari, G.; Sarpong, R. Total Synthesis of Nine Longiborneol Sesquiterpenoids Using a Functionalized Camphor Strategy. *Nat. Chem.* **2022**, *14*, 450–456. (g) Lusi, R. F.; Sennari, G.; Sarpong, R. Strategy Evolution in a Skeletal Remodeling and C–H Functionalization-Based Synthesis of the Longiborneol Sesquiterpenoids. *J. Am. Chem. Soc.* **2022**, *144*, 17277–17294. (h) Newton, J. N.; Fischer, D. F.; Sarpong, R. Synthetic Studies on Pseudo-Dimeric Lycopodium Alkaloids: Total Synthesis of Complanadine B. *Angew. Chem. Int. Ed.* **2013**, *52*, 1726–1730. (i) Sennari, G.; Gardner, K. E.; Wiesler, S.; Haider, M.; Eggert, A.; Sarpong, R. Unified Total Syntheses of Benzenoid Cephalotane-Type Norditerpenoids: Cephanolides and Ceforalides. *J. Am. Chem. Soc.* **2022**, *144*, 19173–19185. (j) West, S. P.; Bisai, A.; Lim, A. D.; Narayan, R. R.; Sarpong, R. Total Synthesis of (+)-Lyconadin A and Related Compounds via Oxidative C−N Bond Formation. *J. Am. Chem. Soc.* **2009**, *131*, 11187–11194.

(3) (a) Bellina, F.; Rossi, R. Transition Metal-Catalyzed Direct Arylation of Substrates with Activated Sp3-Hybridized C−H Bonds and Some of Their Synthetic Equivalents with Aryl Halides and Pseudohalides. *Chem. Rev.* **2010**, *110*, 1082–1146. (b) Che, C.-M.; Lo, V. K.-Y.; Zhou, C.-Y.; Huang, J.-S. Selective Functionalisation of Saturated C–H Bonds with Metalloporphyrin Catalysts. *Chem. Soc. Rev.* **2011**, *40*, 1950. (c) Gensch, T.; N. Hopkinson, M.; Glorius, F.; Wencel-Delord, J. Mild Metal-Catalyzed C–H Activation: Examples and Concepts. *Chem. Soc. Rev.* **2016**, *45*, 2900–2936. (d) Guo, X.-X.; Gu, D.-W.; Wu, Z.; Zhang, W. Copper-Catalyzed C–H Functionalization Reactions: Efficient Synthesis of Heterocycles. *Chem. Rev.* **2015**, *115*, 1622–1651. (e) Hartwig, J. F. Catalyst-Controlled Site-Selective Bond Activation. *Acc. Chem. Res.* **2017**, *50*, 549–555. (f) Lu, H.; Zhang, X. P. Catalytic C–H Functionalization by Metalloporphyrins: Recent Developments and Future Directions. *Chem. Soc. Rev.* **2011**, *40*, 1899–1909. (g) Sun, C.-L.; Li, B.-J.; Shi, Z.-J. Direct C−H Transformation via Iron Catalysis. *Chem. Rev.* **2011**, *111*, 1293–1314. (h) White, M. C.; Zhao, J. Aliphatic C–H Oxidations for Late-Stage Functionalization. *J. Am. Chem. Soc.* **2018**, *140*, 13988–14009. (i) Yamaguchi, J.; Yamaguchi, A. D.; Itami, K. C–H Bond Functionalization: Emerging Synthetic Tools for Natural Products and Pharmaceuticals. *Angew. Chem. Int. Ed.* **2012**, *51*, 8960–9009. (j) Zhou, M.; Crabtree, R. H. C–H Oxidation by Platinum Group Metal Oxo or Peroxo Species. *Chem. Soc. Rev.* **2011**, *40*, 1875.

(4) (a) Green, S. A.; Crossley, S. W. M.; Matos, J. L. M.; Vásquez-Céspedes, S.; Shevick, S. L.; Shenvi, R. A. The High Chemofidelity of Metal-Catalyzed Hydrogen Atom Transfer. *Acc. Chem. Res.* **2018**, *51*, 2628–2640. (b) King, S. M.; Herzon, S. B. Substrate-Modified Functional Group Reactivity: Hasubanan and Acutumine Alkaloid Syntheses. *J. Org. Chem.* **2014**, *79*, 8937–8947. (c) Trost, B. M. Selectivity: A Key to Synthetic Efficiency. *Science* **1983**, *219*, 245–250.

(5) (a) Ishihara, Y.; Baran, P. S. Two-Phase Terpene Total Synthesis: Historical Perspective and Application to the Taxol® Problem. *Synlett* **2010**, *2010*, 1733–1745. (b) Kanda, Y.; Nakamura, H.; Umemiya, S.; Puthukanoori, R. K.; Murthy Appala, V. R.; Gaddamanugu, G. K.; Paraselli, B. R.;

Baran, P. S. Two-Phase Synthesis of Taxol. *J. Am. Chem. Soc.* **2020**, *142*, 10526–10533. (c) Two-Phase Total Synthesis of Taxanes: Tactics and Strategies. *J. Org. Chem* **2020**, *85*, 10293–10320.

(6) Hung, K.; Condakes, M. L.; Novaes, L. F. T.; Harwood, S. J.; Morikawa, T.; Yang, Z.; Maimone, T. J. Development of a Terpene Feedstock-Based Oxidative Synthetic Approach to the Illicium Sesquiterpenes. *J. Am. Chem. Soc.* **2019**, *141*, 3083–3099.

(7) (a) Breslow, R. Biomimetic Control of Chemical Selectivity. *Acc. Chem. Res* **1980**, 8. (b) Gandeepan, P.; Ackermann, L. Transient Directing Groups for Transformative C–H Activation by Synergistic Metal Catalysis. *Chem* **2018**, *4*, 199–222. (c) Lyons, T. W.; Sanford, M. S. Palladium-Catalyzed Ligand-Directed C−H Functionalization Reactions. *Chem. Rev.* **2010**, *110*, 1147–1169. (d) Mo, F.; Tabor, J. R.; Dong, G. Alcohols or Masked Alcohols as Directing Groups for C–H Bond Functionalization. *Chem. Lett.* **2014**, *43*, 264–271. (e) Murali, K.; Machado, L. A.; Carvalho, R. L.; Pedrosa, L. F.; Mukherjee, R.; Da Silva Júnior, E. N.; Maiti, D. Decoding Directing Groups and Their Pivotal Role in C−H Activation. *Eur. J. Chem.* **2021**, *27*, 12453–12508.

(8) Hartwig, J. F.; Larsen, M. A. Undirected, Homogeneous C–H Bond Functionalization: Challenges and Opportunities. *ACS Cent. Sci.* **2016**, *2*, 281–292.

(9) (a) Brill, Z. G.; Condakes, M. L.; Ting, C. P.; Maimone, T. J. Navigating the Chiral Pool in the Total Synthesis of Complex Terpene Natural Products. *Chem. Rev.* **2017**, *117*, 11753–11795. (b) Stout, C. N.; Renata, H. Reinvigorating the Chiral Pool: Chemoenzymatic Approaches to Complex Peptides and Terpenoids. *Acc. Chem. Res.* **2021**, *54*, 1143–1156.

(10) Zhang, X.; King-Smith, E.; Dong, L.-B.; Yang, L.-C.; Rudolf, J. D.; Shen, B.; Renata, H. Divergent Synthesis of Complex Diterpenes through a Hybrid Oxidative Approach. *Science* **2020**, *369*, 799–806.

(11) Hong, Y. J.; Tantillo, D. J. Formation of Beyerene, Kaurene, Trachylobane, and Atiserene Diterpenes by Rearrangements That Avoid Secondary Carbocations. *J. Am. Chem. Soc.* **2010**, *132*, 5375–5386.

(12) Li, C.; Lee, D.; Graf, T. N.; Phifer, S. S.; Nakanishi, Y.; Burgess, J. P.; Riswan, S.; Setyowati, F. M.; Saribi, A. M.; Soejarto, D. D.; Farnsworth, N. R.; Falkinham, J. O.; Kroll, D. J.; Kinghorn, A. D.; Wani, M. C.; Oberlies, N. H. A Hexacyclic Ent-Trachylobane Diterpenoid Possessing an Oxetane Ring from Mitrephora Glabra. *Org. Lett.* **2005**, *7*, 5709–5712.

(13) (a) Groves, J. T.; McClusky, G. A.; White, R. E.; Coon, M. J. Aliphatic Hydroxylation by Highly Purified Liver Microsomal Cytochrome P-450. Evidence for a Carbon Radical Intermediate. *Biochem. Biophys. Res. Commun.* **1978**, *81*, 154–160. (b) Loskot, S. A.; Romney, D. K.; Arnold, F. H.; Stoltz, B. M. Enantioselective Total Synthesis of Nigelladine A via Late-Stage C–H Oxidation Enabled by an Engineered P450 Enzyme. *J. Am. Chem. Soc.* **2017**, *139*, 10196–10199. (c) Sheldon, R. A.; Brady, D.; Bode, M. L. The Hitchhiker's Guide to Biocatalysis: Recent Advances in the Use of

Enzymes in Organic Synthesis. *Chem. Sci.* **2020**, *11*, 2587–2605. (d) Winkler, C. K.; Schrittwieser, J. H.; Kroutil, W. Power of Biocatalysis for Organic Synthesis. *ACS Cent. Sci.* **2021**, *7*, 55–71.

(14) (a) Arnold, F. H. Directed Evolution: Bringing New Chemistry to Life. *Angew. Chem. Int. Ed.* **2018**, *57*, 4143–4148. (b) Wang, Y.; Xue, P.; Cao, M.; Yu, T.; Lane, S. T.; Zhao, H. Directed Evolution: Methodologies and Applications. *Chem. Rev.* **2021**, *121*, 12384–12444. (15) (a) Dong, L.-B.; Zhang, X.; Rudolf, J. D.; Deng, M.-R.; Kalkreuter, E.; Cepeda, A. J.; Renata, H.; Shen, B. Cryptic and Stereospecific Hydroxylation, Oxidation, and Reduction in Platensimycin and Platencin Biosynthesis. *J. Am. Chem. Soc.* **2019**, *141*, 4043–4050. (b) Rudolf, J. D.; Dong, L.-B.; Zhang, X.; Renata, H.; Shen, B. Cytochrome P450-Catalyzed Hydroxylation Initiating Ether Formation in Platensimycin Biosynthesis. *J. Am. Chem. Soc.* **2018**, *140*, 12349–12353.

(16) (a) Richter, M. J. R.; Schneider, M.; Brandstätter, M.; Krautwald, S.; Carreira, E. M. Total Synthesis of (−)-Mitrephorone A. *J. Am. Chem. Soc.* **2018**, *140*, 16704–16710. (b) Wein, L. A.; Wurst, K.; Angyal, P.; Weisheit, L.; Magauer, T. Synthesis of (−)-Mitrephorone A via a Bioinspired Late Stage C–H Oxidation of (−)-Mitrephorone B. *J. Am. Chem. Soc.* **2019**, *141*, 19589–19593.

(17) (a) Alekseychuk, M.; Adrian, S.; Heinze, R. C.; Heretsch, P. Biogenesis-Inspired, Divergent Synthesis of Spirochensilide A, Spirochensilide B, and Abifarine B Employing a Radical-Polar Crossover Rearrangement Strategy. *J. Am. Chem. Soc.* **2022**, *144*, 11574–11579. (b) Long, X.; Li, J.; Gao, F.; Wu, H.; Deng, J. Bioinspired Synthesis of Spirochensilide A from Lanosterol. *J. Am. Chem. Soc.* **2022**, *144*, 16292–16297.

(18) Long, X.; Li, J.; Gao, F.; Wu, H.; Deng, J. Bioinspired Synthesis of Spirochensilide A from Lanosterol. *J. Am. Chem. Soc.* **2022**, *144*, 16292–16297.

(19) Zhao, Q.-Q.; Song, Q.-Y.; Jiang, K.; Li, G.-D.; Wei, W.-J.; Li, Y.; Gao, K. Spirochensilides A and B, Two New Rearranged Triterpenoids from Abies Chensiensis. *Org. Lett.* **2015**, *17*, 2760–2763.

(20) Wappes, E. A.; Fosu, S. C.; Chopko, T. C.; Nagib, D. A. Triiodide-Mediated δ-Amination of Secondary C−H Bonds. *Angew. Chem. Int. Ed.* **2016**, *55*, 9974–9978.

(21) Liang, X.-T.; Chen, J.-H.; Yang, Z. Asymmetric Total Synthesis of (−)-Spirochensilide A. *J. Am. Chem. Soc.* **2020**, *142*, 8116–8121.

(22) (a) Kasuya, S.; Kamijo, S.; Inoue, M. Direct Construction of 1,3-Diaxial Diol Derivatives by C−H Hydroxylation. *Org. Lett.* **2009**, *11*, 3630–3632.

(b) Wong, M.-K.; Chung, N.-W.; He, L.; Yang, D. Substituent Effects on Regioselective Intramolecular Oxidation of Unactivated C−H Bonds: Stereoselective Synthesis of Substituted Tetrahydropyrans. *J. Am. Chem. Soc.* **2003**, *125*, 158–162.

(c) Wong, M.-K.; Chung, N.-W.; He, L.; Wang, X.-C.; Yan, Z.; Tang, Y.-C.; Yang, D. Investigation on the Regioselectivities of Intramolecular Oxidation of Unactivated C−H Bonds by Dioxiranes Generated in Situ. *J. Org. Chem.* **2003**, *68*, 6321–6328.

(d) Yang, D.; Wong, M.-K.; Wang, X.-C.; Tang, Y.-C. Regioselective Intramolecular Oxidation of Unactivated C−H Bonds by Dioxiranes Generated in Situ. *J. Am. Chem. Soc.* **1998**, *120*, 6611–6612.

(23) (a) Fukuyama, Y.; Huang, J.-M. Chemistry and Neurotrophic Activity of Seco-Prezizaane- and Anislactone-Type Sesquiterpenes from Illicium Species. In *Studies in Natural Products Chemistry*; Atta-ur-Rahman, Ed.; Bioactive Natural Products (Part L); Elsevier, 2005; pp 395–427. (b) Lane, J. F.; Koch, W. T.; Leeds, N. S.; Gorin, G. On the Toxin of Illicium Anisatum. I. The Isolation and Characterization of a Convulsant Principle: Anisatin1. *J. Am. Chem. Soc.* **1952**, *74*, 3211–3215.

(24) Martín, A.; Pérez-Martín, I.; Suárez, E. Intramolecular Hydrogen Abstraction Promoted by Amidyl Radicals. Evidence for Electronic Factors in the Nucleophilic Cyclization of Ambident Amides to Oxocarbenium Ions. *Org. Lett.* **2005**, *7*, 2027–2030.

(25) Chen, M. S.; White, M. C. A Predictably Selective Aliphatic C–H Oxidation Reaction for Complex Molecule Synthesis. *Science* **2007**, *318*, 783–787.

(26) (a) Condakes, M. L.; Hung, K.; Harwood, S. J.; Maimone, T. J. Total Syntheses of (−)-Majucin and (−)-Jiadifenoxolane A, Complex Majucin-Type Illicium Sesquiterpenes. *J. Am. Chem. Soc.* **2017**, *139*, 17783–17786. (b) Condakes, M. L.; Novaes, L. F. T.; Maimone, T. J. Contemporary Synthetic Strategies toward Seco-Prezizaane Sesquiterpenes from Illicium Species. *J. Org. Chem.* **2018**, *83*, 14843–14852.

(27) Shen, Y.; Li, L.; Xiao, X.; Yang, S.; Hua, Y.; Wang, Y.; Zhang, Y.; Zhang, Y. Site-Specific Photochemical Desaturation Enables Divergent Syntheses of Illicium Sesquiterpenes. *J. Am. Chem. Soc.* **2021**, *143*, 3256–3263.

(28) Johnson, J. A.; Li, N.; Sames, D. Total Synthesis of (−)-Rhazinilam: Asymmetric C−H Bond Activation via the Use of a Chiral Auxiliary. *J. Am. Chem. Soc.* **2002**, *124*, 6900–6903.

(29) (a) Camelio, A. M.; Barton, T.; Guo, F.; Shaw, T.; Siegel, D. Hydroxyl-Directed Cyclizations of 1,6-Enynes. *Org. Lett.* **2011**, *13*, 1517–1519. (b) Marco-Martínez, J.; López-Carrillo, V.; Buñuel, E.; Simancas, R.; Cárdenas, D. J. Pd-Catalyzed Borylative Cyclization of 1,6-Enynes. *J. Am. Chem. Soc.* **2007**, *129*, 1874–1875.

(30) Berkessel, A.; Adrio, J. A.; Hüttenhain, D.; Neudörfl, J. M. Unveiling the “Booster Effect” of Fluorinated Alcohol Solvents: Aggregation-Induced Conformational Changes and Cooperatively Enhanced H-Bonding. *J. Am. Chem. Soc.* **2006**, *128*, 8421–8426.

(31) Huang, J.; Yokoyama, R.; Yang, C.; Fukuyama, Y. Merrilactone A, a Novel Neurotrophic Sesquiterpene Dilactone from Illicium Merrillianum. *Tetrahedron Lett.* **2000**, *41*, 6111–6114.

(32) Kouno, I.; Mori, K.; Okamoto, S.; Sato, S. Structures of Anislactone A and B; Novel Type of Sesquiterpene Lactones from the Pericarps of Illicium Anisatum. *Chem. Pharm. Bull.* **1990**, *38*, 3060–3063.

(33) (a) Chen, J.; Gao, P.; Yu, F.; Yang, Y.; Zhu, S.; Zhai, H. Total Synthesis of (±)-Merrilactone A. *Angew. Chem. Int. Ed.* **2012**, *51*, 5897–5899. (b) Inoue, M.; Sato, T.; Hirama, M. Asymmetric Total Synthesis of (−)-Merrilactone A: Use of a Bulky Protecting Group as Long-Range Stereocontrolling Element. *Angew. Chem. Int. Ed.* **2006**, *45*, 4843–4848.

(34) (a) Breslow, R.; Baldwin, S.; Flechtner, T.; Kalicky, P.; Liu, S.; Washburn, W. Remote Oxidation of Steroids by Photolysis of Attached Benzophenone Groups. *J. Am. Chem. Soc.* **1973**, *95*, 3251–3262. (b) Barton, D. H. R.; Beaton, J. M. A Synthesis of Aldosterone Acetate. *J. Am. Chem. Soc.* **1960**, *82*, 2641–2641.

(35) Huang, J.-M.; Yang, C.-S.; Tanaka, M.; Fukuyama, Y. Structures of Merrilactones B and C, Novel Anislactone-Type Sesquiterpenes from Illicium Merrillianum, and Chemical Conversion of Anislactone B to Merrilactone A. *Tetrahedron* **2001**, *57*, 4691–4698.

(36) Crossley, S. W. M.; Tong, G.; Lambrecht, M. J.; Burdge, H. E.; Shenvi, R. A. Synthesis of (−)-Picrotoxinin by Late-Stage Strong Bond Activation. *J. Am. Chem. Soc.* **2020**, *142*, 11376–11381.

(37) Porter, L. A. Picrotoxinin and Related Substances. *Chem. Rev.* **1967**, *67*, 441–464.

(38) (a) Cao, J.; Thor, W.; Yang, S.; Zhang, M.; Bao, W.; Zhu, L.; Yang, W.; Cheng, Y.-K.; Lee, C.-S. Synthesis of the Tricyclic Picrotoxane Motif by an Oxidative Cascade Cyclization. *Org. Lett.* **2019**, *21*, 4896–4899. (b) Corey, E. J.; Pearce, H. L. Total Synthesis of Picrotoxinin. *J. Am. Chem. Soc.* **1979**, *101*, 5841–5843. (c) Corey, E. J.; Pearce, H. L. Total Synthesis of Picrotin. *Tetrahedron Lett.* **1980**, *21*, 1823–1824. (d) Miyashita, M.; Suzuki, T.; Yoshikoshi, A. Stereoselective Total Synthesis of (-)-Picrotoxinin and (-)-Picrotin. *J. Am. Chem. Soc.* **1989**, *111*, 3728–3734.(e) Niwa, H.; Wakamatsu, K.; Hida, T.; Niiyama, K.; Kigoshi, H.; Yamada, M.; Nagase, H.; Suzuki, M.; Yamada, K. Stereocontrolled Total Synthesis (-)-Picrotoxinin and (+)-Coriamyrtin via a Common Isotwistane Intermediate. *J. Am. Chem. Soc.* **1984**, *106*, 4547–4552. (f) Trost, B.; Krische, M. J. Palladium-Catalyzed Enyne Cycloisomerization Reaction in an Asymmetric Approach to the Picrotoxane Sesquiterpenes. 2. Second-Generation Total Syntheses of Corianin, Picrotoxinin, Picrotin, and Methyl Picrotoxate. *J. Am. Chem. Soc.* **1999**, *121*, 6131–6141. (g)

Trost, B. M.; Haffner, C. D.; Jebaratnam, D. J.; Krische, M. J.; Thomas, A. P. The Palladium-Catalyzed Enyne Cycloisomerization Reaction in a General Approach to the Asymmetric Syntheses of the Picrotoxane Sesquiterpenes. Part I. First-Generation Total Synthesis of Corianin and Formal Syntheses of Picrotoxinin and Picrotin. *J. Am. Chem. Soc.* **1999**, *121*, 6183–6192. (h) Trost, B. M.; Krische, M. J. General Strategy for the Asymmetric Synthesis of the Picrotoxanes. *J. Am. Chem. Soc.* **1996**, *118*, 233–234.

(39) (a) Hong, B.; Luo, T.; Lei, X. Late-Stage Diversification of Natural Products. *ACS Cent. Sci.* **2020**, *6*, 622–635. (b) Kim, K. E.; Kim, A. N.; McCormick, C. J.; Stoltz, B. M. Late-Stage Diversification: A Motivating Force in Organic Synthesis. *J. Am. Chem. Soc.* **2021**, *143*, 16890–16901.

(40) Gormisky, P. E.; White, M. C. Catalyst-Controlled Aliphatic C–H Oxidations with a Predictive Model for Site-Selectivity. *J. Am. Chem. Soc.* **2013**, *135*, 14052–14055.

(41) Oeschger, R.; Su, B.; Yu, I.; Ehinger, C.; Romero, E.; He, S.; Hartwig, J. Diverse Functionalization of Strong Alkyl C–H Bonds by Undirected Borylation. *Science* **2020**, *368*, 736–741.

(42) Carestia, A. M.; Ravelli, D.; Alexanian, E. J. Reagent-Dictated Site Selectivity in Intermolecular Aliphatic C–H Functionalizations Using Nitrogen-Centered Radicals. *Chem. Sci.* **2018**, *9*, 5360–5365.

(43) Fraga, B. M. The Trachylobane Diterpenes. *Phytochem. Anal.* **1994**, *5*, 49–56.

(44) Wein, L. A.; Wurst, K.; Magauer, T. Total Synthesis and Late-Stage C−H Oxidations of Ent-Trachylobane Natural Products. *Angew. Chem. Int. Ed.* **2022**, *61*, e202113829.

(45) Chen, M. S.; White, M. C. Combined Effects on Selectivity in Fe-Catalyzed Methylene Oxidation. *Science* **2010**, *327*, 566–571.

(46) (a) Bovicelli, P.; Lupattelli, P.; Mincione, E.; Prencipe, T.; Curci, R. Oxidation of Natural Targets by Dioxiranes. 2. Direct Hydroxylation at the Side Chain C-25 of Cholestane Derivatives and of Vitamin D3 Windaus-Grundmann Ketone. *J. Org. Chem.* **1992**, *57*, 5052–5054. (b) Zou, L.; Paton, R. S.; Eschenmoser, A.; Newhouse, T. R.; Baran, P. S.; Houk, K. N. Enhanced Reactivity in Dioxirane C–H Oxidations via Strain Release: A Computational and Experimental Study. *J. Org. Chem.* **2013**, *78*, 4037–4048.

(47) Kawamata, Y.; Yan, M.; Liu, Z.; Bao, D.-H.; Chen, J.; Starr, J. T.; Baran, P. S. Scalable, Electrochemical Oxidation of Unactivated C–H Bonds. *J. Am. Chem. Soc.* **2017**, *139*, 7448–7451.

(48) Wang, C.; Shalyaev, K. V.; Bonchio, M.; Carofiglio, T.; Groves, J. T. Fast Catalytic Hydroxylation of Hydrocarbons with Ruthenium Porphyrins. *Inorg. Chem.* **2006**, *45*, 4769–4782.

(49) Vicens, L.; Bietti, M.; Costas, M. General Access to Modified α-Amino Acids by Bioinspired Stereoselective γ-C−H Bond Lactonization. *Angew. Chem. Int. Ed.* **2021**, *60*, 4740–4746.

(50) Chen, K.; Baran, P. S. Total Synthesis of Eudesmane Terpenes by Site-Selective C–H Oxidations. *Nature* **2009**, *459*, 824–828.

(51) Zhao, P.; Guo, Y.; Luan, X. Total Synthesis of Dalesconol A by Pd(0)/Norbornene-Catalyzed Three-Fold Domino Reaction and Pd(II)-Catalyzed Trihydroxylation. *J. Am. Chem. Soc.* **2021**, *143*, 21270–21274.

(52) Zhang, Y. L.; Ge, H. M.; Zhao, W.; Dong, H.; Xu, Q.; Li, S. H.; Li, J.; Zhang, J.; Song, Y. C.; Tan, R. X. Unprecedented Immunosuppressive Polyketides from Daldinia Eschscholzii, a Mantis-Associated Fungus. *Angew. Chem. Int. Ed.* **2008**, *47*, 5823–5826.

(53) Neufeldt, S. R.; Sanford, M. S. O-Acetyl Oximes as Transformable Directing Groups for Pd-Catalyzed C−H Bond Functionalization. *Org. Lett.* **2010**, *12*, 532–535.

(54) Horwitz, M. A. Local Desymmetrization as an Engine of Stereochemical Elaboration in Total Synthesis. *Tetrahedron Lett.* **2022**, *97*, 153776.

(55) (a) Bai, L.; Liu, J.; Hu, W.; Li, K.; Wang, Y.; Luan, X. Palladium/Norbornene-Catalyzed C−H Alkylation/Alkyne Insertion/Indole Dearomatization Domino Reaction: Assembly of Spiroindolenine-Containing Pentacyclic Frameworks. *Angew. Chem. Int. Ed.* **2018**, *57*, 5151–5155.

(b) Nan, J.; Yuan, Y.; Bai, L.; Liu, J.; Luan, X. Highly Chemoselective Construction of Spiro[4,5]Decane-Embedded Polycyclic Scaffolds by a Palladium/Norbornene-Catalyzed C–H Activation/Arene Dearomatization Reaction. *Org. Lett.* **2018**, *20*, 7731–7734.

(56) Mo, F.; Trzepkowski, L. J.; Dong, G. Synthesis of Ortho-Acylphenols through the Palladium-Catalyzed Ketone-Directed Hydroxylation of Arenes. *Angew. Chem. Int. Ed.* **2012**, *51*, 13075–13079.

(57) Liang, Y.-F.; Wang, X.; Yuan, Y.; Liang, Y.; Li, X.; Jiao, N. Ligand-Promoted Pd-Catalyzed Oxime Ether Directed C–H Hydroxylation of Arenes. *ACS Catal.* **2015**, *5*, 6148–6152.

(58) Diao, T.; Stahl, S. S. Synthesis of Cyclic Enones via Direct Palladium-Catalyzed Aerobic Dehydrogenation of Ketones. *J. Am. Chem. Soc.* **2011**, *133*, 14566–14569.

(59) Kim, J.; Chang, S. Iridium-Catalyzed Direct C–H Amidation with Weakly Coordinating Carbonyl Directing Groups under Mild Conditions. *Angew. Chem. Int. Ed.* **2014**, *53*, 2203–2207.

(60) (a) Bahadoor, A.; Schneiderman, D.; Gemmill, L.; Bosnich, W.; Blackwell, B.; Melanson, J. E.; McRae, G.; Harris, L. J. Hydroxylation of Longiborneol by a Clm2-Encoded CYP450 Monooxygenase to Produce Culmorin in Fusarium graminearum. *J. Nat. Prod.* **2016**, *79*, 81–88. (b) Ashley, J. N.; Hobbs, B. C.; Raistrick, H. Studies in the biochemistry of microorganisms: The crystalline colouring matters of Fusarium culmorum (W. G. Smith) Sacc. And related forms. *Biochem. J.* **1937**, *31*, 385–397. (c) Kasitu, G. C.; ApSimon, J. W.; Blackwell, B. A.; Fielder, D. A.; Greenhalgh, R.; Miller, J. D. Isolation and characterization of culmorin derivatives produced by Fusariumculmorum CMI 14764. *Can. J. Chem.* **1992**, *70*, 1308–1316. (d) Alam, M.; Jones, E. B. G.; Hossain, M. B.; van der Helm, D. Isolation and Structure of Isoculmorin from the Marine Fungus Kallichromaethys. *J. Nat. Prod.* **1996**, *59*, 454–456. (e) R. Barton, D. H.; H. Werstiuk, N. Sesquiterpenoids. Part XIV. The constitution and stereochemistry

of culmorin. *J. Chem. Soc. C: Organic* **1968**, *0*, 148–155. (f) Briggs, L. H. and Sutherland, M. D. The Essential oil of Cupressus Macrocarpa. *J. Org. Chem.* **1942**, *7*, 397–407. (g) Akiyoshi, S.; Erdtman, H.; Kubota, T. Chemistry of the natural order cupressales—XXVI: The identity of junipene, kuromatsuene and longifolene and of juniperol, kuromatsuol, macrocarpol and longiborneol. *Tetrahedron* **1960**, *9*, 237–239.

(61) (a) Lusi, R. F.; Perea, M. A.; Sarpong, R. C–C Bond Cleavage of α-Pinene Derivatives Prepared from Carvone as a General Strategy for Complex Molecule Synthesis. *Acc. Chem. Res.* **2022**, *55*, 746–758.

(b) Masarwa, A.; Weber, M.; Sarpong, R. Selective C–C and C–H Bond Activation/Cleavage of Pinene Derivatives: Synthesis of Enantiopure Cyclohexenone Scaffolds and Mechanistic Insights. *J. Am. Chem. Soc.* **2015**, *137*, 6327–6334.

(62) (a) Simmons, E. M.; Hartwig, J. F. Catalytic functionalization of unactivated primary C–H bonds directed by an alcohol. *Nature* **2012**, *483*, 70–73. b) Li, B.; Driess, M.; Hartwig, J. F. Iridium-Catalyzed Regioselective Silylation of Secondary Alkyl C–H Bonds for the Synthesis of 1,3-Diols. *J. Am. Chem. Soc.* **2014**, *136*, 6586–6589.

(63) Ma, X.; Kucera, R.; Goethe, O. F.; Murphy, S. K.; Herzon, S. B. Directed C–H Bond Oxidation of (+)-Pleuromutilin. *J. Org. Chem.* **2018**, *83*, 6843–6892.

(64) Karmel, C.; Li, B.; Hartwig, J. F. Rhodium-Catalyzed Regioselective Silylation of Alkyl C–H Bonds for the Synthesis of 1,4-Diols. *J. Am. Chem. Soc.* **2018**, *140*, 1460–1470.

(65) Nakazaki, M. & Naemura, K. Photolyses of isobornyl and bornyl nitrites. *Bull. Chem. Soc. Jpn.* **1964**, 37, 532–535.

(66) (a) Renata, H.; Zhou, Q.; Baran, P. S. Strategic Redox Relay Enables A Scalable Synthesis of Ouabagenin, A Bioactive Cardenolide. *Science* **2013**, *339*, 59–63. (b) Berger, M.; Knittl-Frank, C.; Bauer, S.; Winter, G.; Maulide, N. Application of Relay C–H Oxidation Logic to Polyhydroxylated Oleanane Triterpenoids. *Chem* **2020**, *6*, 1183–1189.

(67) Desai, L. V.; Hull, K. L.; Sanford, M. S. Palladium-Catalyzed Oxygenation of Unactivated sp3 C–H Bonds. *J. Am. Chem. Soc.* **2004**, *126*, 9542–9543.

(68) Neufeldt, S. R.; Sanford, M. S. O-Acetyl Oximes as Transformable Directing Groups for Pd-Catalyzed C–H Bond Functionalization. *Org. Lett.* **2010**, *12*, 532–535.

(69) (a) Trotta, A. H. Total Synthesis of Oridamycins A and B. *Org. Lett.* **2015**, *17*, 3358–3361. (b) Trotta, A. H. Toward a Unified Total Synthesis of the Xiamycin and Oridamycin Families of Indolosesquiterpenes. *J. Org. Chem.* **2017**, *82*, 13500–13516.

(70) Corey, E. J.; Niimura, K.; Konishi, Y.; Hashimoto, S.; Hamada, Y. A New Synthetic Route to Prostaglandins. *Tetrahedron Lett.* **1986**, *27* (20), 2199–2202. (see note 14)

(71) Siler, D. A.; Mighion, J. D.; Sorensen, E. J. An Enantiospecific Synthesis of Jiadifenolide. *Angew. Chem. Int. Ed.* **2014**, *53*, 5332–5335.

5.8 Contributors

This chapter includes content reproduced, with permission, from: Bakanas, I.† Lusi, R. F., † Wiesler, S. Sarpong, R.* Strategic Application of C–H Oxidation in Natural Product Total Synthesis *in preparation*. Framework was proposed by R.F.L, sections 5.1-5.3 and 5.6 were written by I.B. 5.4 was written by R.F.L. R.S. and S.W. provided guidance and feedback.

Chapter 6
Progress Toward the Synthesis of Melicolones A & B

6.1 Isolation, biosynthesis, and previous synthesis

Melicolones A & B (**6-1**, **6-2**, Figure 6.1) are rearranged polyprenylated acylphloroglucinol (PPAP) natural products that were isolated in 2015 from the leaves of the deciduous shrub *Melicope ptelefolia* in the southeast of China by Luo, Kong, and coworkers.[1] They feature a unique 9-oxatricyclo[3.2.1.1^{3,8}]nonane core, extensive oxidation, five stereogenic centers, and two all-carbon quaternary centers. Interestingly, they were isolated as a racemic, epimeric, mixture indicative of a non-stereoselective biosynthesis. The absolute configurations of (–)-melicolone A (ent-**6-1**) and (+)-melicolone B (**6-2**) were proven unambiguously by x-ray crystallography. On the basis of previous studies where extracts from the leaves of *Melicope ptelefolia* have been shown to possess antioxidant properties, the isolation chemists tested the melicolones for their protective activity against oxidative stress. Melicolone B showed relatively good activity with nearly 100% cell viability at 5 micromolar dosing compared to the 76% viability of resveratrol as a positive control. The +/– series showed slightly different bioactivity levels, albeit in the expected variance range.

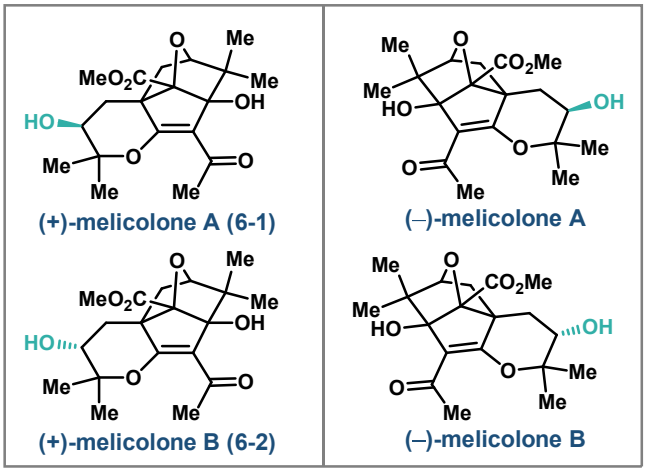

Figure 6.1. The melicolone series of PPAP natural products.

Luo and Kong also proposed a biosynthesis of the melicolones (Scheme 6.1). Prenylated acylphloroglucinol **6-3**, which was detected in the producing organism, was proposed to undergo oxidation and subsequent prenylation to give dearomatized compound **6-4**. Nonselective epoxidation of **6-4** could give epoxide **6-5** as a mixture of four stereoisomers which will eventually lead to the full melicolone series. Intramolecular 6-endo-*tet* cyclization could yield **6-6** containing

the tetrahydropyran ring. Acyloin rearrangement of **6-6** followed by oxidation could provide the [4.3.0] bicyclic acid **6-7**. Prins-type cyclization onto the resulting ketone with concomitant hydration and ether bridge formation (direct etherification is also possible) could then construct the characteristic [3.2.1.1^{3,8}] nonane core of melicolones. Methylation of the acid at this stage would give the melicolones, though the isolation chemists could not rule out the possible incorporation of methanol during extraction.

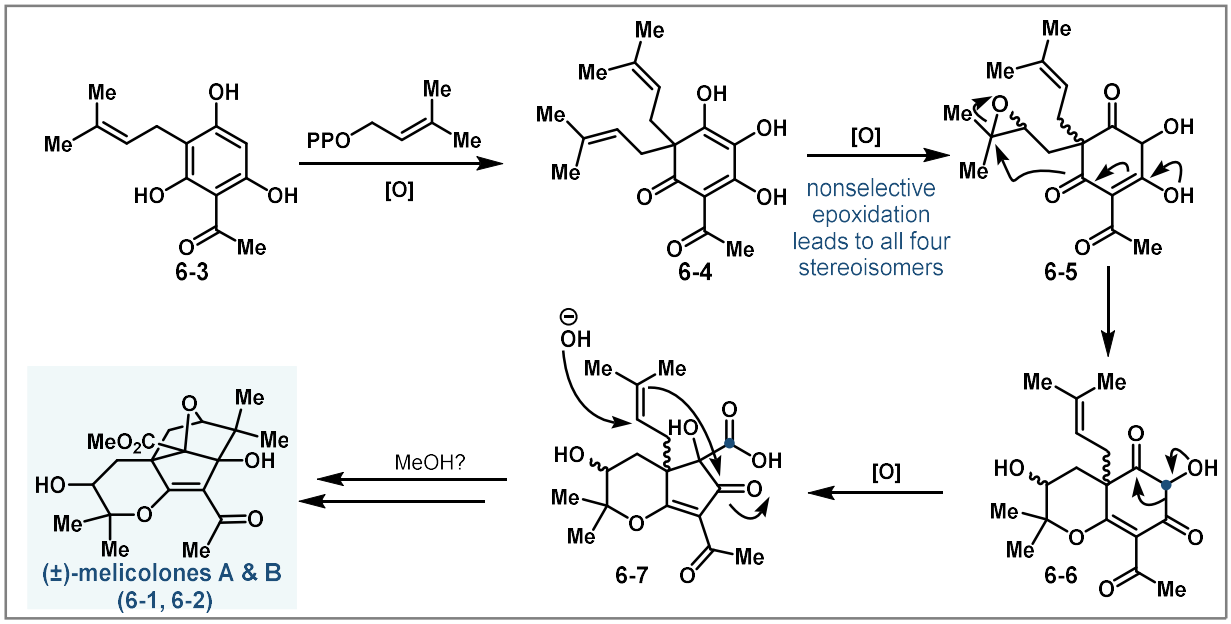

Scheme 6.1. Proposed biosynthesis of melicolones A & B (**6-1**, **6-2**)

There exists one previous synthesis of the melicolones by Wang and Martin (Scheme 6.2) that was reported during the course of our studies in late 2020.[2] Wang and Martin envisioned forming oxabicycle **6-8** through a Rh(II)-catalyzed (3+2) dipolar cycloaddition[3] between enone **6-9** and carbonyl ylide **6-10** (Scheme 6.2A). This disconnection is greatly simplifying and, notably, both **6-9** and **6-10** are achiral so this cycloaddition possessed the potential of rendering the synthesis enantioselective. Their synthesis commenced from enone **6-9**, available in 3 steps from commercial material, and alpha-diazoketoester **6-11**, which is a precursor to carbonyl ylide **6-10** (Scheme 6.2B). After some experimentation, they determined that $Rh_2(NHAc)_4$ was the optimal catalyst for the desired (3+2) cycloaddition, giving bicycle **6-8** in 61% yield along with small amounts of the C-4 epimer (4%) and constitutional isomer (4%). The high regio- and diastereoselectivity was attributed to the steering of the geminal dimethyl group which favors reaction on the less hindered face of enone **6-9** as well as placing the side chain up and away from the endo C-14 methyl group. Formation of the corresponding enolate with NaHMDS followed by alkylation with prenyl iodide proceeded selectively from the exo face—for similar reasons—setting one of the all-carbon quaternary centers as a single diastereomer (see **6-12**) in 65% yield. Vinylogous methyl ester **6-12** was treated with TMSI to cleave the vinylogous ester and induce aldol-cyclization. Epoxidation of the prenyl group was achieved with *m*-CPBA in a non-

stereoselective fashion and the synthesis was completed through acid-mediated cyclization to give the natural products as a 1.1:1 mixture of melicolones A:B. The group sought to render the (3+2) dipolar cycloaddition enantioselective but were unable to achieve this goal using previously reported conditions.

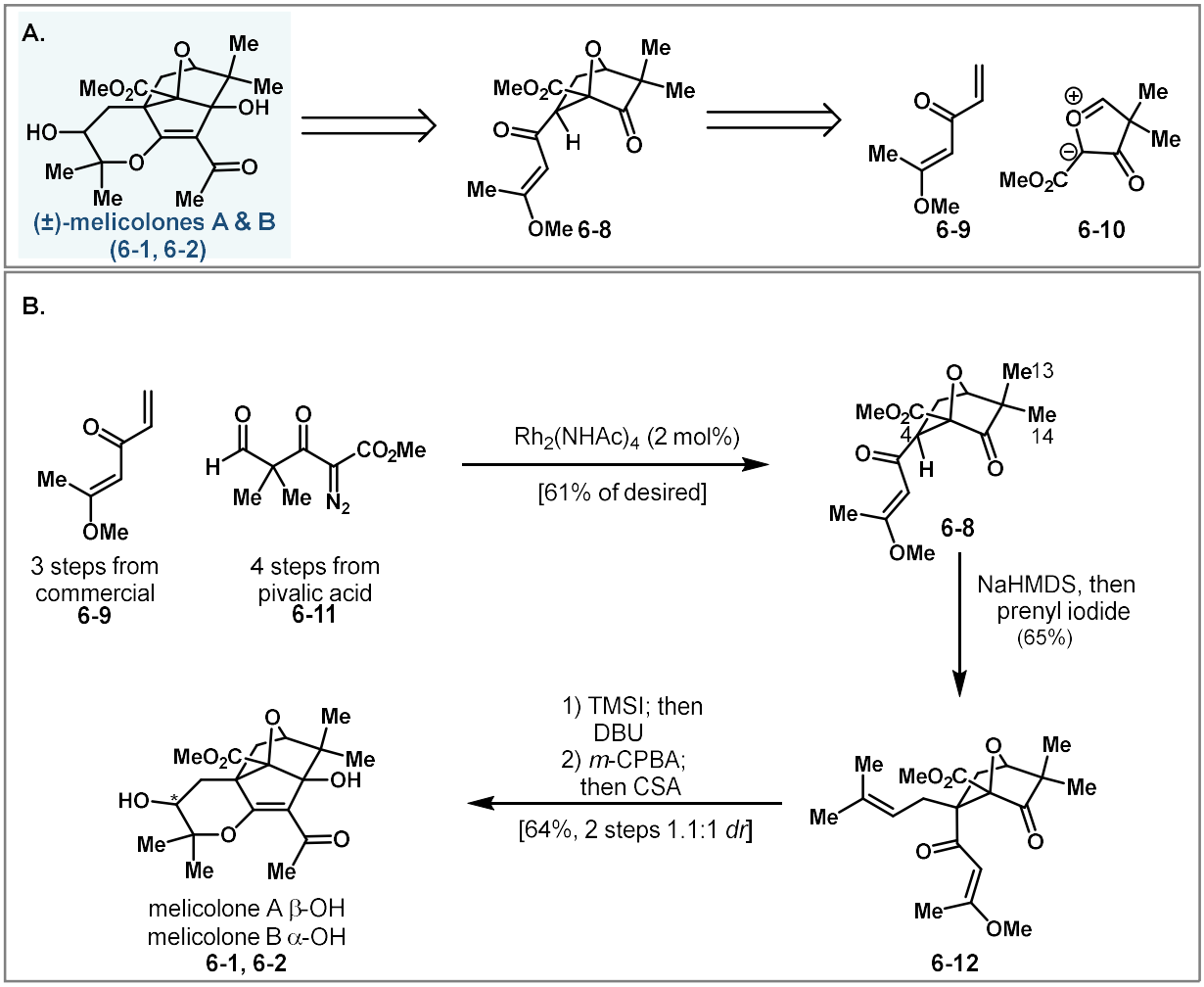

Scheme 6.2 A. Wang and Martin's retrosynthesis of melicolones A & B. **B.** Forward synthesis featuring a key (3+2) dipolar cycloaddition.

The Martin synthesis was instructive for several reasons. First, the epoxidation cyclization sequence to forge the polycyclic ring system of the melicolones was highly efficient and could prove to be a general solution to the formation of the THP ring. It also indicated that the desired THP (from 6-endo cyclization) was formed under acidic conditions preferentially over any THF rings (from 5-exo cyclization). Second, the synthesis illustrates that the (3+2) dipolar cycloaddition disconnection continues to be a powerful way of constructing oxabicycles. In the context of this synthesis, the geminal-dimethyl group steers the diastereoselectivity in constructing the oxabicyclic core. While this synthesis is remarkably efficient, a completely

stereoselective synthesis of these molecules has yet to be accomplished. This became a driving motivation of our synthesis.

6.2 Anionic radical polar crossover (RPC) approach

My retrosynthesis planning was guided primarily by a recognition of hidden symmetry[4] within the melicolone scaffold (Scheme 6.3). The natural products (**6-1** and **6-2)** could be taken back, retrosynthetically, to carbocyclic tricycle **6-13** by removal of some of the peripheral functionality. I hypothesized that **6-13** could be accessed from achiral bisprenylated enedione **6-14** through C–C bond formation from one prenyl group and C–O bond formation from the other. This strategy would not only allow for the rapid assembly of this key tricycle, but also, we could devise a method to do this in a desymmetrizing fashion and access the melicolone core in enantioenriched form for the first time.

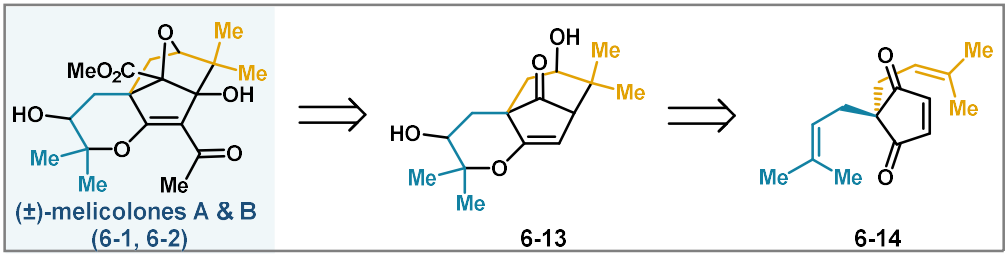

Scheme 6.3. Our hidden symmetry inspired retrosynthesis of the melicolones.

My first foray into this area was inspired by the pioneering work from Gansäuer and coworkers on the desmmetrization of meso epoxides (Scheme 6.4A).[5] Use of a chiral titanocene catalyst allows for the reductive opening of meso epoxide **6-15** and trapping with *t*-butyl acrylate which after trapping with a hydrogen atom or reduction and protonation gives enantioenriched alcohol **6-16** in 61% yield and 82% *ee*. Therefore, I targeted meso-bisepoxide **6-17** (Scheme 6.4B) which could potentially undergo desymmetrizing reductive opening to give tertiary alkyl radical **6-18** that would proceed through Giese-type radical addition into the enedione to give [3.2.1] bicycle **6-19**. In this way, the first C–C bond of our cyclization strategy would be forged. The stabilized radical of **6-18** could undergo further reduction to give carbanion **6-20** which could engage in a bioinspired 6-endo-tet cyclization to form the THP ring of **6-13**. Inclusion of a stoichiometric reductant and acid—to liberate the Ti^{IV} alkoxides—has been shown to allow for catalytic use of titanium in these reactions.[6]

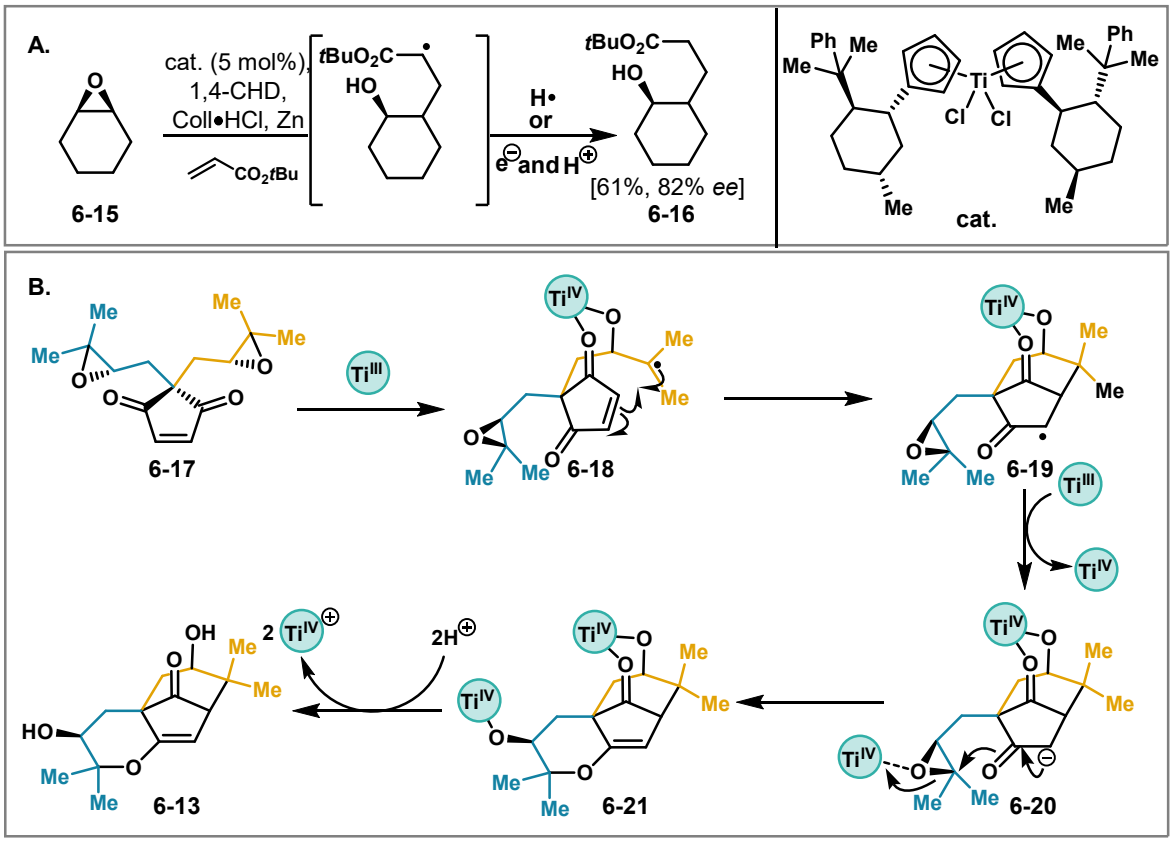

Scheme 6.4 A. Precedent for reductive desymmetrization of meso epoxides. **B.** Proposed cascade

Toward this end, 1,3-cyclopentanedione (**6-22**) underwent bisprenylation with prenyl iodide and Hunig's gase to give dione **6-23** in 70% yield on gram-scale (Scheme 6.5).[7] Notably, this constitutes incorporation of nearly all the carbons of the natural product in a single step! Oxidation with phenyltrimethylammonium tribromide proceeded in 75% yield to give enedione **6-14**. Epoxidation with *m*-CPBA gave 1:1 mixtures of the meso and racemic diastereomers of **6-17** in 91% yield. These diastereomers were found to be inseparable. Nevertheless, I subjected the diastereomeric mixture to the standard reductive radical ring opening reagents—titanocene dichloride reduced in situ with zinc powder—which resulted in undesired reduction of the enedione to give dione **6-24** in 64% yield.

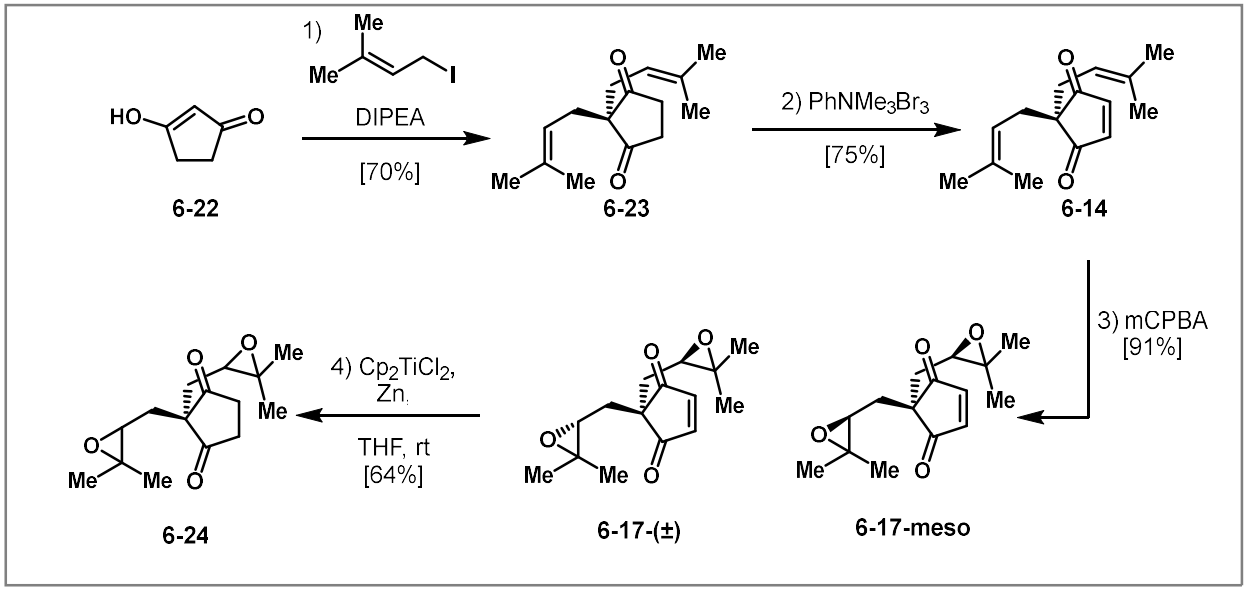

Scheme 6.5 First attempt at reductive radical polar crossover cascade

To overcome the challenge of the reductive lability of the enedione, I sought instead to access the enone variant, which would potentially be less prone to reduction. I could access enone **6-25** in a 4-step procedure from **6-22** (see experimental for details), albeit as a mixture of 3 diastereomers (Scheme 6.6). These diastereomers were subjected to the same reductive radical opening conditions, yielding what was tentatively assigned as the C–C bond formed product **6-26** (the complexity of the diastereomixture made analysis here difficult), as well as the over-reduced product (**6-27)** which was confirmed by X-ray crystallography. Presumably, **6-27** is formed by the radical opening of **6-25**, forming tertiary radical **6-28,** followed by the desired radical cyclization to give **6-29.** Quenching of the radical followed by a reductive opening of the second epoxide to give tertiary radical **6-31** and radical addition into the ketone to give **6-27** after alkoxy radical quenching. Analysis of this system was further complicated by the sensitivity of **6-25** to acid through the formation of various hemiketals. All signs pointed toward a significant problem in this approach—an element of symmetry had been lost resulting in an inseparable mixture of three diastereomers. From this point I considered two plans: 1) alkylation with alkyl iodides that already contained stereo-defined epoxides, or 2) radical cyclizations from a lower oxidation state compound such as enedione **6-14**. I ultimately decided to pursue the latter because the former was similar to work done by the Shair group on the synthesis of structurally distinct PPAP natural products and so while promising,[8] it did not present the same opportunity for discovery.

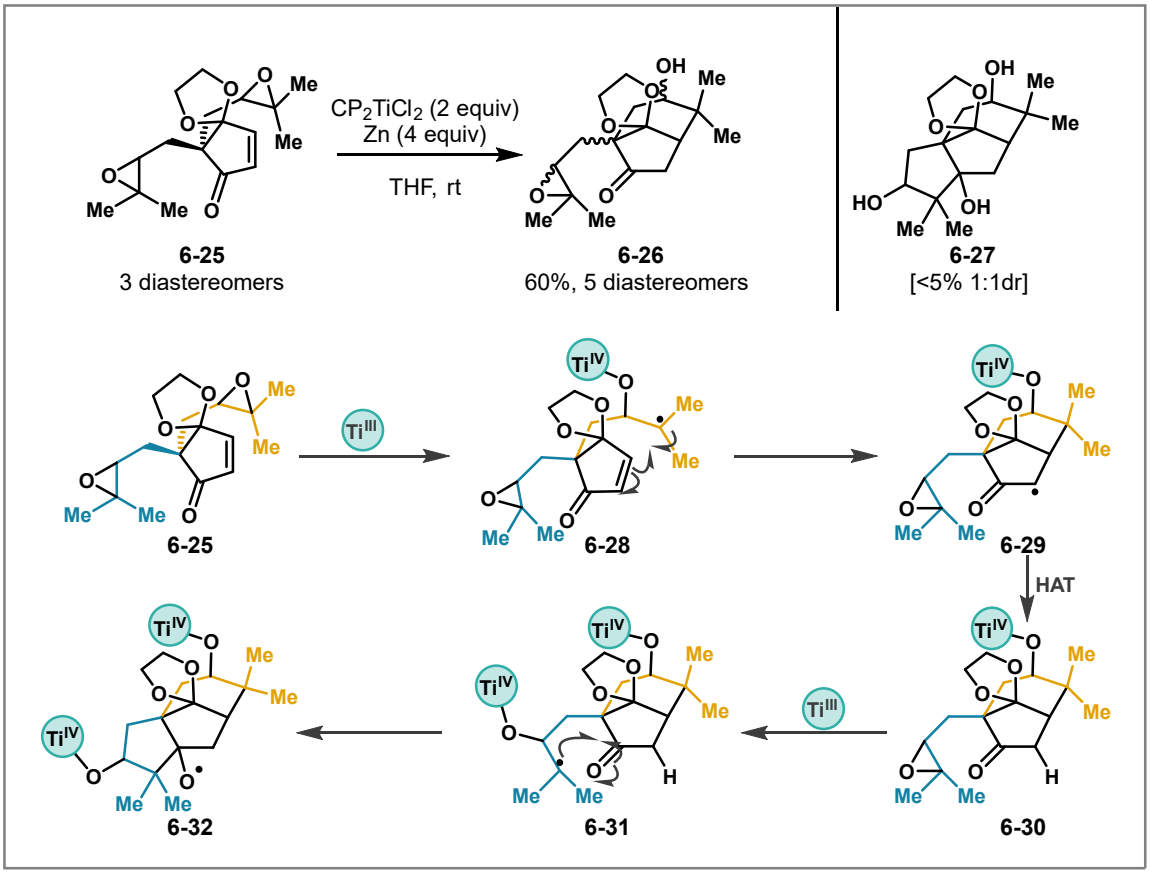

Scheme 6.6 Successful reductive radical cyclization complicated by stereochemical complexity

6.3 Radical Cyclization Followed by C–H Functionalization approach

The stereochemical complexities of the epoxide cyclization approach prompted me to revise our retrosynthesis to utilize the Baran reductive olefin coupling to construct the core from a lower oxidation level (Figure 6.6).[9] Enedione **6-14** could be subjected to $Fe(acac)_3$, $PhSiH_3$ in an ethanol ethylene glycol mixture to afford the carbocyclic core of the melicolones (**6-35**) in a single step. Presumably this transition metal hydrogen atom transfer (TM-HAT) reaction proceeds through the formation of an iron hydride which adds across the alkene through a HAT transition state to yield a tertiary alkyl radical (**6-33**) which undergoes a Giese-type radical cyclization to give stabilized radical **6-34**. The stabilized radical is further reduced and protonated by (or undergoes PCET) to give diketone **6-35**. These methods have gained great popularity in recent years for their ability to form carbon-centered radicals under mild conditions. Furthermore, the dynamic nature of the metal-radical species has large implications for its behavior on the basis of the persistent radical effect.[10]

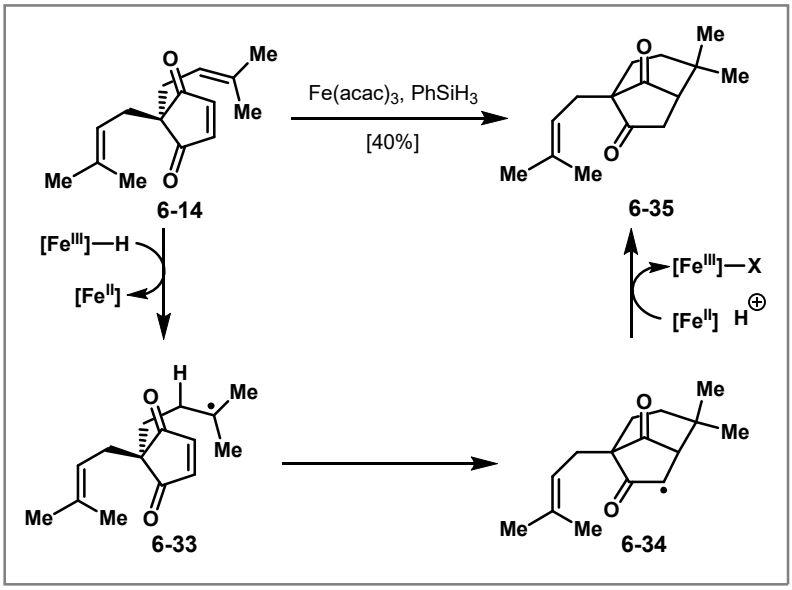

Scheme 6.6 Reductive olefin coupling to form the bicyclo[3.2.1]octane core of the melicolones

While this reaction was very efficient in constructing the carbocycle, the strategy required oxidation of an unactivated C–H bond (Scheme 6.7). We devised C–H functionalization strategies, either undirected through manipulation of substrate electronics or directed using the inherent functional groups of **6-35** as directing groups.[11]

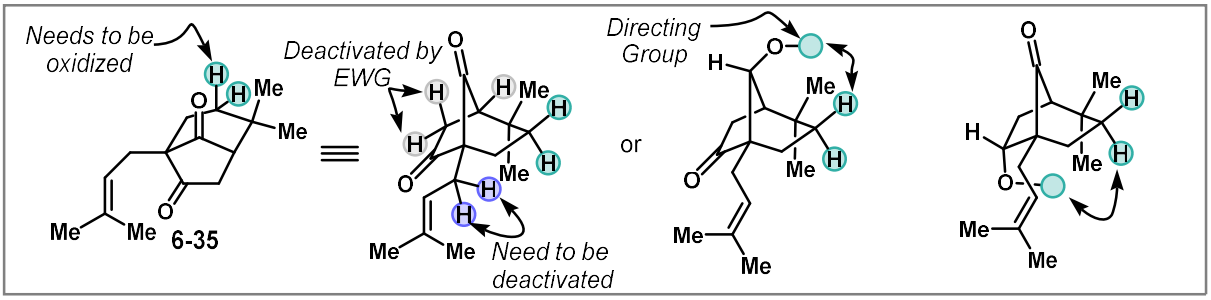

Scheme 6.7 Strategic overview of C–H oxidation tactics to access melicolone oxidation level

First, we initiated studies on the undirected C–H functionalization of **6-35**(Scheme 6.8). It was immediately apparent that the double bond of **6-35** would present a major obstacle as not only are the allylic C–H bonds activated, but also, the double bond could react preferentially with any electrophilic oxidant. Therefore, **6-35** was dihydroxylated using catalytic OsO_4 with NMO as a stoichiometric oxidant to give a 1:1 mixture of hemiketal **6-36** and diol **6-37** in 83% yield. The α-O C–H bond of **6-36** was found to be a liability in undirected C–H functionalization reactions, so diol **6-37** was pursued instead and was protected as either acetonide **6-38** or carbonate **6-39**. I hypothesized that **6-39** would be the ideal substrate and the presence of the carbonyl groups would inductively deactivate undesired positions. However, the substrate was found to be entirely too deactivated! Treatment with the White-Chen catalyst,[12] TFDO,[13] TBADT,[14] chlorine

radical,[15] xanthyl radical,[16] NBS acetophenone and light,[17] among others all led to no reaction. There is significant precedence for the deactivating nature of carbonyls influencing reactivity, but even the conditions developed by Sigman and coworkers to combat this challenge were unsuccessful.[18] I spent some time looking to reengineer this substrate, but ultimately any reduction of the carbonyl groups resulted in either introduction of an oxidizable hydrogen, or introduction of a new electron-withdrawing group (acetate etc.).

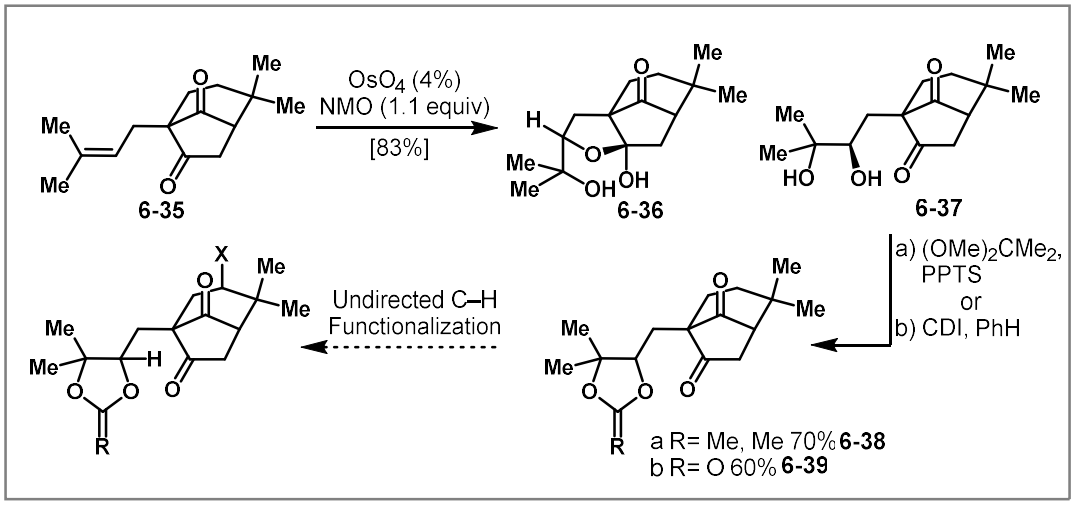

Scheme 6.8 Preparation of substrates **6-38** and **6-39** and exploration of undirected C–H functionalization.

We then investigated directed C–H functionalizations as outlined in Scheme 6.7. Some highlights from this approach are discussed here. I proceeded from hemiketal **6-36** as it provided a simple way to differentiate between the two carbonyls (Scheme 6.9). TMS protection of the hemiketal with TMSOTf followed by LAH reduction gave alcohol **6-40** as a single diastereomer. Presumably the gem-dimethyl group blocks approach of LAH from the back face. We then investigated a series of functional handles and directing groups from this alcohol. Most notable among them was the halomethylsilyl group developed by Gevorgyan and coworkers.[19] Alcohol **6-40** was silylated with (bromomethyl)dimethylsilyl chloride followed by displacement of the bromide with NaI to give iodomethylsilyl ether **6-41** in 86% over 2 steps. This 2-step procedure was found to be more reproducible and efficient than the alternative 1-step procedure starting from (iodomethyl)dimethylsilyl chloride. Treatment of **6-42** with $Pd(OAc)_2$, Cs_2CO_3, a bisphosphine ligand, and irradiation with blue LED presumably allows for the formation of the α-Si radical which can undergo a 1,7-HAT to abstract a distal hydrogen. The resulting alkyl radical then recombines with Pd setting the stage for β-hydride elimination to achieve remote desaturation. Gevorgyan has shown that this reaction is selective for methylenes or methyne protons over methyl groups, due to the slightly lower BDE of the α-Si C–H bond (~103 kcal/mol). However, in this case, no desaturation was observed (**6-3**). Instead, dehalogenation (**6-44**), a known side product of the Gevorgyan process, was observed.

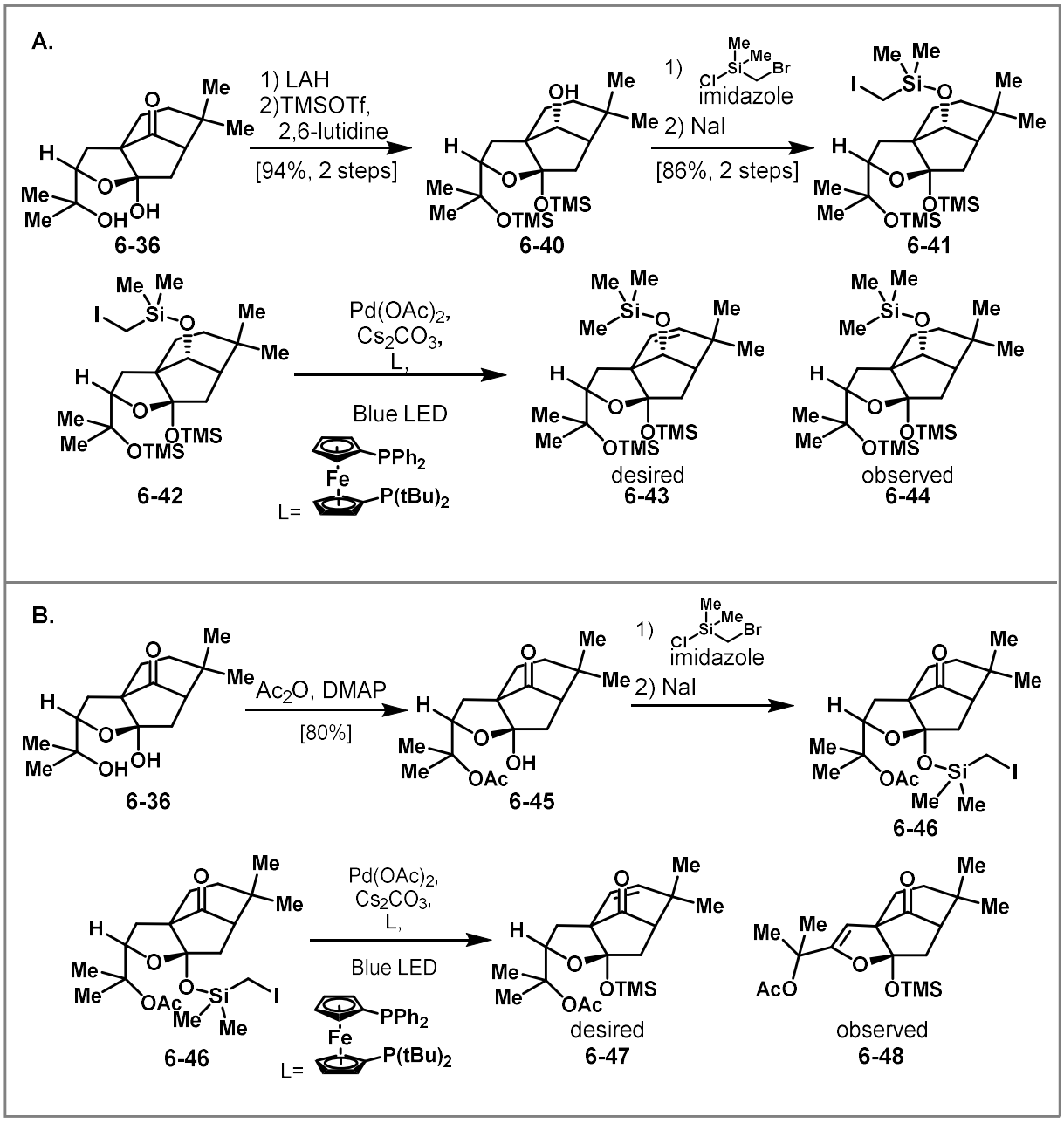

Scheme 6.9A. Directed desaturation studies using functional handles on the northern portion of the molecule **B.** Directed desaturation from the southern portion of the molecule

Undeterred, we investigated the same reaction from the bottom side of the molecule. Acetylation of the tertiary hydroxy group of **6-36** resulted in acetate **6-45**. The same 2-step installation of the iodomethyl silyl group could then be performed on the hemiacetal to give silyl ketal **6-46**. Notably, Gevorgyan has yet to show this reaction from a silyl ketal, and incorporating it into our protective group strategy could be highly efficient (similar tactics were attempted from

the silyl cyanohydrin). However, the remote desaturation from **6-46** led to only undesired desaturation of the 5-membered ring (**6-48**). We anticipated this possibility since the silylmethyl group of **6-46** appeared equidistant from the desired and undesired positions from examination of simple models.

We hypothesized that direct formation of the alkoxy radical could result in the desired oxidation. Treatment of **6-40** with PIDA, I_2, and irradiation with a sunlamp led to selective Suarez etherification to give **6-49** in 75% yield.[20] While both the methyl hydrogen and desired methylene hydrogen could both participate in facile 1,5 HAT, the bicycle conformation clearly places the methyl group closer to the hydroxy group. Further selectivity in this oxidation was shown through lactonization to give **6-50** when the oxidant was changed from PIDA to Pb(OAc)4 along with adding Ca_2CO_3. Total conversion required the use of recrystallized $Pb(OAc)_4$. I attempted to leverage this lactone through a redox-relay strategy wherein saponification and a subsequent directed oxidation could give the desired oxidation. However, these attempts were not successful and lead me to reevaluate the strategy again.

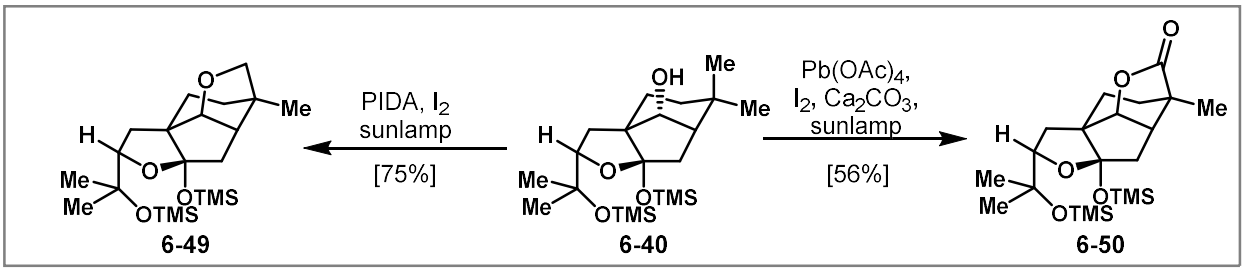

Scheme 6.10 Select directed oxidation studies resulting in undesired methyl group oxidation

6.4 C–C cleavage approach

My final approach was the product of a serendipitous discovery while investigating light-promoted thiol-ene reactions of enone **6-51**. After careful experimentation, I found that **6-51** could undergo [2+2]-photocycloaddition to give tricycle **6-52** as a single positional isomer—though at the time unconfirmed—in excellent yield (Scheme 6.11A). This inspired a new strategy: the extra, strained C–C bond could be leveraged as an oxidation surrogate. In this way we would form the C–C bond of the [3.2.1] bicycle while also functionalizing the distal carbon that we had targeted during the C–H functionalization studies.

Upon forming the [2+2] photoadduct, it was not immediately obvious whether we had obtained the head-to-tail isomer (**6-52)** or the head-to-head isomer (**6-53**, Scheme 6.11B). It was more apparent that **6-52** could undergo nucleophilic fragmentation (see bolded bonds Scheme 6.11B) to give a stabilized carbanion and deliver the desired [3.2.1] bicycle. However, after careful NMR analysis (and corroborating reactivity), the cycloadduct was determined to be the lesser desired head-to-head isomer (i.e., **6-52**). Here, I applied thinking based on symmetry tactics. The head-to-head isomer could be converted to the enantiomer of the head-to-tail isomer through

protecting group manipulation due to the pseudosymmetric nature of their functional groups. Toward this goal, I was able to convert **6-52** to silyl cyanohydrin **6-54**, but subsequent ketal cleavage was unsuccessful. Other explorations on this scaffold revealed several intriguing C–C cleavage reactions as the functionalized strained scaffold readily fragmented. These findings will be discussed in detail in Chapter 7.

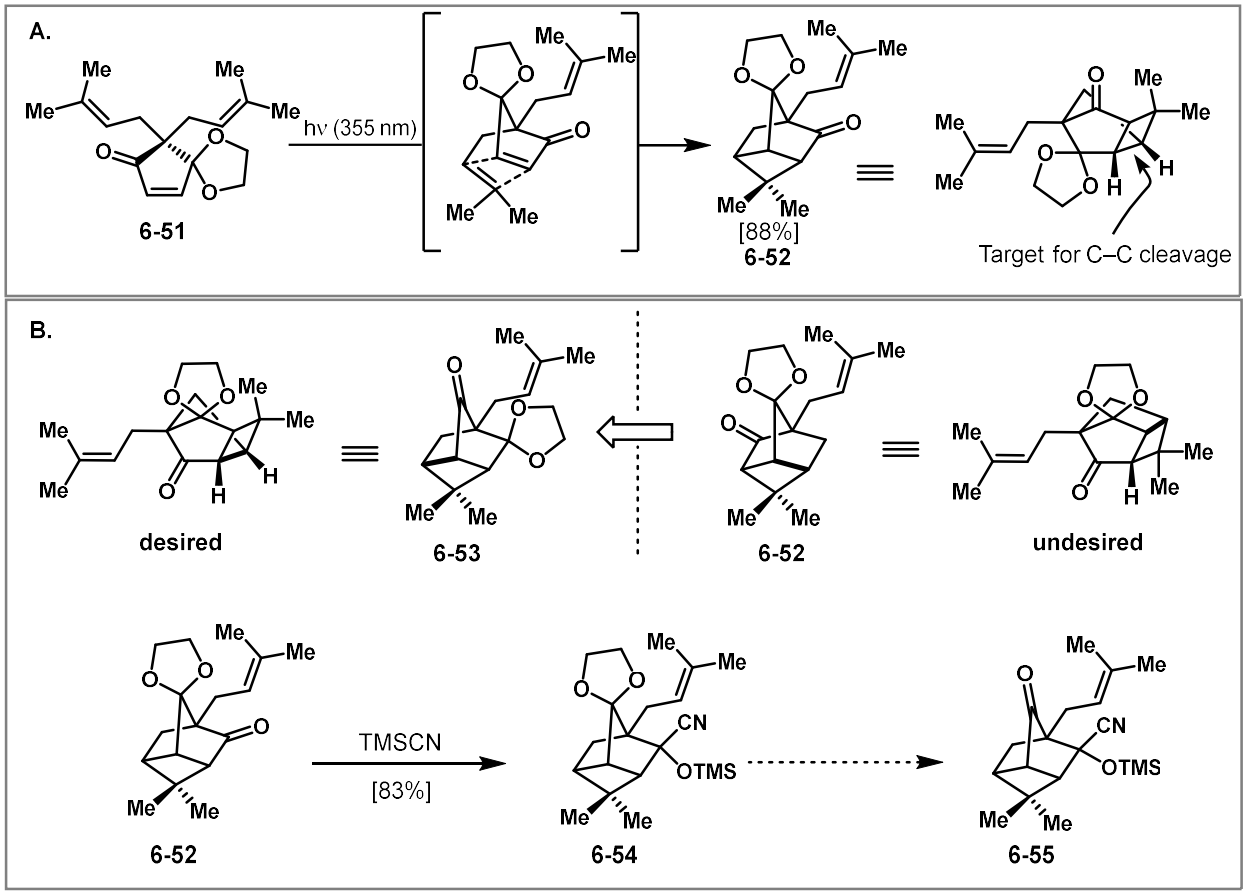

Scheme 6.11A. Discovery of a [2+2] photocycloaddition. **B.** Attempts to access a substrate for selective cleavage of the cyclobutane.

6.5 Conclusion and outlook

If the goal of organic synthesis is to achieve complete programmable control of reactions, then the totally selective synthesis of the melicolones remains an ongoing challenge. I sought to take advantage of the hidden symmetry within their scaffold in designing a retrosynthesis that took the natural products back to achiral building blocks. The end goal of this study was to devise a method for desymmetrization—to do something not even nature has done—to complete a totally stereoselective synthesis of the melicolones.

My first approach utilizing a reductive radical polar crossover cyclization (Section 6.2) failed due to the stereochemical complexity of the system. The strategy became mired in

complications as protecting group manipulations were required and the advantages of a symmetry-based approach was lost.

The second approach sought to combine a rapid synthesis of the [3.2.1] tricycle with C–H oxidation logic to accomplish the synthesis. Enantioselective desymmetrization proved challenging in this system. We had envisioned the development of asymmetric TM-HAT transformations to achieve this goal, but the lack of precedent and a strong theoretical basis dissuaded us from further investigation in this direction. Ultimately, the C–H oxidation proved to be too challenging due to the substrate conformation and the highly electron-deficient nature of the scaffold. Perhaps, further developments in the oxidation of electron-deficient substrates would enable the successful execution this planned route in the future.

Our final approach fit squarely into the "break-it-to-make-it" canon of the group wherein a strained tricycle could undergo fragmentation to the desired core with the desired oxidation pattern. The promise of this strategy was two-fold, assembly of the core in an efficient fashion, but also the wealth of precedent on the enantioselective [2+2] photocycloaddition—ultimately an unsuccessful endeavor. The desired C–C cleavage was illusive but led us to the discoveries detailed in Chapter 7.

Our symmetry-inspired approach to control in the synthesis of the melicolones was fraught with challenges, but also opportunities. Each approach showed definitive promise and given infinite time, I think each still has an opportunity to succeed. Still, these collective studies give us insight into the application of symmetry tactics and strategies, C–H oxidation logic, as well as C–C cleavage logic. Hopefully, these can inform future synthesis planning.

6.6 Experimental

General Methods

Unless otherwise noted, all reactions were performed in flame or oven-dried glassware fitted with rubber septa under a positive pressure of nitrogen using standard Schlenk techniques. Air- and moisture-sensitive liquids were transferred via syringe or stainless steel cannula through rubber septa. Solids were added under inert gas or were dissolved in appropriate solvents. Low temperature-reactions were carried out in a Dewar vessel filled with a cooling agent: acetone/dry ice (−78 °C), H_2O/ice (0 °C). Reaction temperatures above 23 °C were conducted in an oil bath or in a heated metal block (reactions conducted in vials). The reactions were magnetically stirred and monitored by NMR spectroscopy or analytical thin-layer chromatography (TLC), using glass plates precoated with silica gel (Silicycle Siliaplates, glass backed, extra hard layer, 60 Å, 250 µm thickness, F254 indicator). TLC plates were visualized by exposure to ultraviolet light (254 nm), were stained by submersion in aqueous potassium permanganate solution (KMnO4), p-anisaldehyde, or ceric ammonium molybdate solution (CAM), and were developed by heating with a heat gun. Flash-column chromatography on silica gel was performed as described by Still et al.,1 employing silica gel (Silicycle silica gel, 40–63 µm particle size). Organic solutions were concentrated under reduced pressure on a temperature-controlled rotary evaporator equipped with a dry ice/isopropanol condenser. The yields refer to chromatographically and spectroscopically (^{1}H and ^{13}C NMR) pure material.

Materials

Unless noted below, commercial reagents were purchased from Sigma Aldrich, Acros Organics, ChemImpex, Oakwood Chemical, Combi-blocks, TCI, and/or Alfa Aesar, and used without additional purification. Solvents were purchased from Fisher Scientific, Acros Organics, Alfa Aesar, and Sigma Aldrich. Tetrahydrofuran (THF), diethyl ether (Et_2O), acetonitrile (CH_3CN), benzene, toluene (PhMe), methanol (MeOH), and triethylamine (Et_3N) were sparged with argon and dried by passing through alumina columns using argon in a Glass Contour solvent purification system. Dichloromethane (CH_2Cl_2, DCM) was freshly distilled over calcium hydride under a N_2 atmosphere prior to each use.

NMR spectroscopy

NMR spectral data were obtained using deuterated solvents, obtained from Cambridge Isotope Laboratories, Inc. ^{1}H NMR and ^{13}C NMR data were recorded on Bruker AVB-400, AVQ-400, AV-500, NEO-500, AV-600 or AV-700 spectrometers operating at 400 MHz, 400 MHz, 500 MHz, 500 MHz, 600 MHz, 700 MHz for proton nuclei (100 MHz, 100 MHz, 125 MHz, 125 MHz, 150 MHz, 175 MHz for carbon nuclei), respectively. Proton chemical shifts are expressed in parts per million (ppm, δ scale) and are referenced to residual protium in the NMR solvent ($CHCl_3$: δ 7.26). Carbon chemical shifts are expressed in parts per million (δ scale, assigned carbon atom) and are referenced to the carbon resonance of the NMR solvent ($CDCl_3$: δ 77.16). ^{1}H NMR spectroscopic

data are reported as follows: Chemical shift in ppm (multiplicity, coupling constants J (Hz), integration) (e.g. "5.21 (t, 3 J = 7.3 Hz, ^{1}H)"). The multiplicities are abbreviated with s (singlet), br s (broad singlet), d (doublet), t (triplet), q (quartet), p (pentet), se (sextet), h (heptet), m (multiplet) and app (apparent multiplicity). In case of combined multiplicities, the multiplicity with the larger coupling constant is stated first. Except for multiplets, the chemical shift of all signals, as well for centrosymmetric multiplets, is reported as the center of the resonance range. Data for ^{13}C spectroscopy are reported in terms of chemical shift (δ ppm). Additionally to 1D NMR experiments, 2D NMR techniques such as homonuclear correlation spectroscopy (COSY), heteronuclear single quantum coherence (HSQC), heteronuclear multiple bond coherence (HMBC) and nuclear Overhauser enhancement spectroscopy (NOESY) were used to assist structure elucidation. All raw FID files were processed and the spectra analyzed using the program MestReNOVA 11.0 from Mestrelab Research S. L.

Note: The AVB-400, AVQ-400, AV-500, DRX-500 and AV-600 instruments were partially supported by NIH grants SRR023679A, RR02424A-01, S10RR03353-01 and 1S10RR016634-01, and NSF grants CHE-9633007, CHE-8208992, CHE-0130862, and CHE-8703048. The AV-700 instrument was supported by the Berkeley College of Chemistry NMR facility.

Mass spectrometry

Mass spectral data were obtained from the Mass Spectral Facility at the University of California, Berkeley, on a Finnigan/Thermo LTQ-FT instrument (ESI). Data acquisition and processing were performed using the XcaliburTM software.

IR spectroscopy

IR spectroscopic data were recorded on a Bruker ALPHA FT-IR spectrophotometer using a diamond attenuated total reflectance (ATR) accessory. If required, substances were dissolved in dichloromethane prior to direct application on the ATR unit. Data are represented as follows: frequency of absorption (cm^{-1}), and intensity of absorption (s = strong, m = medium, w = weak, br = broad).

X-ray analysis

Single-crystal X-ray diffraction experiments were performed at the UC Berkeley CHEXRAY crystallographic facility. Measurements of all compounds were performed on a Rigaku XtaLAB P200 rotating anode equipped with a Pilatus 200K hybrid pixel array detector. Data were collected using Cu Kα radiation (λ = 1.54184 Å). Crystals were kept at 100(2) K throughout collection. Data collection was performed with CrysAlisPro. 2 Data processing was done using CrysAlisPro and included either a multi-scan absorption or faceindexed absorption correction applied using the SCALE3 ABSPACK scaling algorithm within CrysAlisPro. All structures were solved with SHELXT.3 Structures were refined with SHELXL.4 All non-hydrogen atoms were refined anisotropically, and hydrogen atoms were either included at the geometrically calculated positions and refined using a riding model or located as Q peaks in the Fourier difference map.

Synthetic procedures and analytical data

Synthesis of bisprenylated cyclopentane-1,3-dione 6-23

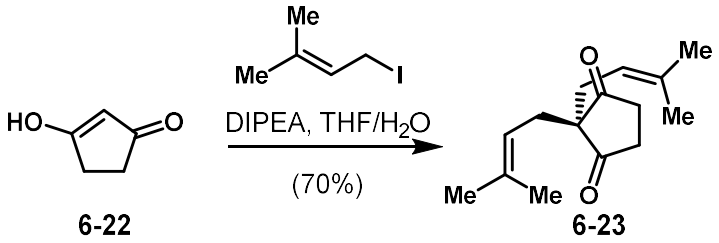

6-22 6-23

Synthesis of prenyl iodide:

To a solution of prenyl bromide (20.0 g, 134 mmol, 2.8 equiv) in acetone (200 mL) was added sodium iodide (24.1 g, 161 mmol, 3.0 equiv). The reaction was stirred for 5 minutes during which a white precipitate formed. The mixture was filtered through a plug of silica and the solvent was evaporated carefully *in vacuo*. The brown crude residue was dissolved in Et_2O (100 mL) and the solution was washed with sat. aq. $NaHCO_3$ (50 mL) and sat. aq. $Na_2S_2O_3$ (10 %, 50 mL), which decolored the solution from brown to pale yellow. The organic layer was dried over Na_2SO_4 and concentrated *in vacuo*. Crude prenyl iodide was directly used in the following reaction without further purification.

Notes: Prenyl bromide and iodide decompose under moisture and air. Using freshly opened or synthesized prenyl bromide ensures reproducibility of experiments. Prenyl iodide is light-sensitive and needs to be used rapidly after synthesis. Blocking light and ensuring a N_2 atmosphere reduces decomposition visibly.

To a solution of 1,3-cyclopentanedione (**S-6** 4.99 g, 50.9 mmol, 1 equiv) in a THF/water mixture (4:1, 400 mL) at 0 °C was slowly added DIPEA (18.2 mL, 104 mmol. 2.1 equiv) and prenyl iodide (crude as above, 134 mmol, 2.6 equiv). The reaction mixture was allowed to warm to room temperature and stirred for 18 hours. THF was then removed by rotary evaporation. To the remaining mixture was added DCM and saturated sodium bicarbonate solution. The aqueous phase was extracted with DCM two times. The combined organic phases were washed with brine, dried over Na_2SO_4 and concentrated *in vacuo*. The crude residue was purified by flash chromatography (Hex/EtOAc = 9/1) to give diketone **S7-7** (8.34 g, 70%).

R_f = 0.50 (hexane:EtOAc = 10:1), UV-active spot (*p*-anisaldehyde)

^{1}H NMR (500 MHz, $CDCl_3$) δ 4.87 (tt, J = 7.7, 1.5 Hz, 1H), 2.55 (s, 2H), 2.34 (d, J = 7.9 Hz, 2H), 1.62 (s, 3H), 1.56 (s, 3H) ppm.

^{13}C NMR (126 MHz, $CDCl_3$) δ 218.0, 136.5, 117.4, 61.6, 36.8, 34.5, 26.0, 17.9 ppm.

Spectral data consistent with those found in the literature[21]

Synthesis of bisprenylated cyclopentene-1,3-dione 6-14

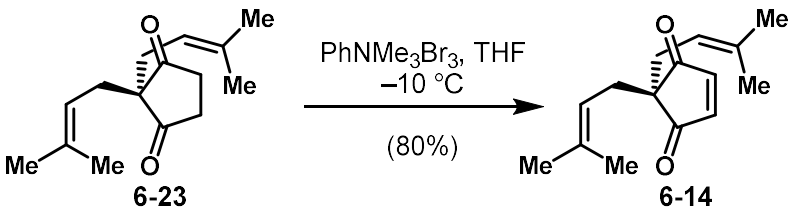

A solution of **S-5** (3.00 g, 12.8 mmol, 1 equiv) in THF (130 mL) was cooled to –10 °C. To this cooled solution was added phenyltrimethylammonium tribromide (4.7 g, 17 mmol, 1 equiv) in four portions. After each addition the solution turned bright yellow and cloudy. Portions were added in 30 minute intervals. Completion of the reaction was judged by TLC, around three hours. Upon completion the reaction was diluted with diethyl ether and quenched with sat. aq. $NaHCO_3$ and sat. aq. $Na_2S_2O_3$ (4:1). The layers were separated, and the aqueous layer was extracted two further times with diethyl ether. The combined organic layers were dried over Na_2SO_4, filtered, and concentrated *in vacuo*. The crude reaction mixture was purified by silica gel flash chromatography (gradient 5:1 pentane: diethyl ether to 1:1 pentane: diethyl ether) to yield **36** as a bright yellow solid (2.38 g, 80%).

R_f = 0.5 (hexane:EtOAc = 10:1), green streak (*p*-anisaldehyde)

^{1}H NMR (700 MHz, $CDCl_3$) δ 5.22 (tt, *J* = 7.5, 1.5 Hz, 1H), 3.22 (t, *J* = 4.4 Hz, 1H), 2.98 (t, *J* = 4.9 Hz, 1H), 2.59 (dt, *J* = 6.7, 5.0 Hz, 1H), 2.42 – 2.37 (m, 1H), 2.30 (dd, *J* = 15.5, 7.5 Hz, 1H), 2.24 (dd, *J* = 12.6, 6.7 Hz, 1H), 2.09 (d, *J* = 12.7 Hz, 1H), 1.70 (d, *J* = 1.5 Hz, 3H), 1.65 (s, 3H), 1.45 (s, 3H), 0.97 (s, 3H) ppm.

^{13}C NMR (176 MHz, $CDCl_3$) δ 208.6, 207.0, 134.4, 118.5, 62.9, 61.5, 46.7, 45.7, 41.4, 32.3, 28.5, 26.0, 21.9, 21.5, 17.9 ppm.

IR (neat) *v*: 2966, 2934, 1776, 1715, 1452, 1386, 1375, 1246, 1222, 1169, 1110, 1058, 983, 910, 720, 647.

Synthesis of bisepoxide 6-17

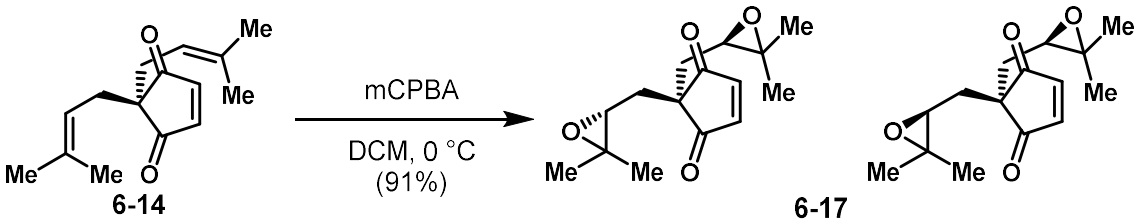

A flame-dried flask was charged with enedione **6-14** (50 mg, 0.22 mmol, 1 equiv) and DCM (2.2 mL). The solution was cooled to 0 °C after which *m*CPBA (108 mg, 0.44 mmol, 2 equiv) was added in two portions. The cloudy pink reaction mixture was stirred until complete consumption of starting material was noted by TLC, about 2 h. The reaction mixture was quenched by addition of sat. aq. $NaHCO_3$ and sat. aq. $Na_2S_2O_3$, separated, and the aqueous layer was extracted three times with EtOAc. The combined organic layers were washed two more times with sat. aq. $NaHCO_3$, followed by sat. aq. NaCl, dried over Na_2SO_4, filtered, and concentrated *in vacuo*. The crude residue **6-17** was sufficiently pure for use in subsequent reaction (53 mg, 91%).

$\mathbf{R_f}$ = 0.2 (hexane:EtOAc = 2:1), purple spot (*p*-anisaldehyde)

^{1}H NMR (400 MHz, $CDCl_3$) δ 7.41 (d, *J* = 6.1 Hz, 1H), 7.37 (s, 2H), 7.31 (d, *J* = 6.1 Hz, 1H), 2.64 (dt, *J* = 8.8, 4.5 Hz, 4H), 2.07 – 1.97 (m, 4H), 1.95 – 1.83 (m, 4H), 1.20 (s, 24H) ppm.

^{13}C NMR (101 MHz, $CDCl_3$) δ 206.5, 206.0, 205.2, 150.1, 149.0, 147.7, 128.3, 59.5, 59.5, 58.9, 58.9, 51.8, 51.7, 33.0 2X, 24.4, 18.5 ppm.

Synthesis of dione 6-24

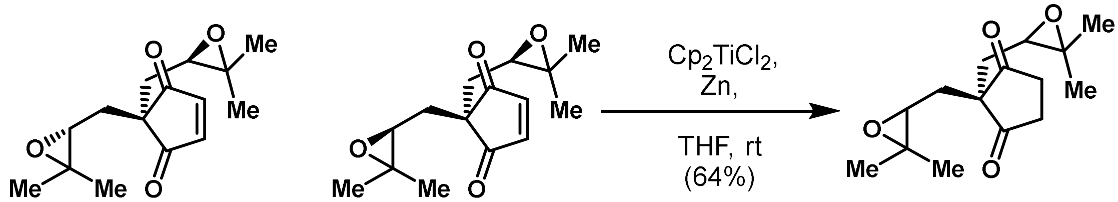

6-17 6-24

A flame-dried vial was charged with Cp_2TiCl_2 (4.7 mg, 0.019 mmol, 1 equiv), and zinc powder (2.5 mg, 0.038 mmol, 2 equiv). The vial was evacuated and back-filled with N_2 three times. Degassed THF (0.4 mL sparged with N_2 for 2 h) was added to the flask and the mixture was stirred for 30 minutes. The red solution quickly turned green in color. Bisepoxide **6-17** (5 mg, 0.019 mmol, 1 equiv) was added dropwise as a solution in degassed THF (0.2 mL). The green solution decolored to red upon addition, and the reaction mixture was stirred for an additional 30 min. The reaction was stopped by exposure to air and quenched with addition of sat. aq. Na_2HPO_4, filtered through plug of Celite, and extracted with EtOAc. The crude reaction mixture was purified by preparatory TLC (hexanes/EtOAc:2/1) to give dione **6-24** as a clear oil (3.1 mg, 64%).

$\mathbf{R_f}$ = 0.18 (hexane:EtOAc = 2:1), purple spot (*p*-anisaldehyde)

^{1}H NMR (500 MHz, $CDCl_3$) δ 3.02 – 2.80 (m, 4H), 2.73 (ddd, *J* = 17.6, 8.5, 4.8 Hz, 2H), 2.03 – 1.86 (m, 4H), 1.22 (m, 12H) ppm.

Synthesis of ketal S6-1

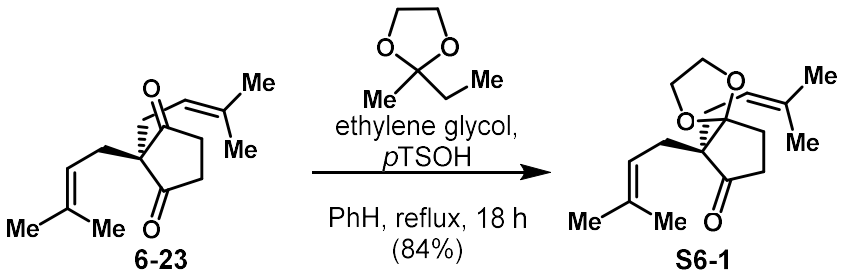

To a solution of dione **6-23** (2.00 g, 8.53 mmol, 1.0 equiv) in benzene (100 mL) was added ethylene glycol (10.0 mL, 179 mmol, 21 equiv) and *para*-toluenesulfonic acid monohydrate (162 mg, 853 µmol, 0.1 equiv). A Dean-Stark apparatus was affixed to the flask and the mixture was heated at reflux (oil bath temperature: 100 °C) for 18 hours. The reaction mixture was then allowed to cool to room temperature, whereupon sat. aq. $NaHCO_3$ and ethyl acetate were added. The aqueous layer was extracted two times with ethyl acetate. The combined organic layers were washed with sat. aq. NaCl, dried over Na_2SO_4, and concentrated *in vacuo* to give the crude residue which was purified by silica gel flash chromatography (*n*Hex/EtOAc = 9/1). The title compound **S6-1** (1.97 g, 7.08 mmol, 84%) was received as a colorless oil.

$\mathbf{R_f}$ = 0.2 (hexane:EtOAc = 9:1), purple spot (*p*-anisaldehyde)

^{1}H NMR (600 MHz, $CDCl_3$) δ 5.09 (ddt, *J* = 8.1, 6.7, 1.5 Hz, 2H), 3.98 – 3.88 (m, 4H), 2.35 – 2.29 (m, 4H), 2.22 (ddt, *J* = 15.1, 6.9, 1.3 Hz, 2H), 2.04 (dd, *J* = 8.7, 7.7 Hz, 2H), 1.67 (q, *J* = 1.4 Hz, 6H), 1.56 (d, *J* = 1.5 Hz, 6H) ppm.

^{13}C NMR (151 MHz, $CDCl_3$) δ 217.5, 133.5, 119.3, 116.4, 64.6, 57.6, 35.3, 30.7, 28.3, 26.2, 17.9 ppm.

HRMS (m/z): EI [M]+ calculated for $C_{17}H_{26}O_3$: 278.1882, found: 278.1880.

Synthesis of enol ether S6-2

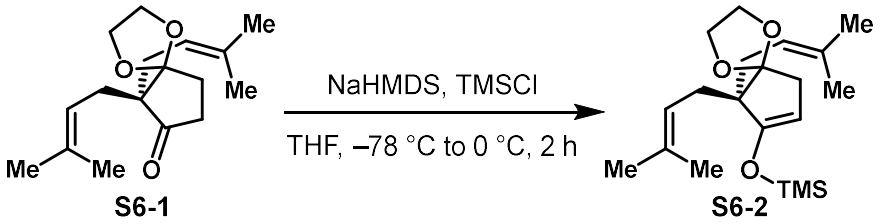

Ketal **S6-1** (548 mg, 1.97 mmol, 1.0 equiv) was dissolved in THF (20 mL) and cooled to –78 °C, whereupon NaHMDS (1.08 mL, 2.17 mmol, 2 M in THF, 1.1 equiv) was added dropwise. The reaction mixture immediately turned orange and was warmed to 0 °C and stirred for 30 minutes at that temperature. The reaction mixture was then cooled back to –78 °C, after which TMSCl (263 µL, 225 mg, 2.07 mmol, 1.05 equiv) was added in a dropwise fashion. After 20 minutes at –78 °C, the reaction was warmed up to 0 °C and stirred at that temperature for 1 h, displaying a slow disappearance of color. The reaction was quenched by the addition of sat. aq. $NaHCO_3$ and ethyl acetate. The aqueous layer was extracted two times with Et_2O. The combined organic layers were washed with sat. aq. NaCl, dried over Na_2SO_4, filtered, and concentrated *in vacuo* to give crude product **S6-2**. The crude product was not stable to silica gel chromatography, but was sufficiently pure to be used in the next step.

^{1}H NMR (400 MHz, $CDCl_3$) δ 5.28 – 5.17 (m, 2H), 4.45 (t, *J* = 2.4 Hz, 1H), 3.89 (m, 4H), 2.30 (d, *J* = 2.4 Hz, 2H), 2.22 (d, *J* = 7.2 Hz, 4H), 1.68 (d, *J* = 1.5 Hz, 6H), 1.59 (d, *J* = 1.3 Hz, 6H), 0.19 (s, 9H). ppm.

Synthesis of enone 6-51

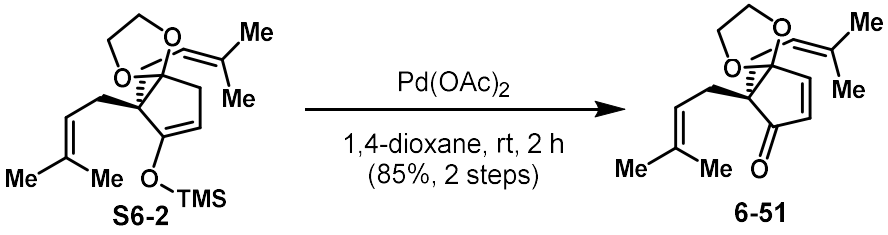

Crude silyl enol ether **S6-2** (1.97 mmol, 1.0 equiv) was dissolved in 1,4-dioxane (20 mL). $Pd(OAc)_2$ (444 mg, 1.98 mmol, 1.0 equiv) was added and the reaction mixture was stirred for 2 hours during which the color deepened from orange to black. After full conversion was noted by TLC, the reaction mixture was filtered two times through a silica plug and eluted with Et_2O to remove bulk palladium. The crude product was subjected to flash chromatography (*n*Hex/EtOAc = 9/1) to give the title compound **6-51** (464 mg, 1.68 mmol, 85 %, over two steps) as a pale yellow oil.

R_f = 0.35 (hexane:EtOAc = 4:1), purple spot (*p*-anisaldehyde)

^{1}H NMR (700 MHz, $CDCl_3$) δ 7.16 (d, *J* = 6.0 Hz, 1H), 6.13 (d, *J* = 5.9 Hz, 1H), 5.09 (tdd, *J* = 6.4, 3.0, 1.5 Hz, 2H), 4.06 – 3.97 (m, 4H), 2.35 – 2.31 (m, 2H), 2.27 – 2.22 (m, 2H), 1.67 (q, *J* = 1.4 Hz, 6H), 1.57 (s, 6H) ppm.

^{13}C NMR (176 MHz, $CDCl_3$) δ 209.2, 155.5, 133.6, 133.1, 119.9, 114.7, 65.4, 56.1, 30.7, 26.2, 17.9 ppm.

HRMS (m/z): EI [M]+ calculated for $C_{17}H_{24}O_3$: 276.1725, found: 276.1721.

Synthesis of diepoxide 6-25

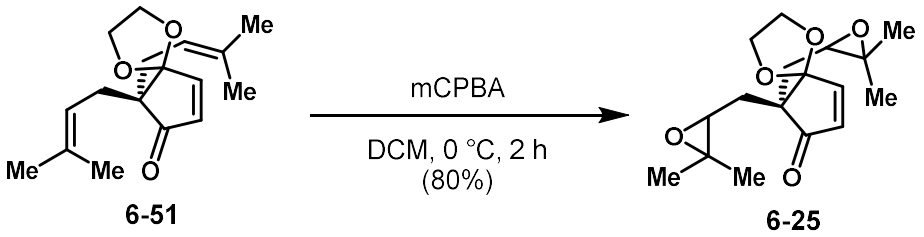

6-51 **6-25**

A flame-dried flask was charged with enedione **6-51** (50 mg, 0.18 mmol, 1 equiv) and DCM (1.8 mL). The solution was cooled to 0 °C after which *m*CPBA (88mg, 0.36 mmol, 2 equiv) was added in two portions. The cloudy pink reaction mixture was stirred for until complete consumption of starting material was noted by TLC, about 2 h. The reaction mixture was quenched by addition of sat. aq. $NaHCO_3$ and sat. aq. $Na_2S_2O_3$, separated, and the aqueous layer was extracted three times with EtOAc. The combined organic layers were washed two further times with sat. aq. $NaHCO_3$, then sat. aq. NaCl, dried over Na_2SO_4, filtered and concentrated *in vacuo*. The crude residue was sufficiently pure for use in subsequent reaction (44 mg, 80% inseparable mixture of diastereomers).

R_f = 0.2 (hexane:EtOAc = 2:1), purple spot (*p*-anisaldehyde)

^{1}H NMR (400 MHz, $CDCl_3$) δ 7.29 (dd, *J* = 5.9, 3.9 Hz, 1H), 6.30 – 6.23 (m, 1H), 4.12 (tdd, *J* = 6.5, 3.6, 1.7 Hz, 4H), 2.89 (dd, *J* = 6.5, 5.1 Hz, 1H), 2.80 (dt, *J* = 9.6, 5.5 Hz, 1H), 2.00 (dd, *J* = 14.6, 5.0 Hz, 1H), 1.94 – 1.85 (m, 3H), 1.27 – 1.21 (m, 12H) ppm.

Synthesis of [3.2.1] bicycle 6-26 and tricycle 6-27

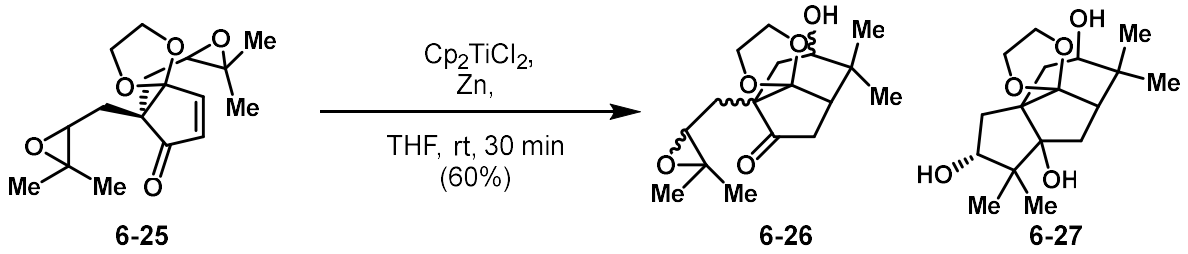

6-25 **6-26** **6-27**

A flame-dried flask was charged with Cp_2TiCl_2 (25 mg, 0.081 mmol, 1 equiv), and zinc powder (10.4 mg, 0.16 mmol, 2 equiv). The flask was evacuated and back-filled with N_2 three times. Degassed THF (1.6 mL sparged with N_2 for 2 h) was added to the flask and the mixture was stirred for 30 minutes. The red solution quickly turned green in color. This mixture of Cp_2TiCl was added dropwise to a solution of Bisepoxide **6-25** (25 mg, 0.081 mmol, 1 equiv) in degassed THF (0.8 mL). The green solution decolored to red upon addition, and the reaction mixture was stirred for an additional 30 min. The reaction was stopped by exposure to air and quenched with addition of sat. aq. Na_2HPO_4, filtered through plug of Celite, and extracted three times with EtOAc. The combined organic layers were washed with sat. aq. NaCl, dried over Na_2SO_4, filtered, and concentrated *in vacuo*. The crude reaction mixture was purified by preparatory TLC (hexanes/EtOAc:2/1) to tentatively give epoxide **6-26** (15 mg, 60% as sparingly separable diastereomers) as well as **6-26** (1.3 mg, 5%) as a clear crystal. After 5 preparatory TLC runs, two diastereomers were separated from the bulk material.

6-26 diastereomer 1: ^{1}H NMR (700 MHz, $CDCl_3$) δ 4.19 (d, *J* = 4.8 Hz, 1H), 4.01 – 3.97 (m, 1H), 3.95 – 3.90 (m, 1H), 3.84 (dd, *J* = 7.5, 6.6 Hz, 1H), 3.79 (dd, *J* = 11.3, 5.8 Hz, 1H), 2.25 (dd, *J* = 15.4, 7.4 Hz, 1H), 2.16 – 2.13 (m, 1H), 2.07 – 2.01 (m, 1H), 2.00 – 1.95 (m, 1H), 1.91 (d, *J* = 7.3 Hz, 1H), 1.52 (d, *J* = 12.7 Hz, 1H), 1.45 – 1.33 (m, 3H), 1.34 – 1.32 (m, 1H), 1.26 (s, 3H), 1.12 (s, 3H), 1.00 (s, 3H) ppm.

diastereomer 2: ^{1}H NMR (700 MHz, $CDCl_3$) δ 4.86 (s, 1H), 4.13 – 4.10 (m, 1H), 4.03 (q, *J* = 7.1 Hz, 1H), 3.99 – 3.96 (m, 1H), 3.87 (q, *J* = 7.1 Hz, 1H), 3.54 (d, *J* = 10.9 Hz, 1H), 3.49 (dd, *J* = 12.4, 5.6 Hz, 1H), 2.55 (dd, *J* = 19.1, 7.7 Hz, 1H), 2.39 (d, *J* = 19.2 Hz, 1H), 2.14 – 2.10 (m, 2H), 1.93 (t, *J* = 12.3 Hz, 1H), 1.29 – 1.25 (m, 2H), 1.20 (s, 6H), 1.15 (s, 3H), 1.05 (s, 3H) ppm.

6-27 ^{1}H NMR (700 MHz, MeOD) δ 4.48 (dd, *J* = 10.3, 7.0 Hz, 1H), 4.00 (ddd, *J* = 15.1, 6.4, 4.5 Hz, 2H), 3.97 – 3.94 (m, 1H), 3.87 – 3.80 (m, 3H), 2.23 – 2.17 (m, 2H), 1.93 (dd, *J* = 13.0, 6.5 Hz, 2H), 1.69 (d, *J* = 7.2 Hz, 1H), 1.55 (d, *J* = 14.5 Hz, 1H), 1.25 – 1.21 (m, 1H), 1.15 (s, 3H), 1.10 (s, 3H), 1.00 (s, 3H), 0.96 (s, 3H) ppm.

The structure of **6-27** was further confirmed through single crystal x-ray analysis from hexanes ethyl acetate mixture (vapor diffusion)

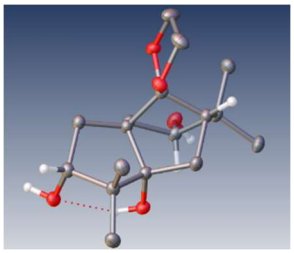

Synthesis of [3.2.1] bicycle 6-35

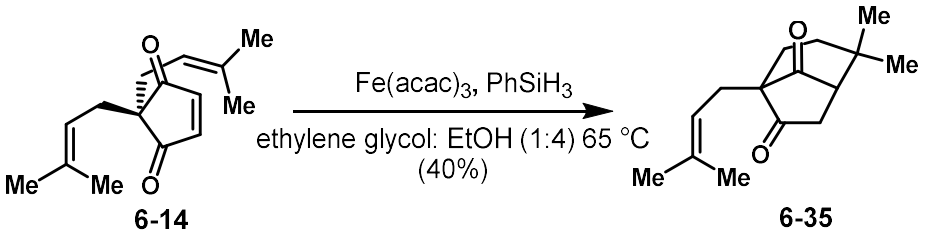

To a flame-dried flask under air was added enedione **6-14** (3.7 g, 16 mmol, 1 equiv), followed by $Fe(acac)_3$ (1.7 g, 4.7 mmol, 0.3 equiv), ethanol (40 mL), and ethylene glycol (10 mL). Phenylsilane (1.9 mL, 16 mmol, 1 equiv) was then added and the reaction mixture was moved to a preheated oil bath at 65 °C. Note: some H_2 evolution was observed. The dark red-brown reaction mixture was stirred for 15 minutes at this temperature wherein full conversion was noted by TLC and the formation of a red foam was visible. The mixture was removed from the oil bath and cooled to room temperature, after which sat. aq. NaCl was added to quench the reaction mixture. The aqueous layer was extracted three times with EtOAc. The combined organic layers were dried over Na_2SO_4, filtered, and concentrated *in vacuo*. The crude residue was purified by silica gel flash chromatography (hexanes:EtOAc = 4:1) to give [3.2.1] bicycle **6-35** (1.5 g, 40% in 80% purity).

R_f = 0.4 (hexane:EtOAc = 4:1), purple spot (*p*-anisaldehyde)

^{1}H NMR (500 MHz, $CDCl_3$) δ 5.06 (ddt, *J* = 8.9, 5.9, 1.5 Hz, 1H), 2.77 (d, *J* = 18.9 Hz, 1H), 2.53 – 2.45 (m, 1H), 2.42 (d, *J* = 7.7 Hz, 1H), 2.38 (d, *J* = 7.9 Hz, 1H), 2.28 (d, *J* = 7.4 Hz, 2H), 2.00 – 1.94 (m, 1H), 1.88 (s, 1H), 1.67 (dd, *J* = 9.0, 1.3 Hz, 6H), 1.39 – 1.35 (m, 1H), 1.09 (d, *J* = 8.5 Hz, 6H) ppm.

Synthesis of hemiketal 6-36 and diol 6-37

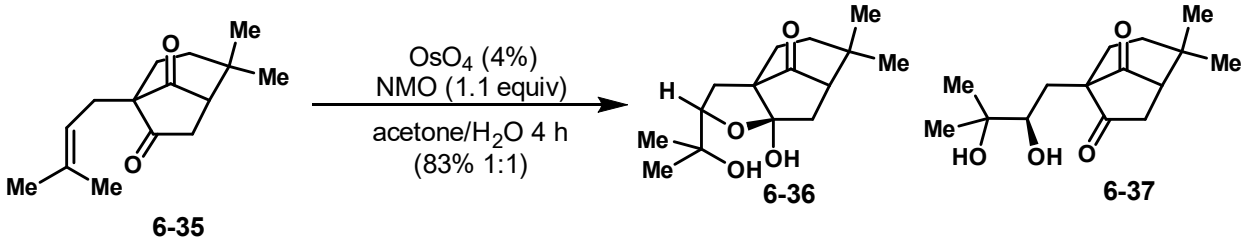

A round-bottomed flask was charged with bicycle **6-35** (1.7 g, 7.3 mmol, 1 equiv) and acetone (37 mL). No effort was made to exclude moisture or air from this reaction. N-methyl morpholine oxide (NMO, 3.4 mL, 7.3 mmol, 1, equiv, 50 wt% in H_2O) was added followed by OsO_4 (1.8 mL, 0.29 mmol, 0.04 equiv, 4 wt% in H_2O). The stirring solution briefly turned black then decolored to orange for the duration of the reaction. Reaction progress was monitored by TLC, judging completion by disappearance of starting material, approximately 4 h. The reaction was quenched by addition of sat. aq. $NaHCO_3$ and sat. aq. $Na_2S_2O_3$ and diluted with EtOAc. The aqueous layer was extracted five times with EtOAc. The organic layers were combined, washed with sat. aq. NaCl, dried over Na_2SO_4, filtered, and concentrated *in vacuo*. The crude residue was purified by silica gel chromatography (hexanes:EtOAc 2:1 to 1:1) to yield hemiketal **6-36** as a yellow solid (800 mg, 41%) and **6-37** as a white solid (820 mg, 42%).

6-36 $\mathbf{R_f}$ = 0.4 (hexane:EtOAc = 2:1), purple spot (*p*-anisaldehyde)

^{1}H NMR (500 MHz, $CDCl_3$) δ 3.87 – 3.80 (m, 1H), 2.44 – 2.34 (m, 1H), 2.29 (dd, *J* = 14.2, 7.5 Hz, 1H), 2.17 – 2.11 (m, 2H), 1.93 (dd, *J* = 13.3, 7.2 Hz, 1H), 1.86 – 1.78 (m, 2H), 1.67 – 1.61 (m, 2H), 1.32 (s, 3H), 1.13 (d, *J* = 1.2 Hz, 3H), 1.00 (d, *J* = 1.2 Hz, 3H), 0.96 (s, 3H) ppm.

^{13}C NMR (126 MHz, $CDCl_3$) δ 215.6, 106.6, 85.2, 71.7, 61.1, 58.6, 41.7, 35.9, 31.2, 30.3, 28.1, 27.9, 27.4, 25.8, 25.6 ppm.

$\mathbf{R_f}$ = 0.3 (hexane:EtOAc = 1:1), purple spot (*p*-anisaldehyde)

^{1}H NMR (700 MHz, $CDCl_3$) δ 4.15 (d, *J* = 5.2 Hz, 1H), 2.59 (dd, *J* = 18.4, 6.5 Hz, 1H), 2.36 – 2.27 (m, 2H), 2.09 – 2.03 (m, 1H), 1.90 (dt, *J* = 13.0, 6.5 Hz, 1H), 1.83 (d, *J* = 13.1 Hz, 1H), 1.77 – 1.69 (m, 1H), 1.35 – 1.20 (m, 11H), 0.97 (s, 3H) ppm.

The structure of **6-36** was further confirmed through single crystal x-ray analysis (vide infre) from hexanes ethyl acetate mixture

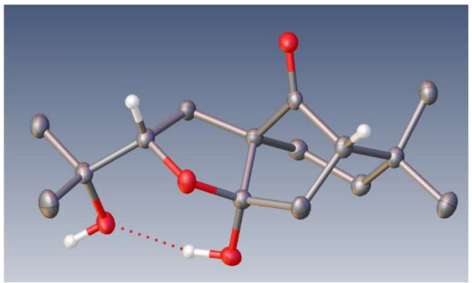

Synthesis of acetonide 6-38

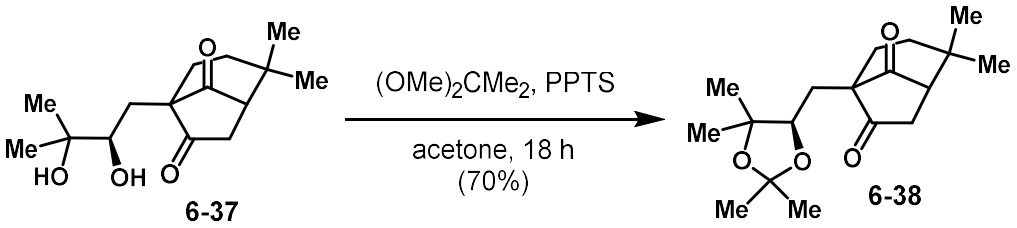

A flame-dried flask was charged with diol **6-37** (200 mg, 0.75 mmol, 1 equiv) followed by acetone (15 mL). To this clear solution was added 2,2-dimethoxypropane (4.6 mL, 37 mmol, 50 equiv) followed by pyridinium p-toluenesulfonate (10 mg, 0.037 mmol, 0.05 equiv). The clear reaction mixture was stirred under an atmosphere of nitrogen for 18 h. The reaction was quenched by addition of sat. aq. $NaHCO_3$ and diluted with EtOAc. The aqueous layer was extracted two times with EtOAc. The organic layers were combined, washed with sat. aq. NaCl, dried over Na_2SO_4, filtered, and concentrated *in vacuo*. The crude residue was purified by silica gel chromatography (hexanes:EtOAc 2:1) to give acetonide **6-38** as a clear oil (160 mg, 70%).

R_f = 0.5 (hexane:EtOAc = 2:1), purple spot (*p*-anisaldehyde)

^{1}H NMR (700 MHz, $CDCl_3$) δ 4.13 (dd, *J* = 10.8, 3.4 Hz, 1H), 2.73 (d, *J* = 18.5 Hz, 1H), 2.59 (dd, *J* = 18.5, 7.5 Hz, 1H), 2.40 (d, *J* = 7.4 Hz, 1H), 1.97 (dd, *J* = 14.0, 10.8 Hz, 1H), 1.94 – 1.89 (m, 2H), 1.55 (ddd, *J* = 17.4, 13.8, 5.1 Hz, 2H), 1.33 (d, *J* = 15.3 Hz, 1H), 1.29 (s, 3H), 1.24 (s, 3H), 1.19 (s, 3H), 1.11 (s, 3H), 1.07 (d, *J* = 10.1 Hz, 6H) ppm.

Synthesis of carbonate 6-39

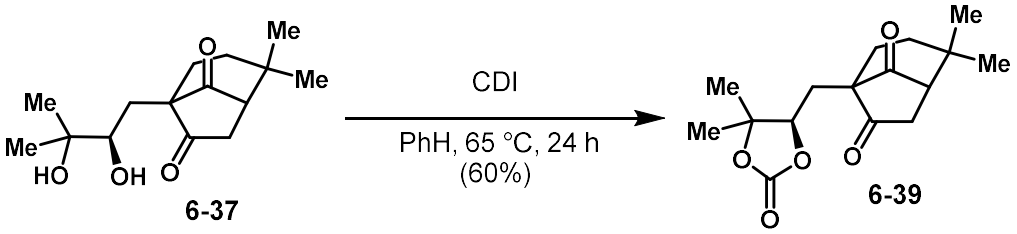

A flame-dried flask was charged with diol **6-37** (200 mg, 0.75 mmol, 1 equiv) followed by benzene (7.5 mL). To this clear solution was added carbonyldiimidazole (121 mg, 0.75 mmol, 1 equiv). The reaction mixture was moved to a preheated oil bath at 65 °C. The reaction mixture was stirred at this temperature for 24 h. The flask was removed from the oil bath and cooled to room temperature whereupon the reaction mixture was quenched by addition of sat. aq. $NaHCO_3$ and diluted with EtOAc. The aqueous layer was extracted two times with EtOAc. The organic layers were combined, washed with sat. aq. NaCl, dried over Na_2SO_4, filtered, and concentrated *in vacuo*. The crude residue was purified by silica gel chromatography (hexanes:EtOAc 2:1) to give carbonate **6-39** as a clear oil (154 mg, 70%).

R_f = 0.4 (hexane:EtOAc = 4:1), purple spot (*p*-anisaldehyde)

^{1}H NMR (400 MHz, $CDCl_3$) δ 4.65 (dd, *J* = 11.1, 2.5 Hz, 1H), 2.80 (d, *J* = 19.2 Hz, 1H), 2.61 (dd, *J* = 19.2, 7.5 Hz, 1H), 2.50 (d, *J* = 7.5 Hz, 1H), 2.19 (dd, *J* = 14.8, 11.1 Hz, 1H), 2.15 – 2.08 (m, 1H), 1.91 (ddd, *J* = 13.0, 5.7, 1.5 Hz, 1H), 1.64 (dd, *J* = 14.6, 5.7 Hz, 1H), 1.56 (dd, *J* = 14.8, 2.6 Hz, 1H), 1.50 (s, 3H), 1.43 (d, *J* = 5.6 Hz, 1H), 1.40 (s, 3H), 1.09 (s, 6H) ppm.

Synthesis of silyl ether S6-3

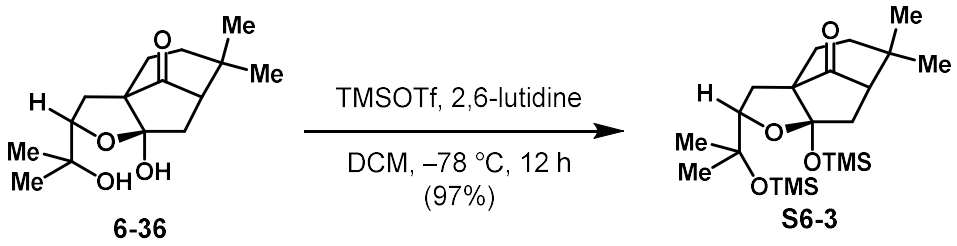

A flame-dried flask was charged with hemiketal **6-36** (200 mg, 0.75 mmol, 1 equiv) followed by DCM (7.5 mL). To this clear solution was added 2,6-lutidine (0.52 mL , 4.5 mmol, 6 equiv). The clear reaction mixture was cooled to –78 °C after which TMSOTf was added (0.30 mL, 1.65 mmol, 2.2 equiv). The reaction mixture was stirred at this temperature for 12 h. The flask was warmed to room temperature whereupon the reaction mixture was quenched by addition of sat. aq. NH_4Cl and diluted with EtOAc. The aqueous layer was extracted two times with EtOAc. The organic layers were combined, washed with sat. aq. NaCl, dried over Na_2SO_4, filtered, and concentrated *in vacuo*. The crude residue was purified by silica gel chromatography (hexanes:EtOAc 4:1) to give silyl hemiketal **S6-3** as a clear oil (300 mg, 97%).

$\mathbf{R_f}$ = 0.6 (hexane:EtOAc = 4:1), purple spot (*p*-anisaldehyde)

^{1}H NMR (400 MHz, $CDCl_3$) δ 3.75 (dd, *J* = 10.2, 6.2 Hz, 1H), 2.38 (dd, *J* = 13.7, 7.4 Hz, 1H), 2.29 – 2.17 (m, 2H), 2.11 (d, *J* = 7.4 Hz, 1H), 1.83 (t, *J* = 2.2 Hz, 2H), 1.50 (dd, *J* = 12.2, 10.1 Hz, 1H), 1.29 (d, *J* = 1.4 Hz, 2H), 1.24 (s, 3H), 1.17 (s, 3H), 1.01 (d, *J* = 7.1 Hz, 6H), 0.28 (s, 9H), 0.14 (d, *J* = 2.8 Hz, 9H) ppm.

Synthesis of alcohol 6-40

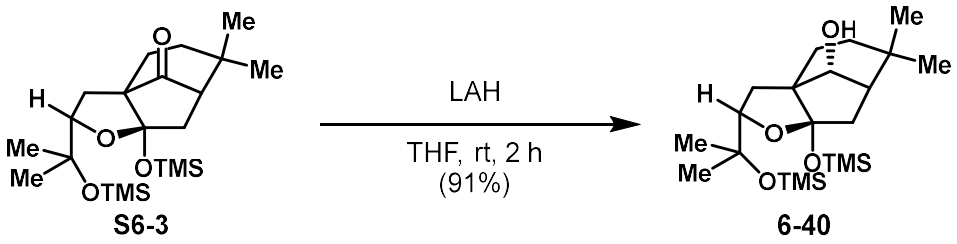

A flame-dried flask was charged with silyl hemiketal **S6-3** (553 mg, 1.34 mmol, 1 equiv) followed by THF (13.4 mL). This clear solution was cooled 0 °C in an ice bath, after which lithium aluminum hydride (0.67 mL, 1.34 mmol, 2 M solution in hexanes) was added dropwise. After addition the reaction mixture was warmed up to room temperature and allowed to stir for 1 h. The reaction mixture was quenched by addition of sat. aq. NaCl and diluted with EtOAc. The aqueous layer was extracted 4 times with EtOAc. The organic layers were combined, washed further with sat. aq. NaCl, dried over Na_2SO_4, filtered, and concentrated *in vacuo*. The crude residue was purified by silica gel chromatography (hexanes:EtOAc 4:1) to give alcohol **6-39** as a white solid (510 mg, 97%).

R_f = 0.6 (hexane:EtOAc = 4:1), purple spot (*p*-anisaldehyde)

^{1}H NMR (700 MHz, $CDCl_3$) δ 3.96 – 3.91 (m, 2H), 2.07 (dd, *J* = 14.1, 6.8 Hz, 1H), 1.97 (s, 1H), 1.95 – 1.90 (m, 1H), 1.85 (d, *J* = 5.8 Hz, 1H), 1.81 (dd, *J* = 12.7, 6.3 Hz, 1H), 1.67 (dd, *J* = 13.4, 5.9 Hz, 1H), 1.50 – 1.46 (m, 1H), 1.25 (d, *J* = 7.6 Hz, 5H), 1.22 (s, 3H), 1.16 (s, 3H), 0.83 (s, 3H), 0.19 (s, 9H), 0.10 (s, 9H) ppm.

Synthesis of (bromomethyl)dimethylsilyl ether S6-4

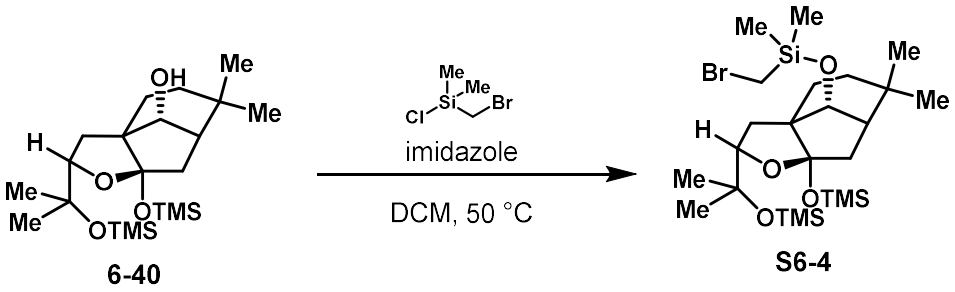

A flame-dried vial was charged alcohol **6-40** (10 mg, 0.024 mmol, 1 equiv) followed by DCM (1 mL). To this clear solution was added imidazole (6.5 mg, 0.096 mmol, 4 equiv) and (bromomethyl)dimethyl silane (6.5 µL, 0.048 mmol, 2 equiv) whereupon a white precipitate formed. The vial was moved to a preheated vial block at 50 °C and stirred for 14 h. The reaction mixture was cooled back to room temperature, quenched by addition of sat. aq. NaCl, and diluted with EtOAc. The aqueous layer was extracted two times with EtOAc. The organic layers were combined, washed further with sat. aq. NaCl, dried over Na_2SO_4, filtered, and concentrated *in vacuo*. The crude residue was sufficiently pure for the next reaction and unstable to silica gel chromatography.

R_f = 0.5 (hexane:EtOAc = 8:1), purple spot (*p*-anisaldehyde)

^{1}H NMR (400 MHz, $CDCl_3$) δ 3.89 (d, *J* = 5.3 Hz, 2H), 2.48 (s, 2H), 2.44 (s, 2H), 2.03 (d, *J* = 7.0 Hz, 1H), 1.98 – 1.87 (m, 2H), 1.76 – 1.67 (m, 2H), 1.67 – 1.57 (m, 2H), 1.42 (dd, *J* = 12.7, 10.3 Hz, 1H), 1.24 (s, 4H), 1.15 (d, *J* = 3.4 Hz, 7H), 0.80 (s, 3H), 0.28 (s, 6H), 0.25 (s, 6H), 0.18 (s, 9H), 0.10 (s, 9H) ppm.

Synthesis of (iodomethyl)dimethylsilyl ether 6-41

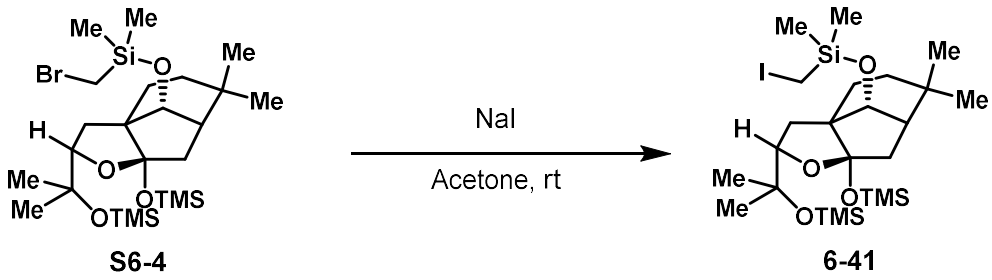

S6-4 **6-41**

A flame-dried vial was charged with crude **S6-4** followed by acetone (1 mL). Sodium iodide (10 mg, 0.067 mmol, 2.8 equiv) was added as a solid and the reaction was stirred for 24 hours at room temperature under air turning orange in color. The reaction mixture was quenched by addition of sat. aq. $NaHCO_3$ and sat. aq. $Na_2S_2O_3$ then diluted with EtOAc. The aqueous layer was extracted two times with EtOAc. The organic layers were combined, washed with sat. aq. NaCl, dried over Na_2SO_4, filtered, and concentrated *in vacuo*. The crude residue was purified by preparatory thin-layer silica gel chromatography (hexanes:EtOAc 4:1) to yield silyl ether **6-41** (12.6 mg, 86%, 2 steps).

$\mathbf{R_f}$ = 0.6 (hexane:EtOAc = 4:1), purple spot (*p*-anisaldehyde)

^{1}H NMR (400 MHz, $CDCl_3$) δ 3.88 (t, *J* = 4.9 Hz, 2H), 2.04 – 2.00 (m, 3H), 1.94 (d, *J* = 14.3 Hz, 2H), 1.81 – 1.69 (m, 2H), 1.67 – 1.60 (m, 1H), 1.44 (d, *J* = 10.7 Hz, 1H), 1.25 (s, 3H), 1.15 (d, *J* = 4.7 Hz, 6H), 0.80 (s, 3H), 0.31 (s, 6H), 0.18 (d, *J* = 1.4 Hz, 9H), 0.10 (d, *J* = 1.3 Hz, 9H) ppm.

Attempted remote desaturation of 6-41

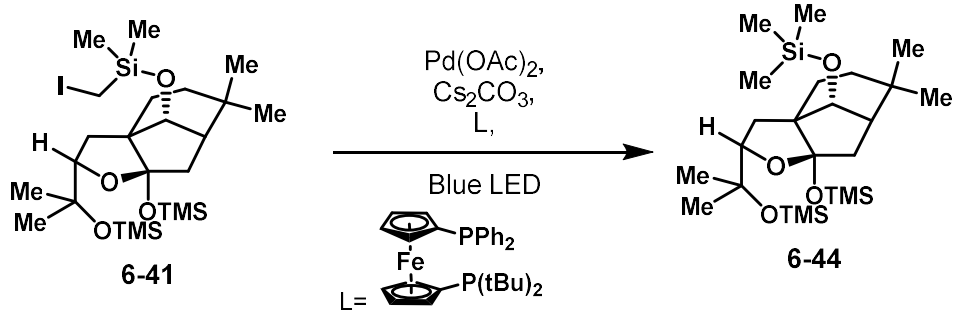

A flame-dried vial was charged with silyl ether **6-41** (10 mg, 0.016 mmol, 1 equiv) and palladium acetate (0.36 mg, 0.0016 mmol, 0.1 equiv). The vial was moved into a glove box wherein 1-diphenylphosphino-1'-(di-tert-butylphosphino)ferrocene (0.16 mg, 0.0032 mmol, 0.2 equiv), cesium carbonate (10 mg, 0.032 mmol, 2 equiv), and degassed benzene (0.1 mL) were added. The vial was sealed and removed from the glovebox. The vial was positioned 3 cm away from a tuna blue Kessil lamp and irradiated for 16 h with a constant stream of air over the vial to maintain temperature. The crude reaction mixture was filtered through a silica plug, but no desired product was observed by NMR analysis.

Synthesis of acetate 6-45

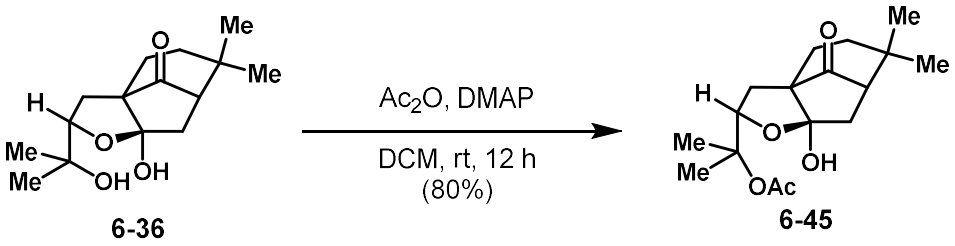

A flame-dried vial was charged with hemiketal **6-40** (10 mg, 0.037 mmol, 1 equiv) followed by DCM (1 mL). To this clear solution was added DMAP (4.5 mg, 0.037 mmol, 1 equiv) and acetic anhydride (175 µL, 1.85 mmol, 50 equiv). The clear reaction mixture was allowed to stir for 12 h whereupon it was quenched by the addition of sat. aq. NH_4Cl and diluted with EtOAc. The aqueous layer was extracted 2 times with EtOAc. The organic layers were combined, washed with sat. aq. NaCl, dried over Na_2SO_4, filtered, and concentrated *in vacuo*. The crude residue was purified by preparatory thin layer chromatography (hexanes:EtOAc 2:1) to give hemiketal **6-45** (9.2 mg, 80%).

R_f = 0.5 (hexane:EtOAc = 2:1), purple spot (*p*-anisaldehyde)

^{1}H NMR (700 MHz, $CDCl_3$) δ 3.96 – 3.93 (m, 1H), 2.75 – 2.71 (m, 1H), 2.47 (d, *J* = 15.3 Hz, 1H), 2.30 – 2.27 (m, 1H), 2.14 (d, *J* = 7.6 Hz, 1H), 2.10 (s, 3H), 1.97 – 1.93 (m, 1H), 1.90 (dd, *J* = 13.0, 5.7 Hz, 1H), 1.72 (dt, *J* = 13.5, 6.7 Hz, 1H), 1.65 – 1.61 (m, 1H), 1.26 (q, *J* = 6.5, 6.1 Hz, 2H), 1.20 (d, *J* = 6.5 Hz, 1H), 1.17 (s, 3H), 1.07 (s, 4H), 0.98 (d, *J* = 13.8 Hz, 6H) ppm.

Synthesis of (bromomethyl)dimethylsilyl ether S6-5

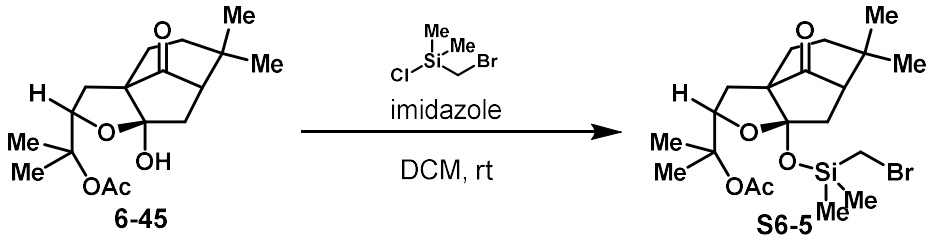

A flame-dried vial was charged with hemiketal **6-45** (5mg, 0.019 mmol, 1 equiv) followed by DCM (1 mL). To this clear solution was added imidazole (5 mg, 0.076 mmol, 4 equiv) and (bromomethyl)dimethyl silane (5 µL, 0.038 mmol, 2 equiv) whereupon a white precipitate formed. The vial was moved to a preheated vial block at 50 °C and stirred for 14 h. The reaction mixture was cooled back to room temperature, quenched by addition of sat. aq. NaCl, and diluted with EtOAc. The aqueous layer was extracted 2 times with EtOAc. The organic layers were combined, washed further with sat. aq. NaCl, dried over Na_2SO_4, filtered, and concentrated *in vacuo*. The crude residue was sufficiently pure for the next reaction and unstable to silica gel chromatography.

R_f = 0.5(hexane:EtOAc = 4:1), purple spot (*p*-anisaldehyde)

^{1}H NMR (700 MHz, $CDCl_3$) δ 3.85 (dd, *J* = 9.9, 6.5 Hz, 1H), 2.68 (dd, *J* = 15.3, 7.5 Hz, 1H), 2.43 (d, *J* = 15.1 Hz, 1H), 2.27 (dd, *J* = 12.5, 6.5 Hz, 1H), 2.12 (d, *J* = 7.4 Hz, 1H), 2.07 (s, 3H), 2.01 (s, 2H), 1.95 – 1.91 (m, 1H), 1.88 – 1.85 (m, 1H), 1.71 (d, *J* = 6.4 Hz, 1H), 1.62 – 1.57 (m, 1H), 1.15 (s, 3H), 1.13 (s, 3H), 0.98 (s, 3H), 0.96 (s, 3H), 0.27 (m, 6H) ppm.

Synthesis of (iodomethyl)dimethylsilyl ether 6-46

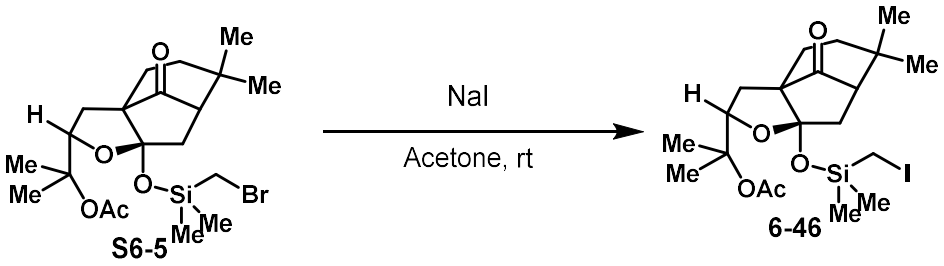

A flame-dried vial was charged with crude **S6-4** followed by acetone (0.5 mL). Sodium iodide (5.6 mg, 0.038 mmol, 2 equiv) was added as a solid and the reaction was stirred for 24 hours at room temperature under air turning orange in color. The reaction mixture was quenched by addition of sat. aq. $NaHCO_3$ and sat. aq. $Na_2S_2O_3$ and diluted with EtOAc. The aqueous layer was extracted two times with EtOAc. The organic layers were combined, washed with sat. aq. NaCl, dried over Na_2SO_4, filtered, and concentrated *in vacuo*. The crude residue was purified by preparatory thin-layer silica gel chromatography (hexanes:EtOAc 4:1) to yield silyl ether **6-46** over 2 steps.

R_f = 0.5(hexane:EtOAc = 4:1), purple spot (*p*-anisaldehyde)

^{1}H NMR (700 MHz, $CDCl_3$) δ 4.11 (q, *J* = 7.2 Hz, 1H), 2.79 (dd, *J* = 15.9, 7.4 Hz, 1H), 2.66 (d, *J* = 15.9 Hz, 1H), 2.13 (d, *J* = 7.3 Hz, 1H), 2.08 (s, 3H), 2.04 (s, 2H), 1.76 (td, *J* = 13.6, 5.9 Hz, 1H), 1.33 (s, 6H), 1.09 – 1.05 (m, 2H), 0.98 (dd, *J* = 22.3, 9.3 Hz, 6H), 0.11 (s, 6H) ppm.

Synthesis of enol ether 6-48

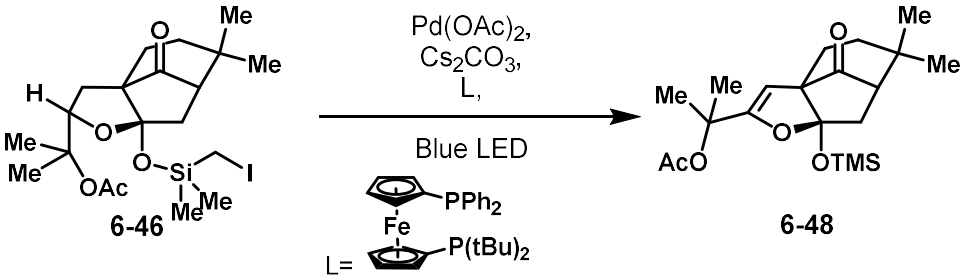

A flame-dried vial was charged with silyl ether **6-46** (3 mg, 0.006 mmol, 1 equiv) and palladium acetate (0.13 mg, 0.0006 mmol, 0.1 equiv). The vial was moved into a glove box wherein L (0.0 6 mg, 0.0012 mmol, 0.2 equiv), cesium carbonate (5 mg, 0.012 mmol, 2 equiv), and degassed benzene (0.1 mL) were added. The vial was sealed and removed from the glovebox. The vial was positioned 3 cm away from a tuna blue Kessil lamp and irradiated for 16 h with a constant stream of air over the vial to maintain temperature. The crude reaction mixture was loaded directly onto a preparatory TLC plate and eluted (hexanes:EtOAc 4:1). Enol ether **6-48** was isolated as a clear oil.

R_f = 0.55 (hexane:EtOAc = 4:1), purple spot (*p*-anisaldehyde)

^{1}H NMR (700 MHz, $CDCl_3$) δ 4.95 (s, 1H), 2.79 (dd, *J* = 15.8, 7.4 Hz, 1H), 2.67 (d, *J* = 15.8 Hz, 1H), 2.14 (d, *J* = 7.5 Hz, 1H), 2.09 (s, 3H), 2.02 (dd, *J* = 12.9, 5.7 Hz, 1H), 1.77 (dt, *J* = 13.4, 6.7 Hz, 1H), 1.33 (s, 6H), 1.00 (d, *J* = 8.0 Hz, 6H), 0.11 (s, 9H) ppm.

Synthesis of ether 6-49

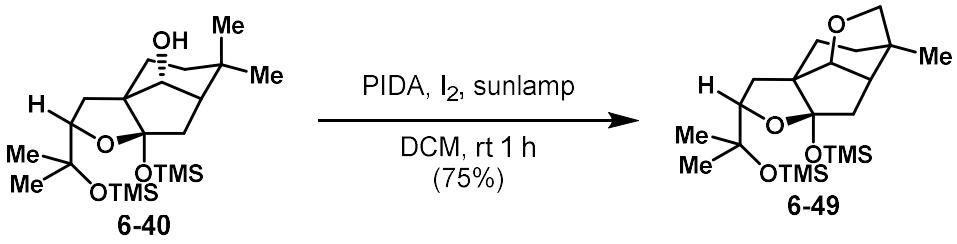

A flame-dried vial was charged with alcohol **6-40** (100 mg, 0.24 mmol, 1 equiv) followed by DCM (2.4 mL). To this clear solution was added PIDA (78 mg, 0.24 mmol, 1 equiv) and molecular iodine (31 mg, 0.12 mmol, 0.5 equiv). The solution immediately turned pink-purple in color. The stirring reaction mixture was irradiated by sunlamp (CFL 6 w) for 1 h. The reaction mixture was quenched by addition of sat. aq. $NaHCO_3$ and sat. aq. $Na_2S_2O_3$ and diluted with EtOAc. The aqueous layer was extracted two times with EtOAc. The organic layers were combined, washed with sat. aq. NaCl, dried over Na_2SO_4, filtered, and concentrated *in vacuo*. The crude residue was purified by flash silica gel chromatography (hexanes:EtOAc 4:1) to yield ether **6-49** (75 mg, 75%) as a yellow solid.

R_f = 0.6 (hexane:EtOAc = 4:1), purple spot (*p*-anisaldehyde)

^{1}H NMR (700 MHz, $CDCl_3$) δ 4.24 (d, *J* = 5.9 Hz, 1H), 3.95 (dd, *J* = 10.3, 6.2 Hz, 1H), 3.81 (d, *J* = 7.7 Hz, 1H), 3.68 (dd, *J* = 7.7, 2.8 Hz, 1H), 2.28 – 2.21 (m, 2H), 1.86 (d, *J* = 13.2 Hz, 1H), 1.79 (tt, *J* = 12.3, 6.5 Hz, 2H), 1.48 (dd, *J* = 12.5, 10.3 Hz, 2H), 1.41 (dd, *J* = 12.7, 6.5 Hz, 1H), 1.27 (s, 3H), 1.15 (s, 3H), 0.93 (s, 3H), 0.21 (s, 9H), 0.12 (s, 9H) ppm.

Synthesis of lactone 6-50

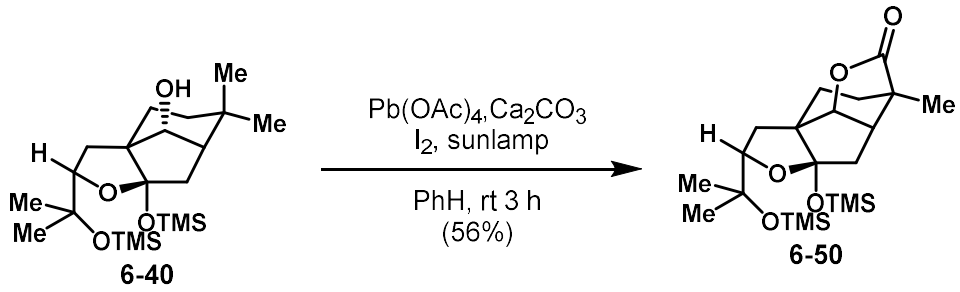

A flame-dried vial was charged with alcohol **6-40** (100 mg, 0.24 mmol, 1 equiv) followed by benzene (3 mL). To this clear solution was added freshly recrystallized lead tetraacetate (321 mg, 0.72 mmol, 3 equiv), molecular iodine (184 mg, 0.72 mmol, 3 equiv) and calcium carbonate (241 mg, 2.41 mmol, 10 equiv). The solution immediately turned dark brown pink-purple in color. The stirring reaction mixture was irradiated by sunlamp (CFL 6 w) for 1 h. The reaction mixture was quenched by addition of sat. aq. $NaHCO_3$ and sat. aq. $Na_2S_2O_3$ and diluted with EtOAc. The aqueous layer was extracted two times with EtOAc. The organic layers were combined, washed with sat. aq. NaCl, dried over Na_2SO_4, filtered, and concentrated *in vacuo*. The crude residue was purified by flash silica gel chromatography (hexanes:EtOAc 4:1) to yield ether **6-49** (58 mg, 56%) as a yellow solid.

$\mathbf{R_f}$ = 0.55 (hexane:EtOAc = 4:1), purple spot (*p*-anisaldehyde)

^{1}H NMR (700 MHz, $CDCl_3$) δ 4.60 (d, *J* = 6.3 Hz, 1H), 4.00 (dd, *J* = 10.4, 6.1 Hz, 1H), 2.60 (t, *J* = 6.9 Hz, 1H), 2.39 – 2.30 (m, 2H), 1.94 – 1.87 (m, 2H), 1.67 (dd, *J* = 10.7, 4.5 Hz, 2H), 1.48 – 1.44 (m, 2H), 1.28 (s, 3H), 1.18 (s, 3H), 1.12 (s, 3H), 0.23 (s, 9H), 0.13 (s, 9H) ppm.

Synthesis of [3.2.1.0^{3,6}] tricycle 6-52

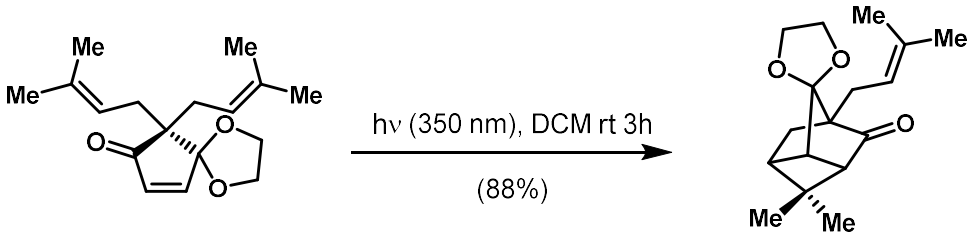

6-51 6-52

Irradiation precursor (12 mg, 0.042 mmol) was dissolved in degassed DCM (0.84 mL). The solution was moved into a Luzchem photobox and irradiated at 350 nm (UVB) for four hours. The dissolved crude mixtures were then purified by prepTLC (*n*Hex/EtOAc = 9/1) to give the title compound as yellow oil (10.6 mg, 88%).

R_f = 0.2(hexane:EtOAc = 9:1), purple streak (*p*-anisaldehyde)

^{1}H NMR (500 MHz, $CDCl_3$) δ 5.32 (ddt, *J* = 8.2, 6.8, 1.5 Hz, 1H), 4.03 – 3.83 (m, 4H), 2.98 (t, *J* = 4.4 Hz, 1H), 2.56 (t, *J* = 4.7 Hz, 1H), 2.37 – 2.18 (m, 4H), 2.15 – 2.01 (m, 1H), 1.71 (d, *J* = 1.5 Hz, 3H), 1.66 (d, *J* = 23.8 Hz, 4H), 1.30 (s, 3H), 0.81 (s, 3H) ppm.

^{13}C NMR (151 MHz, $CDCl_3$) δ 212.9, 132.4, 119.9, 116.5, 65.4, 65.5, 64.5, 60.0, 57.0, 44.5, 43.4, 41.0, 31.9, 30.9, 28.3, 26.1, 25.9, 22.0, 21.0, 17.7 2X ppm.

HRMS EI [M]+ calculated for $C_{17}H_{24}O_3$: 276.1725, found: 276.1725.

Synthesis of silyl cyanohydrin 6-55

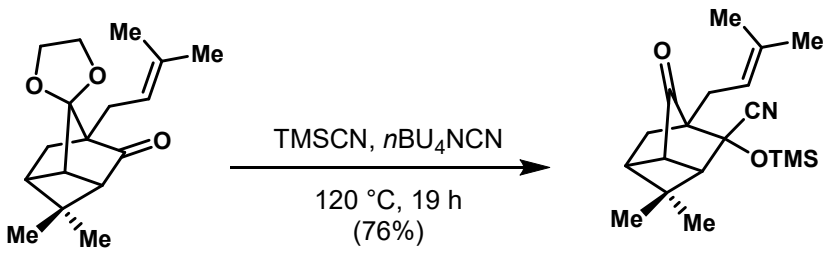

6-52 **6-55**

A flame-dried vial was charged with cyclobutene **6-52** (30 mg, 0.11 mmol, 1 equiv), TMSCN (100 mg, 1.01 mmol, 9.3 equiv), and tetrabutylammonium cyanide (6 mg, 0.02 mmol, 0.2 equiv). The reaction mixture was moved to a preheated vial block at 120 °C and stirred for 19 h. The reaction mixture was then cooled to room temperature and quenched by the addition of sat. aq. NaCl and diluted with EtOAc. The aqueous layer was extracted two times with EtOAc. The organic layers were combined, washed with sat. aq. NaCl, dried over Na_2SO_4, filtered, and concentrated *in vacuo*. The crude residue was purified by flash silica gel chromatography (hexanes:EtOAc 4:1) to yield ether silyl cyanohydrin **6-55** (31 mg, 76%) as a clear oil with recovered starting material (6 mg, 20%).

R_f = 0.6 (hexane:EtOAc = 4:1), purple spot (*p*-anisaldehyde)

^{1}H NMR (700 MHz, $CDCl_3$) δ 5.35 – 5.29 (m, 1H), 4.01 – 3.84 (m, 4H), 2.98 (t, *J* = 4.5 Hz, 1H), 2.56 (t, *J* = 4.8 Hz, 1H), 2.35 – 2.28 (m, 2H), 2.26 – 2.21 (m, 1H), 2.11 (dd, *J* = 14.9, 7.9 Hz, 1H), 1.76 (d, *J* = 12.4 Hz, 1H), 1.70 (dd, *J* = 3.5, 1.9 Hz, 3H), 1.66 – 1.61 (m, 3H), 1.30 (s, 3H), 0.81 (s, 3H), 0.24 (s, 9H) ppm.

X-ray Crystallographic data

A colorless block 0.18 x 0.16 x 0.11 mm in size was mounted on a Cryoloop with Paratone oil. Data were collected in a nitrogen gas stream at 100(2) K using omega scans. Crystal-to-detector distance was 30.23 mm and exposure time was 0.50 seconds per frame using a scan width of 0.5°. Data collection was 100% complete to 74.000° in θ. A total of 52325 reflections were collected covering the indices -15<=h<=15, -11<=k<=11, -17<=l<=17. 3203 reflections were found to be symmetry independent, with an R_{int} of 0.0672. Indexing and unit cell refinement indicated a primitive, monoclinic lattice. The space group was found to be P 21/n (No. 14). The data were integrated using the CrysAlis^{Pro} 1.171.40.71a software program and scaled using the SCALE3 ABSPACK scaling algorithm. Solution by intrinsic phasing (SHELXT-2015) produced a heavy-atom phasing model consistent with the proposed structure. All non-hydrogen atoms were refined anisotropically by full-matrix least-squares (SHELXL-2014). All hydrogen atoms were placed using a riding model. Their positions were constrained relative to their parent atom using the appropriate HFIX command in SHELXL-2014.

Table 1. Crystal data and structure refinement for IB003_Sarpong.

Identification code	IB003_Sarpong
Empirical formula	C17 H28 O5
Formula weight	312.39
Temperature	100(2) K
Wavelength	1.54184 Å
Crystal system	Monoclinic
Space group	P 21/n
Unit cell dimensions	a = 12.63730(10) Å a= 90°.
	b = 9.50810(10) Å b= 114.7090(10)°.
	c = 14.40200(10) Å g = 90°.
Volume	1572.06(3) Å3
Z	4
Density (calculated)	1.320 Mg/m3
Absorption coefficient	0.780 mm-1
F(000)	680

Crystal size	0.180 x 0.160 x 0.110 mm3
Theta range for data collection	3.920 to 74.486°.
Index ranges	-15<=h<=15, -11<=k<=11, -17<=l<=17
Reflections collected	52325
Independent reflections	3203 [R(int) = 0.0672]
Completeness to theta = 74.000°	99.8 %
Absorption correction	Semi-empirical from equivalents
Max. and min. transmission	1.00000 and 0.82376
Refinement method	Full-matrix least-squares on F2
Data / restraints / parameters	3203 / 0 / 215
Goodness-of-fit on F2	1.081
Final R indices [I>2sigma(I)]	R1 = 0.0393, wR2 = 0.1020
R indices (all data)	R1 = 0.0400, wR2 = 0.1025
Extinction coefficient	n/a
Largest diff. peak and hole	0.361 and -0.276 e.Å-3

Table 2. Atomic coordinates (x 104) and equivalent isotropic displacement parameters (Å2x 103)

for ib003_sarpong. U(eq) is defined as one third of the trace of the orthogonalized Uij tensor.

	x	y	z	U(eq)
C(1)	1317(1)	10330(1)	3805(1)	18(1)
C(2)	703(1)	11760(1)	3614(1)	19(1)
C(3)	-594(1)	11439(1)	2927(1)	19(1)
C(4)	-1291(1)	12753(1)	2397(1)	24(1)
C(5)	-1165(1)	10853(1)	3603(1)	23(1)
C(6)	-445(1)	10366(1)	2157(1)	17(1)
C(7)	688(1)	9508(1)	2802(1)	16(1)
C(8)	1437(1)	9244(1)	2200(1)	18(1)
C(9)	742(1)	8649(1)	1120(1)	18(1)
C(10)	-139(1)	7468(1)	1043(1)	19(1)
C(11)	443(1)	6012(1)	1264(1)	24(1)
C(12)	-1100(1)	7422(1)	-57(1)	23(1)
C(13)	-703(1)	7802(1)	1792(1)	18(1)
C(14)	-1366(1)	9229(1)	1613(1)	20(1)
C(15)	218(1)	8045(1)	2895(1)	18(1)
C(16)	789(1)	5990(2)	3810(1)	31(1)
C(17)	-294(1)	6567(1)	3880(1)	28(1)
O(1)	1131(1)	12658(1)	3044(1)	22(1)
O(2)	-312(1)	11198(1)	1372(1)	20(1)
O(3)	1571(1)	8208(1)	729(1)	21(1)

O(4)	1141(1)	7066(1)	3312(1)	20(1)
O(5)	-333(1)	8002(1)	3583(1)	21(1)

Table 3. Bond lengths [Å] and angles [°] for ib003_sarpong.

_____

C(1)-C(2)	1.5330(16)
C(1)-C(7)	1.5391(15)
C(1)-H(1A)	0.9900
C(1)-H(1B)	0.9900
C(2)-O(1)	1.4371(14)
C(2)-C(3)	1.5511(16)
C(2)-H(2A)	1.0000
C(3)-C(4)	1.5353(17)
C(3)-C(5)	1.5376(16)
C(3)-C(6)	1.5742(16)
C(4)-H(4A)	0.9800
C(4)-H(4B)	0.9800
C(4)-H(4C)	0.9800
C(5)-H(5A)	0.9800
C(5)-H(5B)	0.9800
C(5)-H(5C)	0.9800
C(6)-O(2)	1.4456(14)
C(6)-C(14)	1.5417(16)
C(6)-C(7)	1.5708(15)
C(7)-C(15)	1.5399(16)
C(7)-C(8)	1.5487(15)
C(8)-C(9)	1.5386(15)
C(8)-H(8A)	0.9900
C(8)-H(8B)	0.9900
C(9)-O(3)	1.4448(13)

C(9)-C(10)	1.5517(16)
C(9)-H(9)	1.0000
C(10)-C(11)	1.5369(17)
C(10)-C(12)	1.5415(15)
C(10)-C(13)	1.5545(16)
C(11)-H(11A)	0.9800
C(11)-H(11B)	0.9800
C(11)-H(11C)	0.9800
C(12)-H(12A)	0.9800
C(12)-H(12B)	0.9800
C(12)-H(12C)	0.9800
C(13)-C(15)	1.5455(15)
C(13)-C(14)	1.5581(16)
C(13)-H(13)	1.0000
C(14)-H(14A)	0.9900
C(14)-H(14B)	0.9900
C(15)-O(4)	1.4141(14)
C(15)-O(5)	1.4308(14)
C(16)-O(4)	1.4235(16)
C(16)-C(17)	1.5166(19)
C(16)-H(16A)	0.9900
C(16)-H(16B)	0.9900
C(17)-O(5)	1.4247(15)
C(17)-H(17A)	0.9900
C(17)-H(17B)	0.9900
O(1)-H(1)	0.89(2)
O(2)-H(2)	0.87(2)

O(3)-H(3) 0.89(2)

C(2)-C(1)-C(7) 104.96(9)
C(2)-C(1)-H(1A) 110.8
C(7)-C(1)-H(1A) 110.8
C(2)-C(1)-H(1B) 110.8
C(7)-C(1)-H(1B) 110.8
H(1A)-C(1)-H(1B) 108.8
O(1)-C(2)-C(1) 110.28(9)
O(1)-C(2)-C(3) 107.62(9)
C(1)-C(2)-C(3) 105.07(9)
O(1)-C(2)-H(2A) 111.2
C(1)-C(2)-H(2A) 111.2
C(3)-C(2)-H(2A) 111.2
C(4)-C(3)-C(5) 106.64(10)
C(4)-C(3)-C(2) 112.95(10)
C(5)-C(3)-C(2) 108.55(10)
C(4)-C(3)-C(6) 112.92(10)
C(5)-C(3)-C(6) 115.95(10)
C(2)-C(3)-C(6) 99.84(9)
C(3)-C(4)-H(4A) 109.5
C(3)-C(4)-H(4B) 109.5
H(4A)-C(4)-H(4B) 109.5
C(3)-C(4)-H(4C) 109.5
H(4A)-C(4)-H(4C) 109.5
H(4B)-C(4)-H(4C) 109.5
C(3)-C(5)-H(5A) 109.5

C(3)-C(5)-H(5B) 109.5

H(5A)-C(5)-H(5B) 109.5

C(3)-C(5)-H(5C) 109.5

H(5A)-C(5)-H(5C) 109.5

H(5B)-C(5)-H(5C) 109.5

O(2)-C(6)-C(14) 107.23(9)

O(2)-C(6)-C(7) 111.81(9)

C(14)-C(6)-C(7) 104.11(9)

O(2)-C(6)-C(3) 106.49(9)

C(14)-C(6)-C(3) 121.64(9)

C(7)-C(6)-C(3) 105.57(9)

C(1)-C(7)-C(15) 116.33(9)

C(1)-C(7)-C(8) 114.27(9)

C(15)-C(7)-C(8) 104.54(9)

C(1)-C(7)-C(6) 106.05(9)

C(15)-C(7)-C(6) 103.39(9)

C(8)-C(7)-C(6) 111.86(9)

C(9)-C(8)-C(7) 113.61(9)

C(9)-C(8)-H(8A) 108.8

C(7)-C(8)-H(8A) 108.8

C(9)-C(8)-H(8B) 108.8

C(7)-C(8)-H(8B) 108.8

H(8A)-C(8)-H(8B) 107.7

O(3)-C(9)-C(8) 107.44(9)

O(3)-C(9)-C(10) 112.14(10)

C(8)-C(9)-C(10) 115.40(9)

O(3)-C(9)-H(9) 107.2

C(8)-C(9)-H(9)	107.2
C(10)-C(9)-H(9)	107.2
C(11)-C(10)-C(12)	106.91(10)
C(11)-C(10)-C(9)	111.77(9)
C(12)-C(10)-C(9)	109.12(10)
C(11)-C(10)-C(13)	111.04(10)
C(12)-C(10)-C(13)	108.98(9)
C(9)-C(10)-C(13)	108.96(9)
C(10)-C(11)-H(11A)	109.5
C(10)-C(11)-H(11B)	109.5
H(11A)-C(11)-H(11B)	109.5
C(10)-C(11)-H(11C)	109.5
H(11A)-C(11)-H(11C)	109.5
H(11B)-C(11)-H(11C)	109.5
C(10)-C(12)-H(12A)	109.5
C(10)-C(12)-H(12B)	109.5
H(12A)-C(12)-H(12B)	109.5
C(10)-C(12)-H(12C)	109.5
H(12A)-C(12)-H(12C)	109.5
H(12B)-C(12)-H(12C)	109.5
C(15)-C(13)-C(10)	112.16(9)
C(15)-C(13)-C(14)	99.29(9)
C(10)-C(13)-C(14)	115.78(10)
C(15)-C(13)-H(13)	109.7
C(10)-C(13)-H(13)	109.7
C(14)-C(13)-H(13)	109.7
C(6)-C(14)-C(13)	106.70(9)

C(6)-C(14)-H(14A)	110.4
C(13)-C(14)-H(14A)	110.4
C(6)-C(14)-H(14B)	110.4
C(13)-C(14)-H(14B)	110.4
H(14A)-C(14)-H(14B)	108.6
O(4)-C(15)-O(5)	103.95(9)
O(4)-C(15)-C(7)	110.60(9)
O(5)-C(15)-C(7)	113.77(9)
O(4)-C(15)-C(13)	118.11(10)
O(5)-C(15)-C(13)	109.42(9)
C(7)-C(15)-C(13)	101.39(9)
O(4)-C(16)-C(17)	104.72(10)
O(4)-C(16)-H(16A)	110.8
C(17)-C(16)-H(16A)	110.8
O(4)-C(16)-H(16B)	110.8
C(17)-C(16)-H(16B)	110.8
H(16A)-C(16)-H(16B)	108.9
O(5)-C(17)-C(16)	104.22(10)
O(5)-C(17)-H(17A)	110.9
C(16)-C(17)-H(17A)	110.9
O(5)-C(17)-H(17B)	110.9
C(16)-C(17)-H(17B)	110.9
H(17A)-C(17)-H(17B)	108.9
C(2)-O(1)-H(1)	106.9(14)
C(6)-O(2)-H(2)	105.7(13)
C(9)-O(3)-H(3)	109.0(13)
C(15)-O(4)-C(16)	108.14(9)

C(17)-O(5)-C(15) 105.60(9)

Symmetry transformations used to generate equivalent atoms:

Table 4. Anisotropic displacement parameters (Å2x 103)for ib003_sarpong. The anisotropic displacement factor exponent takes the form: -2p2[h2a*2U11 + ... + 2 h k a* b* U12]

	U11	U22	U33	U23	U13	U12
C(1)	17(1)	20(1)	17(1)	-1(1)	7(1)	-1(1)
C(2)	19(1)	20(1)	20(1)	-2(1)	9(1)	-2(1)
C(3)	17(1)	19(1)	22(1)	-2(1)	9(1)	0(1)
C(4)	19(1)	21(1)	31(1)	-1(1)	11(1)	2(1)
C(5)	21(1)	24(1)	27(1)	-3(1)	14(1)	-1(1)
C(6)	14(1)	19(1)	18(1)	1(1)	7(1)	1(1)
C(7)	14(1)	17(1)	17(1)	-1(1)	6(1)	0(1)
C(8)	13(1)	22(1)	17(1)	-1(1)	6(1)	0(1)
C(9)	14(1)	23(1)	17(1)	-2(1)	7(1)	2(1)
C(10)	16(1)	22(1)	16(1)	-2(1)	5(1)	0(1)
C(11)	26(1)	21(1)	23(1)	-3(1)	10(1)	1(1)
C(12)	19(1)	28(1)	19(1)	-3(1)	5(1)	-4(1)
C(13)	15(1)	19(1)	19(1)	-1(1)	6(1)	-1(1)
C(14)	14(1)	22(1)	21(1)	-2(1)	6(1)	0(1)
C(15)	17(1)	20(1)	17(1)	0(1)	7(1)	1(1)
C(16)	26(1)	26(1)	36(1)	12(1)	10(1)	2(1)
C(17)	40(1)	20(1)	32(1)	1(1)	22(1)	-3(1)
O(1)	18(1)	21(1)	25(1)	1(1)	8(1)	-3(1)
O(2)	19(1)	21(1)	18(1)	3(1)	7(1)	1(1)
O(3)	16(1)	31(1)	18(1)	-2(1)	8(1)	3(1)
O(4)	19(1)	19(1)	20(1)	3(1)	6(1)	3(1)
O(5)	25(1)	20(1)	23(1)	0(1)	14(1)	-2(1)

Table 5. Hydrogen coordinates (x 104) and isotropic displacement parameters (Å2x 103) for ib003_sarpong.

	x	y	z	U(eq)
H(1A)	1246	9836	4382	22
H(1B)	2154	10445	3963	22
H(2A)	795	12213	4270	23
H(4A)	-917	13207	2000	35
H(4B)	-1312	13410	2913	35
H(4C)	-2087	12480	1938	35
H(5A)	-1207	11596	4058	34
H(5B)	-699	10068	4012	34
H(5C)	-1953	10523	3169	34
H(8A)	1803	10142	2143	21
H(8B)	2070	8578	2590	21
H(9)	285	9445	682	21
H(11A)	-107	5313	1304	35
H(11B)	1136	6039	1915	35
H(11C)	670	5755	713	35
H(12A)	-1416	8370	-264	35
H(12B)	-1724	6790	-83	35
H(12C)	-771	7079	-521	35
H(13)	-1233	7016	1783	22
H(14A)	-1769	9434	873	24

H(14B)	-1953	9195	1902	24
H(16A)	1407	5799	4499	37
H(16B)	611	5109	3407	37
H(17A)	-998	6057	3412	34
H(17B)	-234	6490	4586	34

H(1)	1880(20)	12800(20)	3432(16)	54(6)
H(2)	230(17)	11810(20)	1695(15)	44(5)
H(3)	1267(17)	8350(20)	59(16)	48(5)

Table 6. Torsion angles [°] for ib003_sarpong.

C(7)-C(1)-C(2)-O(1)	-80.22(11)
C(7)-C(1)-C(2)-C(3)	35.49(11)
O(1)-C(2)-C(3)-C(4)	-45.87(13)
C(1)-C(2)-C(3)-C(4)	-163.40(10)
O(1)-C(2)-C(3)-C(5)	-163.91(9)
C(1)-C(2)-C(3)-C(5)	78.56(11)
O(1)-C(2)-C(3)-C(6)	74.31(11)
C(1)-C(2)-C(3)-C(6)	-43.21(11)
C(4)-C(3)-C(6)-O(2)	35.96(12)
C(5)-C(3)-C(6)-O(2)	159.44(9)
C(2)-C(3)-C(6)-O(2)	-84.23(10)
C(4)-C(3)-C(6)-C(14)	-87.08(13)
C(5)-C(3)-C(6)-C(14)	36.39(15)
C(2)-C(3)-C(6)-C(14)	152.72(10)
C(4)-C(3)-C(6)-C(7)	154.96(9)
C(5)-C(3)-C(6)-C(7)	-81.57(11)
C(2)-C(3)-C(6)-C(7)	34.76(11)
C(2)-C(1)-C(7)-C(15)	-126.75(10)
C(2)-C(1)-C(7)-C(8)	111.21(10)
C(2)-C(1)-C(7)-C(6)	-12.47(11)
O(2)-C(6)-C(7)-C(1)	101.00(10)
C(14)-C(6)-C(7)-C(1)	-143.55(9)
C(3)-C(6)-C(7)-C(1)	-14.39(11)
O(2)-C(6)-C(7)-C(15)	-136.12(9)
C(14)-C(6)-C(7)-C(15)	-20.67(11)

C(3)-C(6)-C(7)-C(15)	108.49(10)
O(2)-C(6)-C(7)-C(8)	-24.18(13)
C(14)-C(6)-C(7)-C(8)	91.26(11)
C(3)-C(6)-C(7)-C(8)	-139.58(9)
C(1)-C(7)-C(8)-C(9)	-170.21(10)
C(15)-C(7)-C(8)-C(9)	61.51(12)
C(6)-C(7)-C(8)-C(9)	-49.71(13)
C(7)-C(8)-C(9)-O(3)	-169.25(9)
C(7)-C(8)-C(9)-C(10)	-43.34(14)
O(3)-C(9)-C(10)-C(11)	37.48(13)
C(8)-C(9)-C(10)-C(11)	-85.98(12)
O(3)-C(9)-C(10)-C(12)	-80.56(12)
C(8)-C(9)-C(10)-C(12)	155.99(10)
O(3)-C(9)-C(10)-C(13)	160.56(9)
C(8)-C(9)-C(10)-C(13)	37.10(13)
C(11)-C(10)-C(13)-C(15)	69.46(12)
C(12)-C(10)-C(13)-C(15)	-173.03(10)
C(9)-C(10)-C(13)-C(15)	-54.06(12)
C(11)-C(10)-C(13)-C(14)	-177.57(9)
C(12)-C(10)-C(13)-C(14)	-60.07(13)
C(9)-C(10)-C(13)-C(14)	58.91(12)
O(2)-C(6)-C(14)-C(13)	108.45(10)
C(7)-C(6)-C(14)-C(13)	-10.18(11)
C(3)-C(6)-C(14)-C(13)	-128.85(11)
C(15)-C(13)-C(14)-C(6)	36.68(11)
C(10)-C(13)-C(14)-C(6)	-83.54(12)
C(1)-C(7)-C(15)-O(4)	-74.03(12)

C(8)-C(7)-C(15)-O(4) 53.00(11)

C(6)-C(7)-C(15)-O(4) 170.20(9)

C(1)-C(7)-C(15)-O(5) 42.53(13)

C(8)-C(7)-C(15)-O(5) 169.55(9)

C(6)-C(7)-C(15)-O(5) -73.25(11)

C(1)-C(7)-C(15)-C(13) 159.87(9)

C(8)-C(7)-C(15)-C(13) -73.11(10)

C(6)-C(7)-C(15)-C(13) 44.09(10)

C(10)-C(13)-C(15)-O(4) -47.32(14)

C(14)-C(13)-C(15)-O(4) -170.17(9)

C(10)-C(13)-C(15)-O(5) -165.88(9)

C(14)-C(13)-C(15)-O(5) 71.27(11)

C(10)-C(13)-C(15)-C(7) 73.65(11)

C(14)-C(13)-C(15)-C(7) -49.20(10)

O(4)-C(16)-C(17)-O(5) -10.02(14)

O(5)-C(15)-O(4)-C(16) 31.11(12)

C(7)-C(15)-O(4)-C(16) 153.60(10)

C(13)-C(15)-O(4)-C(16) -90.29(12)

C(17)-C(16)-O(4)-C(15) -12.98(14)

C(16)-C(17)-O(5)-C(15) 29.04(13)

O(4)-C(15)-O(5)-C(17) -37.52(11)

C(7)-C(15)-O(5)-C(17) -157.89(10)

C(13)-C(15)-O(5)-C(17) 89.52(11)

Symmetry transformations used to generate equivalent atoms:

A colorless block 0.19 x 0.16 x 0.13 mm in size was mounted on a Cryoloop with Paratone oil. Data were collected in a nitrogen gas stream at 100(2) K using omega scans. Crystal-to-detector distance was 30.23 mm and exposure time was 0.50 seconds per frame at low and high angles, using a scan width of 0.5°. Data collection was 100% complete to 74.000° in θ. A total of 14728 reflections were collected covering the indices -10<=h<=10, -26<=k<=26, -10<=l<=10. 2847 reflections were founded to be symmetry independent, with an R_{int} of 0.0294. Indexing and unit cell refinement indicated a primitive, monoclinic lattice. The space group was found to be P 21/c (No. 14). The data were integrated using the CrysAlis^{Pro} 1.171.40.84a software program and scaled using the SCALE3 ABSPACK scaling algorithm. Solution by intrinsic phasing (SHELXT-2015) produced a heavy-atom phasing model consistent with the proposed structure. All non-hydrogen atoms were refined anisotropically by full-matrix least-squares (SHELXL-2014). All hydrogen atoms were placed using a riding model. Their positions were constrained relative to their parent atom using the appropriate HFIX command in SHELXL-2014.

Table 7. Crystal data and structure refinement for IB004_Sarpong.

Identification code	IB004_Sarpong
Empirical formula	C15 H24 O4
Formula weight	268.34
Temperature	100(2) K
Wavelength	1.54184 Å
Crystal system	Monoclinic
Space group	P 21/c
Unit cell dimensions	a = 8.03280(10) Å a= 90°.
	b = 20.9375(3) Å b= 95.3720(10)°.
	c = 8.34830(10) Å g = 90°.
Volume	1397.91(3) Å3
Z	4
Density (calculated)	1.275 Mg/m3
Absorption coefficient	0.738 mm-1

F(000) 584

Crystal size 0.190 x 0.160 x 0.130 mm3

Theta range for data collection 4.223 to 74.488°.

Index ranges -10<=h<=10, -26<=k<=26, -10<=l<=10

Reflections collected 14728

Independent reflections 2847 [R(int) = 0.0294]

Completeness to theta = 74.000° 99.8 %

Absorption correction Semi-empirical from equivalents

Max. and min. transmission 1.00000 and 0.80096

Refinement method Full-matrix least-squares on F2

Data / restraints / parameters 2847 / 0 / 184

Goodness-of-fit on F2 1.081

Final R indices [I>2sigma(I)] R1 = 0.0378, wR2 = 0.0992

R indices (all data) R1 = 0.0397, wR2 = 0.1005

Extinction coefficient n/a

Largest diff. peak and hole 0.308 and -0.180 e.Å-3

Table 8. Atomic coordinates (x 104) and equivalent isotropic displacement parameters (Å2x 103)

for ib004_sarpong. U(eq) is defined as one third of the trace of the orthogonalized Uij tensor.

	x	y	z	U(eq)
O(1)	5186(1)	5968(1)	6266(1)	23(1)
O(2)	2366(1)	6616(1)	1333(1)	22(1)
O(3)	5050(1)	6820(1)	2552(1)	20(1)
O(4)	4823(1)	6156(1)	-443(1)	24(1)
C(1)	4059(1)	6160(1)	5311(1)	17(1)
C(2)	2714(1)	6640(1)	5590(1)	19(1)
C(3)	1067(1)	6248(1)	5710(1)	19(1)
C(4)	1305(2)	5782(1)	7129(1)	23(1)
C(5)	-369(2)	6701(1)	5998(2)	27(1)
C(6)	647(1)	5887(1)	4116(1)	20(1)
C(7)	2131(1)	5531(1)	3495(1)	19(1)
C(8)	3705(1)	5951(1)	3571(1)	17(1)
C(9)	3399(1)	6614(1)	2783(1)	18(1)
C(10)	2674(2)	7046(1)	4036(1)	22(1)
C(11)	6088(1)	6278(1)	2225(1)	19(1)
C(12)	6426(1)	6257(1)	445(1)	20(1)
C(13)	7173(2)	6887(1)	-51(2)	30(1)
C(14)	7581(2)	5701(1)	142(1)	25(1)
C(15)	5198(1)	5681(1)	2808(1)	19(1)

Table 9. Bond lengths [Å] and angles [°] for ib004_sarpong.

_____

O(1)-C(1)	1.2170(14)
O(2)-C(9)	1.4018(13)
O(3)-C(9)	1.4244(13)
O(3)-C(11)	1.4490(13)
O(4)-C(12)	1.4397(14)
C(1)-C(2)	1.5094(15)
C(1)-C(8)	1.5186(14)
C(2)-C(10)	1.5492(16)
C(2)-C(3)	1.5684(15)
C(3)-C(5)	1.5304(16)
C(3)-C(4)	1.5320(16)
C(3)-C(6)	1.5399(15)
C(6)-C(7)	1.5365(15)
C(7)-C(8)	1.5363(15)
C(8)-C(15)	1.5183(14)
C(8)-C(9)	1.5452(15)
C(9)-C(10)	1.5384(15)
C(11)-C(12)	1.5361(15)
C(11)-C(15)	1.5423(15)
C(12)-C(13)	1.5232(17)
C(12)-C(14)	1.5236(17)

C(9)-O(3)-C(11)	110.36(8)
O(1)-C(1)-C(2)	128.18(10)
O(1)-C(1)-C(8)	126.33(10)

C(2)-C(1)-C(8) 105.49(9)

C(1)-C(2)-C(10) 101.22(8)

C(1)-C(2)-C(3) 106.38(9)

C(10)-C(2)-C(3) 112.92(9)

C(5)-C(3)-C(4) 108.35(9)

C(5)-C(3)-C(6) 109.42(9)

C(4)-C(3)-C(6) 110.98(10)

C(5)-C(3)-C(2) 109.76(10)

C(4)-C(3)-C(2) 109.72(9)

C(6)-C(3)-C(2) 108.60(9)

C(7)-C(6)-C(3) 114.54(9)

C(8)-C(7)-C(6) 111.73(9)

C(15)-C(8)-C(1) 115.09(9)

C(15)-C(8)-C(7) 116.65(9)

C(1)-C(8)-C(7) 106.51(8)

C(15)-C(8)-C(9) 104.88(9)

C(1)-C(8)-C(9) 99.00(9)

C(7)-C(8)-C(9) 113.48(9)

O(2)-C(9)-O(3) 111.42(9)

O(2)-C(9)-C(10) 110.70(9)

O(3)-C(9)-C(10) 109.29(9)

O(2)-C(9)-C(8) 115.39(9)

O(3)-C(9)-C(8) 102.51(8)

C(10)-C(9)-C(8) 107.10(9)

C(9)-C(10)-C(2) 105.51(9)

O(3)-C(11)-C(12) 111.19(9)

O(3)-C(11)-C(15) 106.45(8)

C(12)-C(11)-C(15)	114.26(9)
O(4)-C(12)-C(13)	110.04(10)
O(4)-C(12)-C(14)	109.37(9)
C(13)-C(12)-C(14)	110.77(10)
O(4)-C(12)-C(11)	105.82(9)
C(13)-C(12)-C(11)	110.33(10)
C(14)-C(12)-C(11)	110.39(9)
C(8)-C(15)-C(11)	103.75(9)

Symmetry transformations used to generate equivalent atoms:

Table 10. Anisotropic displacement parameters (Å2x 103)for ib004_sarpong. The anisotropic displacement factor exponent takes the form: -2p2[h2a*2U11 + ... + 2 h k a* b* U12]

	U11	U22	U33	U23	U13	U12
O(1)	19(1)	34(1)	16(1)	1(1)	1(1)	2(1)
O(2)	23(1)	27(1)	16(1)	3(1)	1(1)	4(1)
O(3)	22(1)	19(1)	22(1)	-2(1)	7(1)	-2(1)
O(4)	20(1)	41(1)	13(1)	-2(1)	2(1)	-1(1)
C(1)	15(1)	20(1)	16(1)	0(1)	4(1)	-3(1)
C(2)	20(1)	19(1)	18(1)	-4(1)	4(1)	-1(1)
C(3)	17(1)	21(1)	19(1)	-3(1)	4(1)	1(1)
C(4)	22(1)	28(1)	20(1)	-1(1)	6(1)	-3(1)
C(5)	22(1)	29(1)	31(1)	-6(1)	8(1)	3(1)
C(6)	17(1)	22(1)	21(1)	-2(1)	2(1)	-2(1)
C(7)	22(1)	18(1)	17(1)	-2(1)	3(1)	-1(1)
C(8)	18(1)	18(1)	15(1)	0(1)	3(1)	2(1)
C(9)	19(1)	18(1)	17(1)	0(1)	3(1)	0(1)
C(10)	25(1)	17(1)	23(1)	-1(1)	7(1)	2(1)
C(11)	17(1)	23(1)	16(1)	-3(1)	2(1)	0(1)
C(12)	17(1)	27(1)	16(1)	-1(1)	3(1)	-3(1)
C(13)	31(1)	31(1)	30(1)	2(1)	13(1)	-5(1)
C(14)	23(1)	33(1)	20(1)	-3(1)	6(1)	2(1)
C(15)	20(1)	20(1)	16(1)	0(1)	5(1)	3(1)

Table 11. Hydrogen coordinates (x 104) and isotropic displacement parameters (Å2x 103) for ib004_sarpong.

	x	y	z	U(eq)
H(2A)	3012	6902	6577	23
H(4A)	260	5550	7227	34
H(4B)	1615	6021	8122	34
H(4C)	2194	5478	6945	34
H(5A)	-529	7007	5109	41
H(5B)	-101	6932	7010	41
H(5C)	-1398	6455	6060	41
H(6A)	-252	5575	4263	24
H(6B)	206	6197	3285	24
H(7A)	2372	5143	4151	23
H(7B)	1829	5396	2369	23
H(10A)	1514	7173	3668	26
H(10B)	3360	7436	4224	26
H(11)	7184	6324	2889	22
H(13A)	7283	6882	-1210	45
H(13B)	8278	6945	536	45
H(13C)	6439	7240	203	45
H(14A)	7061	5300	434	38
H(14B)	8650	5756	795	38
H(14C)	7775	5691	-1000	38

H(15A)	4833	5396	1896	22
H(15B)	5940	5439	3606	22
H(2)	3030(20)	6456(9)	600(20)	43(5)
H(4)	5010(20)	6119(9)	-1450(20)	43(5)

__Table 12. Torsion angles [°] for ib004_sarpong.

O(1)-C(1)-C(2)-C(10)	137.16(12)
C(8)-C(1)-C(2)-C(10)	-43.78(11)
O(1)-C(1)-C(2)-C(3)	-104.67(13)
C(8)-C(1)-C(2)-C(3)	74.39(10)
C(1)-C(2)-C(3)-C(5)	179.90(9)
C(10)-C(2)-C(3)-C(5)	-69.95(11)
C(1)-C(2)-C(3)-C(4)	60.95(11)
C(10)-C(2)-C(3)-C(4)	171.10(9)
C(1)-C(2)-C(3)-C(6)	-60.52(11)
C(10)-C(2)-C(3)-C(6)	49.63(12)
C(5)-C(3)-C(6)-C(7)	166.99(10)
C(4)-C(3)-C(6)-C(7)	-73.49(12)
C(2)-C(3)-C(6)-C(7)	47.20(13)
C(3)-C(6)-C(7)-C(8)	-46.44(13)
O(1)-C(1)-C(8)-C(15)	-23.73(16)
C(2)-C(1)-C(8)-C(15)	157.18(9)
O(1)-C(1)-C(8)-C(7)	107.21(12)
C(2)-C(1)-C(8)-C(7)	-71.87(11)
O(1)-C(1)-C(8)-C(9)	-134.90(12)
C(2)-C(1)-C(8)-C(9)	46.01(10)

C(6)-C(7)-C(8)-C(15)	-173.02(9)
C(6)-C(7)-C(8)-C(1)	56.92(12)
C(6)-C(7)-C(8)-C(9)	-50.93(12)
C(11)-O(3)-C(9)-O(2)	-91.21(10)
C(11)-O(3)-C(9)-C(10)	146.14(9)
C(11)-O(3)-C(9)-C(8)	32.76(10)
C(15)-C(8)-C(9)-O(2)	87.14(11)
C(1)-C(8)-C(9)-O(2)	-153.77(9)
C(7)-C(8)-C(9)-O(2)	-41.29(12)
C(15)-C(8)-C(9)-O(3)	-34.16(10)
C(1)-C(8)-C(9)-O(3)	84.94(9)
C(7)-C(8)-C(9)-O(3)	-162.58(8)
C(15)-C(8)-C(9)-C(10)	-149.13(9)
C(1)-C(8)-C(9)-C(10)	-30.04(11)
C(7)-C(8)-C(9)-C(10)	82.44(11)
O(2)-C(9)-C(10)-C(2)	131.31(9)
O(3)-C(9)-C(10)-C(2)	-105.61(10)
C(8)-C(9)-C(10)-C(2)	4.74(12)
C(1)-C(2)-C(10)-C(9)	22.89(11)
C(3)-C(2)-C(10)-C(9)	-90.43(11)
C(9)-O(3)-C(11)-C(12)	106.42(10)
C(9)-O(3)-C(11)-C(15)	-18.60(11)
O(3)-C(11)-C(12)-O(4)	-64.23(11)
C(15)-C(11)-C(12)-O(4)	56.29(12)
O(3)-C(11)-C(12)-C(13)	54.77(12)
C(15)-C(11)-C(12)-C(13)	175.29(10)
O(3)-C(11)-C(12)-C(14)	177.54(9)

C(15)-C(11)-C(12)-C(14) -61.94(12)

C(1)-C(8)-C(15)-C(11) -84.54(11)

C(7)-C(8)-C(15)-C(11) 149.58(9)

C(9)-C(8)-C(15)-C(11) 23.10(11)

O(3)-C(11)-C(15)-C(8) -4.15(11)

C(12)-C(11)-C(15)-C(8) -127.28(10)

Symmetry transformations used to generate equivalent atoms:

Copies of NMR Spectra

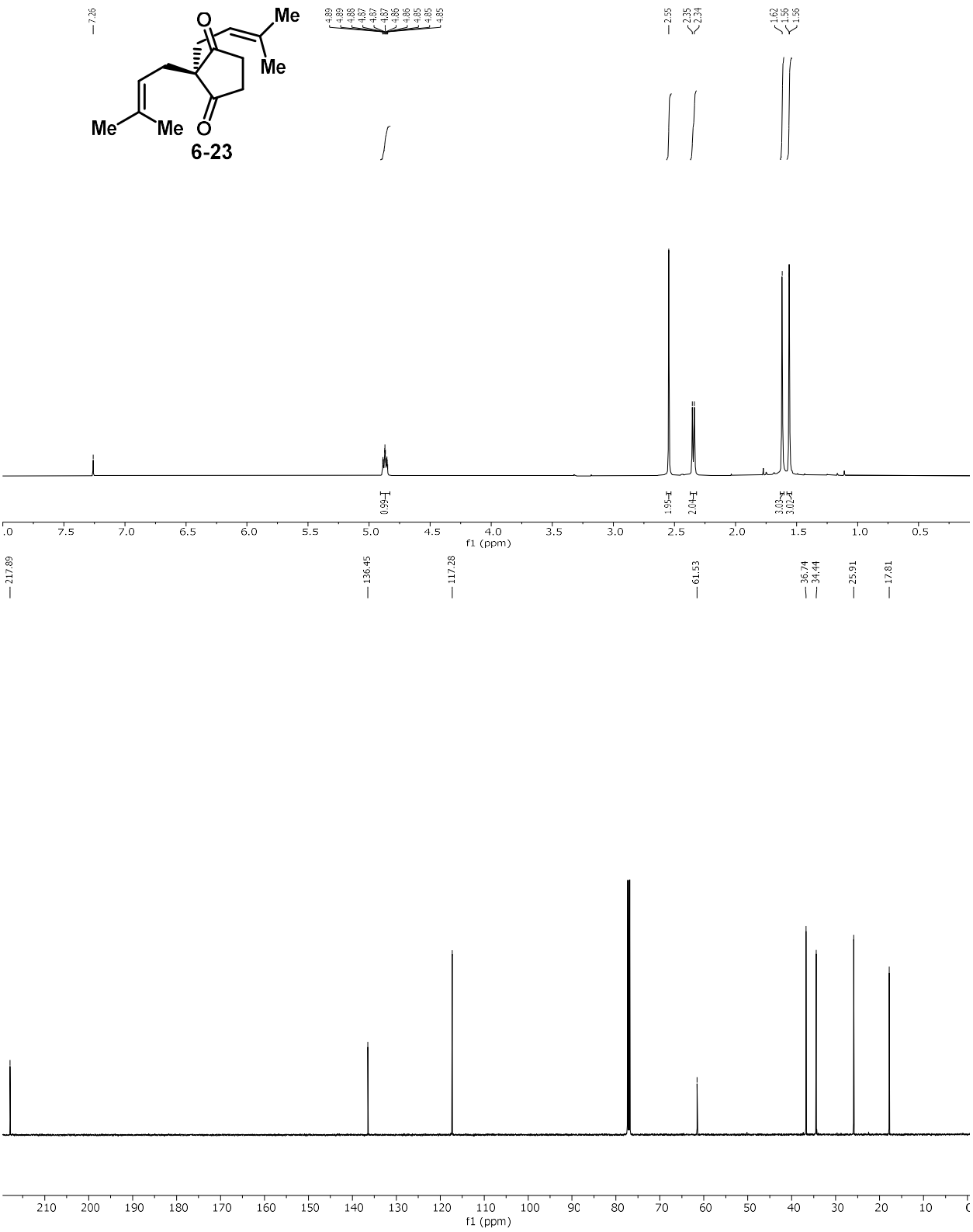

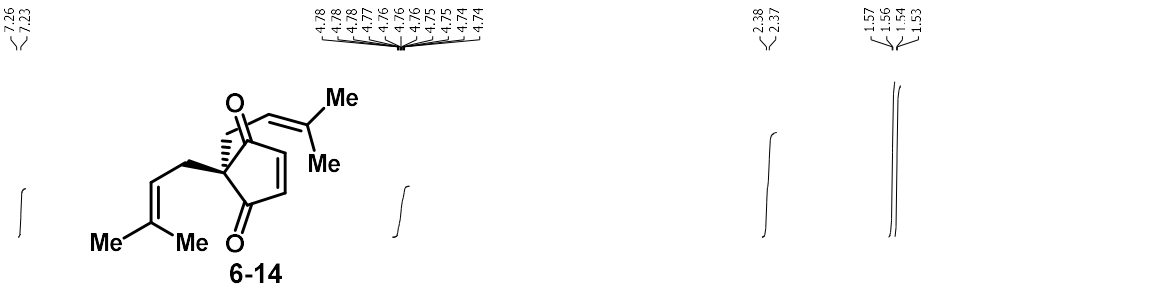
7.26
7.23
4.78
4.78
4.78
4.77
4.76
4.76
4.76
4.75
4.75
4.74
4.74
2.38
2.37
1.57
1.56
1.54
1.53
O
Me
Me
Me
Me
O

6-14

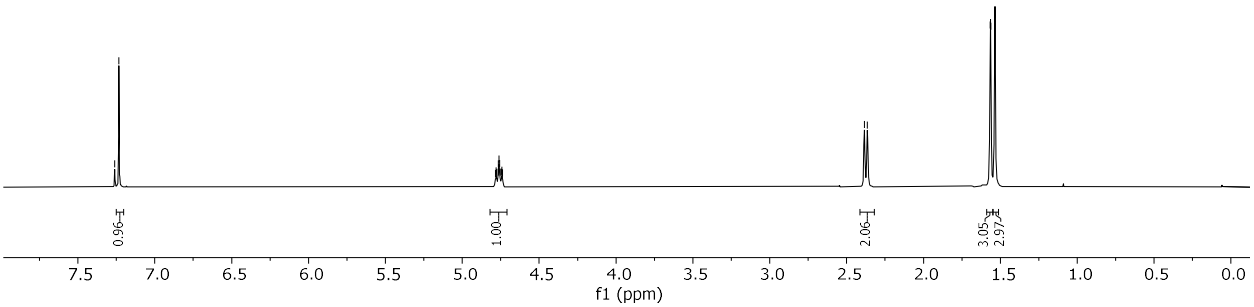
0.96
1.00
2.06
3.05
2.97
7.5
7.0
6.5
6.0
5.5
5.0
4.5
4.0
3.5
3.0
2.5
2.0
1.5
1.0
0.5
0.0
f1 (ppm)

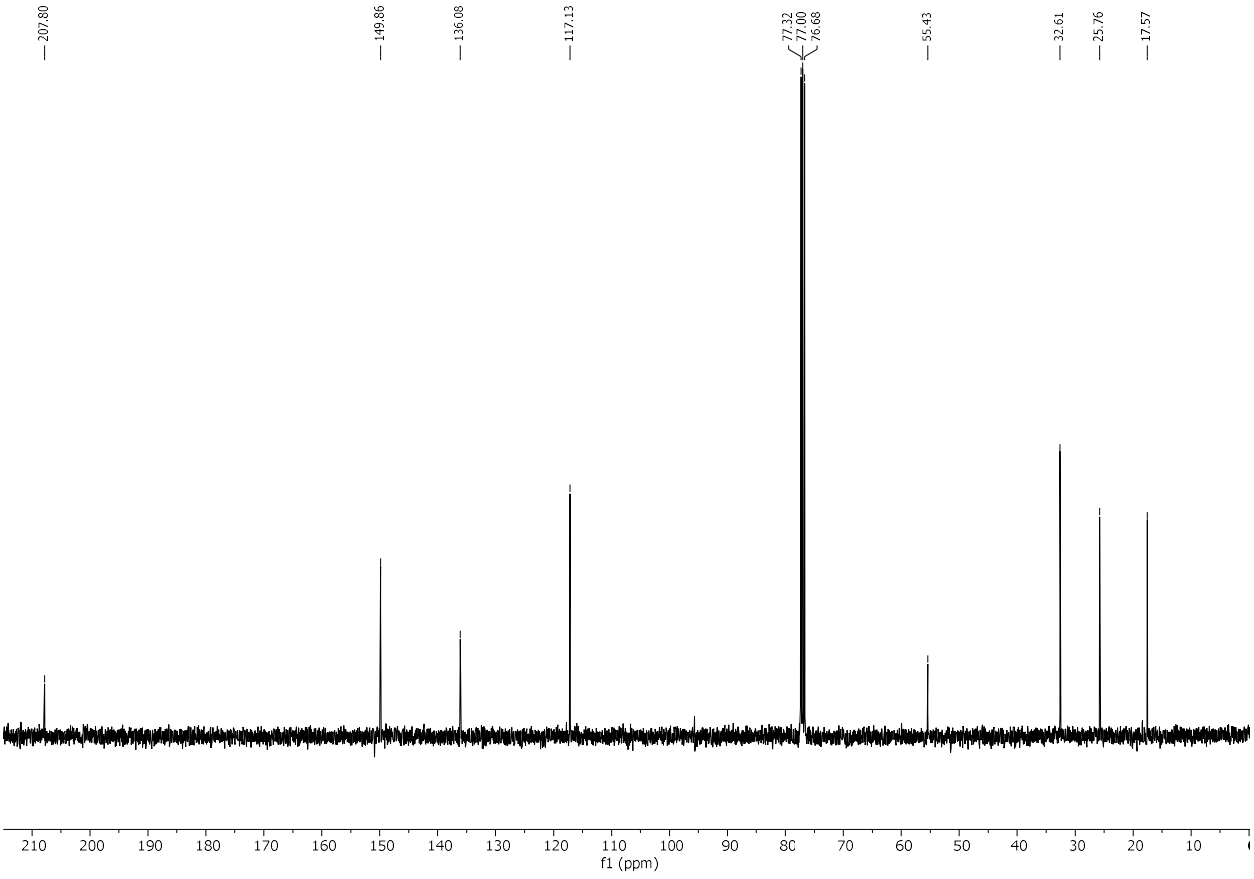
207.80
149.86
136.08
117.13
77.32
77.00
76.68
55.43
32.61
25.76
17.57
210
200
190
180
170
160
150
140
130
120
110
100
90
80
70
60
50
40
30
20
10
f1 (ppm)

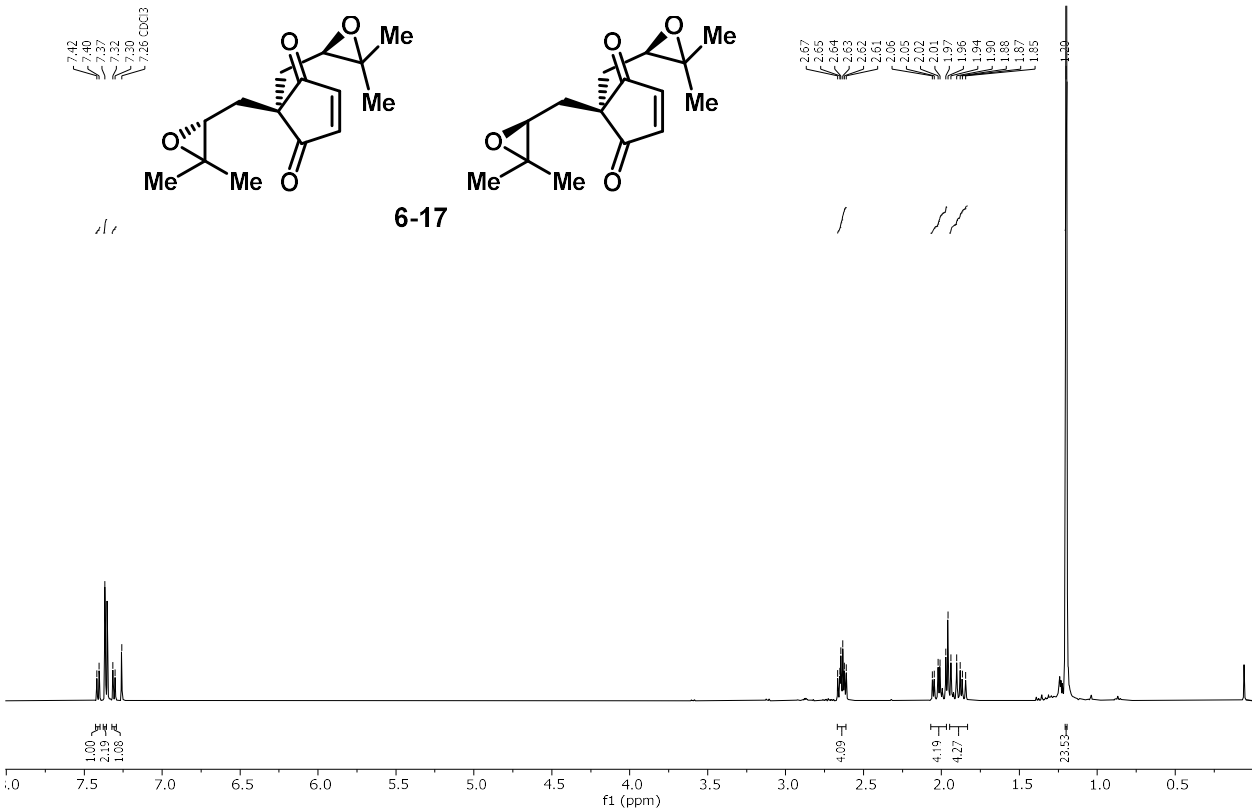
7.42
7.40
7.37
7.32
7.30
7.26 CDCl3
Me
Me
Me
Me
O
O
O
O
O
6-17
2.67
2.65
2.64
2.63
2.62
2.61
2.06
2.05
2.02
2.01
1.97
1.96
1.94
1.90
1.88
1.87
1.85
1.39
1.00
2.19
1.08
4.09
4.19
4.27
23.53
f1 (ppm)

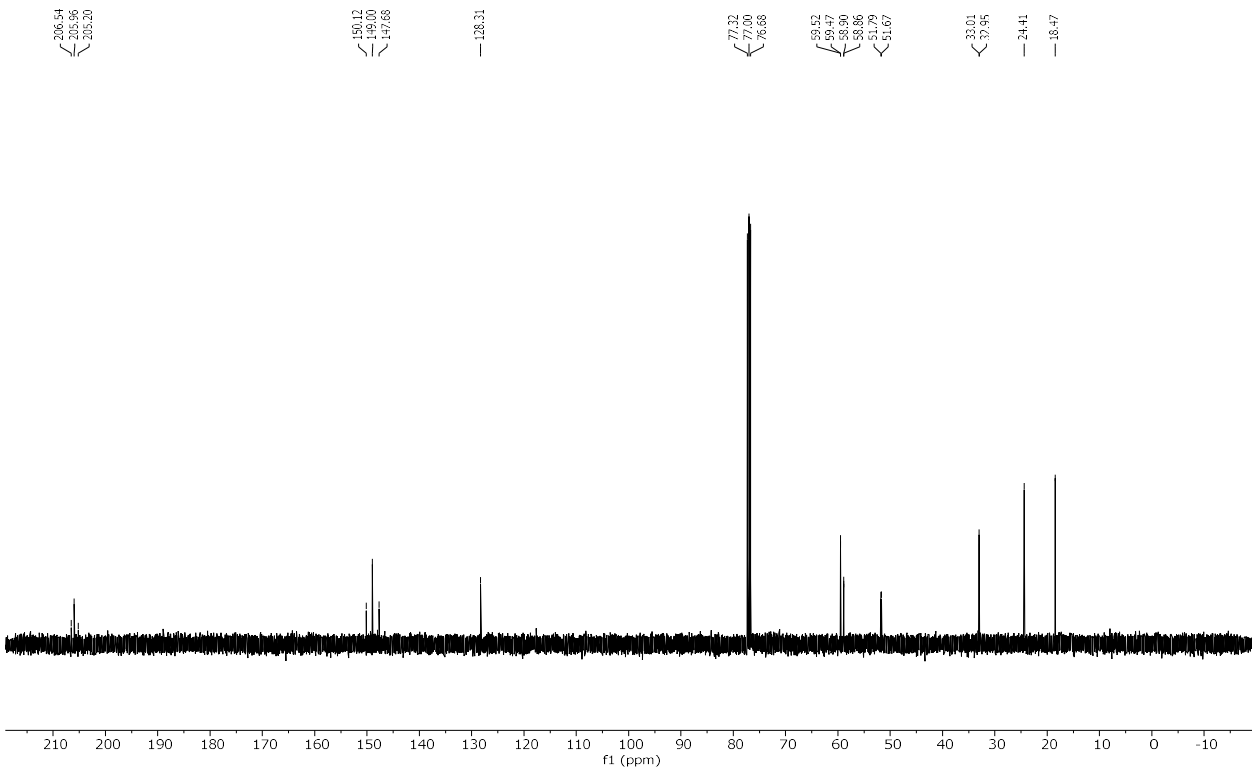
206.54
205.96
205.20
150.12
149.00
147.68
128.31
77.32
77.00
76.68
59.52
59.47
58.90
58.86
51.79
51.67
33.01
32.95
24.41
18.47
f1 (ppm)

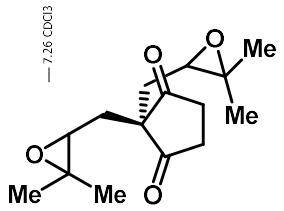
7.26 CDCl3
O
O
Me
Me
O
Me
Me
O

6-24

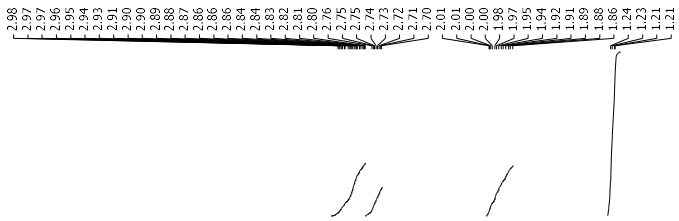
2.98
2.97
2.97
2.96
2.95
2.94
2.93
2.91
2.90
2.90
2.89
2.88
2.87
2.86
2.86
2.86
2.84
2.84
2.83
2.82
2.81
2.80
2.76
2.75
2.75
2.74
2.73
2.72
2.71
2.70
2.01
2.01
2.00
2.00
1.98
1.97
1.95
1.94
1.92
1.91
1.89
1.88
1.86
1.24
1.23
1.21
1.21

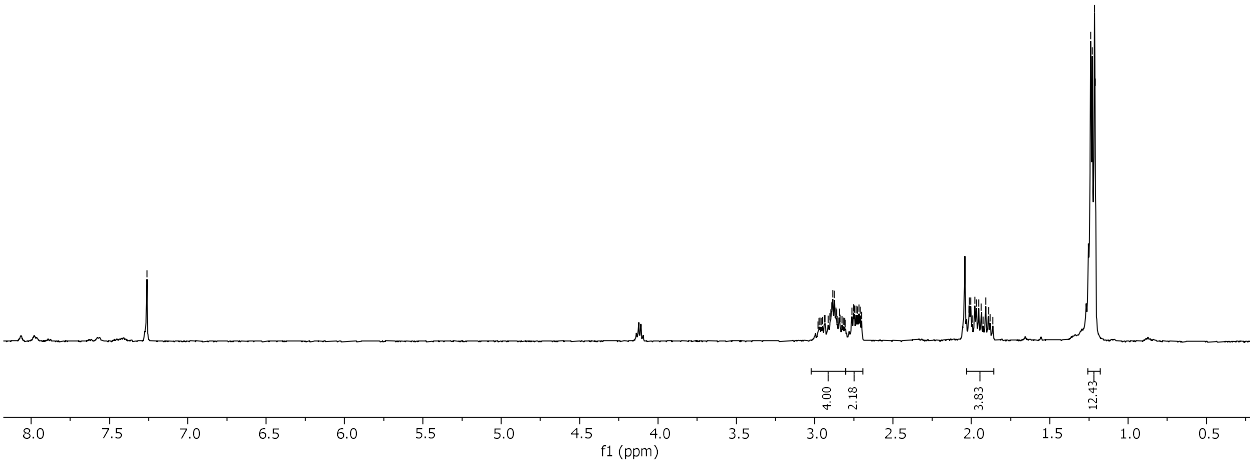
4.00
2.18
3.83
12.43
8.0
7.5
7.0
6.5
6.0
5.5
5.0
4.5
4.0
3.5
3.0
2.5
2.0
1.5
1.0
0.5
f1 (ppm)

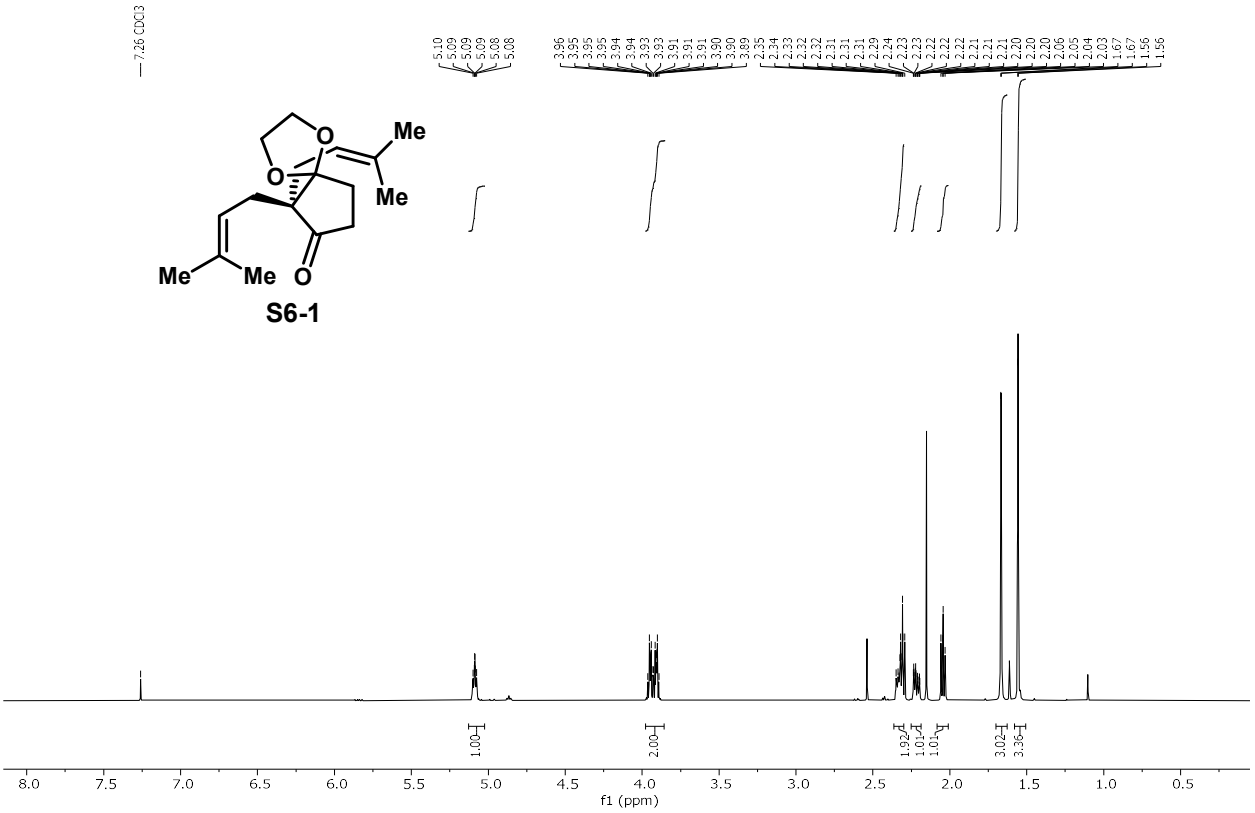
7.26 CDCl3
5.10
5.09
5.09
5.09
5.08
5.08
3.96
3.95
3.95
3.95
3.94
3.94
3.93
3.93
3.91
3.91
3.91
3.90
3.90
3.89
2.35
2.34
2.33
2.32
2.32
2.31
2.31
2.29
2.24
2.23
2.23
2.22
2.22
2.21
2.21
2.21
2.20
2.20
2.20
2.06
2.05
2.04
2.03
1.67
1.67
1.56
1.56
Me
Me
Me
Me
O
O
O
S6-1
1.00
2.00
1.92
1.01
1.01
3.02
3.36
8.0
7.5
7.0
6.5
6.0
5.5
5.0
4.5
4.0
3.5
3.0
2.5
2.0
1.5
1.0
0.5
f1 (ppm)

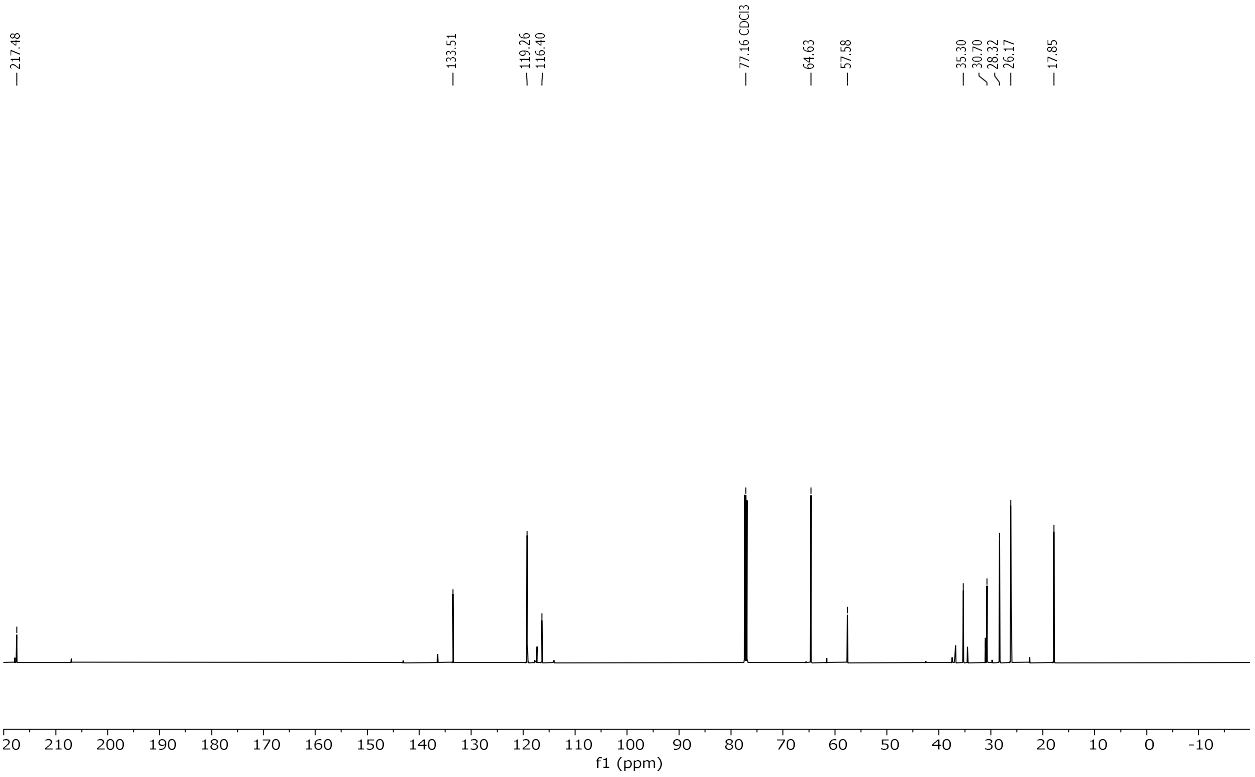
217.48
133.51
119.26
116.40
77.16 CDCl3
64.63
57.58
35.30
30.70
28.32
26.17
17.85
20
210
200
190
180
170
160
150
140
130
120
110
100
90
80
70
60
50
40
30
20
10
0
-10
f1 (ppm)

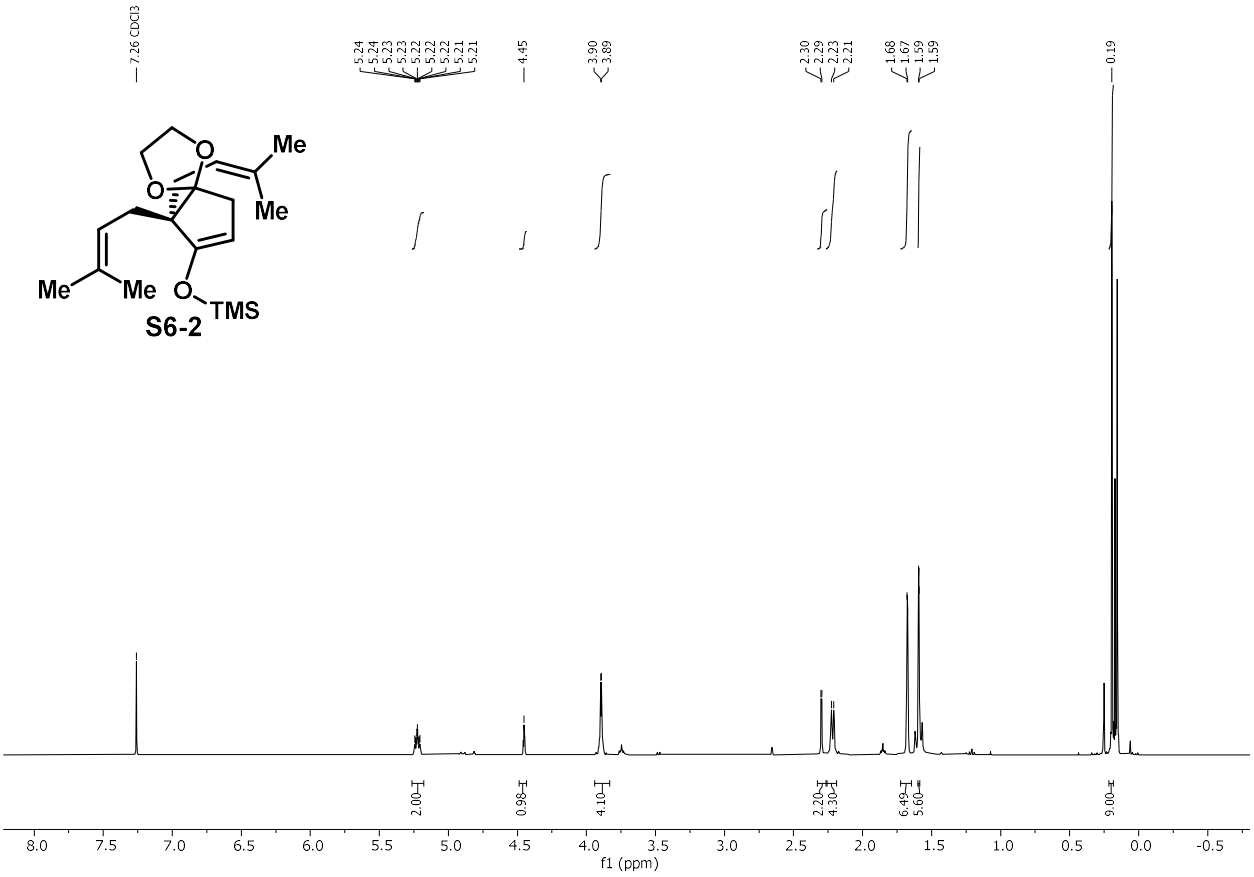
7.26 CDCl3
5.24
5.24
5.23
5.23
5.22
5.22
5.22
5.21
5.21
5.21
4.45
3.90
3.89
2.30
2.29
2.23
2.21
1.68
1.67
1.59
1.59
0.19
Me
Me
Me
Me
O
O
O
TMS
S6-2
2.00
0.98
4.10
2.20
4.30
6.49
5.60
9.00
8.0
7.5
7.0
6.5
6.0
5.5
5.0
4.5
4.0
3.5
3.0
2.5
2.0
1.5
1.0
0.5
0.0
-0.5
f1 (ppm)

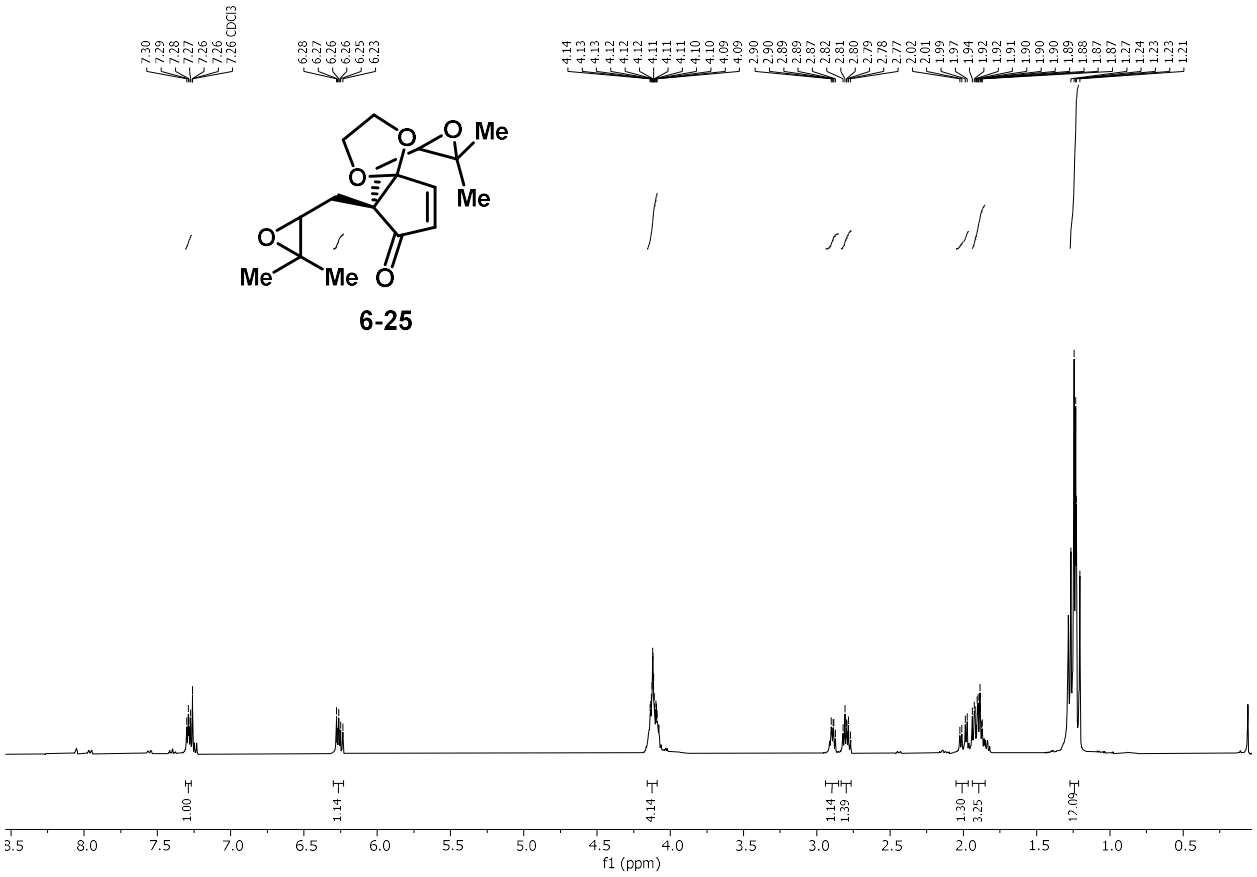
7.30
7.29
7.28
7.27
7.26
7.26
7.26 CDCl3
6.28
6.27
6.26
6.26
6.25
6.23
4.14
4.13
4.13
4.12
4.12
4.12
4.11
4.11
4.11
4.10
4.10
4.09
4.09
2.90
2.90
2.89
2.89
2.87
2.82
2.81
2.80
2.79
2.78
2.77
2.02
2.01
1.99
1.97
1.94
1.92
1.92
1.91
1.90
1.90
1.90
1.90
1.89
1.88
1.87
1.87
1.27
1.24
1.23
1.23
1.21
Me
Me
Me
Me
O
O
O
O
O
1.00
1.14
4.14
1.14
1.39
1.30
3.25
12.09
3.5
8.0
7.5
7.0
6.5
6.0
5.5
5.0
4.5
4.0
3.5
3.0
2.5
2.0
1.5
1.0
0.5
f1 (ppm)

6-25

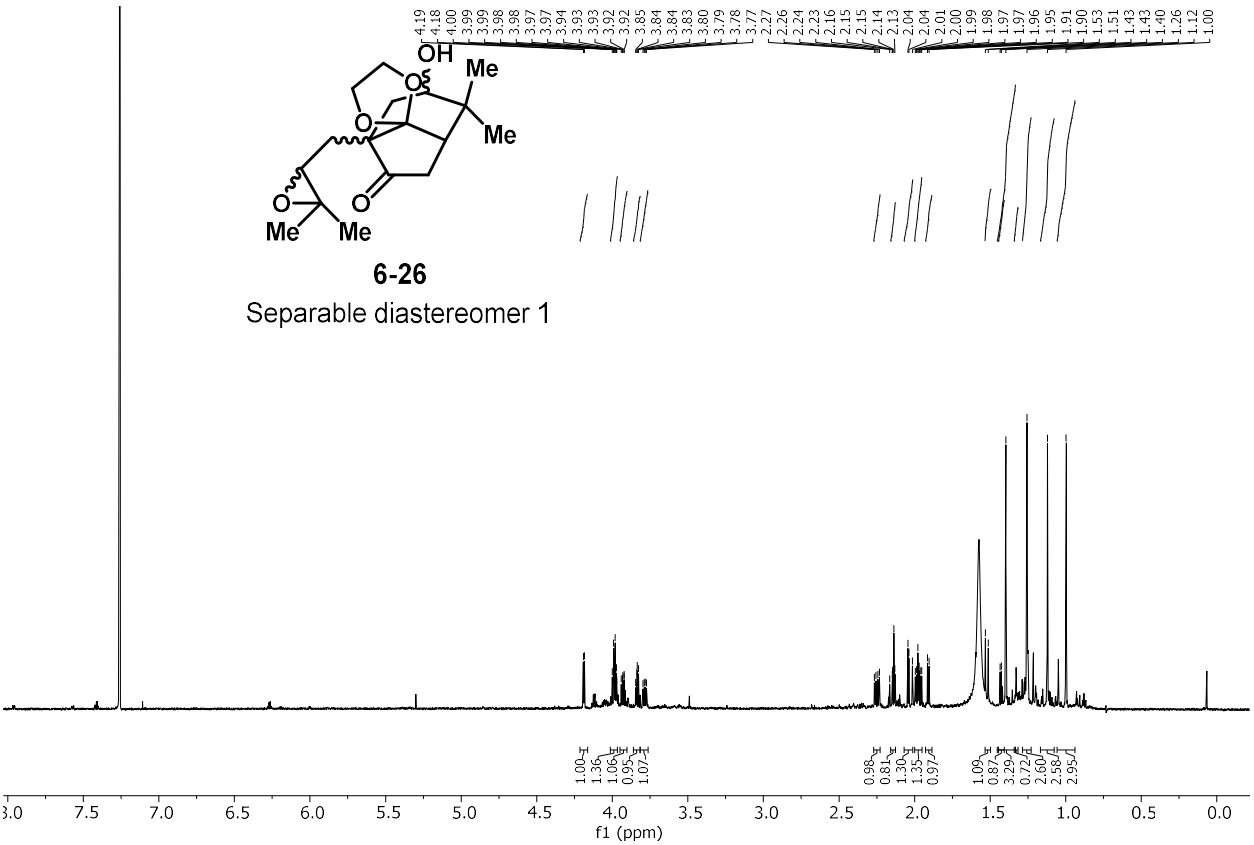

6-26

Separable diastereomer 1

Separable diastereomer 2

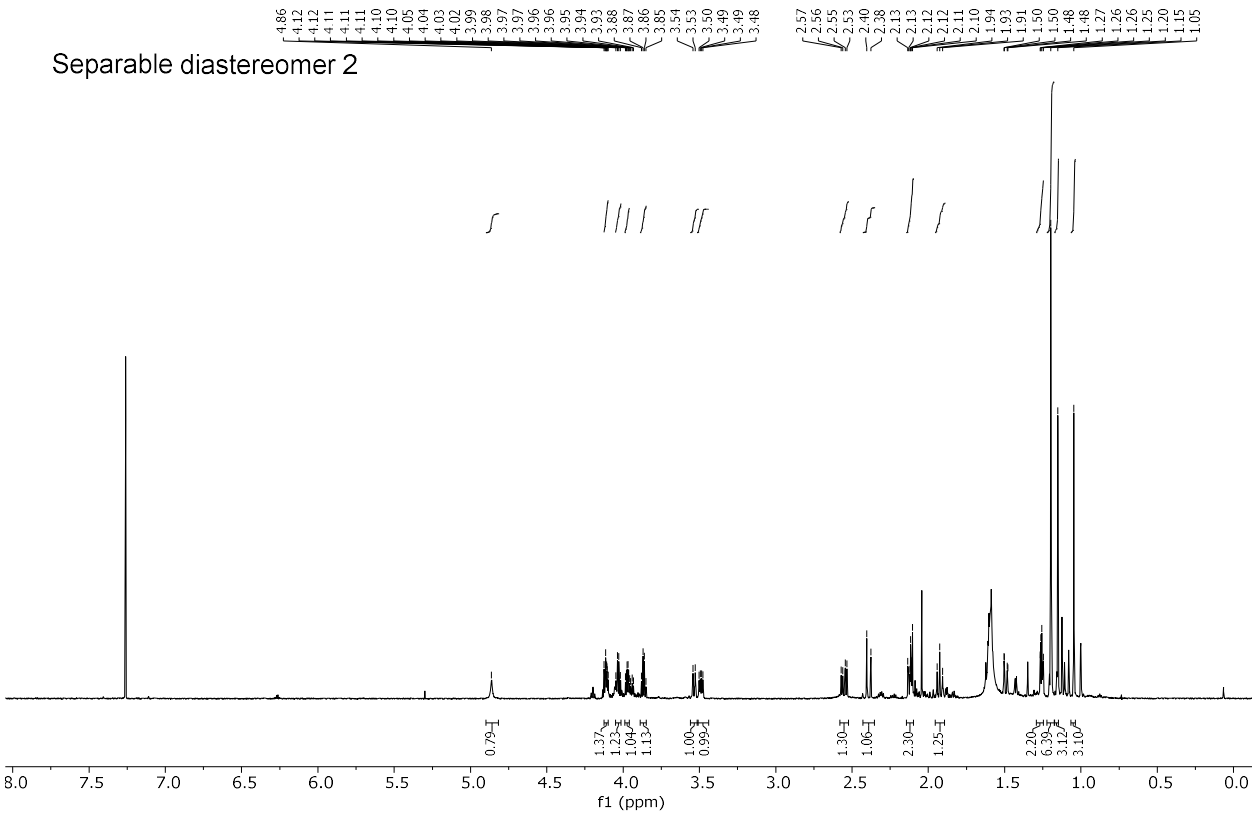

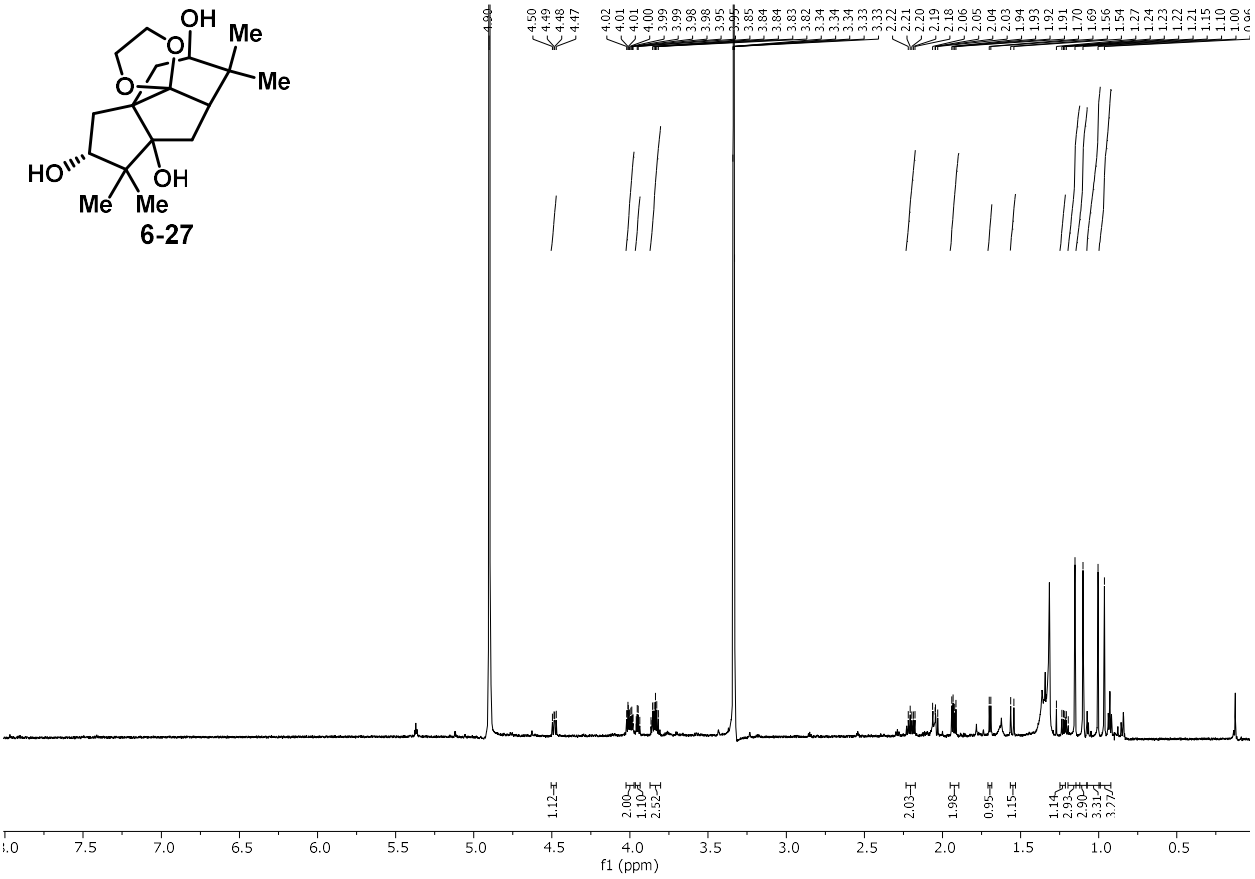
OH
Me
Me
O
O
HO
OH
Me
Me
6-27
f1 (ppm)

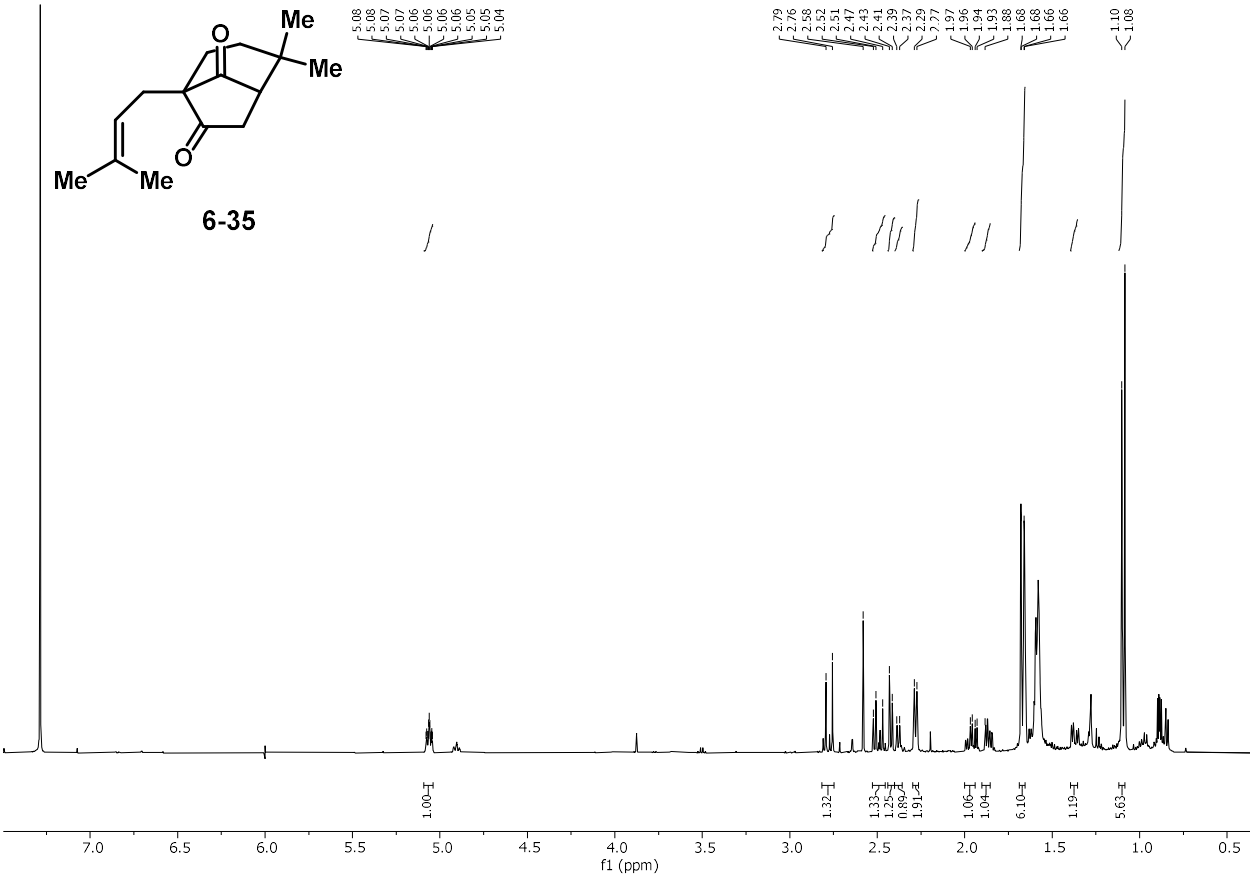
Me
O
Me
O
Me
Me
6-35
5.08
5.08
5.07
5.07
5.06
5.06
5.06
5.06
5.05
5.05
5.04
2.79
2.76
2.58
2.52
2.51
2.47
2.43
2.41
2.39
2.37
2.29
1.97
1.96
1.94
1.93
1.88
1.68
1.68
1.66
1.66
1.10
1.08
1.00
1.32
1.33
1.25
0.89
1.91
1.06
1.04
6.10
1.19
5.63
7.0
6.5
6.0
5.5
5.0
4.5
4.0
3.5
3.0
2.5
2.0
1.5
1.0
0.5
f1 (ppm)

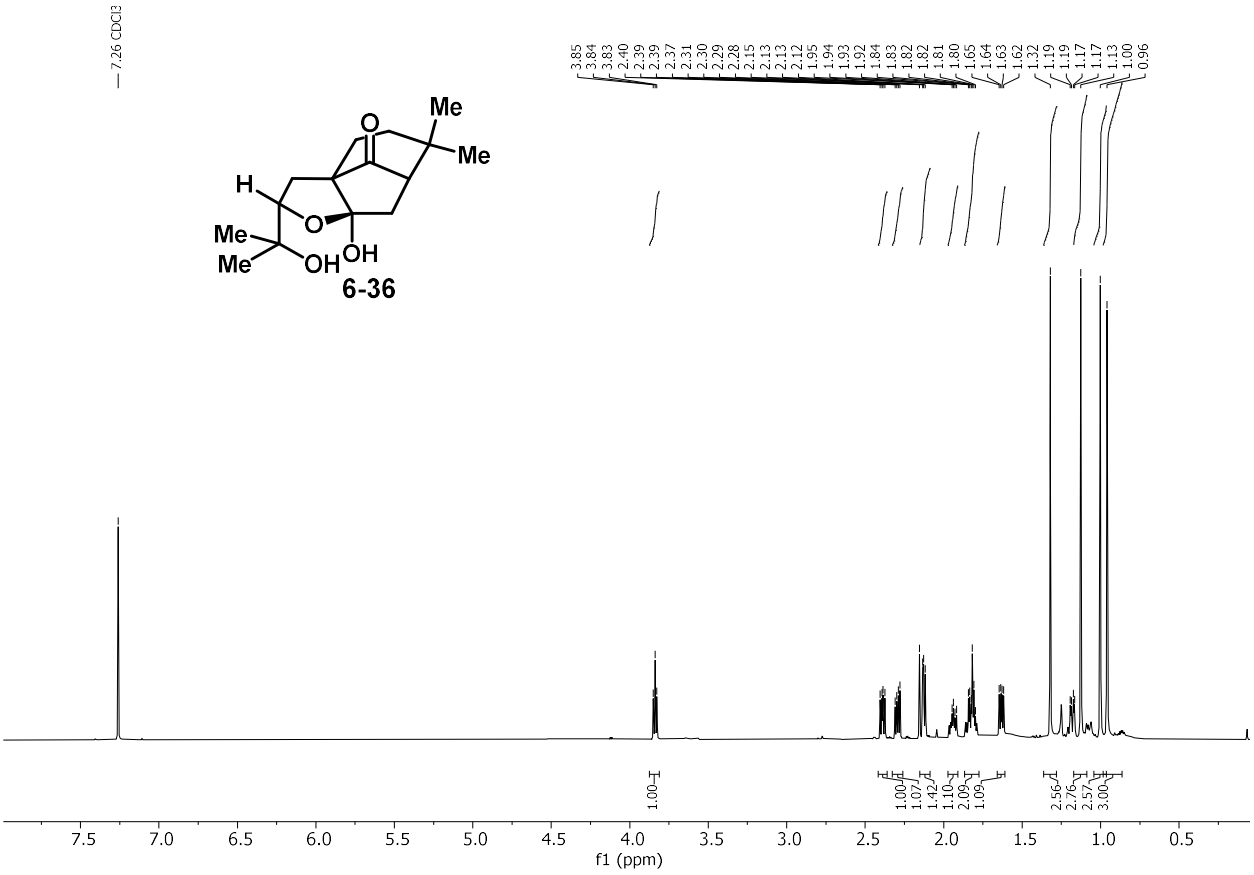
7.26 CDCl3
3.85
3.84
3.83
2.40
2.39
2.39
2.37
2.31
2.30
2.29
2.28
2.15
2.13
2.13
2.12
1.95
1.94
1.93
1.92
1.84
1.83
1.82
1.82
1.81
1.80
1.65
1.64
1.63
1.62
1.32
1.19
1.19
1.17
1.17
1.13
1.00
0.96
Me
Me
O
H
O
Me
Me
OH
OH
6-36
1.00
1.00
1.07
1.42
1.10
2.09
1.09
2.56
2.76
2.57
3.00
7.5
7.0
6.5
6.0
5.5
5.0
4.5
4.0
3.5
3.0
2.5
2.0
1.5
1.0
0.5
f1 (ppm)

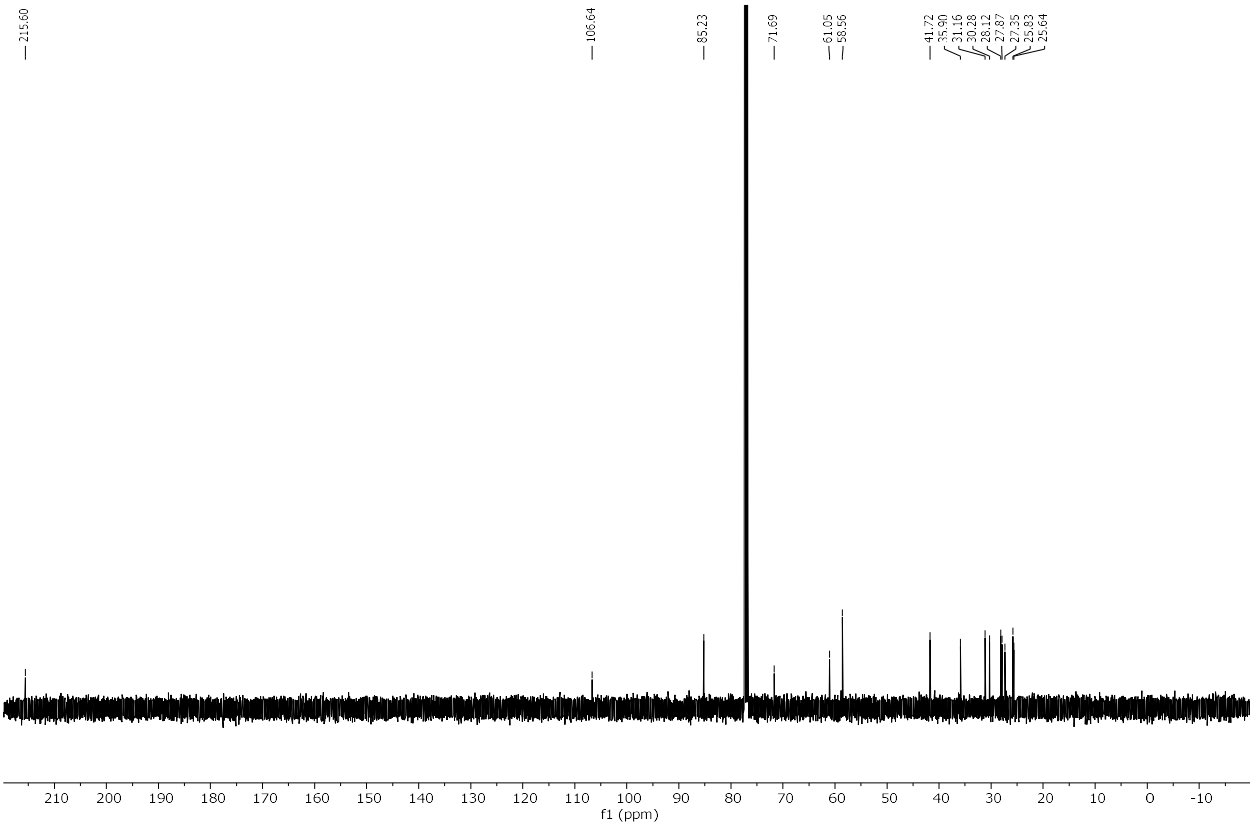
215.60
106.64
85.23
71.69
61.05
58.56
41.72
35.90
31.16
30.28
28.12
27.87
27.25
25.83
25.64
210
200
190
180
170
160
150
140
130
120
110
100
90
80
70
60
50
40
30
20
10
0
-10
f1 (ppm)

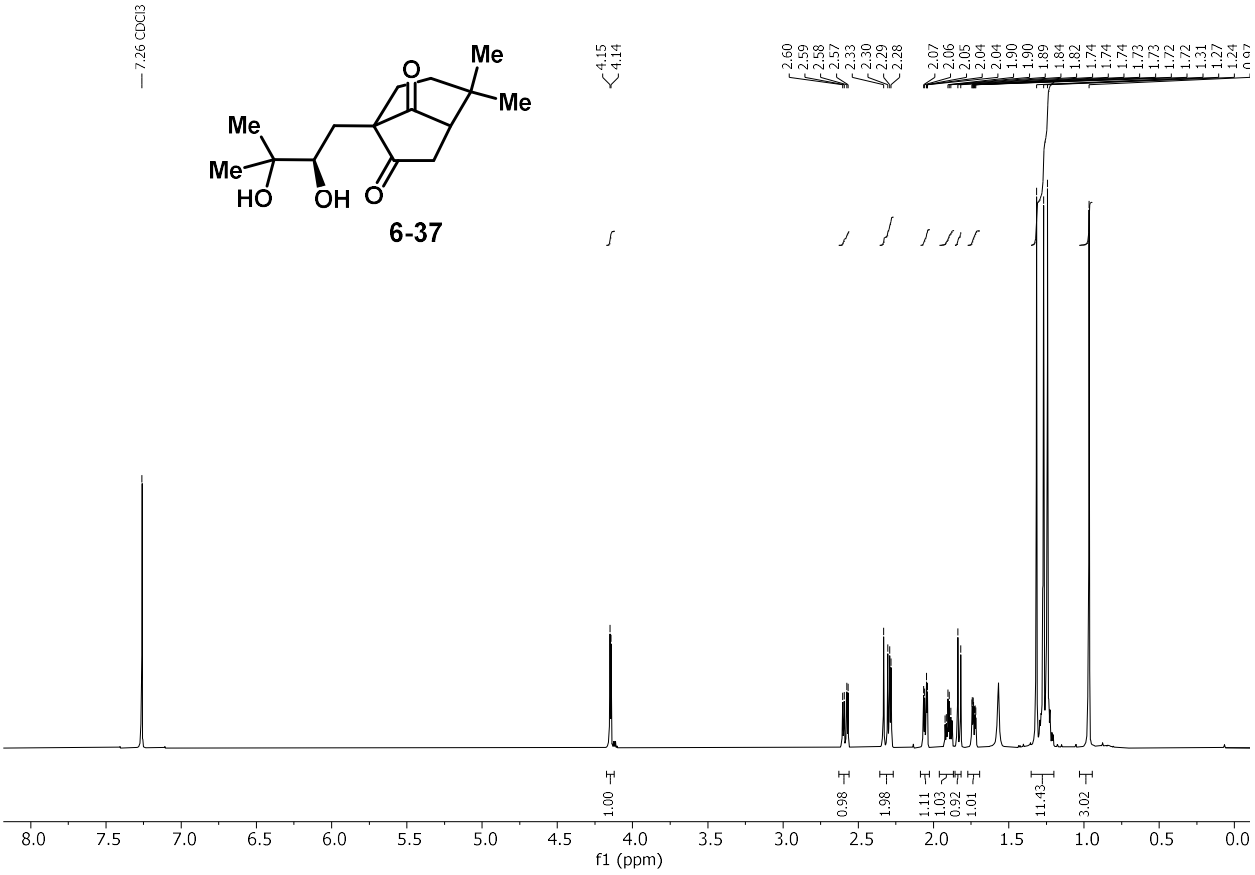
7.26 CDCl3
Me
Me
Me
Me
HO
OH
O
O
6-37
4.15
4.14
2.60
2.59
2.58
2.57
2.33
2.30
2.29
2.28
2.07
2.06
2.05
2.04
2.04
1.90
1.90
1.89
1.84
1.82
1.74
1.74
1.74
1.73
1.73
1.72
1.72
1.31
1.27
1.24
1.00
0.98
1.98
1.11
1.03
0.92
1.01
11.43
3.02
8.0
7.5
7.0
6.5
6.0
5.5
5.0
4.5
4.0
3.5
3.0
2.5
2.0
1.5
1.0
0.5
0.0
f1 (ppm)

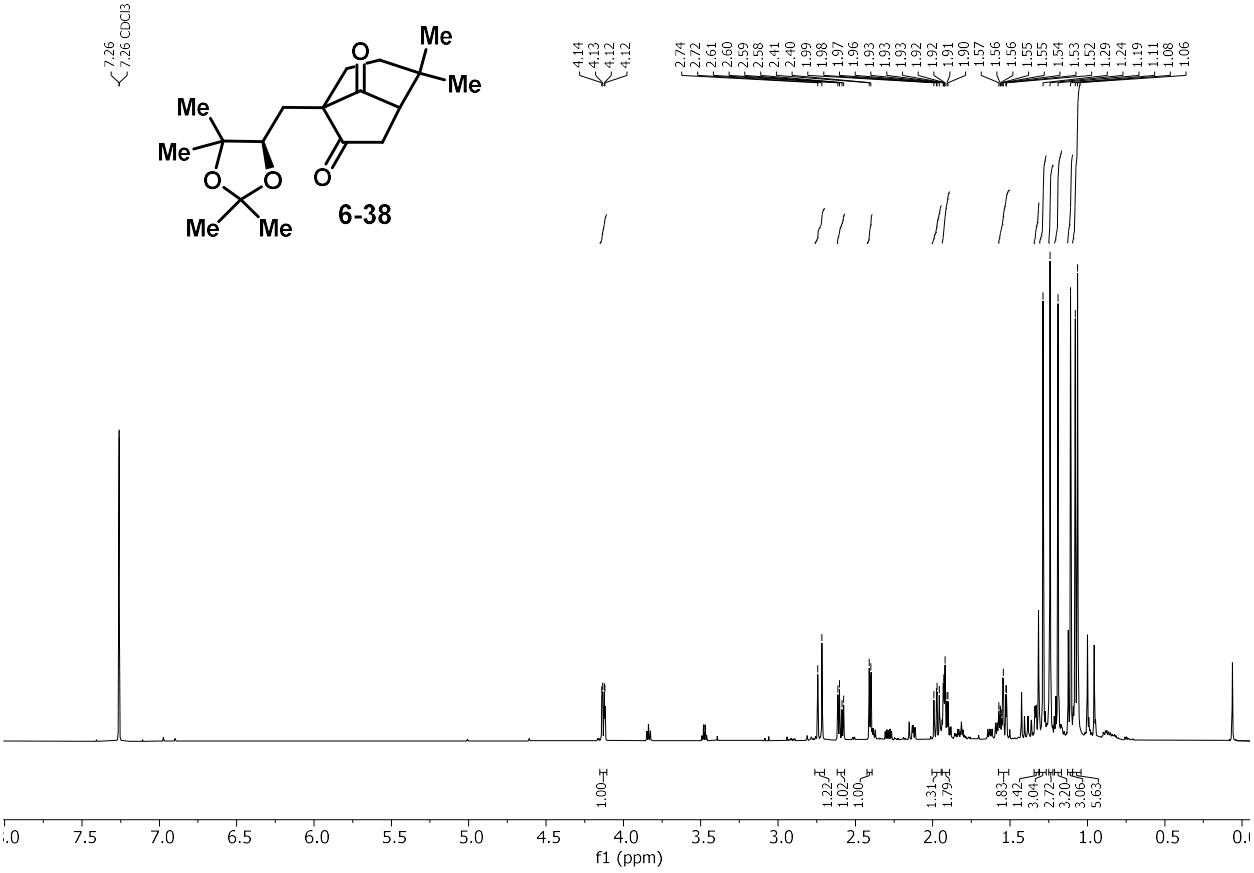
7.26
7.26 CDCl3
Me
Me
Me
Me
Me
Me
O
O
O
O
6-38
4.14
4.13
4.12
4.12
2.74
2.72
2.61
2.60
2.59
2.58
2.41
2.40
1.99
1.98
1.97
1.96
1.93
1.93
1.93
1.92
1.92
1.91
1.90
1.57
1.56
1.56
1.55
1.55
1.54
1.53
1.52
1.29
1.24
1.19
1.11
1.08
1.06
1.00
1.22
1.02
1.00
1.31
1.79
1.83
1.42
3.04
2.72
3.20
3.06
5.63
7.5
7.0
6.5
6.0
5.5
5.0
4.5
4.0
3.5
3.0
2.5
2.0
1.5
1.0
0.5
f1 (ppm)

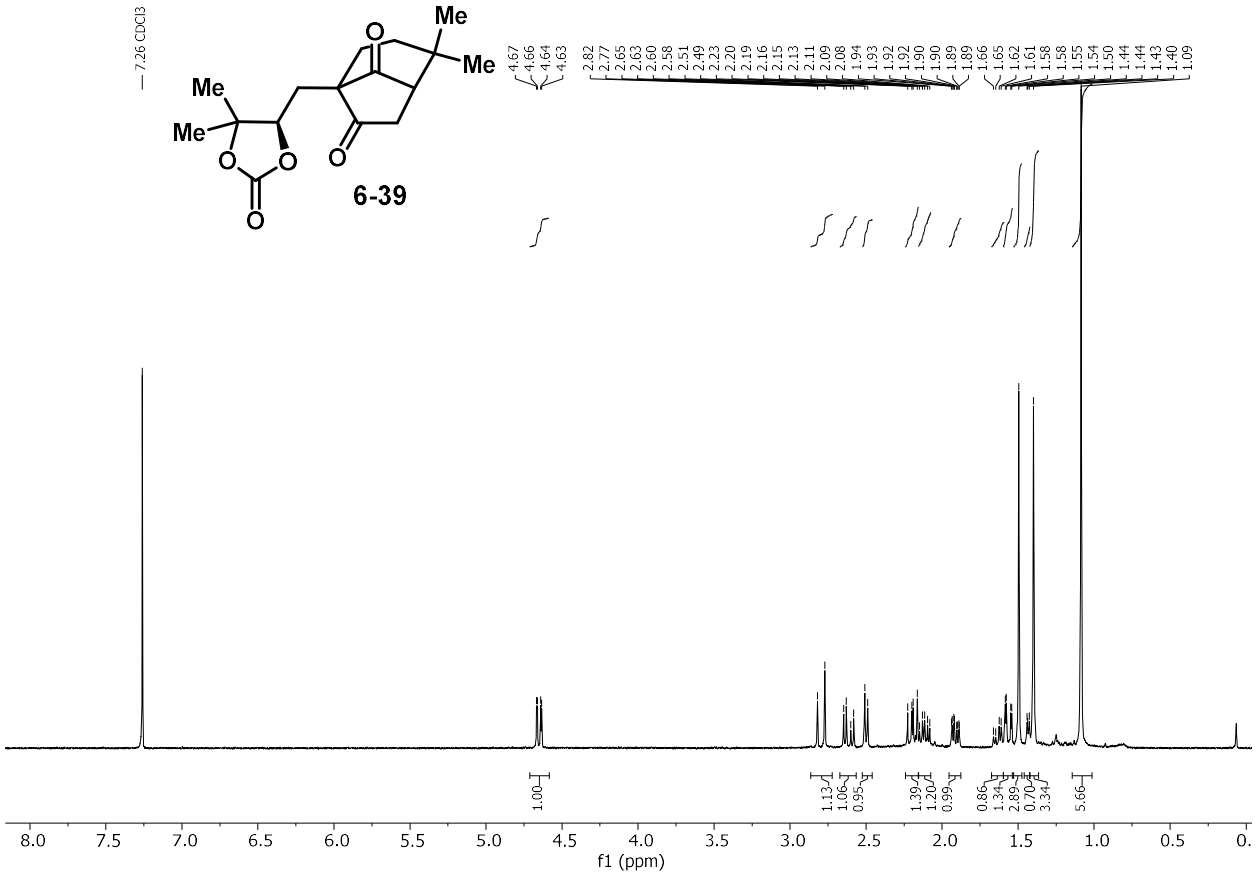
7.26 CDCl3
Me
Me
Me
Me
O
O
O
O
O
6-39
4.67
4.66
4.64
4.63
2.82
2.77
2.65
2.63
2.60
2.58
2.51
2.49
2.23
2.20
2.19
2.16
2.15
2.13
2.11
2.09
2.08
1.94
1.93
1.92
1.92
1.90
1.90
1.89
1.89
1.66
1.65
1.62
1.61
1.58
1.58
1.55
1.54
1.50
1.44
1.44
1.43
1.40
1.09
1.00
1.13
1.06
0.95
1.39
1.20
0.99
0.86
1.34
2.89
0.70
3.34
5.66
8.0
7.5
7.0
6.5
6.0
5.5
5.0
4.5
4.0
3.5
3.0
2.5
2.0
1.5
1.0
0.5
0.
f1 (ppm)

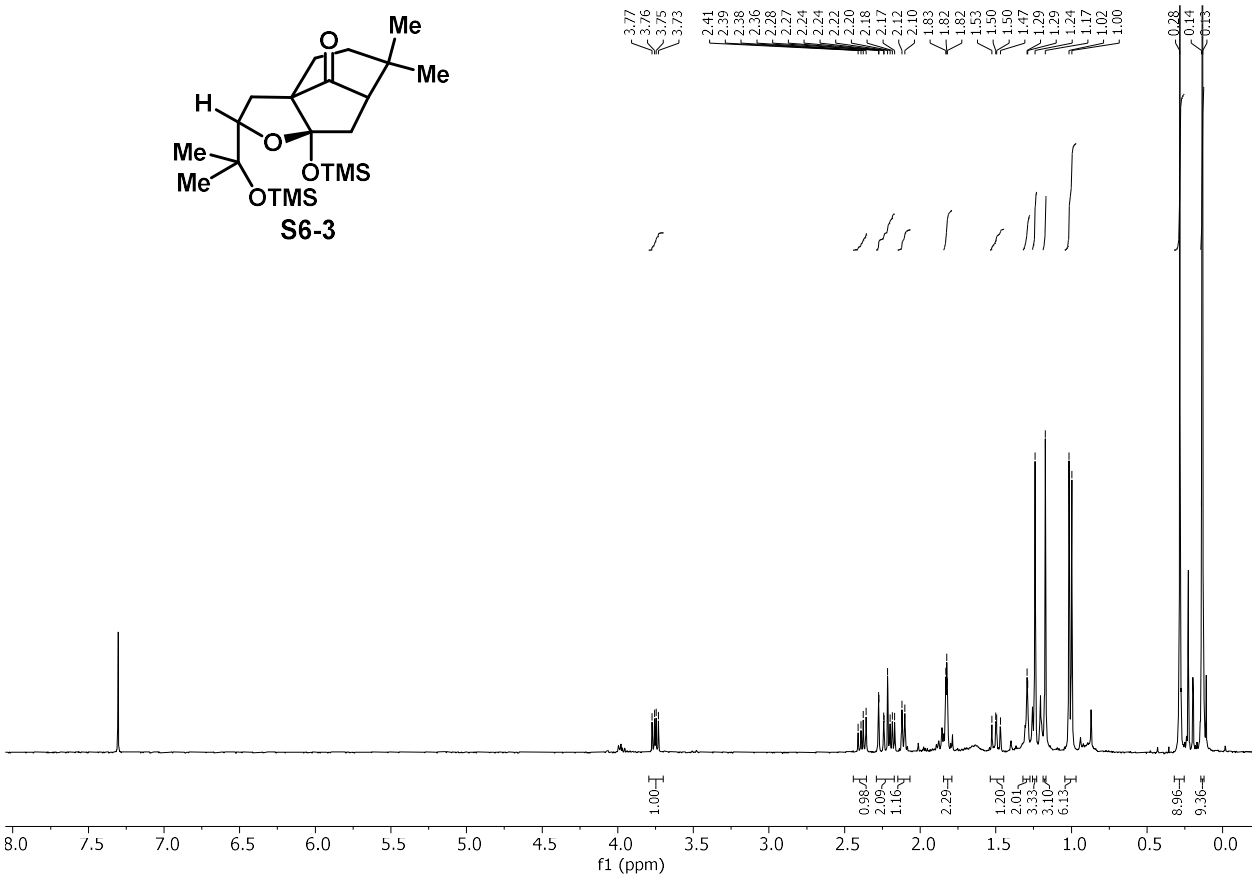
Me
Me
O
H
O
Me
Me
OTMS
OTMS
S6-3
f1 (ppm)

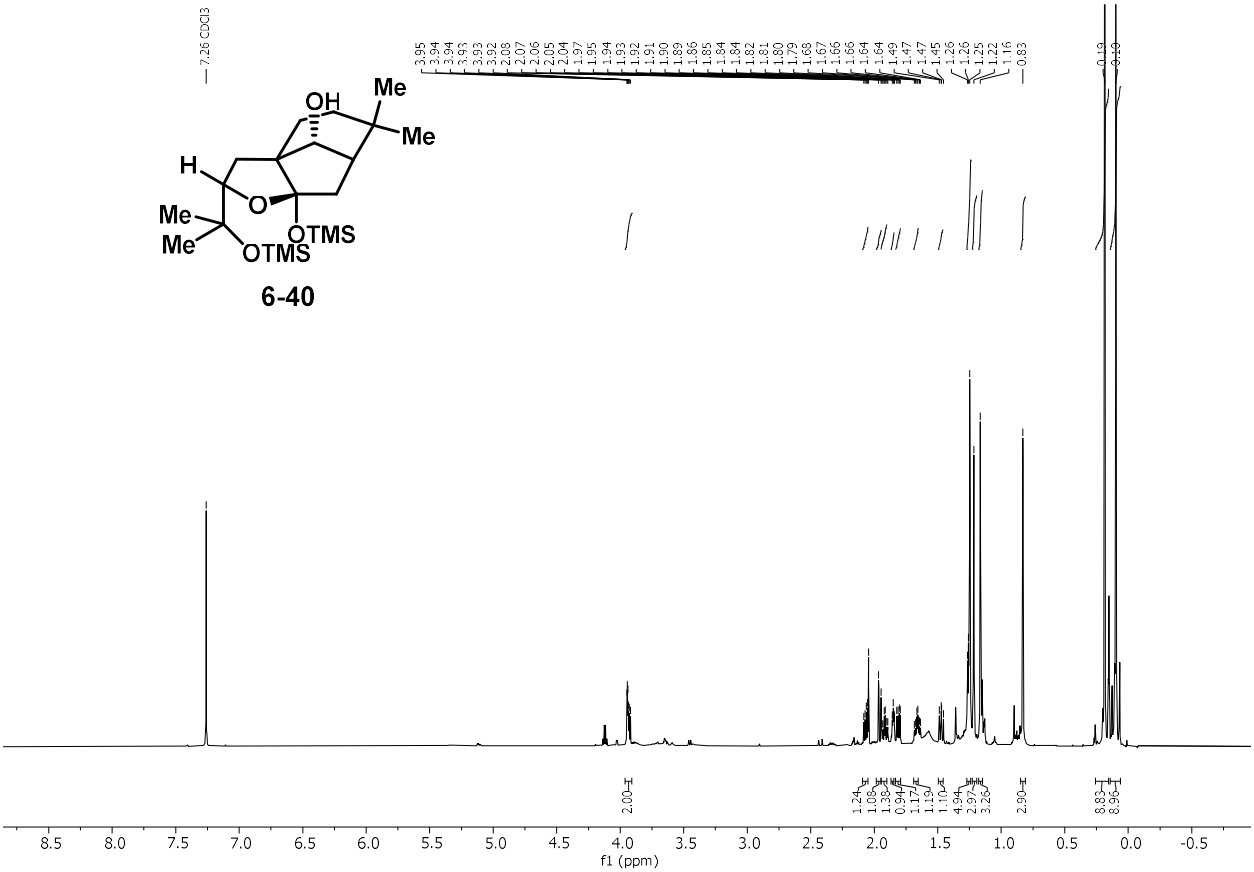
7.26 CDCl3
3.95
3.94
3.94
3.93
3.93
3.92
2.08
2.07
2.06
2.05
2.04
1.97
1.95
1.94
1.93
1.92
1.91
1.90
1.89
1.86
1.85
1.84
1.84
1.82
1.81
1.80
1.79
1.68
1.67
1.66
1.66
1.64
1.64
1.49
1.47
1.47
1.45
1.26
1.26
1.25
1.22
1.16
0.83
0.19
0.19
OH
Me
Me
H
O
Me
Me
OTMS
OTMS
6-40
2.00
1.24
1.08
1.38
0.94
1.17
1.19
1.10
4.94
2.97
3.26
2.90
8.83
8.96
8.5
8.0
7.5
7.0
6.5
6.0
5.5
5.0
4.5
4.0
3.5
3.0
2.5
2.0
1.5
1.0
0.5
0.0
-0.5
f1 (ppm)

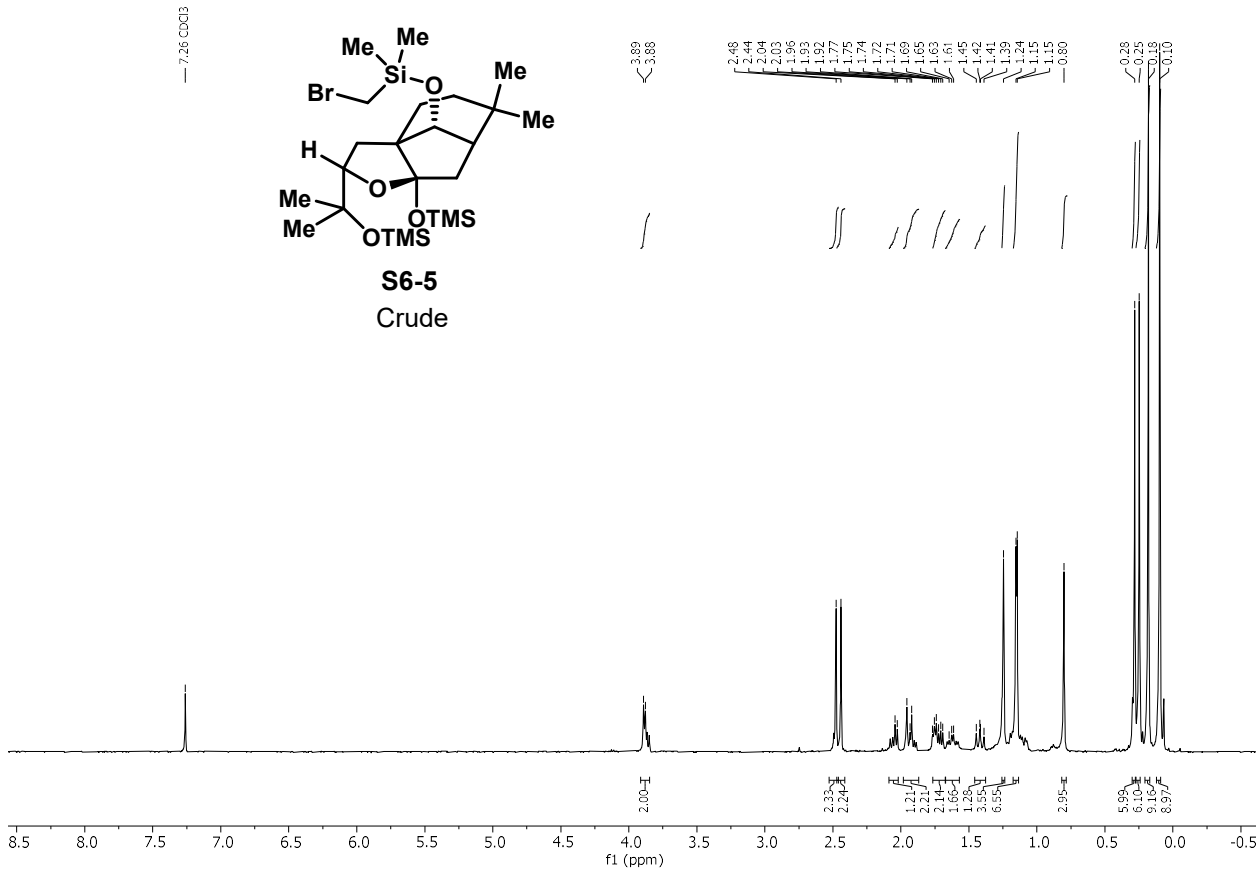
Me
Me
Si
O
Br
Me
Me
H
O
Me
Me
OTMS
OTMS
7.26 CDCl3
3.89
3.88
2.48
2.44
2.04
2.03
1.96
1.93
1.92
1.77
1.75
1.74
1.72
1.71
1.69
1.65
1.63
1.61
1.45
1.42
1.41
1.39
1.24
1.15
1.15
0.80
0.28
0.25
0.18
0.10
2.00
2.33
2.24
1.21
2.21
2.14
1.66
1.28
3.55
6.55
2.95
5.99
6.10
9.16
8.97
8.5
8.0
7.5
7.0
6.5
6.0
5.5
5.0
4.5
4.0
3.5
3.0
2.5
2.0
1.5
1.0
0.5
0.0
-0.5
f1 (ppm)

S6-5

Crude

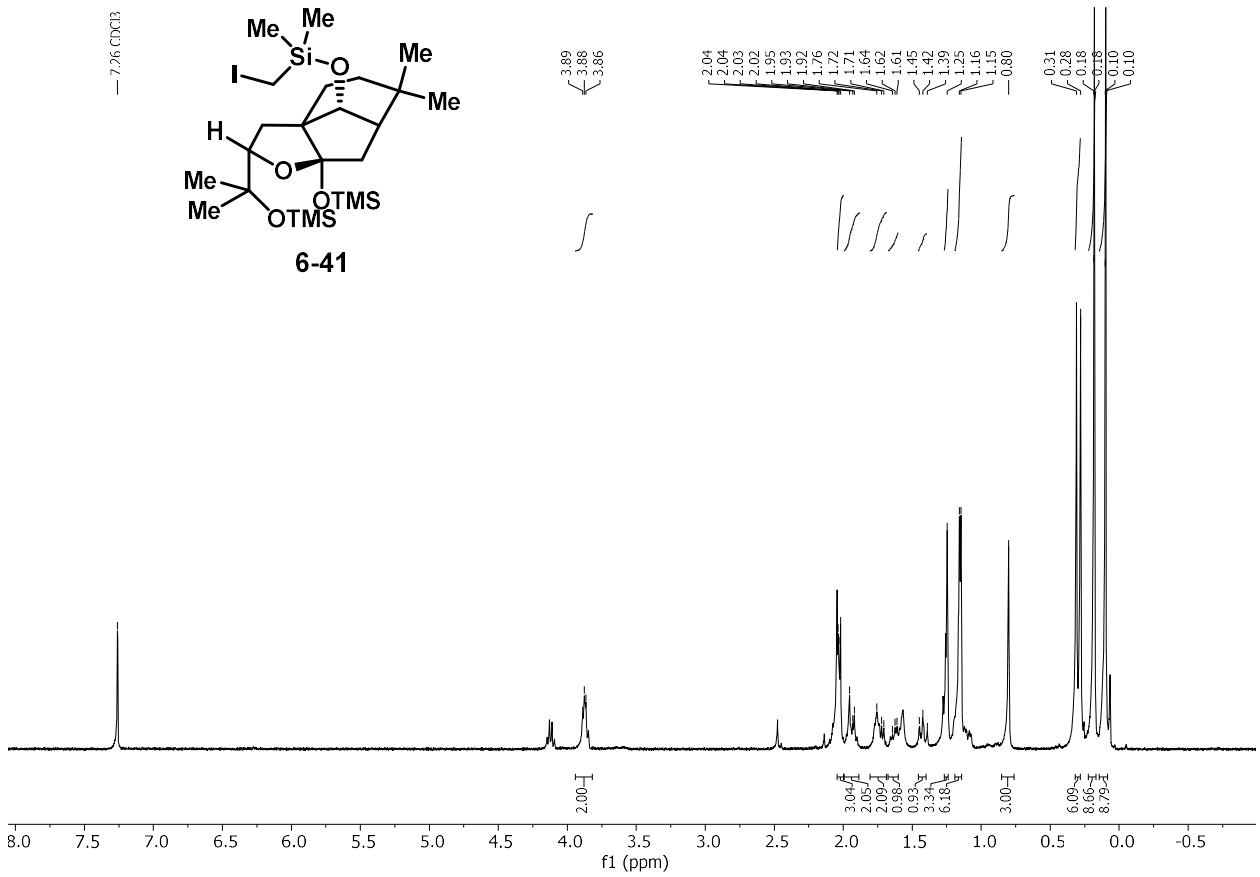
7.26 CDCl3
Me
Me
Si
O
Me
I
Me
H
O
Me
Me
OTMS
OTMS
6-41
3.89
3.88
3.86
2.04
2.04
2.03
2.02
1.95
1.93
1.92
1.76
1.72
1.71
1.64
1.62
1.61
1.45
1.42
1.39
1.25
1.16
1.15
0.80
0.31
0.28
0.18
0.18
0.10
0.10
2.00
3.04
2.05
2.09
0.98
0.93
3.34
6.18
3.00
6.09
8.66
8.79
8.0
7.5
7.0
6.5
6.0
5.5
5.0
4.5
4.0
3.5
3.0
2.5
2.0
1.5
1.0
0.5
0.0
-0.5
f1 (ppm)

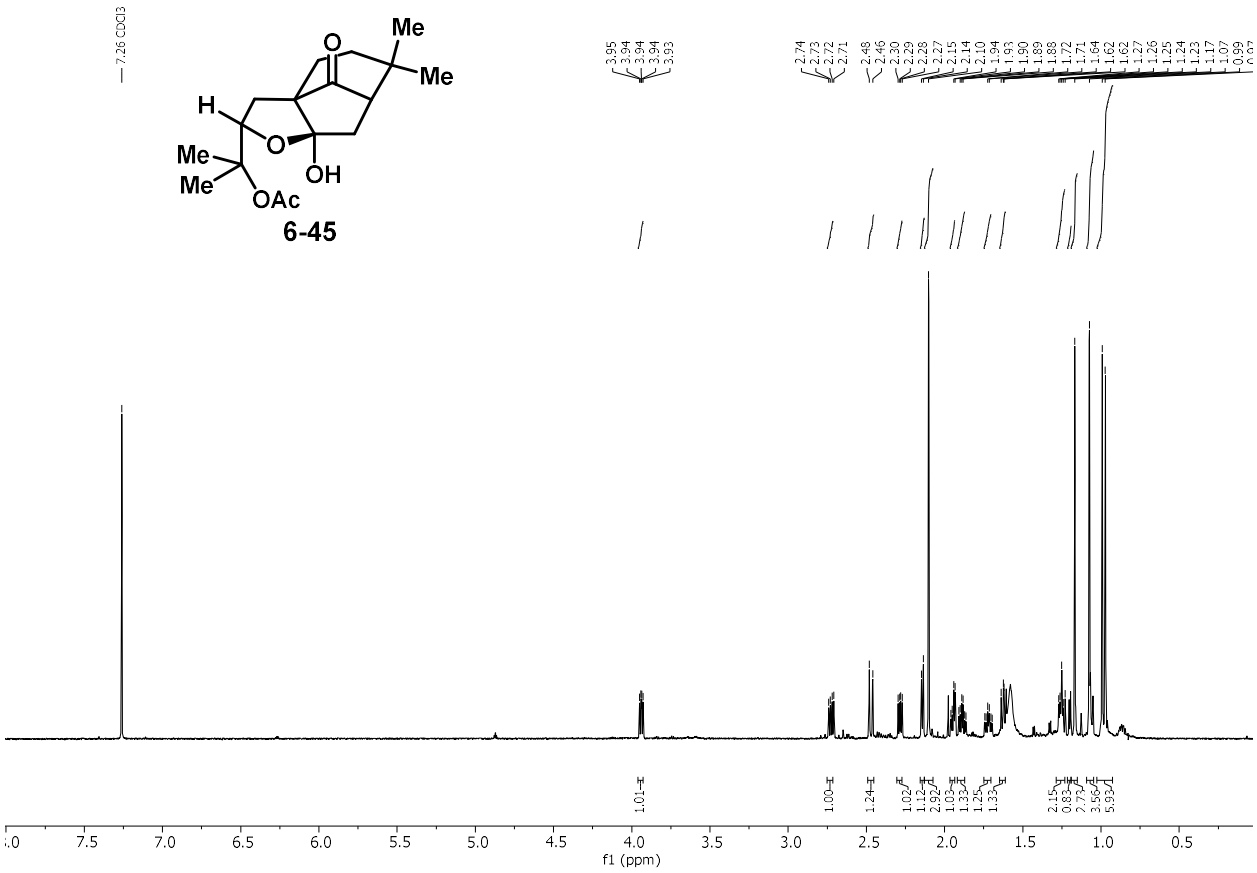
7.26 CDCl3
O
Me
Me
H
O
Me
Me
OAc
OH
6-45
f1 (ppm)

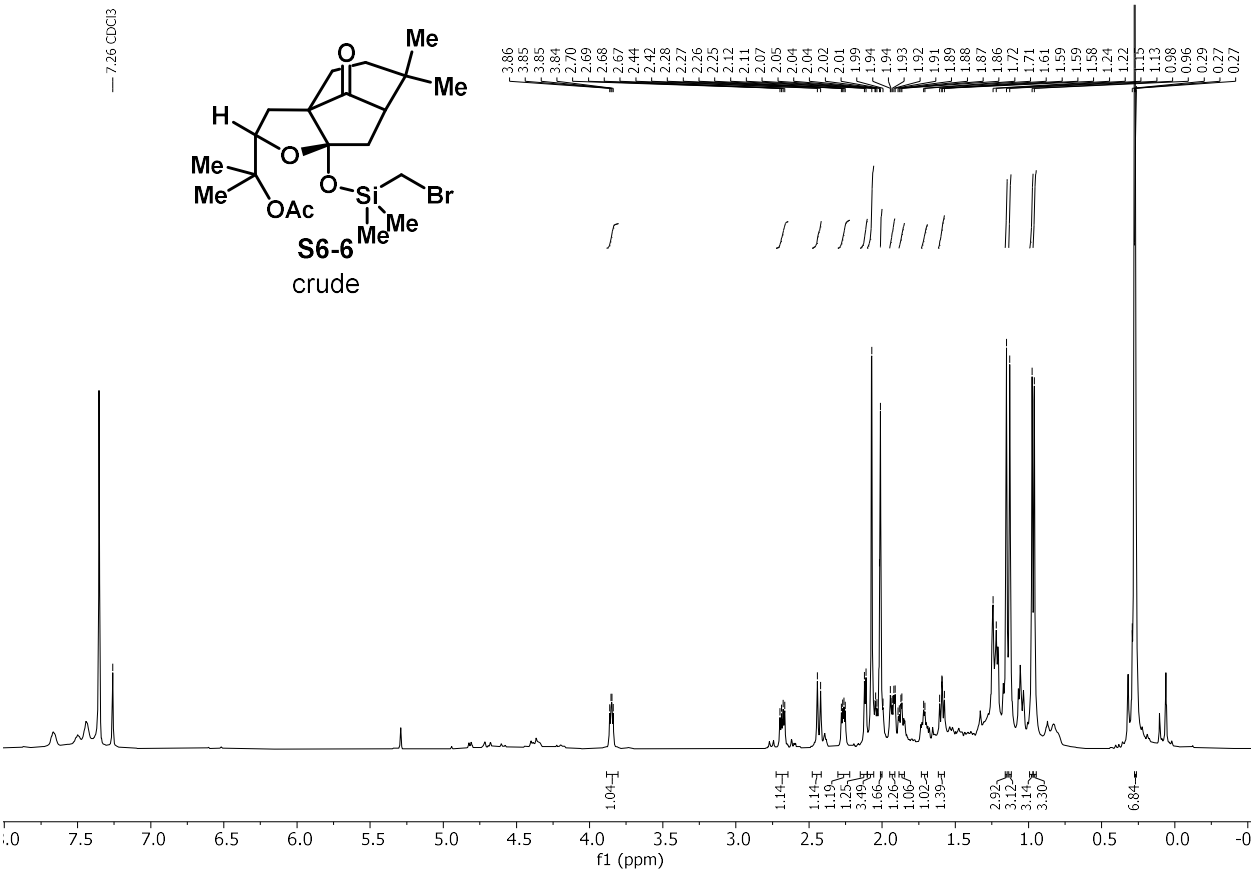
— 7.26 CDCl3
O
Me
Me
H
O
Me
Me
OAc
O
Si
Me
Me
Br
S6-6
crude
3.86
3.85
3.85
3.84
2.70
2.69
2.68
2.67
2.44
2.42
2.28
2.27
2.26
2.25
2.12
2.11
2.07
2.05
2.04
2.04
2.02
2.01
1.99
1.94
1.94
1.93
1.92
1.91
1.89
1.88
1.87
1.86
1.72
1.71
1.61
1.59
1.59
1.58
1.24
1.22
1.15
1.13
0.98
0.96
0.29
0.27
0.27
1.04
1.14
1.14
1.19
1.25
3.49
1.66
1.26
1.06
1.02
1.39
2.92
3.12
3.14
3.30
6.84
7.5
7.0
6.5
6.0
5.5
5.0
4.5
4.0
3.5
3.0
2.5
2.0
1.5
1.0
0.5
0.0
-0
f1 (ppm)

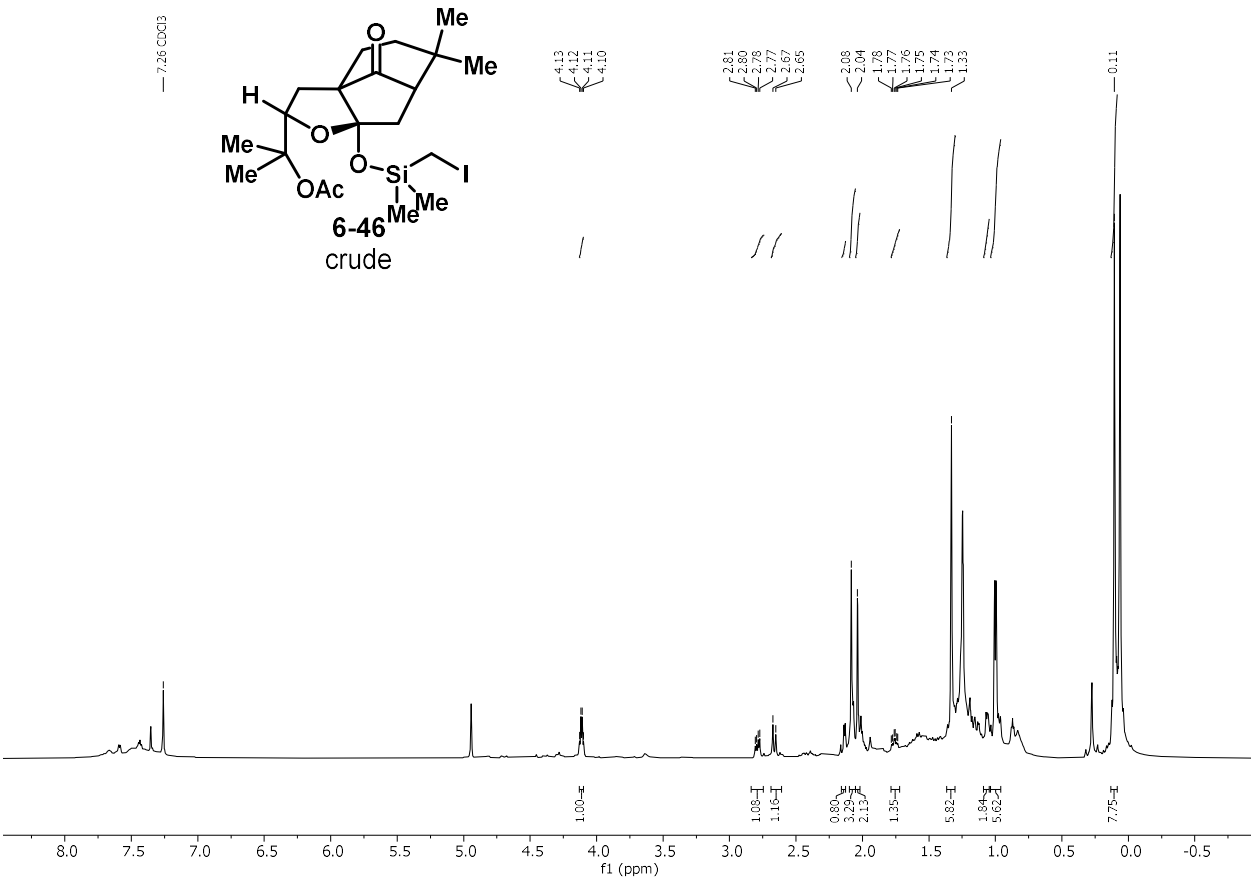
7.26 CDCl3
4.13
4.12
4.11
4.10
2.81
2.80
2.78
2.77
2.67
2.65
2.08
2.04
1.78
1.77
1.76
1.75
1.74
1.73
1.33
0.11
Me
Me
O
H
O
Me
Me
OAc
O
Si
I
Me
Me
6-46
crude
1.00
1.08
1.16
0.80
3.29
2.13
1.35
5.82
1.84
5.62
7.75
8.0
7.5
7.0
6.5
6.0
5.5
5.0
4.5
4.0
3.5
3.0
2.5
2.0
1.5
1.0
0.5
0.0
-0.5
f1 (ppm)

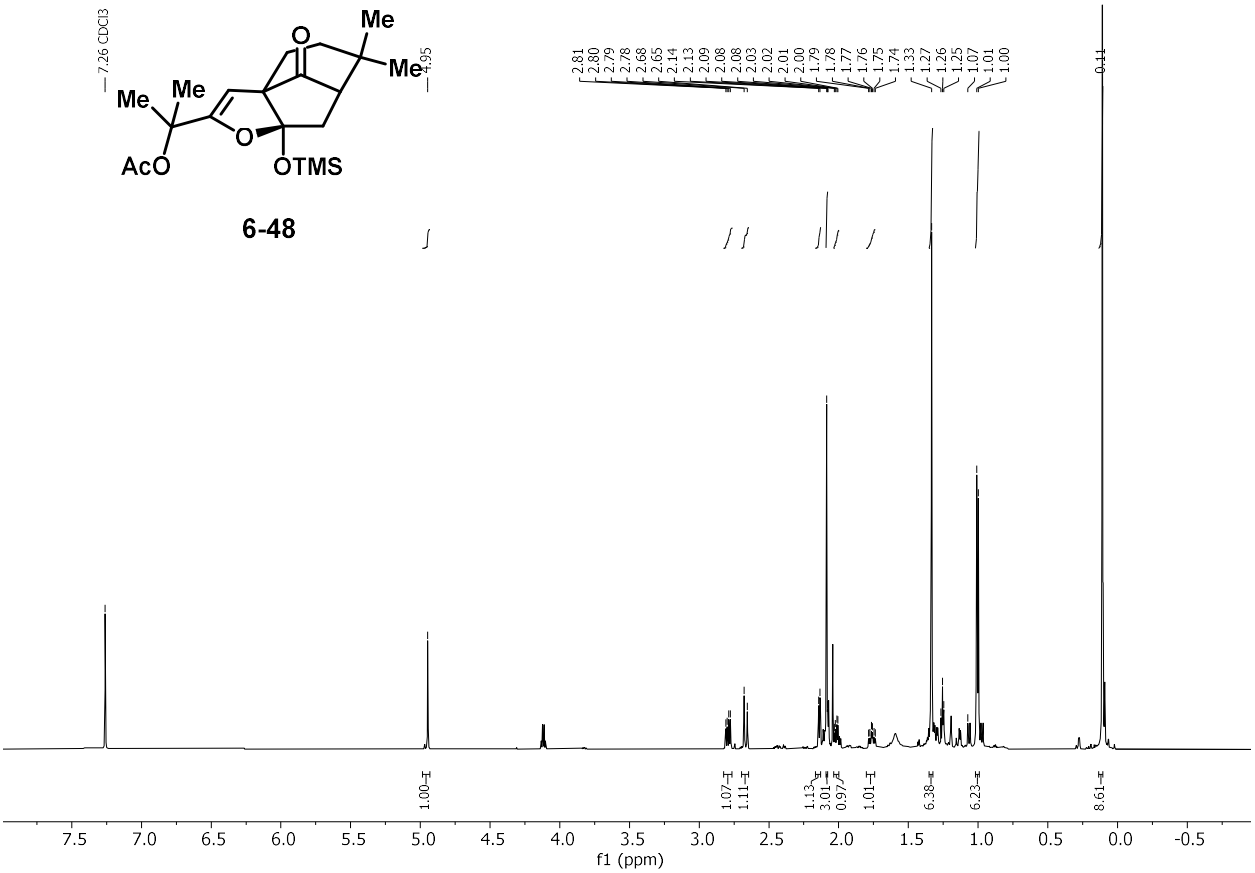
7.26 CDCl3
4.95
Me
Me
Me
Me
O
O
AcO
OTMS
2.81
2.80
2.79
2.78
2.68
2.65
2.14
2.13
2.09
2.08
2.08
2.03
2.02
2.01
2.00
1.79
1.78
1.77
1.76
1.75
1.74
1.33
1.27
1.26
1.25
1.07
1.01
1.00
0.11
1.00
1.07
1.11
1.13
3.01
0.97
1.01
6.38
6.23
8.61
7.5
7.0
6.5
6.0
5.5
5.0
4.5
4.0
3.5
3.0
2.5
2.0
1.5
1.0
0.5
0.0
-0.5
f1 (ppm)

6-48

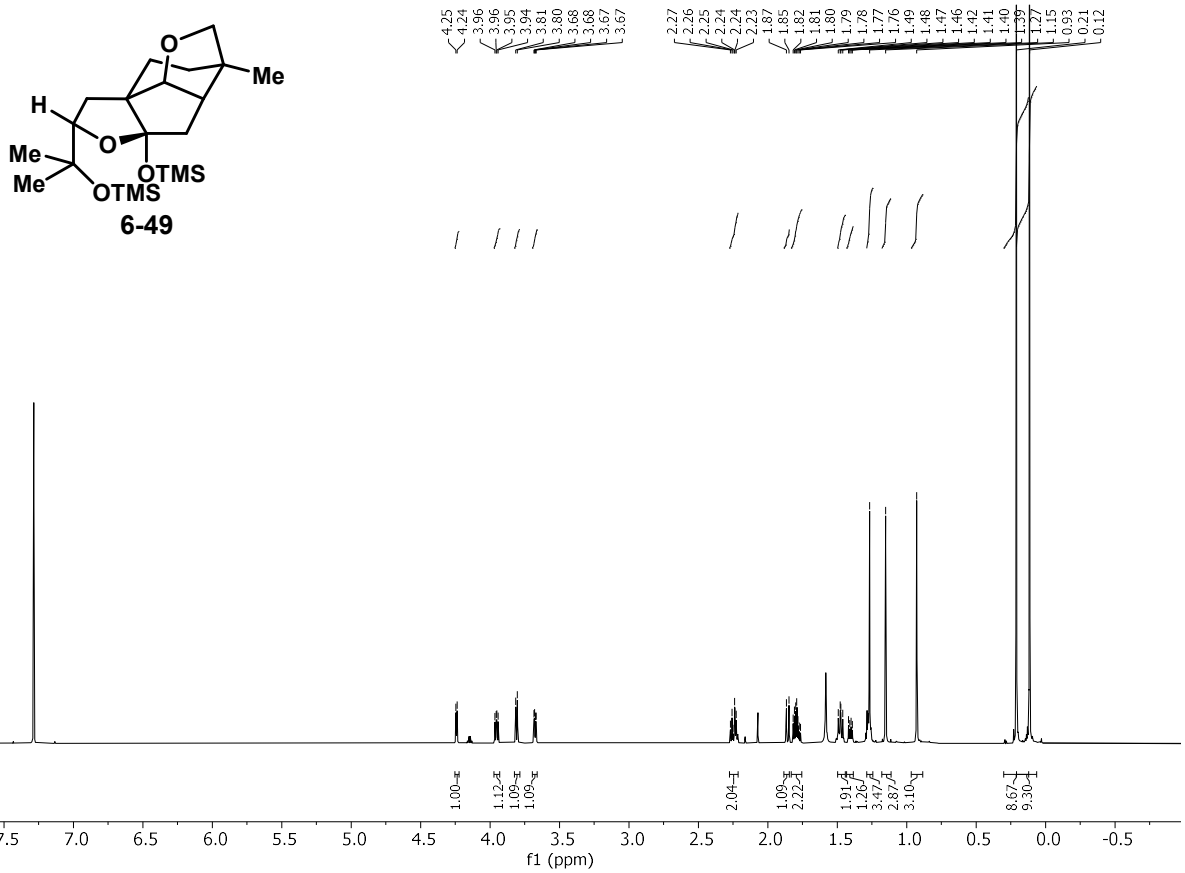
O
Me
H
O
Me
Me
OTMS
OTMS
6-49
f1 (ppm)

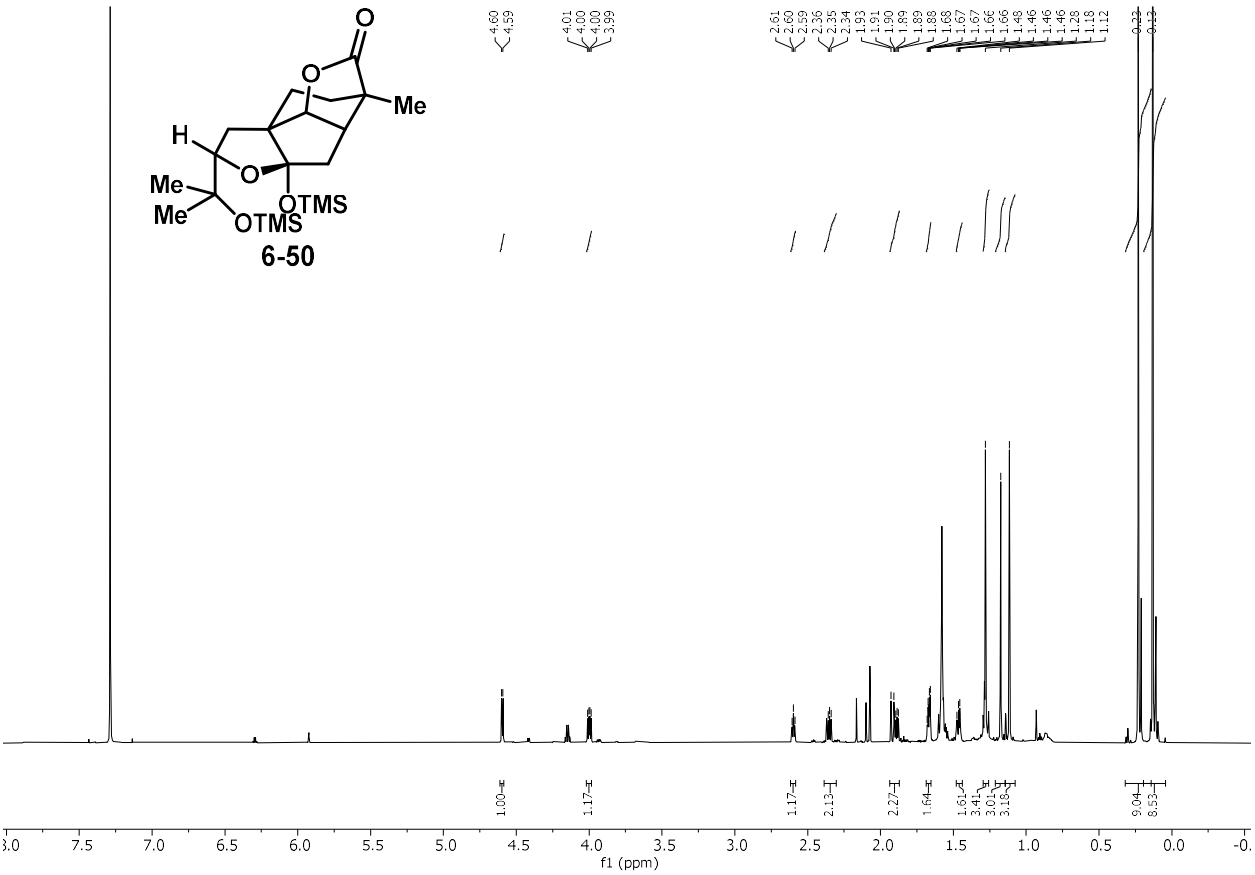
O
O
Me
H
O
Me
Me
OTMS
OTMS
6-50
4.60
4.59
4.01
4.00
4.00
3.99
2.61
2.60
2.59
2.36
2.35
2.34
1.93
1.91
1.90
1.89
1.89
1.88
1.68
1.67
1.67
1.66
1.66
1.48
1.46
1.46
1.46
1.28
1.18
1.12
0.22
0.12
1.00
1.17
1.17
2.13
2.27
1.64
1.61
3.41
3.01
3.18
9.04
8.53
7.5
7.0
6.5
6.0
5.5
5.0
4.5
4.0
3.5
3.0
2.5
2.0
1.5
1.0
0.5
0.0
f1 (ppm)

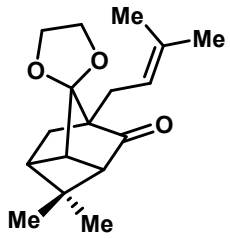
Me
Me
O
O
O
Me
Me

6-52

1.00
4.48
0.93
0.91
4.21
1.49
3.14
3.59
3.41
3.02
7.5
7.0
6.5
6.0
5.5
5.0
4.5
4.0
3.5
3.0
2.5
2.0
1.5
1.0
0.5
0.0
f1 (ppm)

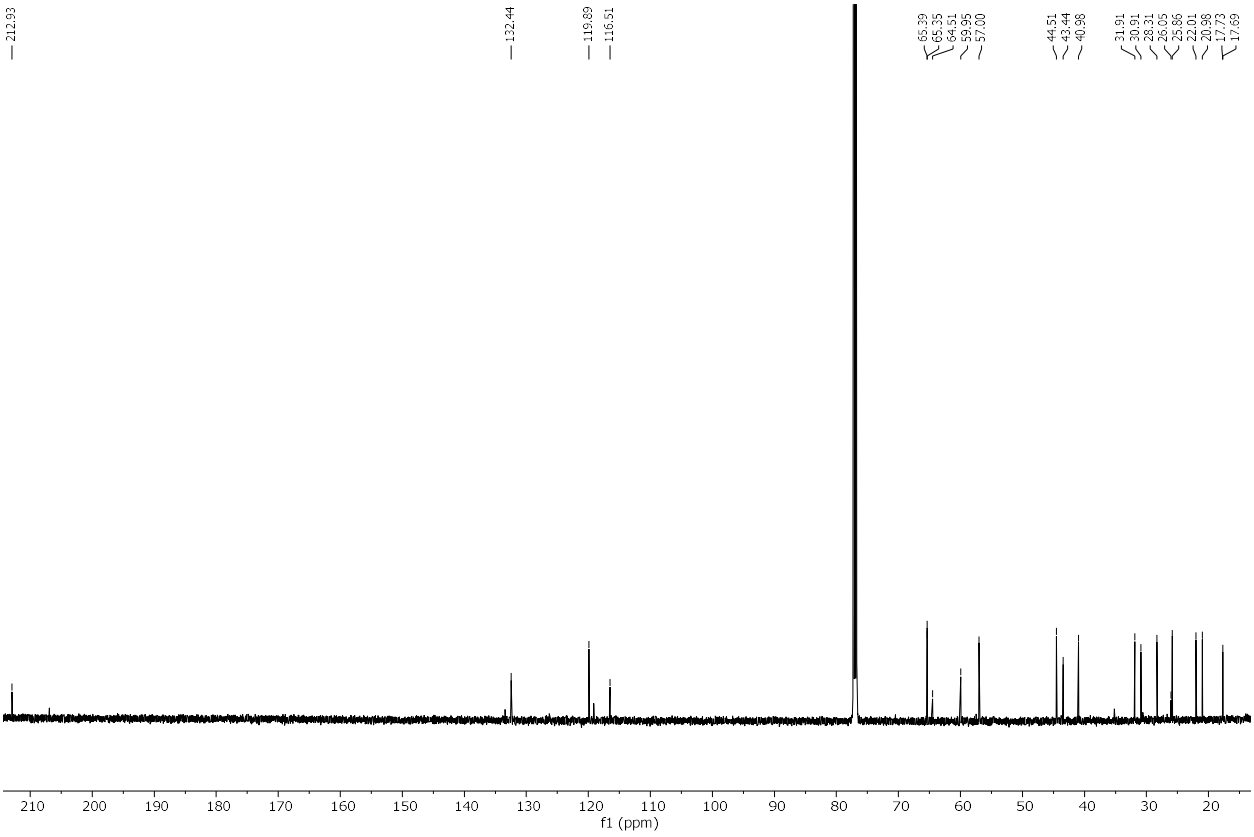
212.93
132.44
119.89
116.51
65.39
65.35
64.51
59.95
57.00
44.51
43.44
40.98
31.91
30.91
28.31
26.05
25.86
22.01
20.98
17.73
17.69
210
200
190
180
170
160
150
140
130
120
110
100
90
80
70
60
50
40
30
20
f1 (ppm)

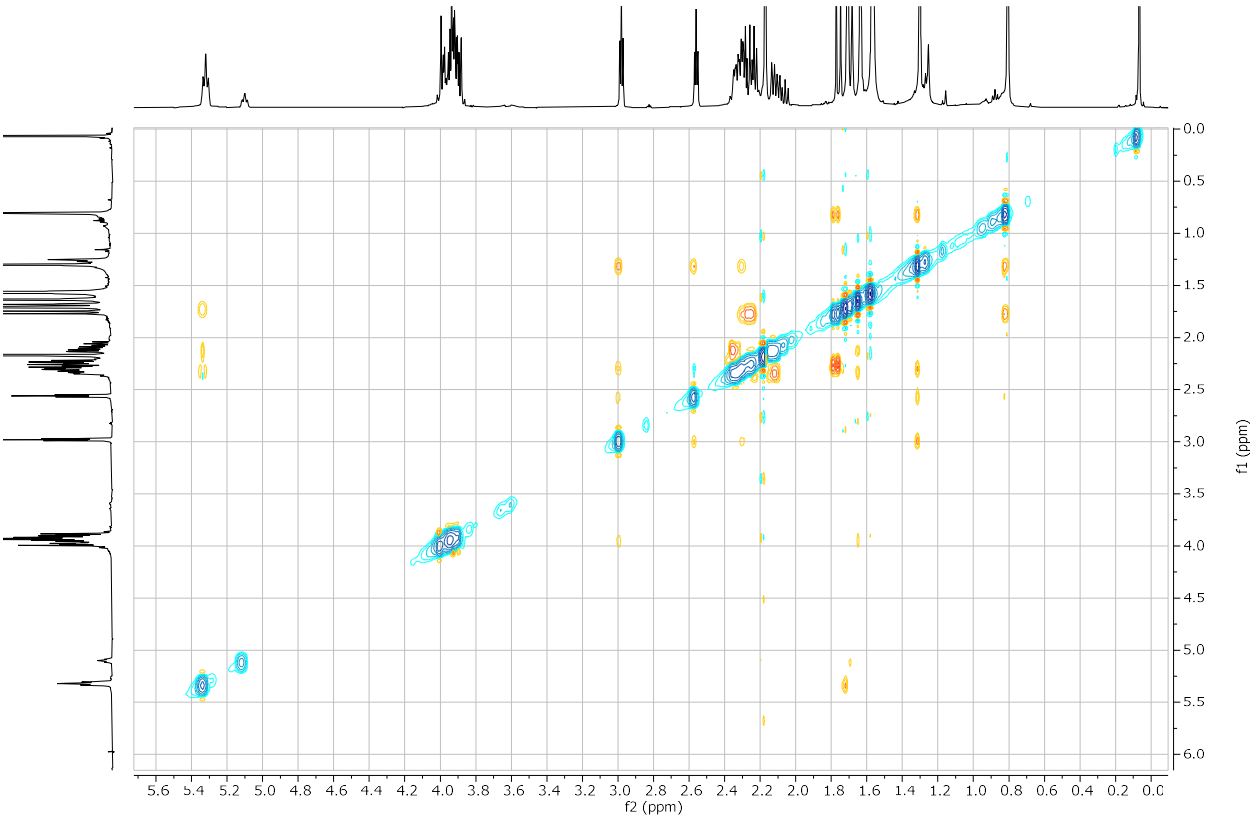
f2 (ppm)
f1 (ppm)

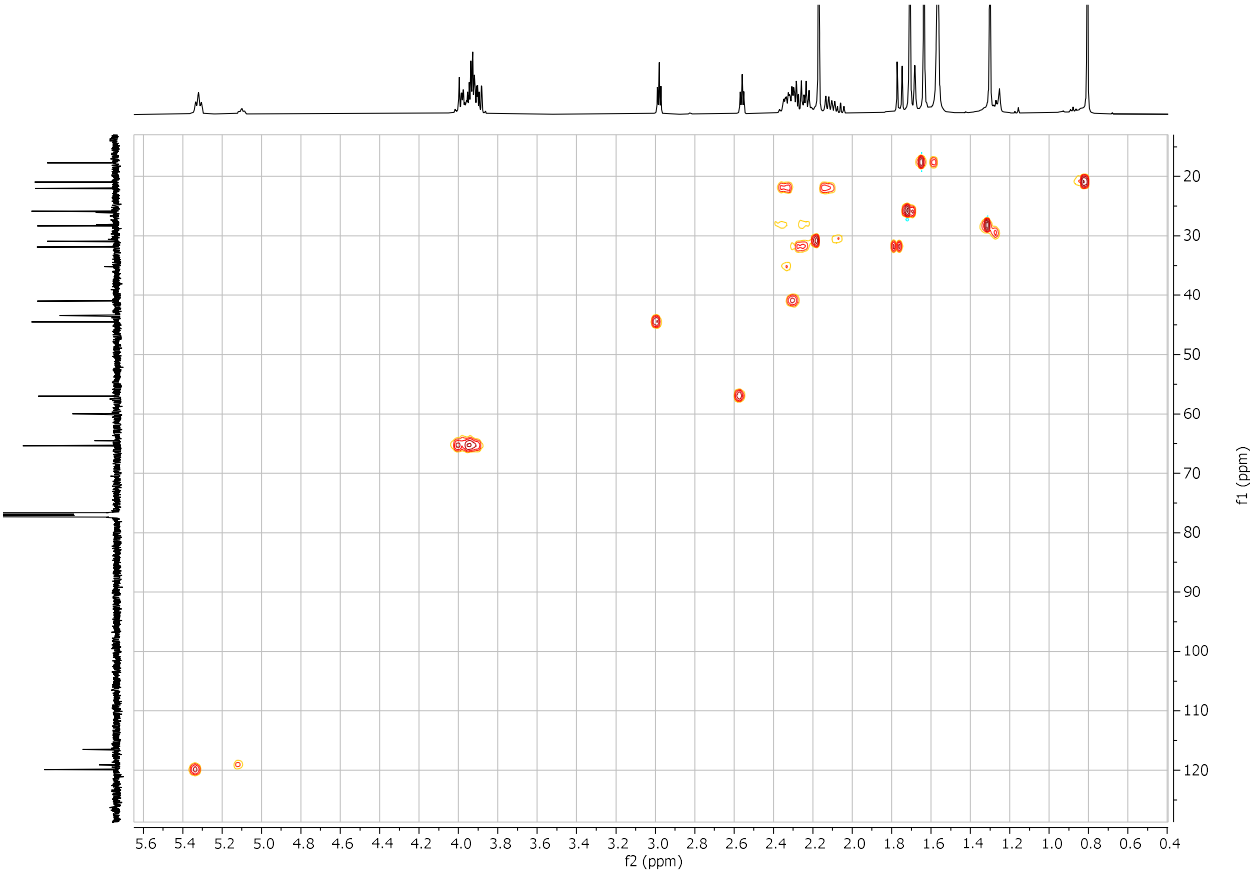
f2 (ppm)
f1 (ppm)

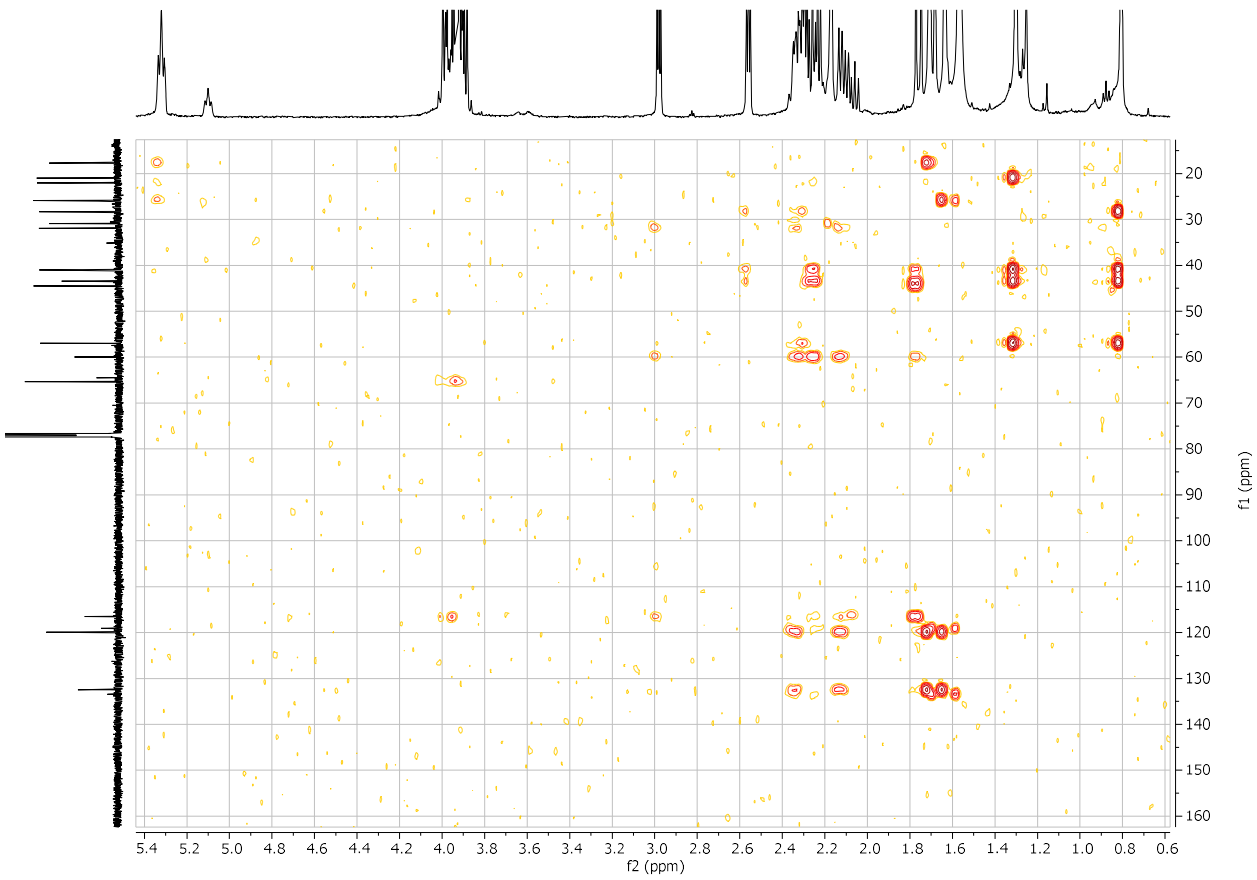
f1 (ppm)
f2 (ppm)

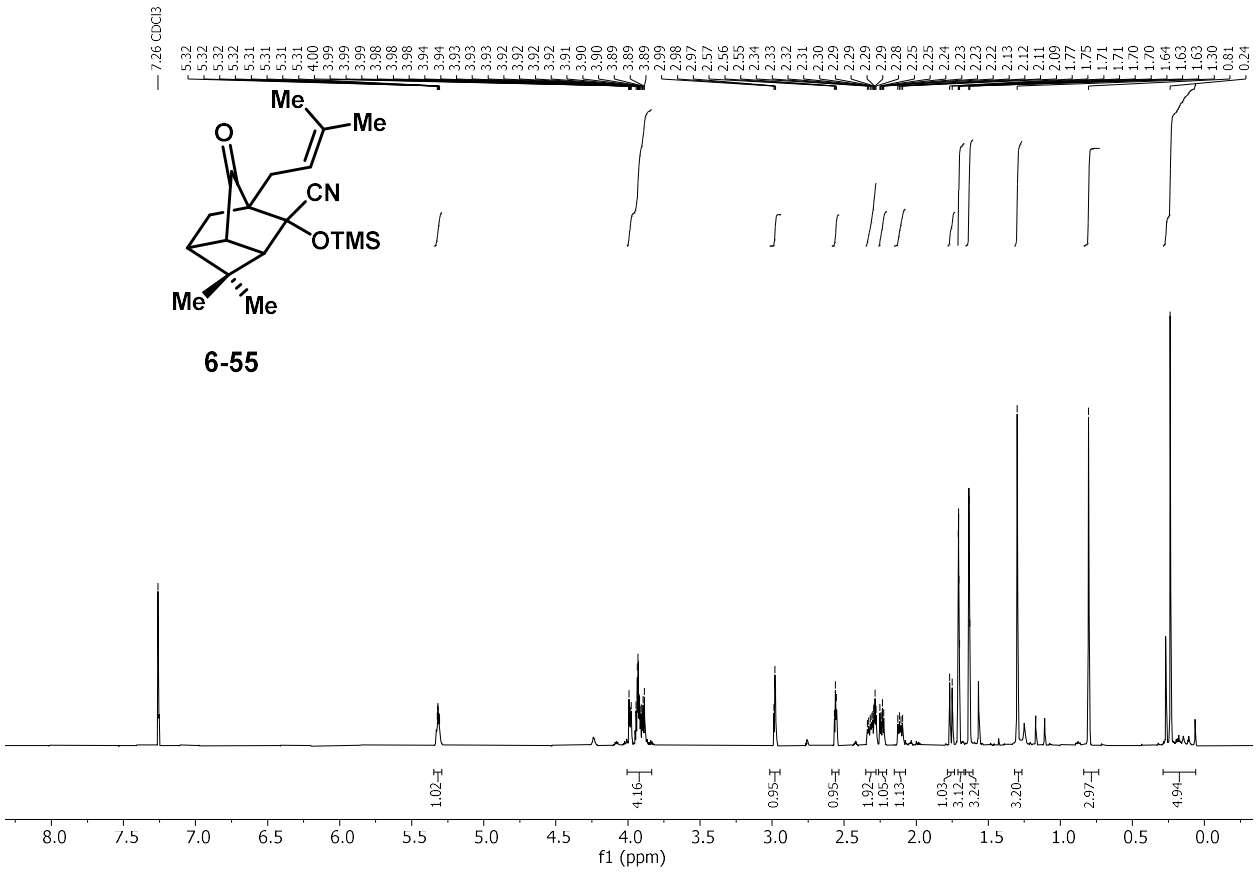
7.26 CDCl3
Me
Me
O
CN
OTMS
Me
Me
6-55
1.02
4.16
0.95
0.95
1.92
1.05
1.13
1.03
3.12
3.24
3.20
2.97
4.94
8.0
7.5
7.0
6.5
6.0
5.5
5.0
4.5
4.0
3.5
3.0
2.5
2.0
1.5
1.0
0.5
0.0
f1 (ppm)

6.7 References

(1) (a) Xu, J.-F.; Zhao, H.-J.; Wang, X.-B.; Li, Z.-R.; Luo, J.; Yang, M.-H.; Yang, L.; Yu, W.-Y.; Yao, H.-Q.; Luo, J.-G.; Kong, L.-Y. (±)-Melicolones A and B, Rearranged Prenylated Acetophenone Stereoisomers with an Unusual 9-Oxatricyclo[3.2.1.13,8]Nonane Core from the Leaves of Melicope Ptelefolia. *Org. Lett.* **2015**, *17*, 146–149. (b) Tang, Y.-Q.; Li, Y.-Q.; Xie, Y.-B.; Zhang, J.-S.; Li, W.; Lou, L.-L.; Zhang, G.; Yin, S. Evodialones A and B: Polyprenylated Acylcyclopentanone Racemates with a 3-Ethyl-1,1-Diisopentyl-4-Methylcyclopentane Skeleton from Evodia Lepta. *J. Nat. Prod.* **2018**, *81*, 1483–1487.

(2) (a) Wang, Z.; Martin, S. F. Concise Stereoselective and Stereodivergent Syntheses of (±)-Melicolones A and B. *Tetrahedron* **2022**, *103*, 132551. (b) Wang, Z.; Martin, S. F. Total Syntheses of (±)-Melicolones A and B. *Org. Lett.* **2020**, *22*, 9071–9074. (c) Carreira, E. M.; Fischer, D. M. Total Synthesis of (±)-Melicolones A and B. *Synfacts* **2021**, *17*, 129.

(3) (a) Švenda, J.; Hill, N.; Myers, A. G. A Multiply Convergent Platform for the Synthesis of Trioxacarcins. *PNAS.* **2011**, *108*, 6709–6714. (b) Shimada, N.; Hanari, T.; Kurosaki, Y.; Anada, M.; Nambu, H.; Hashimoto, S. Catalytic Asymmetric Synthesis of Descurainin via 1,3-Dipolar Cycloaddition of a Carbonyl Ylide Using Rh_2(R-TCPTTL)$_4$. *Tetrahedron Lett.* **2010**, *51*, 6572–6575. (c) Shimada, N.; Hanari, T.; Kurosaki, Y.; Takeda, K.; Anada, M.; Nambu, H.; Shiro, M.; Hashimoto, S. Catalytic Asymmetric Synthesis of the Endo-6-Aryl-8-Oxabicyclo[3.2.1]Oct-3-En-2-One Natural Product from Ligusticum Chuanxing via 1,3-Dipolar Cycloaddition of a Formyl-Derived Carbonyl Ylide Using Rh_2(S-TCPTTL)$_4$. *J. Org. Chem.* **2010**, *75*, 6039–6042.

(4) (a) Bai, W.-J.; Wang, X. Appreciation of Symmetry in Natural Product Synthesis. *Nat. Prod. Rep.* **2017**, *34*, 1345–1358. (b) Horwitz, M. A. Local Desymmetrization as an Engine of Stereochemical Elaboration in Total Synthesis. *Tetrahedron Lett.* **2022**, *97*, 153776. (c) Wang, M.; Feng, M.; Tang, B.; Jiang, X. Recent Advances of Desymmetrization Protocol Applied in Natural Product Total Synthesis. *Tetrahedron Lett.* **2014**, *55*, 7147–7155. (d) Schindler, C. S.; Cala, L.; Gaviria, M. A.; Kim, S. L.; Vogel, T. R. Recognition of Symmetry as a Powerful Tool in Natural Product Synthesis. *Synthesis* DOI: 10.1055/a-1702-5062.

(5) (a) Gansäuer, A.; Lauterbach, T.; Bluhm, H.; Noltemeyer, M. A Catalytic Enantioselective Electron Transfer Reaction: Titanocene-Catalyzed Enantioselective Formation of Radicals from Meso-Epoxides. *Angew. Chem. Int. Ed. 38*, 2909–2910. (b) McCallum, T.; Wu, X.; Lin, S. Recent Advances in Titanium Radical Redox Catalysis. *J. Org. Chem.* **2019**, *84*, 14369–14380.

(6) Cha, J. Y.; Yeoman, J. T. S.; Reisman, S. E. A Concise Total Synthesis of (−)-Maoecrystal Z. *J. Am. Chem. Soc.* **2011**, *133*, 14964–14967.

(7) Sreenivas, K.; Khan, F. A. An Unexpected Acid Mediated Rearrangement of Monoethylene Ketal of 2-Methyl-2-(3-Methylbut-2-En-1-Yl)Cyclohex-4-Ene-1,3-Diones to Chromane. *Tetrahedron Lett.* **2018**, *59*, 1244–1248.

(8) (a) Sparling, B. A.; Moebius, D. C.; Shair, M. D. Enantioselective Total Synthesis of Hyperforin. *J. Am. Chem. Soc.* **2013**, *135*, 644–647. (b) Sparling, B. A.; Tucker, J. K.; Moebius, D. C.; Shair, M. D. Total Synthesis of (−)-Nemorosone and (+)-Secohyperforin. *Org. Lett.* **2015**, *17*, 3398–3401.

(9) (a) Lo, J. C.; Yabe, Y.; Baran, P. S. A Practical and Catalytic Reductive Olefin Coupling. *J. Am. Chem. Soc.* **2014**, *136*, 1304–1307. B) Lo, J. C.; Kim, D.; Pan, C.-M.; Edwards, J. T.; Yabe, Y.; Gui, J.; Qin, T.; Gutiérrez, S.; Giacoboni, J.; Smith, M. W.; Holland, P. L.; Baran, P. S. Fe-Catalyzed C–C Bond Construction from Olefins via Radicals. *J. Am. Chem. Soc.* **2017**, *139*, 2484–2503.

(10) (a) Shevick, S. L.; Wilson, C. V.; Kotesova, S.; Kim, D.; Holland, P. L.; Shenvi, R. A. Catalytic Hydrogen Atom Transfer to Alkenes: A Roadmap for Metal Hydrides and Radicals. *Chem. Sci.* **2020**, *11*, 12401–12422. (b) Crossley, S. W. M.; Obradors, C.; Martinez, R. M.; Shenvi, R. A. Mn-, Fe-, and Co-Catalyzed Radical Hydrofunctionalizations of Olefins. *Chem. Rev.* **2016**, *116*, 8912–9000. (c) Green, S. A.; Crossley, S. W. M.; Matos, J. L. M.; Vásquez-Céspedes, S.; Shevick, S. L.; Shenvi, R. A. The High Chemofidelity of Metal-Catalyzed Hydrogen Atom Transfer. *Acc. Chem. Res.* **2018**, *51*, 2628–2640.

(11) See Chapter 5 for additional discussion

(12) (a) Chen, M. S.; White, M. C. A Predictably Selective Aliphatic C–H Oxidation Reaction for Complex Molecule Synthesis. *Science* **2007**, *318*, 783–787.

(13) (a) Zou, L.; Paton, R. S.; Eschenmoser, A.; Newhouse, T. R.; Baran, P. S.; Houk, K. N. Enhanced Reactivity in Dioxirane C–H Oxidations via Strain Release: A Computational and Experimental Study. *J. Org. Chem.* **2013**, *78*, 4037–4048. (b) Bovicelli, P.; Lupattelli, P.; Mincione, E.; Prencipe, T.; Curci, R. Oxidation of Natural Targets by Dioxiranes. 2. Direct Hydroxylation at the Side Chain C-25 of Cholestane Derivatives and of Vitamin D3 Windaus-Grundmann Ketone. *J. Org. Chem.* **1992**, *57*, 5052–5054.

(14) Shen, Y.; Li, L.; Xiao, X.; Yang, S.; Hua, Y.; Wang, Y.; Zhang, Y.; Zhang, Y. Site-Specific Photochemical Desaturation Enables Divergent Syntheses of Illicium Sesquiterpenes. *J. Am. Chem. Soc.* **2021**, *143*, 3256–3263.

(15) Ravelli, D.; Fagnoni, M.; Fukuyama, T.; Nishikawa, T.; Ryu, I. Site-Selective C–H Functionalization by Decatungstate Anion Photocatalysis: Synergistic Control by Polar and Steric Effects Expands the Reaction Scope. *ACS Catal.* **2018**, *8*, 701–713.

(16) Shields, B. J.; Doyle, A. G. Direct C(Sp3)–H Cross Coupling Enabled by Catalytic Generation of Chlorine Radicals. *J. Am. Chem. Soc.* **2016**, *138*, 12719–12722.

(17) Czaplyski, W. L.; Na, C. G.; Alexanian, E. J. C–H Xanthylation: A Synthetic Platform for Alkane Functionalization. *J. Am. Chem. Soc.* **2016**, *138*, 13854–13857.

(18) Griffin, J. D.; Vogt, D. B.; Du Bois, J.; Sigman, M. S. Mechanistic Guidance Leads to Enhanced Site-Selectivity in C–H Oxidation Reactions Catalyzed by Ruthenium Bis(Bipyridine) Complexes. *ACS Catal.* **2021**, *11*, 10479–10486.

(19) (a) Parasram, M.; Chuentragool, P.; Wang, Y.; Shi, Y.; Gevorgyan, V. General, Auxiliary-Enabled Photoinduced Pd-Catalyzed Remote Desaturation of Aliphatic Alcohols. *J. Am. Chem. Soc.* **2017**, *139*, 14857–14860. B) Chuentragool, P.; Parasram, M.; Shi, Y.; Gevorgyan, V. General, Mild, and Selective Method for Desaturation of Aliphatic Amines. *J. Am. Chem. Soc.* **2018**, *140*, 2465–2468.

(20) Martín, A.; Pérez-Martín, I.; Suárez, E. Intramolecular Hydrogen Abstraction Promoted by Amidyl Radicals. Evidence for Electronic Factors in the Nucleophilic Cyclization of Ambident Amides to Oxocarbenium Ions. *Org. Lett.* **2005**, *7*, 2027–2030.

(21) Narender, T.; Sarkar, S.; Venkateswarlu, K.; Kumar, J. K. New Chemical Access for Pyran Core Embedded Derivatives from Bisalkenylated 1,3-Diketones and 1,3-Diketoesters via Tandem C-Dealkenylation and Cyclization. *Tetrahedron Lett.* **2010**, *51*, 6576–6579.

6.8 Experimental contributors

All experiments were carried out by I.B. with guidance from R.S.

Chapter 7
Skeletal Diversification by C–C Cleavage to Access Bicyclic Frameworks from a Common Tricyclooctane Intermediate

7.1 Introduction

The structural complexity of natural products has long served as an inspiration for synthetic chemists to devise strategies and methodologies for their preparation.[1] The three-dimensional topology of natural products have also expanded the chemical space for drug and agrochemical discovery.[2] Our laboratory has been broadly interested in exploiting C–C cleavage reactions to forge new C-sp3 bonds in what we have termed "break-it-to-make-it" strategies.[3] While not immediately obvious, the use of compounds containing extra C–C bonds than a desired target compound can be greatly simplifying in synthesis—especially if the additional bonds are easily introduced en route to the target structure.[4] Cyclopropanation and [2+2] cycloaddition reactions have been a particularly effective means to arrive at these intermediates as they can form sterically congested C–C bonds (e.g., all-carbon quaternary centers) that are also reactive and can be readily functionalized.[5]

Strategies to accomplish manifold C–C cleavages starting from a single substrate to access diverse targets remain underexplored.[6] Through selective cleavage of different bonds in a single polycyclic scaffold, a variety of substructures bearing unique topology can be unveiled. While our group has explored this approach to structural diversification in the remodeling of bicyclic cyclobutanols derived from carvone,[7] these developments have been inherently limited to the starting scaffold. Here, we describe C–C cleavage tactics to access new chemical space using topologically complex—yet simple to synthesize—molecules.

During the course of a total synthesis (Chapter 6), we recognized that the strained [3.2.1.$0^{3,6}$] tricycle **7-1**, an intermediate in our synthesis, contained distinct bicycles that corresponded to substructures of various natural products (Scheme 1). Through deconstruction of the [3.2.1.$0^{3,6}$] tricyclic skeleton, bicyclo[3.2.1]octane and bicyclo[2.2.1]heptane cores could be readily accessed through cleavage of the cyclobutane. Alternatively, bicyclo[3.1.1]- and [3.2.0]heptane scaffolds could be synthesized through cleavage of relatively less strained bonds (i.e., C-1–C-2, C-1–C-7 Figure 7-1). Because all of the target bicycles are well-represented in natural product structures,[8] variations in C–C bond cleavage using **7-1** could unlock a unified strategy to these molecules. To be practical, this strategy would rely on: 1) the efficient and scalable synthesis of tricycle **7-1** and 2) our ability to selectively activate each C–C bond toward cleavage. Herein, we report initial studies in this regard.

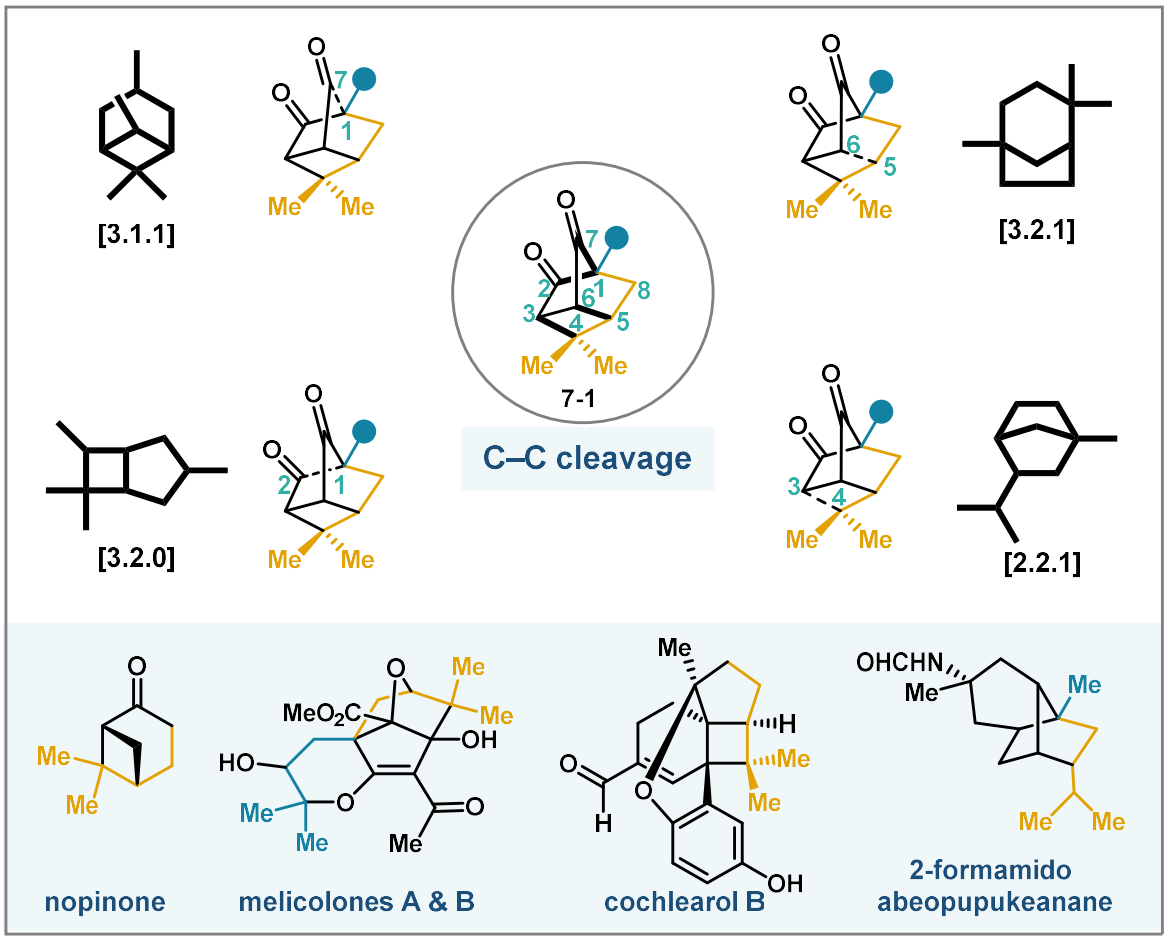

Figure 7.1. Numerous bicyclic terpene-like scaffolds comprise the tricyclic [3.2.1.0^{3,6}] core. Cleavage of select bonds would lead to the [3.2.1] bicyclooctane, [2.2.1] bicyclooctane, [3.2.0] bicycloheptane, and [3.1.1] bicycloheptane skeletons, which are all well-represented in natural products

There are various possible skeletal fragmentations of **7-1**. As such, we devised tactics for selective fragmentation as illustrated in Scheme 2. Consistent with the extensive literature on strained ring opening reactions,[5] we reasoned that incipient charge (either positive or negative), or open shell intermediates would destabilize beta-disposed C–C bonds. Introducing charge at the desired positions (either exocyclic or endocyclic) would reduce the number of possible fragmentations in a pairwise fashion (see **7-2**–**5,** Figure 7-2A). Selective C–C cleavage could be achieved by manipulating the functional groups in **1** (Figure 7-2B). For example, formation of alkoxide **7-6** could lead to selective fragmentation of the C-1–C-7 bond through a retro-aldol cleavage to give enolate **7-7**. Alternatively, formation of a carbon-centered radical at C-7 (see **7-8**) could lead to the selective cleavage of the C-3–C-6 bond. We hypothesized that formation of more stabilized radical **7-9** would be reflected in the selectivity-determining transition state. Furthermore, the C-1–C-2 bond could be targeted through formation of alkoxy radical **7-10**, which could undergo β-scission to form stable tertiary radical **7-11**. Finally, ionization to

carbocation **7-12** could fragment the strained cyclobutane C-3–C-4 bond to give tertiary carbocation **7-13** following rearrangement. To test these envisioned fragmentations, we commenced with the preparation of tricycle **7-1**.

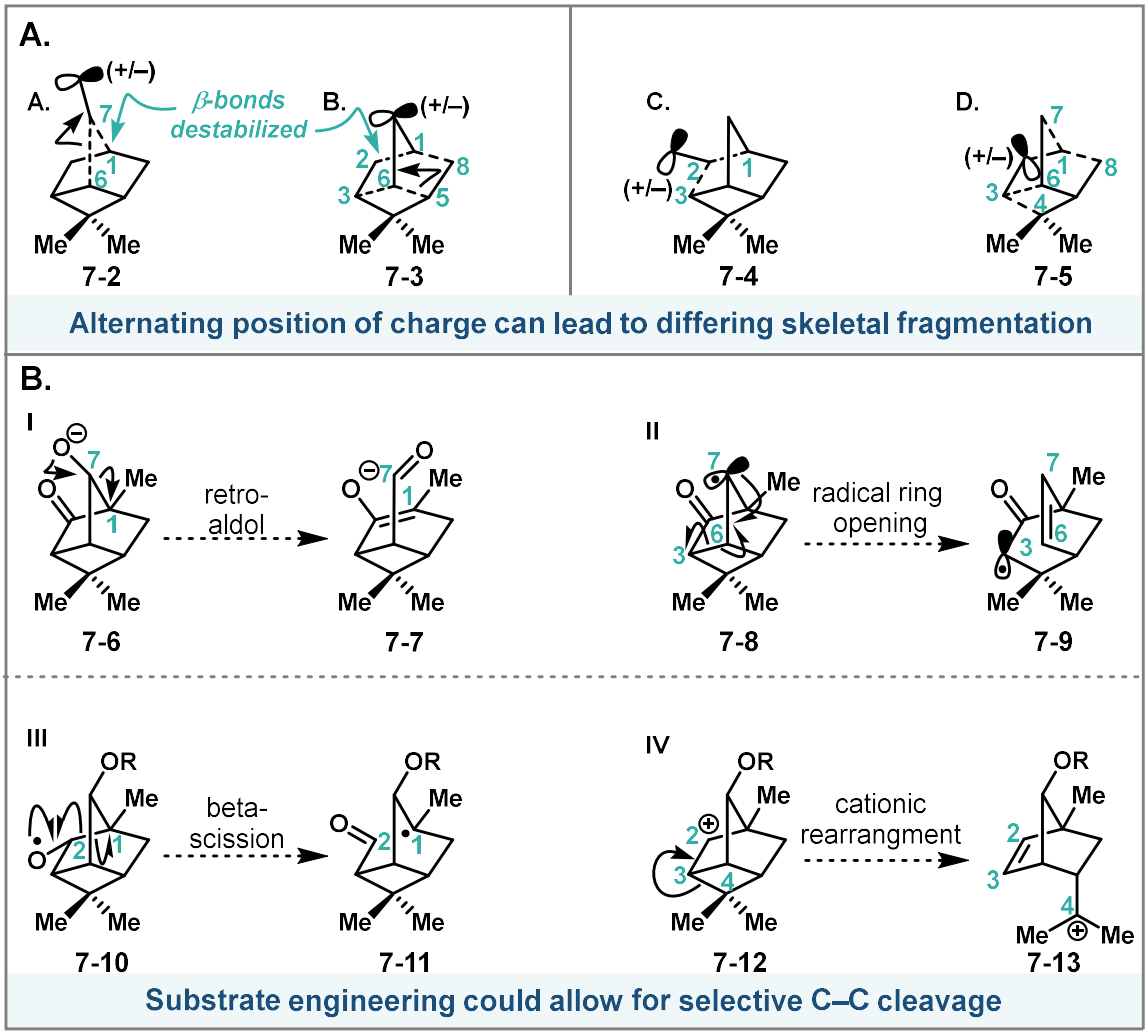

Figure 7.2 A. Conceptual relationship between developing charge or radical and skeletal fragmentation. **B.** Strategies for gaining selectivity in C–C bond cleavage.

7.2 Results and disussion

Tricycles of the general structure **7-1** were readily prepared through the [2+2] cycloaddition of enediones related to **7-14** (Scheme 7-1A and 7-B). In our initial designs, we sought to avoid issues of diastereoselectivity[9] by using achiral, symmetric enediones. The syntheses began with prenylation[10] of commercially available 2-methyl-1,3-cyclopentanedione (**7-15**), followed by desaturation with phenyltrimethylammonium tribromide to give **7-16** in 50% yield over 2 steps on multigram scale. The key [2+2] photocycloaddition to give **7-17** was then investigated (Table 1). Irradiating **7-16** using 254, 310, and 350 nm light resulted in no reaction.

While investigating cycloadditions using visible-light and triplet sensitizers,[11] we observed significant conversion of **7-16**. A control reaction without the triplet sensitizer led to the discovery that blue light irradiation alone was sufficient for achieving full conversion. In fact, irradiation at 420 nm in DCM led to efficient photocycloaddition to give tricycle **7-17** in >95% yield.

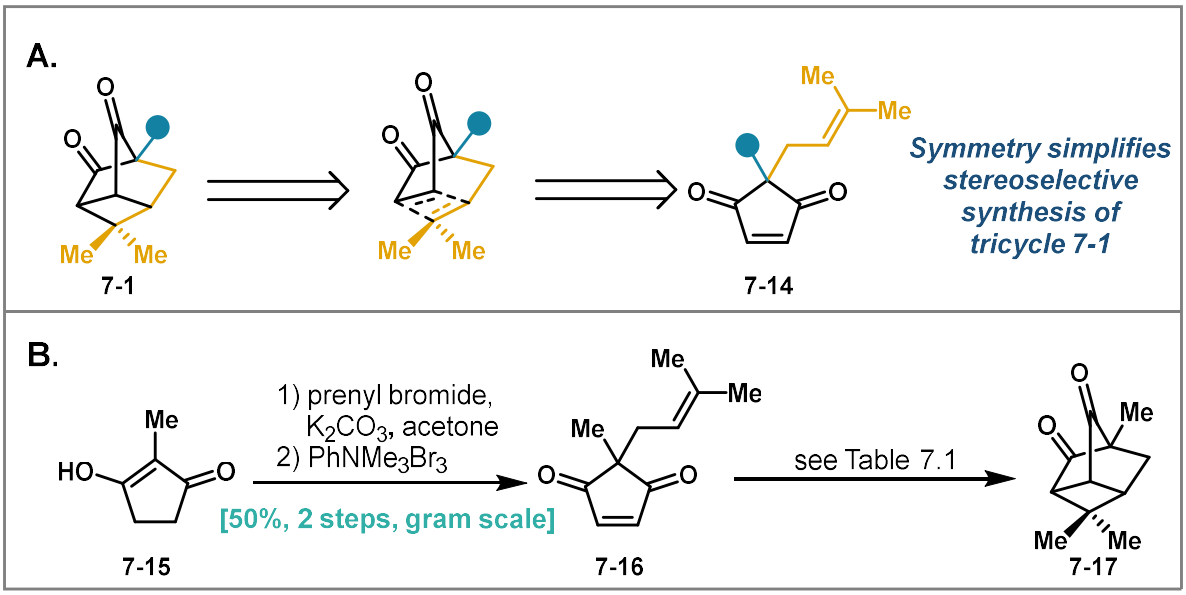

Scheme 7.1 A. Disconnection of key tricycle **7-1** using a [2+2] transform to symmetrical enedione precursor **7-14 B.** Synthesis of enedione **7-16**

The photocycloaddition is tolerant of both air and moisture and proceeds best in aprotic solvents. Interestingly, the UV-vis spectrum of **7-16** shows strong absorption at the unreactive wavelengths of 254 nm and 310 nm, but a smaller trailing absorbance tail at 400-470 nm (visible at relatively high concentrations).[12,13] Consistent with this absorbance profile, reaction at 470 nm proceeded with lower conversion, and no reaction was observed at 520 nm. The photocycloaddition reaction performed faithfully on larger scale, with similar efficiencies observed on gram-scale (entry 12), though the reaction time had to be extended significantly. Prolonged exposure to blue LED irradiation did lead to product decomposition (entry 13). As such, careful monitoring of conversion and exposure window is crucial to success (see the SI for details). The photocycloaddition is tolerant of both air and moisture and proceeds best in aprotic solvents. Interestingly, the UV-vis spectrum of **7-16** shows strong absorption at the unreactive wavelengths of 254 nm and 310 nm, but a smaller trailing absorbance tail at 400-470 nm (visible at relatively high concentrations).[12,13] Consistent with this absorbance profile, reaction at 470 nm proceeded with lower conversion, and no reaction was observed at 520 nm. The photocycloaddition reaction

entry	conditions	conversion (yield)
1	254 nm[a]	0%
2	310 nm[a]	0%
3	350 nm[a]	0%
4	365 nm[b]	100% (58%)
5	385 nm[b]	100% (85%)
6	420 nm[b]	100% (95%[c])
7	450 nm[b]	82% (80%)
8	470 nm[b]	56% (54%)
9	520 nm[b]	0%
10	420 nm, benzene[b]	56% (53%)
11	420 nm, MeOH[b]	100% (<10%)
12	tuna blue kessil lamp, 5 mmol scale	100%[d]
13	420 nm, 50 h[b]	100% (<10%)

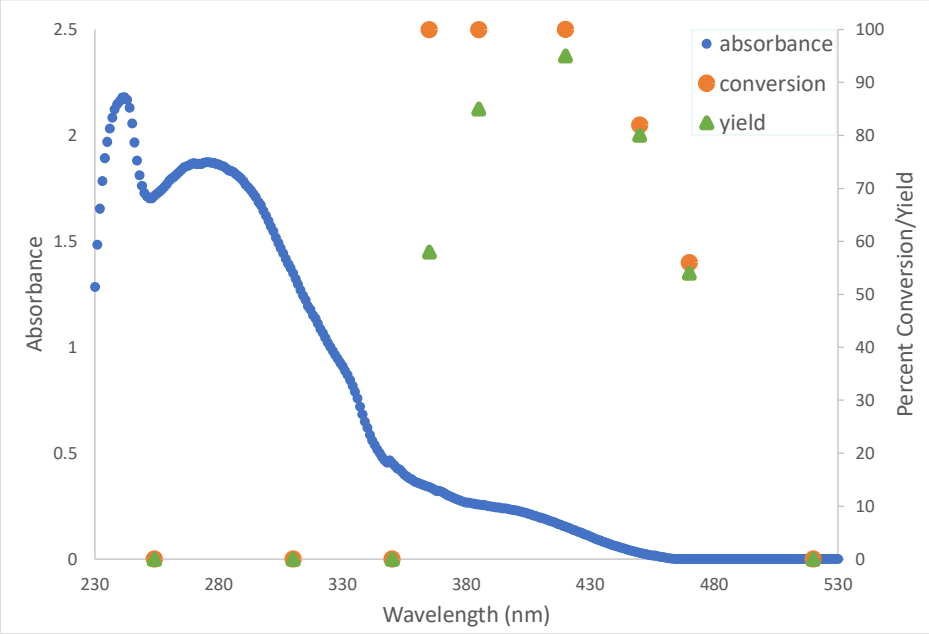

Table 7.1 A. Optimization of the key [2+2] cycloaddition. Percent conversion noted after 10 h of irradiation on 0.05 mmol scale in DCM (0.1 M). Percent yield determined by NMR. [a]Irradiated in a Luzchem photobox with UVA, UVB, or UVC lamps.[b] Penn photoreactor was used and maintained at 23 °C. [c] Average of 3 runs, 0.1 mmol scale. [d]Reaction time extended to 90 h. **B.** UV/Vis absorbance spectrum of **7-16** plotted against yield and conversion at varying wavelengths.

performed faithfully on larger scale, with similar efficiencies observed on gram-scale (entry 12), though the reaction time had to be extended significantly. Prolonged exposure to blue LED irradiation did lead to product decomposition (entry 13). As such, careful monitoring of conversion and exposure window is crucial to success (see the SI for details).

With ready access to sufficient quantities of key tricycle **7-17**, we commenced our studies on its fragmentation. A benefit of the "photon-only" (i.e., "reagentless") cycloaddition is that for most subsequent reactions, the crude reaction mixture only needed to be concentrated and redissolved in the appropriate solvent. We first studied anionic opening reactions (Scheme 7-2A). Addition of several nucleophiles into the northern ketone group of **7-17** led to the selective fragmentation of the C-1–C-7 bond. Most efficient among the nucleophilic reagents that were employed was TMSI[14] (a source of iodide), which first silylates the C-7 carbonyl group to activate it toward iodide addition (see **7-18**). Ensuing fragmentation and hydrolysis gave [3.1.1]-bicyclic acid **7-20** in 78% yield over the two steps. Overall, functionalized [3.1.1] bicycle **7-20**, reminiscent of the pinane scaffold, is accessed in 4 steps (3 purifications) from commercially available material. Engaging the carboxy group of **7-20** in decarboxylative cross coupling reactions[15] could provide access to a wide range of unnatural "pinene-like" compounds possessing unique 3D-topology and vectors for drug discovery.[16]

Next, we investigated the synthesis of the bicyclo[3.2.1]octane core from **7-17**. We first sought to identify direct methods to cleave the C3–C4 bond through the formation of a ketyl radical using dissolving metal reducing conditions or treatment with SmI_2,[17] which led only to reduction of the ketone group or decomposition, respectively. We then sought to form a cation or radical at C-7 of **7-17**. Reduction of the less-hindered C-7 carbonyl group using 1 equivalent of DIBAL at –78 °C yielded the corresponding alcohol in 58% as a single diastereomer. We investigated ionization of this alcohol to give the corresponding carbocation by treatment with various Lewis acids, strong Bronsted acids, as well as solvolysis after treatment with varying activating reagents (Tf_2O, MsCl, etc.) to no avail. We then explored methods for radical formation at C-7. Direct halogenation of the C-7 hydroxy group was unsuccessful and so a two-step iodination protocol was pursued. First, the C-7 alcohol was converted to the mesylate. The choice of pyridine as a solvent and conducting this reaction at 50 °C were crucial to achieving full conversion. Reaction with sodium iodide at 120 °C at that stage resulted in keto-iodide **7-21** in 43% yield over 3 steps as a single diastereomer. Radical dehalogenation reactions (AIBN, Bu_3SnH, TTMSS, photoredox, etc.) of **7-21** gave nonselective mixtures of C–C bond cleavage and dehalogenation products. Notably, dehalogenation indicated that the putative C-7 radical was persistent enough to participate in a bimolecular H-atom abstraction, whereas the resulting C–C bond cleavage was unselective. We then sought to gain selectivity in the C–C bond cleavage of **7-21** through metal-mediated processes. Remarkably, conditions adapted from the pioneering work of Gevorgyan and coworkers for palladium (I)-mediated visible-light catalysis[18] resulted in selective cleavage of the C5–C6 bond to give diene **7-24**. These oxidative additions are proposed to proceed through radical intermediates (**7-22**) and subsequent capture by Pd(I) (see **7-23**). Sequential β-carbon and β-hydride eliminations of **7-23** would then afford **7-24**. Notably, prior

studies have shown that cyclopropenyl iodides undergo radical ring opening under these Pd(I) conditions, which contrasts with our system where the product distribution is different than the free-radical reaction. The conversion of **7-21** to **7-24** is a notable example of the complementary reactivity of metal-radical hybrids which can undergo reactivity distinct from their free radical counterparts.[19] Notably, conversion of **7-21**→ **7-24** does not proceed in the absence of blue LED irradiation, nor in the absence of the Pd catalyst. Diene **7-24** decomposes upon prolonged exposure to blue LED and at elevated temperatures (>35 °C) potentially due to di-pi methane type rearrangements of the skipped diene. Despite these complications, [3.2.1] bicycle **7-24** could be isolated in 26% yield over 4 steps from **7-17**.

We have also explored fragmentations stemming from the southern portion of tricycle **7-17** (Scheme 7-2B). Toward this goal, tricycle **7-17** was reduced with two equivalents of DIBAL at –78 °C to give diol **7-25** (confirmed unambiguously by x-ray crystallographic analysis). Protection of the less-hindered northern hydroxy group proceeded selectively to give silyl ether **7-26** in 75% yield. Notably, stronger silylating agents such as TBSOTf gave appreciable amounts of the bis-silylated product. Using mono-protected diol**26**, we explored the selective formation of an alkoxy radical from the C2 alcohol group, which could undergo beta-scission to yield desired [3.2.0] bicycle **7-28**. Initial screening showed that the Suarez reaction[20] gave trace amounts of the beta-scission product. We then sought to apply conditions for proton coupled electron transfer (PCET)[21] adapted from protocols by Knowles and coworkers. Use of an iridium photocatalyst and phosphonate base presumably effected the selective activation of the O–H bond to form the corresponding alkoxy radical (**7-27**) which underwent the desired cleavage to generate the tertiary alkyl radical followed by trapping with TRIP-thiol to give the desired [3.2.0] bicyclic aldehyde. The resulting aldehyde group was found to be unstable during isolation and so one-pot reduction with $NaBH_4$ was undertaken. The overall sequence gave **7-28** in 53% yield from **7-26**.

Finally, we investigated paired reactivity for C–C cleavage on the southern portion of **7-17**. It was hypothesized that cyclobutyl carbinyl rearrangement of a carbocation or radical at C-2 would selectively cleave the more strained C-3–C-4 bond to form the most stable carbocation or radical. Unfortunately, all the methods for the generation of a radical at C-2 (via the xanthate, halide, etc.) led mostly to decomposition, along with trace cleavage of the undesired C3–C6 bond. We also prepared pivalate **7-29** in anticipation of ionization of the C-2 hydroxy group under strong acid; the TBS ether of **7-26** hydrolyzed under these reactions. Several Lewis and Bronsted acids that were tested (e.g., $AlCl_3$, HCl, pTSOH, H_2SO_4) did not result in any discernible conversion. We observed full conversion of **7-29** to amide **31** upon subjection to H_2SO_4 in MeCN at elevated temperatures. Presumably, in this case, a Ritter reaction results from desired carbocation **30**, which remains resistant to the desired fragmentation.[22] Fragmentation of **7-17** to afford norbornene derivatives such as **7-32** remain the subject of ongoing studies.

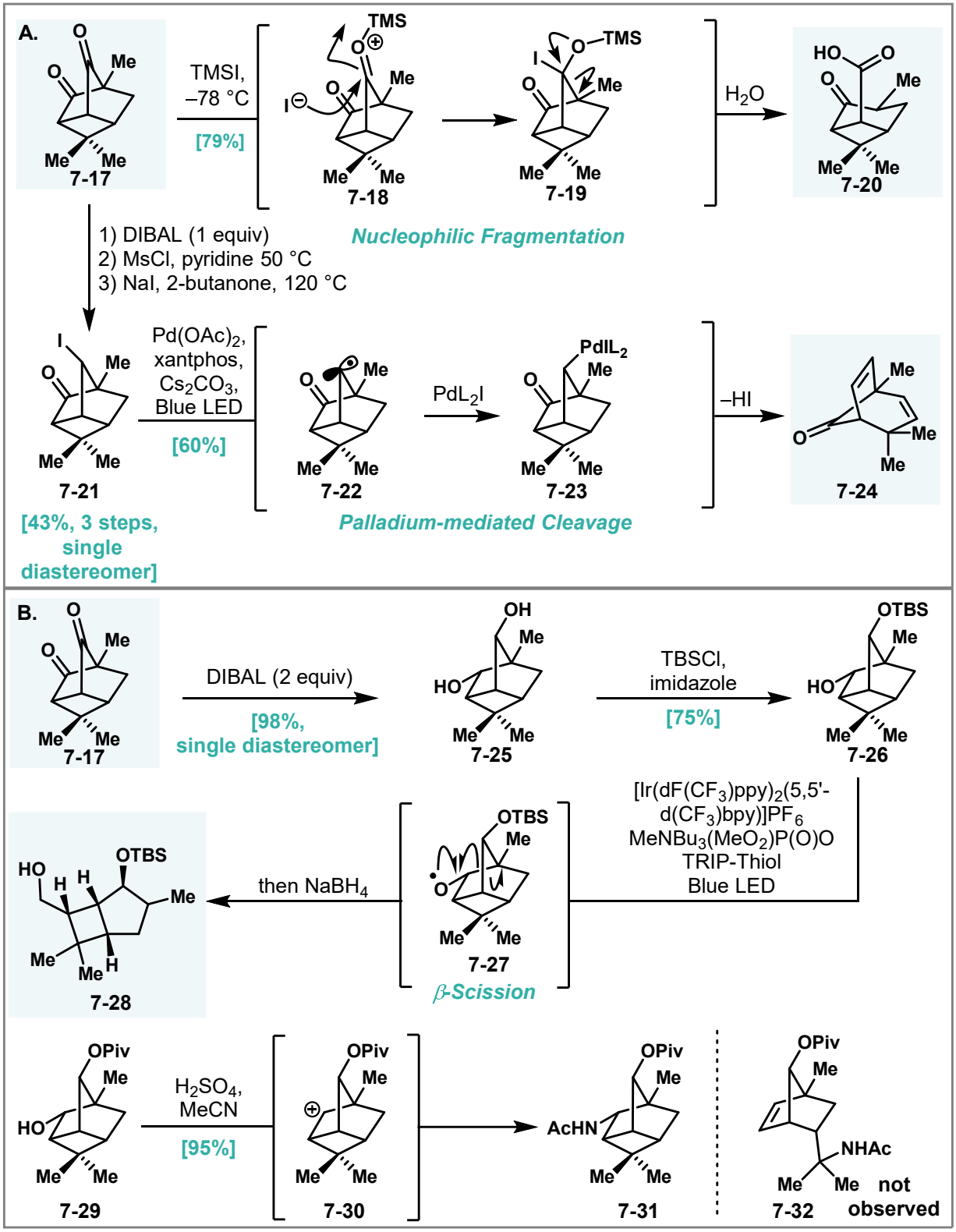

Scheme 7.2 A. Synthesis of the embedded [3.1.1] and [3.2.1] bicycles through divergent skeletal fragmentation. **B.** Synthesis of the [3.2.0] bicycle and attempt at the [2.2.1] bicycle

Finally, we have also explored the formation of other cycloadducts (Scheme 7-3). bromo-enedione **7-33** (a side product of the oxidation of **7-15** to **7-16** at higher temperature) underwent [2+2] cycloaddition under the same conditions in excellent yield to give a 1.3:1 mixture of constitutional isomers **7-34** and **7-35**. Monosubstitution was also tolerated as allyl enedione **7-36** underwent cycloaddition to give tricycle **7-37**. A 1,1-disubstituted alkene to investigate diastereoselectivity. Styrenyl enedione **7-38** underwent cycloaddition to give adduct **7-39** as a single diastereomer. Relating directly to Chapter 6, bisprenyl enedione **7-40** also underwent [2+2] cycloaddition to give tricycle **7-41**, albeit at low temperature since the cycloadduct decomposed under blue LED exposure at room temperature. [2+2]-Cycloadduct **7-41** possesses the carbocyclic core of melicolone A (**7-42**) discussed in Chapter 6.

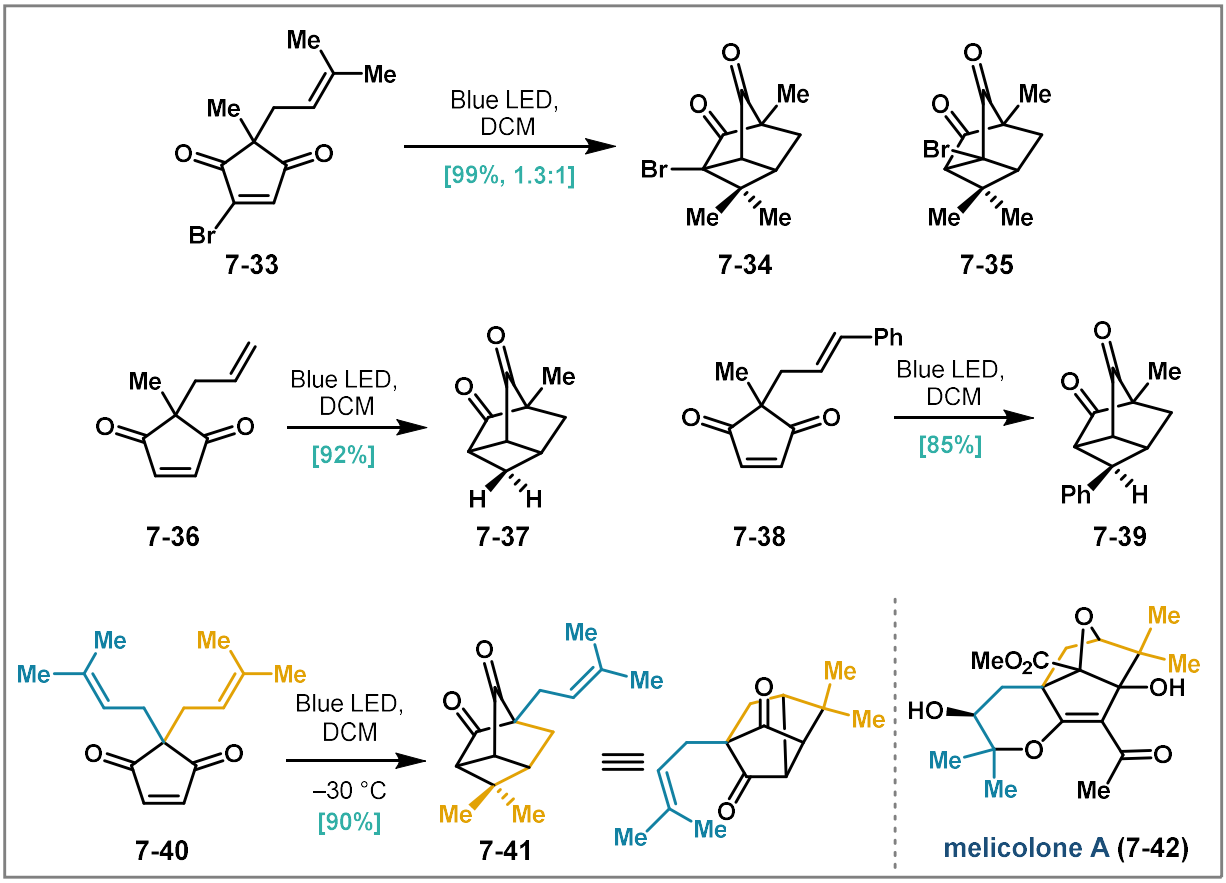

Scheme 7.3 Alternative [2+2] cycloaddition substrates. Reaction tolerates substitution on the enone as well as differing substitution on the double bond showing high diastereoselectivity.

7.3 Conclusion and outlook

In summary, we have achieved a blue-light mediated photocycloaddition of enediones to yield functionalized [3.2.1.0^{3,6}] tricyclooctanes. Recognizing that four distinct bicycles prevalent in natural products are embedded within this tricyclic framework, we have undertaken

fragmentation reactions to access these bicycles. A readily accessible tricyclooctane (**7-17**) was deconstructed into several of these bicycles, providing divergent and selective access to each of the target bicycles. Some key reactions that led to selective C–C bond cleavage include visible-light palladium catalysis and PCET for the mild generation of radical intermediates. The studies reported here lay the groundwork for future studies in natural product synthesis wherein this privileged tricycle may be leveraged to achieve rapid diversification to access different carbon skeletons. A strategic framework for divergent C–C cleavage that relies on the recognition of pairwise charge relationships that form the basis of this work should aid the application of these reactions in synthesis planning.

7.4 Experimental

General Considerations

Unless otherwise noted, all reactions were performed in flame or oven-dried glassware fitted with rubber septa under a positive pressure of nitrogen using standard Schlenk techniques. Air- and moisture-sensitive liquids were transferred via syringe or stainless steel cannula through rubber septa. Solids were added under inert gas or were dissolved in appropriate solvents. Low temperature-reactions were carried out in a Dewar vessel filled with a cooling agent: acetone/dry ice (−78 °C), H_2O/ice (0 °C). Reaction temperatures above 23 °C were conducted in an oil bath or in a heated metal block (reactions conducted in vials). The reactions were magnetically stirred and monitored by NMR spectroscopy or analytical thin-layer chromatography (TLC), using glass plates precoated with silica gel (Silicycle Siliaplates, glass backed, extra hard layer, 60 Å, 250 µm thickness, F254 indicator). TLC plates were visualized by exposure to ultraviolet light (254 nm), were stained by submersion in aqueous potassium permanganate solution (KMnO4), p-anisaldehyde, or ceric ammonium molybdate solution (CAM), and were developed by heating with a heat gun. Flash-column chromatography on silica gel was performed as described by Still et al.,1 employing silica gel (Silicycle silica gel, 40–63 µm particle size). Organic solutions were concentrated under reduced pressure on a temperature-controlled rotary evaporator equipped with a dry ice/isopropanol condenser. The yields refer to chromatographically and spectroscopically (^{1}H and ^{13}C NMR) pure material.

Materials

Unless noted below, commercial reagents were purchased from Sigma Aldrich, Acros Organics, ChemImpex, Oakwood Chemical, Combi-blocks, TCI, and/or Alfa Aesar, and used without additional purification. Solvents were purchased from Fisher Scientific, Acros Organics, Alfa Aesar, and Sigma Aldrich. Tetrahydrofuran (THF), diethyl ether (Et_2O), acetonitrile (CH_3CN), benzene, toluene (PhMe), methanol (MeOH), and triethylamine (Et_3N) were sparged with argon and dried by passing through alumina columns using argon in a Glass Contour solvent purification system. Dichloromethane (CH_2Cl_2, DCM) was freshly distilled over calcium hydride under a N_2 atmosphere prior to each use.

NMR spectroscopy

NMR spectral data were obtained using deuterated solvents, obtained from Cambridge Isotope Laboratories, Inc. ^{1}H NMR and ^{13}C NMR data were recorded on Bruker AVB-400, AVQ-400, AV-500, NEO-500, AV-600 or AV-700 spectrometers operating at 400 MHz, 400 MHz, 500 MHz, 500 MHz, 600 MHz, 700 MHz for proton nuclei (100 MHz, 100 MHz, 125 MHz, 125 MHz, 150 MHz, 175 MHz for carbon nuclei), respectively. Proton chemical shifts are expressed in parts per million (ppm, δ scale) and are referenced to residual protium in the NMR solvent ($CHCl_3$: δ 7.26). Carbon chemical shifts are expressed in parts per million (δ scale, assigned carbon atom) and are referenced to the carbon resonance of the NMR solvent ($CDCl_3$: δ 77.16). ^{1}H NMR spectroscopic

data are reported as follows: Chemical shift in ppm (multiplicity, coupling constants J (Hz), integration) (e.g. "5.21 (t, 3 J = 7.3 Hz, ^{1}H)"). The multiplicities are abbreviated with s (singlet), br s (broad singlet), d (doublet), t (triplet), q (quartet), p (pentet), se (sextet), h (heptet), m (multiplet) and app (apparent multiplicity). In case of combined multiplicities, the multiplicity with the larger coupling constant is stated first. Except for multiplets, the chemical shift of all signals, as well for centrosymmetric multiplets, is reported as the center of the resonance range. Data for ^{13}C spectroscopy are reported in terms of chemical shift (δ ppm). Additionally to 1D NMR experiments, 2D NMR techniques such as homonuclear correlation spectroscopy (COSY), heteronuclear single quantum coherence (HSQC), heteronuclear multiple bond coherence (HMBC) and nuclear Overhauser enhancement spectroscopy (NOESY) were used to assist structure elucidation. All raw FID files were processed and the spectra analyzed using the program MestReNOVA 11.0 from Mestrelab Research S. L.

Note: The AVB-400, AVQ-400, AV-500, DRX-500 and AV-600 instruments were partially supported by NIH grants SRR023679A, RR02424A-01, S10RR03353-01 and 1S10RR016634-01, and NSF grants CHE-9633007, CHE-8208992, CHE-0130862, and CHE-8703048. The AV-700 instrument was supported by the Berkeley College of Chemistry NMR facility.

Mass spectrometry

Mass spectral data were obtained from the Mass Spectral Facility at the University of California, Berkeley, on a Finnigan/Thermo LTQ-FT instrument (ESI). Data acquisition and processing were performed using the XcaliburTM software.

IR spectroscopy

IR spectroscopic data were recorded on a Bruker ALPHA FT-IR spectrophotometer using a diamond attenuated total reflectance (ATR) accessory. If required, substances were dissolved in dichloromethane prior to direct application on the ATR unit. Data are represented as follows: frequency of absorption (cm^{-1}), and intensity of absorption (s = strong, m = medium, w = weak, br = broad).

X-ray analysis

Single-crystal X-ray diffraction experiments were performed at the UC Berkeley CHEXRAY crystallographic facility. Measurements of all compounds were performed on a Rigaku XtaLAB P200 rotating anode equipped with a Pilatus 200K hybrid pixel array detector. Data were collected using Cu Kα radiation (λ = 1.54184 Å). Crystals were kept at 100(2) K throughout collection. Data collection was performed with CrysAlisPro. 2 Data processing was done using CrysAlisPro and included either a multi-scan absorption or faceindexed absorption correction applied using the SCALE3 ABSPACK scaling algorithm within CrysAlisPro. All structures were solved with SHELXT.3 Structures were refined with SHELXL.4 All non-hydrogen atoms were refined anisotropically, and hydrogen atoms were either included at the geometrically calculated positions and refined using a riding model or located as Q peaks in the Fourier difference map.

Note: The instruments are supported by an NIH Shared Instrumentation Grant S10-RR027172.

UV-Vis spectroscopy

UV-Vis spectroscopy was performed on a Varian 5000 UV-Vis-NIR spectrometer using quartz cuvettes with a path length of 1 cm. Data were collected using DCM as a solvent with an absorbance window between 230 and 650 nm.

Experimental Details

Synthesis of prenylated 2-methylcyclopentane-1,3-dione S7-1

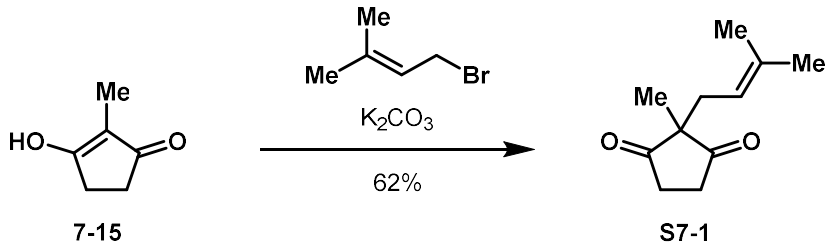

7-15 **S7-1**

A flame-dried flask was charged with 2-methylcyclopentane-1,3-dione (**7-15**, 5.0 g, 45 mmol, 1 equvi) followed by acetone (200 mL). To this orange stirring suspension was added potassium carbonate (9.2 g, 67 mmol, 1.5 equiv) as a single portion followed by the stream-wise addition of 1-bromo-3methylbut-2-ene (10 mL, 89 mmol, 2 equiv). The cloudy light-brown reaction mixture was stirred under an atmosphere of nitrogen for 24 h. The reaction mixture was then concentrated *in vacuo*, resuspended in ether, and mixed with a solution of sat. aq. NaCl. The aqueous layer was extracted two times with ether. Combined organic fractions were dried over Na_2SO_4 and concentrated *in vacuo*. The crude reaction mixture was purified by silica gel flash chromatography (gradient 5:1 pentane: diethyl ether to 1:1 pentane: diethyl ether) to yield **S7-1** as a pale yellow oil (5.1 g, 62%).

R_f = 0.55 (hexane:EtOAc = 10:1), UV-active, blue spot (*p*-anisaldehyde)

^{1}H NMR (500 MHz, CDCl3) δ 4.91 (tt, *J* = 7.8, 1.6 Hz, 1H), 2.75 – 2.61 (m, 4H), 2.31 (d, *J* = 7.9 Hz, 2H), 1.64 (s, 3H), 1.55 (s, 3H), 1.08 (s, 3H) ppm.

^{13}C NMR (126 MHz, $CDCl_3$) δ 217.1, 136.8, 117.2, 57.1, 35.7, 35.5, 26.0, 18.5, 17.9 ppm.
Spectral data were consistent with those found in the literature.[23]

Synthesis of enedione 7-16

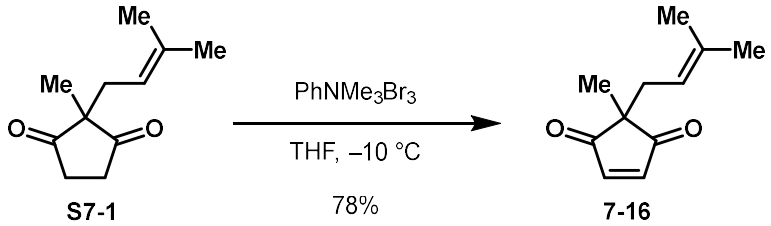

A solution of **S7-1** (3.0 g, 17 mmol, 1 equiv) in THF (170 mL) was cooled to –10 °C. To this cooled solution was added phenyltrimethylammonium tribromide (6.3 g, 17 mmol, 1 equiv) in four portions after which the solution turned bright and cloudy yellow orange. Portions were added in 30 minute intervals. Completion of the reaction was judged by TLC, usually three hours. Upon completion the reaction miture was diluted with diethyl ether and quenched with sat. aq. $NaHCO_3$ and sat. aq. $Na_2S_2O_3$ (4:1). The layers were separated and the aqueous layer was extracted two times with diethyl ether. The combined organic layers were dried over Na_2SO_4, filtered, and concentrated *in vacuo*. The crude reaction mixture was purified by silica gel flash chromatography (gradient 5:1 pentane: diethyl ether to 1:1 pentane: diethyl ether) to yield **7-16** as a bright yellow oil (2.3 g, 78%).

At temperatures above 0 °C bromo-enedione **7-33** was isolated in 15% yield (0.44 g) as a yellow solid. Lowering the temperature completely suppressed formation of this product (see below for analytical data).

R_f = 0.55 (hexane:EtOAc = 10:1), UV-active, blue-green spot (*p*-anisaldehyde)

^{1}H NMR (500 MHz, CDCl3) δ 7.21 (s, 2H), 4.83 – 4.75 (m, 1H), 2.36 (d, *J* = 7.8 Hz, 2H), 1.58 (s, 3H), 1.54 (s, 3H) 1.13 (s, 3H) ppm.

^{13}C NMR (126 MHz, CDCl3) δ 208.0, 148.6, 136.4, 117.5, 51.0, 33.5, 25.9, 18.7, 17.7 ppm.

Spectral data was consistent with those found in the literature.[24]

Preparative-scale Synthesis of [3.2.1.0^{3,6}] tricyclooctane 7-17

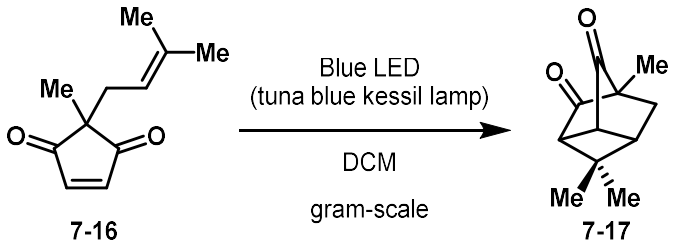

7-16 7-17

Enedione **7-16** (1.0 g, 5.6 mmol) was dissolved in DCM (100 mL) under air in a round-bottomed flask. The resulting pale-yellow solution was then moved to a photoreactor containing two tuna blue Kessil lamps (see below). The pale-yellow reaction mixture was irradiated at maximum intensity under a constant stream of air to maintain room temperature. After complete consumption of the starting material (monitored by NMR), the now clear reaction mixture was concentrated *in vacuo* to yield title compound **7-17**.

Note: reaction time was heavily dependent on reaction scale. Reaction time was optimized for a given scale through careful monitoring of the reactions progress by NMR. Prolonged exposure increased the presence of baseline impurities and decreased yield of desired tricycle.

Slight impurities could be washed away through washing with heptanes and filtration (the impurities are not soluble in heptanes) yielding pure **7-17** as a pale-yellow amorphous solid. The resulting tricycle was not stable to silica gel chromatography but was of sufficient purity to be used directly in the subsequent reactions without purification.

Optimization scale: Reaction at 0.1 mmol was performed in Penn1A-photreactor (see below) Irradiation at 420 nm for 10 h led to complete conversion at this scale and set-up. Reaction efficiency was confirmed by NMR yield (95%, average of 3 trials).

R$_f$ = 0.4 (hexane:EtOAc = 10:1), green streak (*p*-anisaldehyde)

^{1}H NMR (500 MHz, CDCl3) δ 3.25 (t, *J* = 4.4 Hz, 1H), 3.00 (t, *J* = 4.8 Hz, 1H), 2.61 (dd, *J* = 5.2, 4.7 Hz, 1H), 2.23 – 2.15 (m, 2H), 1.47 (s, 3H), 1.13 (s, 3H), 0.98 (s, 3H) ppm.

^{13}C NMR (151 MHz, CDCl3) δ 208.8, 207.1, 61.4, 59.4, 46.7, 45.6, 41.5, 35.2, 28.6, 21.9, 7.0 ppm.

IR (neat): ν = 2970, 2880, 1737, 1726, 1453, 1367, 1229, 1217, 1145, 118, 1099, and 527.

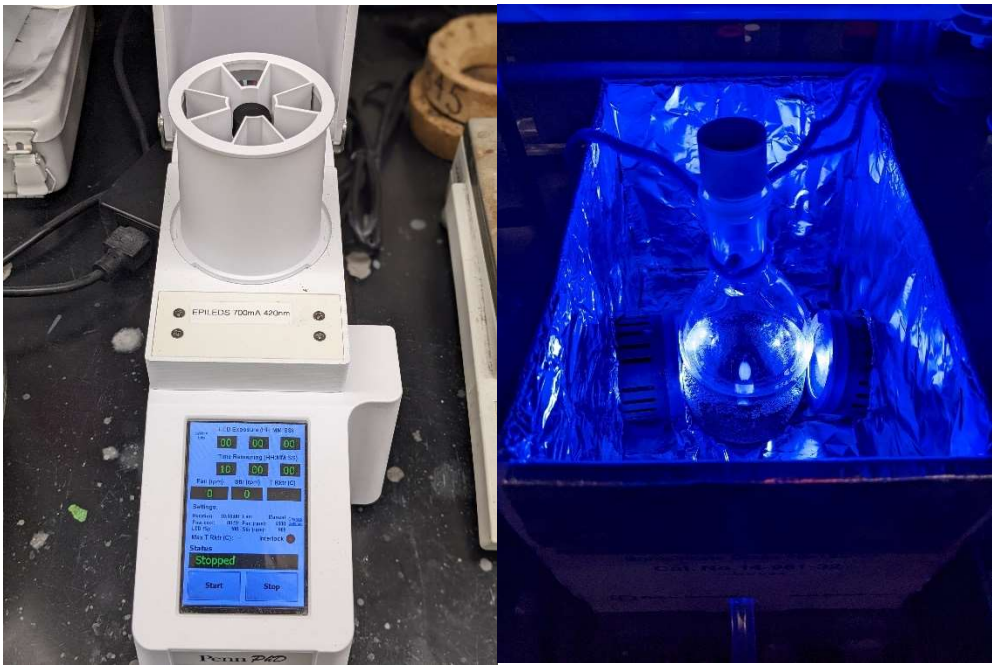

Left: Standard Penn photoreactor setup for optimization scale. Fan 68000 rpm, Stir 909 rpm, LED% 100. Right: preparative-scale reaction full intensity irradiation with two tuna blue Kessil lamps and constant stream of air

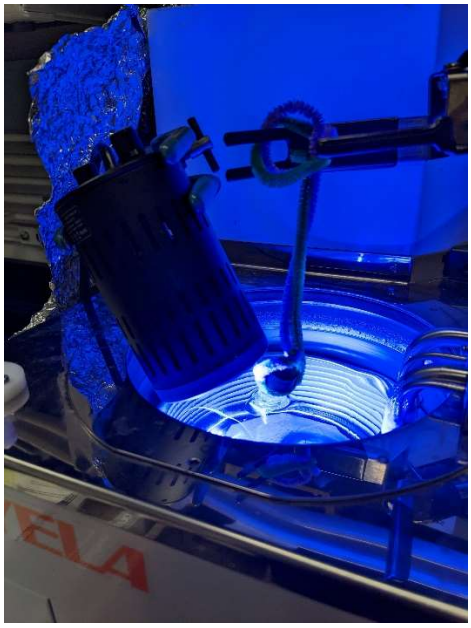

Low temperature LED setup. Cooling bath set to –30 °C and irradiated at full intensity with tuna blue Kessil lamp

Synthesis of bicyclo [3.1.1]heptane 7-20

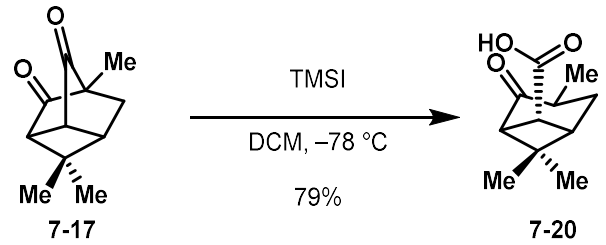

7-17 7-20

A solution of tricycle **7-17** (50 mg, 0.28 mmol, 1 equiv) in DCM (2.8 mL) was cooled to –78 °C. TMSI (40 µL, 0.28 mmol, 1 equiv) was added to the cooled solution. The orange reaction mixture was stirred for 1 h and then quenched by the addition of sat. aq. NaCl and diluted with EtOAc. The layers were separated and the aqueous layer was extracted two times with EtOAc. The combined organic layers were dried over Na_2SO_4, filtered, and concentrated *in vacuo*. The crude residue was purified by silica gel flash chromatography (hexanes: EtOAc 1:2) to afford **7-20** as an orange oil (43 mg, 0.22 mmol, 79%).

R_f = 0.4 (hexane:EtOAc = 1:1), yellow streak (*p*-anisaldehyde)

^{1}H NMR (500 MHz, CDCl3) δ 3.58 (t, *J* = 5.8 Hz, 1H), 2.92 (t, *J* = 5.2 Hz, 1H), 2.64 – 2.51 (m, 2H), 2.34 (dt, *J* = 10.0, 6.9 Hz, 1H), 1.59 – 1.45 (m, 1H), 1.34 (s, 3H), 1.16 (d, *J* = 6.8 Hz, 3H), 0.77 (s, 3H) ppm.

^{13}C NMR (126 MHz, $CDCl_3$) δ 214.6, 179.1, 60.4, 45.1, 40.5, 39.3, 37.8, 28.8, 26.1, 21.3, 14.9 ppm.

IR (neat): ν = 3454, 2962, 2937, 2877, 1711, 1455,1378, 1253, 1230, 1216, 1146, 1119, 1099, 1056, 1013, 987, 953, 913, 864, 841, and 723.

HRMS (ESI, *m/z*): for $[M–H]^-$ calcd. for $C_{11}H_{15}O_3$ 195.1027; found 195.1027.

Synthesis of ketoalcohol S7-2

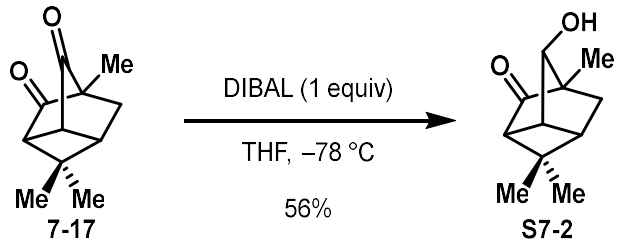

A flame-dried flask was charged with tricycle **7-17** (400 mg, 2.24 mmol, 1 equiv) and THF (22 mL). The clear solution was cooled to –78 °C. DIBAL (2.24 mL, 1M in hexanes, 1 equiv) was added dropwise to the cooled solution. The reaction mixture was stirred for 1 h then quenched by the addition of sat. aq. NaCl and diluted with EtOAc. The layers were separated and the aqueous layer was extracted two times with EtOAc. The combined organic layers were dried over Na_2SO_4, filtered, and concentrated *in vacuo*. The crude compound was purified by silica gel flash chromatography (hexanes: EtOAc 1:1) to afford **S7-2** as a white solid (230 mg, 1.3 mmol, 56%).

The further reduced diol **7-25** was also isolated in ca. 20% yield, however, a more selective synthesis was later developed using 2 equiv of DIBAL (vide infra). Starting material was also observed and recovered in ca. 10% yield.

R_f = 0.25 (hexane:EtOAc = 4:1), purple spot (*p*-anisaldehyde)

^{1}H NMR (400 MHz, $CDCl_3$) δ 3.57 (d, *J* = 1.9 Hz, 1H), 3.12 (td, *J* = 4.4, 1.9 Hz, 1H), 2.37 (m, 2H), 2.18 (dd, *J* = 12.5, 6.6 Hz, 1H), 1.57 (d, *J* = 12.5 Hz, 1H), 1.29 (s, 3H), 1.08 (s, 3H), 0.75 (s, 3H) ppm.

^{13}C NMR (101 MHz, $CDCl_3$) δ 215.6, 77.7, 57.9, 56.5, 44.4, 43.4, 43.2, 32.6, 28.4, 20.9, 10.1 ppm.

IR (neat): ν = 3418, 2958, 2870, 1720, 1454, 1277, 1124, 1094, 1061, 877, and 564.

HRMS (ESI, *m/z*): for $[M+H]^+$ calcd. for $C_{11}H_{17}O_2$ 181.1223; found 181.1223.

M.p. = 68 °C

Synthesis of mesylate S7-3

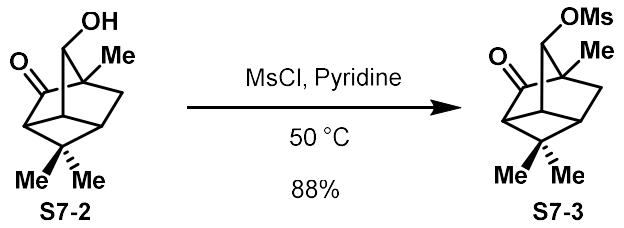

A flame-dried vial was charged with ketoalcohol **S7-2** (160 mg, 0.89 mmol, 1 equiv) and pyridine (1.79 mL, 22.2 mmol, 25 equiv). Mesityl chloride (0.14 mL, 1.8 mmol, 2 equiv) was added to the resulting solution. The vial was moved to a pre-heated vial block at 50 °C. After three hours stirring at this temperature the reaction mixture was cooled back to room temperature then quenched by the addition of sat. aq. NH_4Cl and diluted with EtOAc. The layers were separated and the aqueous layer was extracted two times with EtOAc. The combined organic layers were dried over Na_2SO_4, filtered, and concentrated *in vacuo*. The crude residue was purified by silica gel flash chromatography (hexanes: EtOAc 2:1) to afford **S7-3** as an pale amorphous solid (200 mg, 0.78 mmol, 88%). Notably the elevated temperature and choice of pyridine as solvent was crucial for reproducibility.

R_f = 0.30 (hexane:EtOAc = 4:1), blue spot (*p*-anisaldehyde)

^{1}H NMR (400 MHz, $CDCl_3$) δ 4.42 (d, *J* = 1.9 Hz, 1H), 3.46 (td, *J* = 4.4, 1.9 Hz, 1H), 3.04 (s, 3H), 2.56 – 2.46 (m, 2H), 2.20 (dd, *J* = 13.0, 6.3 Hz, 1H), 1.72 (d, *J* = 12.9 Hz, 1H), 1.33 (s, 3H), 1.18 (s, 3H), 0.80 (s, 3H) ppm.

^{13}C NMR (101 MHz, $CDCl_3$) δ 210.8, 85.0, 57.2, 57.1, 43.8, 43.3, 38.7, 33.5, 28.2, 20.8, 10.1 ppm.

IR (neat): ν = 3022, 2958, 2872, 1742, 1457, 1354, 1174, 1064, 959, 884, 856, 812, 770, 693, 595, 561, 520, and 491.

HRMS (ESI, *m/z*): for $[M+Na]^+$ calcd. for $C_{12}H_{18}NaO_4S_1$ 281.0818; found 281.0818.

Synthesis of iodide 7-21

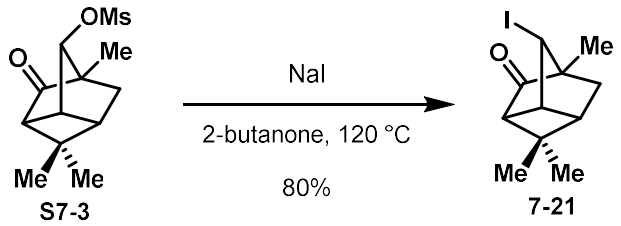

A flame-dried vial was charged with ketomesylate **S7-3** (50 mg, 0.19 mmol, 1 equiv) and 2-butanone (2 mL). Sodium iodide (87 mg, 0.58 mmol, 3 equiv) was added to the solution resulting in a slightly orange heterogeneous reaction mixture. The vial was sealed and moved to a preheated vial block at 120 °C. After 14 hours at this temperature the reaction mixture was cooled back to room temperature then quenched by the addition of sat. aq. $NaHCO_3$ and sat. aq. $Na_2S_2O_3$ (4:1) and diluted with EtOAc. The layers were separated and the aqueous layer was extracted two times with EtOAc. The combined organic layers were dried over Na_2SO_4, filtered, and concentrated *in vacuo*. The crude residue was purified by silica gel flash chromatography (hexanes: EtOAc 4:1) to afford **7-21** as a pale orange solid (45 mg, 0.15 mmol, 80%).

R_f = 0.75 (hexane:EtOAc = 4:1), UV-active, purple spot (*p*-anisaldehyde)

^{1}H NMR (500 MHz, $CDCl_3$) δ 3.98 (d, *J* = 2.3 Hz, 1H), 3.42 (td, *J* = 4.3, 2.3 Hz, 1H), 2.45 (t, *J* = 4.6 Hz, 1H), 2.30 (q, *J* = 4.6 Hz, 1H), 1.78 – 1.72 (m, 2H), 1.31 (s, 3H), 1.16 (s, 3H), 0.80 (s, 3H) ppm.

^{13}C NMR (126 MHz, $CDCl_3$) δ 213.2, 58.2, 55.9, 46.8, 43.3, 41.2, 40.2, 35.2, 28.1, 19.6, 13.4 ppm.

IR (neat): ν = 2958, 2927, 2868, 1746, 1461, 1381, 1296, 1278, 1252, 1203, 1149, 1074, 1054, 1019, 905, 856, 836, 735, and 703.

M.p = 40 °C

Synthesis of bicyclo[3.2.1]octane 7-24

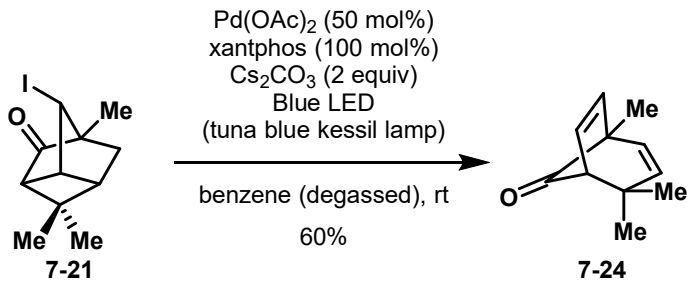

7-21 **7-24**

Ketoiodide **7-21** (8 mg, 0.028 mmol, 1 equiv), $Pd(OAc)_2$ (3.1 mg, 0.014 mmol, 0.5 equiv), and xantphos (16 mg, 0.028 mmol, 1 equiv) were added to a flame-dried vial. The reaction vessel was moved into the glove box, after which Cs_2CO_3 (18 mg, 0.055 mmol, 2 equiv) and degassed benzene (0.11 mL, free-pump-thaw) were added. The vial was sealed and removed from the glove box then moved to a photoreactor containing two tuna blue Kessil lamps (see above). The light orange reaction mixture was irradiated at maximum intensity under a constant stream of air to maintain room temperature. The reaction mixture immediately starts to darken in color becoming brown-black after about thirty minutes. After 3 hours the crude reaction mixture was removed from the photoreactor and loaded directly onto a pipette silica gel column and purified (pentane:ether 10:1) to afford **7-24** (3 mg, 0.017 mmol, 60% adjusted for BHT impurity (from Et_2O stablilizer) in NMR) as a clear oil.

Note: 7-24 is sensitive to temperature and prolonged LED exposure. Concentration on the rotovap at elevated temperatures (>35 °C) led to complete decomposition.

$\mathbf{R_f}$ = 0.77 (hexane:EtOAc = 4:1), UV-active, purple spot (*p*-anisaldehyde)

^{1}H NMR (500 MHz, C_6D_6) δ 6.17 (d, *J* = 6.8 Hz, 1H), 5.75 (dd, *J* = 6.8, 3.2 Hz, 1H), 5.43 (d, *J* = 9.4 Hz, 1H), 4.90 (dd, *J* = 9.4, 1.9 Hz, 1H), 2.44 (dd, *J* = 3.4, 1.9 Hz, 1H), 1.07 (s, 3H), 1.04 (s, 3H), 0.72 (s, 3H) ppm.

^{13}C NMR (151 MHz, C_6D_6) δ 210.2, 145.5, 137.2, 135.4, 129.4, 59.4, 47.8, 41.4, 27.3, 24.7, 14.2 ppm.

IR (neat): ν = 2901, 1824, 1777, 1324, 1244, 1151, 859, 726, and 588.

Synthesis of diol 7-25

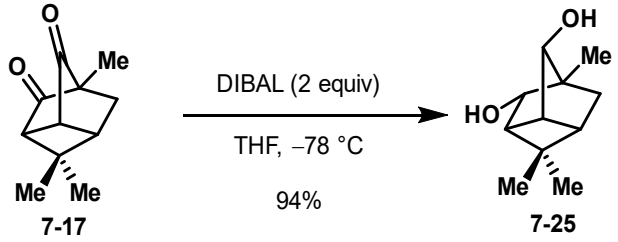

A flame-dried flask was charged with tricycle **7-17** (500 mg, 2.81 mmol, 1 equiv) and THF (44 mL). The clear solution was cooled to –78 °C. DIBAL (5.62 mL, 1M in hexanes, 2 equiv) was added dropwise to the cooled solution. The reaction mixture was stirred for 1 h then quenched by the addition of sat. aq. NaCl and diluted with EtOAc. The layers were separated and the aqueous layer was extracted two times with EtOAc. The combined organic layers were dried over Na_2SO_4, filtered, and concentrated *in vacuo*. The crude compound was purified by silica gel flash chromatography (hexanes: EtOAc 1:1) to afford **7-25** as a white solid (480 mg, 2.6 mmol, 94%).

Suitable crystals for x-ray analysis could be grown through slow diffusion from a pentane EtOAc solution.

R_f = 0.55 (hexane:EtOAc = 1:1), blue spot (*p*-anisaldehyde)

^{1}H NMR (400 MHz, $CDCl_3$) δ 3.76 (dd, *J* = 6.9, 2.2 Hz, 1H), 3.48 (d, *J* = 1.9 Hz, 1H), 2.81 (td, *J* = 4.4, 1.9 Hz, 1H), 2.14 (ddd, *J* = 11.4, 6.9, 4.4 Hz, 2H), 1.98 (d, *J* = 12.8 Hz, 1H), 1.71 – 1.64 (m, 1H), 1.14 (s, 3H), 1.13 (s, 3H) 1.04 (s, 3H) ppm.

^{13}C NMR (101 MHz, $CDCl_3$) δ 79.5, 78.3, 49.6, 47.0, 45.8, 43.9, 39.0, 30.2, 30.1, 22.7, 14.3 ppm.

IR (neat): ν = 3370, 2995, 2946, 2924, 2867, 1461, 1366, 1281, 1217, 1108, 1095, 179, 1032, and 666.

HRMS (ESI, *m/z*): for $[M+H]^+$ calcd. for $C_{12}H_{17}O_2$ 181.1234; found 181.1235.

M.p. = 89 °C

X-ray structure:

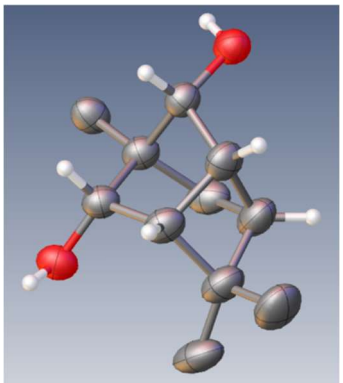

Synthesis of silyl ether 7-26

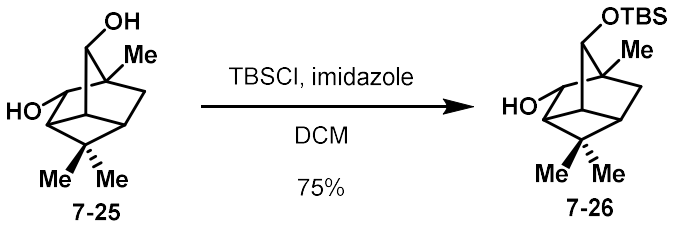

A flame-dried flask was charged with diol **7-25** (60 mg, 0.329 mmol, 1 equiv), DCM (3.3 mL) and imidazole (67 mg, 0.99 mmol, 3 equiv). To the stirring suspension was added TBSCl (60 mg, 0.40 mmol, 1.2 equiv) upon which a white precipitate formed. The reaction mixture was stirred for 14 h at room temperature then quenched by the addition of sat. aq. NaCl and diluted with EtOAc. The layers were separated and the aqueous layer was extracted two times with EtOAc. The combined organic layers were dried over Na_2SO_4, filtered, and concentrated *in vacuo*. The crude compound was purified by silica gel flash chromatography (hexanes: EtOAc 4:1) to afford **7-26** as a clear oil (73 mg, 0.25 mmol, 75%).

R_f = 0.7 (hexane:EtOAc = 4:1), UV-active, blue spot (*p*-anisaldehyde)

^{1}H NMR (500 MHz, $CDCl_3$) δ 3.74 (dd, *J* = 6.6, 2.2 Hz, 1H), 3.40 (d, *J* = 2.0 Hz, 1H), 2.67 (td, *J* = 4.4, 1.8 Hz, 1H), 2.13 – 2.04 (m, 2H), 1.86 (d, *J* = 12.2 Hz, 1H), 1.75 (ddd, *J* = 12.2, 7.3, 2.3 Hz, 1H), 1.13 (s, 3H), 1.12 (s, 3H), 0.98 (s, 3H), 0.87 (s, 9H), 0.03 (s, 3H), 0.02 (s, 3H) ppm.

^{13}C NMR (101 MHz, $CDCl_3$) δ 79.5, 78.4, 49.9, 47.7, 45.8, 44.3, 38.9, 30.6, 30.3, 25.9, 22.8, 18.2, 14.6, –4.3, –4.7 ppm.

IR (neat): ν = 3436, 2927, 2998, 2895, 2859, 1739, 1462, 1366, 1256, 1137, 1118, 1084, 1061, 867, 836, and 775.

HRMS (ESI, *m/z*): for $[M+Na]^+$ calcd. for $C_{17}H_{32}NaO_2Si$ 319.2064; found 319.2063.

Synthesis of [3.2.0] bicycloheptane 7-28

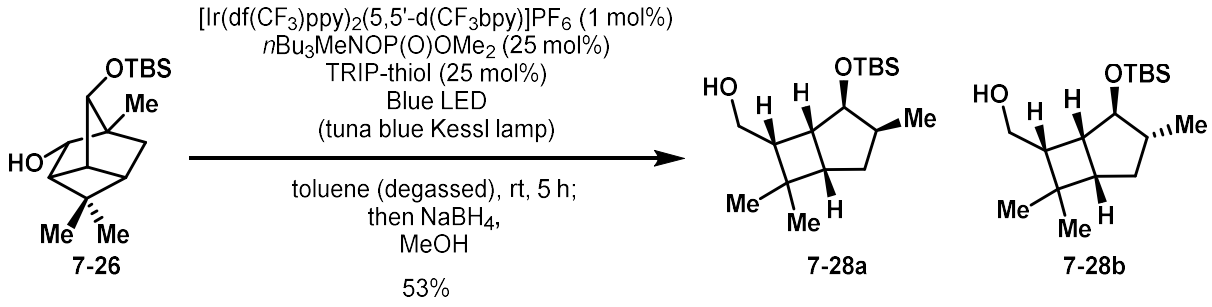

A flame-dried vial was charged with alcohol **7-26** (20 mg, 0.067 mmol, 1 equiv), $[Ir(df(CF_3)ppy)_2(5,5'\text{-}d(CF_3bpy)]PF_6$ (0.07 mg, 0.00067 mmol, 0.01 equiv), and TRIP-thiol (4.0 mg, 0.017 mmol, 0.25 equiv) then moved into a glovebox. Therein, nBu$_3$MeNOP(O)OMe$_2$ (5.5 mg, 0.017 mmol, 0.25 equiv) and degassed toluene (0.67 mL) were added. The vial was moved from the glovebox a photoreactor containing two tuna blue Kessil lamps (see above). The orange reaction mixture was irradiated at maximum intensity under a constant stream of air to maintain room temperature. After five hours the vial was removed from the photoreactor and placed under nitrogen.

To the crude reaction mixture under an atmosphere of nitrogen was added a solution of $NaBH_4$ (5.1 mg, 0.13 mmol, 2 equiv) in methanol (0.13 mL). The bubbling reaction mixture was stirred for 30 minutes after which it was quenched with sat. aq. NH_4Cl and diluted with EtOAc. The layers were separated and the aqueous layer was extracted twice with EtOAc. The combined organic layers were washed with sat. aq. NaCl, dried over Na_2SO_4, filtered, and concentrated *in vacuo*. The crude residue was purified by preparative thin layer chromatography (hexanes:EtOAc 1:1) to yield **7-28a** and **7-28b** as clear oils (11 mg, 0.036 mmol, 53% 1:1 *dr*).

Diastereomer **7-28a**

R_f = 0.65 (hexane:EtOAc = 4:1), blue spot (*p*-anisaldehyde)

^{1}H NMR (500 MHz, $CDCl_3$) δ 3.95 (d, *J* = 4.3 Hz, 1H), 3.69 – 3.58 (m, 2H), 2.63 (dd, *J* = 10.3, 8.0 Hz, 1H), 2.36 (t, *J* = 8.2 Hz, 1H), 2.25 (q, *J* = 8.8 Hz, 1H), 2.07 (dt, *J* = 12.0, 5.9 Hz, 1H), 1.64 – 1.60 (m, 1H), 1.39 (td, *J* = 12.6, 8.4 Hz, 1H), 1.16 (s, 3H), 0.97 (d, *J* = 6.5 Hz, 3H), 0.93 – 0.84 (m, 12H), 0.02 (s, 6H) ppm.

^{13}C NMR (151 MHz, $CDCl_3$) δ 76.7, 60.6, 46.2, 45.6, 44.3, 42.0, 35.4, 34.9, 33.5, 29.9, 26.0, 18.35, 18.2, 14.5, –4.6, –4.7 ppm.

HRMS (ESI, *m/z*): for $[M+Na]^+$ calcd. for $C_{17}H_{34}NaO_2Si$ 321.3220; found 321.3219.

IR (neat): ν = 3322, 2953, 2930, 2857, 1462, 1385, 1362, 1253, 1117, 1095, 1057, 1018, 864, 833, 773, and 670.

Diastereomer **7-28b**

R_f = 0.63 (hexane:EtOAc = 4:1), blue spot (*p*-anisaldehyde)

^{1}H NMR (500 MHz, $CDCl_3$) δ 3.82 – 3.74 (m, 2H), 3.71 (dt, *J* = 8.3, 4.3 Hz, 1H), 2.50 (td, *J* = 9.3, 5.0 Hz, 1H), 2.31 – 2.17 (m, 2H), 1.82 – 1.71 (m, 2H), 1.18 (s, 3H), 1.15 – 1.08 (m, 1H), 1.03 (d, *J* = 6.1 Hz, 3H), 0.90 (s, 3H), 0.87 (s, 9H), 0.06 (s, 3H), 0.04 (s, 3H) ppm.

^{13}C NMR (126 MHz, $CDCl_3$) δ 81.09, 62.84, 46.70, 45.41, 44.01, 36.00, 33.35, 33.08, 26.04, 19.58, 18.24, 17.12, –4.00, –4.16 ppm.

IR (neat) *v*: 3346, 2970, 2951, 2929, 2857, 1738, 1462, 1365, 1252, 1229, 1217, 1206, 1117, 1094, 1058, 1018, 864, 833, 800, 773, 670, 610, and 539.

HRMS (ESI, *m/z*): for $[M+Na]^+$ calcd. for $C_{17}H_{34}NaO_2Si$ 321.3220; found 321.3220.

Synthesis of Pivalate alcohol 7-29

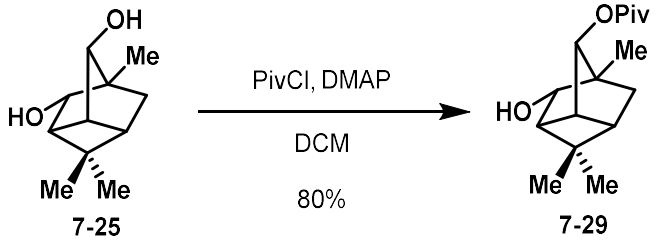

A flame-dried flask was charged with diol **7-25** (90 mg, 0.49 mmol, 1 equiv), DCM (5 mL) and DMAP (72 mg, 0.59 mmol, 1.2 equiv), followed by PivCl (60 mg, 0.4 mmol, 1 equiv). The reaction mixture was stirred until consumption of starting material was noted by TLC, about three hours. The reaction mixture was quenched by the addition of sat. aq. NH_4Cl and diluted with EtOAc. The layers were separated and the aqueous layer was extracted two times with EtOAc. The combined organic layers were washed with sat. aq. NaCl, dried over Na_2SO_4, filtered, and concentrated *in vacuo*. The crude compound was purified by silica gel flash chromatography (hexanes: EtOAc 2:1) to afford **7-29** as a yellow solid (110 mg, 0.40 mmol, 80%).

R_f = 0.50 (hexane:EtOAc = 2:1), blue spot (*p*-anisaldehyde)

^{1}H NMR (500 MHz, $CDCl_3$) δ 4.46 (d, *J* = 1.9 Hz, 1H), 3.87 (dd, *J* = 7.2, 2.2 Hz, 1H), 2.91 (td, *J* = 4.4, 1.9 Hz, 1H), 2.16 (td, *J* = 6.6, 4.8 Hz, 1H), 2.13 – 2.03 (m, 2H), 1.72 (ddd, *J* = 12.7, 7.8, 2.3 Hz, 1H), 1.17 (d, *J* = 1.3 Hz, 9H), 1.12 (s, 6H), 1.00 (s, 3H) ppm.

^{13}C NMR (126 MHz, $CDCl_3$) δ 178.5, 79.7, 78.7, 49.0, 46.0, 44.8, 43.8, 39.3, 39.1, 31.3, 30.0, 27.3, 22.7, 14.51 ppm.

IR (neat): ν = 3462, 3008, 2970, 2873, 1712, 1480, 1461, 1420, 1359, 1285, 1220, 1160, 1096, 1031, 989, 905, 962, and 529.

HRMS (ESI, *m/z*): for $[M+Na]^+$ calcd. for $C_{16}H_{26}NaO_3$ 289.1774; found 289.1174.

Synthesis of pivalate amide 7-31

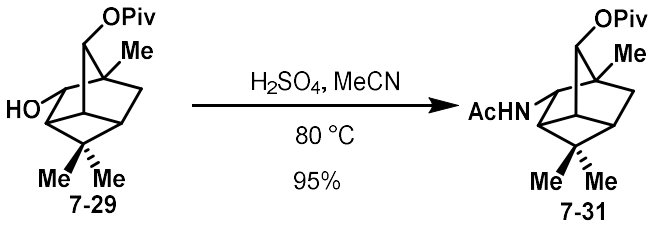

A vial was charged with pivalate **7-29** (4 mg, 0.015 mmol, 1 equiv) and acetonitrile (0.3 mL). No effort was made to exclude moisture. To the stirring yellow solution was added conc. H_2SO_4 (5 µL). The reaction mixture was moved to a preheated vial block at 80 °C. The reaction mixture stirred at this temperature until complete consumption of starting material was noted by TLC, about 30 minutes. The reaction mixture was cooled to room temperature then quenched by the addition of sat. aq. $NaHCO_3$ and diluted with EtOAc. The layers were separated and the aqueous layer was extracted three times with EtOAc. The combined organic layers were washed with sat. aq. NaCl, dried over Na_2SO_4, filtered, and concentrated *in vacuo* to give amide **7-31** (4.4 mg, 0.014 mmol, 95%) as a white amorphous solid of suitable purity.

R_f = 0.1 (hexane:EtOAc = 1:3), purple spot (*p*-anisaldehyde)

^{1}H NMR (500 MHz, MeOD) δ 4.52 (d, *J* = 1.9 Hz, 1H), 4.40 (dd, *J* = 7.2, 2.1 Hz, 1H), 2.93 (d, *J* = 2.1 Hz, 1H), 2.43 – 2.36 (m, 1H), 2.14 – 2.06 (m, 2H), 1.93 (s, 3H), 1.76 (ddd, *J* = 12.7, 7.9, 2.2 Hz, 1H), 1.16 (m, 15H), 1.05 (s, 3H) ppm.

^{13}C NMR (151 MHz, MeOD) δ 179.8, 176.4, 84.0, 80.6, 49.7, 46.1, 45.6, 45.0, 40.5, 40.0, 32.6, 30.2, 27.6, 22.8, 22.1, 14.9 ppm.

IR (neat): ν = 3452, 3010, 2960, 2930, 2871, 1730, 1670, 1480, 1462, 1289, 1217, 1166, 1030, 992, 872, 847, 668, 587.

HRMS (ESI, *m/z*): for $[M+Na]^+$ calcd. for $C_{18}H_{29}NaO_3N$ 330.2040; found 330.2039.

Synthesis of bromo tricyclo[3.2.1.0^{3,6}]octane 7-34 and 7-35

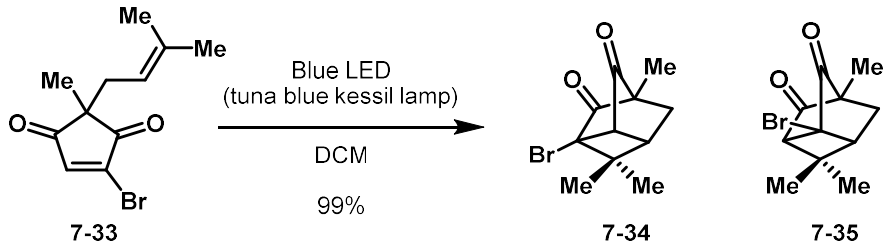

7-33 7-34 7-35

Enedione **7-33** (50 mg, 0.14 mmol) was dissolved in DCM (2.8 mL) under air in a 1 dr vial. The resulting pale yellow solution was then moved to a photoreactor containing two tuna blue Kessil lamps (see above). The light orange reaction mixture was irradiated at maximum intensity under a constant stream of air to maintain room temperature. After complete consumption of the starting material (monitored by NMR), the clear reaction mixture was concentrated *in vacuo* to yield title compounds **7-34** and **7-35** (50 mg, 0.14 mmol, 99%, 1.3:1).

33 R_f = 0.75 (hexane:EtOAc = 4:1), UV-active blue spot (*p*-anisaldehyde)

^{1}H NMR (500 MHz, $CDCl_3$) δ 7.44 (s, 2H), 4.78 (t, *J* = 7.9 Hz, 2H), 2.41 (dd, *J* = 7.8, 5.6 Hz, 4H), 1.60 (s, 6H), 1.53 (s, 6H), 1.20 (s, 6H).

^{13}C NMR (126 MHz, $CDCl_3$) δ 203.2, 200.3, 148.3, 148.1 137.2, 116.9, 52.8, 34.0, 25.9, 18.7, 17.7.

IR (neat): ν = 2971, 2931, 2873, 1753, 1709, 1562, 1452, 1377, 1315, 1229, 1118, 1078, 833, 790, and 413.

34 & 35 R_f = 0.75 (hexane:EtOAc = 4:1), UV-active blue streak (*p*-anisaldehyde)

^{1}H NMR (500 MHz, $CDCl_3$) δ 3.47 – 3.39 (m, 1H), 3.13 (d, *J* = 5.7 Hz, 1H), 2.94 (td, *J* = 5.0, 2.4 Hz, 1H), 2.80 (t, *J* = 6.0 Hz, 1H), 2.33 (dd, *J* = 12.4, 6.5 Hz, 1H), 2.24 (d, *J* = 12.5 Hz, 1H), 2.19 – 2.11 (m, 2H), 1.85 (d, *J* = 1.6 Hz, 3H), 1.49 (d, *J* = 1.6 Hz, 3H), 1.24 – 1.15 (m, 6H), 1.04 – 0.93 (m, 6H) ppm.

^{13}C NMR (126 MHz, $CDCl_3$) δ 205.7, 203.3, 201.9, 201.0, 70.4, 68.1, 60.0, 58.2, 56.9, 54.9, 51.3, 49.4, 46.5, 40.5, 35.5, 33.6, 28.1, 28.1, 23.4, 20.0, 7.5, 7.4 ppm.

IR (neat): ν = 2966, 2938, 2878, 1717, 1457, 1391, 1250, 1222, 1147, 1097, 1059, 1018, 999, 056, 913, 866, 921, 768, 660, and 597.

M.p: 85 °C

Synthesis of methyl allyl 1,3-cyclopentanedione S7-4

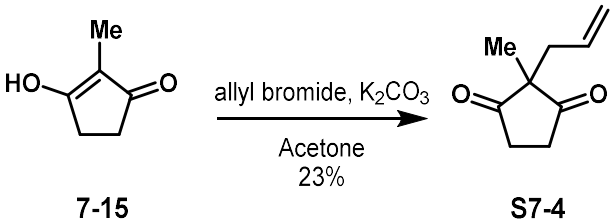

7-15 **S7-4**

To a solution of 2-methylcyclopentane-1,3-dione **7-15** (5.0 g, 45 mmol, 1equiv) in acetone (200 ml) was added potassium carbonate (9.2 g, 67 mmol, 1.5 equiv) in a single portion followed by allyl bromide (10 ml, 89 mmol, 2 equiv) dropwise via syringe. The mixture turned turbid during the addition of bromide. The reaction mixture was stirred under nitrogen for 24 hours then concentrated by rotary evaporation and resuspended in Et_2O. The suspension was then by addition of sat. aq. NaCl. The layers were separated and the aqueous layer was extracted two times with Et_2O. The combined organic layers were dried over Na_2SO_4, filtered, and concentrated in *vacuo*. The crude residue was purified by silica gel flash chromatography (hexanes: EtOAc 4:1) to afford **S7-4** as a colorless to pale yellow oil (1.54 g, 10 mmol, 23%).

R_f = 0.38 (hexane:EtOAc = 4:1), UV-active blue spot (*p*-anisaldehyde)

^{1}H NMR (500 MHz, $CDCl_3$) δ 5.63 – 5.54 (m, 1H), 5.09 – 5.03 (m, 2H), 2.80 – 2.64 (m, 4H), 2.35 (d, *J* = 7.5 Hz, 2H), 1.12 (s, 3H) ppm.

^{13}C NMR (126 MHz, $CDCl_3$) δ 216.4, 131.6, 120.0, 56.9, 40.2, 35.5, 19.0 ppm.

Spectral data were consistent with those found in the literature[23]

Synthesis of enedione 7-36

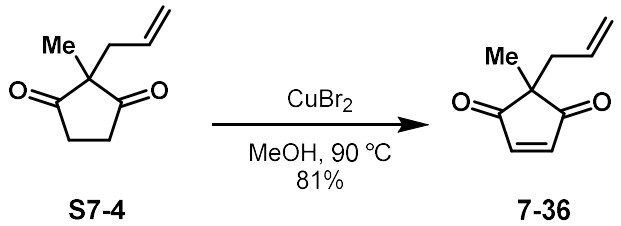

S7-4 **7-36**

To a solution of 2-allyl-2-methylcyclopentane-1,3-dione **S7-4** (1.0 g, 1 Eq, 6.6 mmol) in MeOH (45 mL) was added copper(II) bromide (3.2 g, 2.2 Eq, 14 mmol). The resulting brown solution was moved to a preheated oil bath and stirred at 90 °C under an argon atmosphere. After 1 h the reaction mixture was cooled to room temperature, quenched with 15 mL of distilled water followed by 15 mL of 1 M aq. HCl solution, and diluted with Et_2O. The layers were separated, and the aqueous layer was extracted two times with Et_2O. The combined organic layers were dried over Na_2SO_4, filtered, and concentrated in *vacuo.* The crude residue was purified by silica-gel flash column chromatography (Pentane: diethyl ether = 10:1 to 4:1) to afford **7-36** as a yellow oil (0.80 g, 5.3 mmol, 81%).

R_f = 0.48 (hexane:EtOAc = 4:1), UV-active KMnO4

^{1}H NMR (400 MHz, $CDCl_3$) δ 7.23 (s, 2H), 5.48 (ddt, *J* = 17.6, 10.1, 7.5 Hz, 1H), 5.07 – 4.92 (m, 2H), 2.38 (dt, *J* = 7.5, 1.1 Hz, 2H), 1.15 (s, 3H) ppm.

^{13}C NMR (126 MHz, $CDCl_3$) δ 207.6, 148.7, 131.8, 120.0, 51.0, 39.1, 19.0 ppm.

Spectral data were consistent with those found in the literature[23]

Synthesis of tricycle 7-37

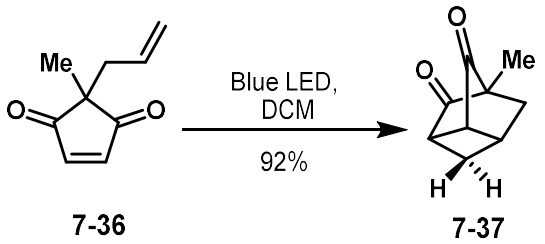

7-36 **7-37**

Enedione **7-36** (16 mg, 0.1 mmol) was dissolved in DCM (1 mL) under air in a 1 dr vial. The resulting pale yellow solution was then moved to the Penn photoreactor affixed with a 420 nm plate (see above). The reaction mixture was irradiated at this wavelength for 12 hours after which it was removed from the photoreactor, and concentrated *in vacuo* to yield tricycle **7-37**. The compound was unstable to silica gel chromatography, so the yield was assessed by ^{1}HNMR, 90%.

R_f = 0.30 (hexane:EtOAc = 4:1), streak KMnO4

^{1}H NMR (500 MHz, $CDCl_3$) δ 3.29 – 3.21 (m, 2H), 3.16 (dddd, *J* = 10.4, 6.3, 4.6, 2.0 Hz, 1H), 2.97 (ddd, *J* = 11.4, 6.6, 4.9 Hz, 1H), 2.40 (ddd, *J* = 12.1, 6.7, 3.0 Hz, 1H), 2.06 (dd, *J* = 25.5, 11.1 Hz, 2H), 1.17 (s, 3H) ppm.

^{13}C NMR (126 MHz, $CDCl_3$) δ 209.7, 208.2, 60.0, 51.4, 48.0, 40.8, 38.0, 32.7, 7.3.

IR (neat): ν = 3453, 2971, 2933, 2871, 1780, 1727, 1451, 1347, 1140, 1063, 1019, 897, 821, 779, 703, 608, 504, and 473 ppm.

Synthesis of dione S7-5

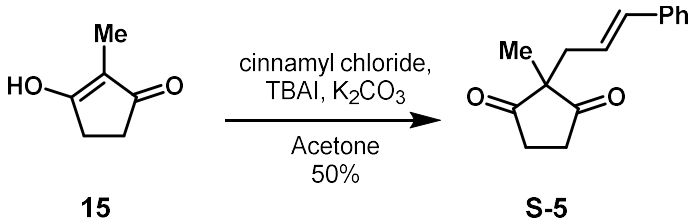

15 **S-5**

A solution of 2-methylcyclopentane-1,3-dione **7-15** (1.0 g, 8.9 mmol, 1equiv) and Tetra-n-butylammonium iodide (33 mg, 8.9µmol, 1 mol%) in dry acetone (40 ml) was added cinnamyl chloride (2.7 g, 18 mmol, 2 equiv) in a portion. The mixture turned turbid while the addition of cinnamyl chloride. After stirred for 5 min, potassium carbonate (1.8 g, 13 mmol, 1.5 equiv) was added to the mixture. Then it was stirred under nitrogen for 24 hours and concentrated by rotary evaporation and resuspended in ether. The mixture was then quenched with Brine. The aqueous layer was further extracted by ether. The combined organic layers were dried over Na_2SO_4, filtered, and concentrated in *vacuo*. The crude residue was purified by silica gel flash chromatography (hexanes: EtOAc 10:1 to 2:1) to afford **S7-5** as a white to pale-yellow solid (1.0 g, 4.4 mmol, 50%).

R_f = 0.50 (hexane:EtOAc = 2:1), UV-active KMnO4

^{1}H NMR (600 MHz, $CDCl_3$) δ 7.32 – 7.27 (m, 4H), 7.24 – 7.20 (m, 1H), 6.41 (dt, *J* = 15.8, 1.3 Hz, 1H), 5.98 (dt, *J* = 15.6, 7.7 Hz, 1H), 2.82 – 2.72 (m, 2H), 2.72 – 2.64 (m, 2H), 2.51 (dd, *J* = 7.7, 1.3 Hz, 2H), 1.17 (s, 3H) ppm.

^{13}C NMR (151 MHz, $CDCl_3$) δ 216.5, 136.8, 134.9, 128.7, 127.9, 126.4, 122.8, 57.2, 39.4, 35.6 , 19.2 ppm.

Spectral data were consistent with those found in the literature[23]

Synthesis of enedione 7-38

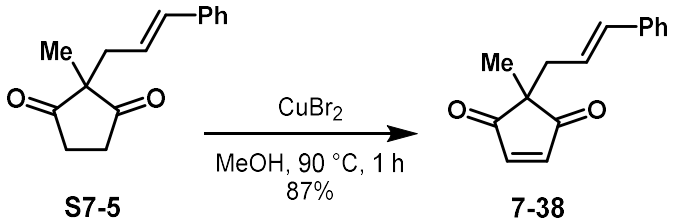

S7-5 **7-38**

To a solution of 2-cinnamyl-2-methylcyclopentane-1,3-dione (**S7-5** 0.5 g, 1 equiv, 2.2 mmol) in MeOH (45 mL) was added copper(II) bromide (1.1 g, 2.2 equiv, 4.8 mmol). The resulting brown solution was moved to a preheated oil bath and stirred at 90 °C under an argon atmosphere. After 1 h the reaction mixture was cooled to room temperature, quenched with 15 mL of distilled water followed by 15 mL of 1 M aq. HCl solution, and diluted with Et_2O. The layers were separated, and the aqueous layer was extracted two times with Et_2O. The combined organic layers were dried over Na_2SO_4, filtered, and concentrated in *vacuo.* The crude residue was purified by silica-gel flash column chromatography (Pentane: diethyl ether = 10:1 to 4:1) to afford **7-38** as a yellow solid (0.43 g, 1.9 mmol, 87%).

R_f = 0.22 (hexane:EtOAc = 10:1), UV-active KMnO4

^{1}H NMR (500 MHz, $CDCl_3$) δ 7.30 (dd, *J* = 4.6, 2.0 Hz, 7H), 7.24 (d, *J* = 3.0 Hz, 2H), 6.44 – 6.35 (m, 1H), 5.91 (dt, *J* = 15.6, 7.7 Hz, 1H), 2.59 (d, *J* = 7.8 Hz, 2H), 1.24 (s, 3H) ppm.

^{13}C NMR (126 MHz, $CDCl_3$) δ 207.4, 148.6, 136.8, 134.7, 128.6, 127.7, 126.4, 122.9, 51.2, 38.1, 18.9 ppm.

Spectral data were consistent with those found in the literature[23]

Synthesis of tricycle 7-39

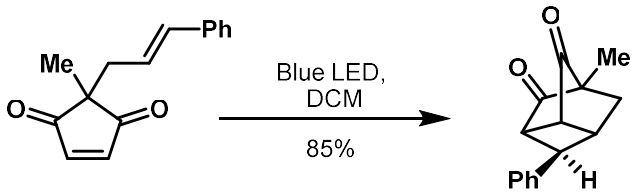

7-38 7-39

Enedione **7-38** (22 mg, 0.1 mmol) was dissolved in DCM (1 mL) under air in a 1 dr vial. The resulting pale-yellow solution was then moved to the Penn photoreactor affixed with a 420 nm plate (see above). The reaction mixture was irradiated at this wavelength for 12 hours after which it was removed from the photoreactor and concentrated *in vacuo* to yield tricycle **7-39**. The compound was unstable to silica gel chromatography, so the yield was assessed by ^{1}HNMR, 85%.

R_f = 0.15 (hexane:EtOAc = 10:1), streak KMnO4

^{1}H NMR (600 MHz, $CDCl_3$) δ 7.45 – 7.38 (m, 2H), 7.36 – 7.33 (m, 2H), 7.33 – 7.29 (m, 1H), 3.48 (s, 1H), 3.43 (dt, *J* = 13.3, 4.7 Hz, 2H), 3.17 (dt, *J* = 6.8, 5.2 Hz, 1H), 2.52 – 2.45 (m, 1H), 2.22 (d, *J* = 12.2 Hz, 1H), 1.25 (s, 3H) ppm.

^{13}C NMR (151 MHz, $CDCl_3$) δ 209.2, 206.7, 140.6, 129.1, 127.4, 126.7, 59.4, 56.2, 55.1, 46.55, 39.5, 37.9, 7.2 ppm.

IR (neat): ν = 2965, 2931, 2870, 1762, 1732, 1602, 1498, 1450, 1261, 1181, 1097, 1044, 802, 749, 699, 660, 597, 561.

HRMS (ESI, *m/z*): for $[M+H]^+$ calcd. for $C_{15}H_{15}O_2$ 227.1067; found 227.1067.

Synthesis of bisprenyl dione S7-7

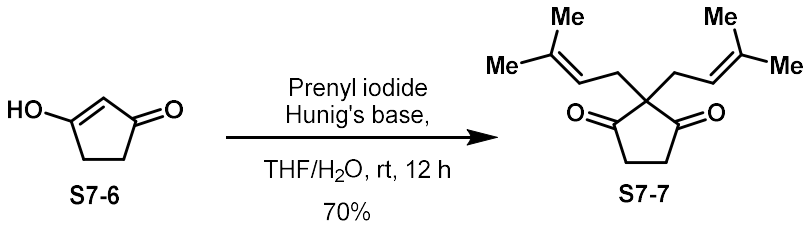

Synthesis of prenyl iodide:

To a solution of prenyl bromide (20.0 g, 134 mmol, 2.8 equiv) in acetone (200 mL) was added sodium iodide (24.1 g, 161 mmol, 3.0 equiv). The reaction was stirred for 5 minutes during which a white precipitate formed. The mixture was filtered through a plug of silica and the solvent was evaporated carefully *in vacuo*. The brown crude residue was dissolved in Et_2O (100 mL) and the solution was washed with sat. aq. $NaHCO_3$ (50 mL) and sat. aq. $Na_2S_2O_3$ (10 %, 50 mL), which decolored the solution from brown to pale yellow. The organic layer was dried over Na_2SO_4 and concentrated *in vacuo*. Crude prenyl iodide was directly used in the following reaction without further purification.

Notes: Prenyl bromide and iodide decompose under moisture and air. Using freshly opened or synthesized prenyl bromide ensures reproducibility of experiments. Prenyl iodide is light-sensitive and needs to be used rapidly after synthesis. Blocking light and ensuring a N_2 atmosphere reduces decomposition visibly.

To a solution of 1,3-cyclopentanedione (**S-6** 4.99 g, 50.9 mmol, 1 equiv) in a THF/water mixture (4:1, 400 mL) at 0 °C was slowly added DIPEA (18.2 mL, 104 mmol. 2.1 equiv) and prenyl iodide (crude as above, 134 mmol, 2.6 equiv). The reaction mixture was allowed to warm to room temperature and stirred for 18 hours. THF was then removed by rotary evaporation. To the remaining mixture was added DCM and saturated sodium bicarbonate solution. The aqueous phase was extracted with DCM two times. The combined organic phases were washed with brine, dried over Na_2SO_4 and concentrated *in vacuo*. The crude residue was purified by flash chromatography (Hex/EtOAc = 9/1) to give diketone **S7-7** (8.34 g, 70%).

R_f = 0.50 (hexane:EtOAc = 10:1), UV-active spot (*p*-anisaldehyde)

^{1}H NMR (500 MHz, $CDCl_3$) δ 4.87 (tt, J = 7.7, 1.5 Hz, 1H), 2.55 (s, 2H), 2.34 (d, J = 7.9 Hz, 2H), 1.62 (s, 3H), 1.56 (s, 3H) ppm.

^{13}C NMR (126 MHz, $CDCl_3$) δ 218.0, 136.5, 117.4, 61.6, 36.8, 34.5, 26.0, 17.9 ppm.

Spectral data consistent with those found in the literature[25]

Synthesis of enedione 7-40

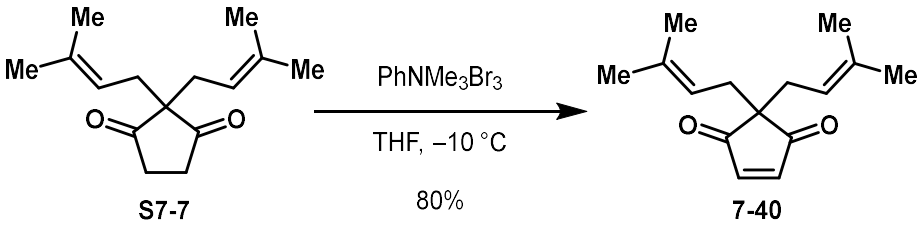

A solution of **S7-7** (3.00 g, 12.8 mmol, 1 equiv) in THF (130 mL) was cooled to –10 °C. To this cooled solution was added phenyltrimethylammonium tribromide (4.7 g, 17 mmol, 1 equiv) in four portions after which the solution turned bright yellow. Portions were added in 30 minute intervals. Completion of the reaction was judged by TLC, circa three hours. Upon completion the reaction was diluted with diethyl ether and quenched with sat. aq. $NaHCO_3$ and sat. aq. $Na_2S_2O_3$ (4:1). The layers were separated and the aqueous layer was extracted two further times with diethyl ether. The combined organic layers were dried over Na_2SO_4, filtered, and concentrated *in vacuo*. The crude reaction mixture was purified by silica gel flash chromatography (gradient 5:1 pentane: diethyl ether to 1:1 pentane: diethyl ether) to yield **7-40** as a bright yellow solid (2.38 g, 80%).

R_f = 0.50 (hexane:EtOAc = 10:1), UV-active blue spot (*p*-anisaldehyde)

^{1}H NMR (400 MHz, $CDCl_3$) δ 7.23 (s, 1H), 4.76 (tt, *J* = 7.8, 1.5 Hz, 1H), 2.37 (d, *J* = 7.8 Hz, 2H), 1.55 (dd, *J* = 11.9, 1.4 Hz, 6H) ppm.

^{13}C NMR (101 MHz, $CDCl_3$) δ 208.0, 150.0, 136.2, 117.3, 55.6, 32.8, 25.9, 17.7 ppm.

IR (neat): ν = 2972, 2914, 2859, 1700, 1441, 1378, 1324, 1231, 1057, 1030, 985, 836, 700, and 577.

M.p: 70 °C

2.23 Synthesis of prenylated tricyclo[3.2.1.0^{3,6}]octane 7-41

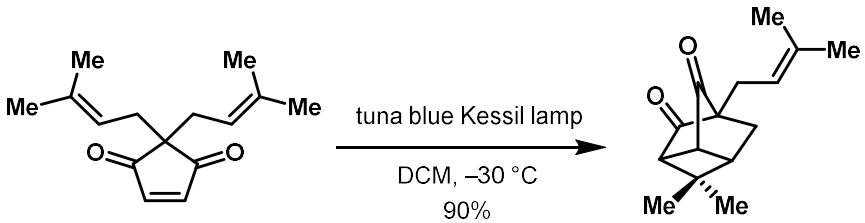

7-40 **7-41**

Enedione **7-40** (100 mg, 0.56 mmol) was dissolved in DCM (5.6 mL) under air in a round-bottomed flask. The resulting pale yellow solution was cooled to –30 °C. A tuna blue Kessil lamp was affixed and the solution was irradiated for 3 h (see above). After complete consumption of the starting material (monitored by NMR), the clear reaction mixture was concentrated *in vacuo* and washed with heptanes to yield title compound **7-41** (90 mg, 0.50 mmol).

R_f = 0.5 (hexane:EtOAc = 10:1), green streak (*p*-anisaldehyde)

^{1}H NMR (700 MHz, $CDCl_3$) δ 5.22 (tt, *J* = 7.5, 1.5 Hz, 1H), 3.22 (t, *J* = 4.4 Hz, 1H), 2.98 (t, *J* = 4.9 Hz, 1H), 2.59 (dt, *J* = 6.7, 5.0 Hz, 1H), 2.42 – 2.37 (m, 1H), 2.30 (dd, *J* = 15.5, 7.5 Hz, 1H), 2.24 (dd, *J* = 12.6, 6.7 Hz, 1H), 2.09 (d, *J* = 12.7 Hz, 1H), 1.70 (d, *J* = 1.5 Hz, 3H), 1.65 (s, 3H), 1.45 (s, 3H), 0.97 (s, 3H) ppm.

^{13}C NMR (176 MHz, $CDCl_3$) δ 208.6, 207.0, 134.4, 118.5, 62.9, 61.5, 46.7, 45.7, 41.4, 32.3, 28.5, 26.0, 21.9, 21.5, 17.9 ppm.

IR (neat): ν = 2966, 2934, 1776, 1715, 1452, 1386, 1375, 1246, 1222, 1169, 1110, 1058, 983, 910, 720, 647.

X-ray crystallographic data

A colorless block 0.12 x 0.07 x 0.04 mm in size was mounted on a Cryoloop with Paratone oil. Data were collected in a nitrogen gas stream at 100(2) K using omega scans. Crystal-to-detector distance was 33.00 mm and exposure time was 3.00 seconds per frame at low angles and 13.00 seconds at high angles, using a scan width of 0.5°. Data collection was 100% complete to 74.000° in θ. A total of 32348 reflections were collected covering the indices -29<=h<=27, -29<=k<=24, -7<=l<=7. 3522 reflections were found to be symmetry independent, with an R_{int} of 0.0438. Indexing and unit cell refinement indicated a primitive, tetragonal lattice. The space group was found to be P 42 nm (No. 102). The data were integrated using the CrysAlis^{Pro} 1.172.42.72a software program and scaled using the SCALE3 ABSPACK scaling algorithm. Solution by intrinsic phasing (SHELXT-2015) produced a heavy-atom phasing model consistent with the proposed structure. All non-hydrogen atoms were refined anisotropically by full-matrix least-squares (SHELXL-2014). All hydrogen atoms were placed using a riding model. Their positions were constrained relative to their parent atom using the appropriate HFIX command in SHELXL-2014. A solvent mask was applied to remove electron density related to an unidentifiable, disordered outer sphere solvent molecule.

Table 1. Crystal data and structure refinement for IB008_Sarpong.

Identification code	IB008_Sarpong	
Empirical formula	C11 H18 O2	
Formula weight	182.25	
Temperature	100(2) K	
Wavelength	1.54184 Å	
Crystal system	Tetragonal	
Space group	P 42 n m	
Unit cell dimensions	a = 23.5301(3) Å	a= 90°.
	b = 23.5301(3) Å	b= 90°.
	c = 5.98071(11) Å	g = 90°.
Volume	3311.31(10) $Å^3$	
Z	12	
Density (calculated)	1.097 Mg/m^3	
Absorption coefficient	0.583 mm^{-1}	
F(000)	1200	
Crystal size	0.120 x 0.070 x 0.040 mm^3	
Theta range for data collection	2.656 to 75.283°.	
Index ranges	-29<=h<=27, -29<=k<=24, -7<=l<=7	
Reflections collected	32348	
Independent reflections	3522 [R(int) = 0.0438]	
Completeness to theta = 74.000°	99.9 %	
Absorption correction	Semi-empirical from equivalents	
Max. and min. transmission	1.00000 and 0.79637	
Refinement method	Full-matrix least-squares on F^2	
Data / restraints / parameters	3522 / 32 / 246	
Goodness-of-fit on F^2	1.086	
Final R indices [I>2sigma(I)]	R1 = 0.0597, wR2 = 0.1670	
R indices (all data)	R1 = 0.0646, wR2 = 0.1725	
Absolute structure parameter	0.0(4)	
Extinction coefficient	n/a	
Largest diff. peak and hole	0.384 and -0.296 $e.Å^{-3}$	

Table 2. Atomic coordinates (x 10^4) and equivalent isotropic displacement parameters ($Å^2$x 10^3)
for ib008_sarpong. U(eq) is defined as one third of the trace of the orthogonalized U^{ij} tensor.

	x	y	z	U(eq)
O(1A)	3776(1)	1465(1)	3551(4)	48(1)
O(2A)	5827(1)	1493(1)	2226(4)	47(1)
C(1A)	4822(1)	1381(1)	3436(6)	42(1)
C(2A)	4277(1)	1554(1)	2229(6)	41(1)
C(3A)	4388(2)	2168(1)	1466(6)	48(1)
C(4A)	4398(2)	2626(2)	3355(8)	59(1)
C(5A)	4460(2)	3215(2)	2285(11)	83(2)
C(6A)	3945(2)	2657(2)	5163(8)	70(1)
C(7A)	4994(2)	2385(2)	3948(8)	60(1)
C(8A)	4961(2)	1823(2)	5239(6)	52(1)
C(9A)	5056(2)	2174(1)	1475(8)	51(1)
C(10A)	5243(1)	1562(1)	1595(6)	42(1)
C(11A)	4858(2)	771(2)	4203(7)	48(1)
O(1B)	7883(3)	3492(3)	5332(12)	46(2)
O(2B)	6600(3)	1886(3)	4886(13)	50(2)
C(1B)	7358(15)	2596(14)	5293(10)	43(3)
C(2B)	7435(6)	3198(9)	4250(40)	43(3)
C(3B)	6841(4)	3463(4)	4537(16)	51(2)
C(4B)	6671(4)	3609(3)	6974(16)	60(2)
C(5B)	7037(4)	3945(3)	8478(16)	61(2)
C(6B)	6050(20)	3890(20)	6950(20)	88(7)
C(7B)	6598(3)	2961(3)	7382(15)	55(2)
C(8B)	7326(3)	2878(3)	7689(12)	45(2)
C(9B)	6465(4)	2902(4)	4809(19)	57(2)
C(10B)	6839(10)	2416(6)	4100(40)	49(3)
C(11B)	7823(8)	2166(6)	4995(11)	60(2)

Table 3. Bond lengths [Å] and angles [°] for ib008_sarpong.

O(1A)-C(2A)	1.437(4)
O(1A)-H(1A)	0.8400
O(2A)-C(10A)	1.435(4)
O(2A)-H(2A)	0.8400
C(1A)-C(11A)	1.509(4)
C(1A)-C(2A)	1.528(4)
C(1A)-C(8A)	1.534(5)
C(1A)-C(10A)	1.540(5)
C(2A)-C(3A)	1.535(5)
C(2A)-H(2AA)	1.0000
C(3A)-C(4A)	1.561(5)
C(3A)-C(9A)	1.573(5)
C(3A)-H(3A)	1.0000
C(4A)-C(6A)	1.520(6)
C(4A)-C(5A)	1.535(6)
C(4A)-C(7A)	1.554(5)
C(5A)-H(5AA)	0.9800
C(5A)-H(5AB)	0.9800
C(5A)-H(5AC)	0.9800
C(6A)-H(6AA)	0.9800
C(6A)-H(6AB)	0.9800
C(6A)-H(6AC)	0.9800
C(7A)-C(8A)	1.532(6)
C(7A)-C(9A)	1.567(6)
C(7A)-H(7A)	1.0000
C(8A)-H(8AA)	0.9900
C(8A)-H(8AB)	0.9900
C(9A)-C(10A)	1.507(4)
C(9A)-H(9A)	1.0000
C(10A)-H(10A)	1.0000
C(11A)-H(11A)	0.9800
C(11A)-H(11B)	0.9800
C(11A)-H(11C)	0.9800
O(1B)-C(2B)	1.42(2)

O(1B)-H(1B)	0.8400
O(2B)-C(10B)	1.45(2)
O(2B)-H(2B)	0.8400
C(1B)-C(10B)	1.48(4)
C(1B)-C(11B)	1.501(9)
C(1B)-C(2B)	1.56(4)
C(1B)-C(8B)	1.581(15)
C(2B)-C(3B)	1.540(15)
C(2B)-H(2BA)	1.0000
C(3B)-C(4B)	1.550(13)
C(3B)-C(9B)	1.598(16)
C(3B)-H(3B)	1.0000
C(4B)-C(5B)	1.474(12)
C(4B)-C(7B)	1.553(10)
C(4B)-C(6B)	1.61(3)
C(5B)-H(5BA)	0.9800
C(5B)-H(5BB)	0.9800
C(5B)-H(5BC)	0.9800
C(6B)-H(6BA)	0.9800
C(6B)-H(6BB)	0.9800
C(6B)-H(6BC)	0.9800
C(7B)-C(9B)	1.577(14)
C(7B)-C(8B)	1.732(8)
C(7B)-H(7B)	1.0000
C(8B)-H(8BA)	0.9900
C(8B)-H(8BB)	0.9900
C(9B)-C(10B)	1.503(18)
C(9B)-H(9B)	1.0000
C(10B)-H(10B)	1.0000
C(11B)-H(11D)	0.9800
C(11B)-H(11E)	0.9800
C(11B)-H(11F)	0.9800

C(2A)-O(1A)-H(1A)	109.5
C(10A)-O(2A)-H(2A)	109.5
C(11A)-C(1A)-C(2A)	116.4(3)

C(11A)-C(1A)-C(8A)	114.8(3)
C(2A)-C(1A)-C(8A)	109.3(2)
C(11A)-C(1A)-C(10A)	116.4(3)
C(2A)-C(1A)-C(10A)	97.3(3)
C(8A)-C(1A)-C(10A)	100.2(3)
O(1A)-C(2A)-C(1A)	113.0(3)
O(1A)-C(2A)-C(3A)	116.1(3)
C(1A)-C(2A)-C(3A)	104.4(3)
O(1A)-C(2A)-H(2AA)	107.6
C(1A)-C(2A)-H(2AA)	107.6
C(3A)-C(2A)-H(2AA)	107.6
C(2A)-C(3A)-C(4A)	115.9(3)
C(2A)-C(3A)-C(9A)	100.2(2)
C(4A)-C(3A)-C(9A)	88.6(3)
C(2A)-C(3A)-H(3A)	116.0
C(4A)-C(3A)-H(3A)	116.0
C(9A)-C(3A)-H(3A)	116.0
C(6A)-C(4A)-C(5A)	108.7(4)
C(6A)-C(4A)-C(7A)	119.2(4)
C(5A)-C(4A)-C(7A)	109.8(4)
C(6A)-C(4A)-C(3A)	122.5(3)
C(5A)-C(4A)-C(3A)	108.9(4)
C(7A)-C(4A)-C(3A)	85.8(3)
C(4A)-C(5A)-H(5AA)	109.5
C(4A)-C(5A)-H(5AB)	109.5
H(5AA)-C(5A)-H(5AB)	109.5
C(4A)-C(5A)-H(5AC)	109.5
H(5AA)-C(5A)-H(5AC)	109.5
H(5AB)-C(5A)-H(5AC)	109.5
C(4A)-C(6A)-H(6AA)	109.5
C(4A)-C(6A)-H(6AB)	109.5
H(6AA)-C(6A)-H(6AB)	109.5
C(4A)-C(6A)-H(6AC)	109.5
H(6AA)-C(6A)-H(6AC)	109.5
H(6AB)-C(6A)-H(6AC)	109.5
C(8A)-C(7A)-C(4A)	112.6(3)

C(8A)-C(7A)-C(9A)	102.0(3)
C(4A)-C(7A)-C(9A)	89.1(3)
C(8A)-C(7A)-H(7A)	116.4
C(4A)-C(7A)-H(7A)	116.4
C(9A)-C(7A)-H(7A)	116.4
C(7A)-C(8A)-C(1A)	104.0(3)
C(7A)-C(8A)-H(8AA)	111.0
C(1A)-C(8A)-H(8AA)	111.0
C(7A)-C(8A)-H(8AB)	111.0
C(1A)-C(8A)-H(8AB)	111.0
H(8AA)-C(8A)-H(8AB)	109.0
C(10A)-C(9A)-C(7A)	106.5(3)
C(10A)-C(9A)-C(3A)	106.4(3)
C(7A)-C(9A)-C(3A)	85.0(3)
C(10A)-C(9A)-H(9A)	117.9
C(7A)-C(9A)-H(9A)	117.9
C(3A)-C(9A)-H(9A)	117.9
O(2A)-C(10A)-C(9A)	113.6(3)
O(2A)-C(10A)-C(1A)	113.4(3)
C(9A)-C(10A)-C(1A)	96.4(3)
O(2A)-C(10A)-H(10A)	110.9
C(9A)-C(10A)-H(10A)	110.9
C(1A)-C(10A)-H(10A)	110.9
C(1A)-C(11A)-H(11A)	109.5
C(1A)-C(11A)-H(11B)	109.5
H(11A)-C(11A)-H(11B)	109.5
C(1A)-C(11A)-H(11C)	109.5
H(11A)-C(11A)-H(11C)	109.5
H(11B)-C(11A)-H(11C)	109.5
C(2B)-O(1B)-H(1B)	109.5
C(10B)-O(2B)-H(2B)	109.5
C(10B)-C(1B)-C(11B)	111(2)
C(10B)-C(1B)-C(2B)	99.5(6)
C(11B)-C(1B)-C(2B)	119(3)
C(10B)-C(1B)-C(8B)	121.1(19)
C(11B)-C(1B)-C(8B)	115.2(11)

C(2B)-C(1B)-C(8B)	89.2(19)
O(1B)-C(2B)-C(3B)	115.2(15)
O(1B)-C(2B)-C(1B)	110.3(19)
C(3B)-C(2B)-C(1B)	102.7(13)
O(1B)-C(2B)-H(2BA)	109.5
C(3B)-C(2B)-H(2BA)	109.5
C(1B)-C(2B)-H(2BA)	109.5
C(2B)-C(3B)-C(4B)	115.4(11)
C(2B)-C(3B)-C(9B)	100.3(10)
C(4B)-C(3B)-C(9B)	86.8(8)
C(2B)-C(3B)-H(3B)	116.5
C(4B)-C(3B)-H(3B)	116.5
C(9B)-C(3B)-H(3B)	116.5
C(5B)-C(4B)-C(3B)	122.8(7)
C(5B)-C(4B)-C(7B)	119.6(8)
C(3B)-C(4B)-C(7B)	87.7(6)
C(5B)-C(4B)-C(6B)	108.6(18)
C(3B)-C(4B)-C(6B)	108.6(8)
C(7B)-C(4B)-C(6B)	108(2)
C(4B)-C(5B)-H(5BA)	109.5
C(4B)-C(5B)-H(5BB)	109.5
H(5BA)-C(5B)-H(5BB)	109.5
C(4B)-C(5B)-H(5BC)	109.5
H(5BA)-C(5B)-H(5BC)	109.5
H(5BB)-C(5B)-H(5BC)	109.5
C(4B)-C(6B)-H(6BA)	109.5
C(4B)-C(6B)-H(6BB)	109.5
H(6BA)-C(6B)-H(6BB)	109.5
C(4B)-C(6B)-H(6BC)	109.5
H(6BA)-C(6B)-H(6BC)	109.5
H(6BB)-C(6B)-H(6BC)	109.5
C(4B)-C(7B)-C(9B)	87.4(7)
C(4B)-C(7B)-C(8B)	91.1(5)
C(9B)-C(7B)-C(8B)	106.9(6)
C(4B)-C(7B)-H(7B)	121.1
C(9B)-C(7B)-H(7B)	121.1

C(8B)-C(7B)-H(7B)	121.1
C(1B)-C(8B)-C(7B)	90.0(12)
C(1B)-C(8B)-H(8BA)	113.6
C(7B)-C(8B)-H(8BA)	113.6
C(1B)-C(8B)-H(8BB)	113.6
C(7B)-C(8B)-H(8BB)	113.6
H(8BA)-C(8B)-H(8BB)	110.9
C(10B)-C(9B)-C(7B)	103.0(11)
C(10B)-C(9B)-C(3B)	106.0(11)
C(7B)-C(9B)-C(3B)	85.2(7)
C(10B)-C(9B)-H(9B)	119.0
C(7B)-C(9B)-H(9B)	119.0
C(3B)-C(9B)-H(9B)	119.0
O(2B)-C(10B)-C(1B)	114(2)
O(2B)-C(10B)-C(9B)	109.8(16)
C(1B)-C(10B)-C(9B)	97.5(11)
O(2B)-C(10B)-H(10B)	111.4
C(1B)-C(10B)-H(10B)	111.4
C(9B)-C(10B)-H(10B)	111.4
C(1B)-C(11B)-H(11D)	109.5
C(1B)-C(11B)-H(11E)	109.5
H(11D)-C(11B)-H(11E)	109.5
C(1B)-C(11B)-H(11F)	109.5
H(11D)-C(11B)-H(11F)	109.5
H(11E)-C(11B)-H(11F)	109.5

Symmetry transformations used to generate equivalent atoms:

Table 4. Anisotropic displacement parameters ($Å^2 x\ 10^3$)for ib008_sarpong. The anisotropic displacement factor exponent takes the form: $-2p^2[\ h^2 a^{*2} U^{11} + ... + 2\ h\ k\ a^*\ b^*\ U^{12}\ ]$

	U^{11}	U^{22}	U^{33}	U^{23}	U^{13}	U^{12}
O(1A)	43(1)	54(1)	46(1)	5(1)	-2(1)	10(1)
O(2A)	46(1)	44(1)	50(1)	-2(1)	-4(1)	5(1)
C(1A)	46(2)	39(2)	41(2)	2(1)	-2(1)	7(1)
C(2A)	45(2)	41(2)	38(1)	1(1)	0(1)	7(1)
C(3A)	57(2)	42(2)	46(2)	1(1)	-4(2)	12(1)
C(4A)	69(2)	44(2)	64(2)	-11(2)	-6(2)	13(2)
C(5A)	92(3)	42(2)	114(4)	-5(2)	-10(3)	14(2)
C(6A)	72(3)	69(3)	68(2)	-26(2)	-12(2)	31(2)
C(7A)	63(2)	44(2)	72(3)	-16(2)	-11(2)	7(2)
C(8A)	50(2)	64(2)	42(2)	-11(2)	-7(2)	14(2)
C(9A)	60(2)	36(2)	59(2)	2(2)	-3(2)	3(1)
C(10A)	46(2)	38(2)	41(2)	1(1)	-4(1)	3(1)
C(11A)	43(2)	47(2)	55(2)	11(1)	-2(2)	6(1)
O(1B)	40(3)	52(3)	45(3)	11(3)	-2(3)	-18(3)
O(2B)	55(4)	47(4)	46(4)	5(3)	-9(3)	-25(3)
C(1B)	52(9)	35(5)	42(2)	2(4)	-5(5)	-6(4)
C(2B)	44(6)	44(5)	41(5)	6(3)	-6(5)	-4(5)
C(3B)	43(4)	42(4)	67(5)	9(3)	-6(3)	-1(3)
C(4B)	63(4)	47(3)	70(5)	-5(3)	6(4)	-7(3)
C(5B)	77(5)	41(3)	64(4)	-3(3)	8(4)	-12(3)
C(6B)	71(15)	61(10)	132(8)	-24(13)	-8(14)	-4(9)
C(7B)	53(4)	46(4)	66(4)	0(4)	12(4)	-8(3)
C(8B)	42(3)	48(3)	46(3)	2(2)	-2(2)	-19(3)
C(9B)	39(4)	50(4)	81(6)	1(4)	-14(4)	-11(4)
C(10B)	56(6)	43(7)	49(6)	12(5)	0(4)	-13(5)
C(11B)	88(11)	33(7)	58(3)	-6(7)	-5(10)	-4(2)

Table 5. Hydrogen coordinates (x 10^4) and isotropic displacement parameters ($Å^2$x 10^3) for ib008_sarpong.

	x	y	z	U(eq)
H(1A)	3486	1510	2749	71
H(2A)	5885	1154	2606	70
H(2AA)	4243	1313	858	50
H(3A)	4202	2284	34	58
H(5AA)	4777	3210	1219	124
H(5AB)	4536	3497	3453	124
H(5AC)	4108	3314	1501	124
H(6AA)	3585	2781	4500	105
H(6AB)	4062	2929	6314	105
H(6AC)	3895	2281	5840	105
H(7A)	5283	2666	4476	72
H(8AA)	4659	1838	6390	62
H(8AB)	5328	1737	5973	62
H(9A)	5254	2428	386	62
H(10A)	5160	1360	161	50
H(11A)	4611	717	5507	72
H(11B)	5251	681	4609	72
H(11C)	4733	519	2992	72
H(1B)	7992	3762	4520	68
H(2B)	6314	1803	4111	75
H(2BA)	7523	3160	2622	52
H(3B)	6718	3738	3357	61
H(5BA)	7410	3761	8602	91
H(5BB)	6861	3967	9960	91
H(5BC)	7084	4329	7871	91
H(6BA)	6054	4239	6064	132
H(6BB)	5931	3977	8487	132
H(6BC)	5776	3621	6292	132

H(7B)	6328	2815	8537	66
H(8BA)	7535	3242	7802	55
H(8BB)	7433	2618	8918	55
H(9B)	6060	2909	4302	68
H(10B)	6897	2412	2449	59
H(11D)	7952	2169	3437	89
H(11E)	7679	1787	5373	89
H(11F)	8142	2260	5981	89

Table 6. Torsion angles [°] for ib008_sarpong.

C(11A)-C(1A)-C(2A)-O(1A)	58.2(4)
C(8A)-C(1A)-C(2A)-O(1A)	-73.9(3)
C(10A)-C(1A)-C(2A)-O(1A)	-177.5(2)
C(11A)-C(1A)-C(2A)-C(3A)	-174.7(3)
C(8A)-C(1A)-C(2A)-C(3A)	53.2(3)
C(10A)-C(1A)-C(2A)-C(3A)	-50.4(3)
O(1A)-C(2A)-C(3A)-C(4A)	53.8(4)
C(1A)-C(2A)-C(3A)-C(4A)	-71.3(3)
O(1A)-C(2A)-C(3A)-C(9A)	147.3(3)
C(1A)-C(2A)-C(3A)-C(9A)	22.1(3)
C(2A)-C(3A)-C(4A)-C(6A)	-46.9(5)
C(9A)-C(3A)-C(4A)-C(6A)	-147.5(4)
C(2A)-C(3A)-C(4A)-C(5A)	-175.1(3)
C(9A)-C(3A)-C(4A)-C(5A)	84.3(4)
C(2A)-C(3A)-C(4A)-C(7A)	75.4(3)
C(9A)-C(3A)-C(4A)-C(7A)	-25.2(3)
C(6A)-C(4A)-C(7A)-C(8A)	47.9(5)
C(5A)-C(4A)-C(7A)-C(8A)	174.1(4)
C(3A)-C(4A)-C(7A)-C(8A)	-77.3(4)
C(6A)-C(4A)-C(7A)-C(9A)	150.5(4)
C(5A)-C(4A)-C(7A)-C(9A)	-83.3(4)
C(3A)-C(4A)-C(7A)-C(9A)	25.3(3)
C(4A)-C(7A)-C(8A)-C(1A)	77.2(4)
C(9A)-C(7A)-C(8A)-C(1A)	-16.8(4)
C(11A)-C(1A)-C(8A)-C(7A)	170.7(3)
C(2A)-C(1A)-C(8A)-C(7A)	-56.4(3)
C(10A)-C(1A)-C(8A)-C(7A)	45.1(3)
C(8A)-C(7A)-C(9A)-C(10A)	-17.9(4)
C(4A)-C(7A)-C(9A)-C(10A)	-130.9(3)
C(8A)-C(7A)-C(9A)-C(3A)	87.7(3)
C(4A)-C(7A)-C(9A)-C(3A)	-25.2(3)
C(2A)-C(3A)-C(9A)-C(10A)	14.8(4)
C(4A)-C(3A)-C(9A)-C(10A)	130.9(3)
C(2A)-C(3A)-C(9A)-C(7A)	-91.0(3)

C(4A)-C(3A)-C(9A)-C(7A)	25.1(3)
C(7A)-C(9A)-C(10A)-O(2A)	-74.3(4)
C(3A)-C(9A)-C(10A)-O(2A)	-164.0(3)
C(7A)-C(9A)-C(10A)-C(1A)	44.6(3)
C(3A)-C(9A)-C(10A)-C(1A)	-45.0(4)
C(11A)-C(1A)-C(10A)-O(2A)	-59.6(4)
C(2A)-C(1A)-C(10A)-O(2A)	176.1(2)
C(8A)-C(1A)-C(10A)-O(2A)	64.9(3)
C(11A)-C(1A)-C(10A)-C(9A)	-178.7(3)
C(2A)-C(1A)-C(10A)-C(9A)	57.0(3)
C(8A)-C(1A)-C(10A)-C(9A)	-54.2(3)
C(10B)-C(1B)-C(2B)-O(1B)	173.4(17)
C(11B)-C(1B)-C(2B)-O(1B)	-67(2)
C(8B)-C(1B)-C(2B)-O(1B)	51.9(17)
C(10B)-C(1B)-C(2B)-C(3B)	50.1(8)
C(11B)-C(1B)-C(2B)-C(3B)	170.1(18)
C(8B)-C(1B)-C(2B)-C(3B)	-71.3(17)
O(1B)-C(2B)-C(3B)-C(4B)	-49.8(16)
C(1B)-C(2B)-C(3B)-C(4B)	70.2(16)
O(1B)-C(2B)-C(3B)-C(9B)	-141.1(13)
C(1B)-C(2B)-C(3B)-C(9B)	-21.2(16)
C(2B)-C(3B)-C(4B)-C(5B)	51.1(13)
C(9B)-C(3B)-C(4B)-C(5B)	151.0(8)
C(2B)-C(3B)-C(4B)-C(7B)	-73.1(10)
C(9B)-C(3B)-C(4B)-C(7B)	26.8(6)
C(2B)-C(3B)-C(4B)-C(6B)	179(3)
C(9B)-C(3B)-C(4B)-C(6B)	-81(2)
C(5B)-C(4B)-C(7B)-C(9B)	-154.1(8)
C(3B)-C(4B)-C(7B)-C(9B)	-27.2(6)
C(6B)-C(4B)-C(7B)-C(9B)	81.5(9)
C(5B)-C(4B)-C(7B)-C(8B)	-47.2(9)
C(3B)-C(4B)-C(7B)-C(8B)	79.6(6)
C(6B)-C(4B)-C(7B)-C(8B)	-171.6(8)
C(10B)-C(1B)-C(8B)-C(7B)	-12(2)
C(11B)-C(1B)-C(8B)-C(7B)	-150(3)
C(2B)-C(1B)-C(8B)-C(7B)	88.2(13)

C(4B)-C(7B)-C(8B)-C(1B)	-105.3(14)
C(9B)-C(7B)-C(8B)-C(1B)	-17.7(15)
C(4B)-C(7B)-C(9B)-C(10B)	131.8(10)
C(8B)-C(7B)-C(9B)-C(10B)	41.4(11)
C(4B)-C(7B)-C(9B)-C(3B)	26.4(6)
C(8B)-C(7B)-C(9B)-C(3B)	-63.9(7)
C(2B)-C(3B)-C(9B)-C(10B)	-13.3(19)
C(4B)-C(3B)-C(9B)-C(10B)	-128.6(12)
C(2B)-C(3B)-C(9B)-C(7B)	88.8(11)
C(4B)-C(3B)-C(9B)-C(7B)	-26.5(6)
C(11B)-C(1B)-C(10B)-O(2B)	61(2)
C(2B)-C(1B)-C(10B)-O(2B)	-172.8(18)
C(8B)-C(1B)-C(10B)-O(2B)	-78(2)
C(11B)-C(1B)-C(10B)-C(9B)	177.3(17)
C(2B)-C(1B)-C(10B)-C(9B)	-56.9(11)
C(8B)-C(1B)-C(10B)-C(9B)	38(2)
C(7B)-C(9B)-C(10B)-O(2B)	74.9(15)
C(3B)-C(9B)-C(10B)-O(2B)	163.6(13)
C(7B)-C(9B)-C(10B)-C(1B)	-44.5(17)
C(3B)-C(9B)-C(10B)-C(1B)	44.2(18)

Symmetry transformations used to generate equivalent atoms:

A yellow block 0.23 x 0.13 x 0.09 mm in size was mounted on a Cryoloop with Paratone oil. Data were collected in a nitrogen gas stream at 100(2) K using omega scans. Crystal-to-detector distance was 33.00 mm and exposure time was 0.50 seconds per frame using a scan width of 0.5°. Data collection was 100% complete to 74.000° in θ. A total of 12788 reflections were collected covering the indices -8<=h<=8, -24<=k<=24, -10<=l<=10. 2325 reflections were found to be symmetry independent, with an R_{int} of 0.0382. Indexing and unit cell refinement indicated a primitive, monoclinic lattice. The space group was found to be P 21/n (No. 14). The data were integrated using the CrysAlis^{Pro} 1.172.42.72a software program and scaled using the SCALE3 ABSPACK scaling algorithm. Solution by intrinsic phasing (SHELXT-2015) produced a heavy-atom phasing model consistent with the proposed structure. All non-hydrogen atoms were refined anisotropically by full-matrix least-squares (SHELXL-2014). All hydrogen atoms were placed using a riding model. Their positions were constrained relative to their parent atom using the appropriate HFIX command in SHELXL-2014.

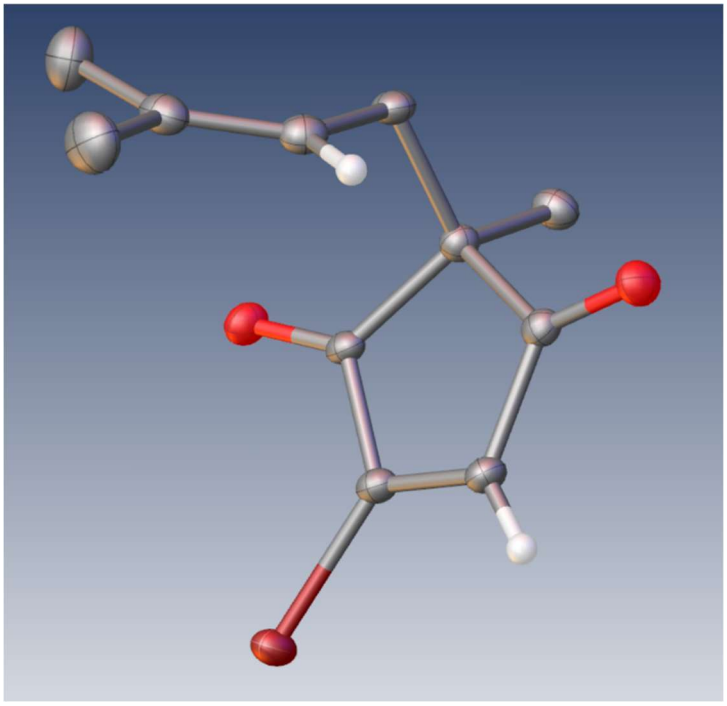

Table 1. Crystal data and structure refinement for IB007_Sarpong.

Identification code	IB007_Sarpong	
Empirical formula	C11 H13 Br O2	
Formula weight	257.12	
Temperature	100(2) K	
Wavelength	1.54184 Å	
Crystal system	Monoclinic	
Space group	P 21/n	
Unit cell dimensions	a = 6.69110(10) Å	a= 90°.
	b = 19.8327(3) Å	b= 99.3160(10)°.
	c = 8.71150(10) Å	g = 90°.
Volume	1140.79(3) $Å^3$	
Z	4	
Density (calculated)	1.497 Mg/m^3	
Absorption coefficient	4.700 mm^{-1}	
F(000)	520	
Crystal size	0.230 x 0.130 x 0.090 mm^3	
Theta range for data collection	4.459 to 74.440°.	
Index ranges	-8<=h<=8, -24<=k<=24, -10<=l<=10	
Reflections collected	12788	
Independent reflections	2325 [R(int) = 0.0382]	
Completeness to theta = 74.000°	99.5 %	
Absorption correction	Semi-empirical from equivalents	
Max. and min. transmission	1.00000 and 0.75728	
Refinement method	Full-matrix least-squares on F^2	
Data / restraints / parameters	2325 / 0 / 130	
Goodness-of-fit on F^2	1.088	
Final R indices [I>2sigma(I)]	R1 = 0.0294, wR2 = 0.0806	
R indices (all data)	R1 = 0.0297, wR2 = 0.0808	
Extinction coefficient	n/a	
Largest diff. peak and hole	0.452 and -0.679 $e.Å^{-3}$	

Table 2. Atomic coordinates (x 10^4) and equivalent isotropic displacement parameters ($Å^2$x 10^3)
for ib007_sarpong. U(eq) is defined as one third of the trace of the orthogonalized U^{ij} tensor.

	x	y	z	U(eq)
Br(1)	7462(1)	6067(1)	8900(1)	20(1)
O(1)	3697(2)	7239(1)	3871(2)	21(1)
O(2)	10182(2)	6625(1)	6437(2)	19(1)
C(1)	6793(3)	6506(1)	6997(2)	16(1)
C(2)	4940(3)	6660(1)	6257(2)	17(1)
C(3)	5115(3)	7039(1)	4815(2)	16(1)
C(4)	7350(3)	7149(1)	4722(2)	15(1)
C(5)	8398(3)	6745(1)	6112(2)	14(1)
C(6)	7894(3)	7900(1)	4963(2)	19(1)
C(7)	7935(3)	6883(1)	3191(2)	17(1)
C(8)	7348(3)	6158(1)	2864(2)	19(1)
C(9)	8572(3)	5631(1)	2783(2)	22(1)
C(10)	10839(4)	5669(1)	3006(3)	31(1)
C(11)	7703(4)	4939(1)	2387(3)	34(1)

Table 3. Bond lengths [Å] and angles [°] for ib007_sarpong.

Br(1)-C(1)	1.8620(19)
O(1)-C(3)	1.217(2)
O(2)-C(5)	1.205(2)
C(1)-C(2)	1.337(3)
C(1)-C(5)	1.497(2)
C(2)-C(3)	1.484(3)
C(2)-H(2)	0.9500
C(3)-C(4)	1.526(3)
C(4)-C(5)	1.525(3)
C(4)-C(6)	1.540(3)
C(4)-C(7)	1.542(3)
C(6)-H(6A)	0.9800
C(6)-H(6B)	0.9800
C(6)-H(6C)	0.9800
C(7)-C(8)	1.506(3)
C(7)-H(7A)	0.9900
C(7)-H(7B)	0.9900
C(8)-C(9)	1.336(3)
C(8)-H(8)	0.9500
C(9)-C(10)	1.499(3)
C(9)-C(11)	1.509(3)
C(10)-H(10A)	0.9800
C(10)-H(10B)	0.9800
C(10)-H(10C)	0.9800
C(11)-H(11A)	0.9800
C(11)-H(11B)	0.9800
C(11)-H(11C)	0.9800
C(2)-C(1)-C(5)	111.46(17)
C(2)-C(1)-Br(1)	127.37(15)
C(5)-C(1)-Br(1)	121.16(14)
C(1)-C(2)-C(3)	109.26(17)
C(1)-C(2)-H(2)	125.4
C(3)-C(2)-H(2)	125.4

O(1)-C(3)-C(2)	125.24(18)
O(1)-C(3)-C(4)	125.52(17)
C(2)-C(3)-C(4)	109.23(16)
C(5)-C(4)-C(3)	102.20(15)
C(5)-C(4)-C(6)	109.35(15)
C(3)-C(4)-C(6)	110.04(16)
C(5)-C(4)-C(7)	111.03(16)
C(3)-C(4)-C(7)	112.66(16)
C(6)-C(4)-C(7)	111.19(16)
O(2)-C(5)-C(1)	125.62(17)
O(2)-C(5)-C(4)	126.95(17)
C(1)-C(5)-C(4)	107.42(15)
C(4)-C(6)-H(6A)	109.5
C(4)-C(6)-H(6B)	109.5
H(6A)-C(6)-H(6B)	109.5
C(4)-C(6)-H(6C)	109.5
H(6A)-C(6)-H(6C)	109.5
H(6B)-C(6)-H(6C)	109.5
C(8)-C(7)-C(4)	113.27(16)
C(8)-C(7)-H(7A)	108.9
C(4)-C(7)-H(7A)	108.9
C(8)-C(7)-H(7B)	108.9
C(4)-C(7)-H(7B)	108.9
H(7A)-C(7)-H(7B)	107.7
C(9)-C(8)-C(7)	127.8(2)
C(9)-C(8)-H(8)	116.1
C(7)-C(8)-H(8)	116.1
C(8)-C(9)-C(10)	124.8(2)
C(8)-C(9)-C(11)	120.4(2)
C(10)-C(9)-C(11)	114.8(2)
C(9)-C(10)-H(10A)	109.5
C(9)-C(10)-H(10B)	109.5
H(10A)-C(10)-H(10B)	109.5
C(9)-C(10)-H(10C)	109.5
H(10A)-C(10)-H(10C)	109.5
H(10B)-C(10)-H(10C)	109.5

C(9)-C(11)-H(11A)	109.5
C(9)-C(11)-H(11B)	109.5
H(11A)-C(11)-H(11B)	109.5
C(9)-C(11)-H(11C)	109.5
H(11A)-C(11)-H(11C)	109.5
H(11B)-C(11)-H(11C)	109.5

Symmetry transformations used to generate equivalent atoms:

Table 4. Anisotropic displacement parameters ($Å^2 x\ 10^3$)for ib007_sarpong. The anisotropic displacement factor exponent takes the form: $-2p^2[\ h^2 a^{*2} U^{11} + ... + 2\ h\ k\ a^*\ b^*\ U^{12}\ ]$

	U^{11}	U^{22}	U^{33}	U^{23}	U^{13}	U^{12}
Br(1)	20(1)	25(1)	16(1)	6(1)	5(1)	1(1)
O(1)	18(1)	25(1)	20(1)	3(1)	1(1)	2(1)
O(2)	13(1)	24(1)	19(1)	0(1)	3(1)	1(1)
C(1)	17(1)	16(1)	15(1)	-1(1)	6(1)	-1(1)
C(2)	16(1)	19(1)	16(1)	0(1)	6(1)	1(1)
C(3)	16(1)	15(1)	16(1)	-2(1)	4(1)	0(1)
C(4)	14(1)	17(1)	15(1)	0(1)	3(1)	-1(1)
C(5)	16(1)	14(1)	13(1)	-1(1)	6(1)	-1(1)
C(6)	23(1)	16(1)	17(1)	1(1)	3(1)	-3(1)
C(7)	20(1)	19(1)	14(1)	0(1)	7(1)	-1(1)
C(8)	20(1)	23(1)	15(1)	-1(1)	3(1)	-3(1)
C(9)	29(1)	20(1)	17(1)	1(1)	5(1)	-2(1)
C(10)	28(1)	27(1)	39(1)	-4(1)	4(1)	5(1)
C(11)	40(1)	21(1)	40(1)	-3(1)	8(1)	-2(1)

Table 5. Hydrogen coordinates (x 10^4) and isotropic displacement parameters (Å^{2}x 10^3) for ib007_sarpong.

	x	y	z	U(eq)
H(2)	3706	6546	6599	20
H(6A)	7549	8051	5959	28
H(6B)	7130	8165	4116	28
H(6C)	9348	7961	4969	28
H(7A)	7269	7166	2319	21
H(7B)	9417	6929	3240	21
H(8)	5937	6063	2694	23
H(10A)	11303	5569	2020	47
H(10B)	11416	5341	3795	47
H(10C)	11278	6124	3350	47
H(11A)	6222	4959	2263	50
H(11B)	8215	4624	3226	50
H(11C)	8108	4784	1414	50

Table 6. Torsion angles [°] for ib007_sarpong.

C(5)-C(1)-C(2)-C(3)	-1.7(2)
Br(1)-C(1)-C(2)-C(3)	177.19(14)
C(1)-C(2)-C(3)-O(1)	178.35(19)
C(1)-C(2)-C(3)-C(4)	-2.7(2)
O(1)-C(3)-C(4)-C(5)	-175.42(18)
C(2)-C(3)-C(4)-C(5)	5.61(19)
O(1)-C(3)-C(4)-C(6)	68.5(2)
C(2)-C(3)-C(4)-C(6)	-110.47(18)
O(1)-C(3)-C(4)-C(7)	-56.2(3)
C(2)-C(3)-C(4)-C(7)	124.83(17)
C(2)-C(1)-C(5)-O(2)	-173.30(19)
Br(1)-C(1)-C(5)-O(2)	7.7(3)
C(2)-C(1)-C(5)-C(4)	5.4(2)
Br(1)-C(1)-C(5)-C(4)	-173.57(13)
C(3)-C(4)-C(5)-O(2)	172.25(19)
C(6)-C(4)-C(5)-O(2)	-71.2(2)
C(7)-C(4)-C(5)-O(2)	51.9(3)
C(3)-C(4)-C(5)-C(1)	-6.42(19)
C(6)-C(4)-C(5)-C(1)	110.16(17)
C(7)-C(4)-C(5)-C(1)	-126.78(16)
C(5)-C(4)-C(7)-C(8)	60.6(2)
C(3)-C(4)-C(7)-C(8)	-53.3(2)
C(6)-C(4)-C(7)-C(8)	-177.40(17)
C(4)-C(7)-C(8)-C(9)	-115.6(2)
C(7)-C(8)-C(9)-C(10)	-0.3(4)
C(7)-C(8)-C(9)-C(11)	-177.9(2)

Symmetry transformations used to generate equivalent atoms:

Copies of NMR Spectra

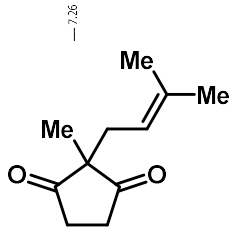

S-1

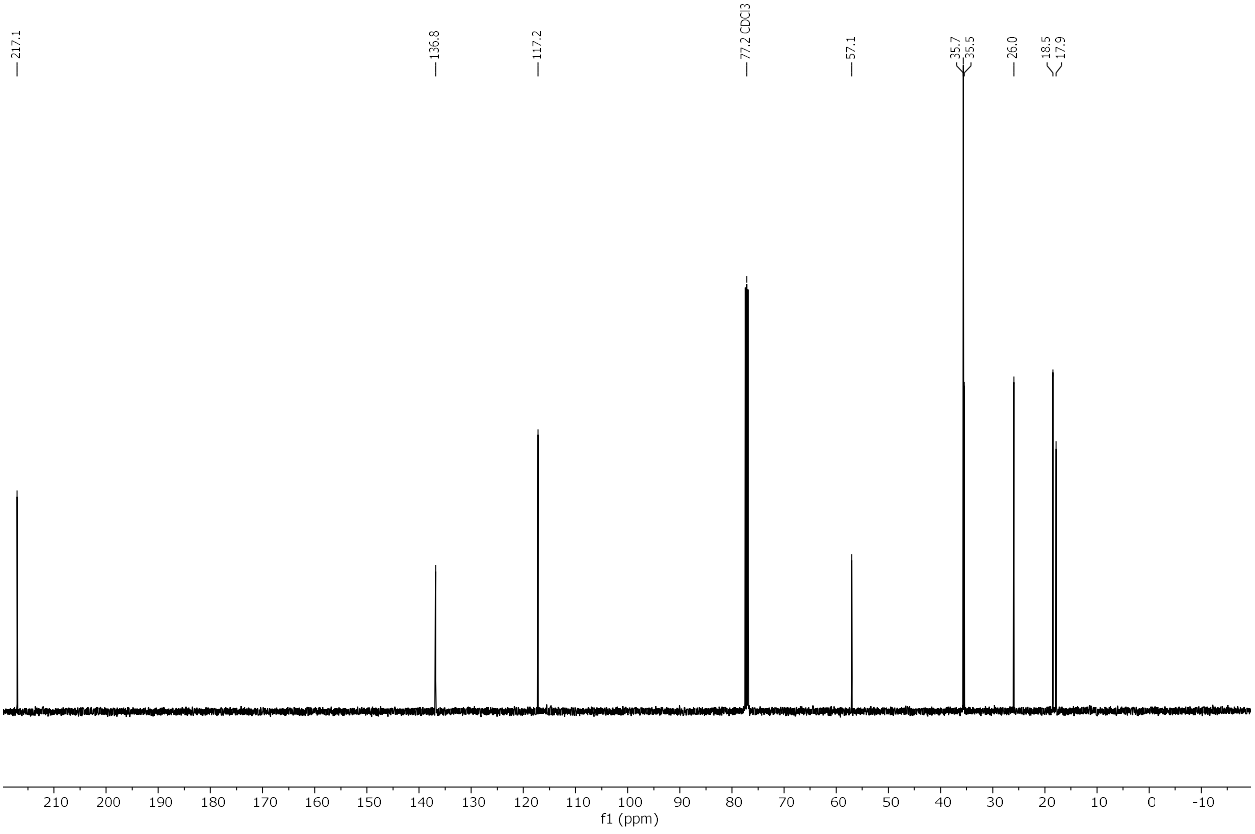

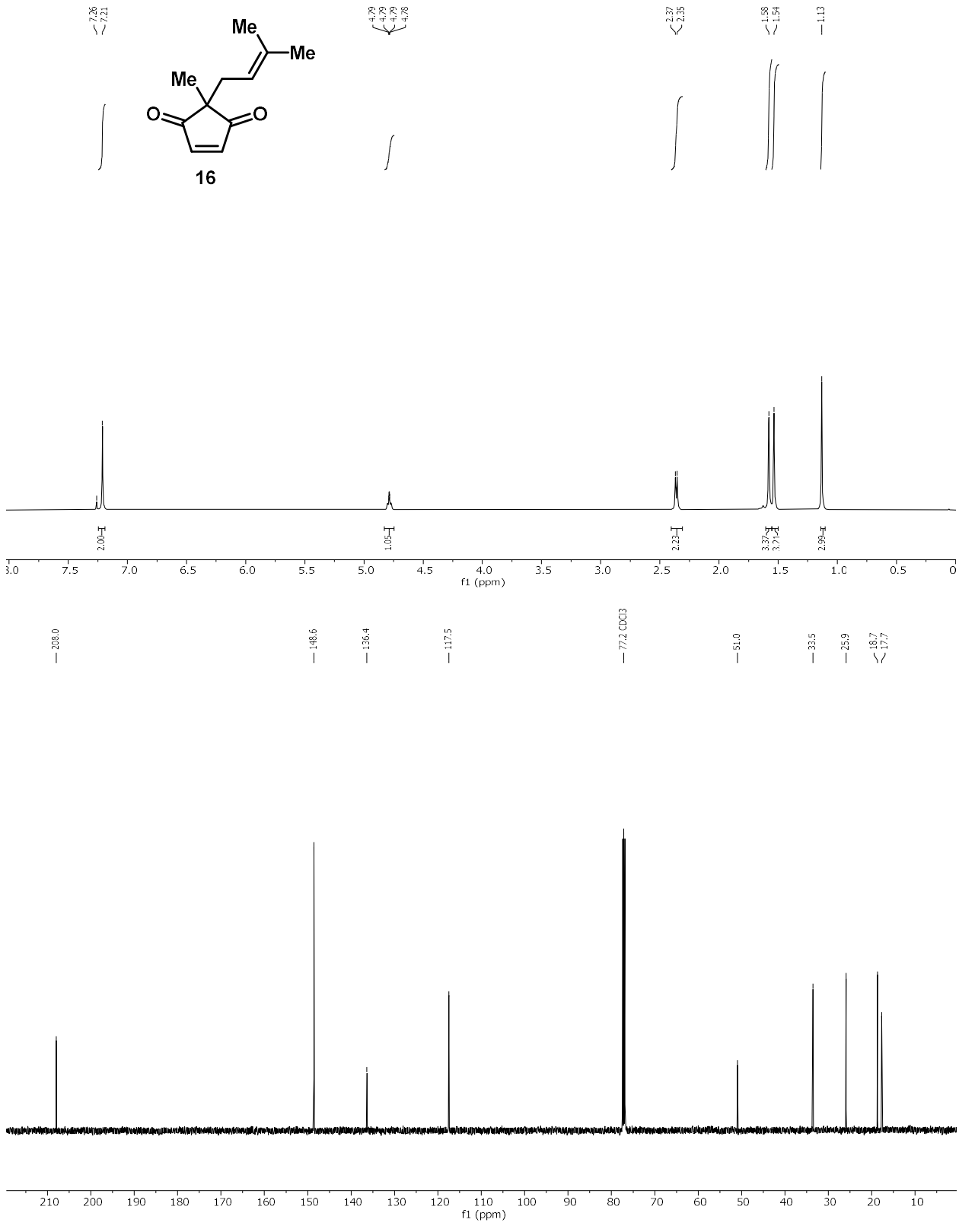
Me
Me
Me
O
O
16
f1 (ppm)
f1 (ppm)

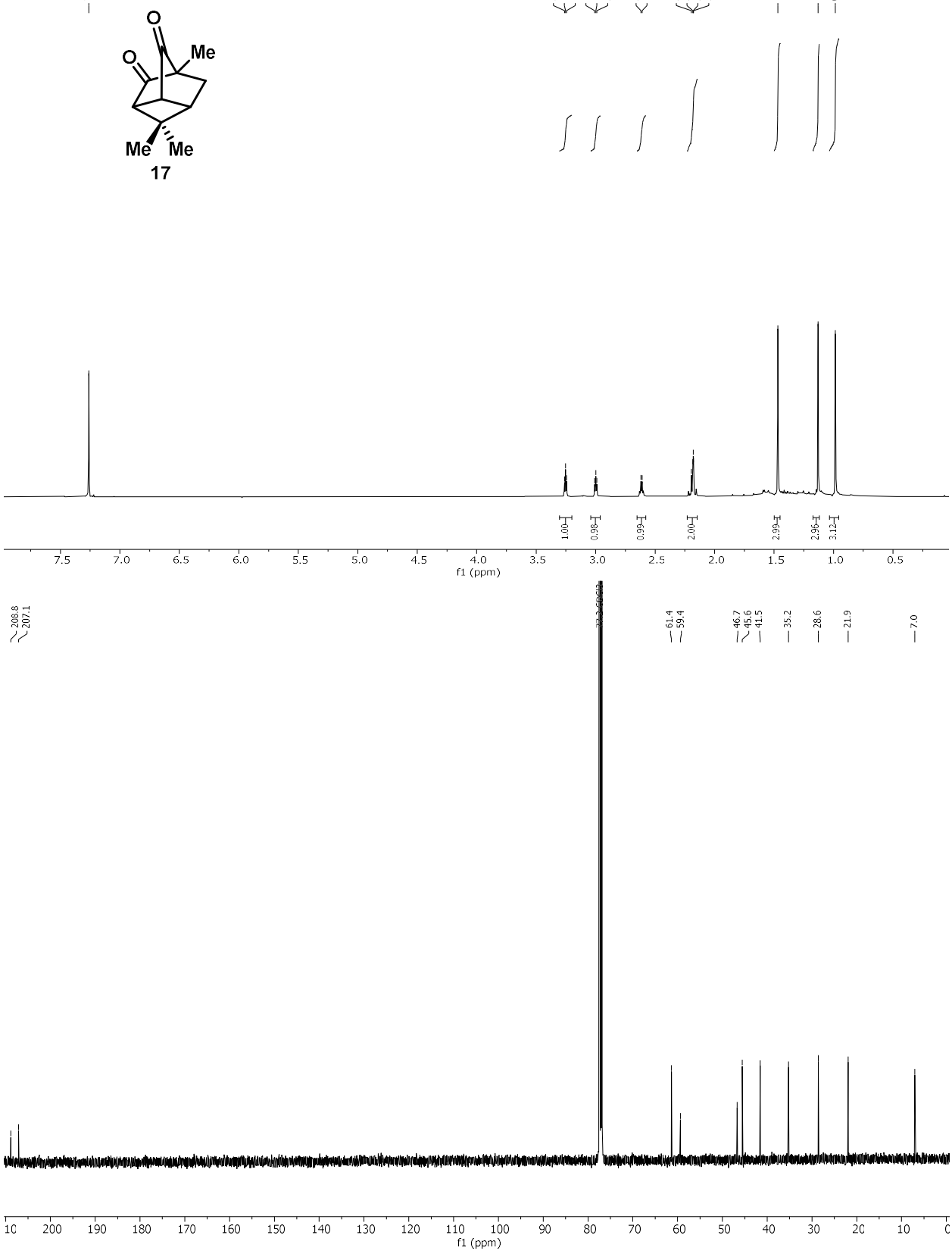
7.26
3.26
3.25
3.24
3.01
3.00
2.99
2.62
2.61
2.19
2.18
2.18
2.18
1.47
1.13
0.98
O
O
Me
Me
Me
17
1.00
0.98
0.99
2.00
2.99
2.96
3.12
7.5
7.0
6.5
6.0
5.5
5.0
4.5
4.0
3.5
3.0
2.5
2.0
1.5
1.0
0.5
f1 (ppm)
208.8
207.1
77.3
77.0
76.8
61.4
59.4
46.7
45.6
41.5
35.2
28.6
21.9
7.0
210
200
190
180
170
160
150
140
130
120
110
100
90
80
70
60
50
40
30
20
10
0
f1 (ppm)

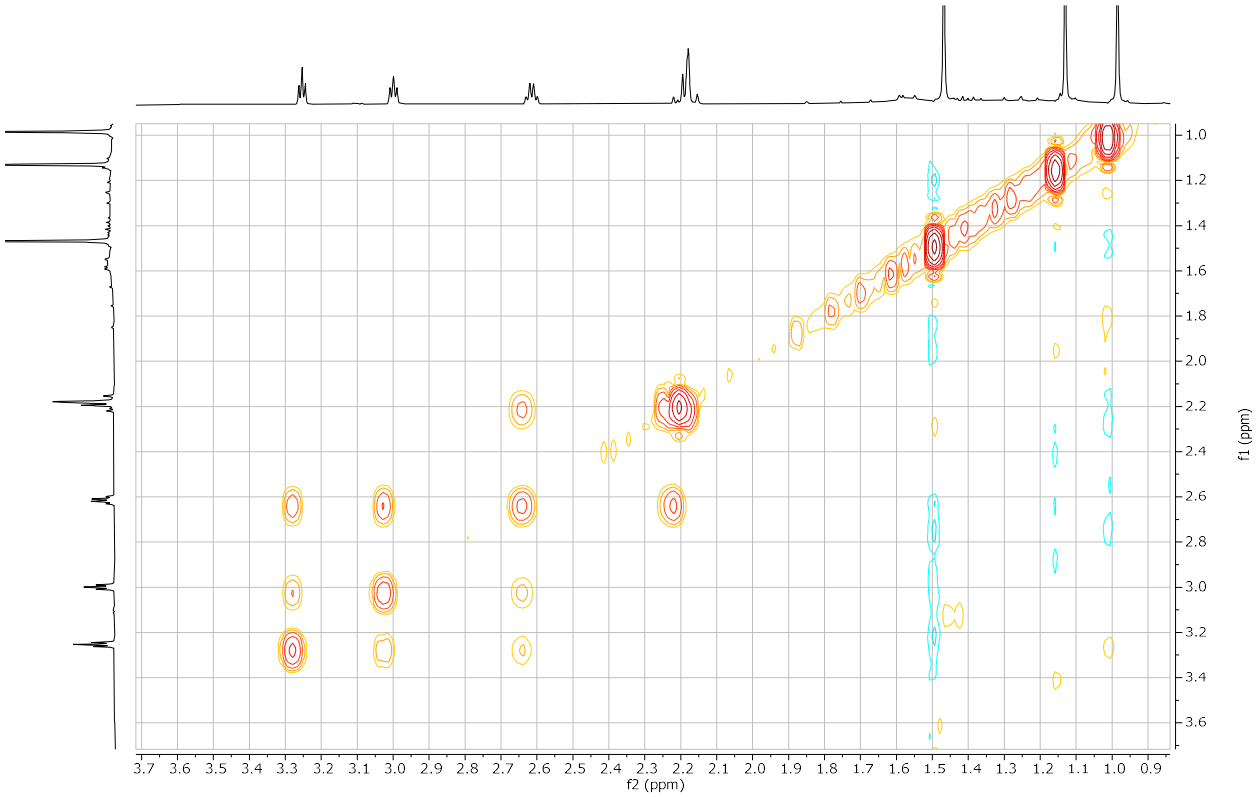
f1 (ppm)
f2 (ppm)

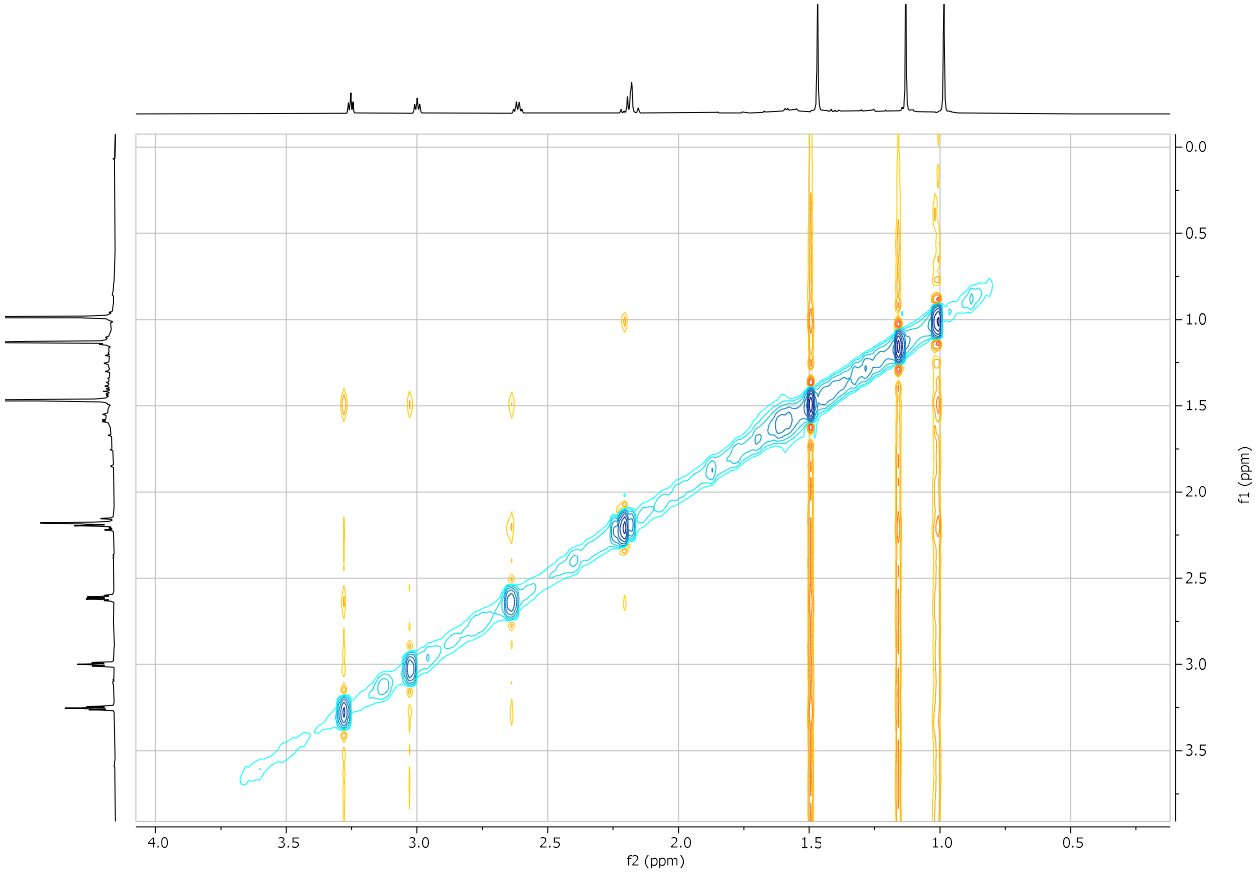
f1 (ppm)
f2 (ppm)

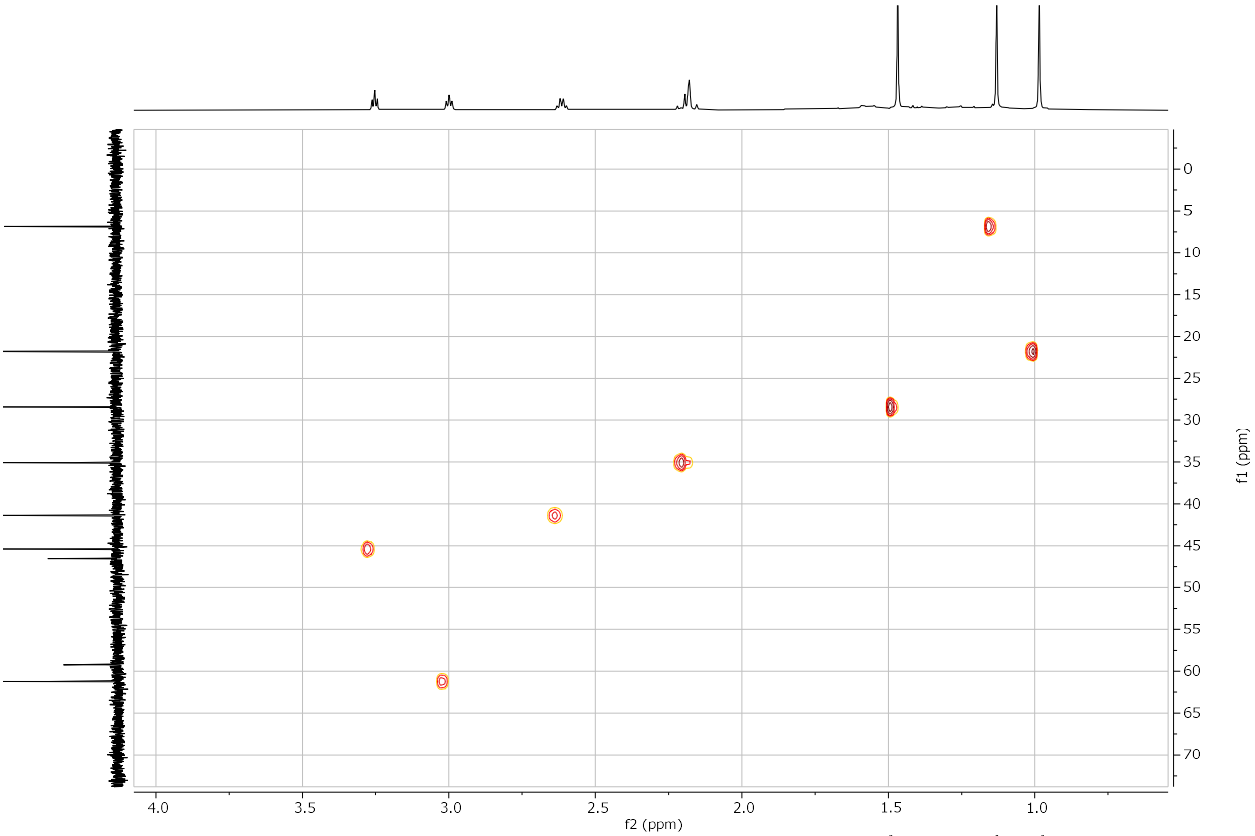
0
5
10
15
20
25
30
35
40
45
50
55
60
65
70
f1 (ppm)
4.0
3.5
3.0
2.5
2.0
1.5
1.0
f2 (ppm)

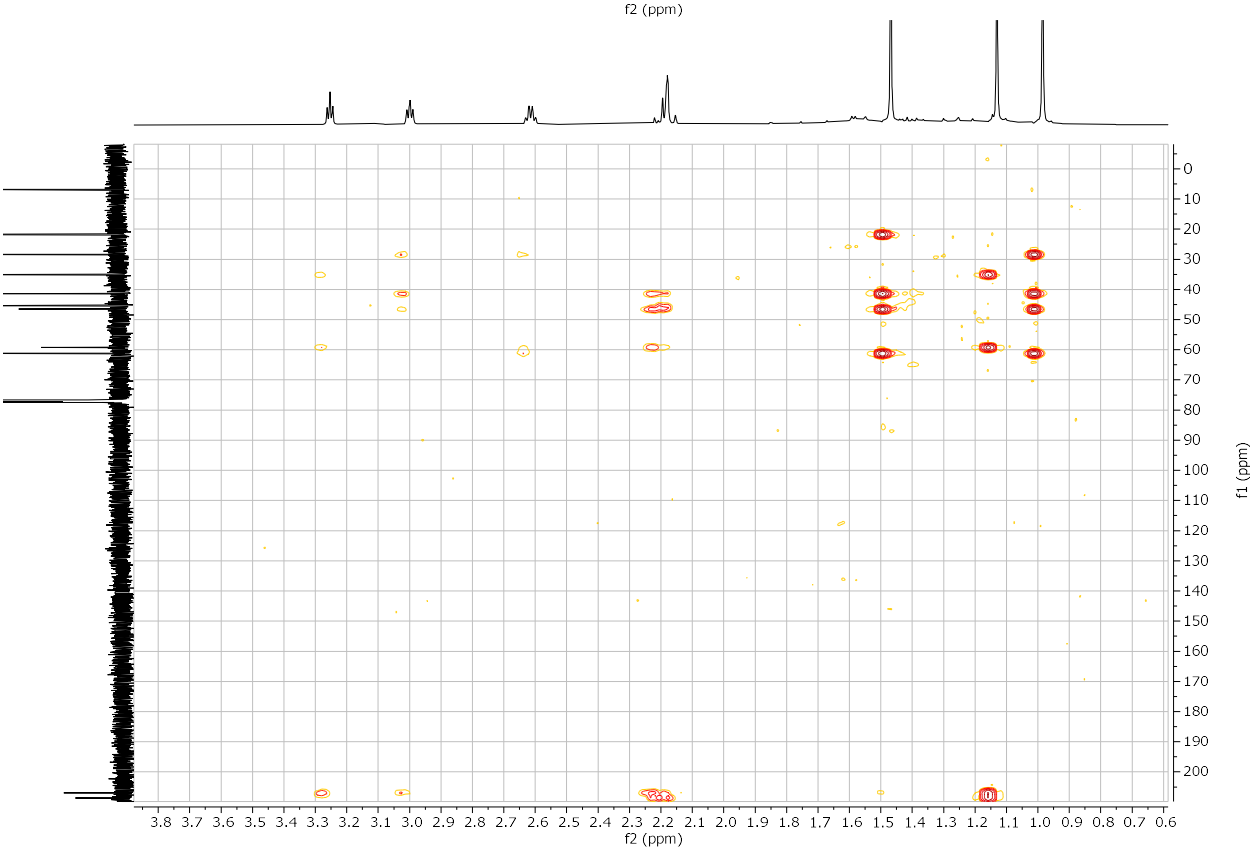
0
10
20
30
40
50
60
70
80
90
100
110
120
130
140
150
160
170
180
190
200
f1 (ppm)
3.8 3.7 3.6 3.5 3.4 3.3 3.2 3.1 3.0 2.9 2.8 2.7 2.6 2.5 2.4 2.3 2.2 2.1 2.0 1.9 1.8 1.7 1.6 1.5 1.4 1.3 1.2 1.1 1.0 0.9 0.8 0.7 0.6
f2 (ppm)

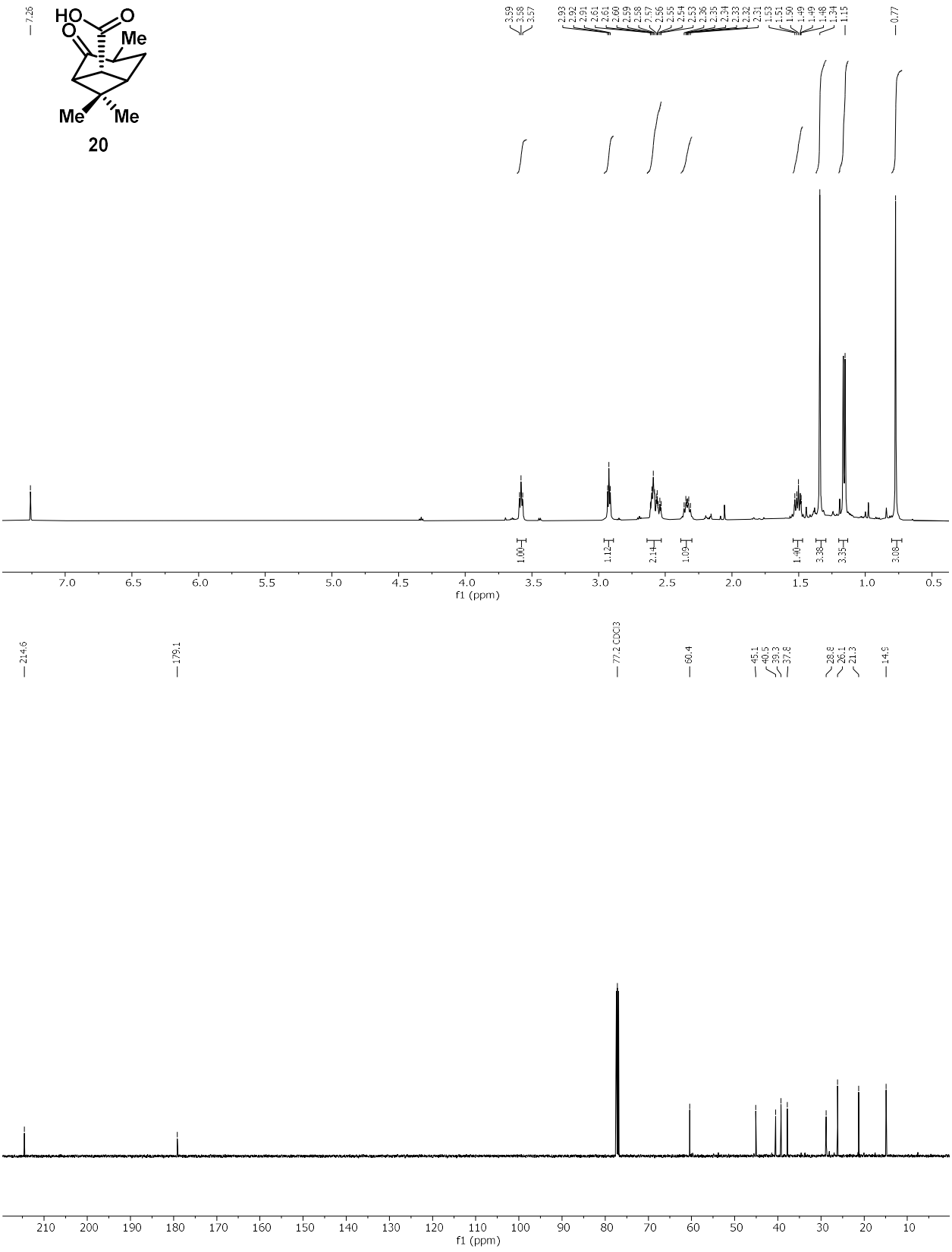
HO
O
O
Me
Me
Me
20
f1 (ppm)
CDCl3
f1 (ppm)

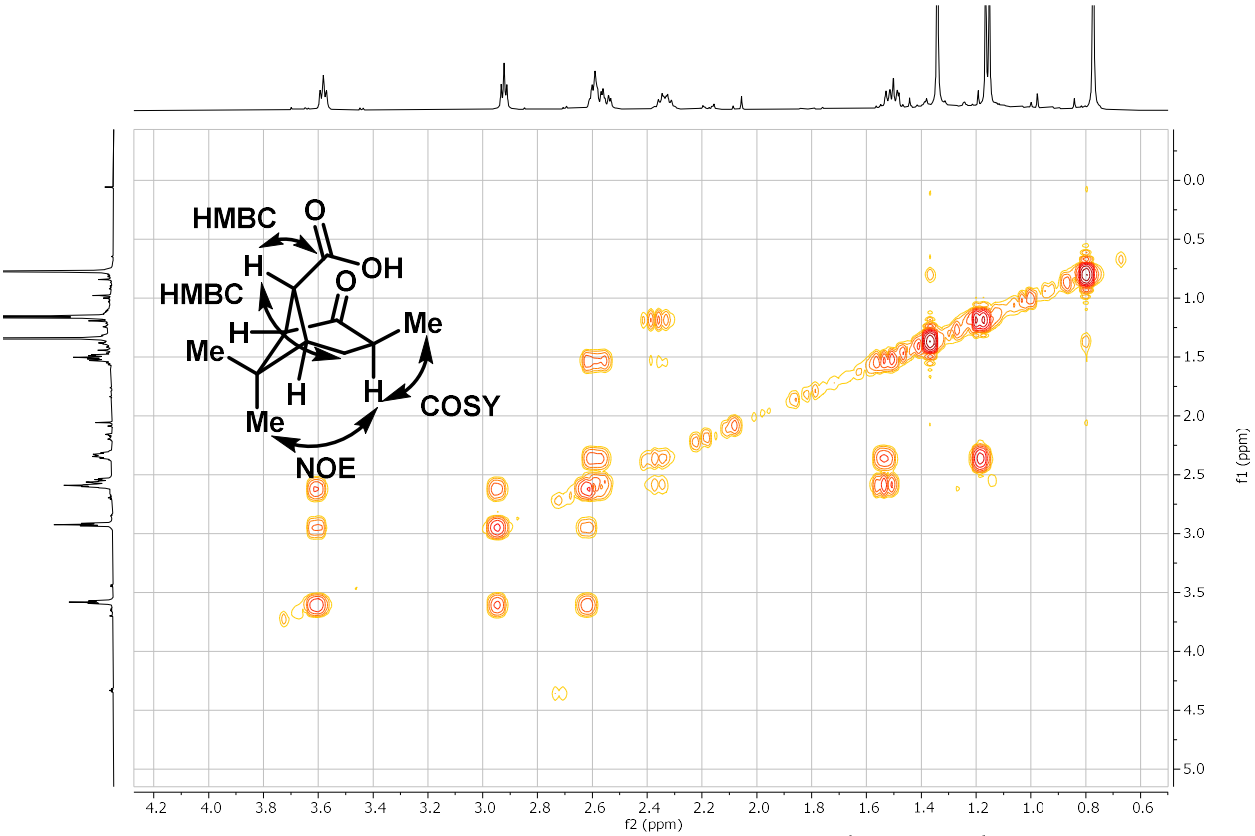
HMBC
O
H
OH
HMBC
O
H
Me
Me
H
H
COSY
Me
NOE
f2 (ppm)
f1 (ppm)

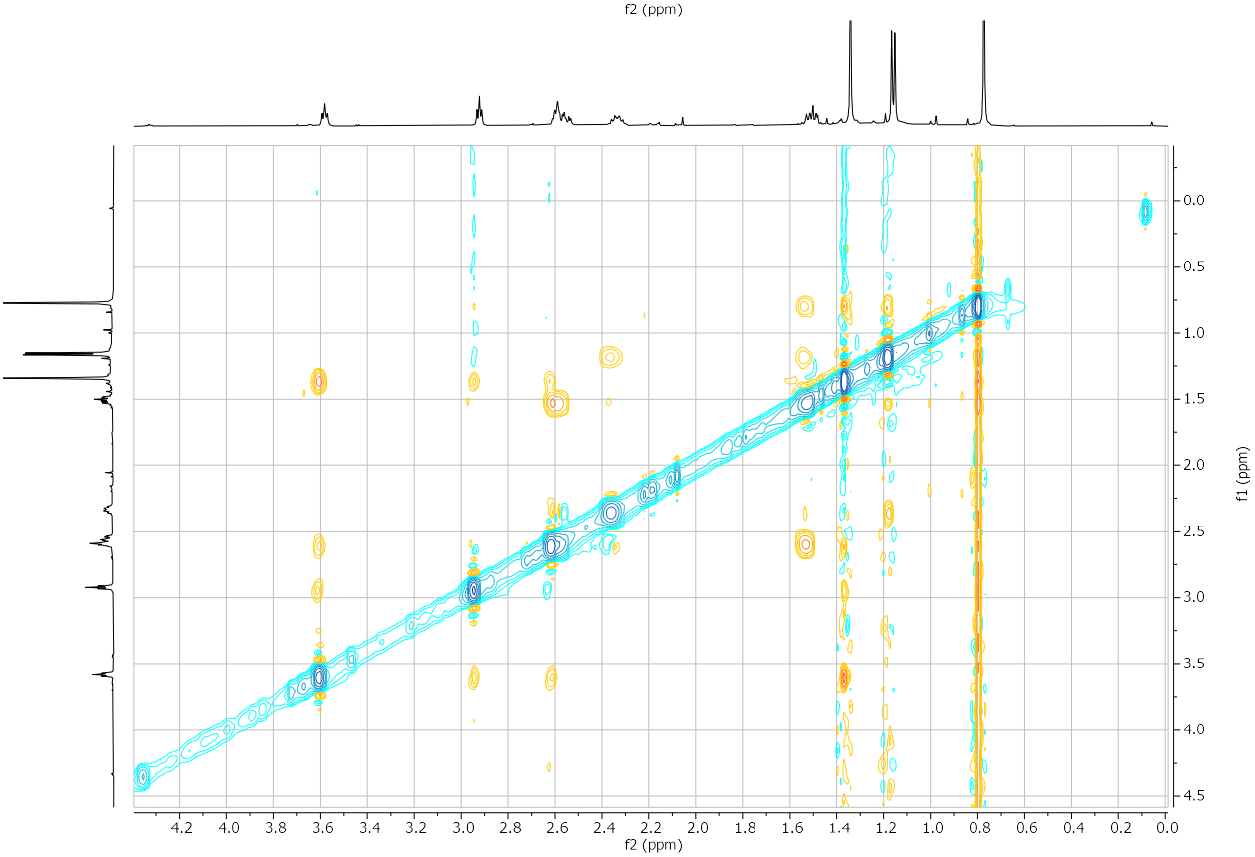
f2 (ppm)
f1 (ppm)

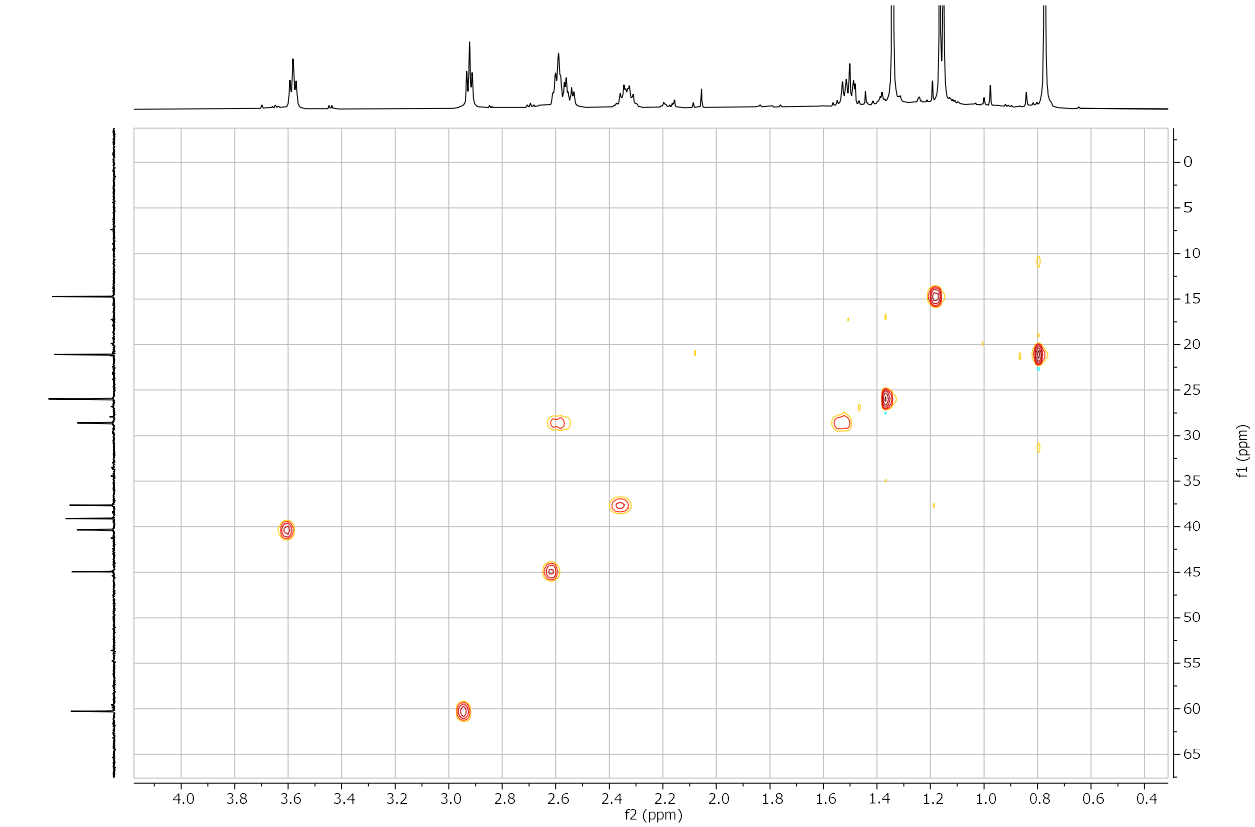
f2 (ppm)
f1 (ppm)

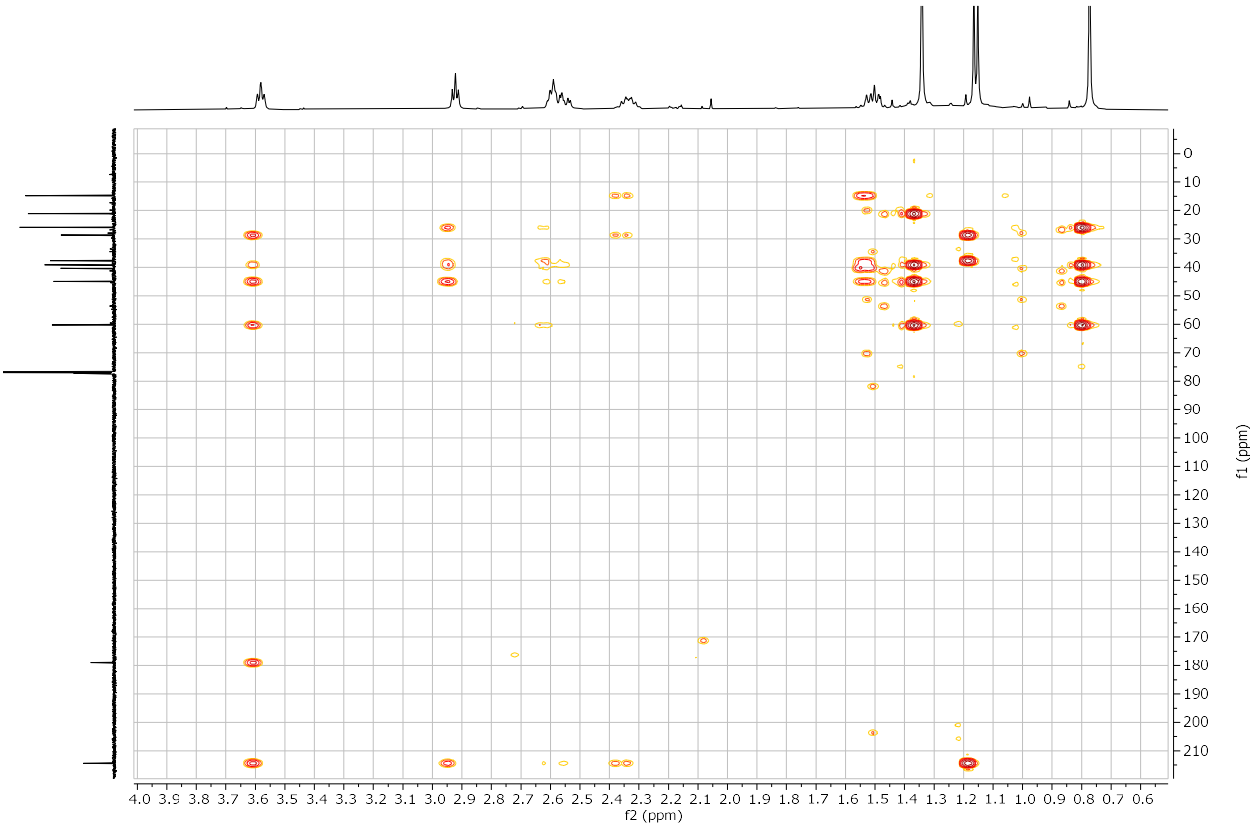
f2 (ppm)
f1 (ppm)

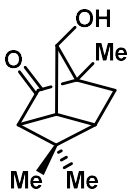
OH
O
Me
Me
Me

S-2

7.26
3.58
3.57
3.14
3.13
3.13
3.12
3.12
3.11
2.40
2.39
2.38
2.38
2.36
2.35
2.34
2.21
2.19
2.17
2.16
1.59
1.56
1.29
1.08
0.75
1.00
1.04
2.39
1.12
1.11
3.25
3.25
3.11
f1 (ppm)

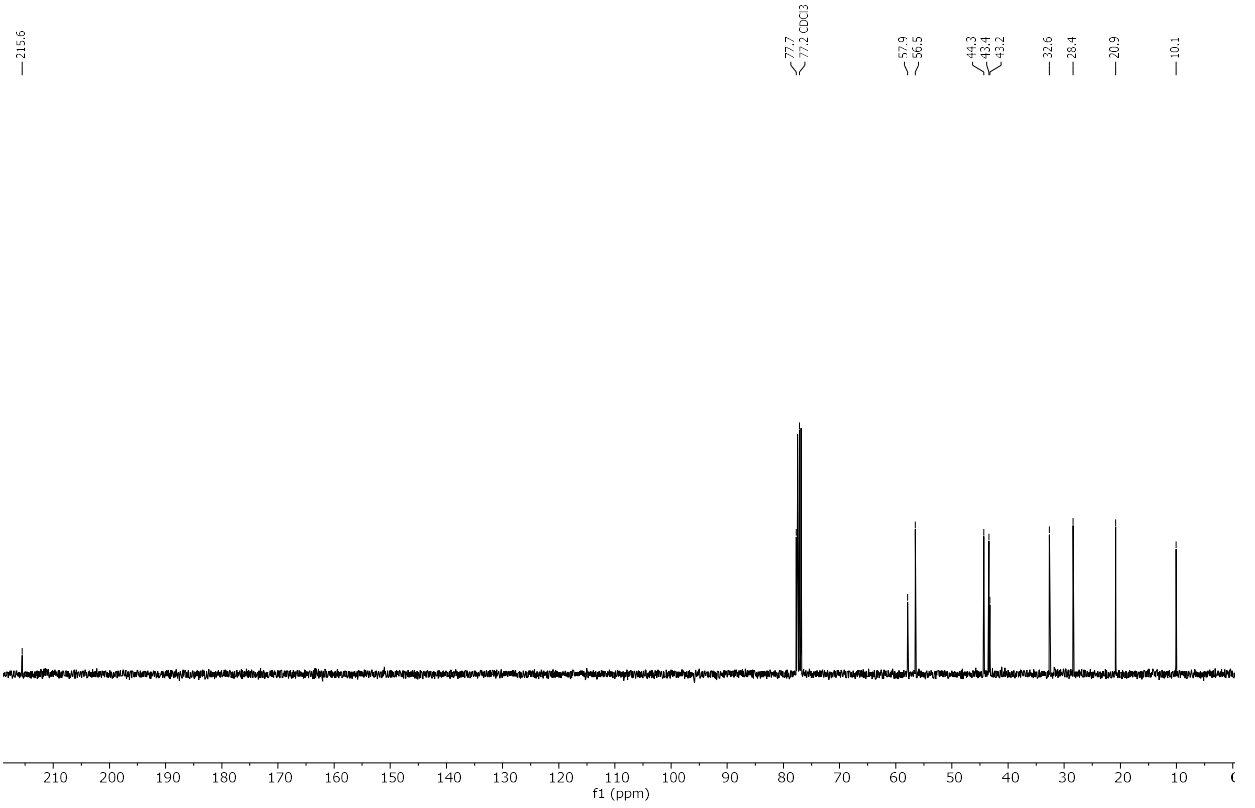
215.6
77.7
77.2 CDCl3
57.9
56.5
44.3
43.4
43.2
32.6
28.4
20.9
10.1
f1 (ppm)

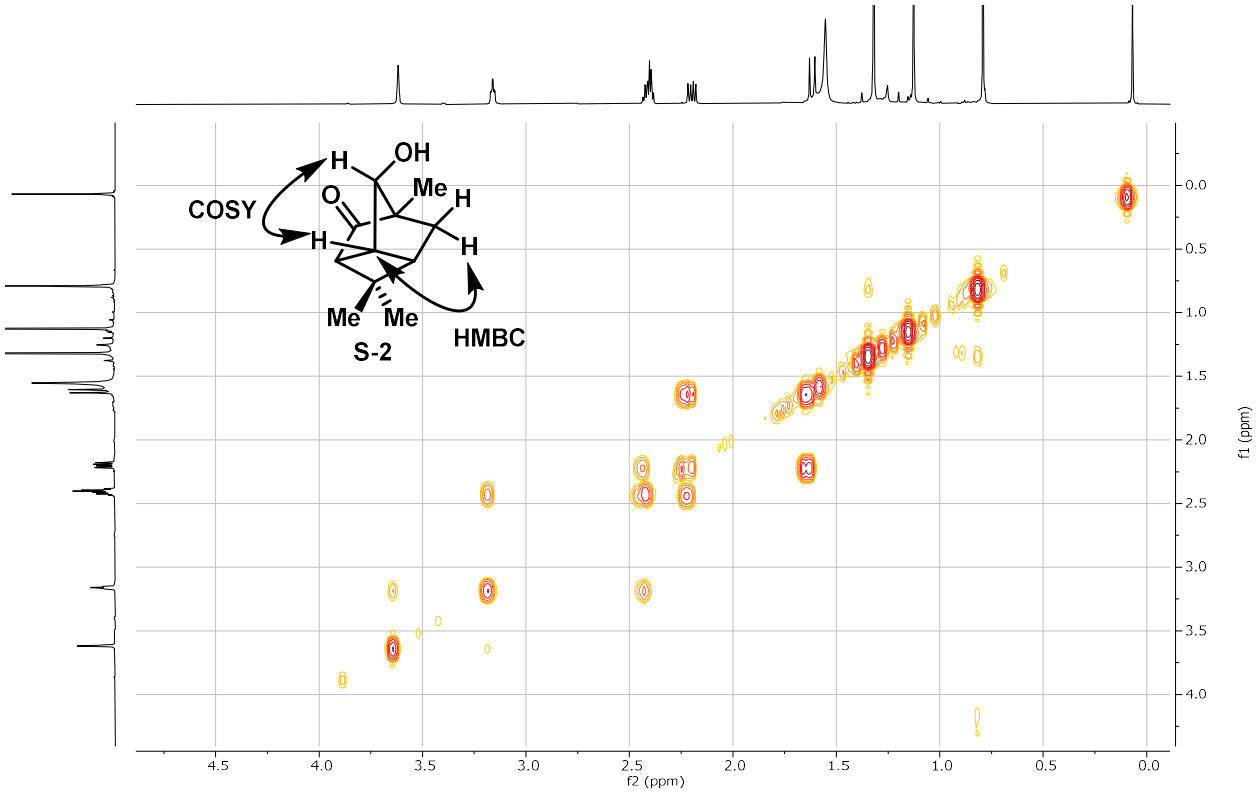
COSY
H
OH
O
Me
H
H
H
Me
Me
HMBC
S-2
f2 (ppm)
f1 (ppm)

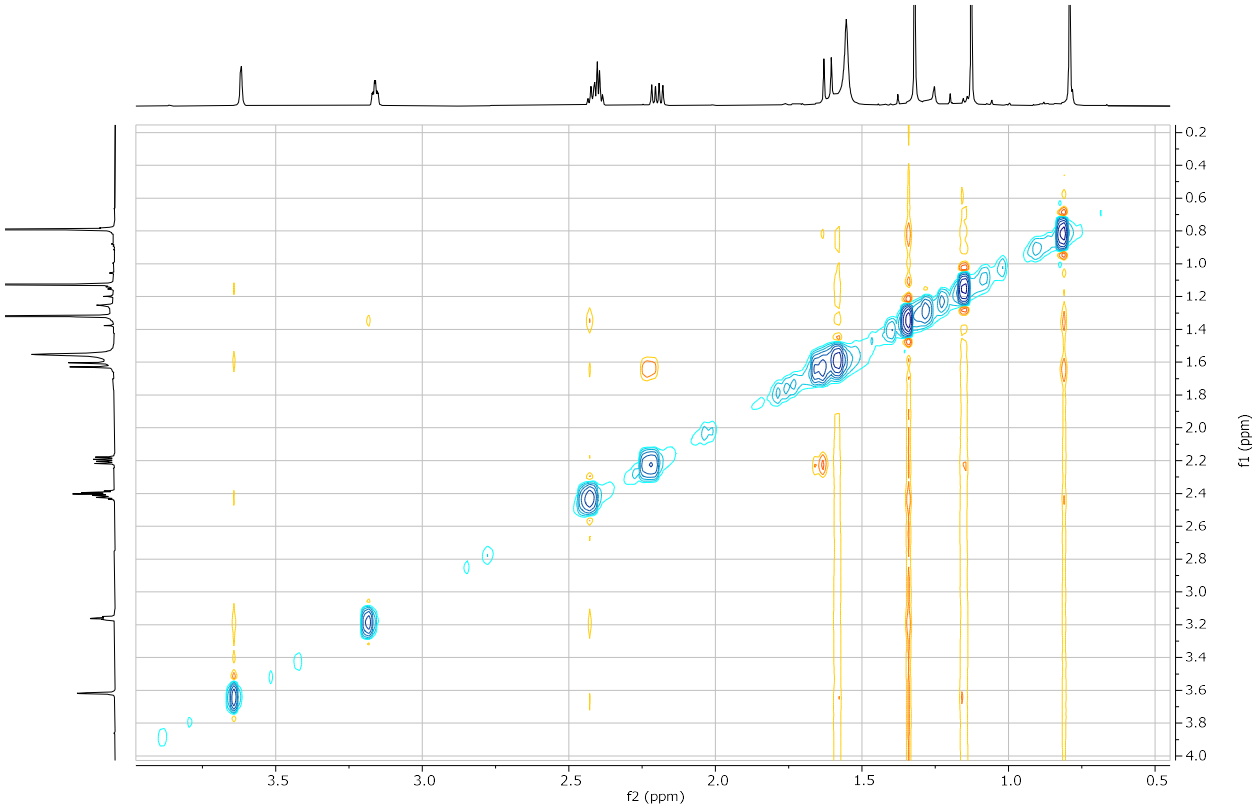
f2 (ppm)
f1 (ppm)

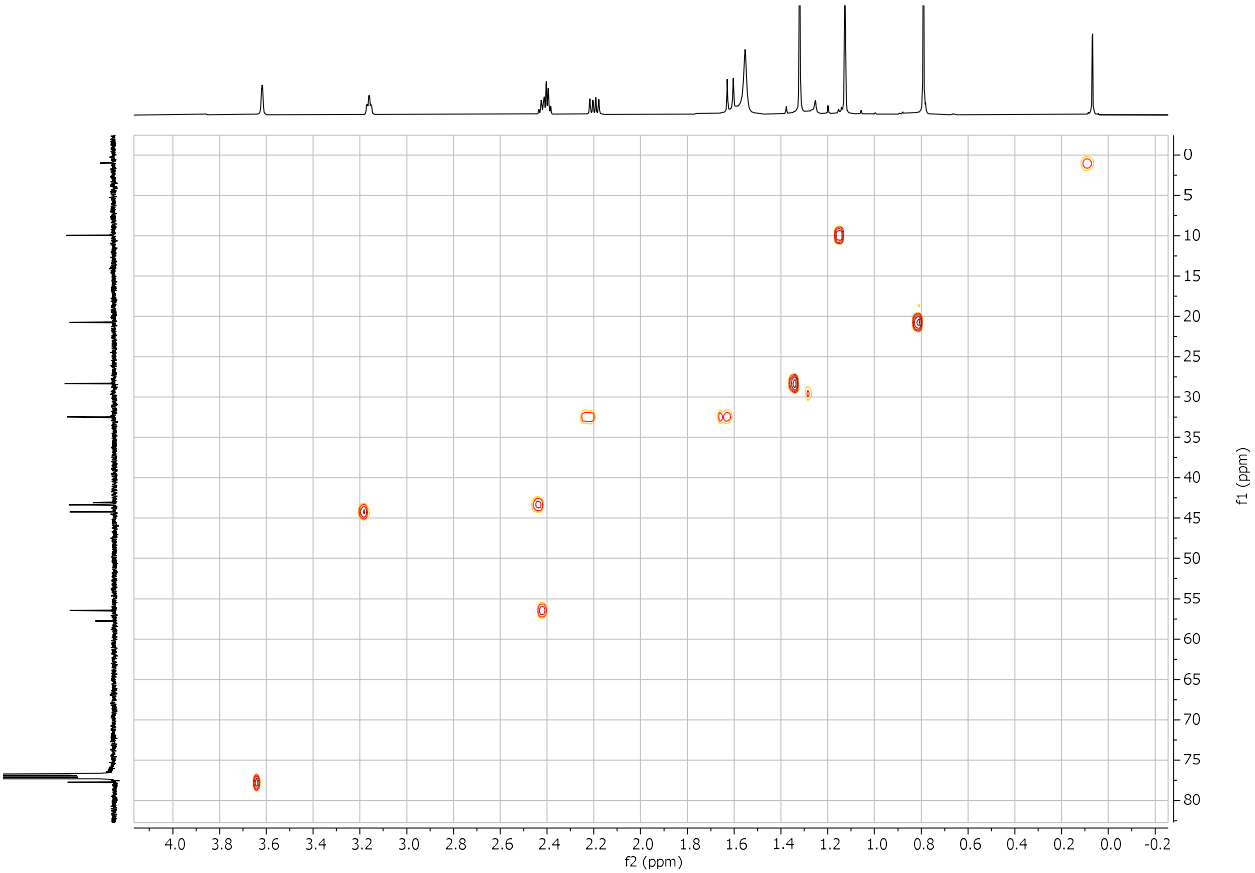
f2 (ppm)
f1 (ppm)

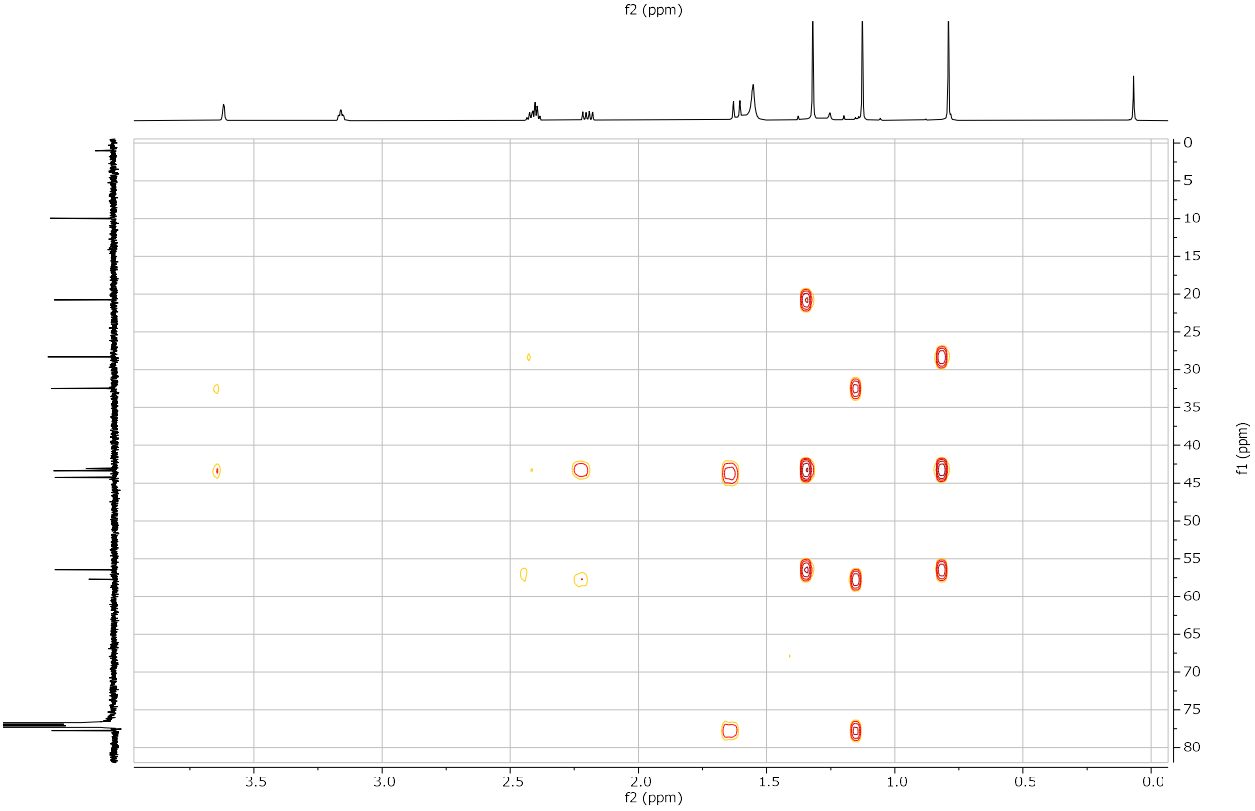
f2 (ppm)
f1 (ppm)

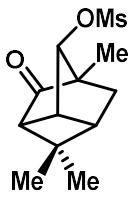
OMs
Me
O
Me
Me

S-3

4.42
4.42
3.47
3.47
3.46
3.46
3.45
3.45
3.04
2.52
2.51
2.50
2.49
2.49
2.48
2.47
2.23
2.21
2.20
2.18
1.74
1.71
1.33
1.18
0.80
1.00
1.07
3.17
2.04
1.14
1.10
3.33
3.30
3.31
f1 (ppm)

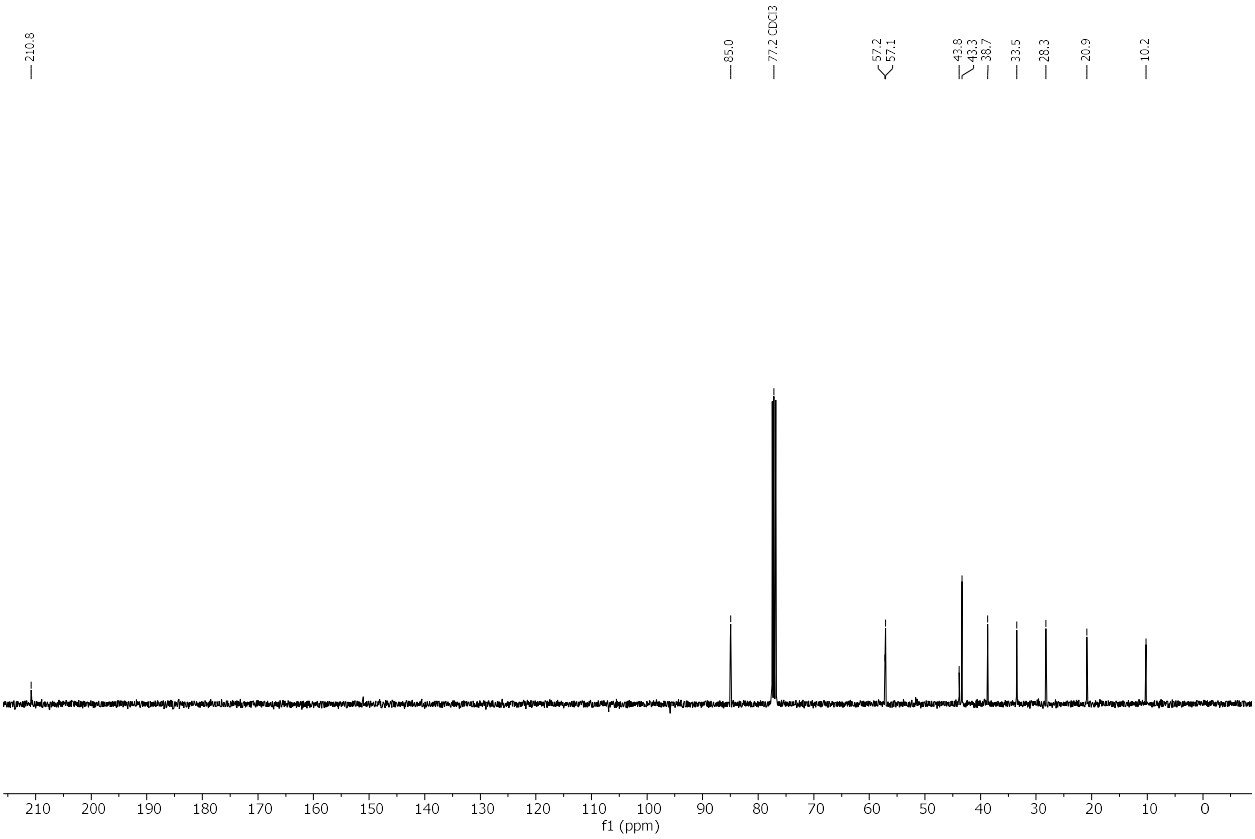
210.8
85.0
77.2 CDCl3
57.2
57.1
43.8
43.3
38.7
33.5
28.3
20.9
10.2
f1 (ppm)

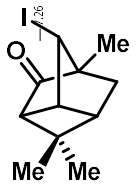
I
O
Me
Me
Me

21

3.99
3.98
3.44
3.43
3.43
3.42
3.42
3.41
2.46
2.45
2.44
2.31
2.30
2.29
2.28
1.75
1.74
1.73
1.31
1.16
0.80
1.00
0.97
1.03
0.96
1.91
3.26
3.04
3.12
f1 (ppm)

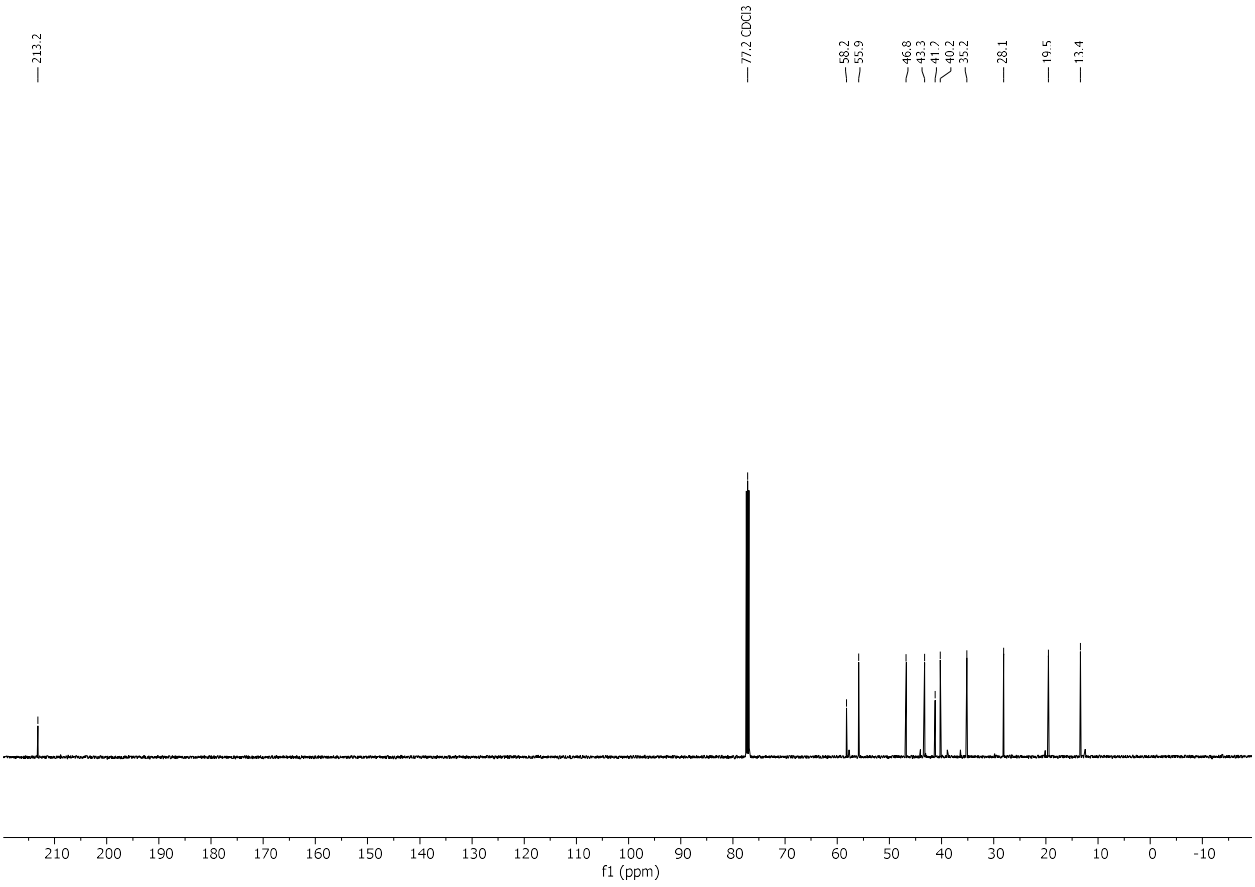
213.2
77.2 CDCl3
58.2
55.9
46.8
43.3
41.7
40.2
35.2
28.1
19.5
13.4
f1 (ppm)

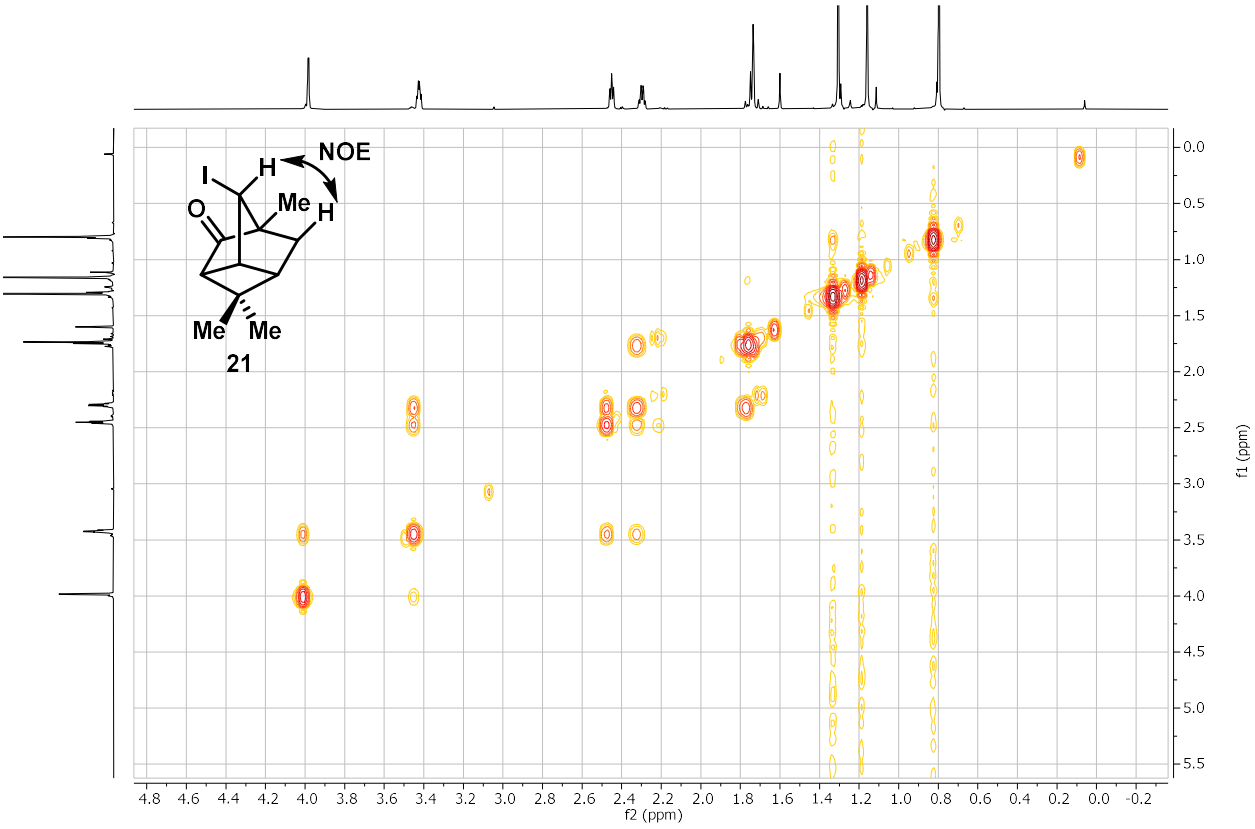
NOE
I
H
O
Me
H
Me
Me
21
f2 (ppm)
f1 (ppm)

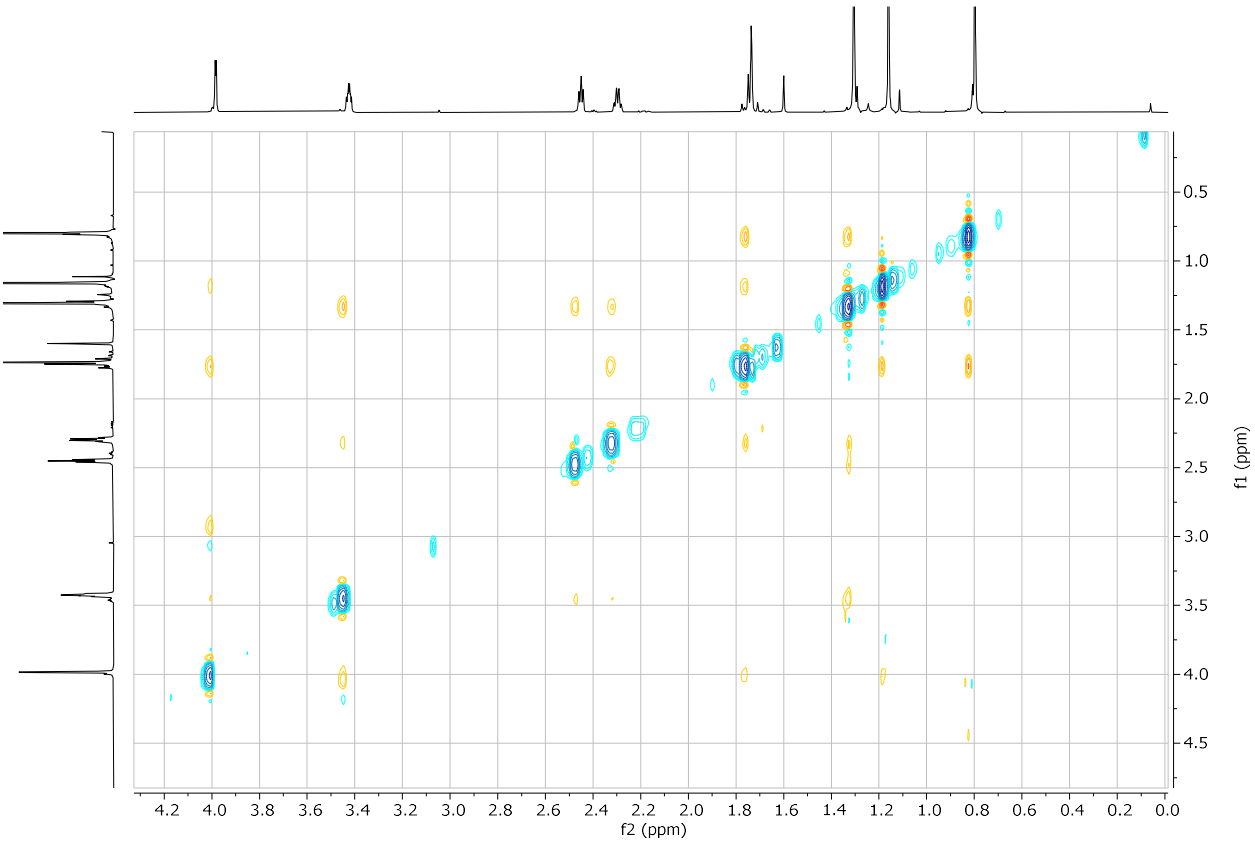
f2 (ppm)
f1 (ppm)

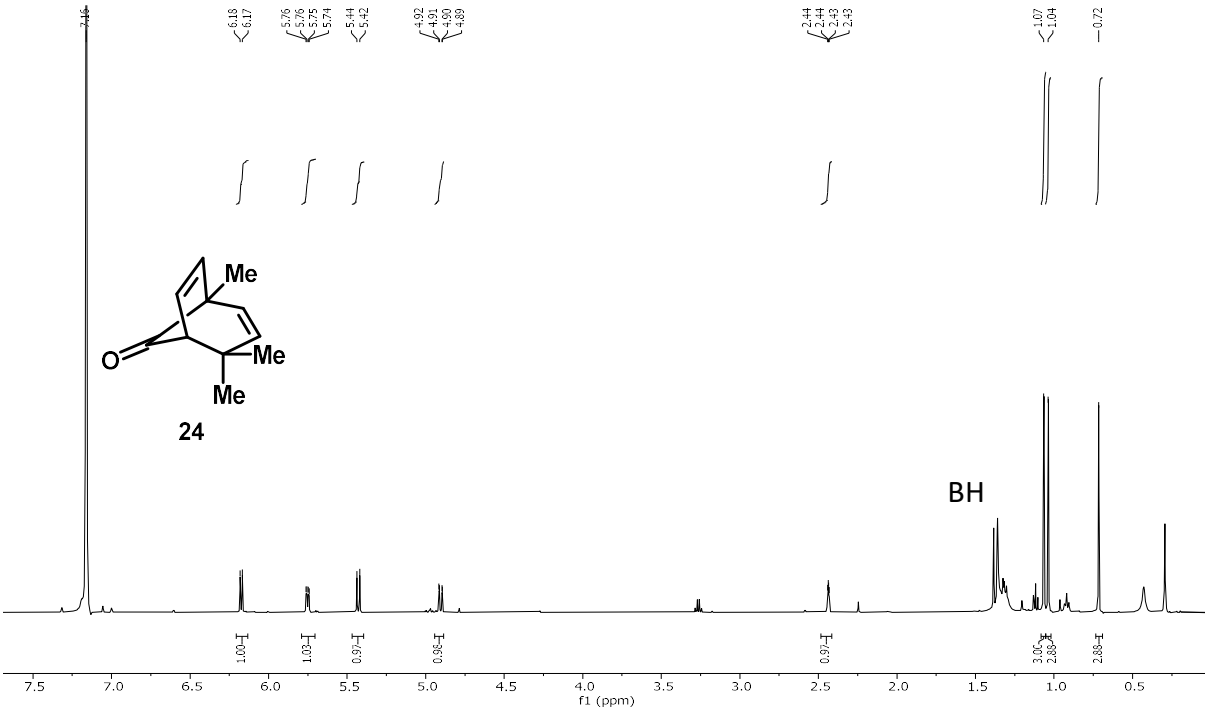
Me
Me
Me
O
24
BH
f1 (ppm)

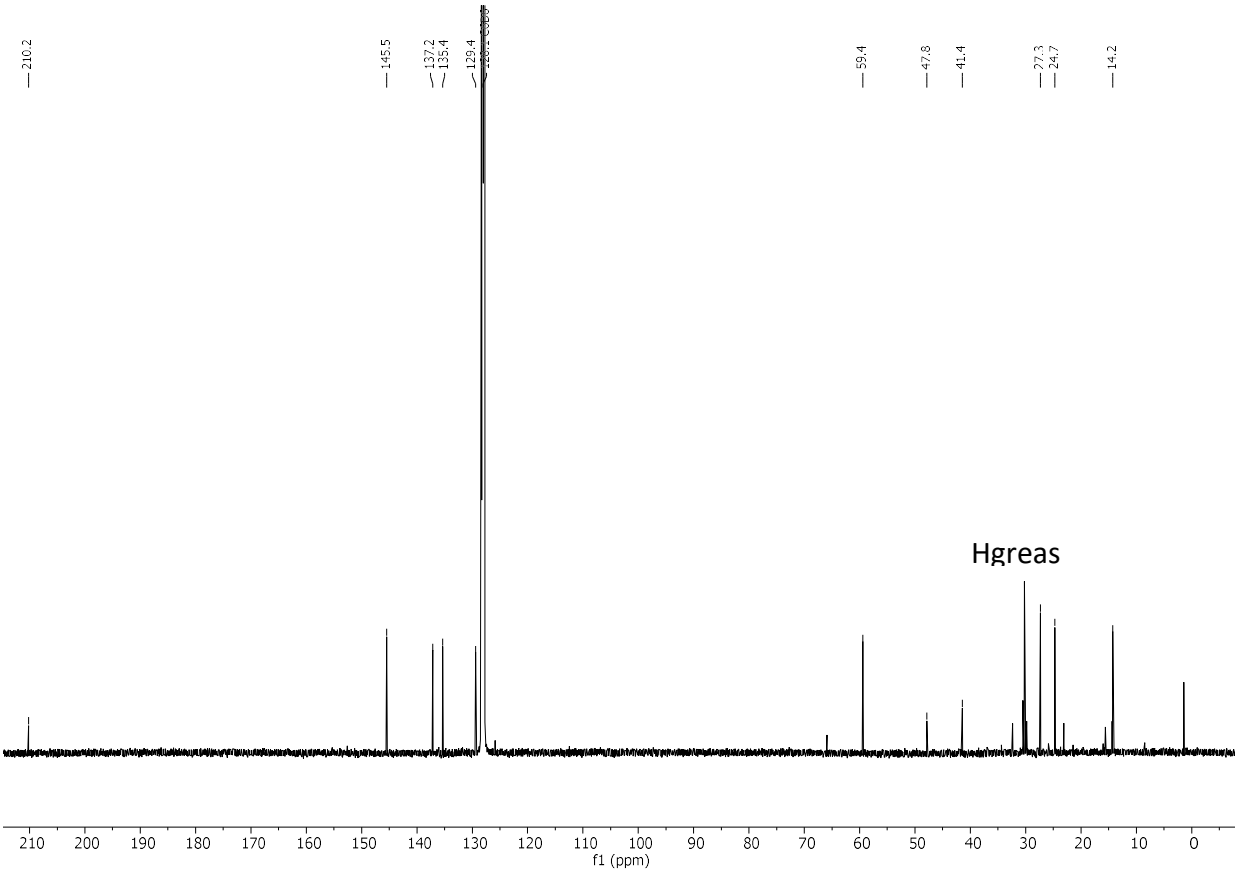
Hgreas
f1 (ppm)

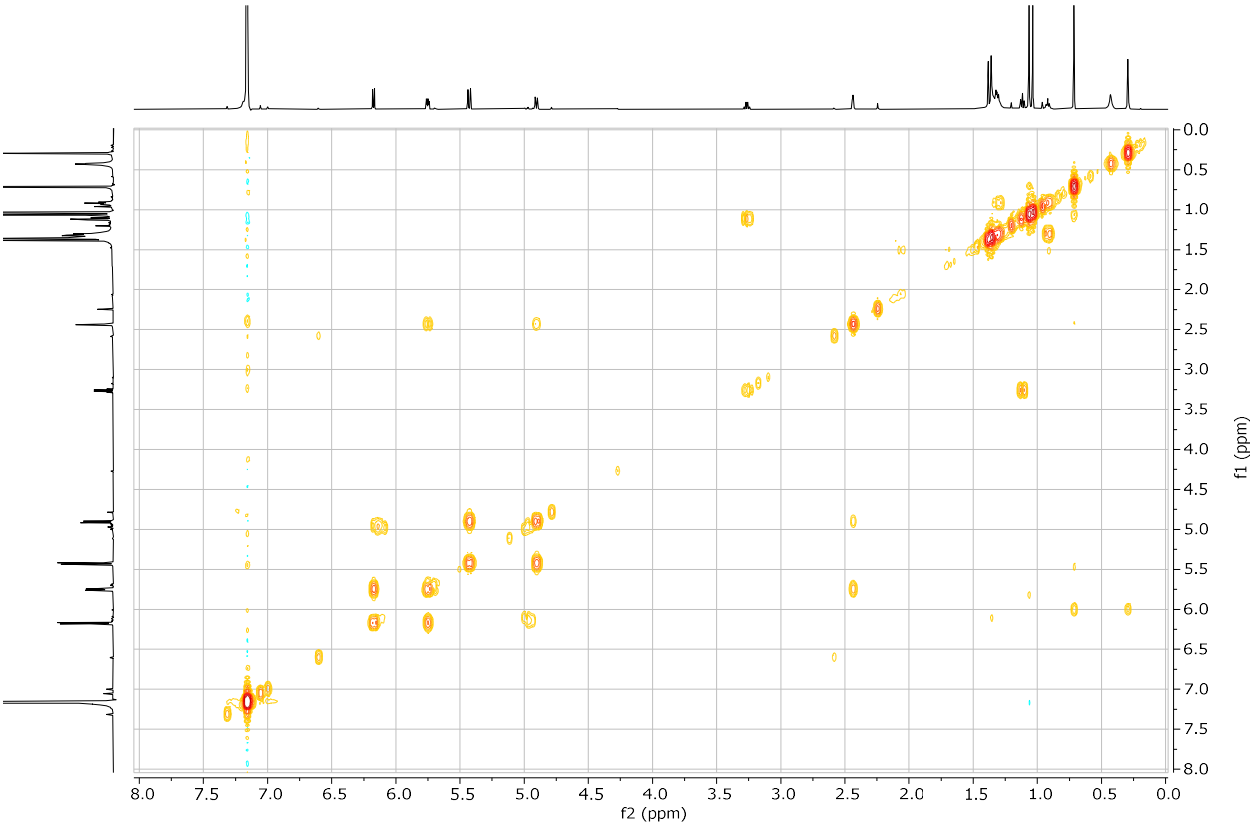
f2 (ppm)
f1 (ppm)

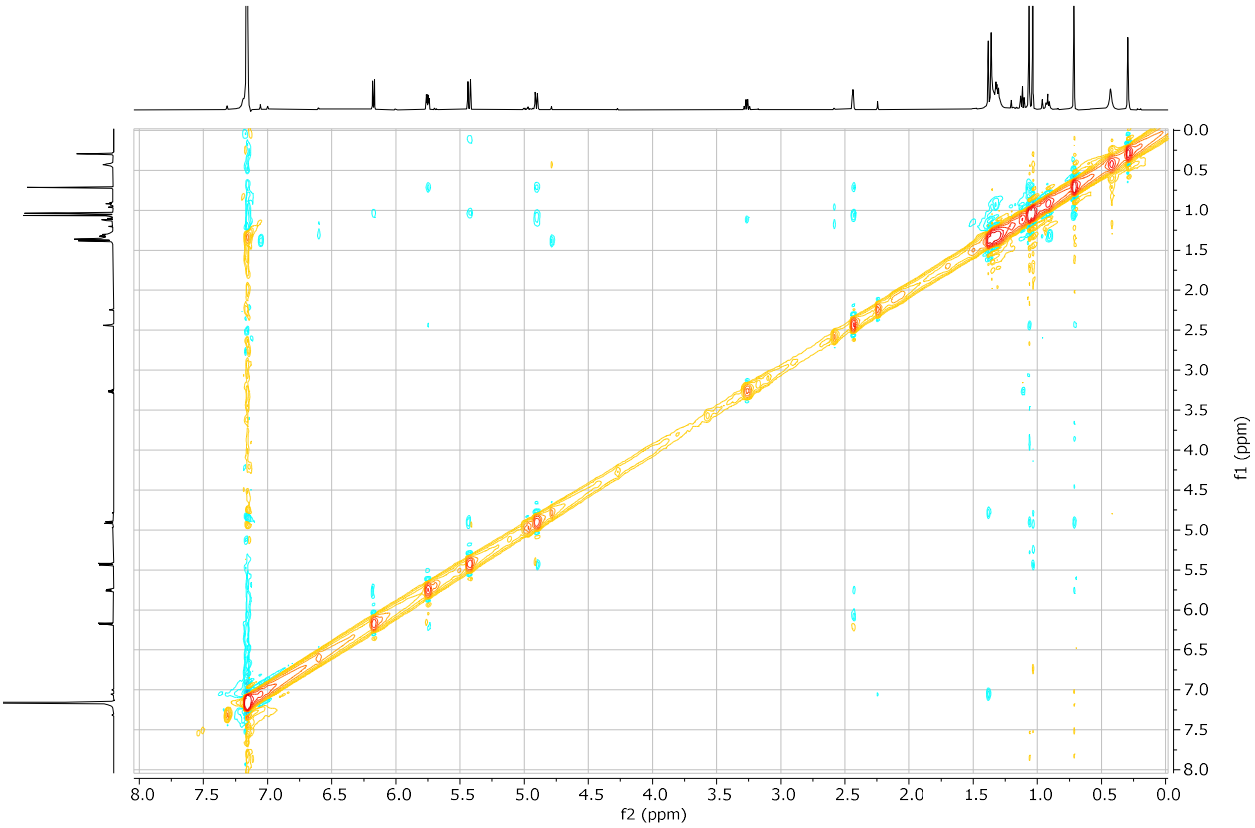
f2 (ppm)
f1 (ppm)

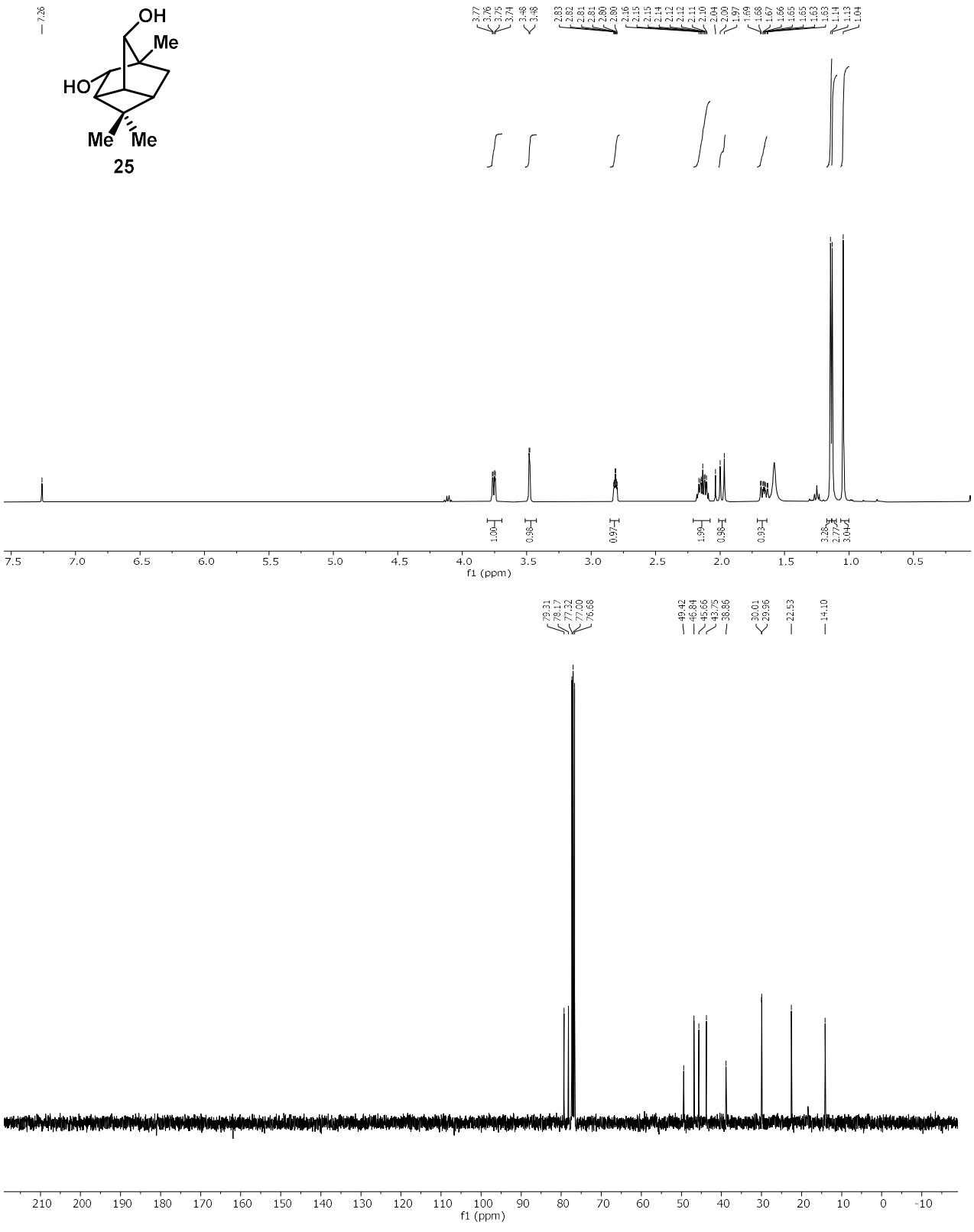
OH
Me
HO
Me
Me
25
f1 (ppm)
f1 (ppm)

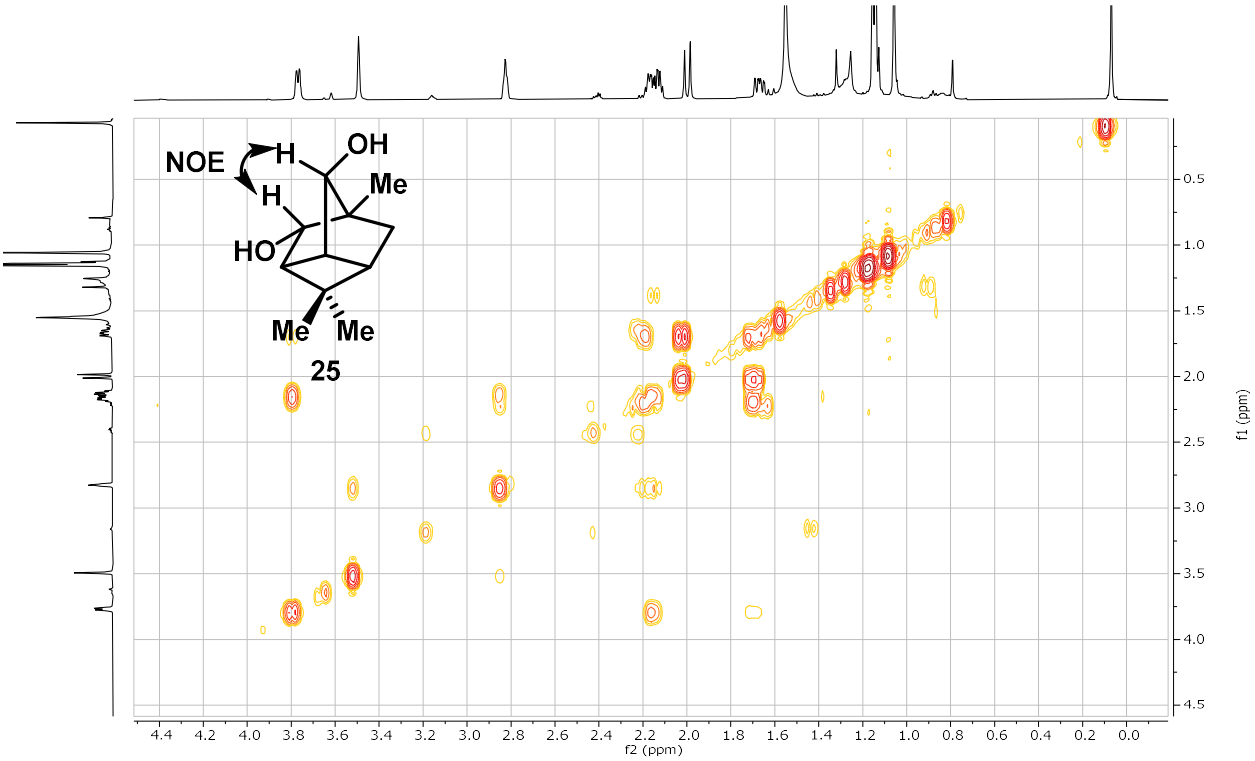
NOE
H
OH
Me
H
HO
Me
Me
25
f2 (ppm)
f1 (ppm)

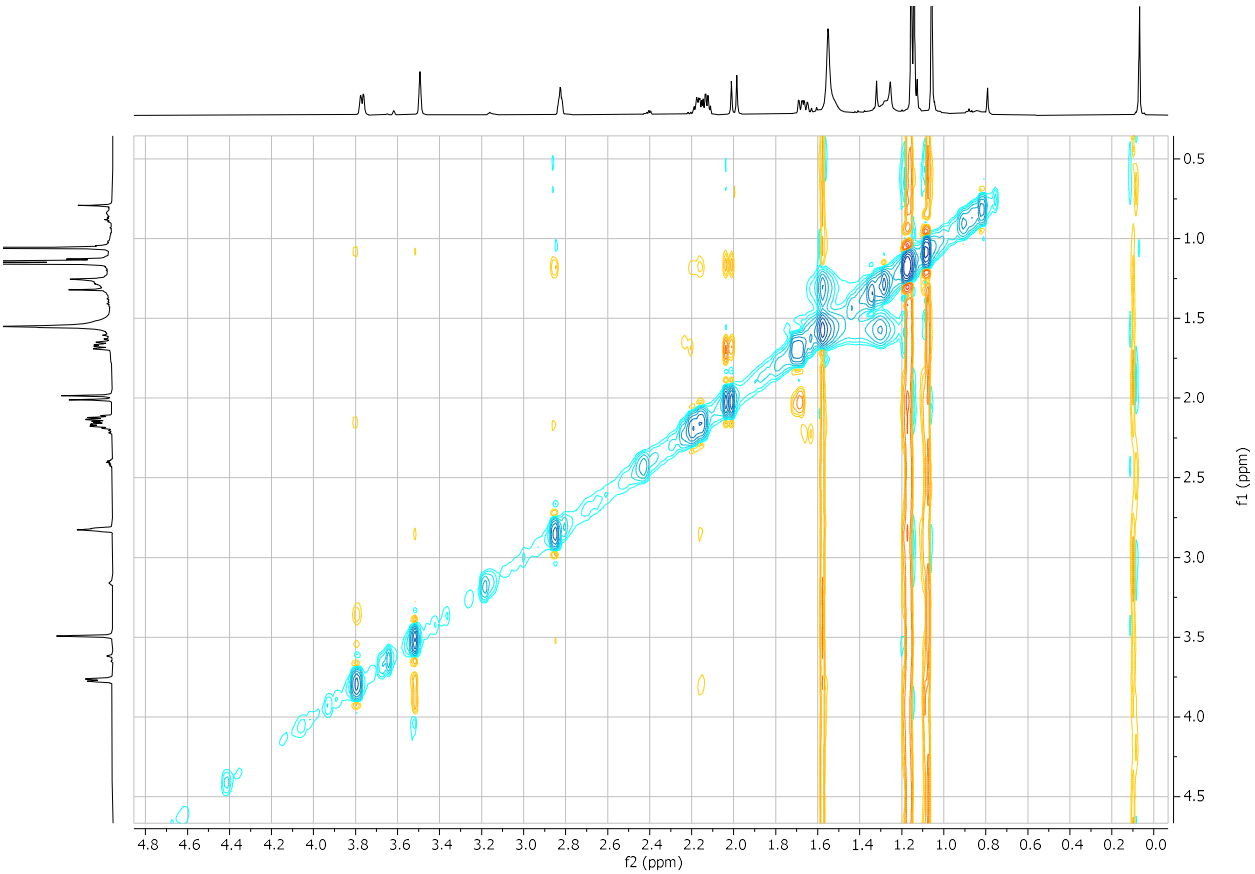
f2 (ppm)
f1 (ppm)

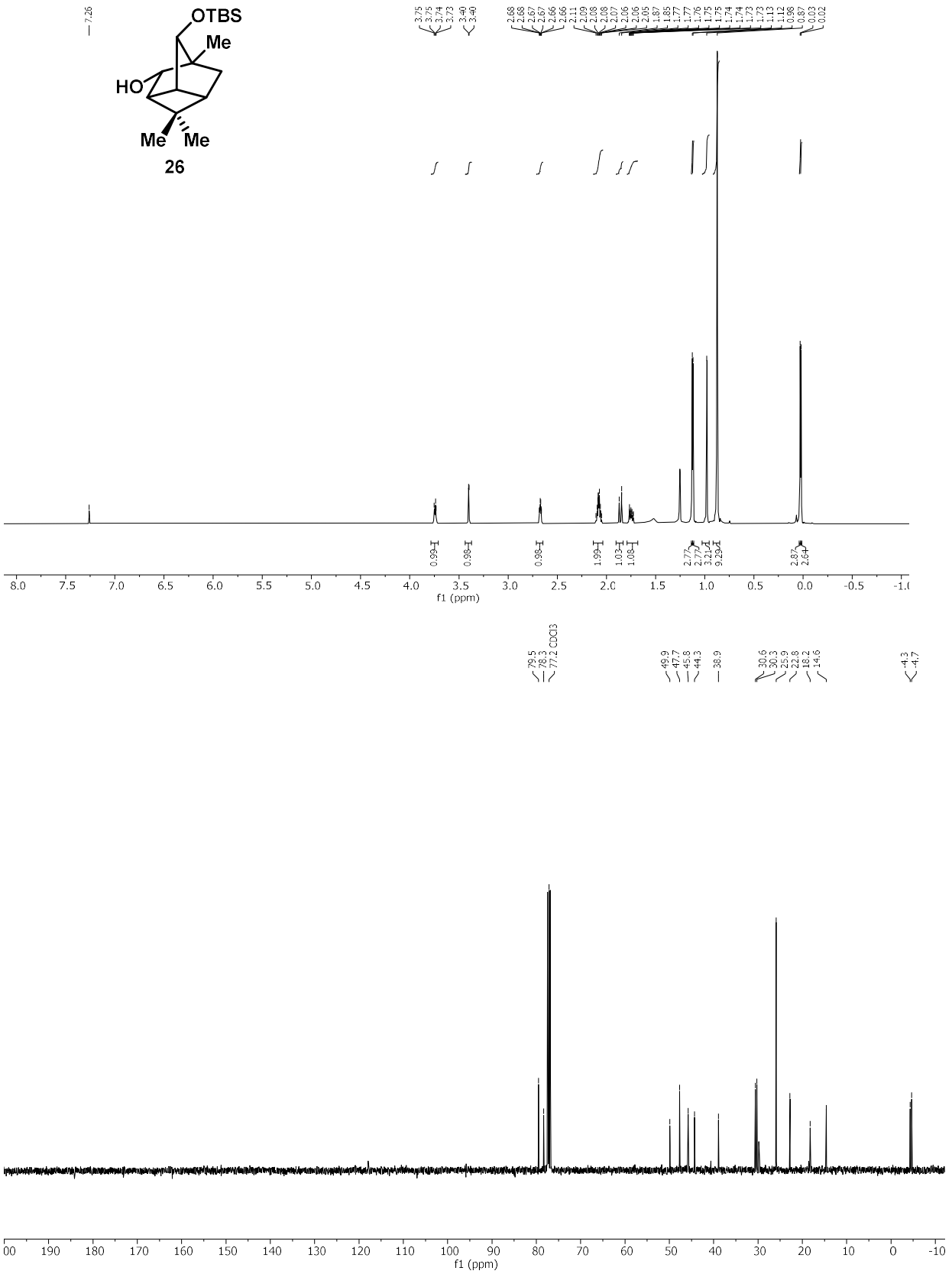
OTBS
Me
HO
Me
Me
26
f1 (ppm)
CDCl3
f1 (ppm)

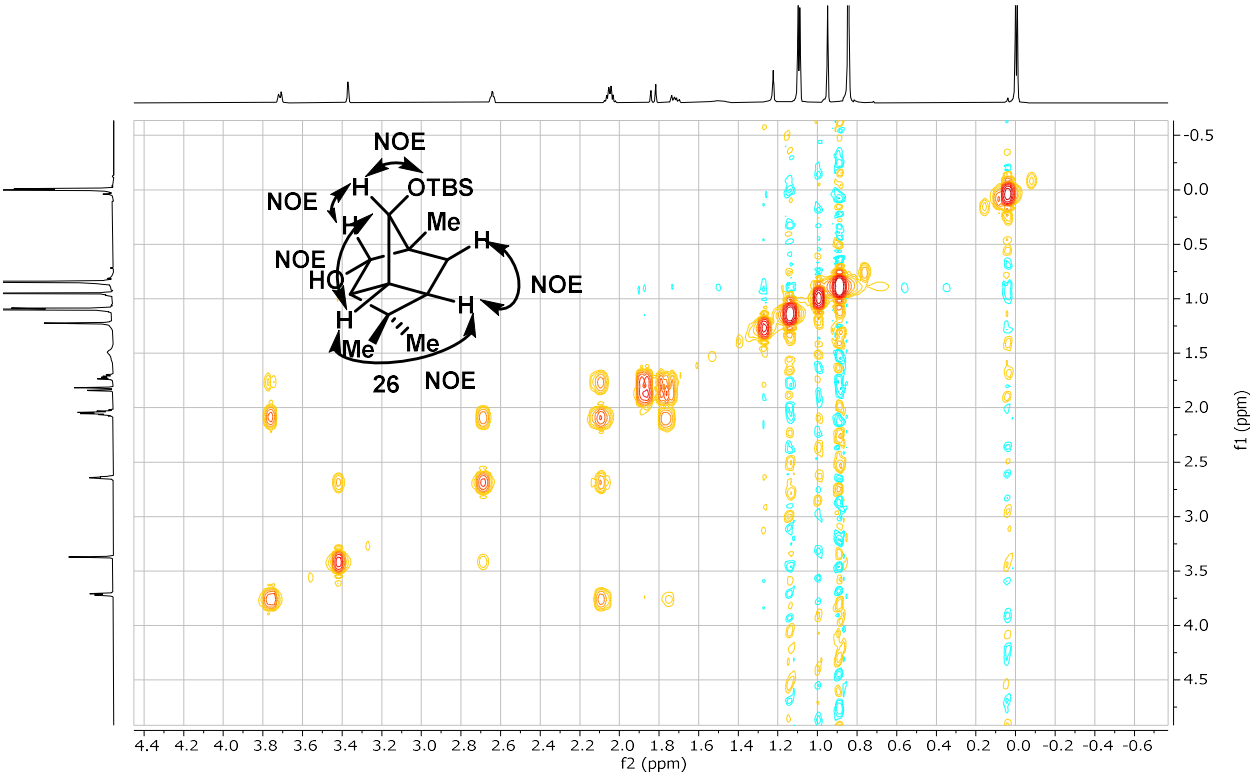
NOE
H
OTBS
NOE
H
Me
H
NOE
HO
NOE
H
H
Me
Me
26
NOE
f2 (ppm)
f1 (ppm)

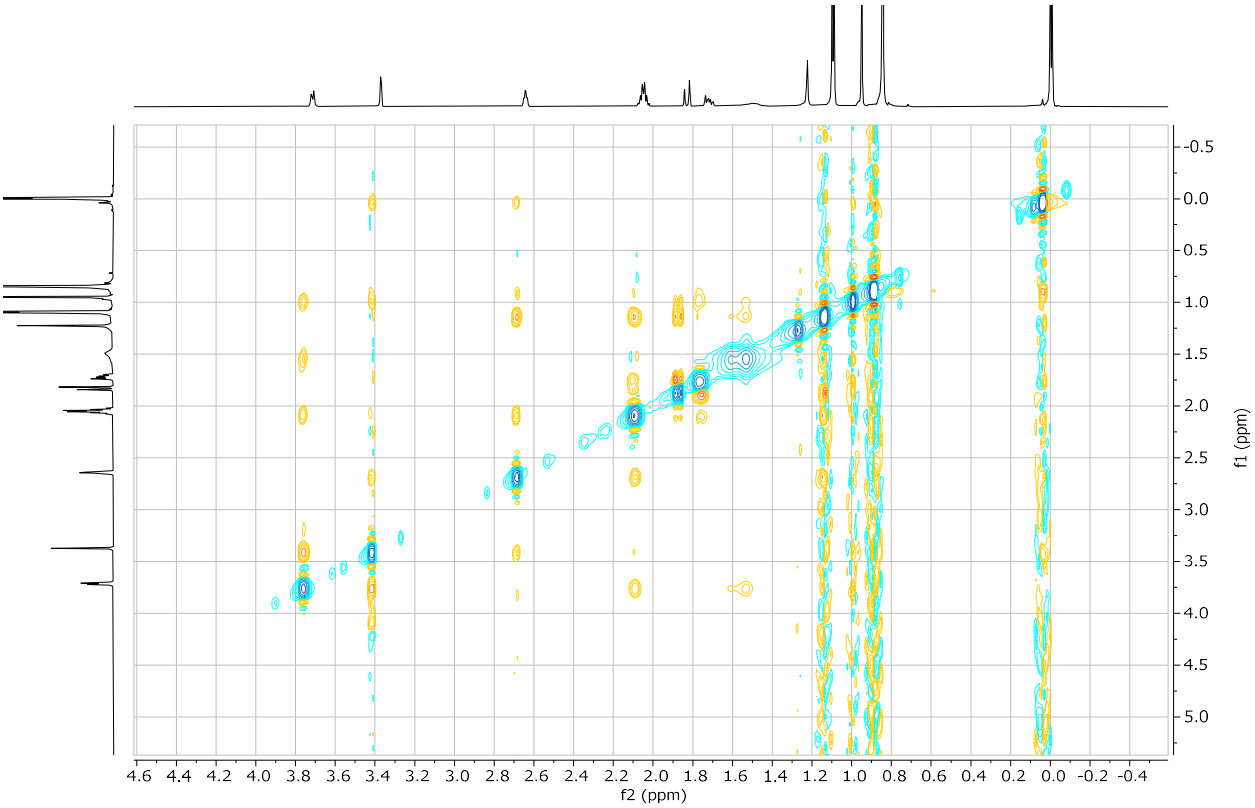
f2 (ppm)
f1 (ppm)

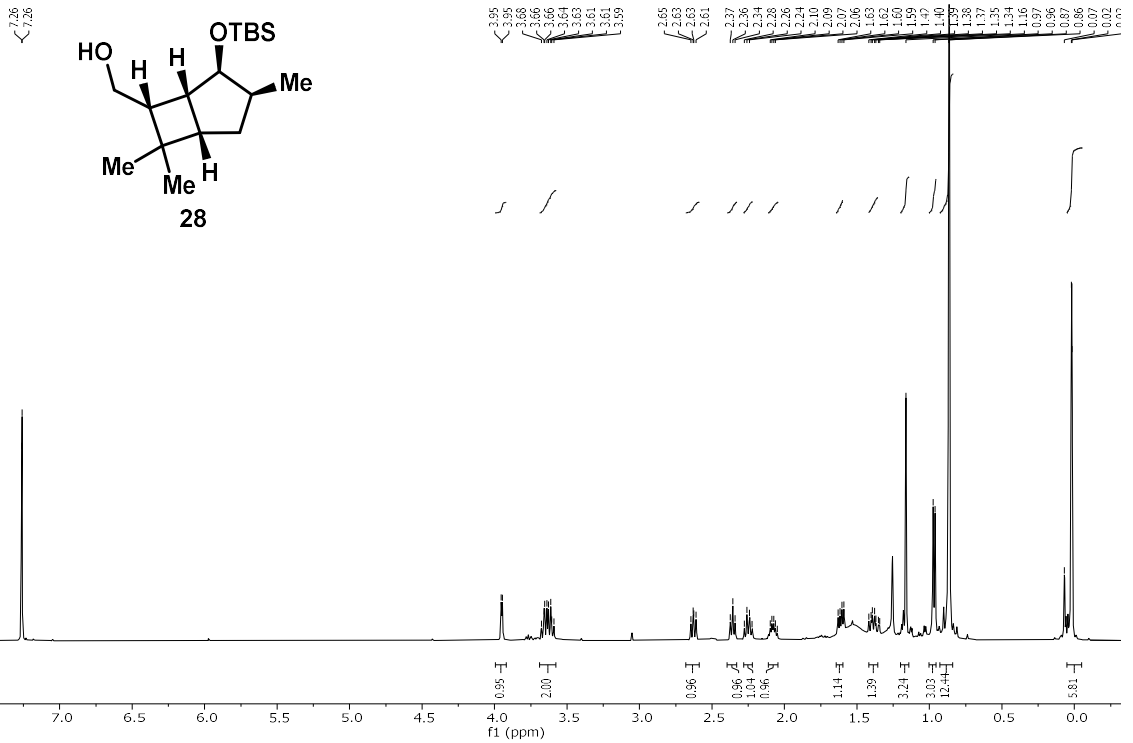
HO
H
H
OTBS
Me
Me
Me
H
28
f1 (ppm)

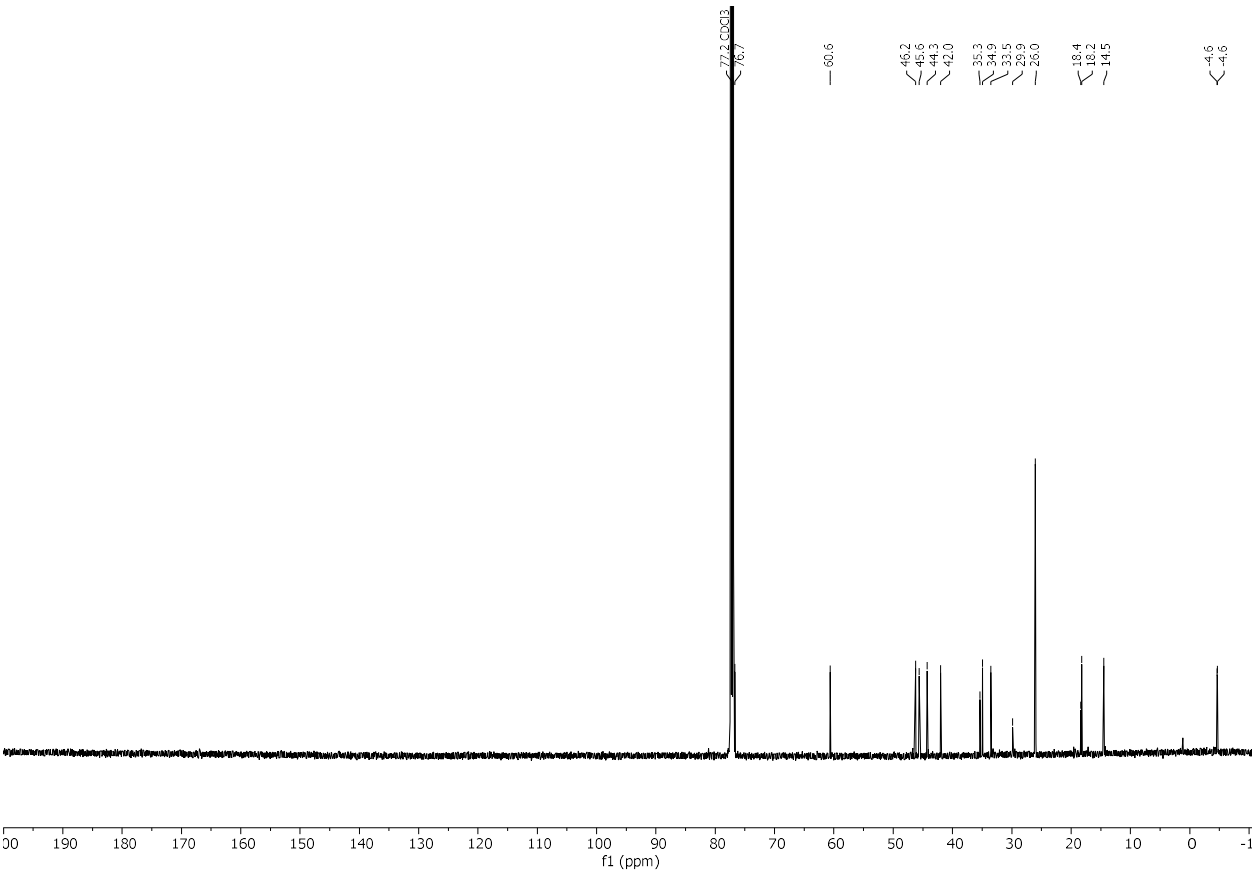
f1 (ppm)

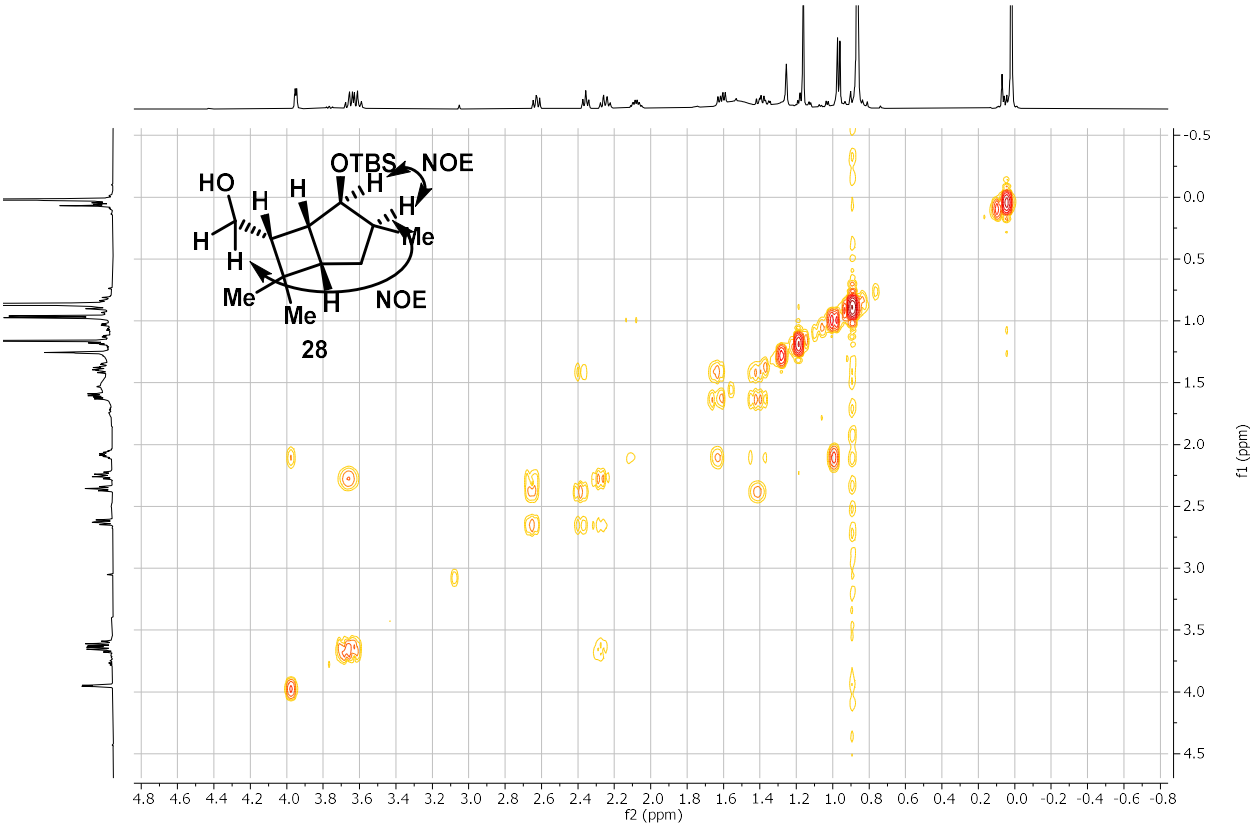
HO
H
H
H
H
H
OTBS
H
NOE
H
Me
Me
Me
H
NOE
28
f2 (ppm)
f1 (ppm)

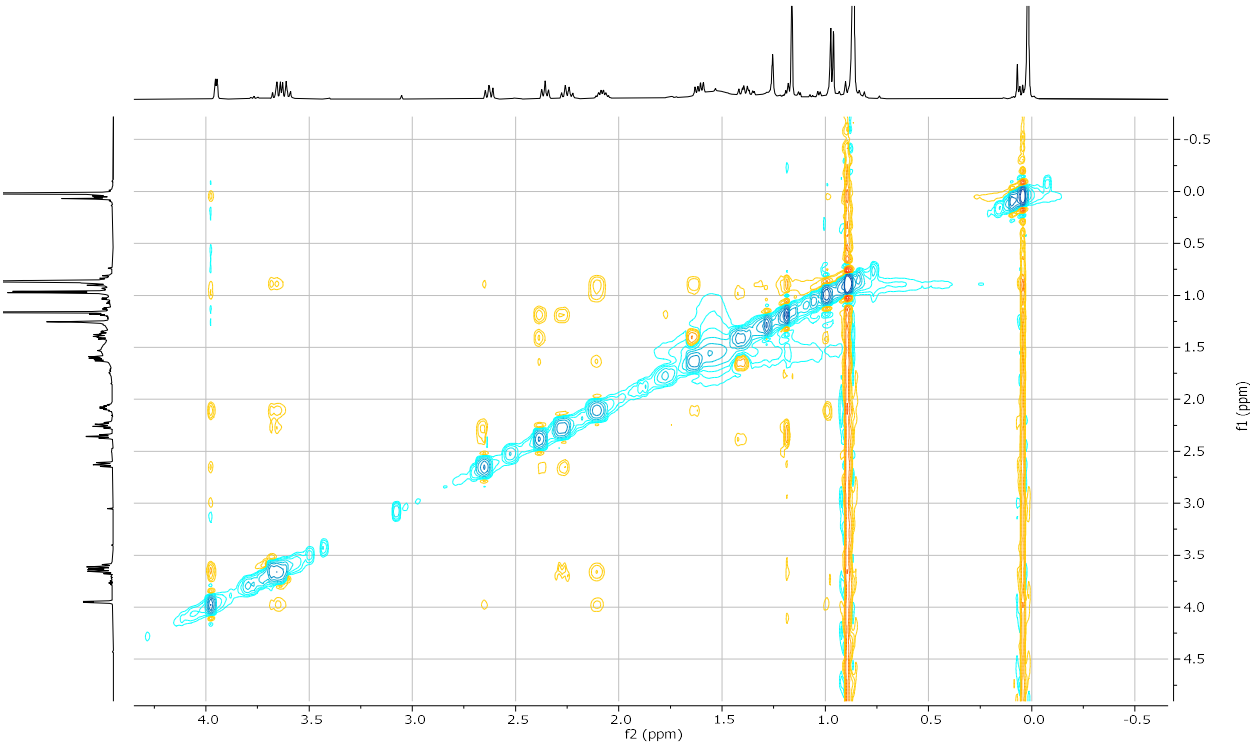
f2 (ppm)
f1 (ppm)

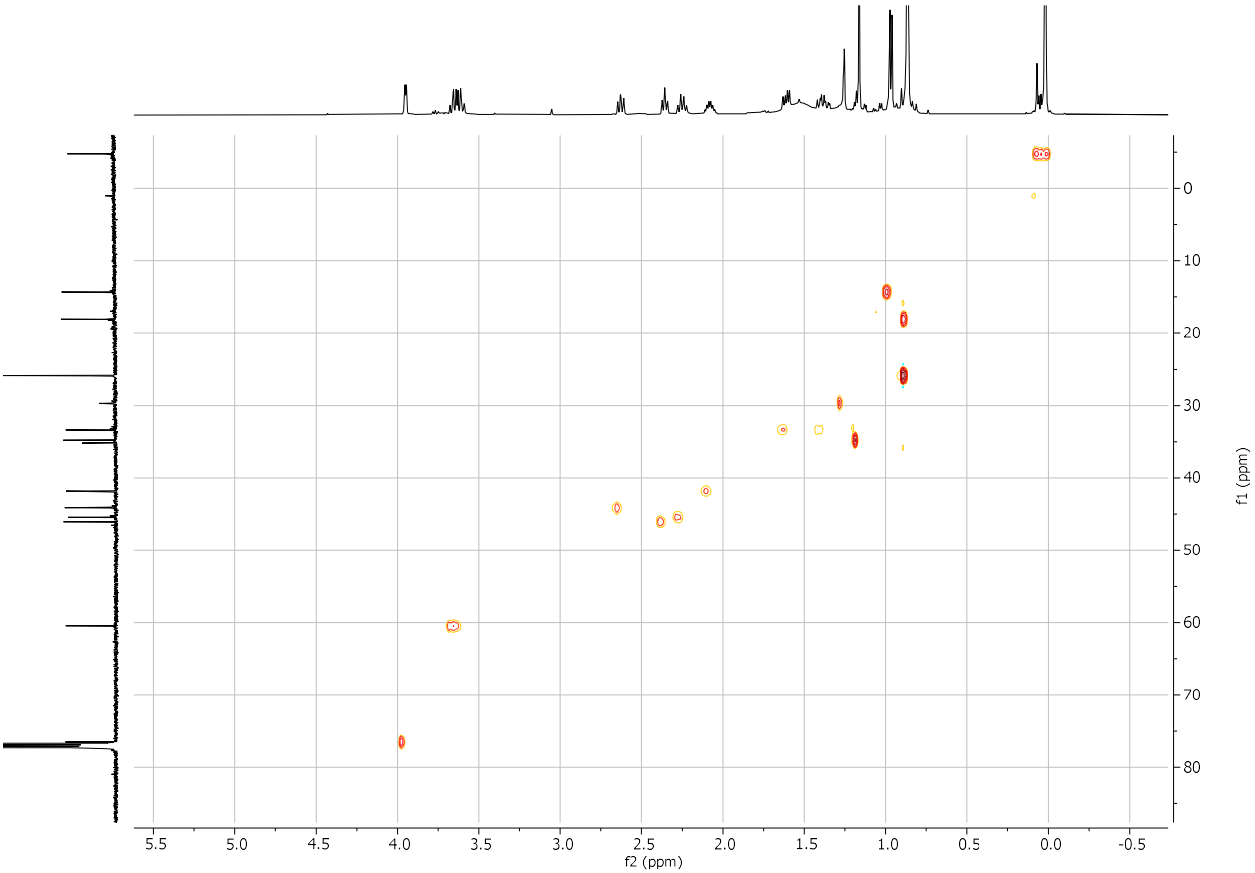
f2 (ppm)
f1 (ppm)

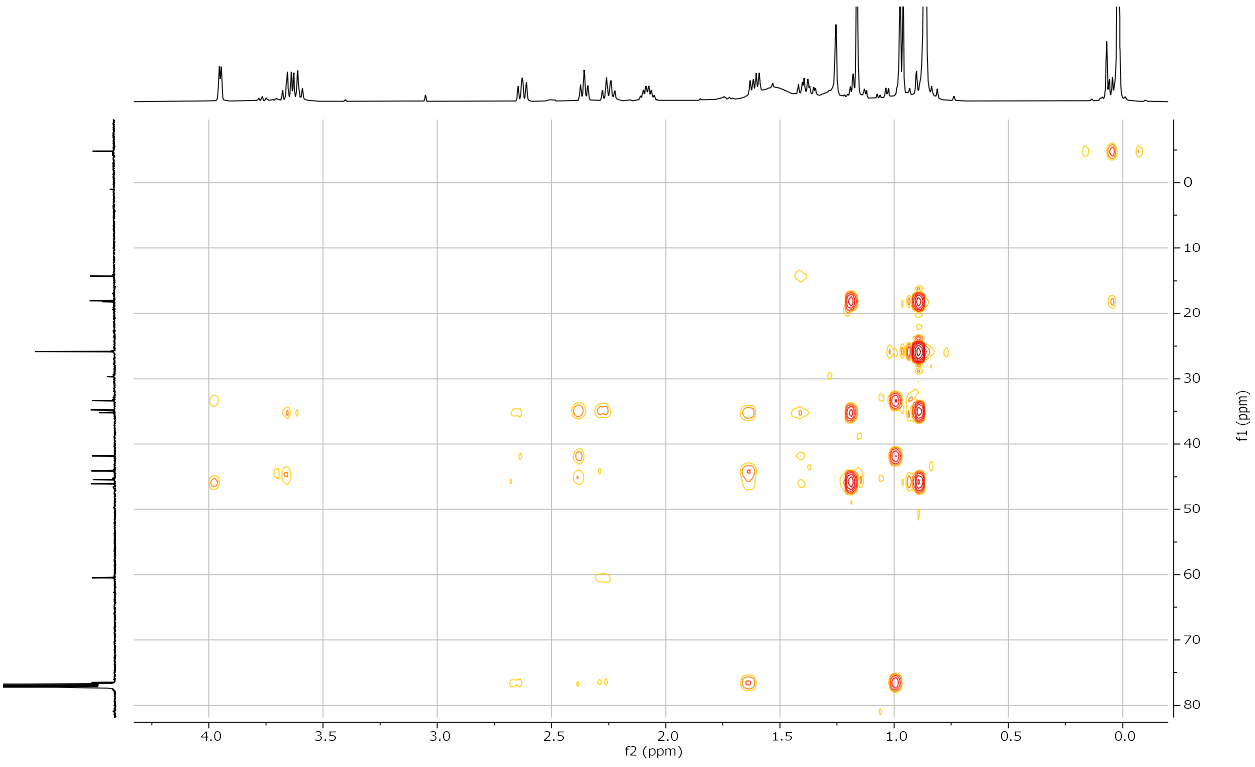
f2 (ppm)
f1 (ppm)

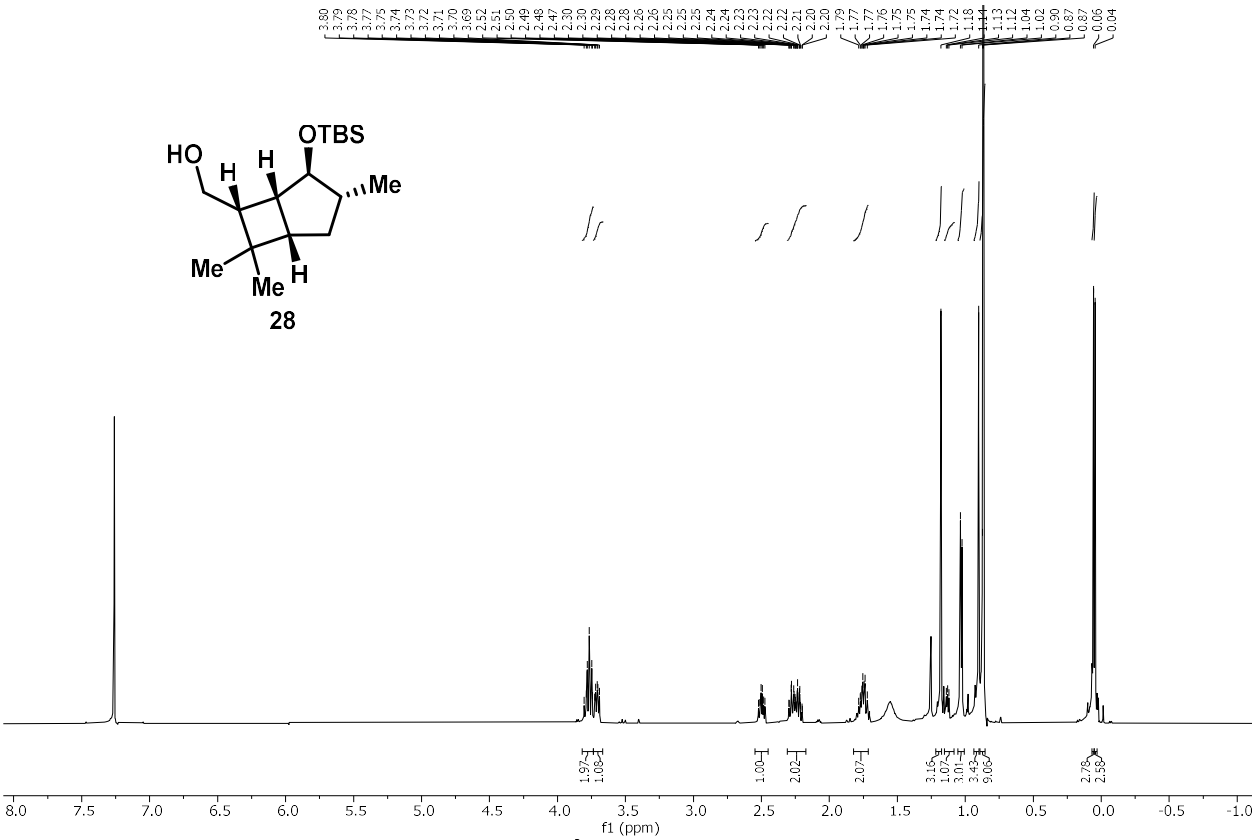
HO
H
H
OTBS
Me
Me
Me
H
28
f1 (ppm)

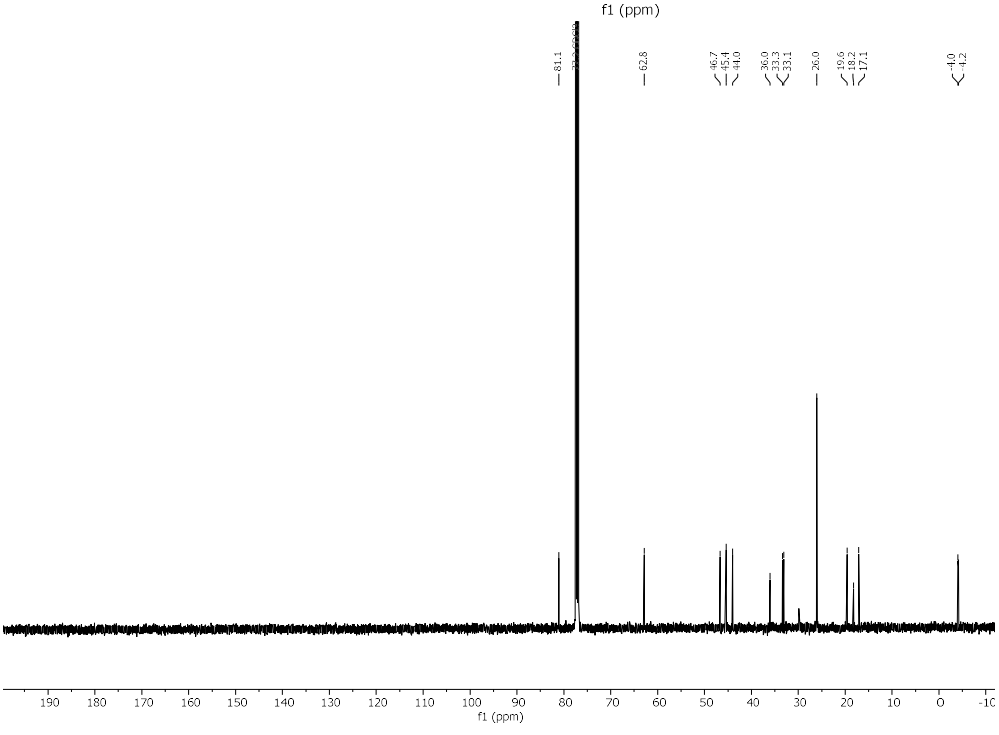
f1 (ppm)

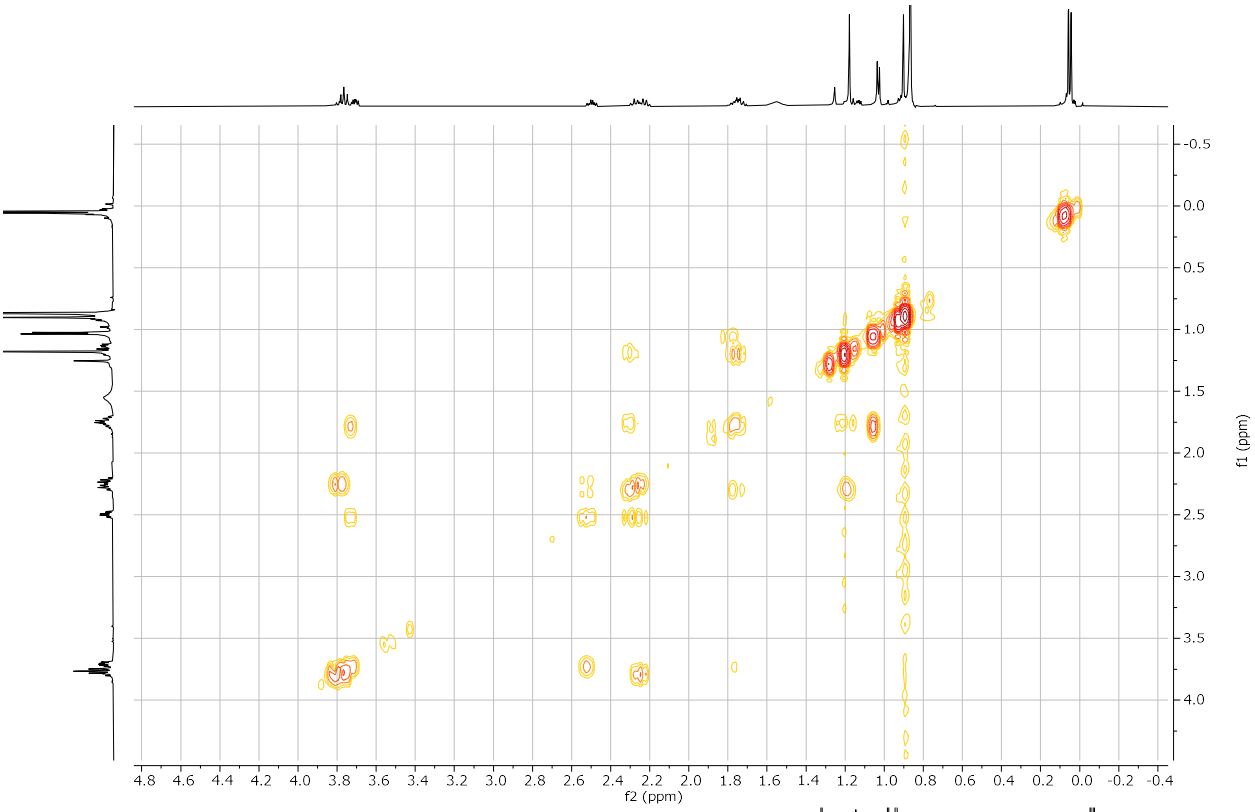
-0.5
0.0
0.5
1.0
1.5
2.0
2.5
3.0
3.5
4.0
f1 (ppm)
4.8 4.6 4.4 4.2 4.0 3.8 3.6 3.4 3.2 3.0 2.8 2.6 2.4 2.2 2.0 1.8 1.6 1.4 1.2 1.0 0.8 0.6 0.4 0.2 0.0 -0.2 -0.4
f2 (ppm)

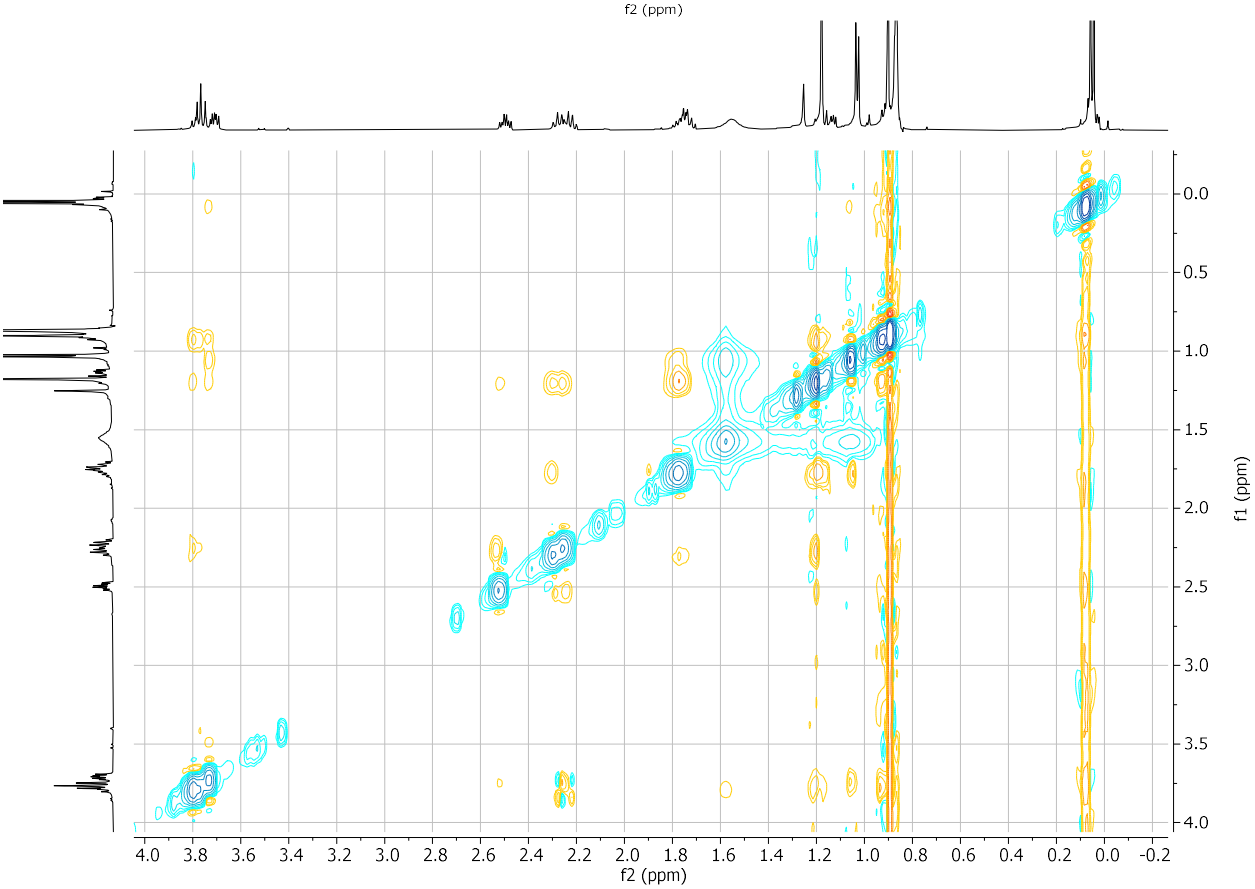
0.0
0.5
1.0
1.5
2.0
2.5
3.0
3.5
4.0
f1 (ppm)
4.0 3.8 3.6 3.4 3.2 3.0 2.8 2.6 2.4 2.2 2.0 1.8 1.6 1.4 1.2 1.0 0.8 0.6 0.4 0.2 0.0 -0.2
f2 (ppm)

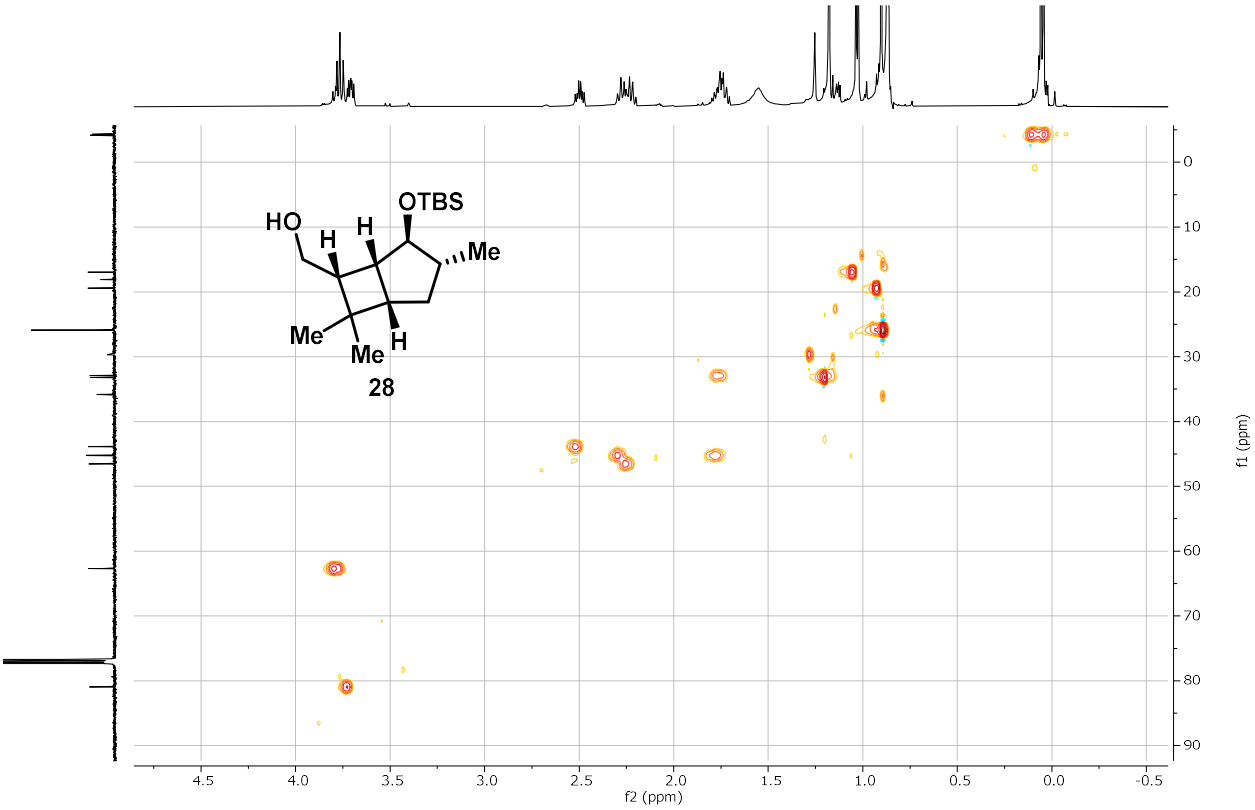
HO
H
H
OTBS
Me
Me
Me
H
28
f2 (ppm)
f1 (ppm)

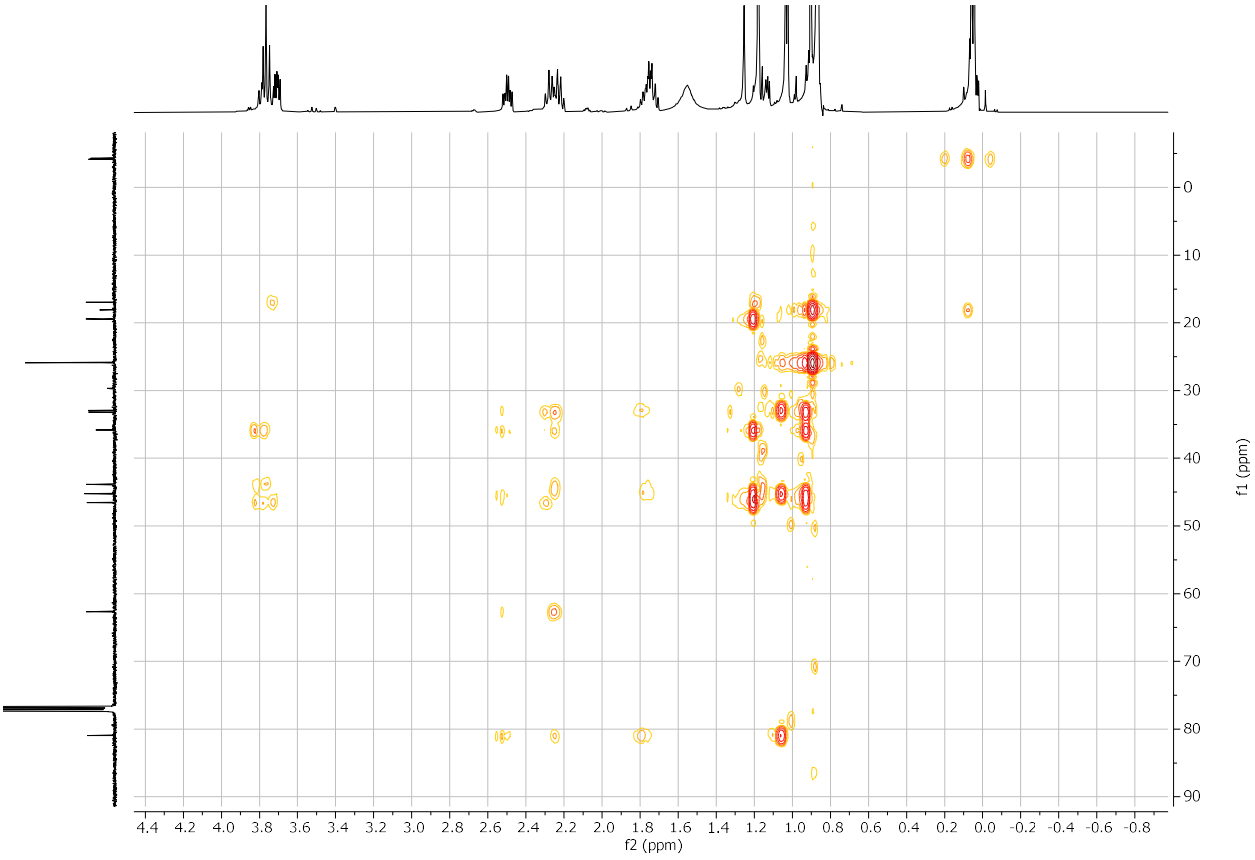
f2 (ppm)
f1 (ppm)

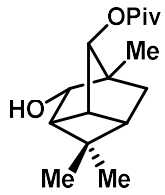

29

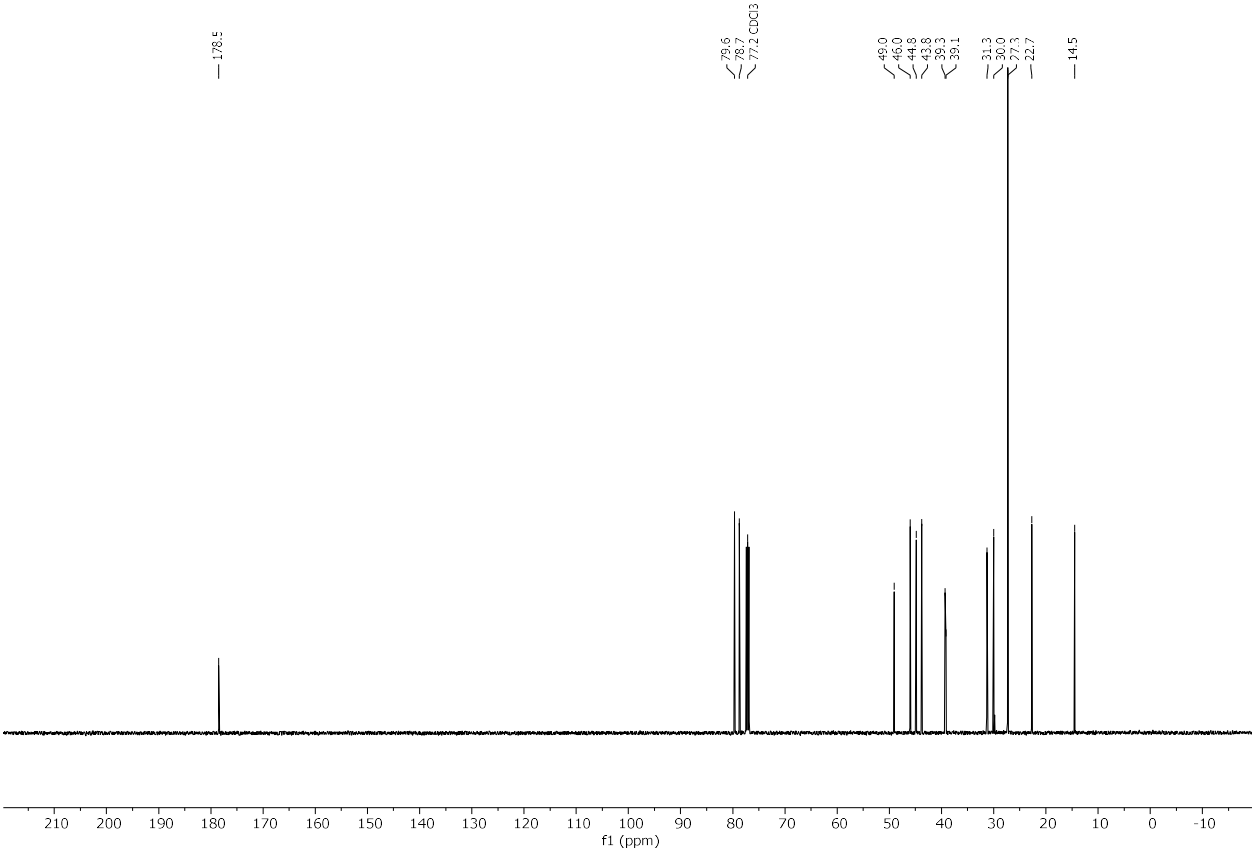

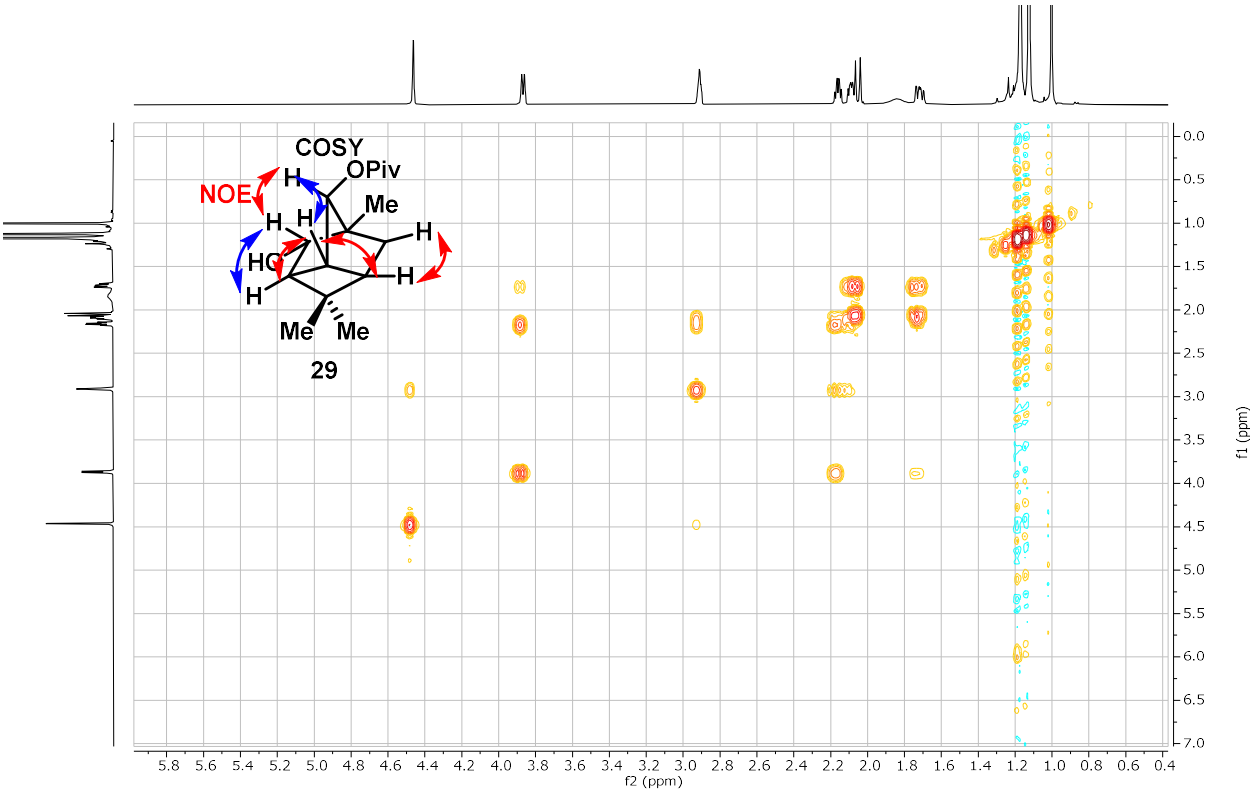
COSY
NOE
OPiv
Me
H
HO
Me
Me
29
f2 (ppm)
f1 (ppm)

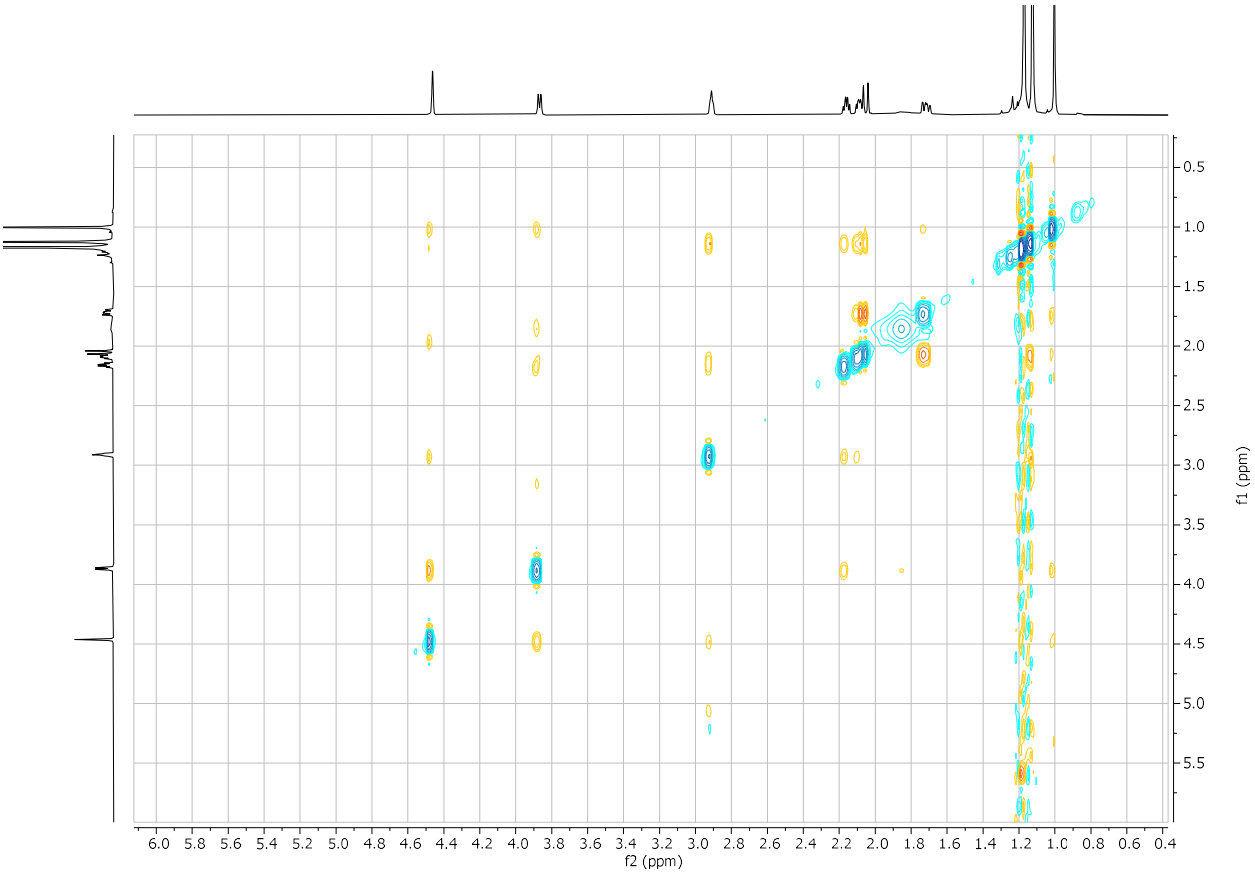
f2 (ppm)
f1 (ppm)

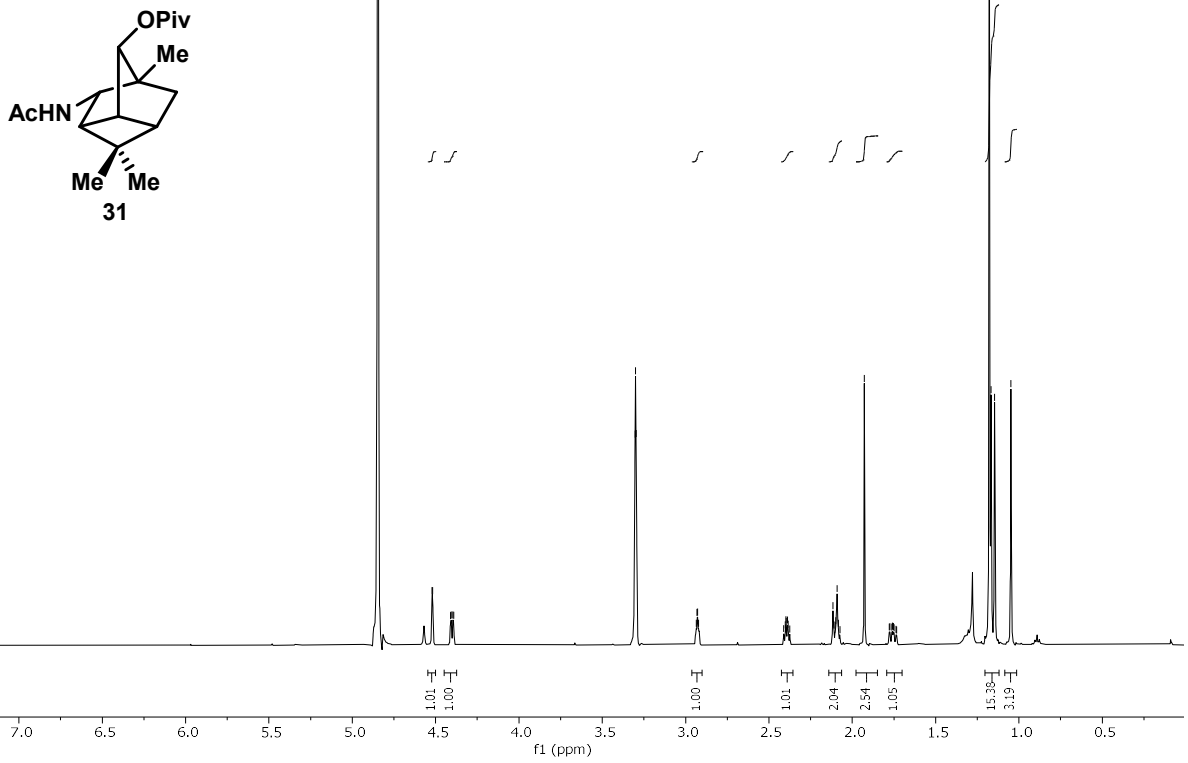
OPiv
Me
AcHN
Me
Me
31
f1 (ppm)

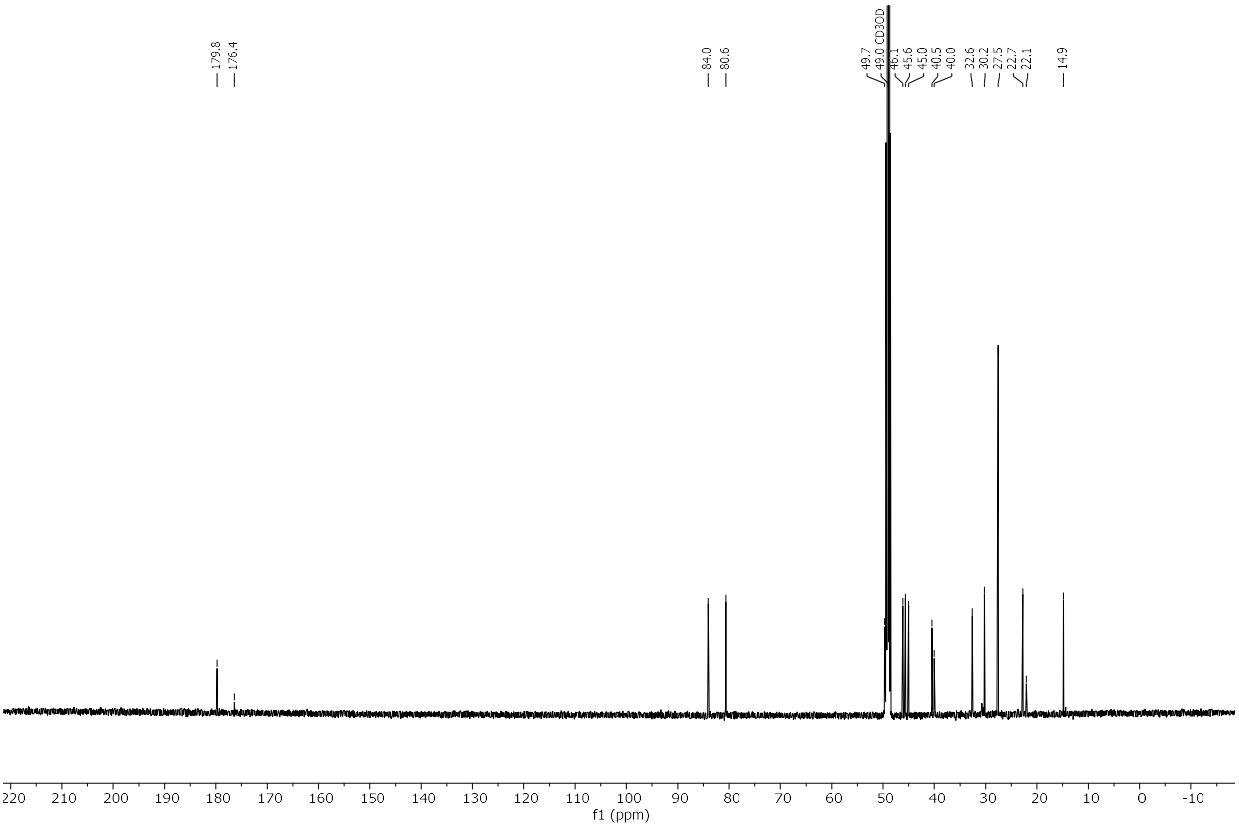
179.8
176.4
84.0
80.6
49.7
49.0 CD3OD
46.1
45.6
45.0
40.5
40.0
32.6
30.2
27.5
22.7
22.1
14.9
f1 (ppm)

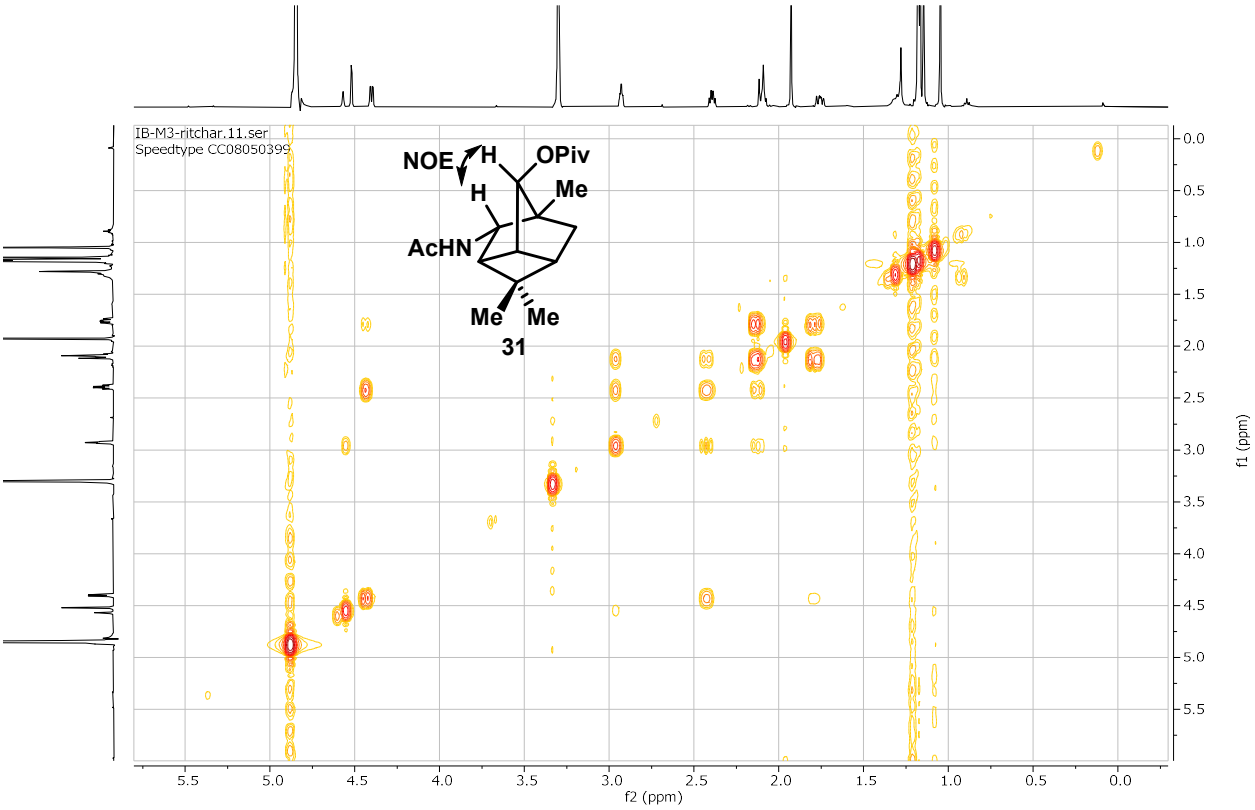
IB-M3-ritchar.11.ser
Speedtype CC08050399
NOE
H
OPiv
H
Me
AcHN
Me
Me
31
f2 (ppm)
f1 (ppm)

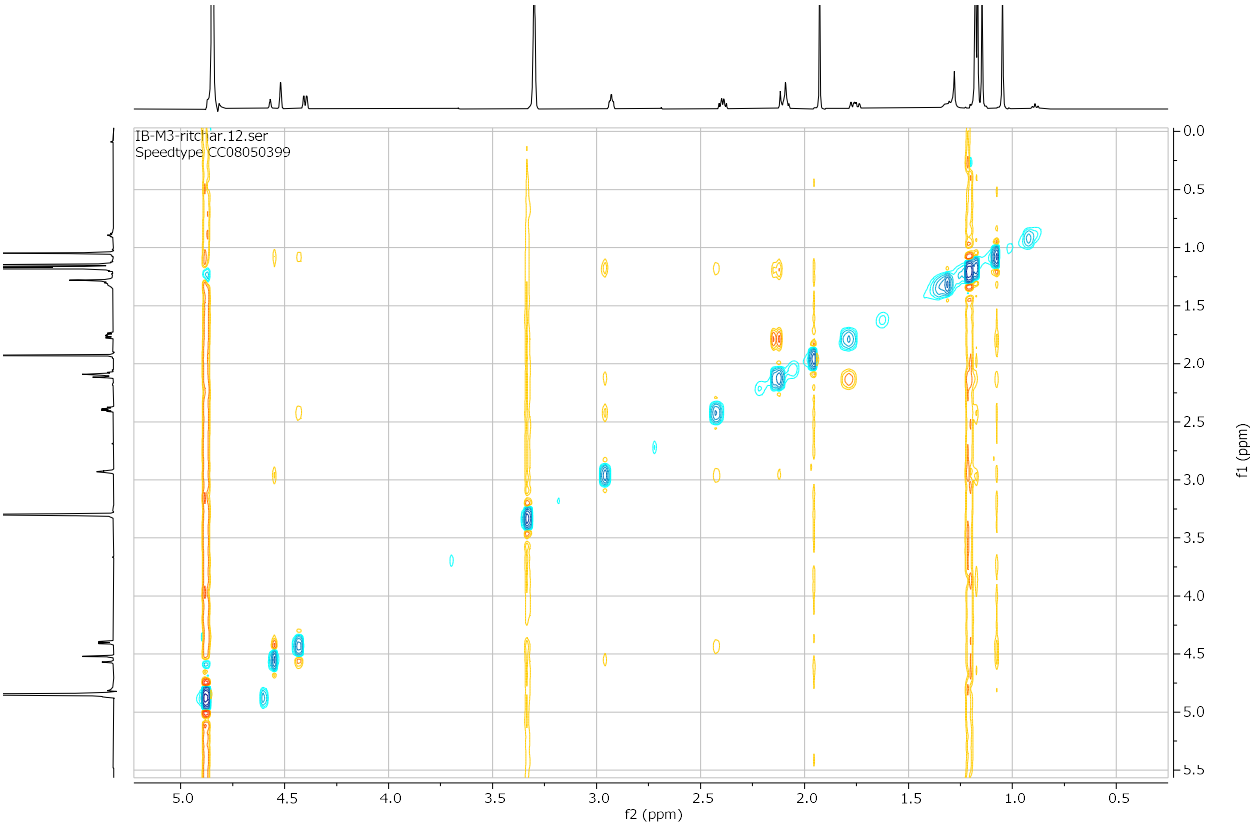
IB-M3-ritchar.12.ser
Speedtype CC08050399
f2 (ppm)
f1 (ppm)

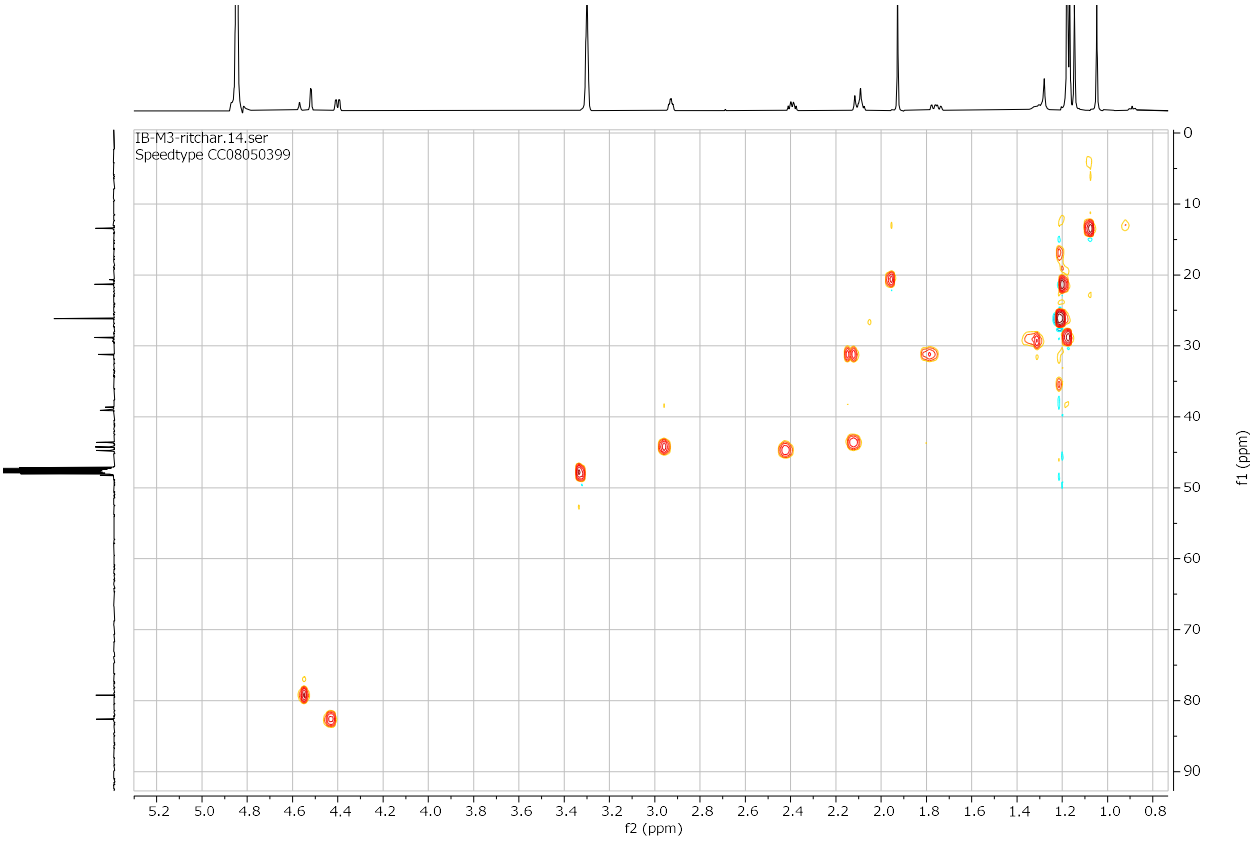
IB-M3-ritchar.14.ser
Speedtype CC08050399
f2 (ppm)
f1 (ppm)

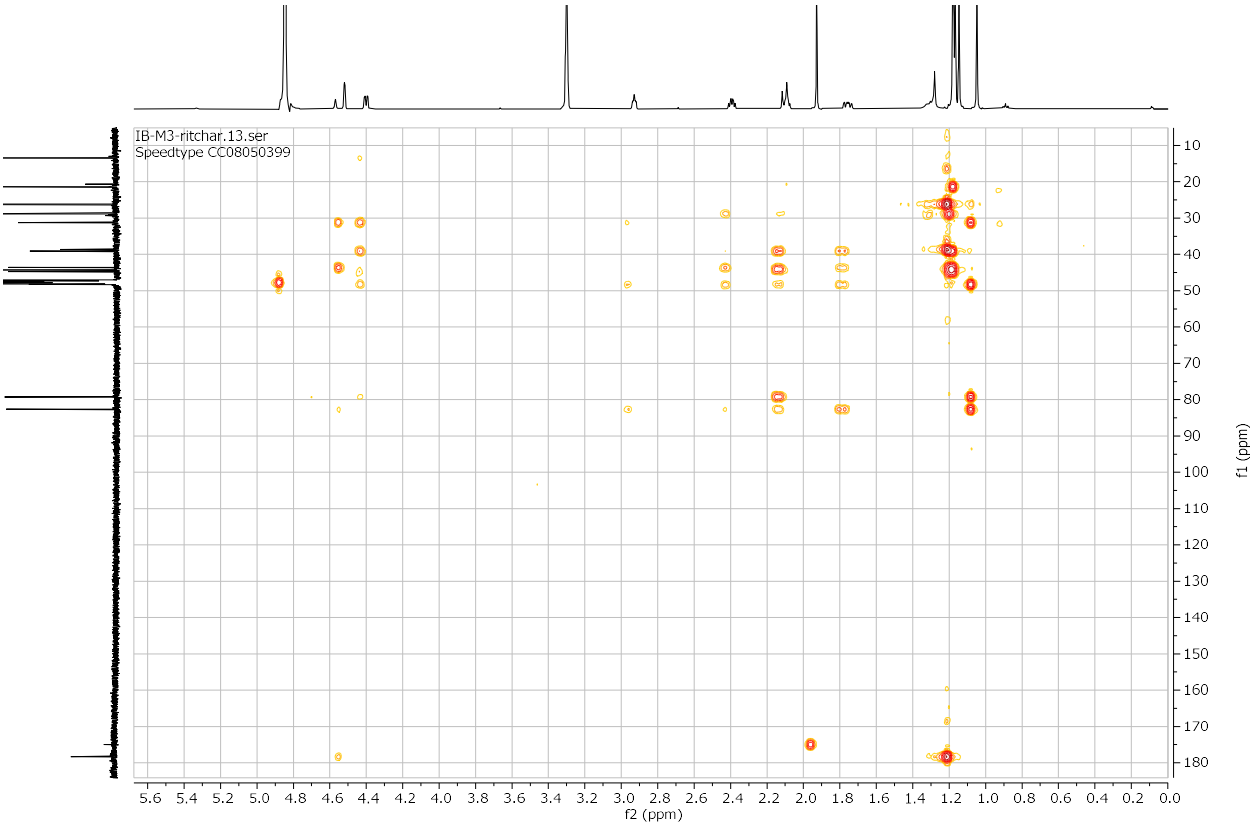
IB-M3-ritchar.13.ser
Speedtype CC08050399
f2 (ppm)
f1 (ppm)

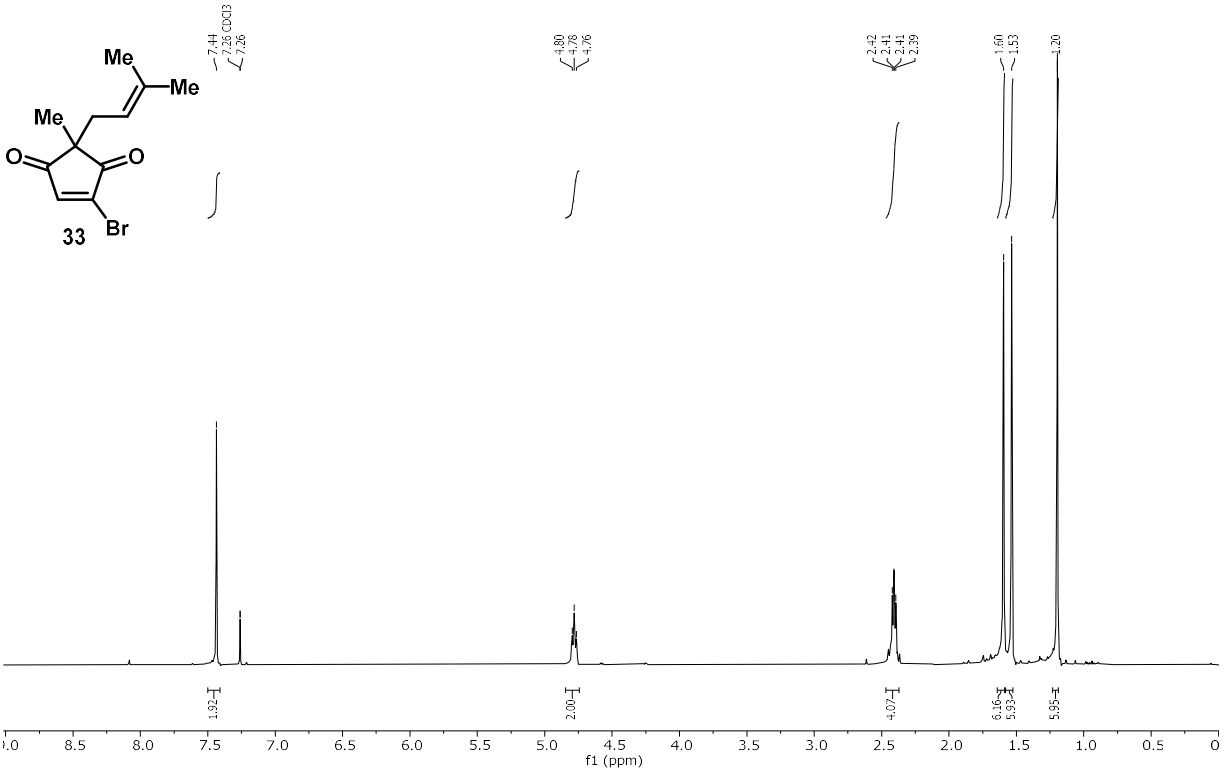
Me
Me
Me
O
O
Br
33
7.44
7.26 CDCl3
7.26
4.80
4.78
4.76
2.42
2.41
2.41
2.39
1.60
1.53
1.20
1.92
2.00
4.07
6.16
5.93
5.85
f1 (ppm)

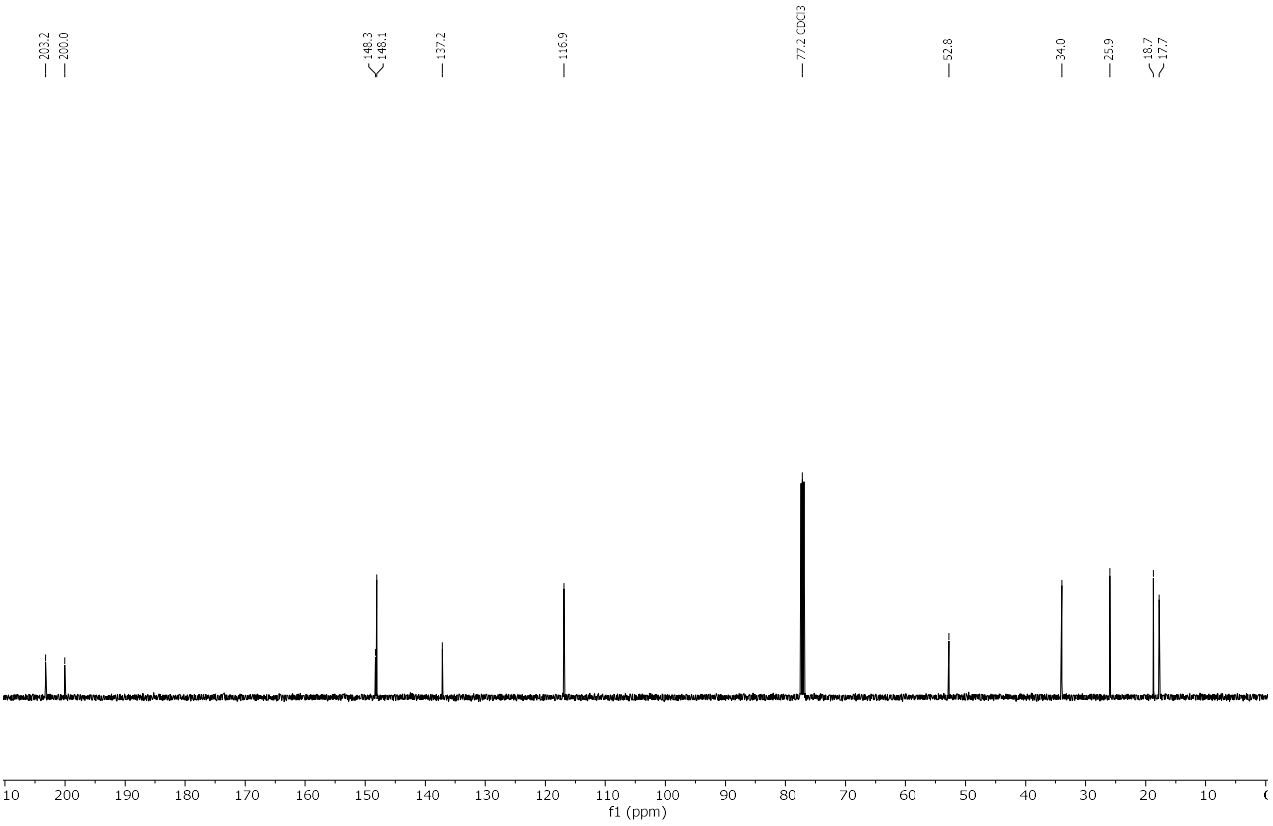
203.2
200.0
148.3
148.1
137.2
116.9
77.2 CDCl3
52.8
34.0
25.9
18.7
17.7
f1 (ppm)

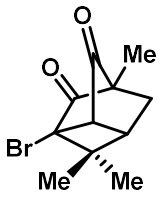
O
O
Me
Br
Me
Me

34

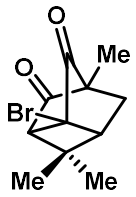
O
O
Me
Br
Me
Me

35

7.26
3.44
3.43
3.42
3.14
3.13
2.96
2.94
2.94
2.93
2.93
2.92
2.15
2.15
2.14
1.49
1.49
1.19
1.18
1.18
0.98
0.97
0.96
1.00
0.74
1.02
0.77
0.98
0.81
2.21
2.72
3.32
5.84
5.95
7.5
7.0
6.5
6.0
5.5
5.0
4.5
4.0
3.5
3.0
2.5
2.0
1.5
1.0
f1 (ppm)

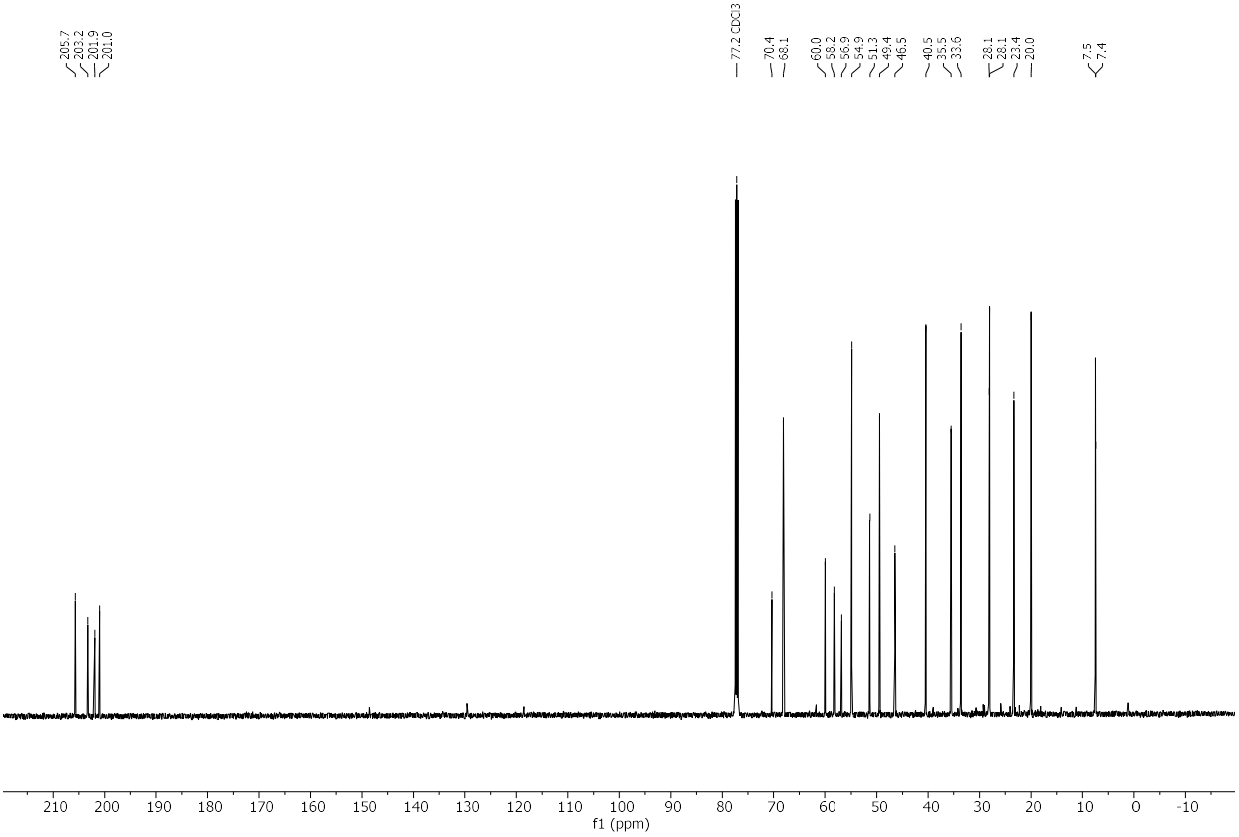
205.7
203.2
201.9
201.0
77.2 CDCl3
70.4
68.1
60.0
58.2
56.9
54.9
51.3
49.4
46.5
40.5
35.5
33.6
28.1
28.1
23.4
20.0
7.5
7.4
210
200
190
180
170
160
150
140
130
120
110
100
90
80
70
60
50
40
30
20
10
0
-10
f1 (ppm)

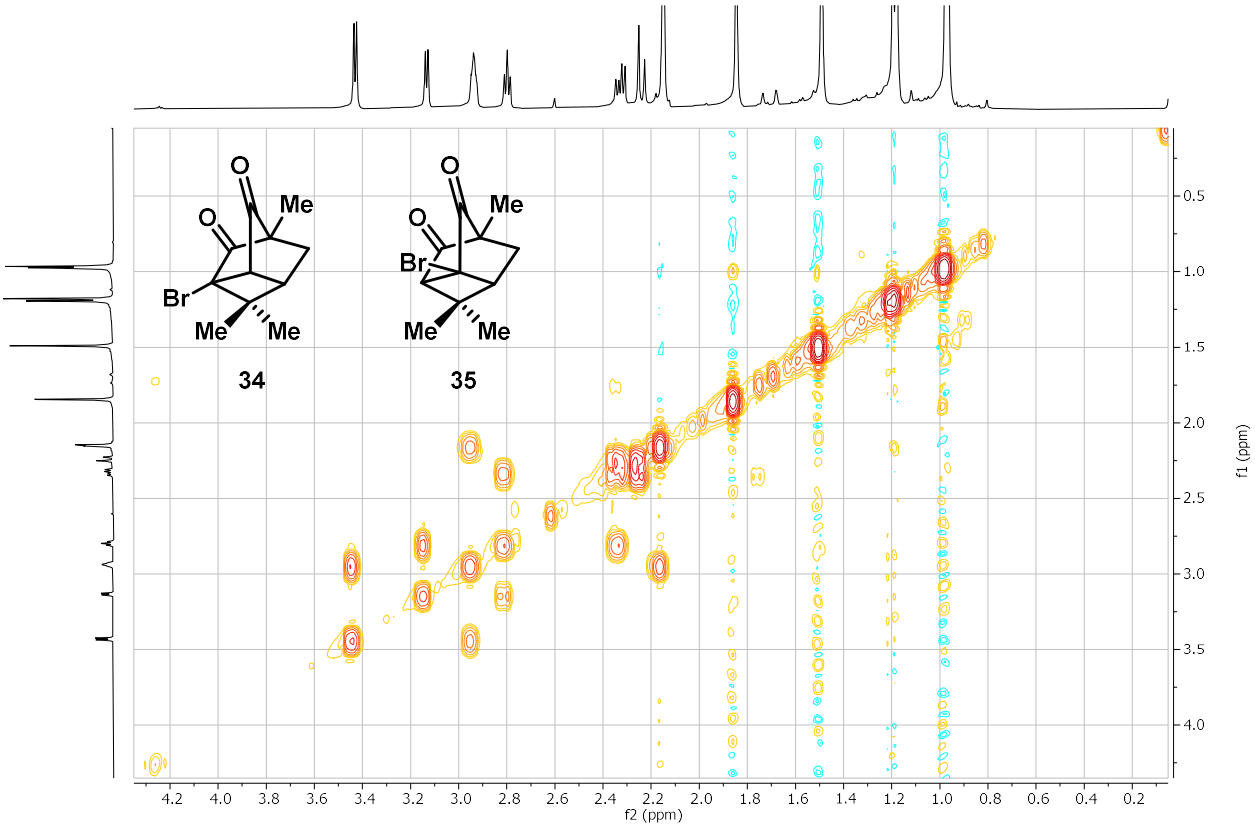
O
Me
O
Br
Me
Me
34
O
Me
O
Br
Me
Me
35
f2 (ppm)
f1 (ppm)

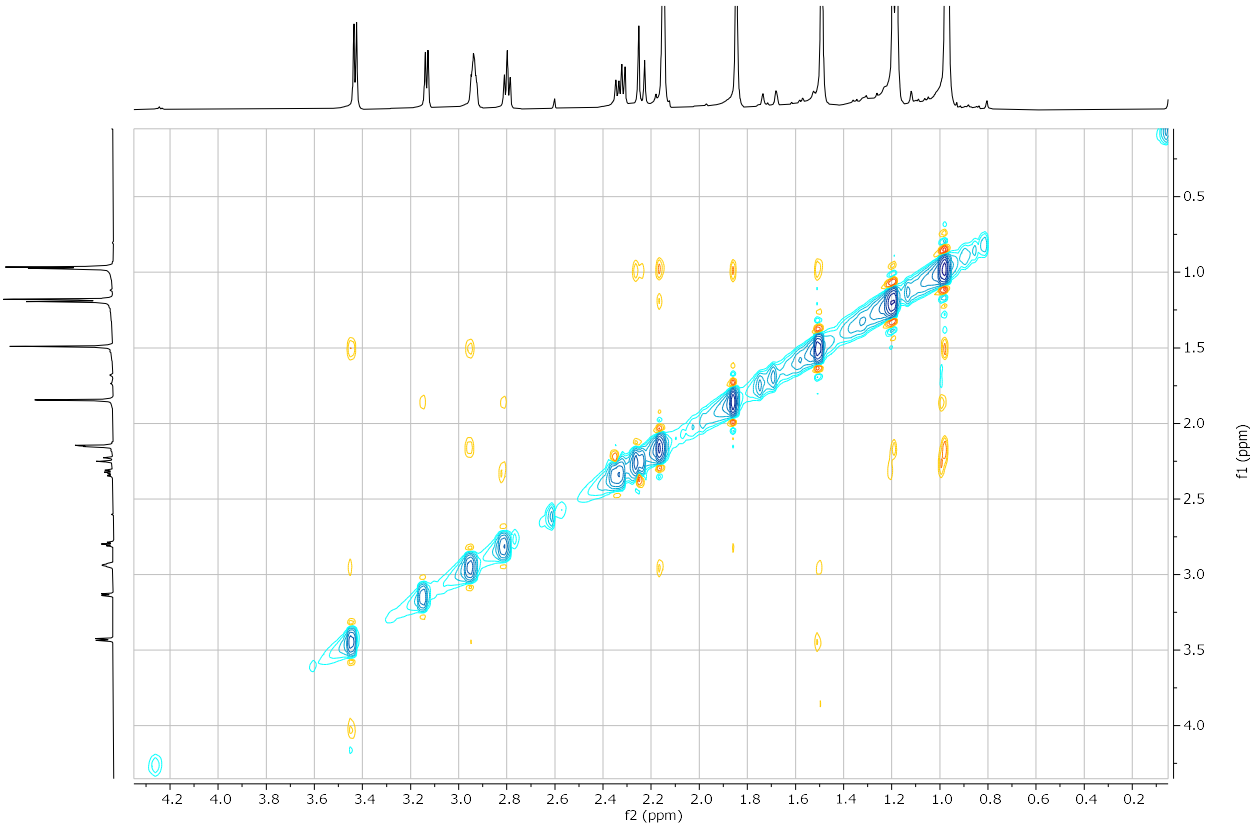
f2 (ppm)
f1 (ppm)

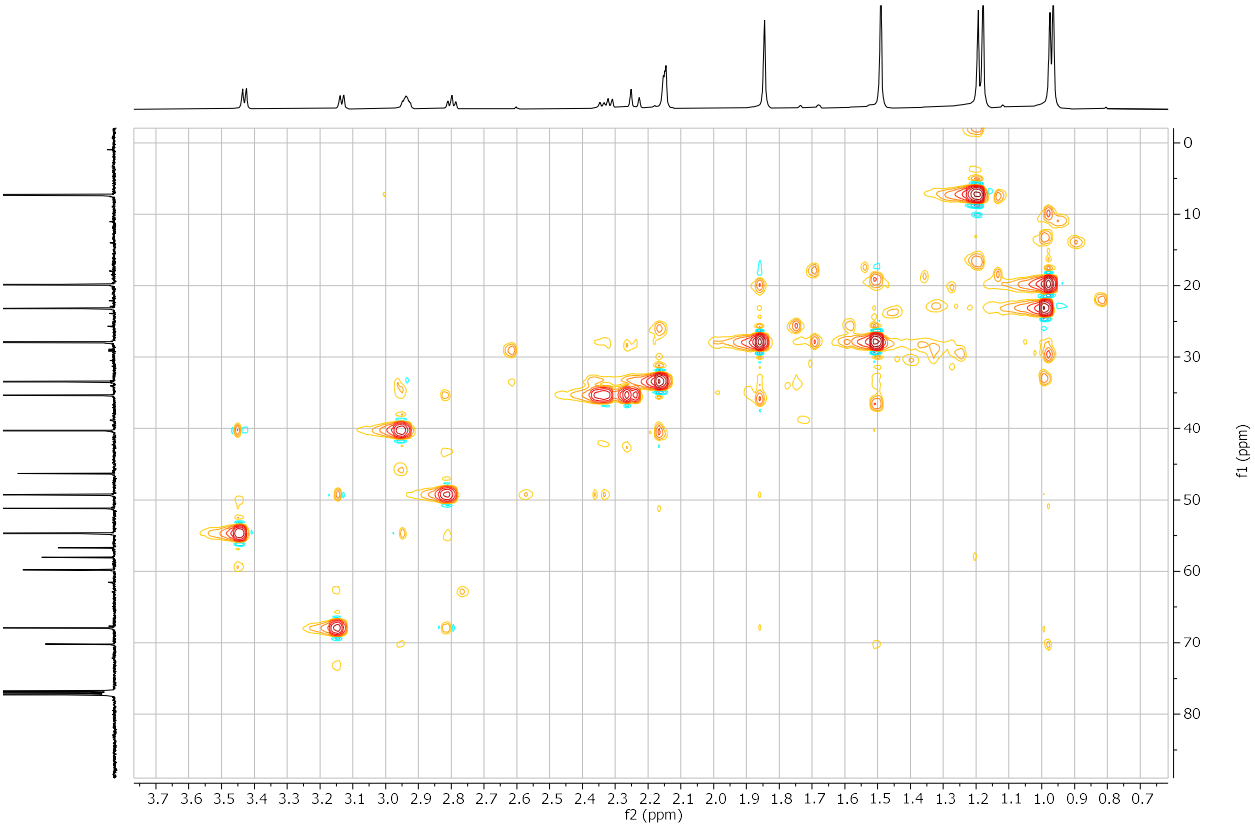
0
10
20
30
40
50
60
70
80
f1 (ppm)
3.7 3.6 3.5 3.4 3.3 3.2 3.1 3.0 2.9 2.8 2.7 2.6 2.5 2.4 2.3 2.2 2.1 2.0 1.9 1.8 1.7 1.6 1.5 1.4 1.3 1.2 1.1 1.0 0.9 0.8 0.7
f2 (ppm)

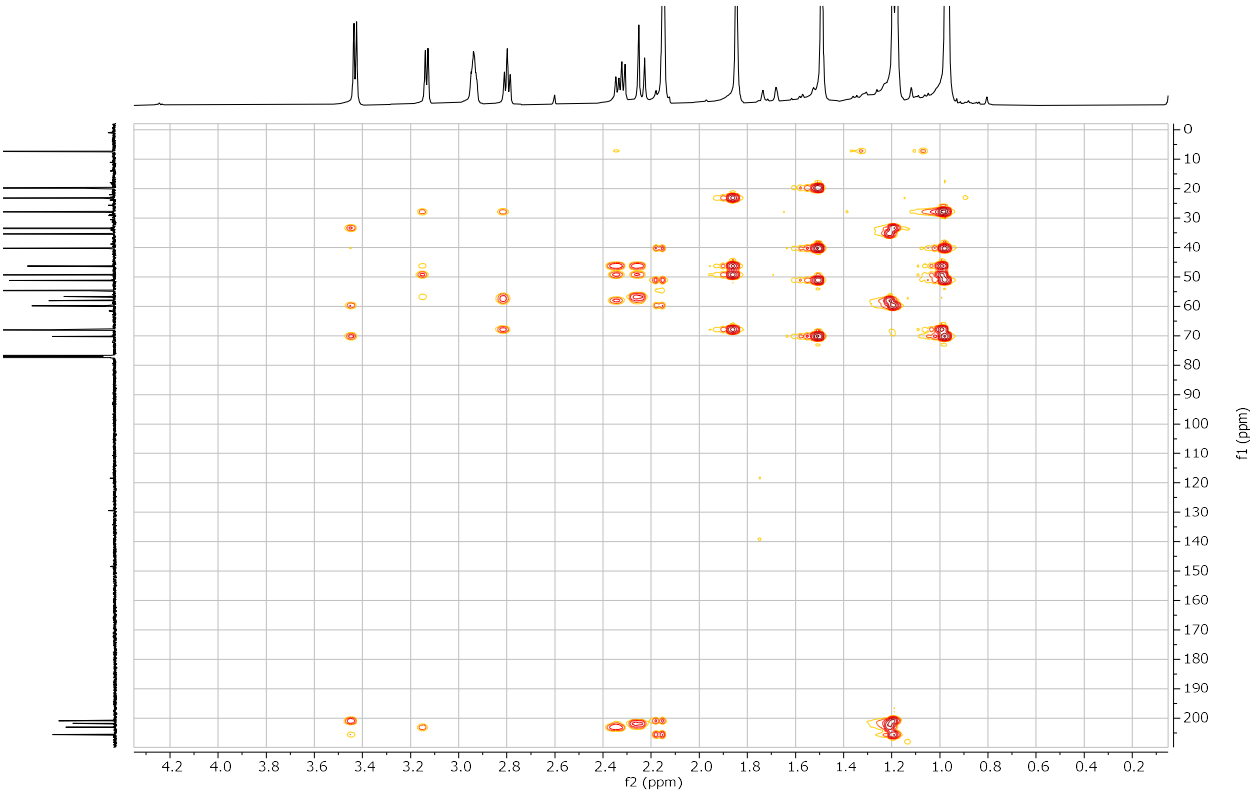
0
10
20
30
40
50
60
70
80
90
100
110
120
130
140
150
160
170
180
190
200
f1 (ppm)
4.2 4.0 3.8 3.6 3.4 3.2 3.0 2.8 2.6 2.4 2.2 2.0 1.8 1.6 1.4 1.2 1.0 0.8 0.6 0.4 0.2
f2 (ppm)

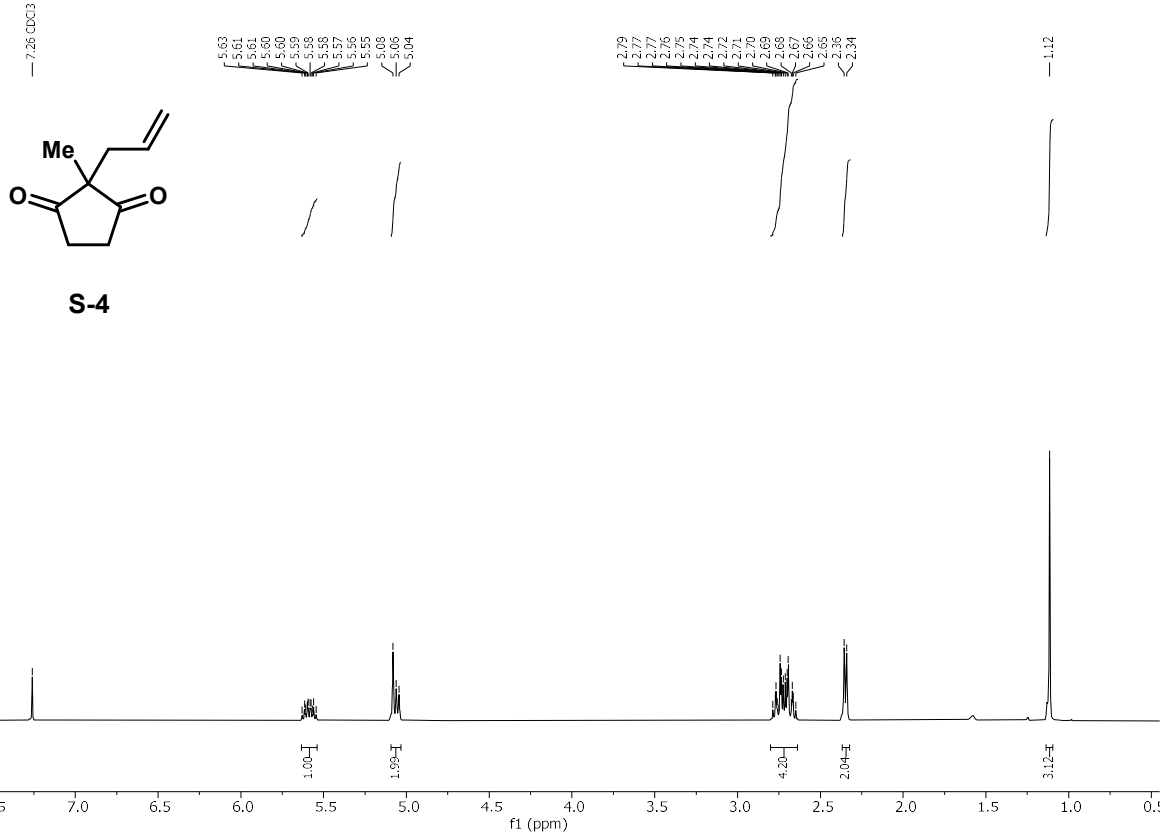
7.26 CDCl3
5.63
5.61
5.61
5.60
5.60
5.59
5.58
5.58
5.57
5.56
5.55
5.08
5.06
5.04
2.79
2.77
2.77
2.76
2.75
2.74
2.74
2.72
2.71
2.70
2.69
2.68
2.67
2.66
2.65
2.36
2.34
1.12
Me
O
O
1.00
1.99
4.20
2.04
3.12
7.5
7.0
6.5
6.0
5.5
5.0
4.5
4.0
3.5
3.0
2.5
2.0
1.5
1.0
f1 (ppm)

S-4

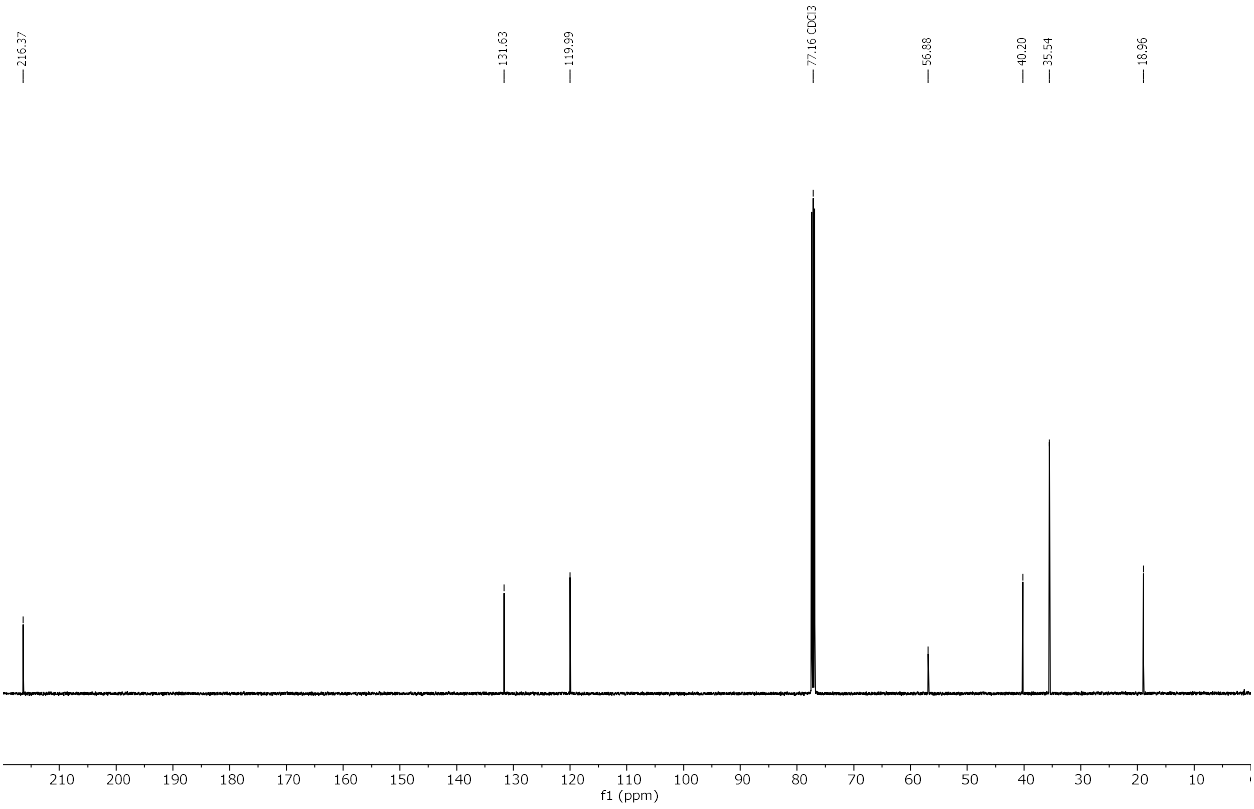
216.37
131.63
119.99
77.16 CDCl3
56.88
40.20
35.54
18.96
210
200
190
180
170
160
150
140
130
120
110
100
90
80
70
60
50
40
30
20
10
f1 (ppm)

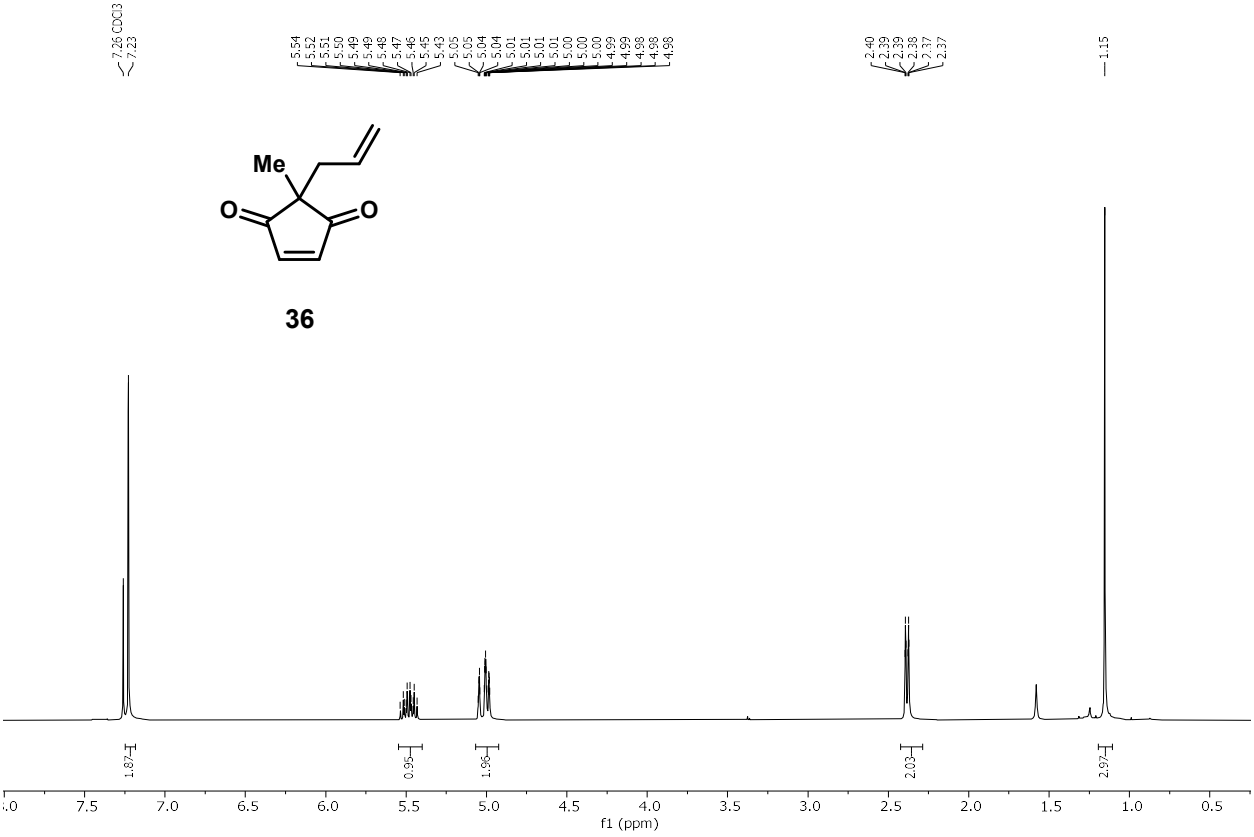
7.26 CDCl3
7.23
5.54
5.52
5.51
5.50
5.49
5.49
5.48
5.47
5.46
5.45
5.43
5.05
5.05
5.04
5.04
5.01
5.01
5.01
5.01
5.00
5.00
5.00
4.99
4.99
4.98
4.98
4.98
2.40
2.39
2.39
2.39
2.38
2.37
2.37
1.15
Me
O
O
36
1.87
0.99
1.98
2.03
2.97
f1 (ppm)

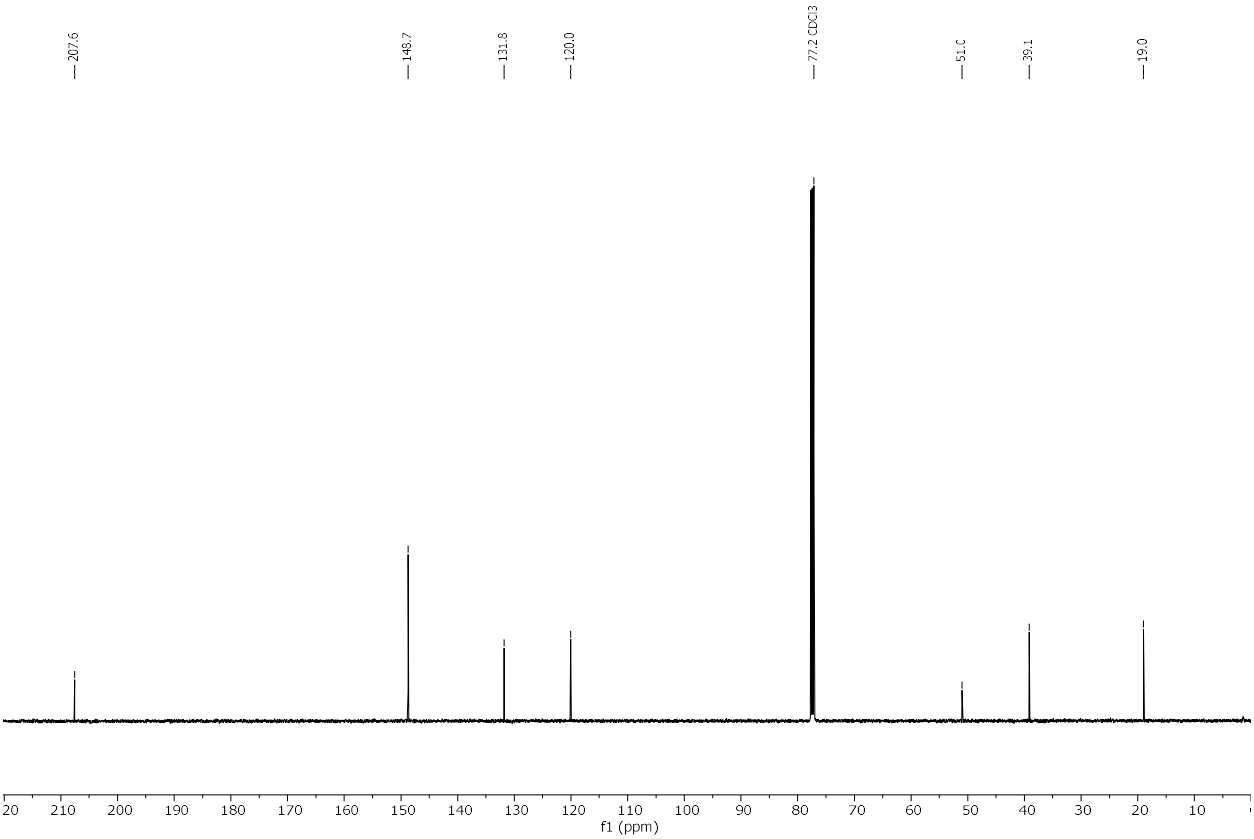
207.6
148.7
131.8
120.0
77.2 CDCl3
51.0
39.1
19.0
f1 (ppm)

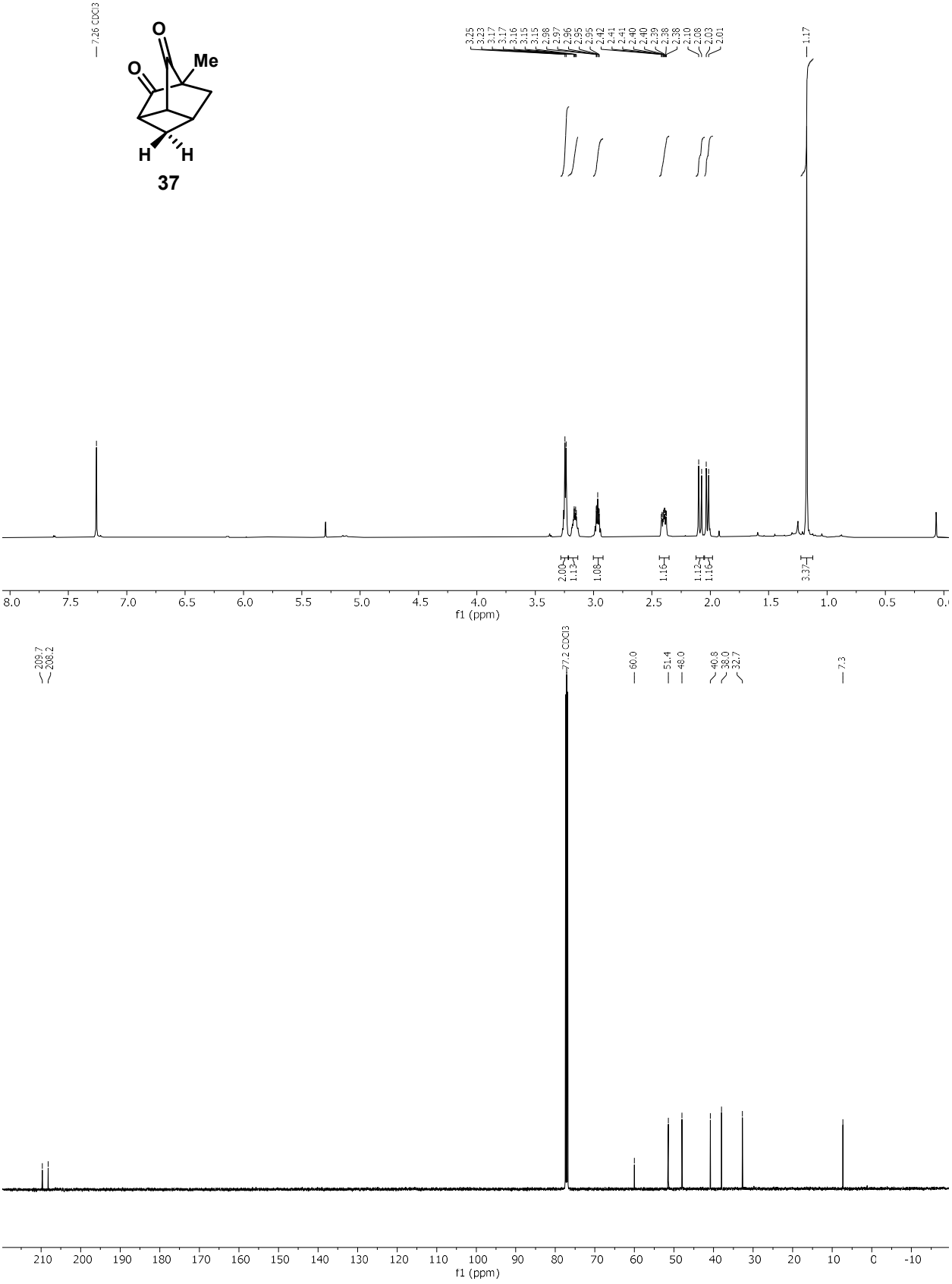
7.26 CDCl3
O
O
Me
H
H
37
3.25
3.23
3.17
3.17
3.16
3.15
3.15
2.98
2.97
2.96
2.95
2.95
2.42
2.41
2.41
2.40
2.40
2.39
2.38
2.38
2.10
2.08
2.03
2.01
1.17
2.00
1.13
1.08
1.16
1.12
1.16
3.37
f1 (ppm)
209.7
208.2
77.2 CDCl3
60.0
51.4
48.0
40.8
38.0
32.7
7.3
f1 (ppm)

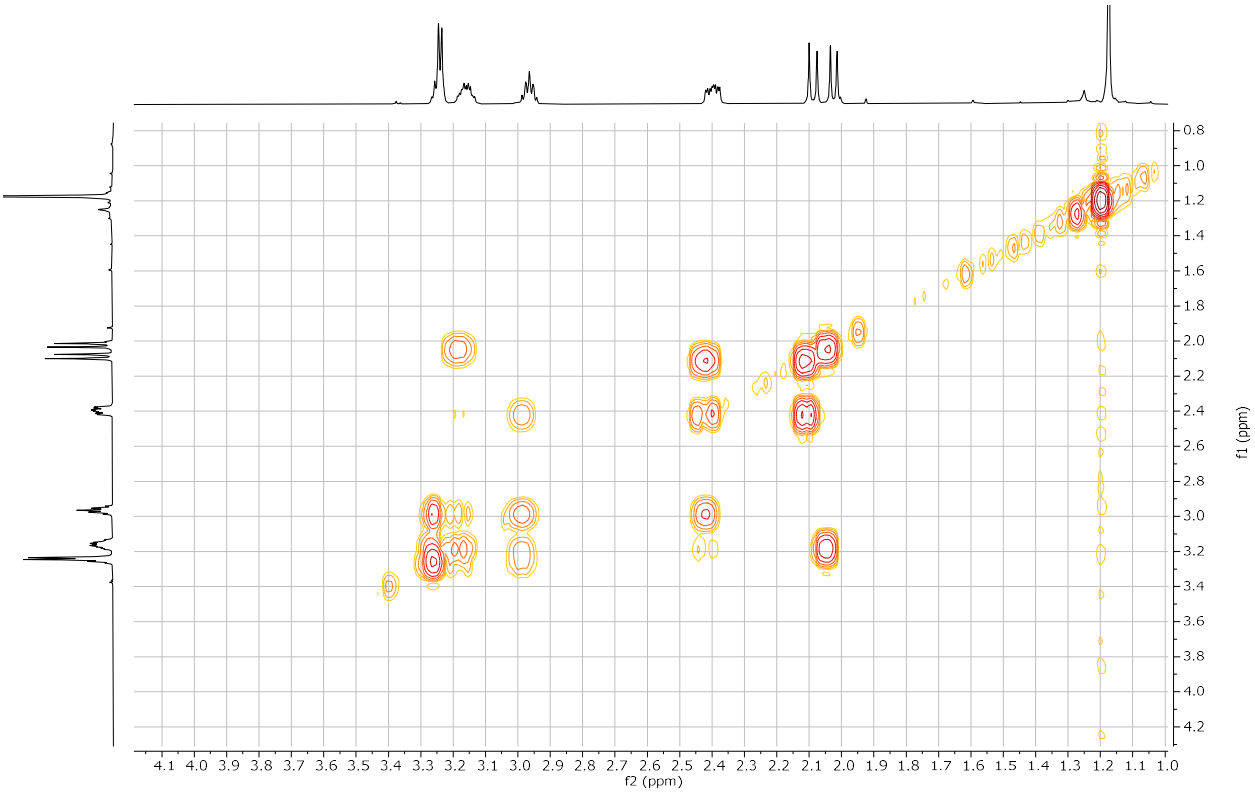
f2 (ppm)
f1 (ppm)

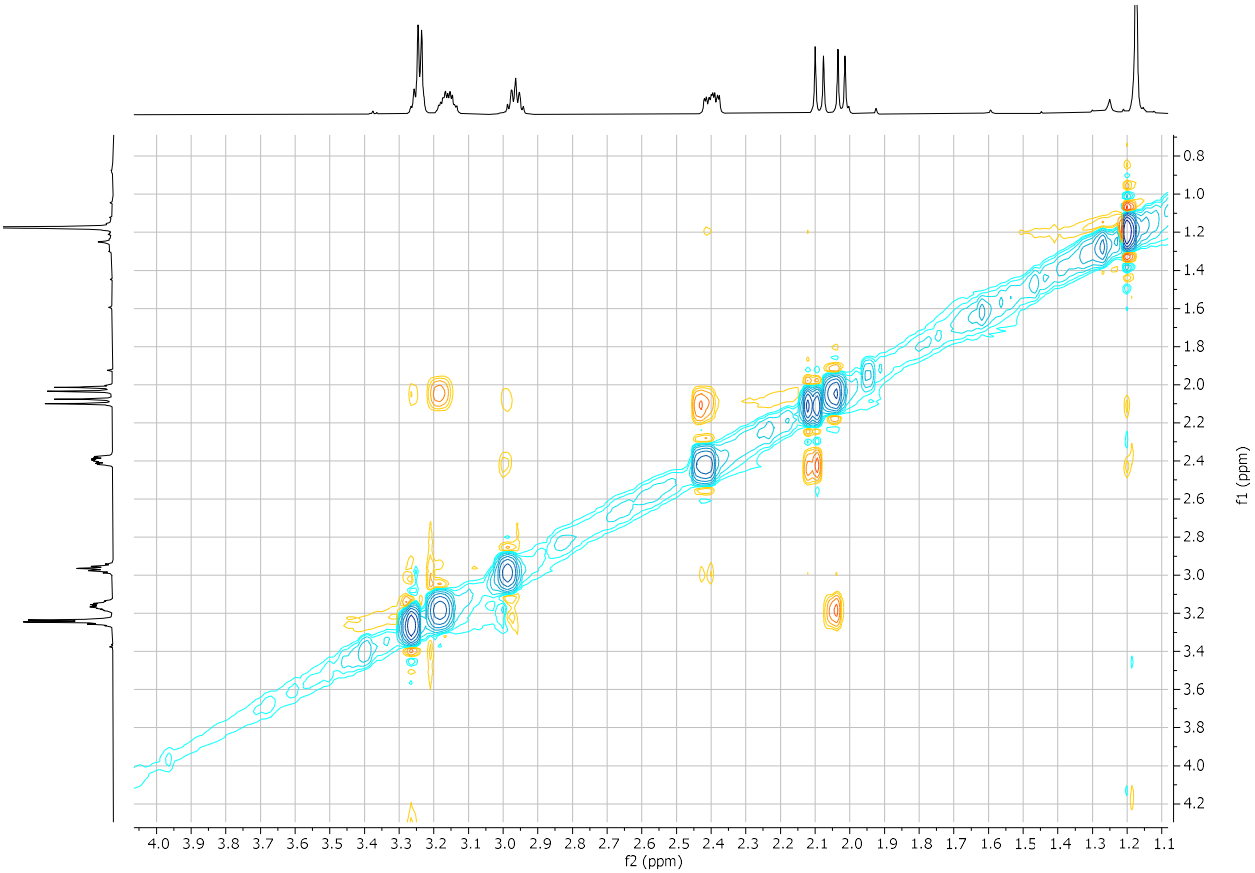
f2 (ppm)
f1 (ppm)

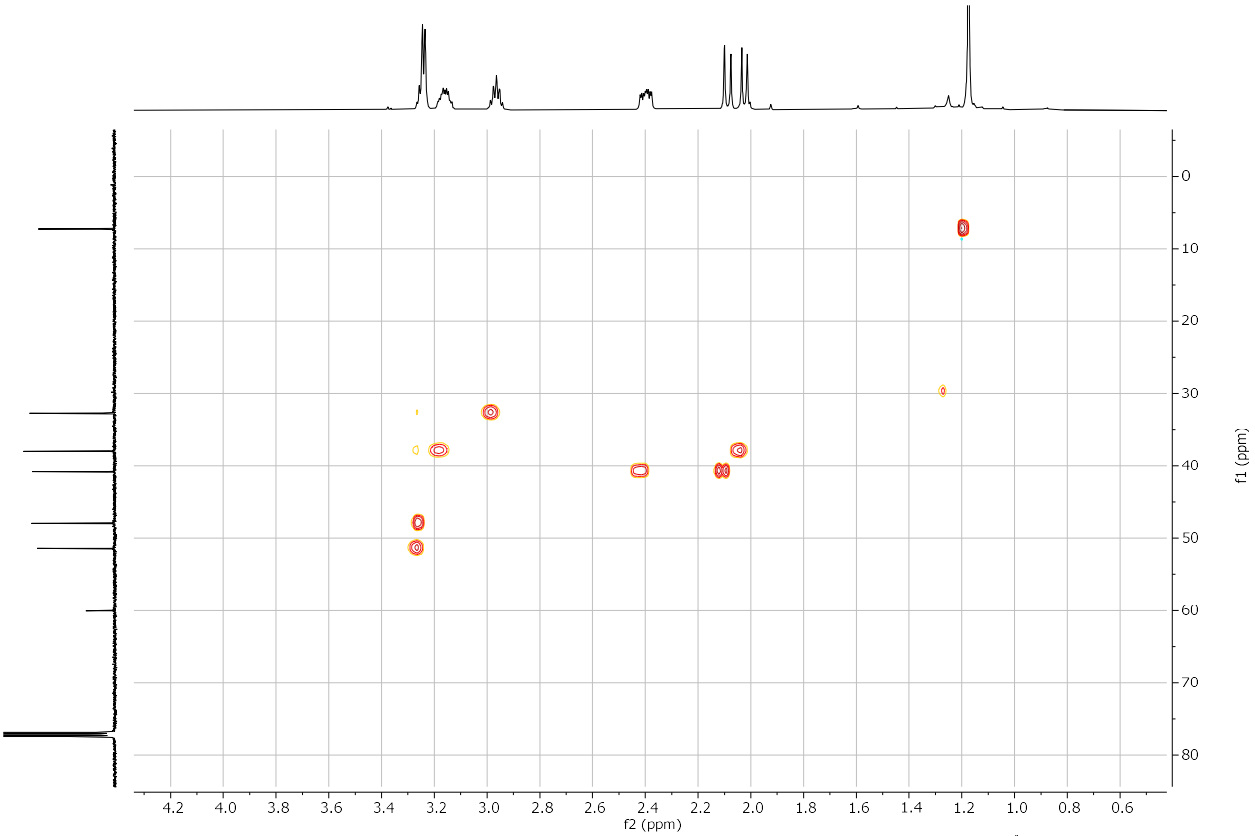
f2 (ppm)
f1 (ppm)

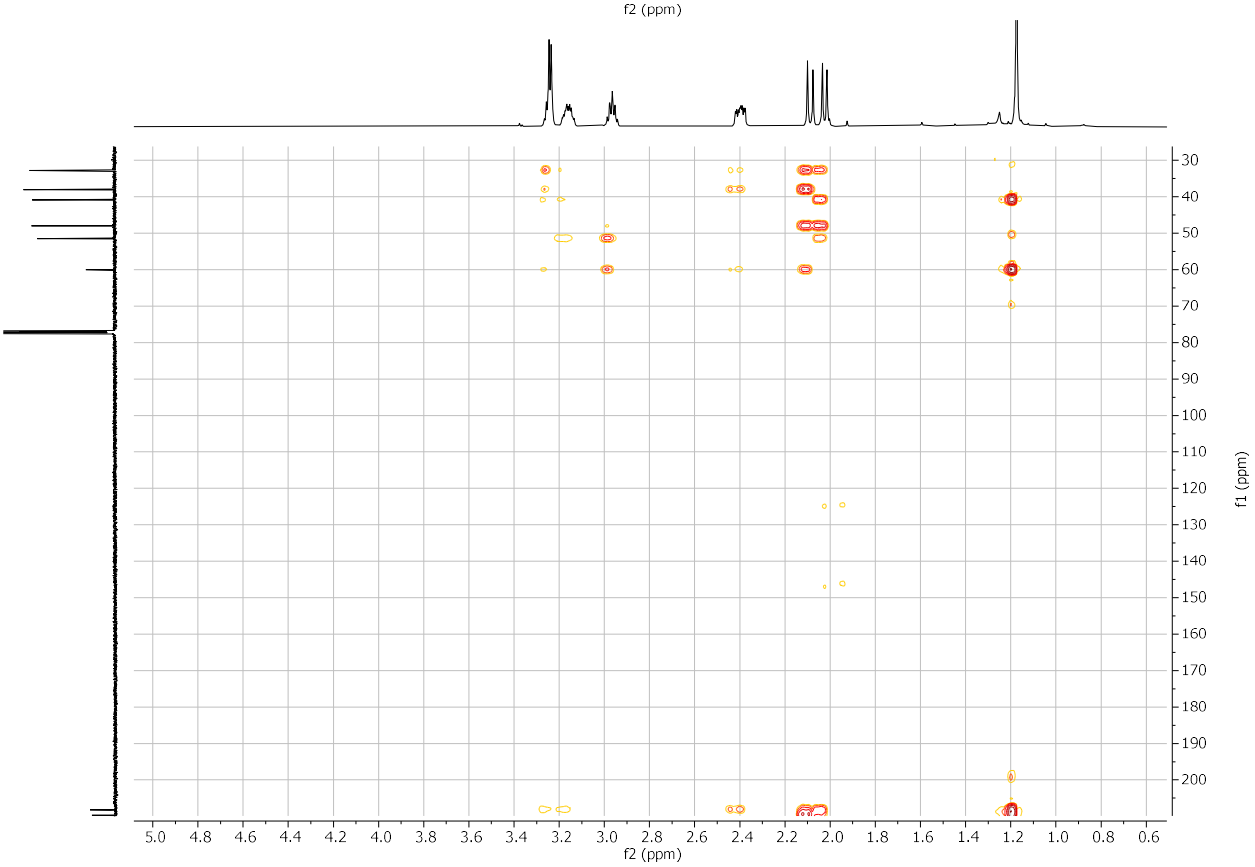
f2 (ppm)
f1 (ppm)

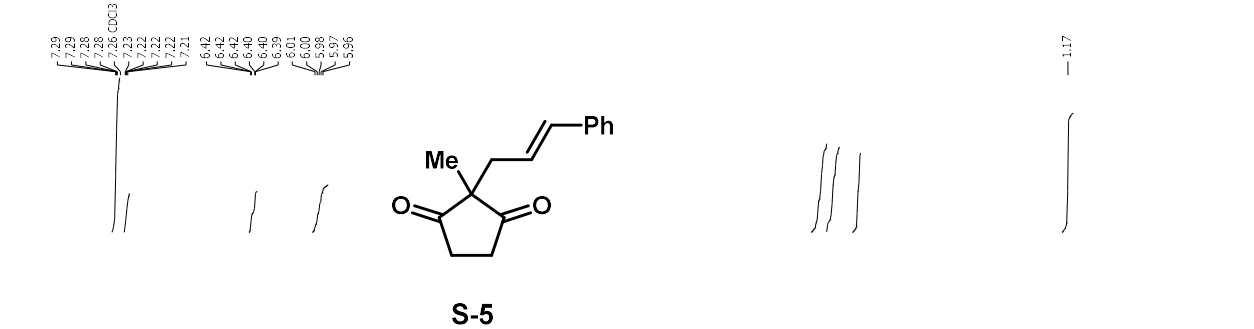

S-5

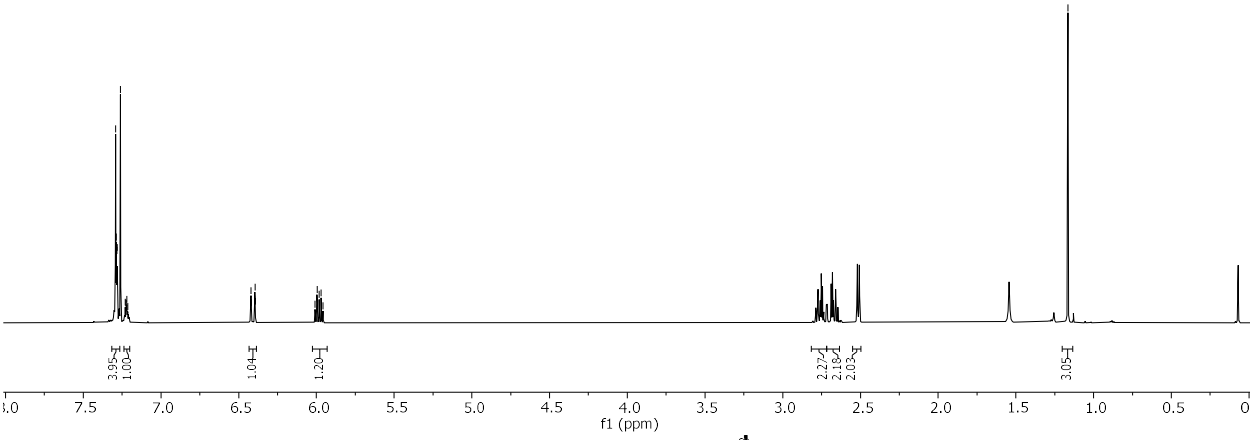

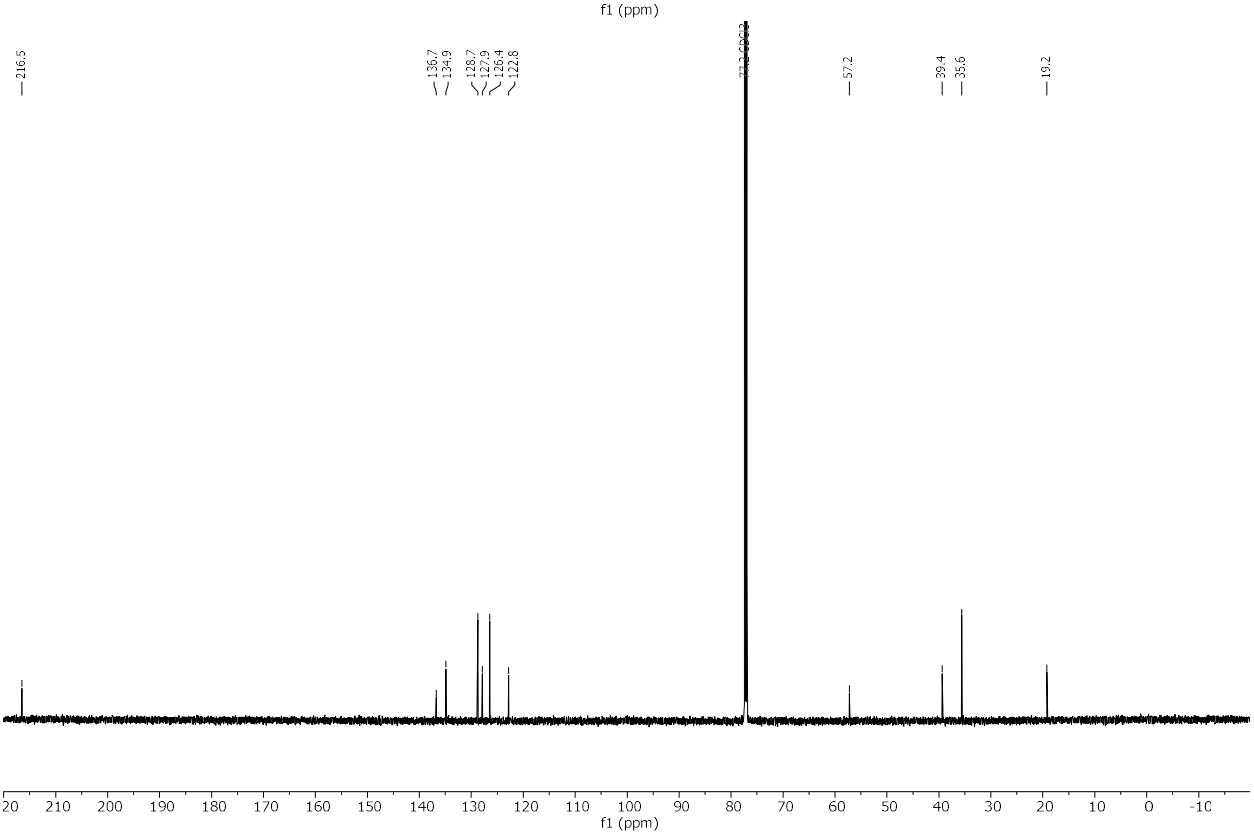

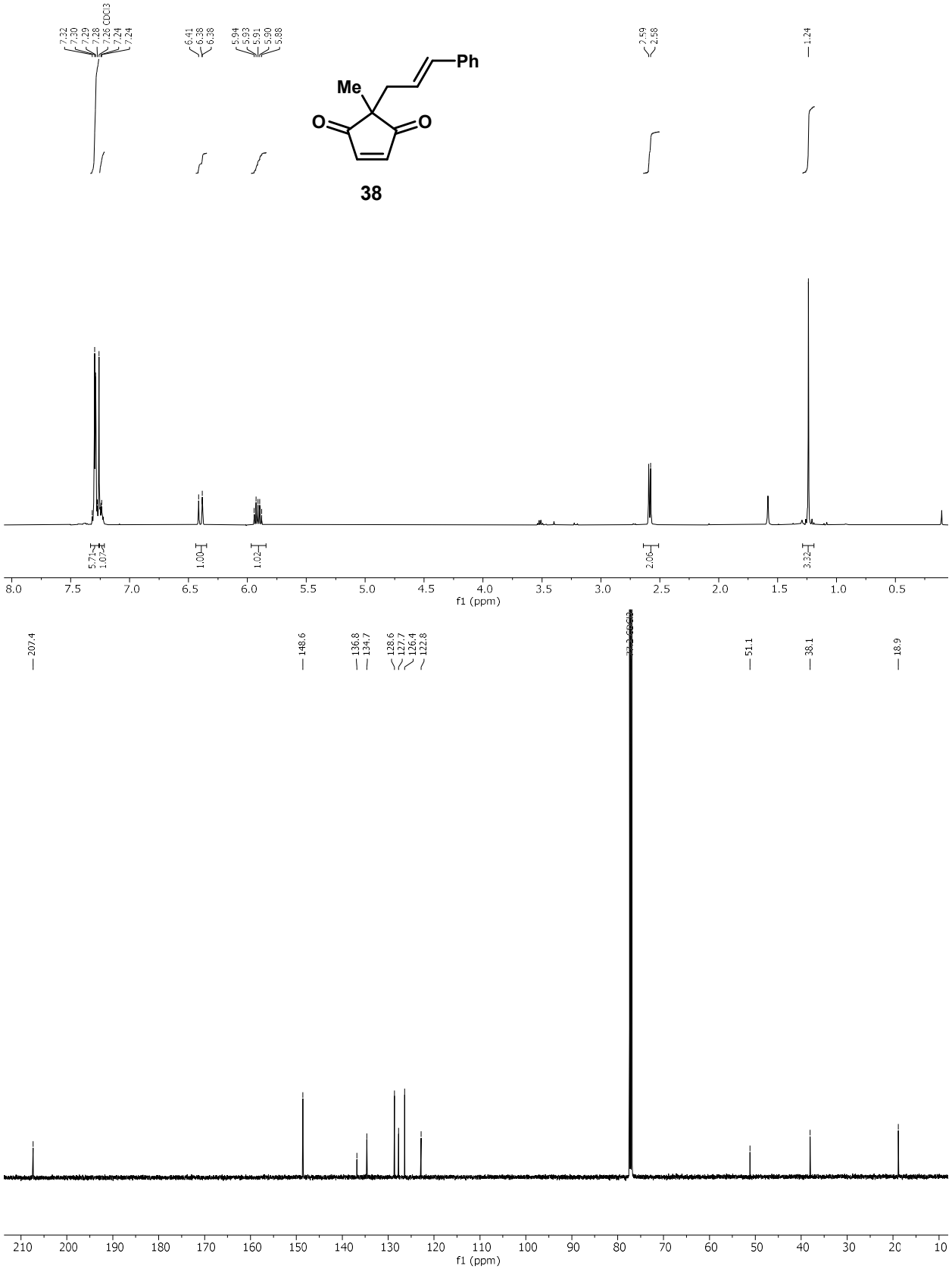
7.32
7.30
7.29
7.28
7.26 CDCl3
7.24
7.24
6.41
6.38
6.38
5.94
5.93
5.91
5.90
5.88
2.59
2.58
1.24
Ph
Me
O
O
38
5.71
1.07
1.00
1.02
2.06
3.32
f1 (ppm)
207.4
148.6
136.8
134.7
128.6
127.7
126.4
122.8
77.3 CDCl3
51.1
38.1
18.9
f1 (ppm)

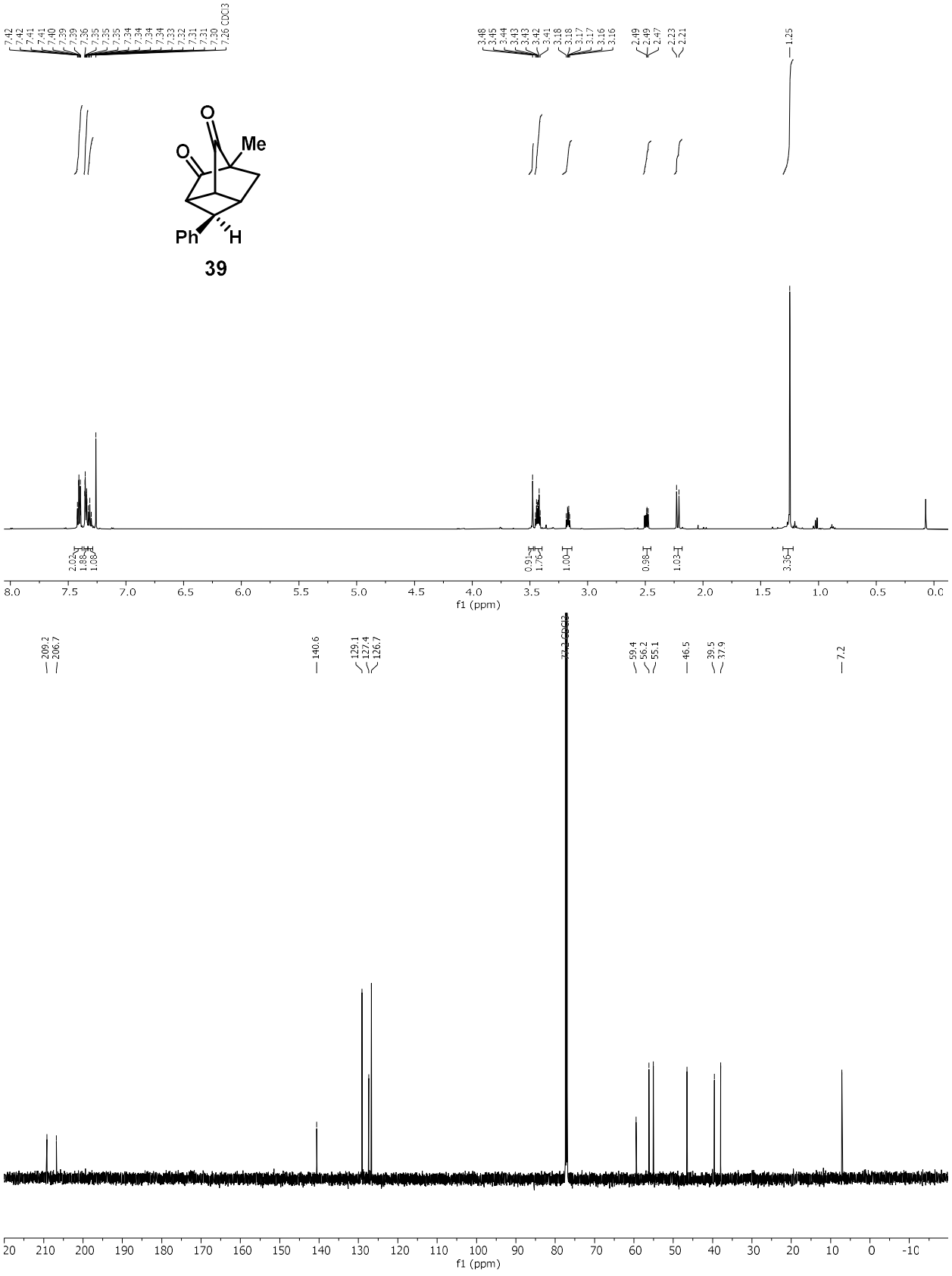
7.42
7.42
7.41
7.41
7.40
7.39
7.39
7.36
7.35
7.35
7.35
7.34
7.34
7.34
7.34
7.33
7.32
7.31
7.31
7.30
7.26 CDCl3
3.48
3.45
3.44
3.43
3.43
3.42
3.41
3.18
3.18
3.17
3.17
3.17
3.16
3.16
2.49
2.49
2.47
2.23
2.21
1.25
O
O
Me
Ph
H
39
2.02
1.88
1.08
0.91
1.76
1.00
0.98
1.03
3.36
f1 (ppm)
209.2
206.7
140.6
129.1
127.4
126.7
77.3 CDCl3
59.4
56.2
55.1
46.5
39.5
37.9
7.2
f1 (ppm)

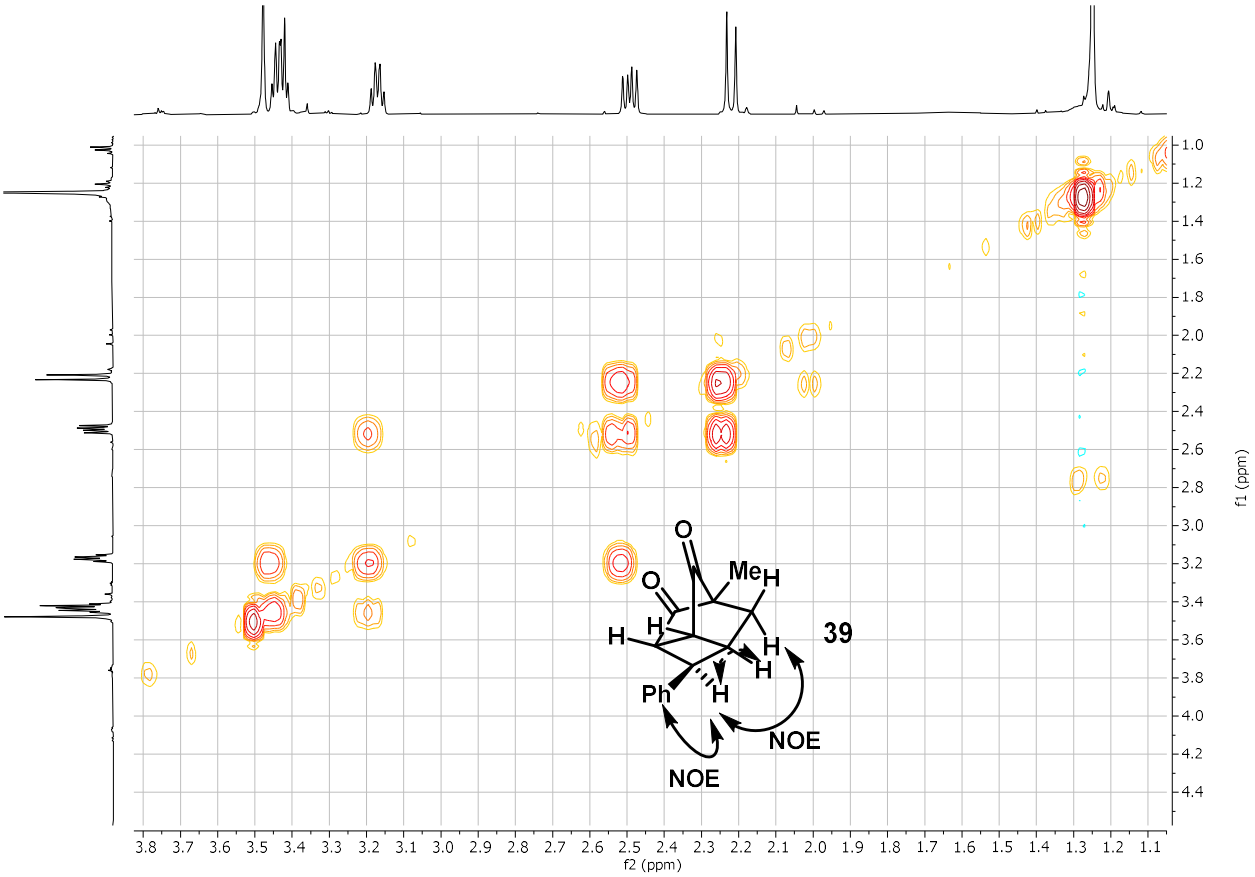
f2 (ppm)
f1 (ppm)
O
O
Me
H
H
H
H
H
Ph
H
39
NOE
NOE

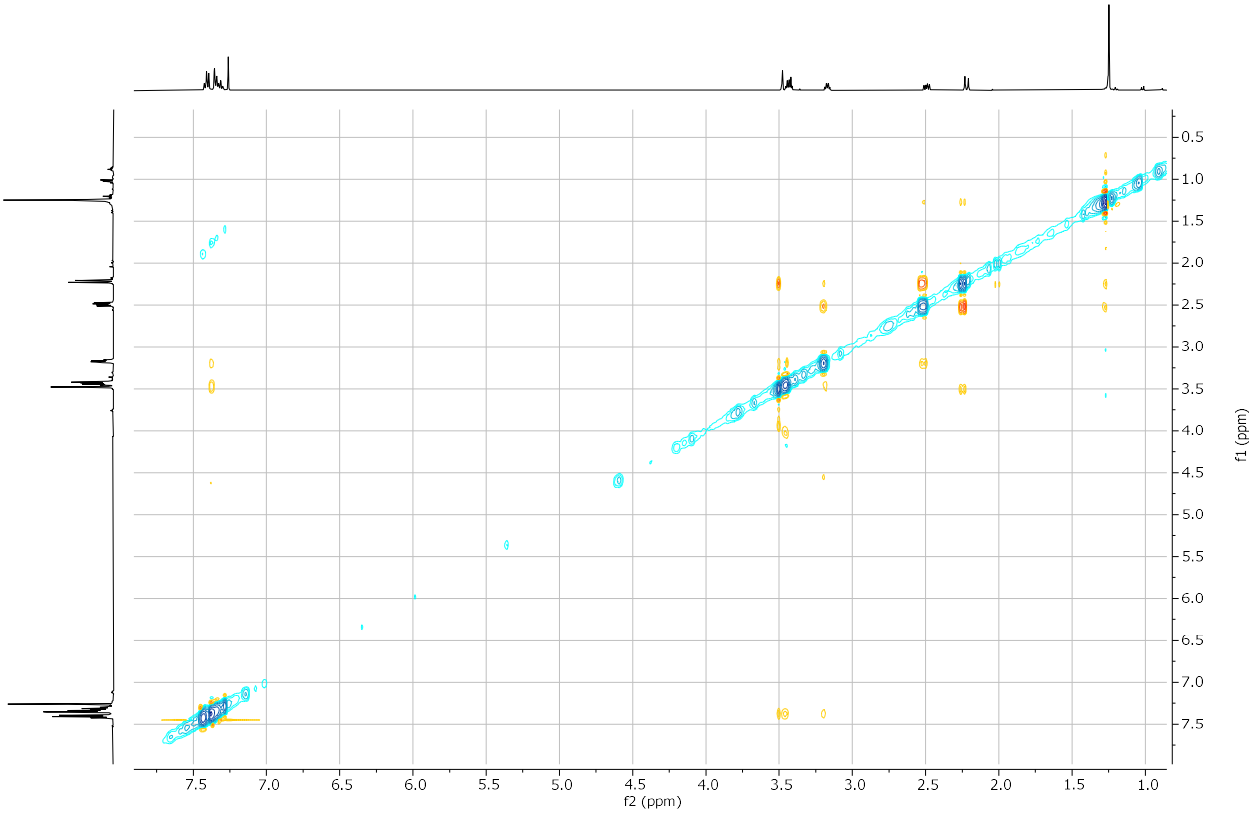
f2 (ppm)
f1 (ppm)

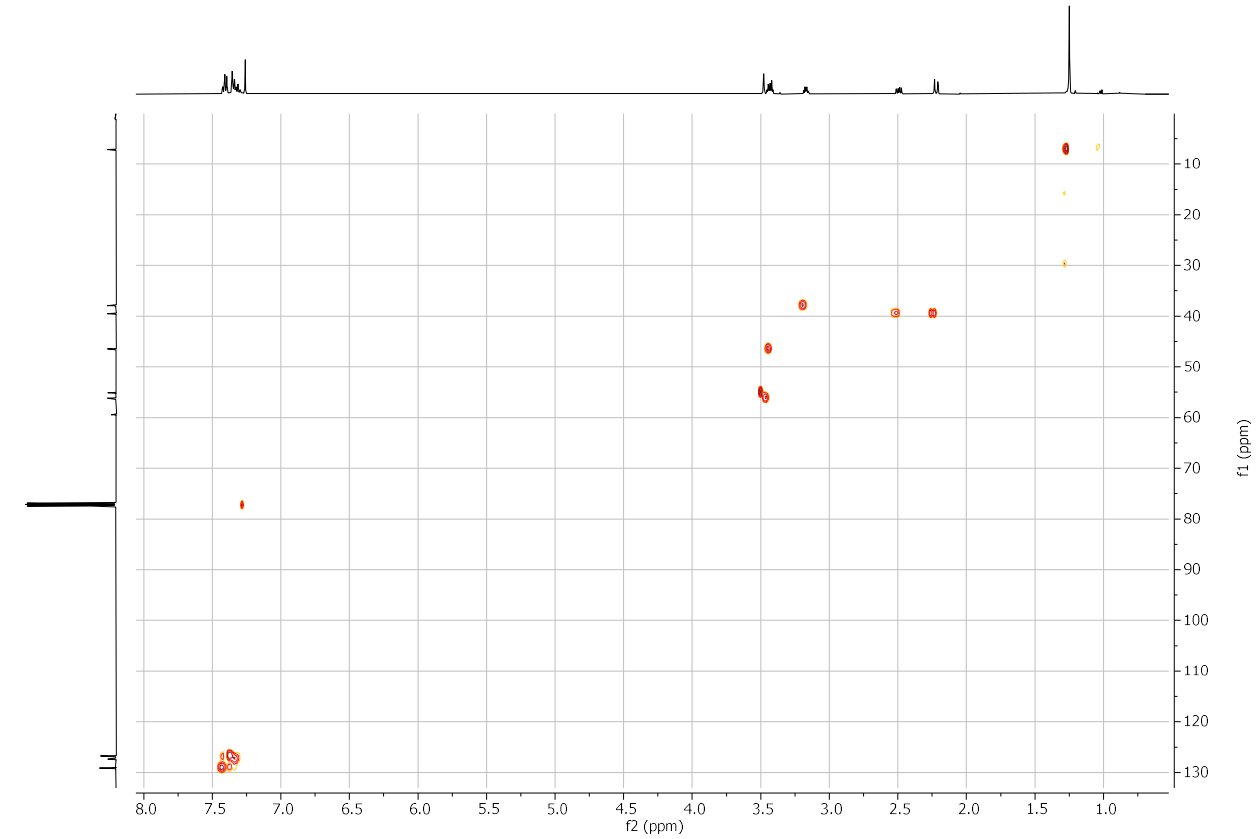
f2 (ppm)
f1 (ppm)

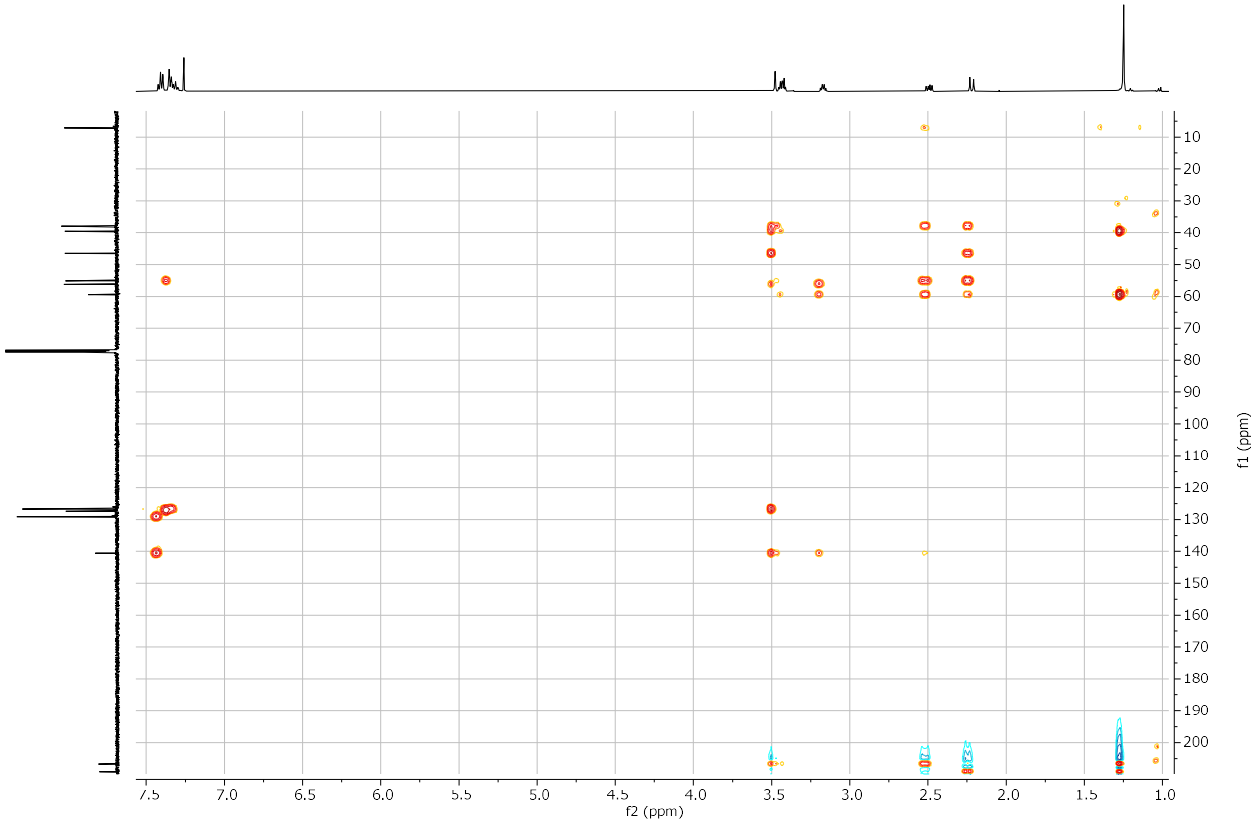
f2 (ppm)
f1 (ppm)

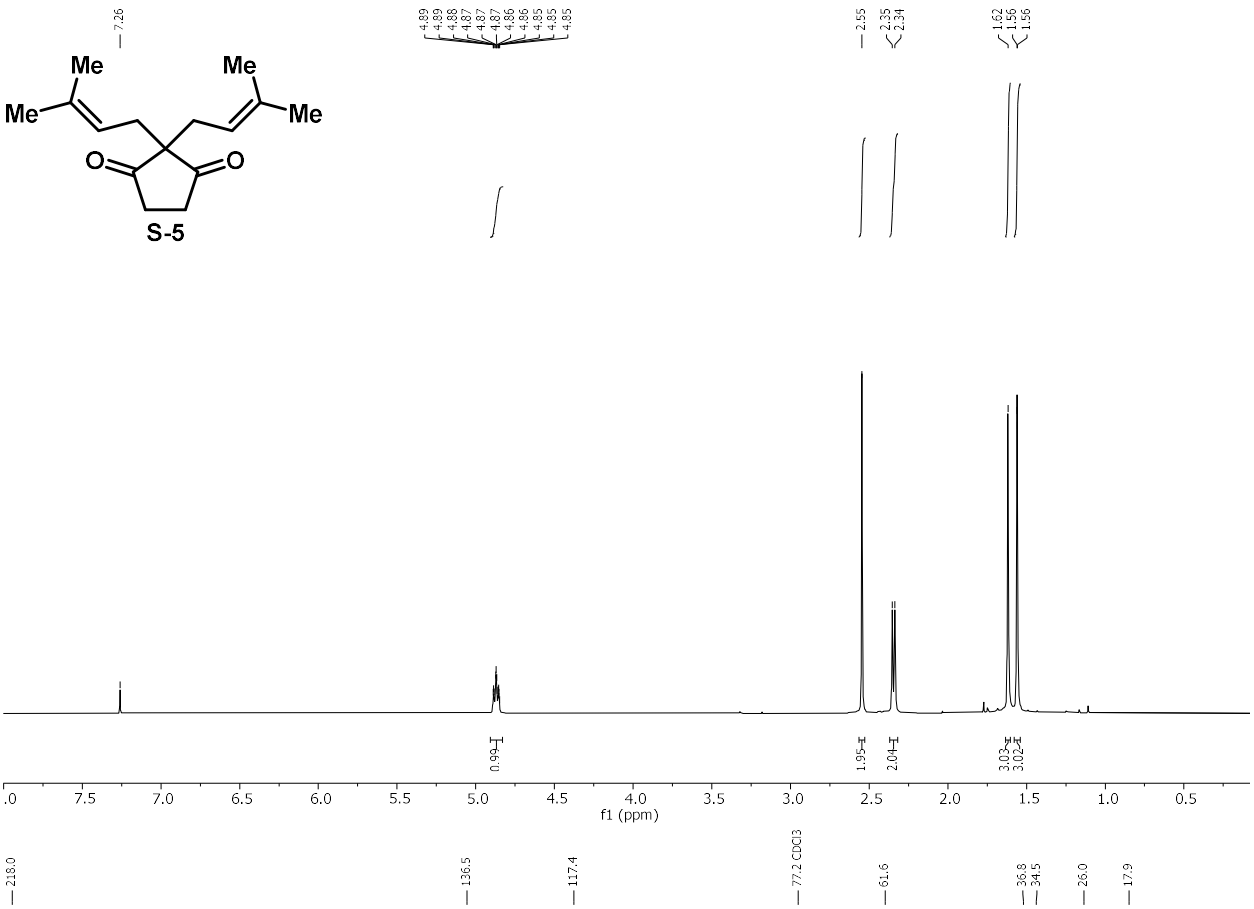
Me
Me
Me
Me
O
O
S-5
7.26
4.89
4.89
4.88
4.87
4.87
4.87
4.86
4.86
4.85
4.85
4.85
2.55
2.35
2.34
1.62
1.56
1.56
0.99
1.95
2.04
3.03
3.02
f1 (ppm)

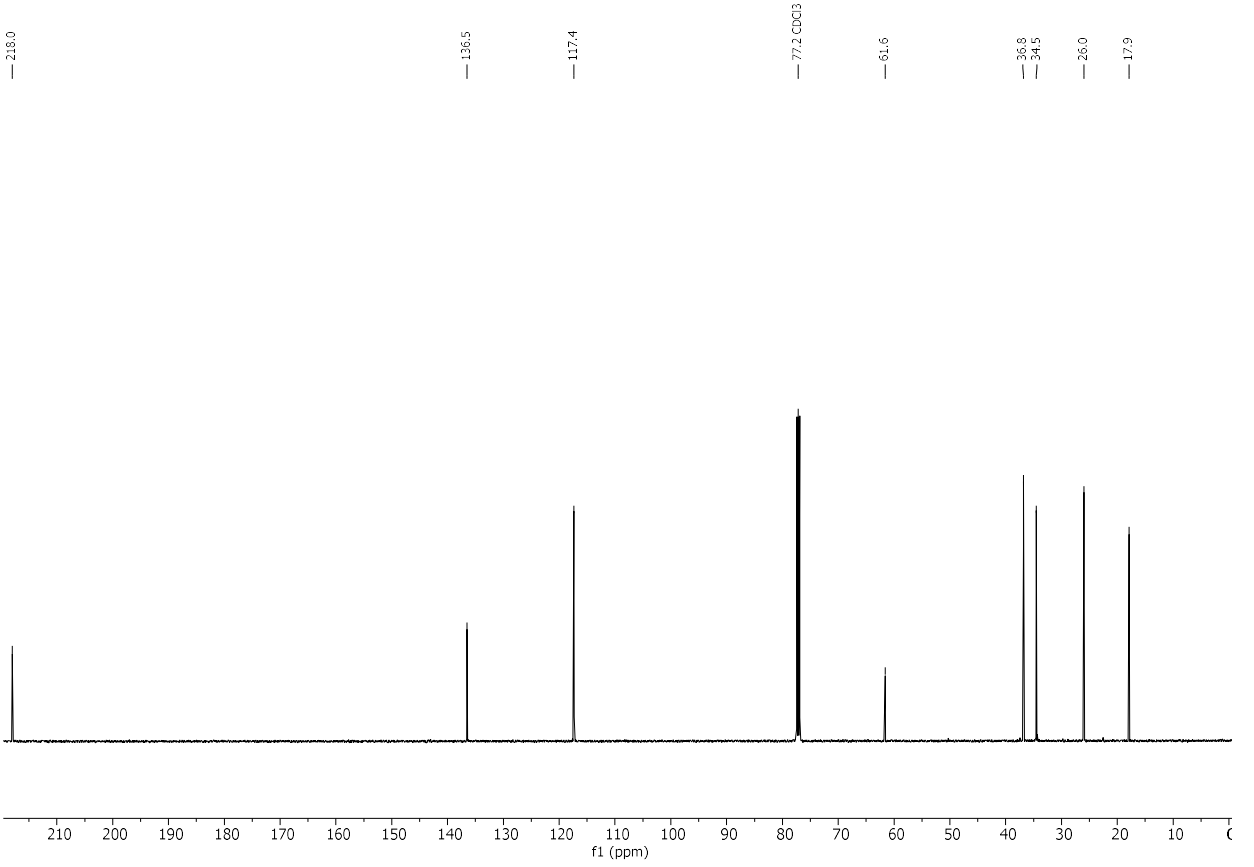
218.0
136.5
117.4
77.2 CDCl3
61.6
36.8
34.5
26.0
17.9
f1 (ppm)

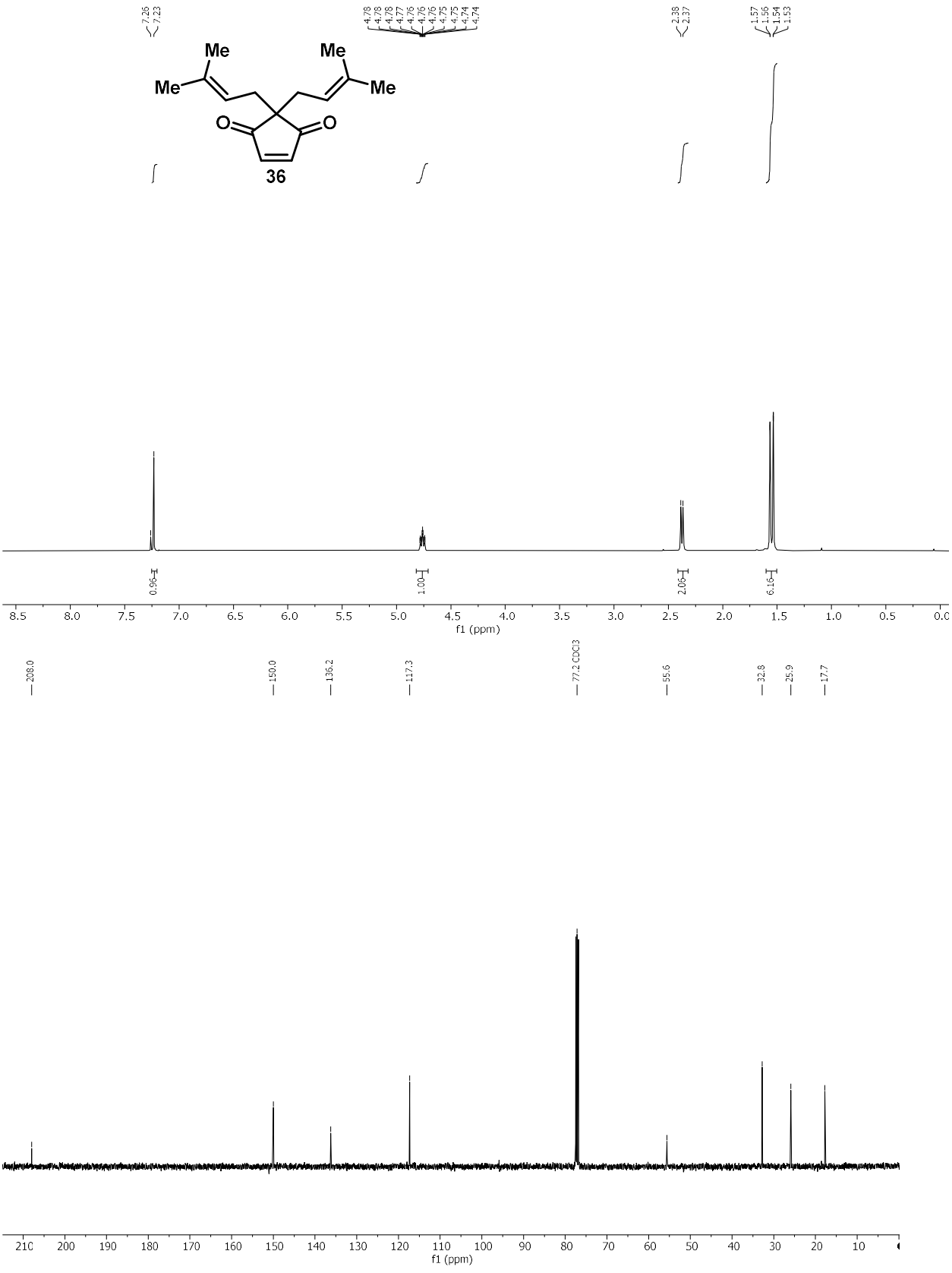
Me
Me
Me
Me
O
O
36
f1 (ppm)
f1 (ppm)

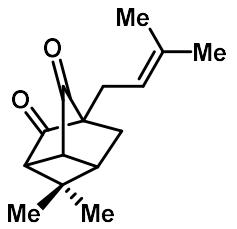

41

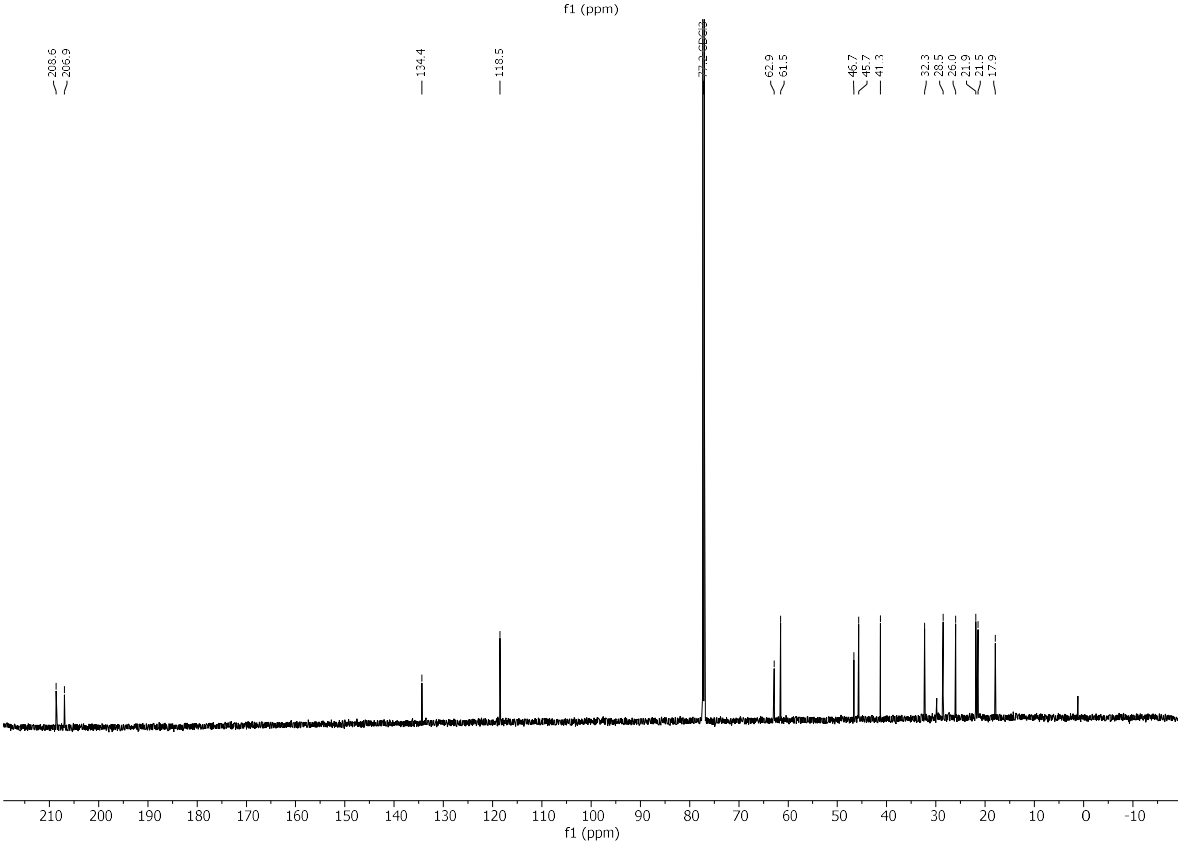

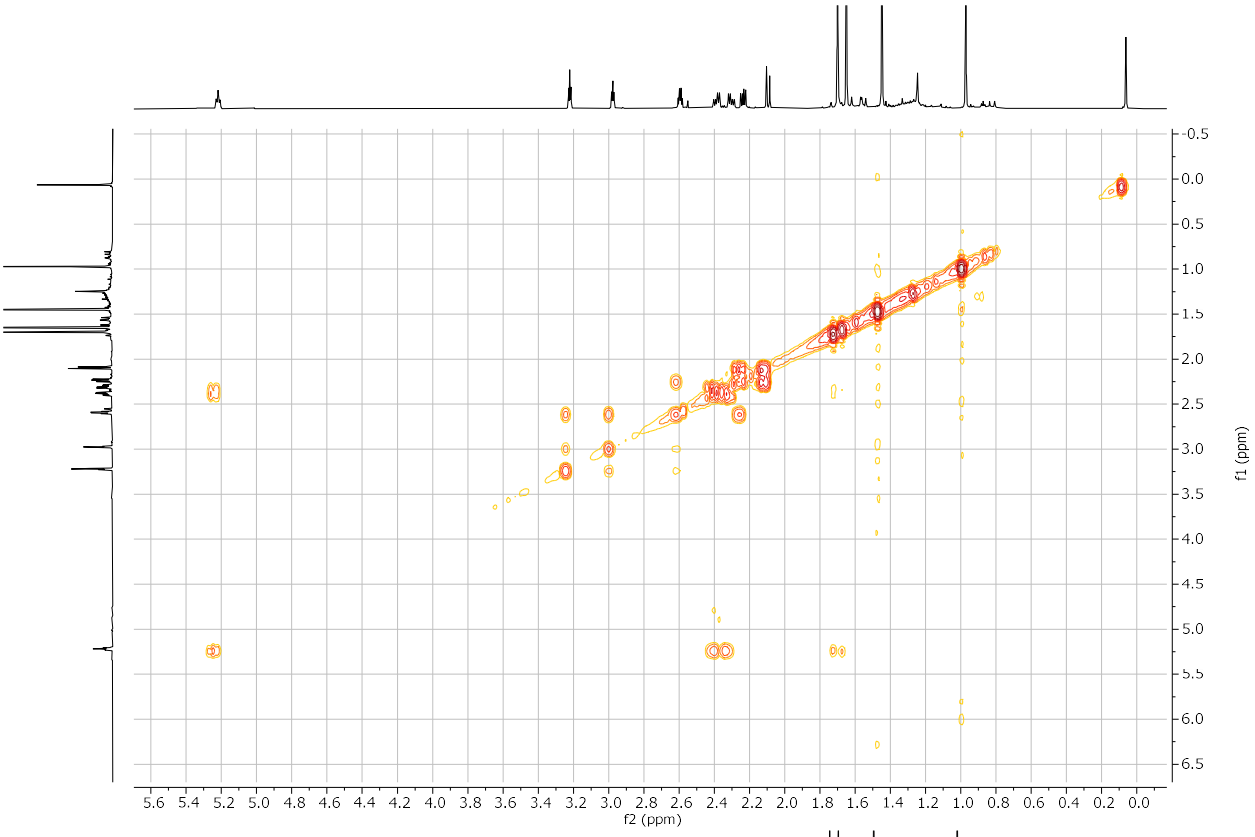
f2 (ppm)
f1 (ppm)

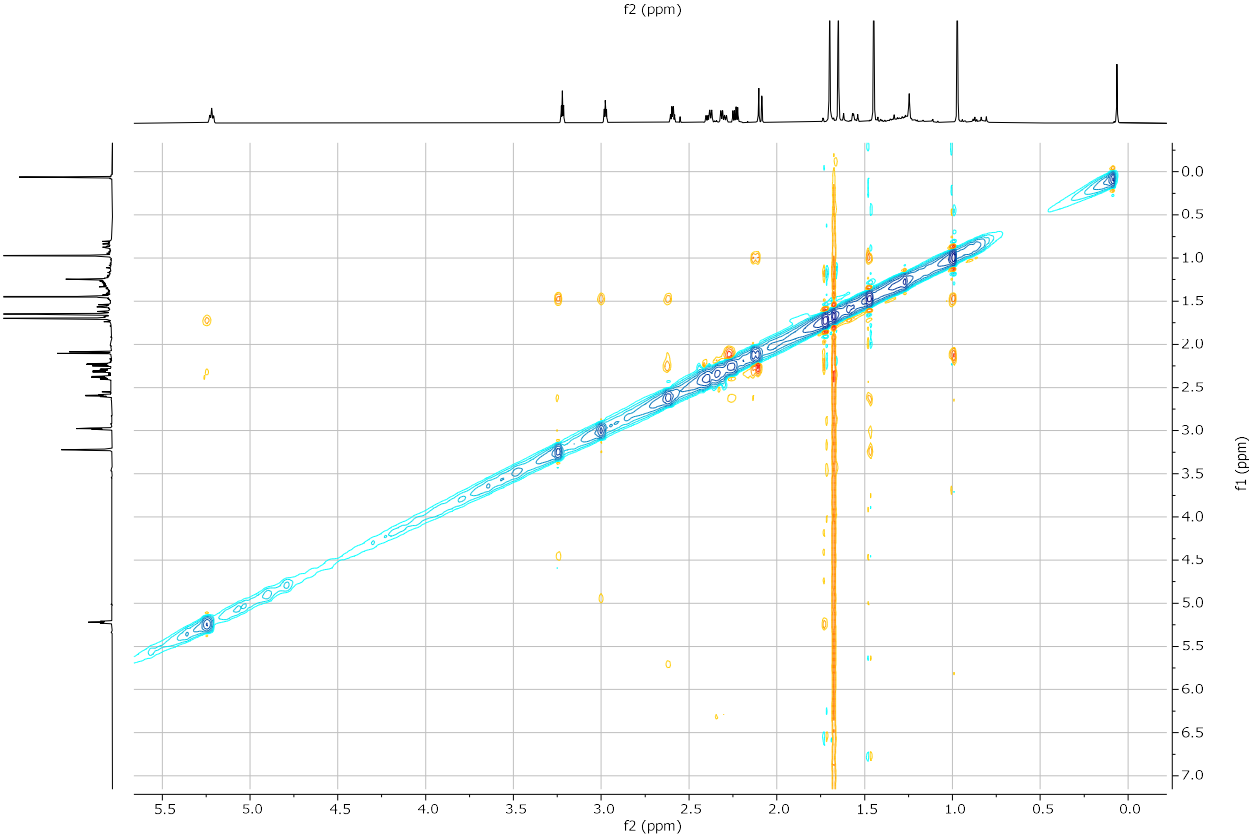
f2 (ppm)
f1 (ppm)

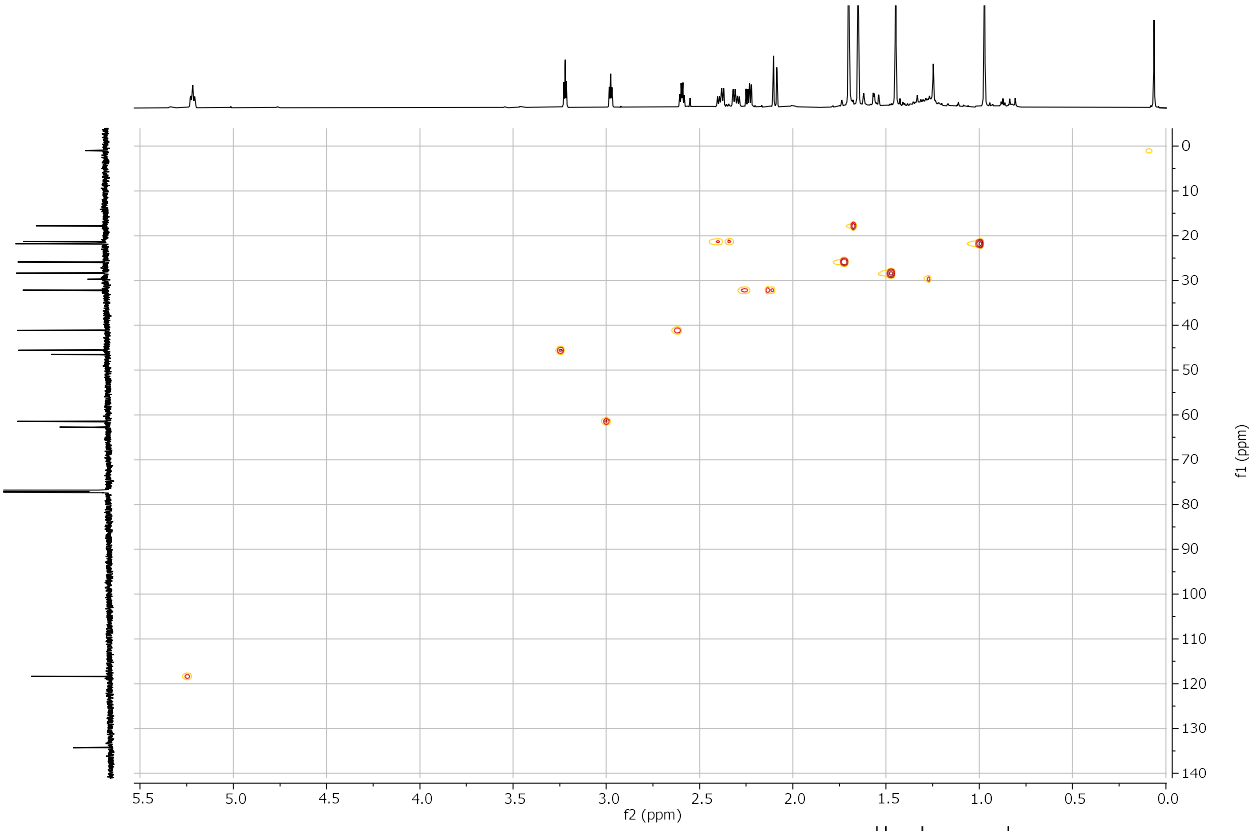
f2 (ppm)
f1 (ppm)

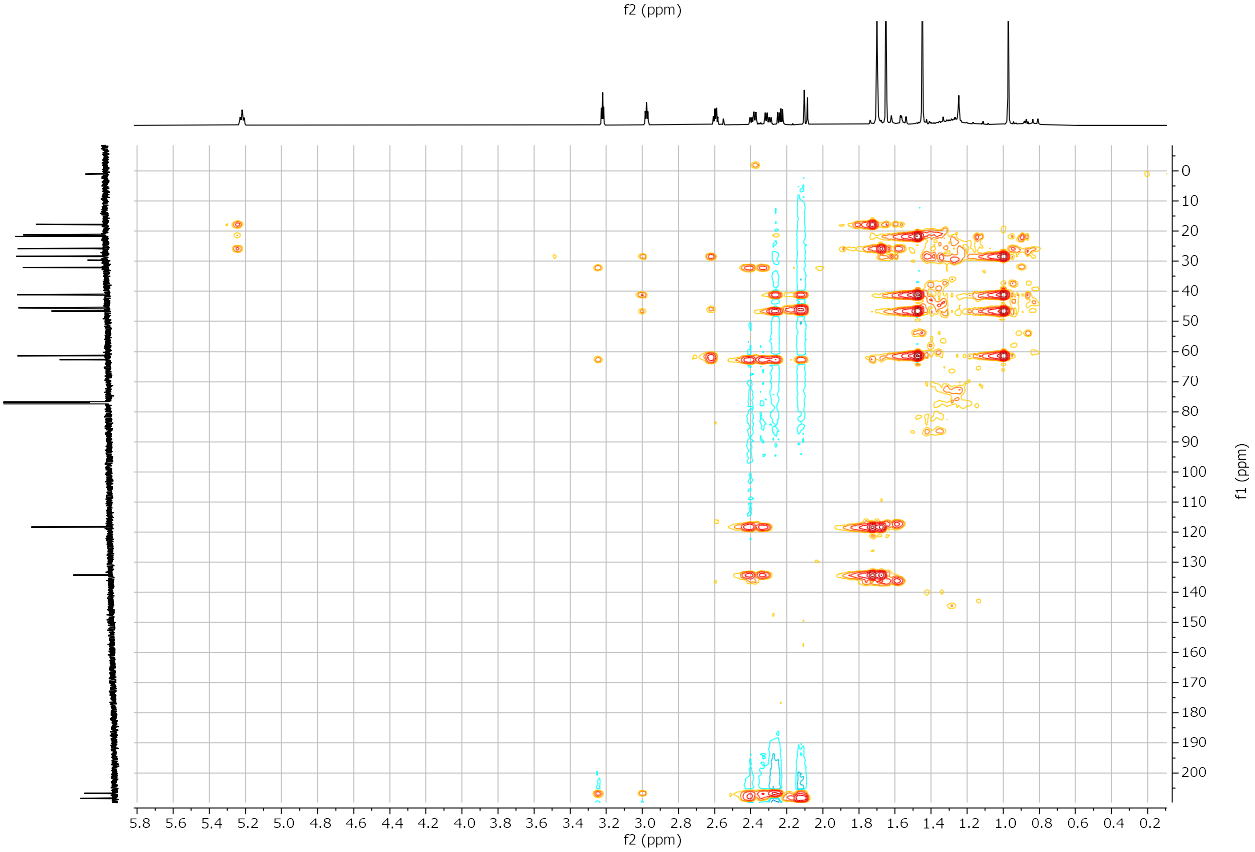
f2 (ppm)
f1 (ppm)

7.5 References

(1) (a) Lovering, F. Escape from Flatland 2: Complexity and Promiscuity. *Med. Chem. Commun.* **2013**, *4*, 515–519. (b) Lovering, F.; Bikker, J.; Humblet, C. Escape from Flatland: Increasing Saturation as an Approach to Improving Clinical Success. *J. Med. Chem.* **2009**, *52*, 6752–6756. (c) Atanasov, A. G.; Zotchev, S. B.; Dirsch, V. M.; Supuran, C. T. Natural Products in Drug Discovery: Advances and Opportunities. *Nat. Rev. Drug. Discov.* **2021**, *20*, 200–216. (d) Sparks, T. C.; Hahn, D. R.; Garizi, N. V. Natural Products, Their Derivatives, Mimics and Synthetic Equivalents: Role in Agrochemical Discovery. *Pest Manag. Sci.* **2017**, *73*, 700–715.

(2) (a) Bertz, S. H. Convergence, Molecular Complexity, and Synthetic Analysis. *J. Am. Chem. Soc.* **1982**, *104*, 5801–5803. (b) Bertz, S. H. The First General Index of Molecular Complexity. *J. Am. Chem. Soc.* **1981**, *103*, 3599–3601.

(3) (a)Haley, H. M. S.; Payer, S. E.; Papidocha, S. M.; Clemens, S.; Nyenhuis, J.; Sarpong, R. Bioinspired Diversification Approach Toward the Total Synthesis of Lycodine-Type Alkaloids. *J. Am. Chem. Soc.* **2021**, *143*, 4732–4740. (b) Jones, K. E.; Park, B.; Doering, N. A.; Baik, M.-H.; Sarpong, R. Rearrangements of the Chrysanthenol Core: Application to a Formal Synthesis of Xishacorene B. *J. Am. Chem. Soc.* **2021**, *143*, 20482–20490. (c) Wang, B.; Perea, M. A.; Sarpong, R. Transition Metal-Mediated C−C Single Bond Cleavage: Making the Cut in Total Synthesis. *Angew. Chem. Int. Ed.* **2020**, *59*, 18898–18919.

(4) Nandy, M.; Das, S.; Nanda, S. Cyclobutane Based “Overbred Intermediates” and Their Exploration in Organic Synthesis. *Org. Biomol. Chem.* **2022**, *20*, 1582–1622.

(5) (a) Murakami, M.; Ishida, N. Cleavage of Carbon–Carbon σ-Bonds of Four-Membered Rings. *Chem. Rev.* **2021**, *121*, 264–299. (b) Kärkäs, M. D.; Porco, J. A. Jr.; Stephenson, C. R. J. Photochemical Approaches to Complex Chemotypes: Applications in Natural Product Synthesis. *Chem. Rev.* **2016**, *116*, 9683–9747. (c) Bach, T.; Hehn, J. P. Photochemical Reactions as Key Steps in Natural Product Synthesis. *Angew. Chem. Int. Ed.* **2011**, *50*, 1000–1045. (d) Marek, I.; Masarwa, A.; Delaye, P.-O.; Leibeling, M. Selective Carbon–Carbon Bond Cleavage for the Stereoselective Synthesis of Acyclic Systems. *Angew. Chem. Int. Ed.* **2015**, *54*, 414–429.

(6) (a)Charaschanya, M.; Aubé, J. Reagent-Controlled Regiodivergent Ring Expansions of Steroids. *Nat. Commun.* **2018**, *9*, 934. (b) Blümel, M.; Nagasawa, S.; Blackford, K.; Hare, S. R.; Tantillo, D. J.; Sarpong, R. Rearrangement of Hydroxylated Pinene Derivatives to Fenchone-Type Frameworks: Computational Evidence for Dynamically-Controlled Selectivity. *J. Am. Chem. Soc.* **2018**, *140*, 9291–9298.

(7) (a)Leger, P. R.; Kuroda, Y.; Chang, S.; Jurczyk, J.; Sarpong, R. C–C Bond Cleavage Approach to Complex Terpenoids: Development of a Unified Total Synthesis of the Phomactins. *J. Am. Chem. Soc.* **2020**, *142*, 15536–15547. (b) Lusi, R. F.; Perea, M. A.; Sarpong, R. C–C Bond Cleavage of α-Pinene Derivatives Prepared from Carvone as a General Strategy for Complex Molecule Synthesis. *Acc. Chem. Res.* **2022**, *55*, 746–758. (c) Weber, M.; Owens, K.; Masarwa, A.; Sarpong, R. Construction of Enantiopure Taxoid and Natural Product-like Scaffolds Using a C–C Bond Cleavage/Arylation Reaction. *Org. Lett.* **2015**, *17*, 5432–5435. (d) Na, C. G.; Kang, S. H.; Sarpong, R. Development of a C–C Bond Cleavage/Vinylation/Mizoroki–Heck Cascade Reaction:

Application to the Total Synthesis of 14- and 15-Hydroxypatchoulol. *J. Am. Chem. Soc.* **2022**, *144*, 19253–19257. (e) Perea, M. A.; Wang, B.; Wyler, B. C.; Ham, J. S.; O'Connor, N. R.; Nagasawa, S.; Kimura, Y.; Manske, C.; Scherübl, M.; Nguyen, J. M.; Sarpong, R. General Synthetic Approach to Diverse Taxane Cores. *J. Am. Chem. Soc.* **2022**, *144*, 21398–21407. (f) Kuroda, Y.; Nicacio, K. J.; da Silva-Jr, I. A.; Leger, P. R.; Chang, S.; Gubiani, J. R.; Deflon, V. M.; Nagashima, N.; Rode, A.; Blackford, K.; Ferreira, A. G.; Sette, L. D.; Williams, D. E.; Andersen, R. J.; Jancar, S.; Berlinck, R. G. S.; Sarpong, R. Isolation, Synthesis and Bioactivity Studies of Phomactin Terpenoids. *Nat. Chem.* **2018**, *10*, 938–945. (g) Masarwa, A.; Weber, M.; Sarpong, R. Selective C–C and C–H Bond Activation/Cleavage of Pinene Derivatives: Synthesis of Enantiopure Cyclohexenone Scaffolds and Mechanistic Insights. *J. Am. Chem. Soc.* **2015**, *137*, 6327–6334. (h) Kerschgens, I.; Rovira, A. R.; Sarpong, R. Total Synthesis of (−)-Xishacorene B from (R)-Carvone Using a C–C Activation Strategy. *J. Am. Chem. Soc.* **2018**, *140*, 9810–9813. (i) Lusi, R. F.; Sennari, G.; Sarpong, R. Total Synthesis of Nine Longiborneol Sesquiterpenoids Using a Functionalized Camphor Strategy. *Nat. Chem.* **2022**, *14*, 450–456.

(8) (a) Xu, J.-F.; Zhao, H.-J.; Wang, X.-B.; Li, Z.-R.; Luo, J.; Yang, M.-H.; Yang, L.; Yu, W.-Y.; Yao, H.-Q.; Luo, J.-G.; Kong, L.-Y. (±)-Melicolones A and B, Rearranged Prenylated Acetophenone Stereoisomers with an Unusual 9-Oxatricyclo[3.2.1.13,8]Nonane Core from the Leaves of Melicope Ptelefolia. *Org. Lett.* **2015**, *17*, 146–149. (b) Dou, M.; Di, L.; Zhou, L.-L.; Yan, Y.-M.; Wang, X.-L.; Zhou, F.-J.; Yang, Z.-L.; Li, R.-T.; Hou, F.-F.; Cheng, Y.-X. Cochlearols A and B, Polycyclic Meroterpenoids from the Fungus Ganoderma Cochlear That Have Renoprotective Activities. *Org. Lett.* **2014**, *16*, 6064–6067. (c) Li, J.; Gao, K.; Bian, M.; Ding, H. Recent Advances in the Total Synthesis of Cyclobutane-Containing Natural Products. *Org. Chem. Front.* **2019**, *7*, 136–154. (d) Chen, Z.-H.; Guo, Y.-W.; Li, X.-W. Recent Advances on Marine Mollusk-Derived Natural Products: Chemistry, Chemical Ecology and Therapeutical Potential. *Nat. Prod. Rep.* **2022**, DOI: 10.1039/d2np00021k

(9) (a) Sauers, R. R.; Weston, C. A.; Dentz, B. I. Rearrangements of Tricyclo[3.2.1.03,6]Octyl Systems. *J. Org. Chem.* **1980**, *45*, 2813–2816.

(a) Barker, A. J.; Pattenden, G. Zizaane Sesquiterpenes. Synthesis of the Coates-Sowerby Tricyclic Ketone. *Tetrahedron Lett.* **1981**, *22*, 2599–2600.

(10) Manna, M. S.; Mukherjee, S. Remarkable Influence of Secondary Catalyst Site on Enantioselective Desymmetrization of Cyclopentenedione. *Chem. Sci.* **2014**, *5*, 1627–1633.

(11) Yoon, T. P.; Ischay, M. A.; Du, J. Visible Light Photocatalysis as a Greener Approach to Photochemical Synthesis. *Nat. Chem.* **2010**, *2*, 527–532.

(12) Christl, M.; Braun, M.; Deeg, O.; Wolff, S. Photochemical Reactions of Chloranil with Cyclooctene, 1,5-Cyclooctadiene, and Cyclohexene Revisited. *Eur. J. Org. Chem.* **2011**, *2011*, 968–982.

(13) (a) Irshadeen, I. M.; Walden, S. L.; Wegener, M.; Truong, V. X.; Frisch, H.; Blinco, J. P.; Barner-Kowollik, C. Action Plots in Action: In-Depth Insights into Photochemical Reactivity. *J. Am. Chem. Soc.* **2021**, *143*, 21113–21126. (b) Menzel, J. P.; Noble, B. B.; Lauer, A.; Coote, M. L.; Blinco,

J. P.; Barner-Kowollik, C. Wavelength Dependence of Light-Induced Cycloadditions. *J. Am. Chem. Soc.* **2017**, *139*, 15812–15820.

(14) (a) Næsborg, L.; Jandl, C.; Zech, A.; Bach, T. Complex Carbocyclic Skeletons from Aryl Ketones through a Three-Photon Cascade Reaction. *Angew. Chem. Int. Ed.* **2020**, *132*, 5705–5708. (b)Rauscher, N.; Næsborg, L.; Jandl, C.; Bach, T. Concise Total Synthesis of Agarozizanol B via a Strained Photocascade Intermediate. *Angew. Chem. Int. Ed.* **2021**, *60*, 24039–24042.

(15) Laudadio, G.; Palkowitz, M. D.; El-Hayek Ewing, T.; Baran, P. S. Decarboxylative Cross-Coupling: A Radical Tool in Medicinal Chemistry. *ACS Med. Chem. Lett.* **2022**, *13*, 1413–1420.

(16) Locke, G. M.; Bernhard, S. S. R.; Senge, M. O. Nonconjugated Hydrocarbons as Rigid-Linear Motifs: Isosteres for Material Sciences and Bioorganic and Medicinal Chemistry. *Eur. J. Chem.* **2019**, *25*, 4590–4647.

(17) Shipe, W. D.; Sorensen, E. J. Convergent, Enantioselective Syntheses of Guanacastepenes A and E Featuring a Selective Cyclobutane Fragmentation1. *J. Am. Chem. Soc.* **2006**, *128*, 7025–7035.

(18) Kurandina, D.; Parasram, M.; Gevorgyan, V. Visible Light-Induced Room-Temperature Heck Reaction of Functionalized Alkyl Halides with Vinyl Arenes/Heteroarenes. *Angew. Chem. Int. Ed.* **2017**, *56*, 14212–14216.

(19) (a)Chuentragool, P.; Kurandina, D.; Gevorgyan, V. Catalysis with Palladium Complexes Photoexcited by Visible Light. *Angew. Chem. Int. Ed.* **2019**, *58*, 11586–11598. (b) Cheung, K. P. S.; Sarkar, S.; Gevorgyan, V. Visible Light-Induced Transition Metal Catalysis. *Chem. Rev.* **2022**, *122*, 1543–1625.

(20) Boto, A.; Betancor, C.; Prange, T.; Suarez, E. Fragmentation of Alkoxy Radicals: Tandem .Beta.-Fragmentation-Cycloperoxyiodination Reaction. *J. Org. Chem.* **1994**, *59*, 4393–4401.

(21) (a) Ota, E.; Wang, H.; Frye, N. L.; Knowles, R. R. A Redox Strategy for Light-Driven, Out-of-Equilibrium Isomerizations and Application to Catalytic C–C Bond Cleavage Reactions. *J. Am. Chem. Soc.* **2019**, *141*, 1457–1462. (b) Gentry, E. C.; Knowles, R. R. Synthetic Applications of Proton-Coupled Electron Transfer. *Acc. Chem. Res.* **2016**, *49*, 1546–1556.

(22) Hartzel, L. W.; Ritter, J. J. A New Reaction of Nitriles. IV. Synthesis of N-Benzoylamino Acids. *J. Am. Chem. Soc.* **1949**, *71*, 4130–4131.

(23) Qin, X.-L.; Li, A.; Han, F.-S. Desymmetric Enantioselective Reduction of Cyclic 1,3-Diketones Catalyzed by a Recyclable P-Chiral Phosphinamide Organocatalyst. *J. Am. Chem. Soc*. **2021**, *143*, 2994–3002.

(24) Manna, M. S.; Mukherjee, S. Remarkable Influence of Secondary Catalyst Site on Enantioselective Desymmetrization of Cyclopentenedione. *Chem. Sci.* **2014**, *5*, 1627–1633.

(25) Narender, T.; Sarkar, S.; Venkateswarlu, K.; Kumar, J. K. New Chemical Access for Pyran Core Embedded Derivatives from Bisalkenylated 1,3-Diketones and 1,3-Diketoesters via Tandem C-Dealkenylation and Cyclization. *Tetrahedron Lett*. **2010**, *51*, 6576–6579.

7.6 Experimental contributors

This chapter includes content reproduced, with permission, from: Bakanas, I. Tang, J, C, Sarpong, R.* Skeletal Diversification by C–C Cleavage to Access Bicyclic Frameworks from a Common Tricyclooctane *in preparation*. Experiments were carried out by I.B. with assistance from J.C.T. with guidance from R.S.